

AD 684334

AD

USAAVLABS TECHNICAL REPORT 68-40

**STOPPED-STOWED ROTOR COMPOSITE
RESEARCH AIRCRAFT**

January 1969

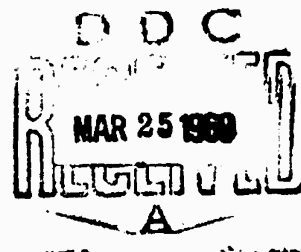
**U. S. ARMY AVIATION MATERIEL LABORATORIES
FORT EUSTIS, VIRGINIA**

**CONTRACT DA 44-177-AMC-372(T)
LOCKHEED-CALIFORNIA COMPANY
A DIVISION OF LOCKHEED AIRCRAFT CORPORATION
BURBANK, CALIFORNIA**

*This document has been approved
for public release and sale; its
distribution is unlimited.*



CLEARINGHOUSE
for the dissemination of information
to the public



440

Disclaimers

The findings in this report are not to be construed as an official Department of the Army position unless so designated by other authorized documents.

When Government drawings, specifications, or other data are used for any purpose other than in connection with a definitely related Government procurement operation, the United States Government thereby incurs no responsibility nor any obligation whatsoever; and the fact that the Government may have formulated, furnished, or in any way supplied the said drawings, specifications, or other data is not to be regarded by implication or otherwise as in any manner licensing the holder or any other person or corporation, or conveying any rights or permission, to manufacture, use, or sell any patented invention that may in any way be related thereto.

Trade names cited in this report do not constitute an official endorsement or approval of the use of such commercial hardware or software.

Disposition Instructions

Destroy this report when no longer needed. Do not return it to the originator.

ACCESSION NO.		
TEST	WRITE SECTION <input checked="" type="checkbox"/>	
DOC	COPY SECTION <input type="checkbox"/>	
ANNOUNCED	<input type="checkbox"/>	
SPECIFICATION		
DISTRIBUTION/AVAILABILITY CODE		
DIST.	AVAIL.	and/or SPECIAL

NTIS DISCLAIMER

- ❖ This document has been reproduced from the very best copy that was furnished by the Source Agency. Although NTIS realizes that parts of this document may be illegible, it is being released in order to make available as much information as possible.



DEPARTMENT OF THE ARMY
U. S. ARMY AVIATION MATERIEL LABORATORIES
FORT BELVOIR, VIRGINIA 22064

This report is a summary of the preliminary design study of a Stopped-Stowed Rotor Composite Research Aircraft (CRA) concept. The general objective of the CRA was to combine into one research aircraft the efficient hovering characteristics of a helicopter and the high-speed cruise characteristics of fixed-wing aircraft.

This study presents one approach to meeting the above objective. This report is published for the dissemination of information and the stimulation of new ideas.

Task 1F163204D15704
Contract DA 44-177-AMC-372(T)
USAAVLABS Technical Report 68-40
January 1969

STOPPED-STOWED ROTOR COMPOSITE
RESEARCH AIRCRAFT

Final Report

Lockheed Report LR 21722

by

Rotary Wing - New Design

Prepared by

Lockheed-California Company
A Division of Lockheed Aircraft Corporation
Burbank, California

for

U. S. ARMY AVIATION MATERIEL LABORATORIES
FORT EUSTIS, VIRGINIA

This document has been approved
for public release and sale; its
distribution is unlimited.

This page intentionally left blank.

SUMMARY

This summary report describes the preliminary design of the Army VTOL Rotary Wing Composite Research Aircraft (CRA). The vehicle is configured to meet the requirements, and satisfy the objectives, of this program.

This CRA design was the result of combining the most desirable features of a helicopter with those of a fixed-wing aircraft. The vehicle derived was capable of hovering as a helicopter with low rotor downwash velocity and yet cruise at high speed with economy and little noise or vibration. Use of the rigid-rotor system supplied positive control moments, in-flight rotor stop/start capability, and a simple blade-folding/stowing mechanism.

The CRA can fly up to the conversion speed in the helicopter mode transfer lift and control to the conventional fixed-wing surfaces, stop the rotor, fold the blades and retract the rotor and blades into the top of the fuselage. This process is reversible to convert from the fixed-wing configuration to the helicopter.

The results of this study indicate that the CRA is feasible and additional study and development should be undertaken.

This page intentionally left blank.

FOREWORD

The Composite Research Aircraft Review draft report was submitted June 1, 1966 to the U. S. Army Aviation Materiel Laboratories in response to the Statement of Work for Contract DA 44-177-AMC-372(T). This report consisted of three volumes: I, Technical; II, Management; and III, Cost. The technical volume was composed of Parts A through P (Data Item 15-004-R), bound in separate books.

Selected portions of these books have been combined and are reproduced herein to provide a summary and condensation of all technical information in a single document.

This page intentionally left blank.

TABLE OF CONTENTS

	<u>Page</u>
SUMMARY	iii
FOREWORD	v
LIST OF ILLUSTRATIONS	xi
LIST OF TABLES	xix
LIST OF SYMBOLS	xxi
INTRODUCTION	1
PART 1 - DESIGN CONCEPT	
COMPOSITE	3
VEHICLE DESCRIPTION	7
Component Design Philosophy	7
General Description	8
Vehicle Characteristics	11
Maintainability Program	18
PART 2 - PERFORMANCE	
AERODYNAMIC DESCRIPTION	26
Optimization of the Configuration	27
PERFORMANCE ANALYSIS	40
Hover and Vertical Flight	40
Forward Flight	53
Mission Analysis	69
POWERPLANT INSTALLATION	81
Main Engines	81
Air Induction System	82
Fuel Systems	86
Engine Mount System	90
Lubrication Systems	90
Powerplant Control System	93
Instrumentation System	102
Starting System	102

TABLE OF CONTENTS (Continued)

	<u>Page</u>
Engine Compartment Cooling	103
Installation Loss Analysis	103
POWER TRANSMISSION SYSTEMS	123
General Description	124
Design Criteria - Transmission System	137
Design Loads - Transmission System	139
Lubrication System	148
VERTICAL LIFT SYSTEM	151
Main Rotor	151
Rotor Folding and Stowing System	159
Antitorque Rotor	164
FORWARD THRUST SYSTEM	171
Propeller Blades	171
Hub and Gearbox	172
PART 4 - WEIGHT AND BALANCE	
ESTIMATED WEIGHT REPORT	173
SUPPLEMENTARY WEIGHT DATA	186
Variations from Optimum Design	186
Equipment Weight Allowances	186
PART 5 - STABILITY, CONTROL AND FLYING QUALITIES	
FLIGHT CONTROL SYSTEMS	187
Rotary-Wing Flight Control System	188
Helicopter Controls	189
Fixed-Wing Flight Control System	190
Transition Controls	191
Propeller Controls	192
STABILITY AND CONTROL ANALYSIS	194
Helicopter Mode	194
Fixed-Wing Mode	233

TABLE OF CONTENTS (Continued)

	<u>Page</u>
PART 6 - STRUCTURES	
STRUCTURAL DESIGN CRITERIA	276
Design Rotor Speeds	276
Design Limit Flight Maneuver Load Factors	278
Design Gust Load Factors	283
Design Landing Conditions	291
Design Taxi and Takeoff Conditions	295
Main Rotor Structural Requirements	297
Tail Rotor Structural Requirements	297
Powerplant Installation	298
Wing Design Criteria	300
Fuselage Design Criteria	300
Empennage Design Criteria	301
Control System	303
Emergency Landing Requirements	304
Fatigue Loading Criteria	304
STRUCTURAL DESIGN LOADS	310
Rotor Dynamic Loads Determination	310
Component Loads	313
PART 7 - HYDRAULIC AND MECHANICAL SYSTEMS	
HYDRAULIC SYSTEMS	339
MECHANICAL SYSTEMS	345
Landing Gear	345
PART 8 - EMERGENCY SYSTEMS AND PROCEDURES	
EMERGENCY SYSTEMS	348
Emergency System Determination	348
Emergency Escape - Crew	352
EMERGENCY PROCEDURES	359
Main Rotor System	359
Powerplant System	360
Drive System	360

TABLE OF CONTENTS (Continued)

	<u>Page</u>
PART 9 - COCKPIT ARRANGEMENT	
GENERAL ARRANGEMENT	362
Pilot Visibility	362
FLIGHT STATION PROVISIONS	367
Instrument Panel	367
Control-Display Arrangement	368
PART 10 - AEROELASTICITY	
COMPOUND HELICOPTER FLIGHT	372
Main Rotor Aeroelastic Stability	372
High-Speed Gyro Characteristics	377
Tail Rotor Aeroelastic Stability	377
Mechanical Stability	378
Vibration	378
Blade Frequency Spectrum	378
TRANSITIONAL FLIGHT	384
Main Rotor Aeroelastic Stability	384
Rotor Contribution to Aircraft Stability	388
STOPPED ROTOR FLIGHT	391
Main Rotor Aeroelastic Stability	391
LITERATURE CITED	403
DISTRIBUTION	407

LIST OF ILLUSTRATIONS

<u>Figure</u>		<u>Page</u>
1	General Arrangement	9
2	Inboard Profile	19
3	Effect of Tip Speed on Solidity Required.	29
4	Required Wing Span as a Function of Equivalent Flat Plate Area	31
5	Effect of Propeller Diameter on Performance and Weight	34
6	Effect of Propeller Tip Speed	35
7	Effect of Propeller Activity Factor	36
8	Results of Tail Rotor Parametric Study.	38
9	Dynamic Pressure Distribution in Rotor Downwash	41
10	Vertical Drag Coefficients	42
11	Main Rotor Thrust Coefficient in Hover.	43
12	Main Rotor Performance in Hover	44
13	Main Rotor Figure of Merit	45
14	Tail Rotor Thrust Coefficient	46
15	Tail Rotor Performance	47
16	Main Rotor Power Required for Hover	48
17	Antitorque Power Required in Hover	49
18	Total Hover Power	50
19	Hover Ceiling	52
20	Effect of Tip Speed on Sea Level Hover.	54
21	Power Required for Vertical Climb	55
22	Equivalent Parasite Area of Complete Airplanes	58
23	Airplane Compressibility Correction	59
24	Parasite Drag Variation	60
25	Total Drag Coefficients	61
26	Propeller Power at Sea Level	63
27	Propeller Power at 10,000 Feet	64

LIST OF ILLUSTRATIONS (Continued)

<u>Figure</u>		<u>Page</u>
28	Power Required for Forward Flight, Flaps Up	65
29	Power Required for Forward Flight, Flaps Down	66
30	Lift Sharing Between Wing and Rotor	67
31	Maximum Speed as a Function of Altitude	70
32	Maximum Rates of Climb	71
33	Specific Range at Sea Level	72
34	Specific Range at 10,000 Feet	73
35	Specific Range at 20,000 Feet	74
36	Specific Endurance at Sea Level	75
37	Landing Distance	76
38	Takeoff Distance	76
39	Payload - Range	77
40	Altitude Effect on Specific Range	78
41	Range as a Function of Takeoff Weight	79
42	Payload - Endurance	80
43	Power Plant Installation with Related Systems	83
44	Fuel System Schematic	87
45	Engine and Propeller Gearbox Oil System Schematic	91
46	Engine Power and Speed Control Schematic	94
47	Flight Station Instrumentation	97
48	Engine Compartmentation Schematic	100
49	Engine Compartment Cooling Schematic	104
50	Estimated CRA Inlet Total Pressure Recovery	105
51	Exhaust System Arrangement	107
52	T64-GE-16 Installed Performance, Sea Level	110
53	T64-GE-16 Installed Performance, Sea Level	111
54	T64-GE-16 Installed Performance, 10,000 Feet	112
55	T64-GE-16 Installed Performance, 10,000 Feet	113
56	T64-GE-16 Installed Performance, 20,000 Feet	114
57	T64-GE-16 Installed Performance, 20,000 Feet	115
58	T64-GE-16 Installed Performance, 30,000 Feet	116

LIST OF ILLUSTRATIONS (Continued)

<u>Figure</u>		<u>Page</u>
59	T64-GE-16 Installed Performance, 30,000 Feet	117
60	T64-GE-16 Installed Performance, Maximum Power	118
61	T64-GE-16 Installed Performance, Military Power	119
62	T64-GE-16 Installed Performance, Normal Power	120
63	T64-GE-16 Installed Performance, Hover in Ground Effect	121
64	T64-GE-16 Installed Performance, Hover out of Ground Effect	122
65	Power Drive System Arrangement	125
66	Main Rotor Transmission Assembly	131
67	Tail Rotor Inplane Bending Moment-Maximum Thrust	143
68	Tail Rotor Flapwise Bending Moment-Maximum Thrust	144
69	Power Transmitted, Hover/VTOL Mode	145
70	Power Transmitted, Hover/VTOL Mode - Emergency	146
71	Power Transmitted, Fixed-Wing Mode	147
72	Main Transmission Oil System Schematic	150
73	Rotor V_t and σ Optimization Map	152
74	Main Rotor Blade Coupled Frequency Spectrum	154
75	Rotor Blade Assembly	157
76	Main Rotor Hub and Blade-Folding Mechanism	161
77	Main Rotor Controls Arrangement	165
78	Tail Rotor Assembly	169
79	Dimensional Data for Reference Axes	174
80	Summary Weight Statement	175
81	Center-of-Gravity Travel Diagram	185
82	Longitudinal Stick Force and Position vs Speed - Helicopter Mode	195
83	Response to Longitudinal Step Inputs in Hover	196
84	Response to a 1-Inch Longitudinal Step Input, 80 Knots, Aft Center-of-Gravity	197
85	Response to a 1-Inch Longitudinal Step Input, 80 Knots, Forward Center-of-Gravity	198

LIST OF ILLUSTRATIONS (Continued)

<u>Figure</u>		<u>Page</u>
86	Response to a 1-Inch Longitudinal Pulse Input at 80 Knots	199
87	Control Power and Damping in Pitch - Helicopter Mode . .	201
88	Maneuvering Stability - Helicopter Mode	203
89	Lateral Stick Position Vs. Sideslip Angle Helicopter Mode	204
90	Rolling Moment Coefficient Vs. Sideslip Angle	204
91	Response to Lateral Step Inputs in Hover	205
92	Response to a 1-Inch Lateral Step Input, 80 Knots . . .	206
93	Response to a 1-Inch Lateral Pulse Input, 80 Knots . . .	207
94	Control Power and Damping in Roll - Helicopter Mode . .	209
95	Pedal Position Vs. Velocity - Helicopter Mode	210
96	Yawing Moment Coefficient Vs. Sideslip Angle	211
97	Pedal Position Vs. Sideslip Angle - Helicopter Mode . .	212
98	Main Rotor Torque Vs. Sideward Velocity	214
99	Tail Rotor Capability and Requirement in Sideward Flight	215
100	Response to a 1-Inch Directional Input, 80 Knots, Aft Center of Gravity	221
101	Time History of Rotor Speed Following Engine Failure in Hover	223
102	Time History of Rotor Speed Following Engine Failure at 140 Knots	229
103	Rate of Descent in Steady Autorotation	231
104	Height-Velocity Curves for Landing in Autorotation . . .	232
105	Lift Curve - $\delta_F = 0^\circ, 20^\circ, 45^\circ$	234
106	Comparison of Wind Tunnel with Estimated Flap Lift Data	235
107	Static Stick-Fixed Stability	237
108	Elevator Required to Trim $C_{L_{max}}$	238
109	Power-On Lift Curve - $\delta_F = 45^\circ$	239
110	Power-On Lift Curve - $\delta_F = 20^\circ$	240
111	Power-On Pitching Moment - $\delta_F = 45^\circ$	241

LIST OF ILLUSTRATIONS (Continued)

<u>Figure</u>		<u>Page</u>
112	Power-On Pitching Moment - $\delta_F = 20^\circ$	242
113	Stick Force per g in Pull-Up	243
114	Stick Force Gradient in Unaccelerated Flight (Takeoff) .	245
115	Stick Force Gradient in Unaccelerated Flight (Transition)	246
116	Stick Force Gradient in Unaccelerated Flight (Approach).	247
117	Stick Force Gradient in Unaccelerated Flight (Cruise) .	248
118	Stick Force Gradient in Unaccelerated Flight (Maximum Speed)	249
119	Time History of Control Motions During Transition from Helicopter to Airplane Mode	252
120	Time History of Control Motions During Transition from Airplane to Helicopter Mode	253
121	Longitudinal Short-Period Damping	258
122	Stopped-Rotor Blade Angle Schedule for Maintaining Zero Rotor Load	259
123	Yawing Moment Coefficient Vs. Sideslip Angle (Flaps Up and Down)	260
124	Side Force Coefficient Vs. Sideslip Angle (Flaps Up and Down)	261
125	Rolling Moment Coefficient Vs. Sideslip Angle (Flaps Up and Down)	262
126	Dihedral Effect (Flaps Up and Down)	263
127	Aileron Effectiveness	265
128	Bank Angle Time History at Transition Speed	266
129	Aileron Hinge Moment Coefficient	267
130	Aileron Stick Force	268
131	Characteristics in Steady-State Sideslip (Approach). .	269
132	Control Forces in Straight Yawed Flight (Approach) . .	270
133	Characteristics in Steady-State Sideslip (Cruise) . .	271
134	Control Forces in Straight Yawed Flight (Cruise) . . .	272
135	Dutch Roll Characteristics	275
136	Minimum Rotor Speed Vs. Cross Weight for 1.0 g Flight. .	277
137	V-n Diagram - Fixed-Wing Mode	279

LIST OF ILLUSTRATIONS (Continued)

<u>Figure</u>		<u>Page</u>
138	Variation of Section Maximum Lift Coefficient with Mach Number	280
139	Maximum Rotor Load Factor Vs. Rotor RPM	281
140	Division of Lift Between Rotor and Vehicle Less Rotor - 1.0 g	282
141	Maximum Collective Pitch Vs. Forward Speed	284
142	V-n Diagram - Compound Mode	285
143	$\Delta C_{T_1}/\sigma$ and $\Delta \lambda$ per 1° Collective Pitch Vs. Advance Ratio	287
144	$dC_{T_1}/d\sigma$ Vs. Advance Ratio	288
145	Nose Landing Gear Load Factor Vs. Strut Stroke	293
146	Landing Gear Capability - Fixed-Wing Mode	296
147	Probability Distribution of Events by Pitching Acceleration	306
148	Typical Fatigue Loading Spectrum Presentations	309
149	Main Rotor Mass and Stiffness Distribution	314
150	Main Rotor Coupled Blade Frequencies - $\theta = 0.15$ RAD . .	316
151	Main Rotor Centrifugal Force Per Ω^2	317
152	Main Rotor Bending Moments Vs. Azimuth Angle - Hover . .	318
153	Main Rotor Bending Moments Vs. Azimuth Angle - V = 100 KEAS	319
154	Main Rotor Bending Moments and Torsion - 1.0 g, Hover 227 RPM	320
155	Main Rotor Bending Moments and Torsion - 1.0 g, V = 100 KEAS, 227 RPM	321
156	Main Rotor Bending Moments and Torsion - 1.0 g, Hover, 265 RPM	322
157	Main Rotor Bending Moments and Torsion - 1.0 g, V = 100 KEAS, 265 RPM	323
158	Main Rotor Bending Moments and Torsion - 1.49 g, Hover, 227 RPM	324
159	Main Rotor Bending Moments and Torsion - 1.93 g, V = 100 KEAS, 227 RPM	325
160	Main Rotor Bending Moments and Torsion - 1.88 g, Hover, 265 RPM	326

LIST OF ILLUSTRATIONS (Continued)

<u>Figure</u>		<u>Page</u>
161	Main Rotor Bending Moments and Torsion - 2.23 g, V = 100 KEAS, 265 RPM	327
162	Main Rotor Flapwise Bending Moments - Slope Terrain Takeoff	328
163	Main Rotor - 1st Mode Flapping Distribution Curve . . .	329
164	Main Rotor Flapwise Bending Moments - Rotor Stopped at V = 140 KEAS	330
165	Main Rotor Flapwise Bending Moments - Rotor Stopped at V = 160 KEAS	331
166	Main Rotor Inplane Bending Moments - Rotor Stopped at V = 140 KEAS	332
167	Main Rotor Inplane Bending Moments - Rotor Stopped at V = 160 KEAS	333
168	Main Rotor Feathering Moments - Rotor Stopped at V = 140 KEAS	335
169	Main Rotor Feathering Moments - Rotor Stopped at V = 160 KEAS	336
170	Tail Rotor Flapwise Bending Moment - Overspeed	337
171	Tail Rotor Inplane Bending Moment - Overspeed	338
172	Hydraulic Systems Schematic	341
173	Hydraulic Systems Components Arrangement	343
174	Flight Station Arrangement	353
175	Ejection-Seat System Sequencing	355
176	Flight Station Visibility Angles	363
177	Mockup Visibility	366
178	Instrument Panel	369
179	Center Control Console	371
180	Whirl Tower Installation of 33-Foot-Diameter Stopped-Rotor Model	373
181	View of 33-Foot-Diameter Stopped-Rotor Model with Blades Folded	374
182	Ames 40 X 80-Foot Wind Tunnel Installation of 33-Foot-Diameter Stopped-Rotor Model	375
183	Mode Shapes Used for Modalization Analyses	376

LIST OF ILLUSTRATIONS (Continued)

<u>Figure</u>		<u>Page</u>
184	Main Rotor First Coupled Mode - CRA	380
185	Main Rotor Second Coupled Mode - CRA	381
186	Main Rotor Third Coupled Mode - CRA	382
187	Main Rotor Frequency Variation with Respect to Collective Angle - CRA	383
188	Time History of Stop-and-Start Sequence for 33-Foot-Diameter at 80 Knots	385
189	Time History of Stop-and-Start Sequence for 33-Foot-Diameter at 120 Knots	386
190	Time History of Stop-and-Start Sequence for 33-Foot-Diameter at 140 Knots	387
191	Rotor Moments During Start Sequences of 33-Foot-Diameter Rotor-System at Several Speeds	390
192	Summary of Nonrotating Flapwise Bending Moments for Stopped-Rotor, 33-Foot-Diameter	392
193	Nonrotating Flapwise Bending Moments as a Function of Rotor Angle for 33-Foot-Diameter Stopped-Rotor Full-Scale Model	393
194	Nonrotating Flapwise Bending Moments as a Function of Collective Angle for 33-Foot-Diameter Stopped-Rotor Full-Scale Model	394
195	Hub Flapwise Bending Moment - 33-Foot-Diameter Rotor	396
196	Hub Flapwise Bending Moment - 33-Foot Diameter Rotor	397
197	CRA Blade Flapwise Elastic Deflection	398
198	CRA Blade Section Shear	399
199	CRA Blade Section Flapwise Moment	400
200	CRA Blade Section Torque	401
201	CRA Blade Divergence Region	402

LIST OF TABLES

<u>Table</u>		<u>Page</u>
I	General Characteristics	11
II	Weight Summary	26
III	Power Losses	51
IV	Estimation of Minimum Drag	56
V	T64 Uninstalled Engine Data	82
VI	Losses Due to Power Extraction	108
VII	Power Transmission System Ratings	127
VIII	Limit Torque/Shaft Horsepower (SHP) Summary - Transmitter System	140
IX	CRA Transmission System - 1200-Hour Power-Time Design Spectrum (Constant RPM)	141
X	Shaft Horsepower (SHP) Distribution	148
XI	Weight and Balance Summary	180
XII	Group Weight and Balance Summary	181
XIII	Gross Weight Balance	182
XIV	Extreme Forward Center-of-Gravity Condition	183
XV	Extreme Aft Center-of-Gravity Condition	184
XVI	Weight Variations from Optimum Design Configuration	186
XVII	Neutral Points	244
XVIII	Longitudinal Dynamic Stability Derivatives	256
XIX	Elevator Stick Force Due to Sudden Deviations from Longitudinal Trim	257
XX	Lateral-Directional Dynamic Stability Derivatives	274
XXI	Design Rotor Speeds	276
XXII	Gust Incremental Load Factor - Main Rotor	289
XXIII	Gust Incremental Load Factor - Vehicle Less Rotor	289
XXIV	Engine Data for Engine Mount Loads	299
XXV	Emergency Landing Load Factors	304

LIST OF TABLES (Continued)

<u>Table</u>		<u>Page</u>
XXVI	Emergency Egress Data	350
XXVII	Start/Stop Sequences Vs. Tunnel- Speed/Angle-of-Attack	388
XXVIII	Significant Properties of 33-Foot-Diameter Stopped-Rotor Vehicle	389

LIST OF SYMBOLS

A	Rotor Disc Area, sq ft
AF	Propeller Blade Activity Factor
AR	Aspect Ratio of Wing
b	Wing Span
C_L	Wing Lift Coefficient
C_{L_i}	Integrated Design Lift Coefficient
C_{D_i}	Induced Drag Coefficient
$C_{D_{ow}}$	Minimum Wing Drag Coefficient
C_{D_P}	Parasite Drag Coefficient
C_{D_C}	Drag Coefficient due to Compressibility Effects
C_T	Coefficient of Thrust
D	Drag, lb
e	Wing Efficiency Factor
f_o	Minimum Equivalent Flat Plate Area, sq ft
H	Horizontal Stabilizer
IGE	In Ground Effect
L	Lift, lb
L/D	Lift-to-Drag Ratio
M	Mach Number
MAC	Mean Aerodynamic Chord
OGE	Out of Ground Effect
q	Dynamic Pressure, psf
r	Blade Radial Station, ft
R	Rotor or Propeller Radius, ft

LIST OF SYMBOLS (Continued)

S_F	Wetted Area, sq ft
sfc	Specific Fuel Consumption
SL	Sea Level
S_W	Wing Area, sq ft
T	Rotor Thrust, lb
V	Velocity, fps; Vertical Stabilizer
V_s	Stall Speed
V_t	Tip Speed, fps
W	Wing
Z	Distance Below Rotor, ft
η_p	Propeller Efficiency
σ	Rotor Solidity
Ω	Rotor or Propeller Rotational Velocity, radians per second

INTRODUCTION

It has long been recognized that the relatively low disc loading of the helicopter has the most efficient hover capabilities of the VTOL (Vertical Takeoff and Landing) type aircraft. It is also recognized that the simple fixed-wing aircraft has the most efficient lift producing system in the 300- to 400-knot speed range. The objective is to combine these characteristics into one research aircraft which will provide a VTOL aircraft with significantly increased productivity, increased range, reduced fuel logistics, and low noise level.

The need for a vehicle of this type has been recognized for many years. In 1950, the Air Force conducted a design competition to evaluate three types of high-speed VTOL aircraft: the XV-1, XV-2, and XV-3. However, the forward speed was limited to only 200 miles per hour. The XV-1, designed and tested by McDonnell Aircraft Corporation, was a compound aircraft with a gross weight of approximately 5000 pounds, and the rotor was driven by a pressure jet system and the vehicle was propelled forward by a pusher propeller. The XV-2 program was limited to a study and wind tunnel test of a stopped-rotor configuration and was conducted by Sikorsky Aircraft Corporation. The XV-3 consisted of a tilt rotor configuration with a gross weight of 5000 pounds, and was tested by Bell Helicopter Corporation.

It is generally agreed that the results of this program established the technical feasibility of the concepts that were flight tested; that is, the XV-1 compound and the XV-3 tilt rotor. The stopped-rotor concept, however, was not carried through a flight test program and therefore has not had the opportunity of a demonstrated acceptance.

Recent development of the rigid-rotor system, which eliminates the need for conventional flapping and lead-lag hinges, offers an opportunity for developing a successful stopped-and stowed-rotor concept. Such programs as the XH-51A helicopter and the testing on a modified compound XH-51A, which led to the award of the Advanced Aerial Fire Support System (AAFSS), form the basis for the design, as presented in this report, of a stopped-rotor system.

Recently, technical feasibility of the stopped-rotor concept was positively confirmed with the successful completion of a wind tunnel test program using a full-scale 33-foot-diameter rotor in the NASA-Ames 40 X 80-foot wind tunnel, reference BuWeps Contract, N0w 66-0246-f. Rotor start and stop testing, with blade folding and extending, was performed in the tunnel tests. Start/stop tests were made at wind tunnel speeds and rotor angles of attack of 80 knots from 0 to 12 degrees, 100 knots from 0 to 6 degrees, 120 knots from 0 to 2 degrees, and 140 knots at 0 degrees. A total of 55 start/stops were successfully completed. In conjunction with the start/stop tests, blade folding and extending tests were conducted at speeds up to 140 knots.

Early testing on this full-size rotor showed that the control system must be stiff during the rotor start and stop phase. Tests with this original model produced blade-bending moments that resulted in blade permanent set. Subsequent to these tests, however, the control system was redesigned and the control actuators were located closely coupled with the swash plate enabling the wind tunnel program to be successfully completed.

Results of these tests can be used to substantiate the analysis and design of the stowed-rotor concept. This wind tunnel test vehicle was designed to transition at a forward speed of 120 knots with a margin over transition to 140 knots.

The preliminary design of the Composite Research Aircraft (CRA) incorporates design features of this test rotor. Control actuators are close coupled with the swashplate. A simple fold mechanism developed on the test rotor has also been employed. These tested mechanical design features, coupled with the successful completion of the wind tunnel tests, provide a high degree of confidence that the stowed-rotor concept will be successfully developed.

The following sections of this report summarize the application of the stopped rotor into a composite aircraft configuration.

PART 1
DESIGN CONCEPT

SECTION 1
COMPOSITE AIRCRAFT CONCEPT

For many years, attention has been directed toward a composite aircraft which would exhibit the VTOL capability of the helicopter and the high forward speed capability and cruise efficiency of the fixed-wing aircraft. A number of military missions exist where vertical takeoff requiring low rotor disc loading in conjunction with maximum forward speed and/or cruise efficiency greater than that of existing helicopters would greatly enhance overall mission effectiveness. Prime examples are logistics, ground troop transport, surveillance, target acquisition, and ASW missions.

During the past 20 years, the helicopter has performed those missions which require VTOL capability. However, helicopter operation in these missions has been inefficient, particularly with regard to high operating costs and low forward speeds. Application of the shaft turbine to the helicopter and improvements in mechanical design have contributed greatly to reducing direct operating costs; and while forward speed capability has improved, significant increases are not in evidence in operational helicopters.

The fundamental characteristics of the helicopter speed constraints have been identified and understood for many years. These constraints are primarily associated with compressibility effects on the advancing rotor blade and stall effects on the retreating rotor blade. While both phenomena increase power required by the main rotor, it is their profound effect on aircraft vibration and rotor stress levels that represents the practical forward speed constraint.

In view of the forward speed requirements of a composite aircraft, i.e., in excess of 300 knots, it is apparent that a successful composite concept must be one in which the forward speed constraints of the conventional rotor are completely removed. While there are a number of configurations which accomplish the combination of VTOL and high-speed capability, there are a limited number of concepts which exhibit VTOL capabilities in conjunction with low disc loading, i.e., less than 10. The low disc loading requirement, which evolves from the need for operational capability from unprepared sites and with low noise signature, clearly indicates the use of a conventional shaft-driven rotor in the VTOL mode.

The requirement for maximum forward speed and/or cruise efficiency comparable to that of the conventional fixed-wing airplane implies overall configuration lift-to-drag ratios of 10 or greater; thus, in the high-speed flight mode, the composite aircraft must closely resemble conventional fixed-wing airplanes.

The most successful direct means of relieving, but not eliminating, the helicopter rotor speed constraints are represented by the compound helicopter. In this configuration a fixed wing is installed to provide lift at high forward speed, and a separate forward propulsion device is provided. While this relief of the rotor speed constraints allows the compound helicopter to fly at speeds much in excess of the conventional helicopter, such unloaded rotors still exhibit a fundamental limitation on forward flight speed.

Thus, the stowed rotor concept evolves as a means of removing the forward flight limitations of the unloaded compound rotor. Stopping and starting a conventional rotor in forward flight has been demonstrated successfully by many investigators. Recently, Lockheed has conducted extensive wind tunnel tests to establish optimum starting and stopping procedures for the rigid-rotor system, and the aeroelastic design criteria imposed by such optimum procedures. Folding a stopped rotor in flight requires automatic folding provisions identical to those required for folding helicopter rotors aboard Navy aircraft carriers. Finally, stowing the folded rotor requires a mechanical linkage similar to that used for retracting a conventional aircraft landing gear. Feasibility of the entire stopping, folding, starting cycle with the rigid rotor has been recently verified in the Ames 40- x 80-foot Wind Tunnel at forward speeds of 80, 120, and 140 knots. The mechanical design evolved for folding and stowing coupled with the success of the wind tunnel tests provides a high confidence level in the successful completion of this CRA concept.

The stowed-rotor configuration retains the excellent hovering capability of the helicopter; and, by relieving the rotor of any forward speed lift or propulsion assignment, the configuration exhibits good high-speed characteristics. Forward speed potential for this concept is comparable to fixed-wing aircraft and simply depends upon the nature of the forward propulsion means, i.e., propellers or turboprops.

This concept not only offers an opportunity for removing the forward flight limitations, but it retains the capability for flying in the compound mode above the transition speeds for stowing. Thus, in a mission application requiring a high dash speed, it is possible to fly the stowed rotor concept up to forward speeds in excess of 200 knots without requiring any form of conversion. This nonconversion characteristic is possible by using a combination of separate lift and propulsion devices that facilitate a high-speed flight similar to a compound configuration while still providing the stowing feature required for higher speed operation in the airplane mode.

Any meaningful concept selection must be based on evaluations which consider the basic objectives and final utilization of a composite aircraft. These basic objectives are to obtain, in a single vehicle, the transport productivity, range capability, and high-speed potential of the fixed-wing aircraft and the low-speed capability (hover endurance) of the helicopter. Further, these composite aircraft performance characteristics are to be

available in special environments where low noise levels must be maintained and where operation from unprepared sites is mandatory. Finally, the intended operating environment introduces fuel logistics as a significant consideration.

Thus, concept selection must be based on the basic premise that many mission profiles will evolve for the composite vehicle, each with varied requirements for:

- High transport productivity
- High-speed capability
- VTOL performance (hovering endurance)

As such, the optimum composite aircraft concept must be one which is free from fundamental constraints on these three basic performance requirements. The stowed rotor concept is free from such constraints and displays the versatility required to yield productive configuration solutions to mission profiles which emphasize, to varying degrees, the three basic performance requirements.

When considering the transport productivity of various vehicles, it is common practice to compare the product of payload and cruise velocity divided by empty weight. Such a comparison may be meaningful if the vehicles being compared are very similar in configuration. While the assumption is generally accepted that payload times velocity is a measure of effectiveness, empty weight is only a measure of "flyaway cost" when configurations are essentially identical. The true measure of transport productivity must reflect all operating costs attendant to transporting a pound of payload at a given cruise velocity.

In the case of the stopped-folded-stowed rotor concept, it is clear that direct operating costs associated with the main and tail rotors and their control systems will not be comparable to conventional rotary-wing components, since they are utilized for a fraction of the total mission time. Further, the weight fractions (i.e., portion of empty weight) of these components are substantially reduced, since they are not required to operate at forward speeds or thrust levels required in conventional rotary-wing flight. While configurations which utilize rotary-wing components in both the VTOL and forward-flight modes exhibit lower total propulsion system weight fractions, they do exhibit direct operating costs similar to those of the helicopter.

Consideration of the high forward speed performance objectives of the composite aircraft, with respect to concept selection, is largely a matter of propulsive systems. Those composite aircraft concepts which utilize common VTOL lifting and forward-flight propulsive means (for acceptable disc loadings) have fundamental forward-speed limitations, while those concepts which separate these functions are limited only by the forward propulsion means selected.

Finally, VTOL performance and low noise level requirements for the composite aircraft can be considered as directly dependent on rotor disc loading; low disc loadings produce efficient hover performance and low noise levels (for shaft-driven rotors). The stowed-rotor concept has no low disc-loading constraint.

Thus, the stopped-stowed rigid-rotor concept utilized in the design of the CRA is a concept which has no basic aerodynamic constraints. This provides the capability to optimize configuration development for missions which involve, to varying degrees, requirements for high transport productivity, high-speed capability, and high VTOL performance.

SECTION 2
VEHICLE DESCRIPTION

COMPONENT DESIGN PHILOSOPHY

The design philosophy employed during the preliminary studies of the composite aircraft is divided into two approaches: (1) to design a light-weight vehicle optimized in accordance with the requirements of the Contract DA44-177-AMC-372(T), and (2) to design a research vehicle that utilizes off-the-shelf equipment, where possible.

The optimum vehicle design is used to determine the design gross weight that may be expected in an operational configuration. The research vehicle design uses off-the-shelf equipment to minimize cost and development risk.

With this approach, both the design gross weight and the empty weight are the same for both the optimum vehicle and the research vehicle. Differences between the component weights of the optimum design and the off-the-shelf equipment are compensated for by adjusting fixed equipment weight in the research vehicle. For example, the required fixed equipment weight in the optimum design provides for 900 pounds of avionics equipment, whereas the research vehicle avionics should not exceed 350 pounds. The total weight differences between the optimum components and the off-the-shelf components is estimated to be 361 pounds.

The CRA research aircraft is designed to include the following off-the-shelf components:

- C-140 nose gear
- P-3A fuel system
- F-104 brake system
- XC-142 propeller gearbox
- XC-142 propeller hub
- Available hydraulic components
- Available electric components
- AH-56A T64-GE-16 engines

The rotor assembly employs a unique stowing requirement and, therefore, does not provide for the use of off-the-shelf equipment. All components relating to the main rotor, transmission assemblies, drive system, and flight control system are optimized for both the research and the optimum vehicle. Therefore, development of this dynamic system on the research aircraft will be applicable to future operational vehicles.

Since the design of the composite aircraft incorporates criteria of both the helicopter and the fixed-wing airplane, criteria compromises are possible. For example, the rotor is not designed for conventional helicopter forward-speed flight conditions, since unloading of the rotor occurs, starting at speeds below 100 knots. Also, the propeller, wing, and landing gear are not designed for airplane type takeoff and landing conditions, thereby providing means for designing lightweight components. Many other criterion compromises are possible which result in a vehicle weight that is less than the weight of combining the conventional helicopter components with the conventional airplane components in accordance with normal design practices.

GENERAL DESCRIPTION

The general arrangement of the CRA vehicle is presented in Figure 1; the inboard profile is presented in Figure 2. This vehicle has a gross weight of 24,500 pounds and a maximum speed of 358 knots at sea level, hovers at 6800 feet on a 95°F day, and includes features making it suitable for a variety of tasks.

Primary power is derived from two T64-GE-16 engines, one mounted in a nacelle under each wing. The engine power is transmitted through a gearbox to 10-foot-diameter 4-bladed propellers for forward thrust. Engine power is also transmitted through gearboxes and shafting to the main transmission to power the main rotor and the antitorque tail rotor.

A major feature of the vehicle is the 60-foot-diameter, 3-bladed main rotor. This rotor is capable of being stopped, folded, and stowed in the top of the fuselage, thus allowing high-speed airplane mode operations. The stopping and folding operation is initiated at approximately 140 knots by declutching and braking the rotor to a stopped position with one blade trailing aft. The other two blades are then mechanically folded to a contiguous aft trailing position. The entire rotor hub and mast assembly is then lowered into the fuselage compartment. Doors, one at each side of the transmission, and articulated by the transmission stowage mechanism, cover the hub and forward part of the rotor blades in the stowed attitude.

The empennage and tail rotor are conventional components, if individually considered. The tail rotor is similar to the AH-56A tail rotor and is conventionally powered by shafting and gearboxes. It provides the antitorque control for helicopter operations. The same control system used for control of the tail rotor is connected to the rudder, which is attached to the vertical fin in a normal airplane manner. The horizontal stabilizer and elevator are conventional and similar to other airplane installations.

The wing is sized to achieve a lift-to-drag (L/D) ratio of 10, as required by the contract. As such, it has a 50-foot span with a 279-square-foot area. The wing is positioned for optimum center of gravity location in all rotor phases (rotating, stopped, folded, and stowed) and for reasonable

MAIN ROTOR

TYPE — LOCKHEED RIGID ROTOR
 DIAMETER — 60 FEET
 NO. OF BLADES — 3
 CHORD — 22 INCHES
 DISC AREA — 2230 SQ FT
 DISC LOADING — 8.67 LB/SQ FT
 TIP SPEED — 753 FT/SEC
 AIRFOIL ROOT — NACA 63A 021 (S.R.S. 72)
 AIRFOIL TIP — NACA 63A 010

TAIL ROTOR

DIAMETER — 13 FT 6 IN.
 NO. OF BLADES — 4
 CHORD — 14 INCHES
 TIP SPEED — 638 FT/SEC
 AIRFOIL ROOT — NACA 63A022.3
 AIRFOIL TIP — NACA 63A012

PROPELLER TWO (2)

DIAMETER — 10 FEET
 NO. OF BLADES — 4
 RPM — 1545
 TIP SPEED — 807 FT/SEC

WING

SPAN — 30 FT 0 IN. (91.4)
 AREA — 279 SQ FT
 ASPECT RATIO — 8.98
 TAPER RATIO — .25
 DIHEDRAL — 0°
 TWIST — 0°
 AIRFOIL ROOT — NACA 64A318
 AIRFOIL TIP — NACA 64A712

HORIZONTAL TAIL

SPAN — 15 FT 0 IN. (45.7)
 AREA — 58 SQ FT
 TAPER RATIO — .47
 DIHEDRAL — 0°
 AIRFOIL ROOT — NACA 64A018
 AIRFOIL TIP — NACA 64A012

VERTICAL TAIL

AREA — 64 SQ FT
 TAPER RATIO — .34
 AIRFOIL ROOT — NACA 64A018
 AIRFOIL TIP — NACA 64A012

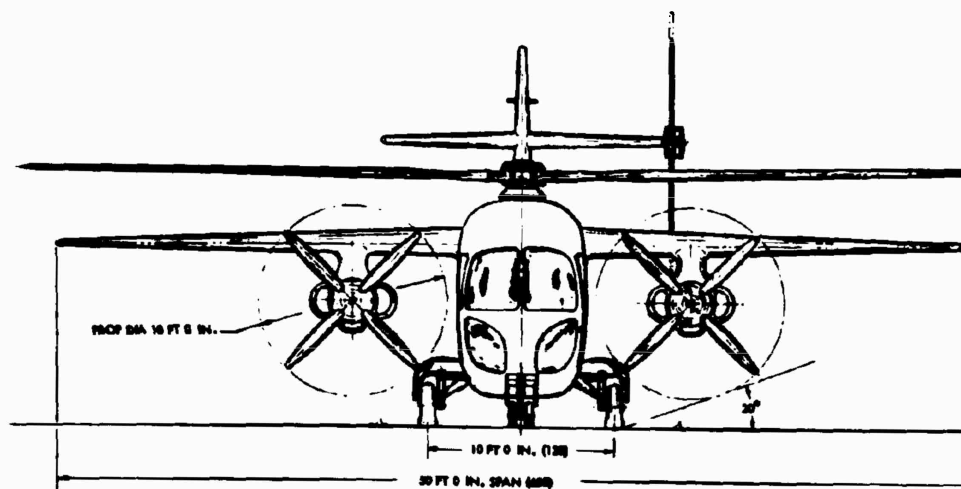
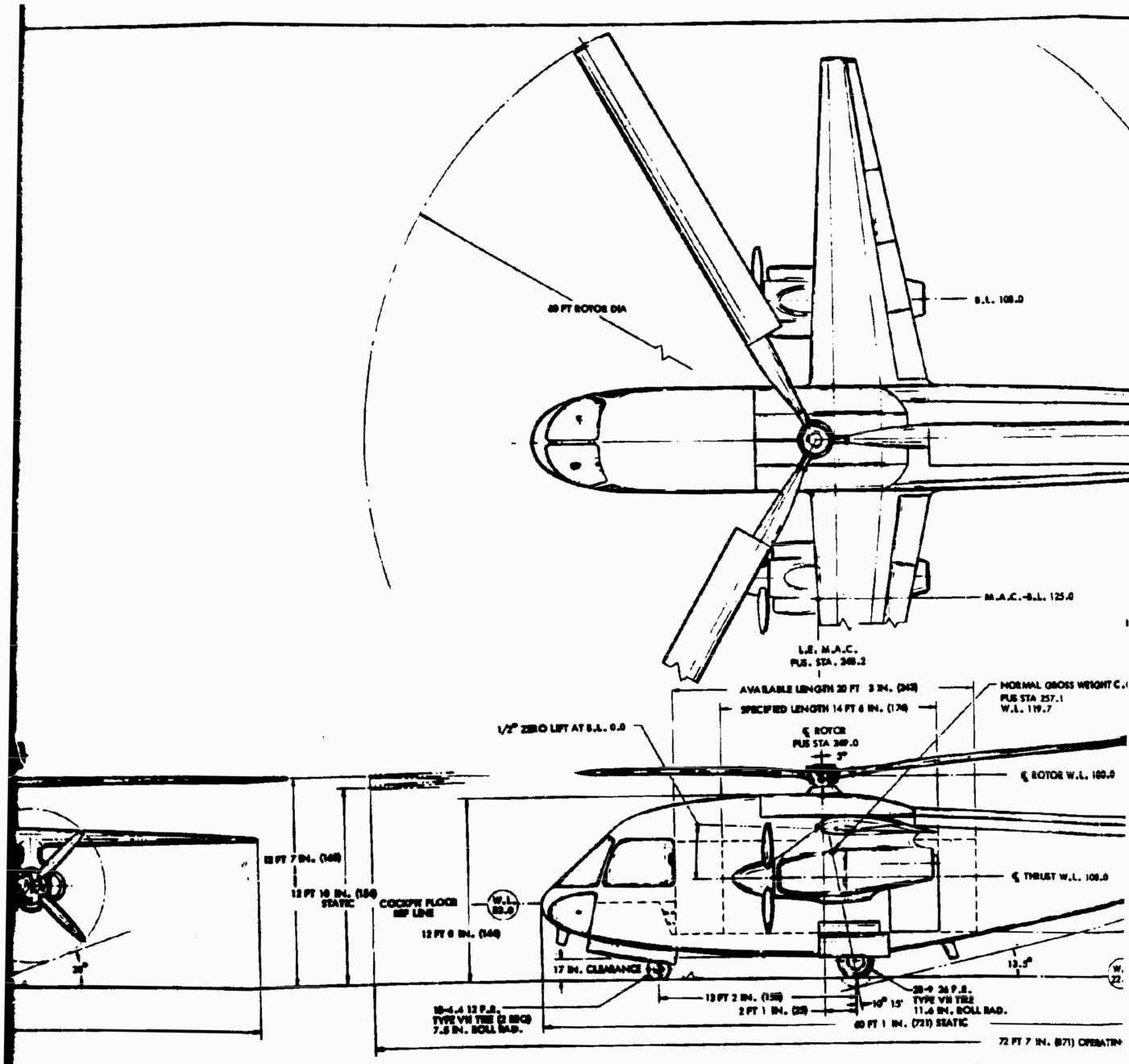
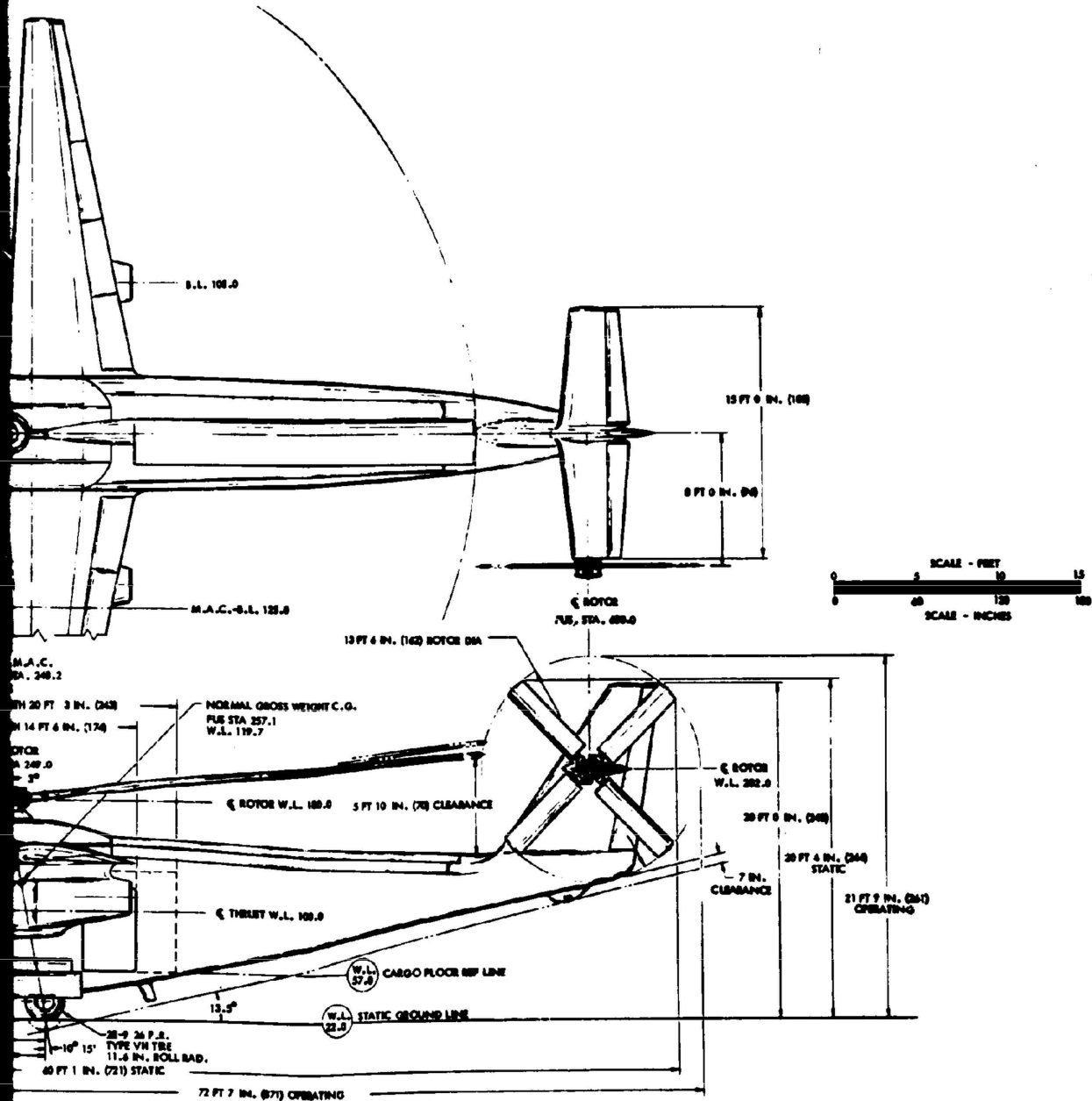


Figure 1. General Arrangement.





Page Intentionally Left Blank

loading regimes in the cabin. An integral fuel tank is included in the wing main structural box outside the fuselage. Slotted flaps and conventional ailerons are installed on the trailing edge of the wing. The flaps can be deflected to minimize the rotor downwash effects during VTOL operations.

The fuselage is a typical high-wing unpressurized structure as shown in Figure 2. The forebody contains the flight station with accommodation for a pilot and a copilot. Crew visibility is good with the maximum amount of transparent area provided. The forebody includes the nosewheel well and space for the APU and electronic equipment. Immediately aft of the flight station is a cargo compartment with approximately 500 cubic feet of capacity and with flooring capable of 175 pounds per square foot loading. Both the floor and the supporting structure are designed to accept the later incorporation of tiedown fittings if desired. There is available volume in the cargo compartment of 670 cubic feet.

The main rotor transmission, the wing carry-through structure, the power-shafting, the hydraulic service center, and the rotor-stowing mechanism and compartment are contained in the fuselage midbody over the cargo compartment.

The portion of the aftbody including the vertical and horizontal stabilizers is designed as an integrally fabricated structure and supports the tail rotor drive mechanism.

A tricycle landing gear is provided with a forward-retracting, swivelling nose wheel and two main wheels which retract inwardly into the belly of the fuselage. Main wheel brakes are utilized for ground steering during taxiing and conventional airplane takeoffs and landings.

VEHICLE CHARACTERISTICS

A summary of the aircraft characteristics for the CRA is presented in Table I.

TABLE I. GENERAL CHARACTERISTICS	
MAIN ROTOR	
Type	Rigid
Number of Blades	3
Rotor Diameter	60 ft
Disc Area	2830 sq ft

TABLE I - Continued

Blade Chord	32 in.
Blade Airfoil Section	
Root (R.S. 72)	NASA 63A021
Tip	NASA 63A010
Blade Twist	0 deg
Blade Sweep (from R.S. 25)	1.5 deg forward
Coning Angle	3.8 deg
Solidity	0.085
Angle of Incidence of Rotor Plane to Fuselage Reference Line	-3 deg
Feathering Axis	30% chord
Feathering Bearings (Blade Station)	
Inboard	13.3 in.
Outboard	25.3 in.
Fold Joint (Blade Station)	11.25 in.
Rotor Polar Moment of Inertia	13,000 slug-ft ²
Collective Pitch Range	0 to 15 deg
Cycle Pitch Range	±8 deg
TAIL ROTOR	
Type	Teeter
Number of Blades	4
Rotor Diameter	13.5 ft
Disc Area	143 sq ft
Blade Chord	16 in.

TABLE I - Continued		
Blade Airfoil Section		
Root at 17% R		NASA 63A022.3
Tip		NASA 63A012
Blade Twist		0 deg
Blade Sweep		0 deg
Coning Angle		0 deg
Solidity		0.251
Feathering Axis		37% chord
Rotor Polar Moment of Inertia		83.6 slug-ft ²
Collective Pitch Range		-10 to +26 deg
Teeter Angle Range		±6 deg
Location of Hub Centerline		
Fuselage Sta.		680
Butt Line		96 L
Water Line		202
WING		
Area		279 sq ft
Span		50 ft
Chord		
Root		107 in.
Tip		27 in.
MAC		75 in.
L.E. of MAC		Fus. Sta. 248.2
Taper Ratio		0.25

TABLE I - Continued

Sweep of 1/4 Chord	-0° 30 min
Dihedral	0 deg
Twist	-3 1/2 deg
Angle of Incidence at Root	+1/2 deg
Angle of Incidence at Tip	-3 deg
Airfoil Section	
Root	NASA 64A518
Tip	NASA 64A712
HORIZONTAL TAIL	
Area	58 sq ft
Span	180 in.
Chord	
Root	55 in.
Tip	37 in.
MAC	46.59 in.
L.E. of MAC	Fus. Sta. 662
Taper Ratio	0.67
Airfoil Section	
Root	NASA 64A018
Tip	NASA 64A012
Dihedral	0 deg
Incidence	0 deg
Distance from	407 in.
MAC _W /4 to MAC _Z /4	

TABLE I - Continued

Elevator	32.3% chord
Area	16 sq ft
Mean Chord, C_e	14.21 in.
Hinge Line Location	75% chord
Deflection Range	
Up	20 deg
Down	30 deg
VERTICAL TAIL	
Area (Total to Top of Fus.)	64 sq ft
Span	10 ft 9 in.
Chord	
Root	107 in.
Tip	36 in.
MAC	77.4 in.
L.E. of MAC	Fus. Sta. 642.1
Taper Ratio	0.34
Airfoil Section	
Root	NASA 64A018
Tip	NASA 64A012
Offset	0 deg
Distance from	394.6 in.
$MAC_{\sqrt{V}}/4$ to $MAC_{\sqrt{V}}/4$	

TABLE I - Continued

Rudder	29.6% chord
Area	17 sq ft
Mean Chord, C_r	23.59 in.
Hinge Line Location	75% chord
Deflection Range	
Left	15 deg
Right	15 deg
AILERONS	32.3% chord
Area (Per Side)	6.25 sq ft
Mean Chord, C_a	10.3 in.
Span	7 ft 6 in.
Spanwise Location	
Inboard	W.S. B.L. 210
Outboard	W.S. B.L. 300
Hinge Line Location	75% chord
Deflection Range	
Up	11 deg
Down	11 deg
FLAPS	
Type	Slotted
Area	21.2 sq ft
Chord	19.06 in.

TABLE I - Continued

Spanwise Location		
Inboard		W.S. B.L. 43.75
Outboard		W.S. B.L. 210
Deflection		45 deg
Span		166 in.
FUSELAGE		
Length		689 in.
Nose		Fus. Sta. 23
Maximum Width		82.5 in.
LANDING GEAR		
	Main	Nose
Axle Location, Static		
F.S.	275	115.5
B.L.	60	5.3
W.L.	32	29.8
Tire Size	28 x 9 Type VII	18 x 4.4 Type VII
Moment of Inertia of Rotating Assem.	44.6 psf	4.2 psf
Strut Stroke	10 in.	12 in.
Strut Extension under Static Load	2 in.	2 in.
Spring Rate of Tire	8200 lb/in.	5600 lb/in.
Direction of Retraction	Inboard	Forward
Angle of F.R.L. to Ground, Static	0 deg	

TABLE I - Continued

POWER PLANT	
Engine Designation	T64-GE-16
Number of Engines	2
Maximum Horsepower	3435
Location, W.S.	108
PROPELLERS	
Number	2
Diameter	10 ft
Disc Area	78.5 ft ²
Location of Hub	
F.S.	195.5
W.S.	108
W.L.	100
Activity Factor	120
Clearance, Blade Tip to Fuselage	7 in.
Polar Moment of Inertia	660 lb-ft ² 20.5 slug-ft ²
Number of Blades	4

MAINTAINABILITY PROGRAM

The systems and components of this aircraft have been designed with a high degree of maintainability as one of the prime objectives. Use of parts and components with a service history of reliable operation, plus qualified equipment currently being used on other aircraft such as the P-3B or F-104, insures high initial reliability; this simplifies the overall maintenance of the vehicle. Since this is a research aircraft, the accent has been placed on developing the stowed rotor concept. During the follow-on phase, every effort will be made to further develop the areas needed to improve maintainability, with special emphasis on the newly developed systems and

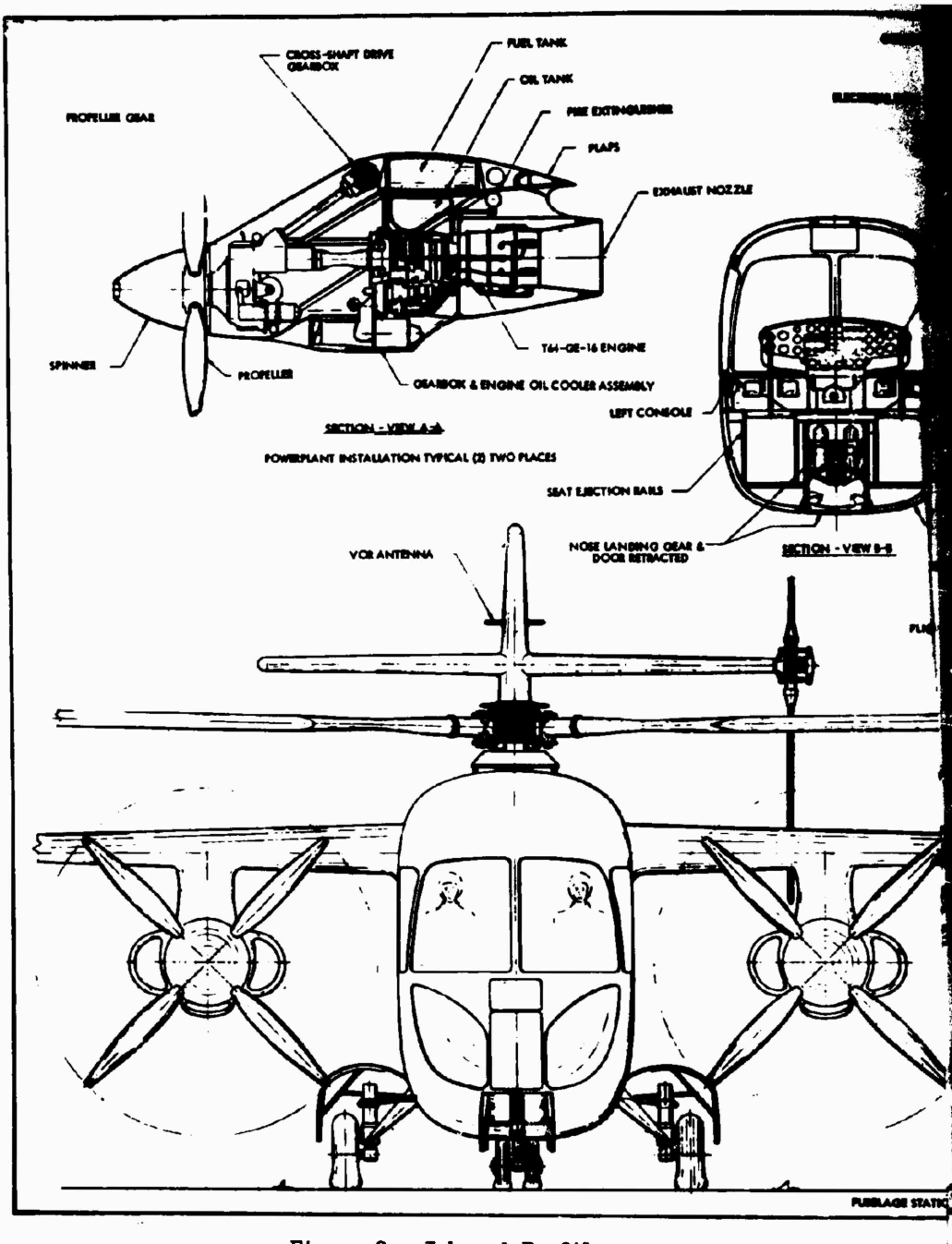
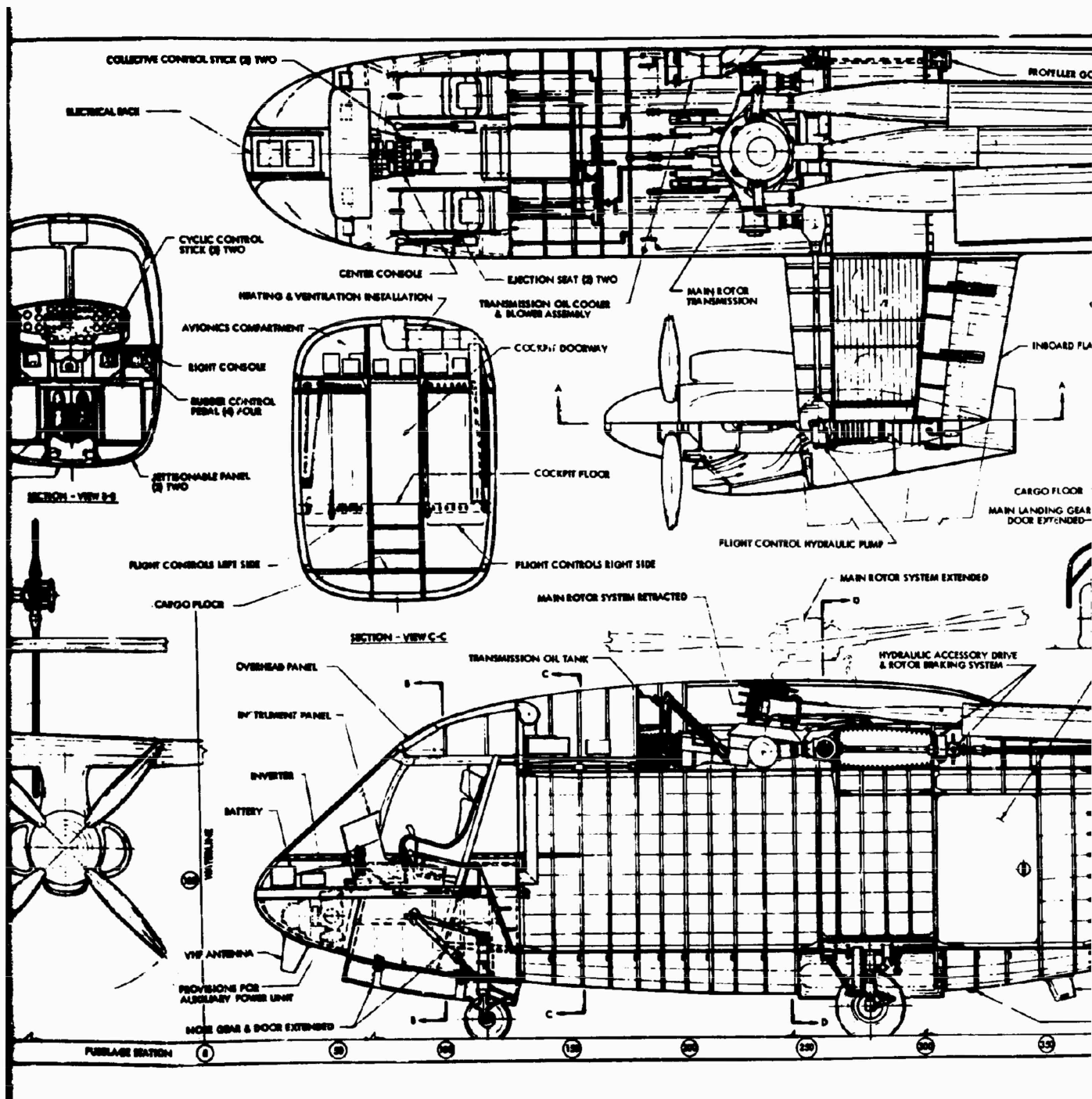
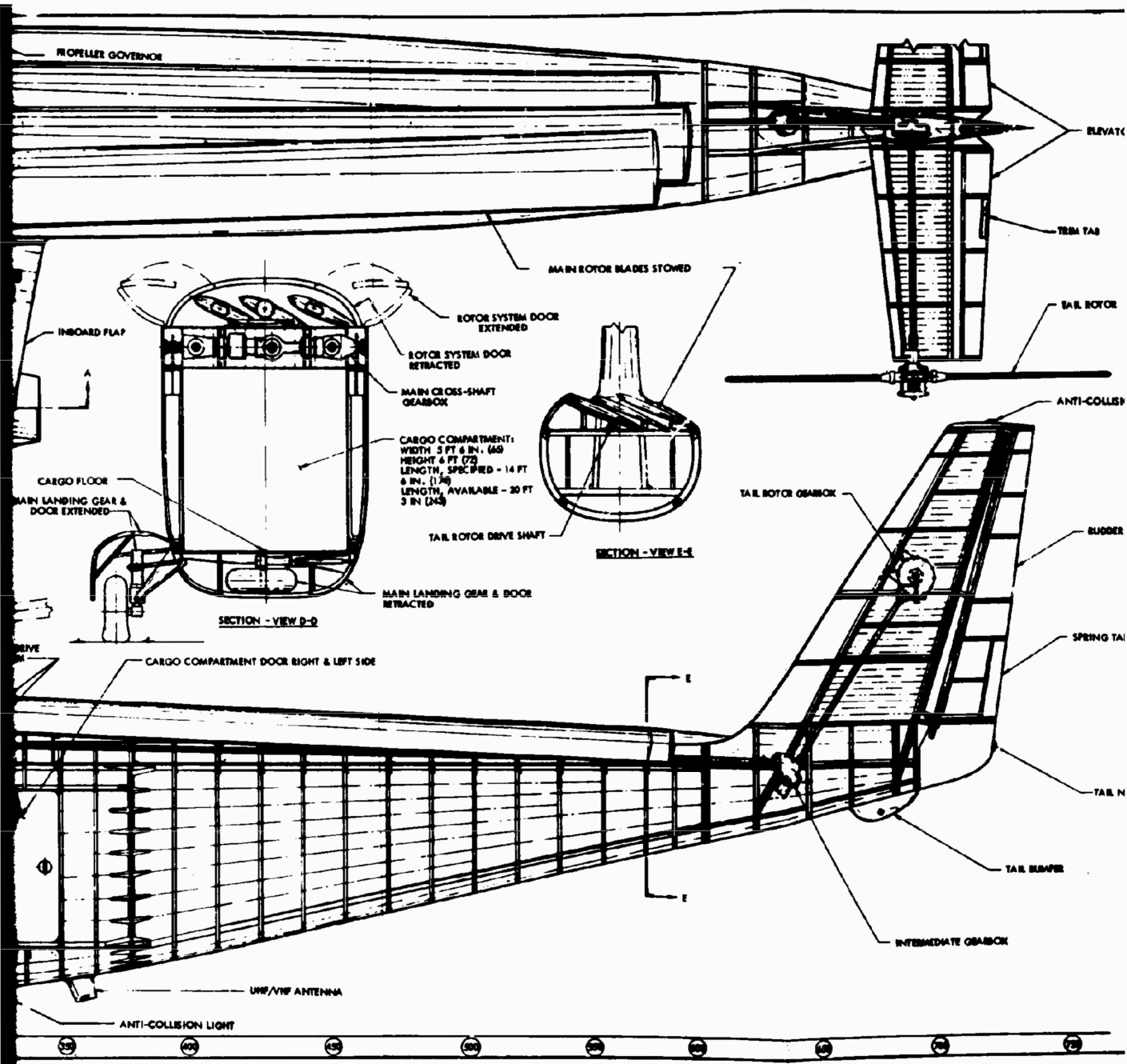
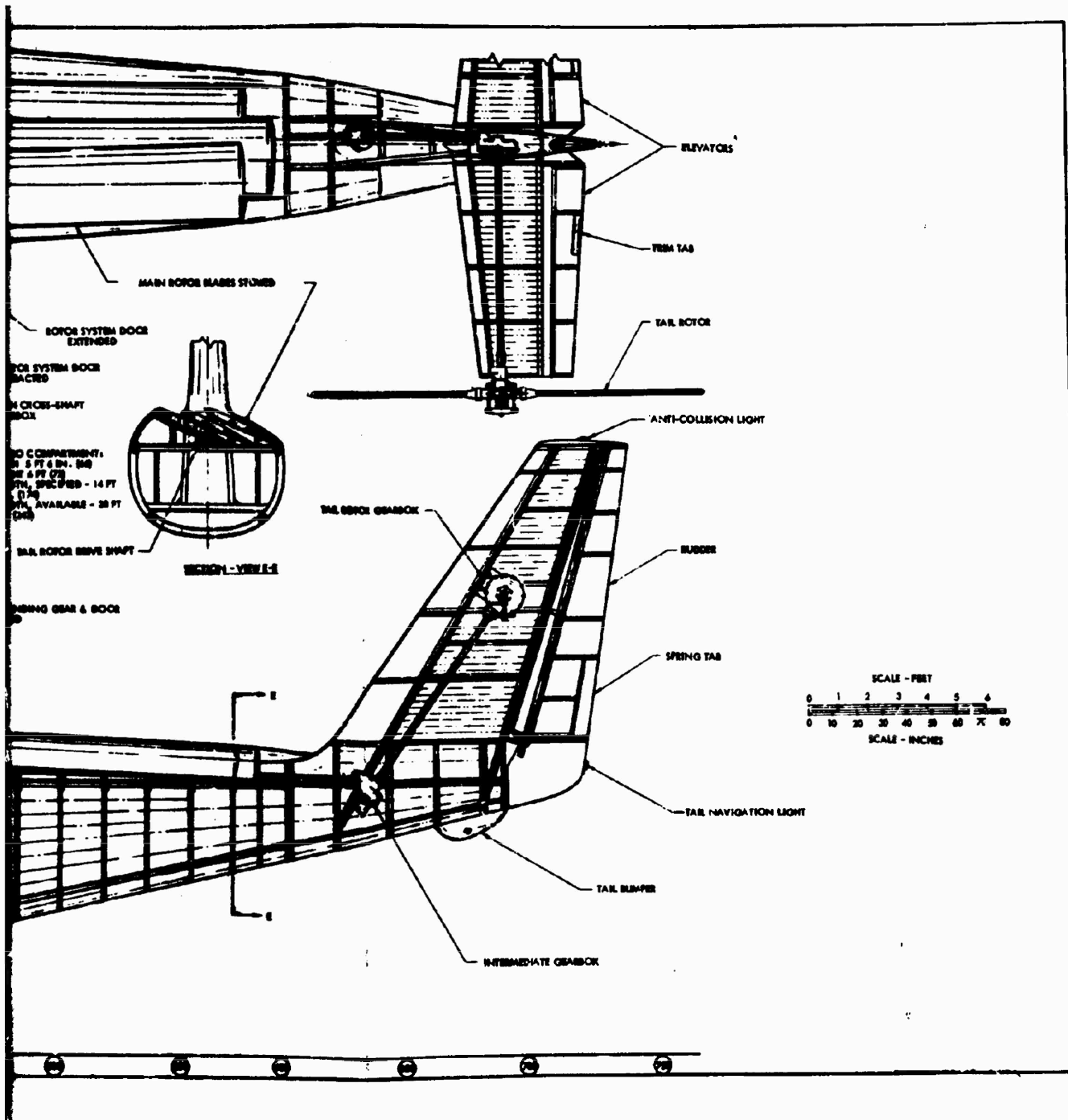


Figure 2. Inboard Profile.



B





C

D

dynamic components; for example, improvements in the inspectability and ease of installation of the main rotor blades. Methods will be developed through redesign, as needed, to provide for simple cross-shaft clutch installation and removal procedures. Studies and trade-offs will be carried out to determine if the tail drive shaft installation can be further simplified. Gearbox designs will be further improved to eliminate the use of dry lubed splines and gear journals as bearing inner races.

Access and Inspection

Accessibility has been stressed throughout the aircraft design. The service center concept has been utilized, grouping like components or those with similar maintenance requirements, to minimize lost time by reducing the number of access doors to be opened during maintenance and by eliminating the need to move from place to place while troubleshooting. Hinged leading edges, hinged spanwise panels in the lower wing trailing edge surface, and tank cover panels provide generous access to controls, fuel system, and drive shafting in the wings. Hinged side cowl and quickly removable panels provide full access to the engines and pylon structure. Main rotor head and blade stowage compartment doors provide access to main and tail rotor drive system components. All components are arranged so that they can be serviced and maintained while installed and so that they are accessible for replacement.

Servicing

The fuel tanks may be serviced through gravity fillers on the wing upper surface. Engine oil level can be checked by an exposed sight gage on each tank located in the engine support pylons. Filler access is through quick fastening doors on the pylons. Hydraulic oil level can be checked by observing level indicators on the hydraulic power package units. Main gearbox, intermediate gearbox, and tail rotor gearbox oil levels are checked by observing their respective sight gages. Engine, hydraulic, and gearbox oil can be replenished directly from 1-quart cans.

Fuel System

Removable covers on the underside of each wing provide access to the interior for maintenance. A dual-element boost/scavenge pump in each surge box supplies fuel to its respective engine, crossfeed system, and surge box. Access cover plates are located in the wing upper surface directly over the pumps. The pumps can be replaced without draining the tanks. The emergency shutoff, tank shutoff, and cross-feed shutoff valves are accessible by opening the hinged wing leading edges; valve bodies are replaced without defueling. Tank drain valves in the low point of each tank allow drainage of water or residual fuel. Valve design permits primary seals to be replaced without defueling. Boost/scavenge pumps and cross-feed and tank shut-off valves are interchangeable within the system.

Wing

Access panels are provided at all inspection, maintenance, replacement, and attachment points. The wing leading edge from the fuselage to the nacelle pylon is hinged downward, exposing the cross-shaft, cross-shaft gearbox, fuel system shutoff and cross-feed valves, and front beam. The rear beam and flap and aileron controls are completely exposed by opening hinged access doors located in the lower skin surface aft of the rear beam.

Power Plant

The power plant installation consists of two nacelle-mounted T64 turboprop engines driving propellers. Each propeller reduction gearbox provides a power takeoff for driving the main rotor gearbox through use of cross-shafting routed through the pylon and wing leading edges. Use of standard hardware and proven components has been maximized. The power plants are configured for interchangeability to either position. To reduce engine replacement time, all fluid lines are equipped with self-sealing quick disconnects. All cable-actuated controls terminate at quadrants at the Q.E.C. disconnect points, permitting push-pull rod actuation of the engine components. This avoids the disconnection of control cables with a resultant disruption of system rigging at the time of engine change. Rigging pinholes are provided to permit the control system to be locked in a neutral position, thereby permitting quick system checkout and adjustment.

Main Rotor and Transmissions

Stainless steel construction and leading-edge abrasion strips provide for minimum main rotor blade maintenance.

The rigid main rotor, by virtue of its design and construction, insures a minimum of assembly/disassembly problems and associated maintenance and inspection tasks. Blade radial thrust loads are carried by lamiflex bearings having no maintenance or lubrication requirements. Accessible and adequate grease points are provided for blade feathering bearings.

The blade fold and locking mechanism is comparatively simple, utilizing a minimum of units. One hydraulic rotary actuator and drum using a multiple cable assembly simultaneously rotates the blades to a trailing position. Teflon bearing surfaces are provided on the hub to minimize friction during blade folding operations.

The main transmission lubrication system provides filters furnished with throw-away elements and pop-out-type filter bypass indicators. Low-pressure screens are installed in the inlets to the pressure pumps to prevent damage or failure resulting from tank contaminant ingestion. Each discharge jet is provided with a screen capable of filtering out contaminants of a size sufficient to clog the orifice. A filter in the scavenge line from the dual clutch assembly prevents clutch disc throw-off from contaminating the rest of the systems. The oil tank filler and sight gage locations provide for ease of servicing.

Shafting and Aft Gearboxes

Steel tail-rotor drive-shafting, joined by dry hyperbolic steel couplings which have no maintenance or lubrication requirements, connects the gearboxes. Shaft-support bearings and ball splines have been provided with grease fittings for ease of lubrication. Intermediate and tail gearboxes have been provided with an accessible filter and chip detector. Lip seals run on wear rings protecting the gear shafts. Both lip seals and gear shaft plug seals are replaceable without box removal or disassembly. The lube pumps are standard "off-the-shelf" items, replaceable as a package when necessary.

Tail Rotor

Grease fittings have been provided for lubrication of hub trunnion and blade cuff bearings. Pitch change links have Teflon-lined rod-end bearings requiring no lubrication or maintenance. The titanium skin on the tail rotor blades is protected from abrasion by nickel cladding the outer half (span-wise) of the leading edge. The replaceable tip caps are protected from abrasion in the same manner.

Fuselage

The simple skin, stringer, and frame construction is maintained and repaired by standard skills and methods. Numerous access doors and openings are provided to service, inspect, and maintain the structure and installed components.

Quick-fastening exterior doors provide access to controls and electronic equipment located beneath the cockpit floor.

Main rotor hub and blade stowage compartment doors provide access to the main and tail rotor drives and control system.

Access to the tail cone is provided for inspection of controls, drive shafting, structure, and empennage. A walkway has been provided in the aft fuselage section to prevent structural damage by maintenance personnel.

Console and Instrument Panel

Instruments are face-mounted, allowing removal without the need to work behind the panel. MS-type quick disconnects are used for electrical connections. The instrument panel is hinged at the bottom and can be tilted aft, providing unrestricted access to the area behind the panel. Radio control panels located in the console are quickly removed through the use of cam locks and quick-disconnect type electrical connections. Removable panels provide access to the propeller quadrant, power quadrant, and cables.

Electrical System

The electrical system uses standard components arranged for maximum accessibility. The primary source of power is supplied by one 20-kva ac brushless generator mounted on the No. 2 engine propeller gearbox. Quick attach/detach mounting provides for rapid change using only standard hand tools. A further maintenance man-hour saving is realized by the elimination of periodic brush inspection and replacement requirements.

One 200-ampere transformer rectifier provides 28 vdc. The use of solid-state circuitry in these units provides a maximum of reliability.

Emergency ac and dc power is provided by a three-phase, 115 vac, 250-volt-ampere inverter and a 22 amp-hour nickel-cadmium battery. Battery and inverter are accessible through a hinged door on the nose of the fuselage.

Hydraulic Power

Hydraulic power is supplied to the helicopter flight control and aircraft utility systems by two completely self-contained power packages. This concept groups all system and maintenance items into one unit, (i.e., reservoir, sight gage, filters, clogged filter indicator, system bleeder, etc.). The throw-away filters are readily accessible and are sized to prevent their inadvertent interchange. A quick attach/detach clamp provides for easy removal and installation of the complete package. Propeller pitch control power is supplied by both hydraulic systems. The hydraulic engine starters receive power from a ground unit through self-sealing quick disconnects and the utility system.

Control System

The control system is an integrated helicopter/fixed-wing arrangement that is both mechanically and hydraulically actuated. The cable-actuated portion employs a maximum of straight runs to minimize the maintenance and inspection potential. Readily accessible clip-locked turnbuckles are used on all cables, reducing time required for safetying. That portion of the system, used in both helicopter and fixed-wing modes, employs push-pull tubes and cranks, providing a minimum of inspection and maintenance. To prevent the inadvertent crossing of controls, adjacent identical connectors have been reversed. Accessible rigging pinholes have been provided for locking the control system in a neutral position, thus permitting quick system checkout, adjustment, and/or component replacement.

Landing Gear

The landing gear is a tricycle type designed to meet the requirements of prepared field and minimum maintenance.

The main landing gear is a single-wheel-per-side configuration, swinging inboard on retraction to lie flat under the floor structure, in the bottom

of the fuselage. The complete main gear installation is interchangeable and may be installed on either side. A standard air-oil shock strut with a readily accessible servicing point is used. For wheel or brake change, a jack pad is provided on the base of the shock strut in addition to the towing/tiedown provisions.

A dual-wheel nose gear fitted with a standard air oil strut retracts forward into the nose. When the nose gear is extended, the open nose gear doors provide unobstructed access for servicing. A jack pad is provided between the wheels; but if only a single wheel change is necessary, the needed elevation is obtained by rolling the opposite wheel up on an inclined block. A quick-disconnect feature on the scissors, with stowing provisions, provides a 360° turning radius for towing.

PART 2
PERFORMANCE

SECTION 3
AERODYNAMIC DESCRIPTION

This section contains a discussion of the trade-off studies that were used to establish the various parameters which affect performance. Section 4 contains an analysis of the performance of the CRA throughout the flight spectrum. The flying qualities of the CRA are presented in Part 5 of this report, entitled "Stability, Control, and Flying Qualities."

The configuration which has been selected for the Composite Research Aircraft satisfies all of the requirements in the Statement of Work. The most important of these requirements are:

- The capability to hover out of ground effect at 6000 feet on a 95°F day.
- Maximum speed of at least 300 knots, with 400 knots desired
- Maximum lift-to-drag (L/D) ratio based on total engine power of at least 10
- Disc loading of 10 psf or less

A summary of the weights for each important design condition is presented in Table II.

TABLE II. WEIGHT SUMMARY	
Condition	Weight (lb)
Empty Weight	17,961
Structural Design Gross Weight	24,500
Overload Gross Weight	28,800
Ferry Takeoff	30,000
Hover IGE SL STD	31,200
Hover OGE SL STD	28,900
Hover OGE 6000 ft, 95°F	24,900

The various dimensions, areas, and other parameters necessary to describe the aerodynamic characteristics of the CRA are shown in Table I, General Characteristics.

OPTIMIZATION OF THE CONFIGURATION

Selection of the Transition Speed

An important decision which affects many components in the selection of the speed at which to make the transition. A low transition speed is desirable to minimize the structural weight of the blades, which must have an aeroelastic divergence speed above the selected transition speed. A high transition speed is desirable to minimize the area and the weight of the wing, which must be large enough to support the entire weight of the aircraft at the transition speed with a margin of lift capability to allow for maneuvering and gust effects.

A trade-off study was conducted in which the additional structural weight required to stabilize the stopped blade was determined as a function of the speed for aeroelastic divergence, and the wing area and weight were determined as a function of transition speed. The results of this study showed that the sum of rotor and wing weights was a minimum when the transition speed was selected in the 120- to 140-knot range. The rotor blades were designed to be stiff enough to have a divergence speed of 168 knots and the wing to have a stall speed, flaps down, of 102 knots, thus providing adequate margin at both ends of the transition range.

Main Rotor

The design requirements of the main rotor are:

- To provide the capability to hover at the design gross weight at 6000 ft, 95°F;
- To have aeroelastic stability when stopped during the transition
- To be capable of being folded and stored.

The selection of the various parameters is discussed in the following paragraphs.

Disc Loading

A low disc loading is desirable when considering requirements for good hovering capability, safe power-off landings, and minimum down-wash velocities. A high disc loading is desirable when considering requirements for small overall size and light empty weight. For the CRA, the upper limit on disc loading is specified as 10 psf by the Statement of Work. In selecting the disc loading for the CRA, as low a disc loading as possible was chosen in order to minimize the operational problems without unduly penalizing the empty weight. These

considerations led to the selection of the disc loading of 8.7 psf with a corresponding rotor radius of 30 feet.

Rotor Tip Speed

The effect of tip speed on the rotor solidity required to hover 24,500 pounds at 6000 feet, 95°F with two T64 is shown in Figure 3. From this figure, it may be seen that the lowest solidity, and thus the lowest rotor weight, occurs at a tip speed of about 750 fps. At the transition speed of 140 knots, this tip speed results in an advancing tip Mach number of 0.88, which is considered to be acceptable for an unloaded rotor with a tip thickness of 10% of the chord. For these reasons, the tip speed of 754 fps, corresponding to 240 rpm, was selected for the CRA.

Airfoil Sections

Thick airfoils, especially at the root of the main rotor blades, are desirable to obtain sufficient stiffness to prevent aeroelastic divergence for a minimum blade weight. Moderately thin airfoils, especially near the blade tip, are desirable for optimum hovering performance and high critical Mach number. These two features have been combined on the CRA blades by tapering the thickness ratio from 21 percent at the 20 percent radius station to 10 percent at the tip. The NASA 63 Airfoil Series has been selected for this rotor because of its high drag divergence Mach number and its high maximum lift coefficient.

Number of Blades

A large number of blades is desirable for high hover efficiency. A small number of blades is desirable for individual blade stiffness and ease of folding and stowing. Two-bladed rigid rotors for stopped rotors were studied, but associated dynamic problems are so difficult that further consideration is unwarranted. Design studies of stowed rotor aircraft comparing four-bladed rotors with three-bladed rotors have shown that with four blades, the weight penalty required for sufficient stiffness to prevent aeroelastic divergence and the mechanical problems of folding and stowing four blades far outweigh the increase in hovering efficiency. For these reasons, a three-bladed rotor has been selected for the CRA.

Twist

High twist is desirable for maximum hovering efficiency. Low twist is desirable for ease of stowage and blade fabrication and for minimum aerodynamic loads during the rotor stopping process. A nontwisted blade has been selected for the CRA in order to minimize the potential problems during stopping and folding.

Solidity

Low solidity is desirable from a rotor stowing standpoint; high solidity is desirable for obtaining minimum blade weight with sufficient

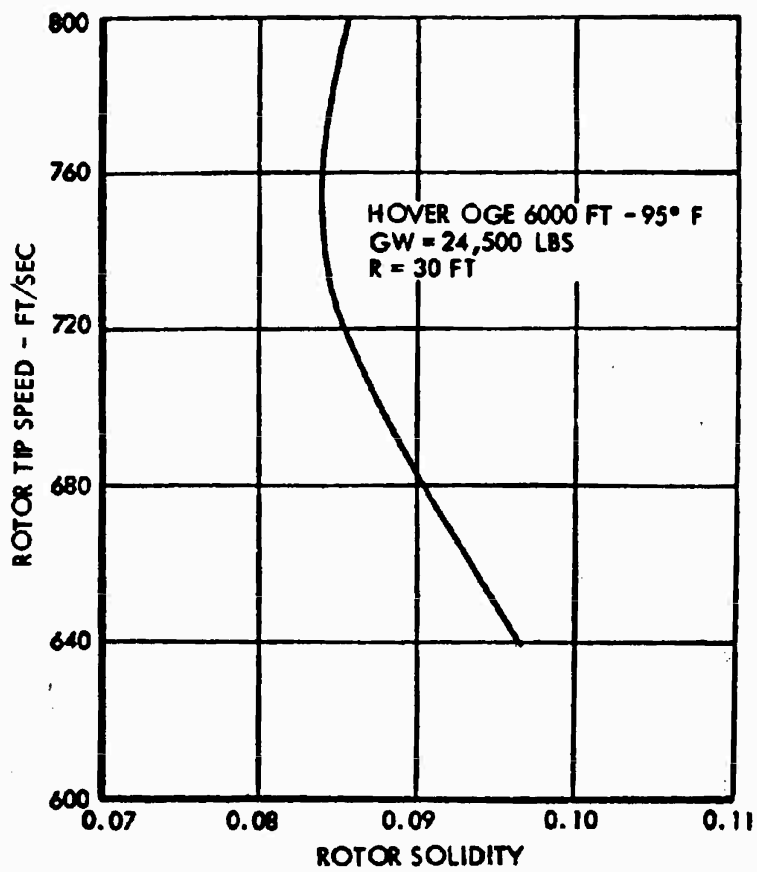


Figure 3. Effect of Tip Speed on Solidity Required.

stiffness to prevent aeroelastic divergence; and a particular value of solidity which permits the rotor to operate at its highest figure of merit is desirable for optimum hovering efficiency.

Figure 3 shows that the selected tip speed of 754 fps corresponds to a solidity of about 0.085. This solidity, which corresponds to the lowest blade weight, was chosen for the CRA. The chord which corresponds to this solidity is 32 inches. These blades can be stowed without undue design problems.

Wing

The design requirements of the wing are:

- To carry the full weight of the aircraft at transition speed
- To achieve an L/D of 10 based on total power
- To have a sufficiently high drag divergence Mach number so that speeds of approximately 400 knots can be achieved without substantial compressibility penalties.

The selection of values for the various parameters is discussed in the following paragraphs.

Flap Configuration

A flap which gives the highest possible increment in maximum lift coefficient is desirable to minimize wing size, wing weight, wing download in hover, and wing drag at high speed. Lockheed has made design studies of wings with no flaps, plain flaps, slotted flaps, and Fowler flaps and has determined that slotted flaps offer the best overall compromise between minimum wing weight and minimum complexity for the research mission of the aircraft. The flap configuration selected is shown in the general arrangement drawing (Figure 1) as a partial-span single-slotted flap, extending from the fuselage sides to the ailerons. This type of flap is capable of developing a maximum lift coefficient of 2.5 at the Reynolds number corresponding to the transition speed.

Wing Span

A large wing span is desirable to produce high performance in the airplane flight mode. A small wing span is desirable to minimize wing structural weight and wing download in hover. The decision on which wing span to use was made after a study of the effect of span on the lift-to-drag ratio. The Statement of Work specifies that the lift-to-drag ratio, based on total power, be at least 10 in the airplane mode. An expression for the wing span, b , can be derived from simple airplane performance equations as a function of the required maximum lift-to-drag ratio and the drag characteristics of the aircraft:

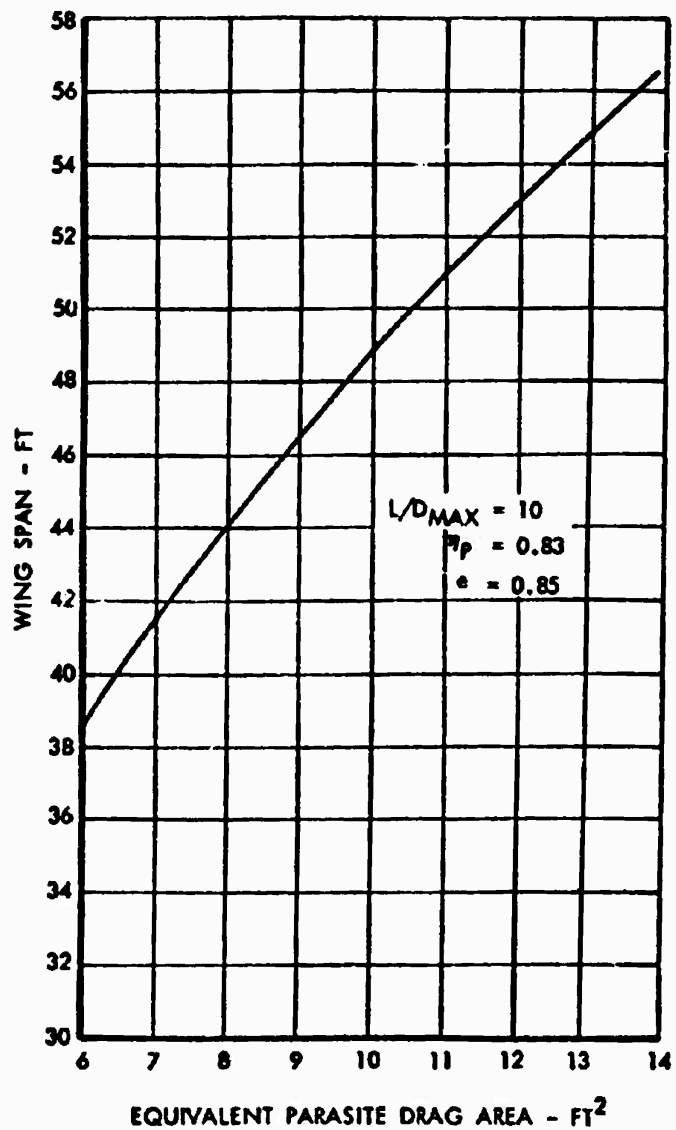


Figure 4. Required Wing Span as a Function of Equivalent Flat Plate Area.

$$b = \frac{(L/D)_{\max}}{\eta_p} \sqrt{\frac{f_0 + C_{D_{OW}} S_w}{\pi e}}$$

This equation has been solved for the span, b , as a function of the parasite drag area, f_0 , for an L/D max of 10, a wing equivalent flat plate area, $C_{D_{OW}} S_w$, of 1 sq ft, an efficiency, e , of 0.85, and a propulsive efficiency, η_p , of 0.83. The results are shown in Figure 4, and were used as a guide in the selection of the span. The wind tunnel tests reported in Reference 1 were performed with a model with a short wing of 40-foot span which produced a maximum airplane lift-to-drag ratio of about 7.7, or a value of about 8.1 when an estimated propulsive efficiency of 83 percent was accounted for. Several design changes were made after the tunnel tests were completed. One change which increased the drag was the substitution of partial doors over the stowed rotor hub and blades for the full doors simulated on the model. To obtain a total lift-to-drag ratio of 10 with partial doors, two design changes were made: the wing was cambered so that the minimum profile drag occurred at a lift coefficient of about 0.7, which is close to the lift coefficient for maximum lift to drag ratio; and the wing span was increased from 40 to 50 feet. A complete discussion of the procedure used to establish camber and span and to estimate the total drag is presented in the section on drag estimation.

Wing Area

The wing area was selected to provide a flaps-down stall speed sufficiently below the minimum transition speed of 120 knots to allow a safe margin. A margin of 15 percent on speed was selected as adequate, giving a stall speed of 102 knots at a lift coefficient of 2.5 and a corresponding wing area of 279 square feet for the CRA.

Wing Airfoil Sections

Thin airfoils are desirable to prevent compressibility losses at high speed. Thick airfoils are desirable to minimize wing structural weight and to produce high maximum lift coefficients. At the maximum estimated speed of about 360 knots at sea level, the Mach number is 0.55. Wind tunnel tests of the C-130 model with NASA 63 series airfoils varying from an 18 percent thickness ratio at the root to a 12 percent thickness ratio at the tip have shown that, up to a Mach number of 0.55, no significant drag divergence could be measured. The thickness distribution of the C-130 was considered to be directly applicable to the CRA from a structural standpoint; thus, a thickness ratio distribution tapering from 18 percent at the root to 12 percent at the tip and the NASA 63 series has been selected for the CRA. Highly cambered sections were selected so that minimum profile drag would occur at the high lift coefficients corresponding to the maximum lift-to-drag ratio. The airfoil sections selected for the CRA wing are the NASA 63A518 at the root and the NASA 63A712 at the tip.

Wing Twist

The wings are twisted to produce good stalling characteristics by delaying stall at the tip until the root portion has stalled. Wind tunnel tests on the C-130 wing indicated that a twist of -3 degrees was sufficient. Since the CRA uses similar airfoils but with higher camber, slightly more twist is felt to be necessary and so a twist of -3.5 degrees is used.

Propellers

In the selection of the optimum propeller for the CRA, three critical flight conditions were considered:

- Maximum speed, where the highest possible thrust at military horsepower was desired.
- Speed for maximum lift-to-drag ratio, where the smallest possible value of power for the required thrust was desired.
- Hover, where the smallest possible value of power dissipated was desired.

The first two requirements are similar in that they both correspond to the highest possible propeller efficiency but at two different airspeeds.

Diameter

A large propeller diameter is desirable for obtaining the highest possible propeller efficiency. A small propeller diameter is desirable for maintaining propeller tip clearance between the rotor and the ground and for minimum weight in the propeller and the propeller gearbox. The effect of propeller diameter on the maximum theoretical efficiency at speeds of 200 and 400 knots is shown in Figure 5. It may be shown that increasing the diameter above 10 feet results in only small increases in efficiency. Figure 5 also shows the effect of propeller diameter on the sum of propeller and propeller gearbox weight. On the basis of these curves, and on consideration of clearance problems, a propeller diameter of 10 feet was selected as the maximum practical for the CRA.

Tip Speed

A high propeller tip speed is desirable to minimize the weight of the propeller and the propeller gearbox. A low tip speed is desirable to minimize noise, compressibility losses at high speeds, and power losses at hover. Figure 6 shows the effect of tip speed on the maximum allowable forward speed. For a maximum speed goal of 400 knots, a tip speed of about 800 fps is the maximum allowable. The tip speed has been selected to minimize the propeller and gearbox weight, which

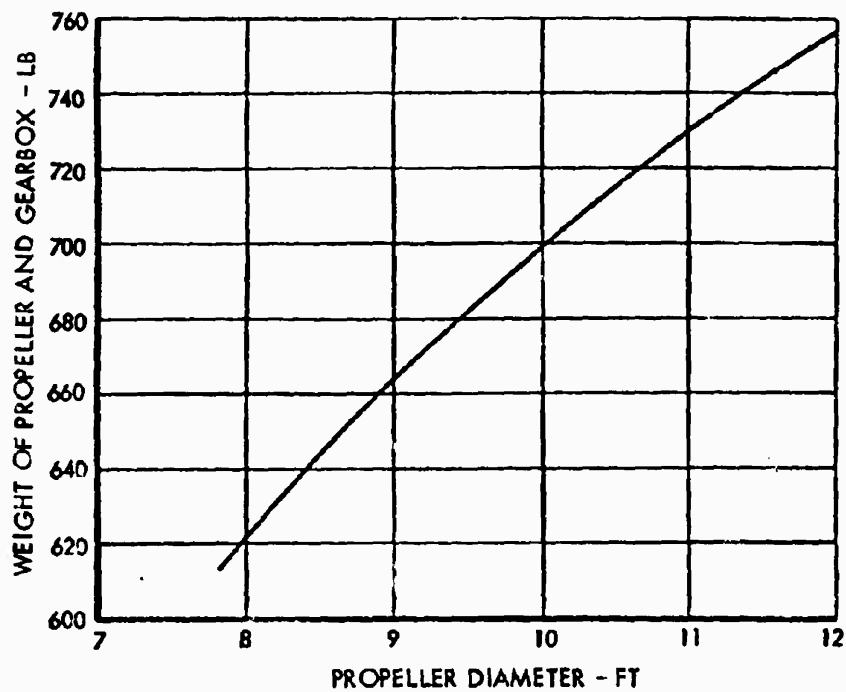
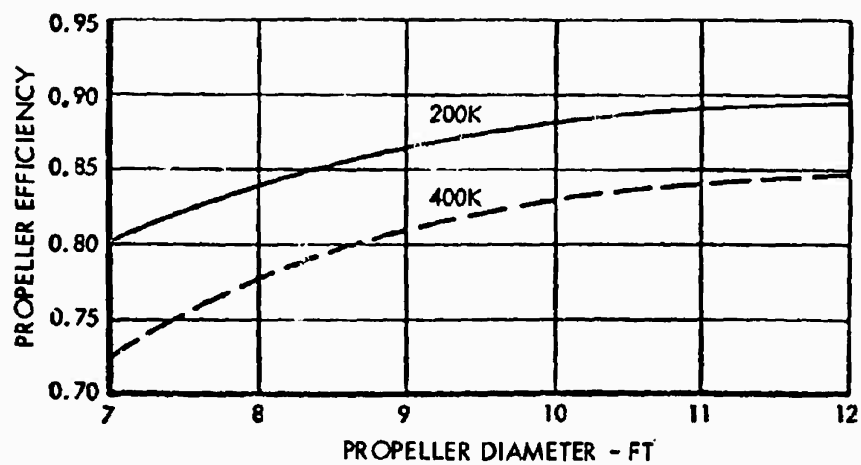


Figure 5. Effect of Propeller Diameter on Performance and Weight.

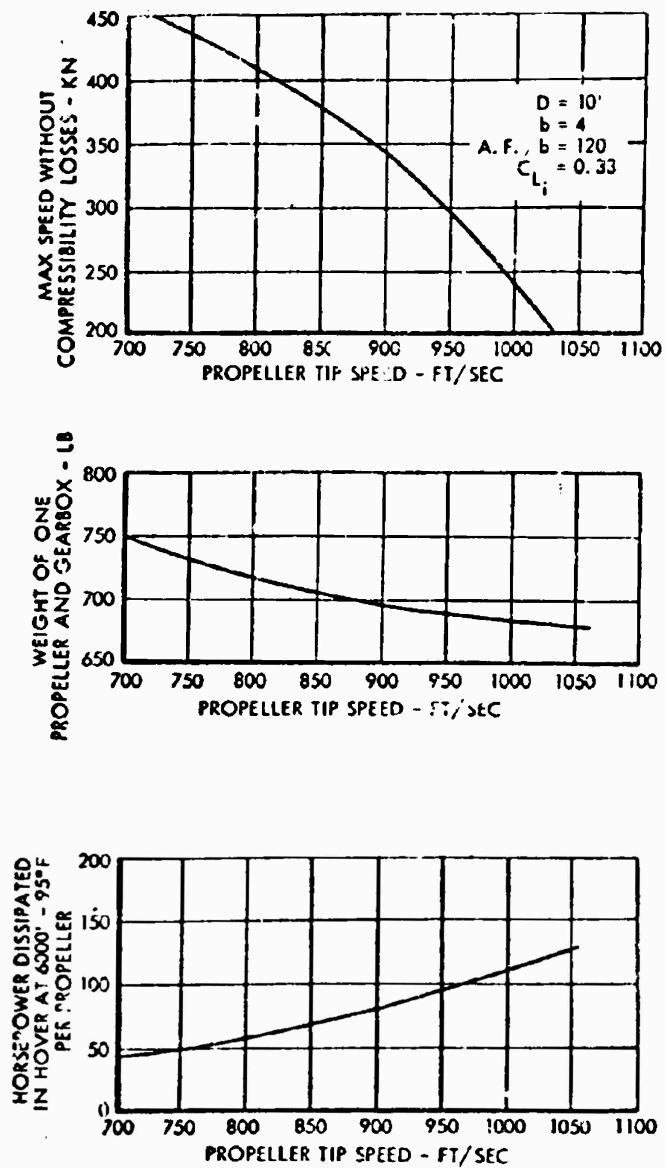


Figure 6. Effect of Propeller Tip Speed.

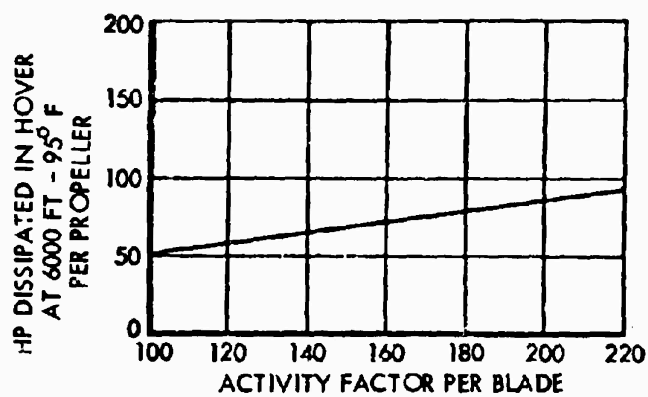
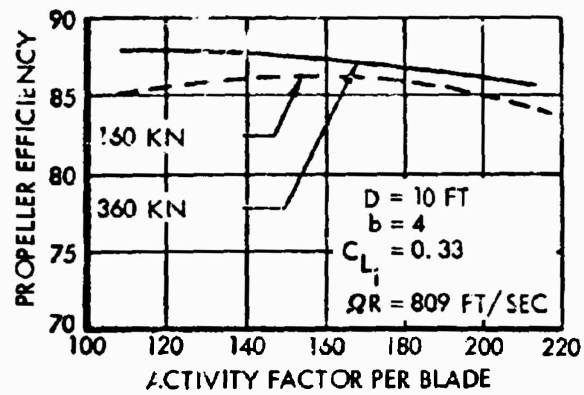


Figure 7. Effect of Propeller Activity Factor .

is also shown on Figure 6. The power dissipated by each propeller in hover is shown on the bottom of Figure 6. It may be seen that low tip speeds require less power, but the weight advantage with high tip speed was considered as the prime consideration in selecting the design tip speed of 809 fps.

Number of Blades

A high number of blades is desirable to maximize the propeller efficiency in forward flight and to minimize noise. A low number of blades is desirable to minimize weight, cost, and complexity. For the CRA a four-bladed propeller was chosen to take advantage of the high efficiency compared with that of three-bladed propellers.

Activity Factor

A low total activity factor is desirable to minimize propeller weight and power dissipated at hover. A moderately high total activity factor is desirable to obtain high efficiency at forward flight. Figure 7 shows the effect of propeller activity factor on efficiency at the speed for maximum lift-to-drag ratio, 160 knots, and at the maximum speed, 260 knots. Also shown in Figure 7 is the effect of activity factor on the power dissipated in hover. An activity factor of 120 per blade has been chosen for the CRA as the best compromise for the three flight conditions shown.

Tail Rotor

The tail rotor must provide both sufficient antitorque moment and adequate directional control while the CRA is flying in the helicopter mode. The design objectives for the tail rotor involve satisfying these requirements with minimum power and minimum weight.

Diameter

To minimize the power required by the tail rotor, it is desirable to use as large a diameter as possible. However, design problems relevant to obtaining suitable ground and rotor clearance and minimum weight place restraints on tail rotor diameter. Figure 8 shows the effect of the tail rotor design parameters on power and on weight. The design decision was to select a diameter of 13.5 feet as the best compromise.

Tip Speed

From Figure 8, it may be seen that for a diameter of 13.5 feet, a tip speed of about 650 fps is optimum for minimizing both power and weight. A tip speed of 638 fps was actually selected to maintain a gear ratio between the main rotor and the tail rotor which would insure that,

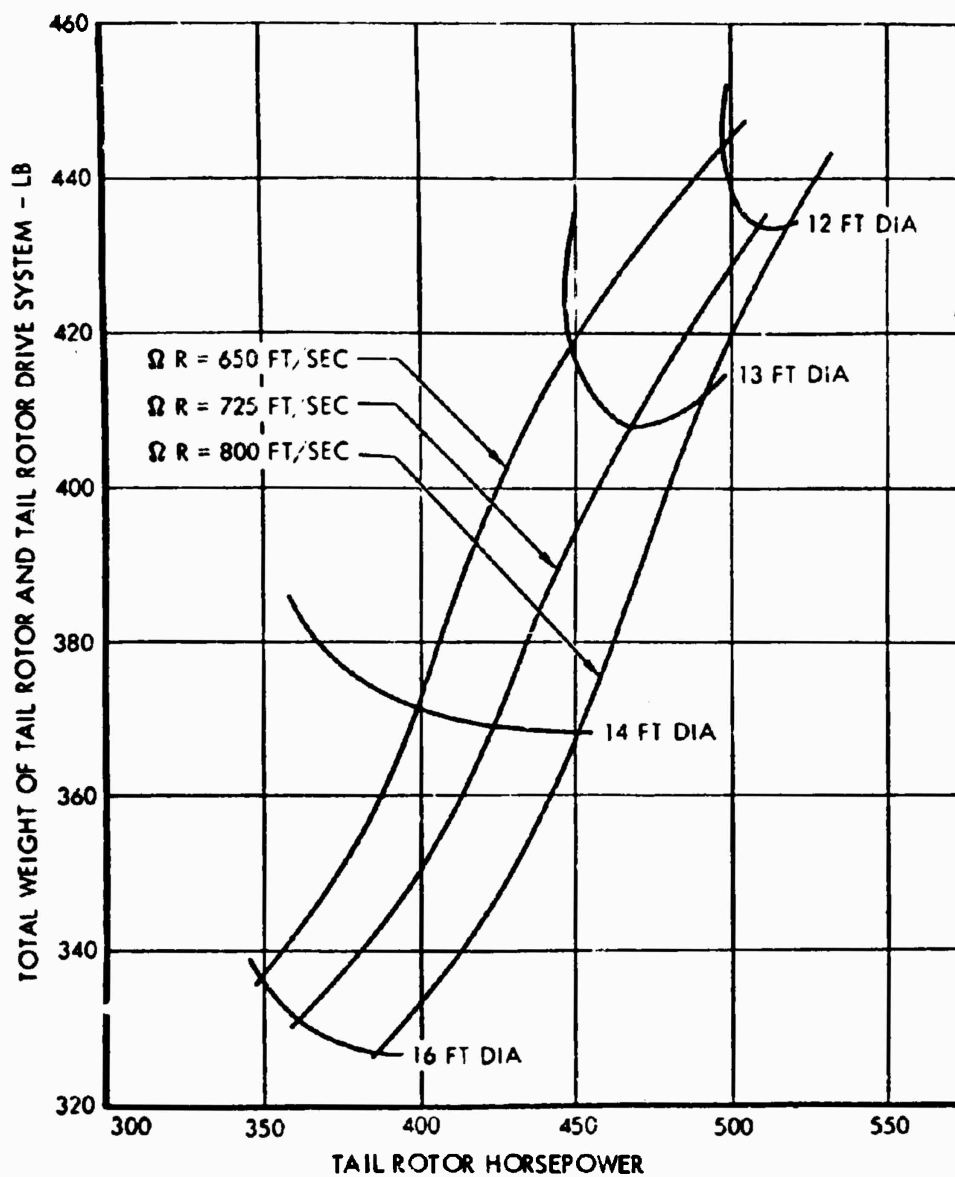


Figure 8. Results of Tail Rotor Parametric Study.

when the main rotor was folded, the tail rotor would be stopped with two blades horizontal and two blades vertical. This would minimize aeroelastic divergence problems.

Solidity

The solidity of the tail rotor was selected to absorb the smallest possible amount of power at 6000 feet, 95°F while generating the thrust required for antitorque. Once the tail rotor diameter and tip speed were selected, a study of power as a function of solidity at the hover condition showed that a solidity of 0.258 was optimum, and this value was selected for the CRA.

Horizontal Stabilizer

The horizontal stabilizer must be adequate to trim and control the aircraft while flying in the airplane mode.

Tail Length

The horizontal stabilizer has been placed halfway up the vertical stabilizer and has been used to carry the tail rotor. This arrangement dictates that the tail length for the horizontal stabilizer be approximately equal to the total of the main rotor and tail rotor radii in order to provide clearance between the two rotors. On the CRA, the tail length between the quarter chords of the wing and the horizontal stabilizers is 33.2 feet.

Area

The horizontal stabilizer area was selected to provide a static margin of approximately 0.06 with the most aft center-of-gravity position in the airplane mode. An area of 58 square feet was verified as giving this margin by the wind tunnel tests reported in Reference 1. Further discussion of the horizontal stabilizer is presented in Part 5.

Vertical Stabilizer

The vertical stabilizer must provide adequate directional stability in the airplane mode. A vertical stabilizer area of 17 square feet has been selected as adequate. Further discussion of the vertical stabilizer is presented in Part 5.

CHAPTER
PERFORMANCE ANALYSIS

HOVER AND VERTICAL FLIGHT

Power Required by Rotors

The hover and vertical flight analysis was performed with a digital computer program which uses a method based on strip analysis, variable induced velocity, and two-dimensional airfoil characteristics as a function of local blade angle of attack, thickness ratio, and Mach number. The airfoil data which are used in this program are based on wind tunnel and whirl tower tests reported in References 7, 8, 9, 10, and 11.

Vertical drag in hover was computed by strip analysis using the variation of dynamic pressure with radius and distance below the rotor as shown in Figure 9, which was constructed from the data in Reference 7. The vertical drag coefficients used for this analysis are shown in Figure 10. Analysis has shown that the vertical drag in hover is 7 percent of the gross weight.

The main rotor performance is shown in nondimensional coefficient form in Figures 11, 12, and 13. These figures show the thrust coefficient as a function of collective pitch, the torque coefficient/solidity as a function of thrust coefficient/solidity, and the figure of merit as a function of thrust coefficient/solidity, respectively. The tail rotor performance is shown in nondimensional form in Figures 14 and 15. These figures show thrust coefficient as a function of collective pitch and torque coefficient/solidity as a function of thrust coefficient/solidity.

The nondimensional results have been used to calculate the main rotor and tail rotor power in hover as a function of aircraft gross weight. The results of these calculations are shown on Figures 16 and 17, respectively.

Power Losses in Hover

Besides the main and tail rotor, several other components absorb power and these losses must be accounted for in computing performance. Table III lists the components and the equations for their respective losses.

Total Power Required to Hover

The total engine shaft power required to hover is the total of main rotor power, tail rotor power, propeller power, and all of the losses shown in Table III. Figure 18 shows the engine shaft horsepower as a function of gross weight for hovering in and out ground effect on a sea level standard day and on a 6000-foot 59°F day.

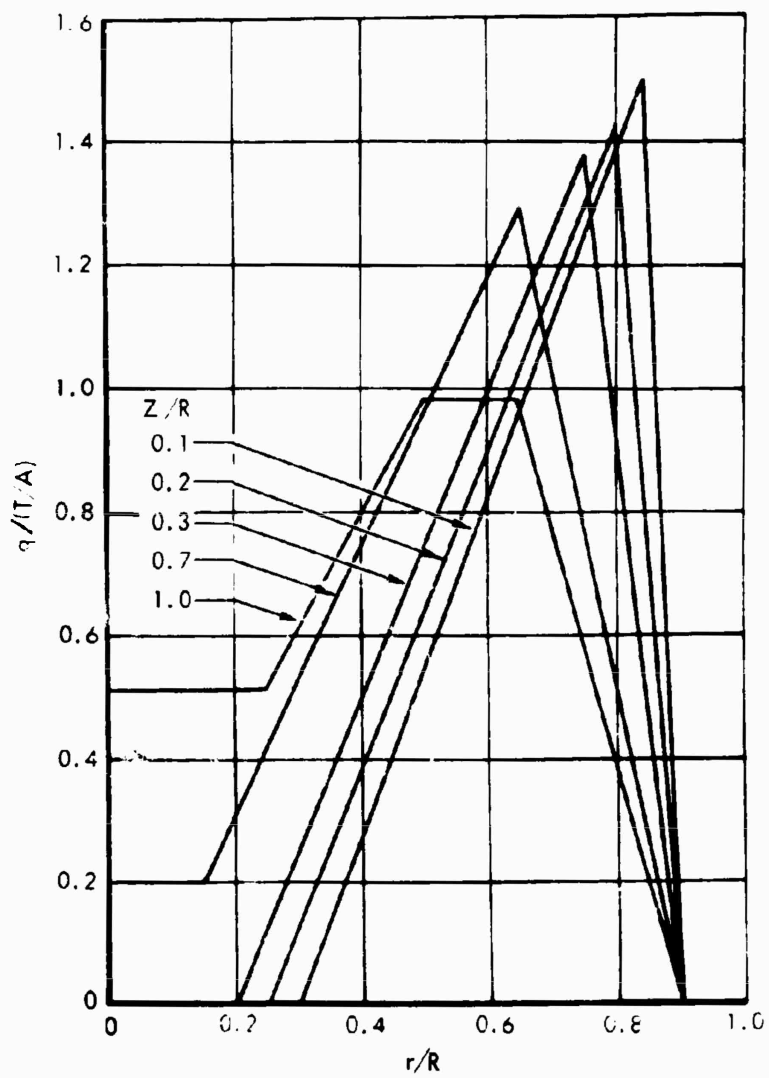


Figure 9. Dynamic Pressure Distribution in Rotor Downwash.

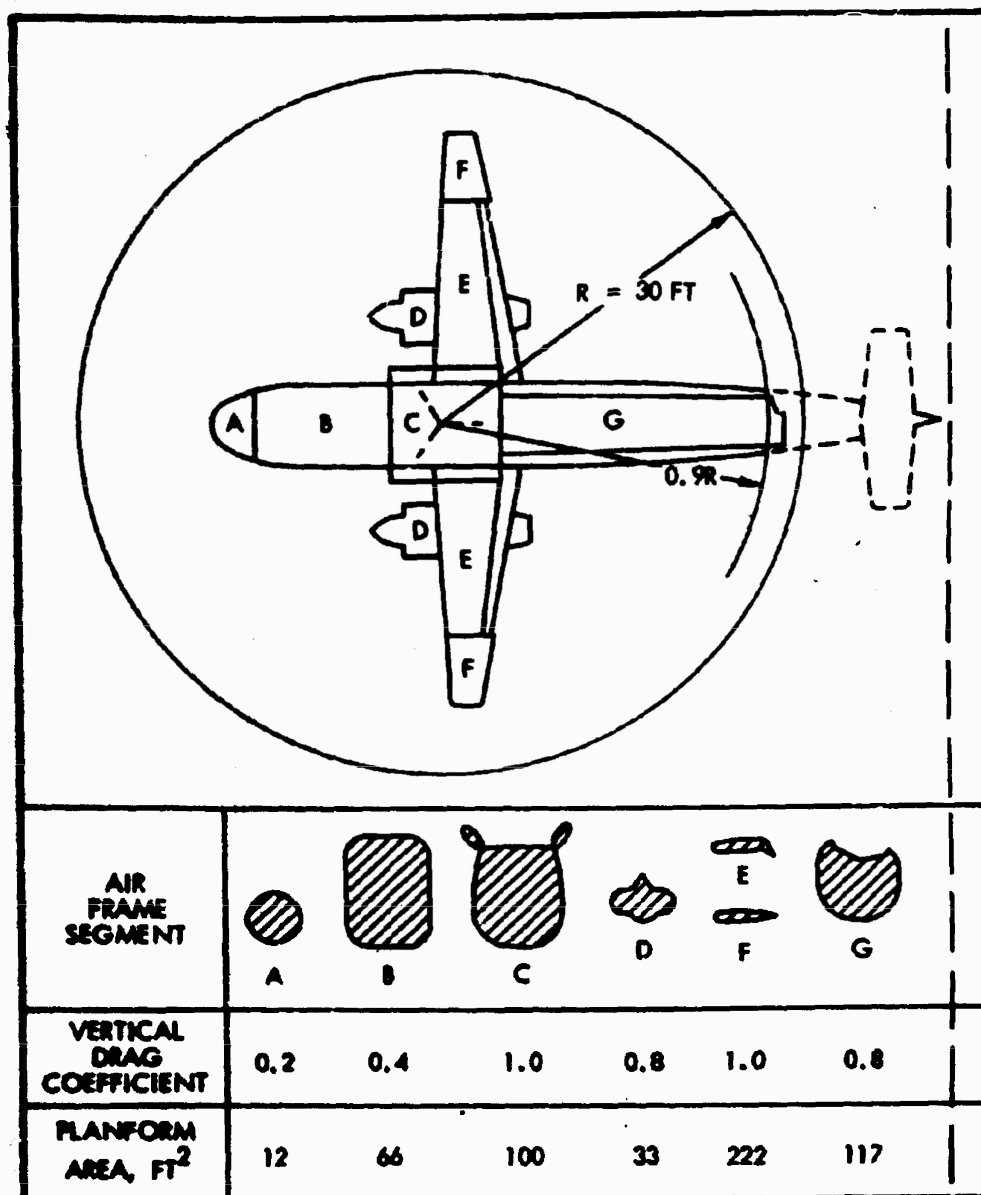


Figure 10. Vertical Drag Coefficients.

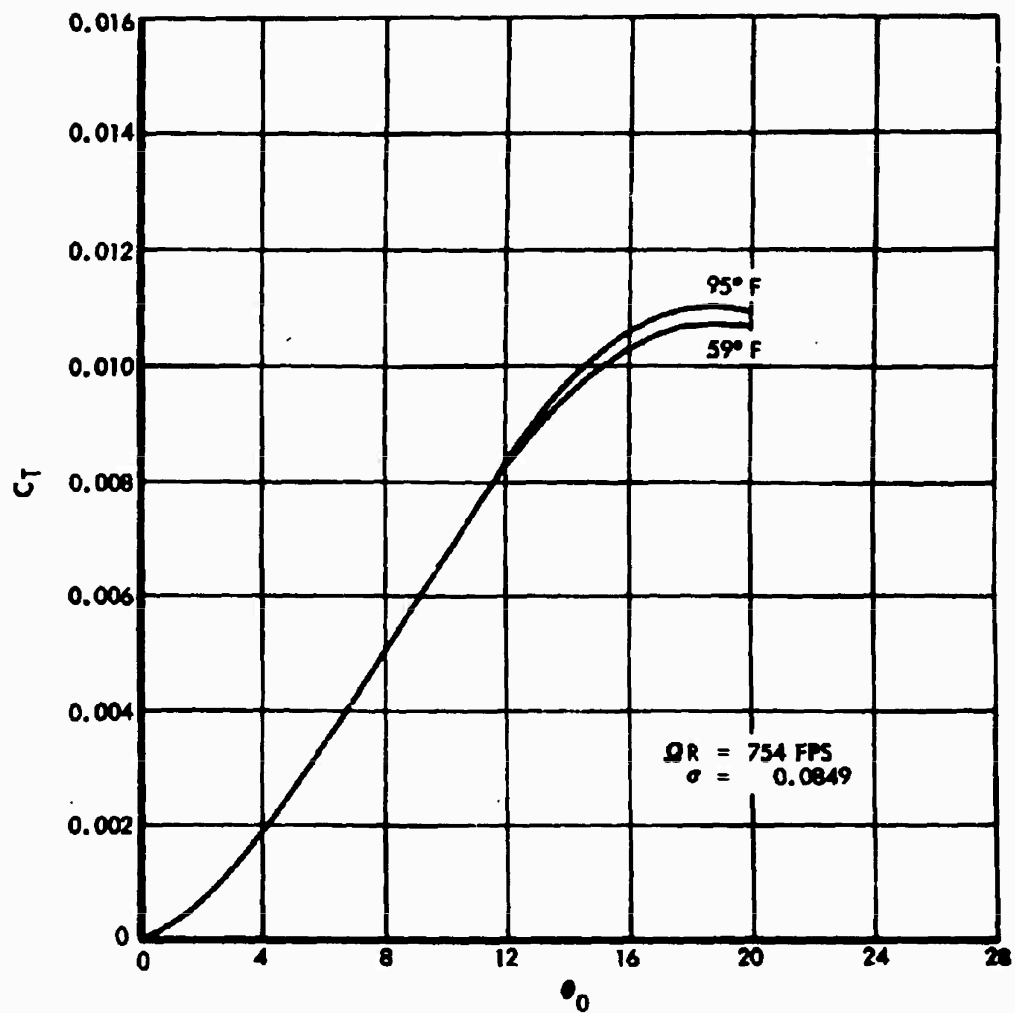


Figure 11. Main Rotor Thrust Coefficient in Hover.

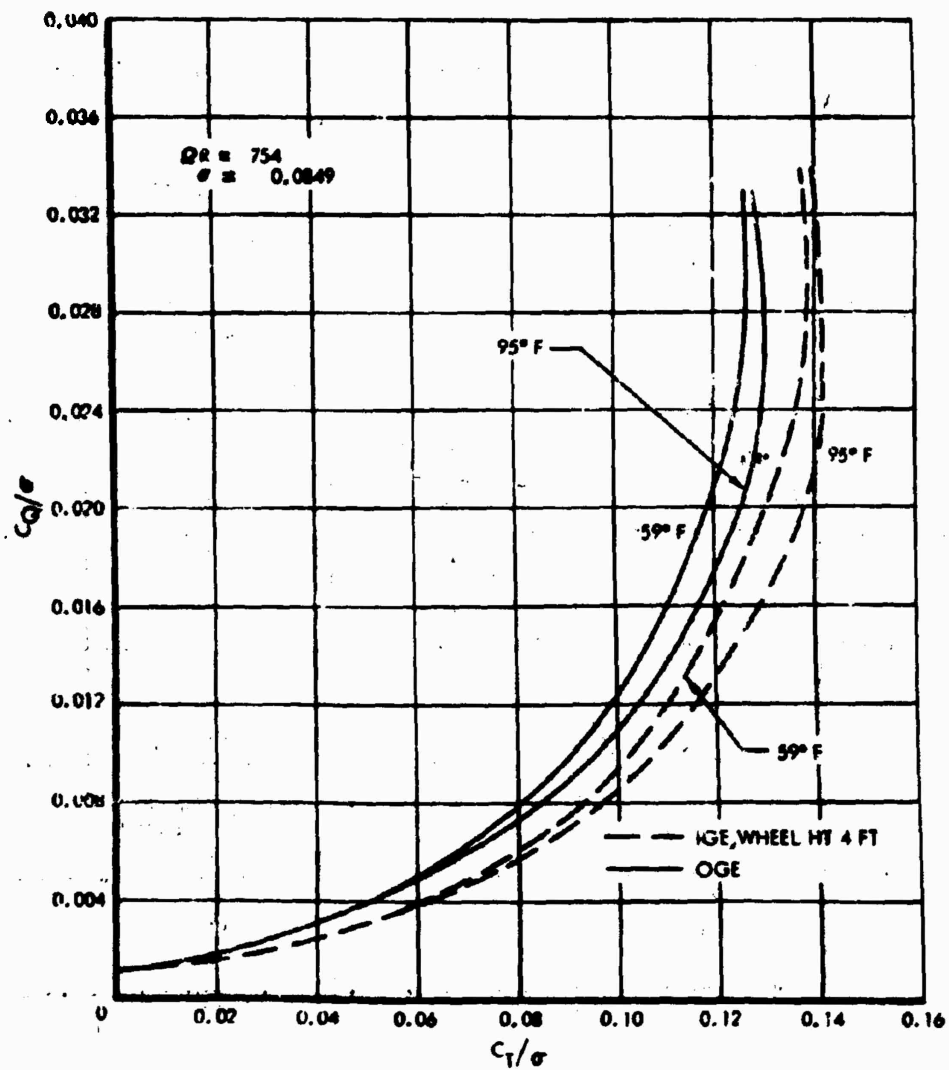


Figure 12. Main Rotor Performance in Hover.

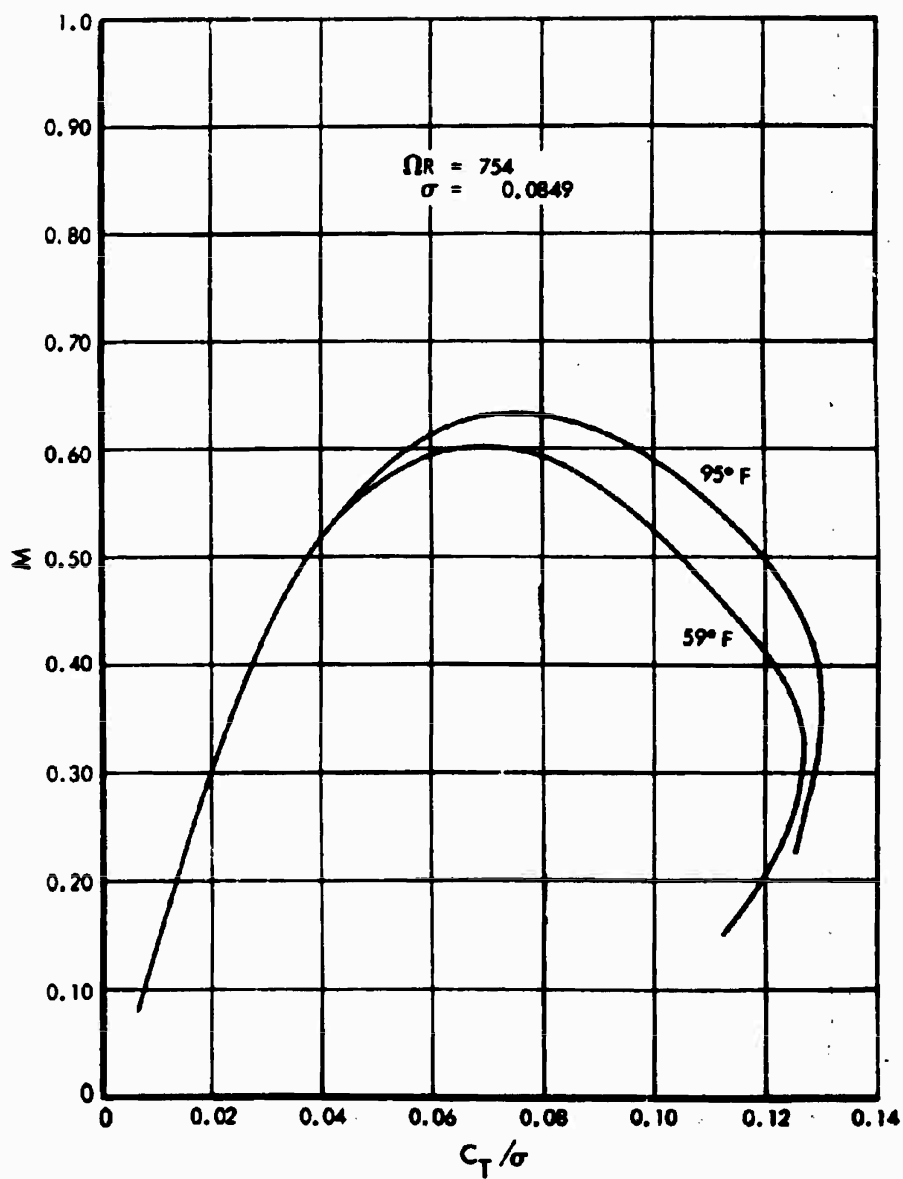


Figure 13. Main Rotor Figure of Merit.

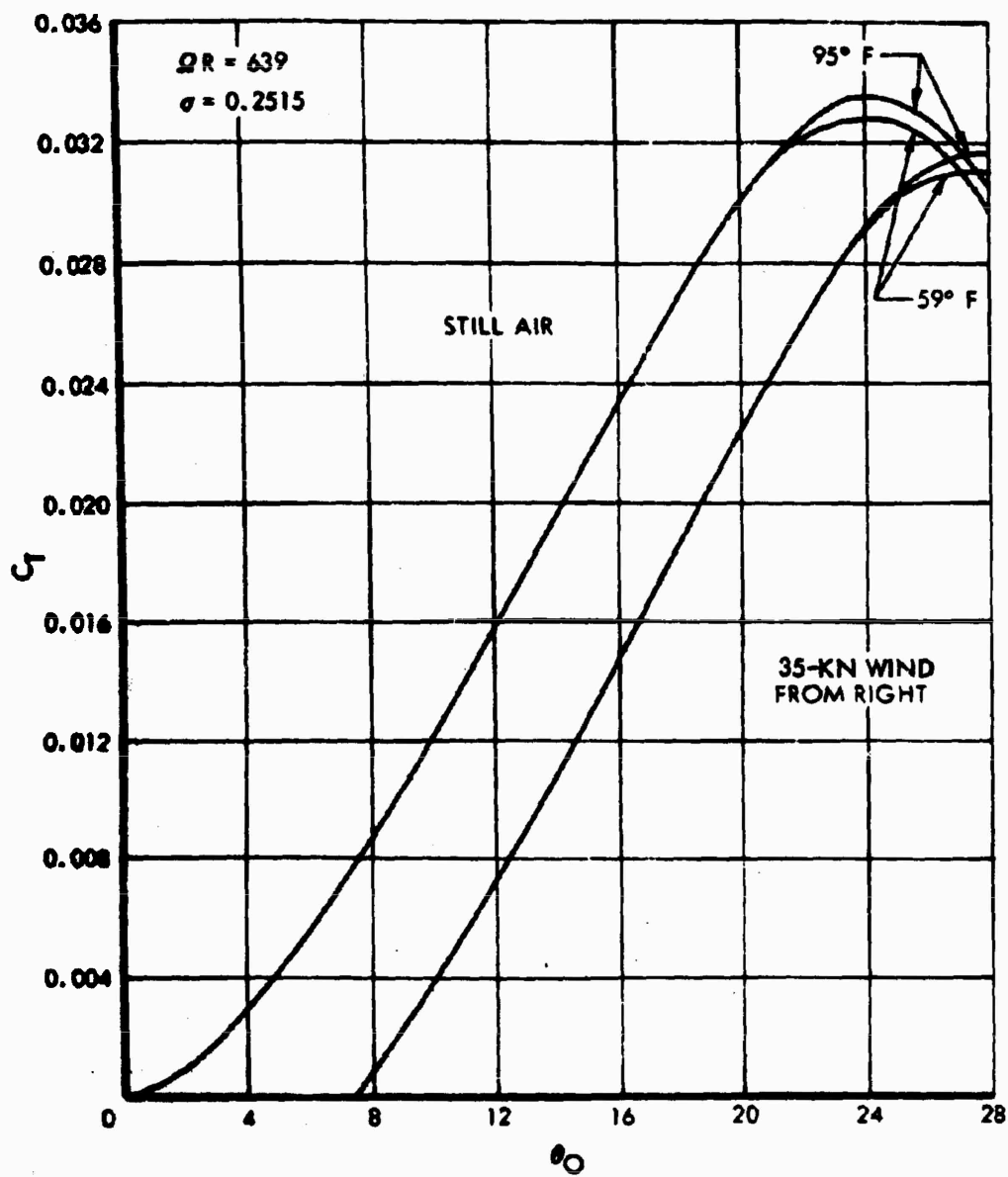


Figure 14. Tail Rotor Thrust Coefficient.

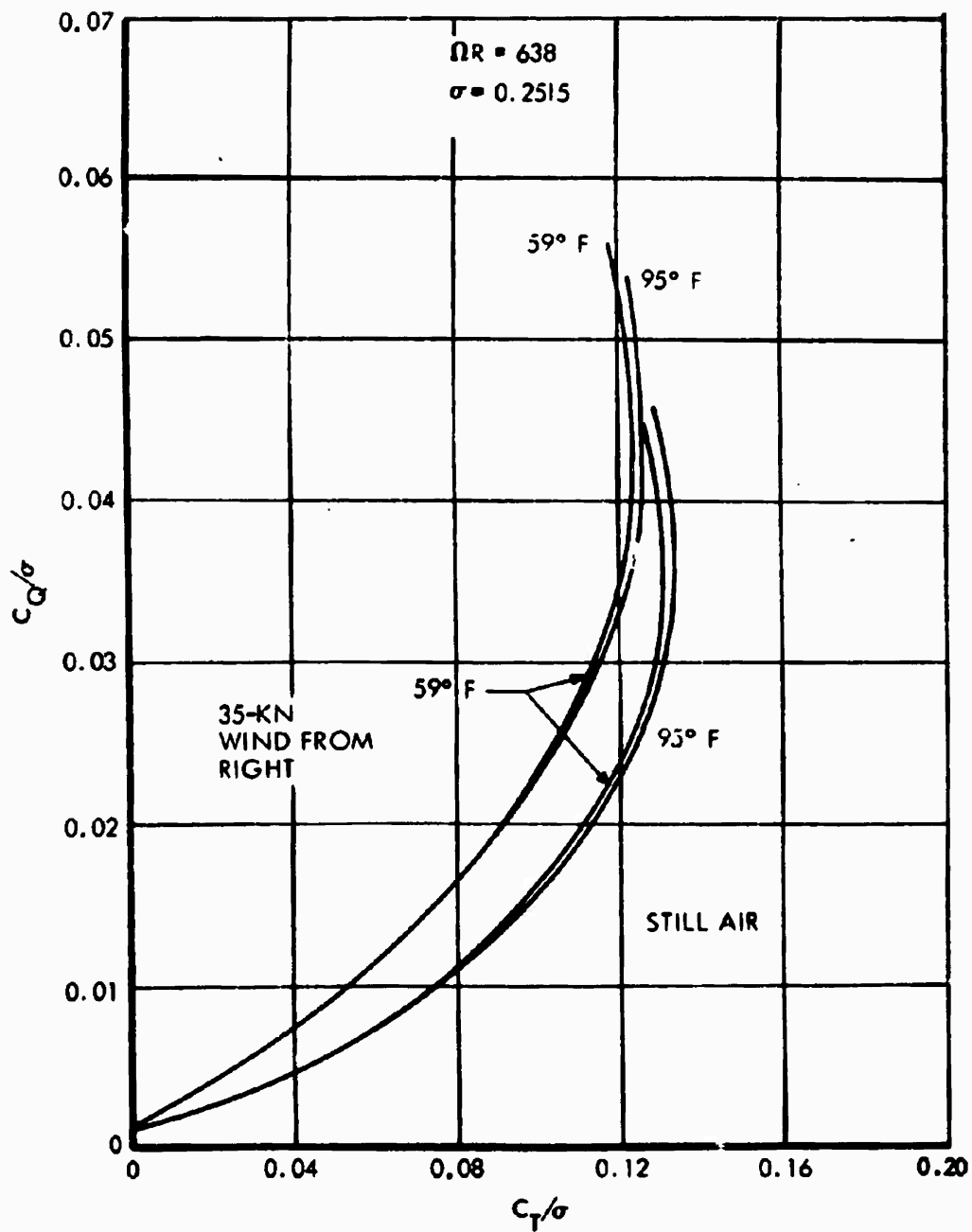


Figure 15. Tail Rotor Performance.

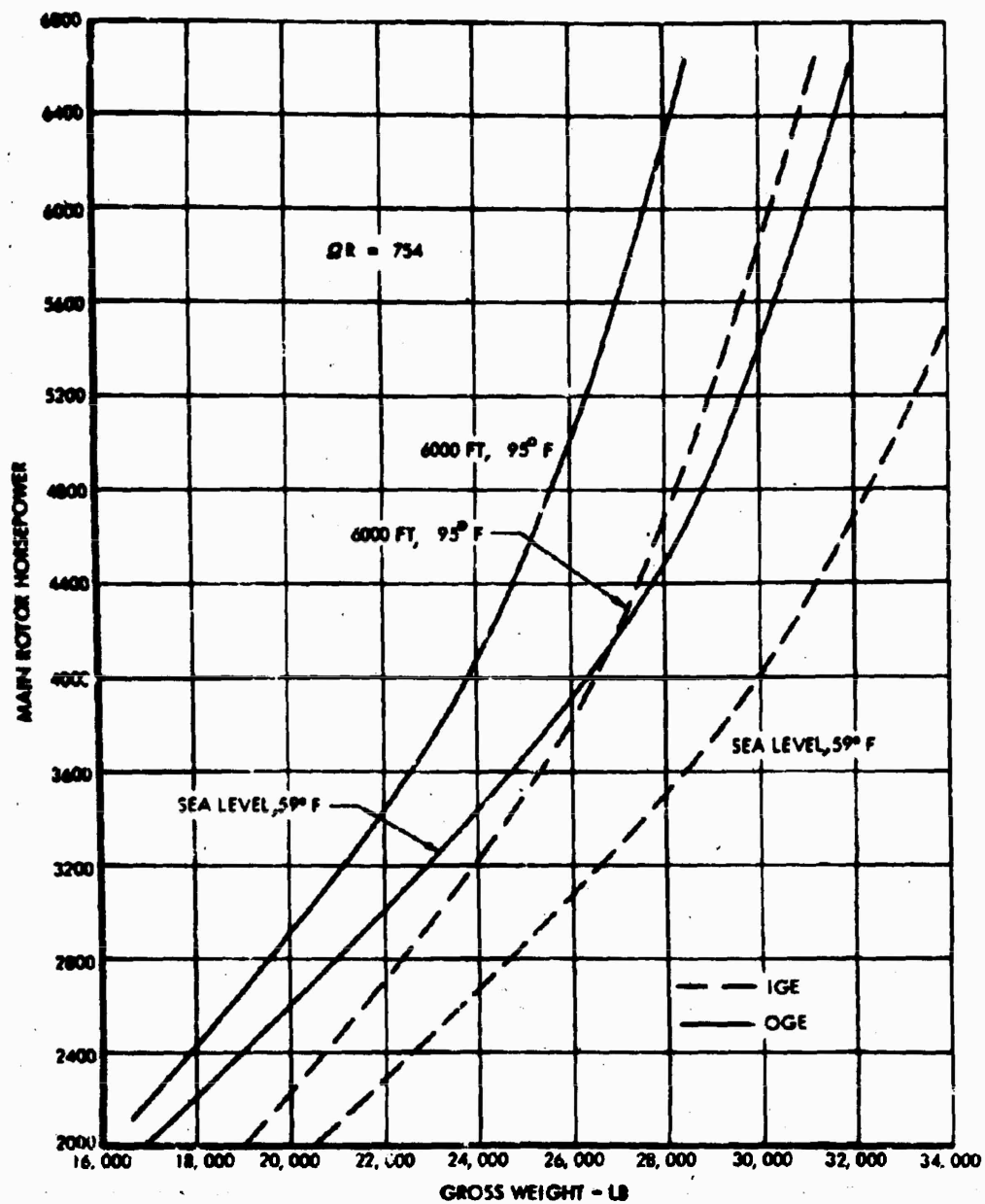


Figure 16. Main Rotor Power Required for Hover.

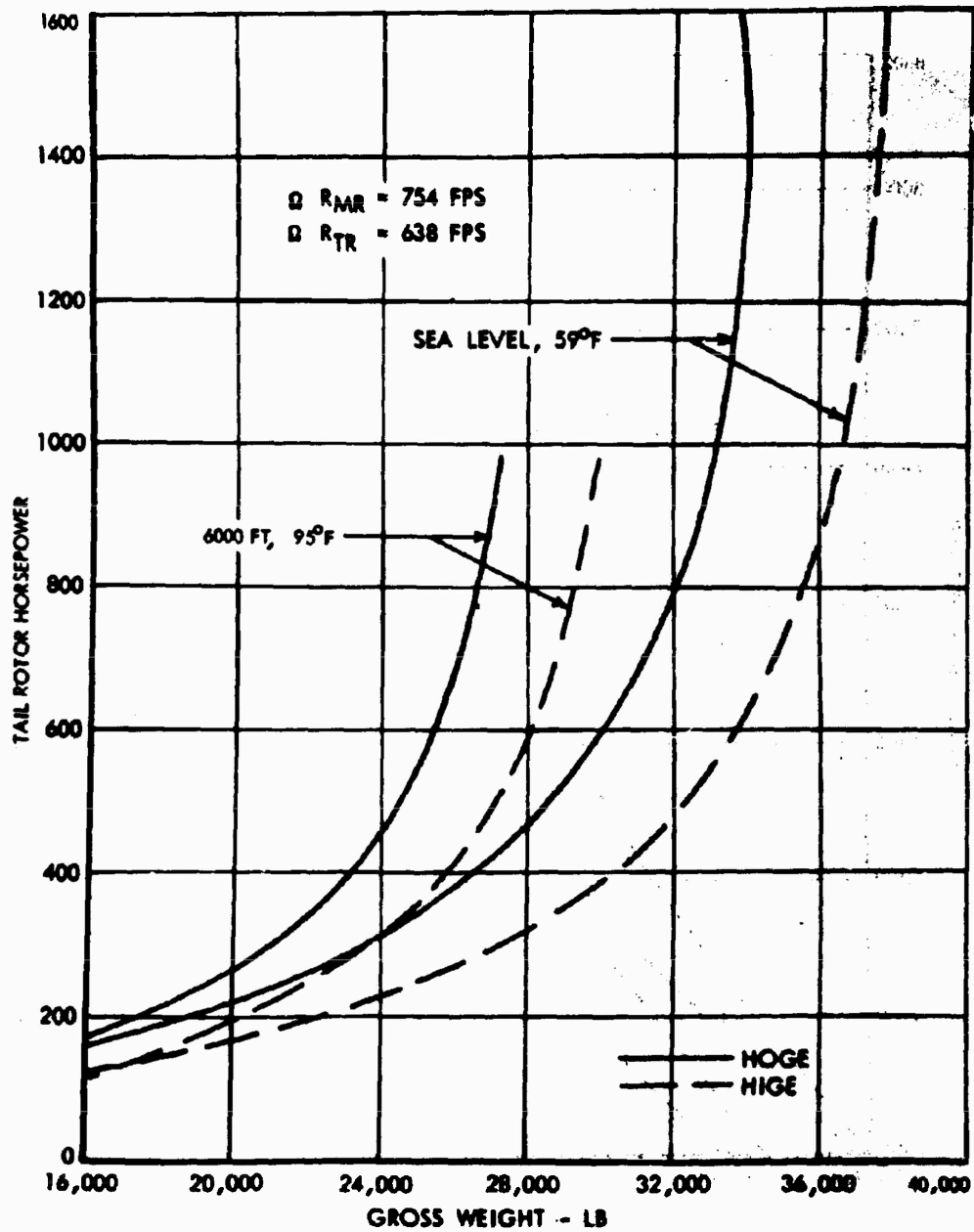


Figure 17. Antitorque Power Required in Hover.

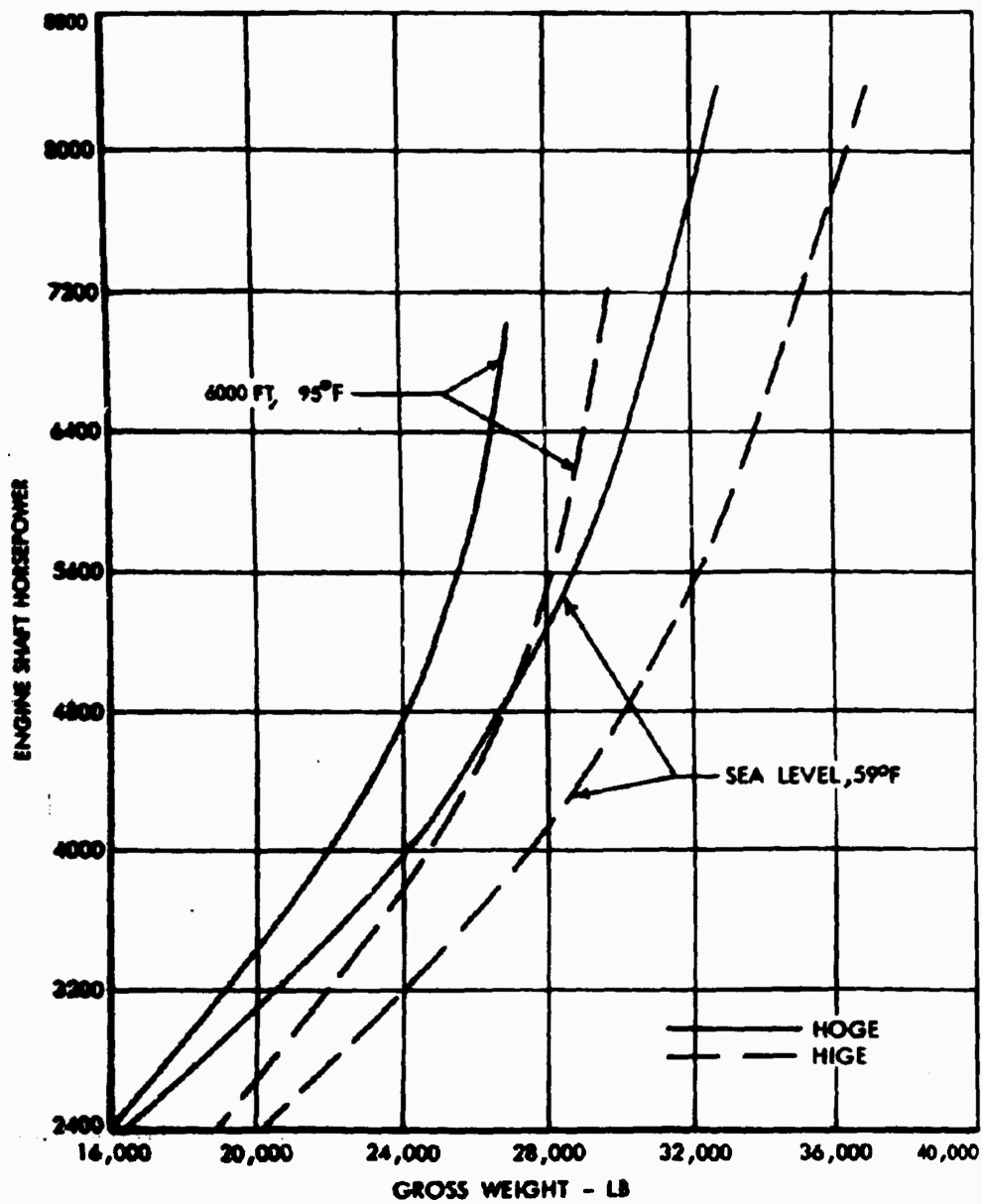


Figure 18. Total Hover Power .

TABLE III. POWER LOSSES				
Item	Equation for Power Loss	Typical Power Losses		
		Hover 6000 Ft 95°F	V = 175 knots	V = 360 knots
Propeller Gearboxes and Cross-Shafting	0.018 (Propeller power)	2	22	133
Main Rotor and Tail Rotor Transmissions	0.028 (Main rotor and tail rotor power)	137	0	0
Hydraulic Pumps	15	15	15	15
Electrical	15	15	15	15
Lubrication	5	5	5	5
Transmission Cooling (in helicopter mode only)	15	15	-	-
Propellers (2) (in hover only)	$156 \frac{P}{0.002378}$	117	-	-
	TOTAL	306	57	168
NOTE: Engine and propeller lubrication is from oil pump on engine accessory drive pad and is accounted for in the power-available calculations.				

Hover Ceiling

By matching the power required as a function of gross weight, altitude, and temperature with the maximum engine power available as a function of altitude and temperature, hover ceilings were established. Figure 19 shows hover ceilings in and out of ground effect as a function of gross weight on standard days and on 95°F days. It may be seen that at the design gross weight of 24,500 pounds, the CRA can hover out of ground effect on an altitude of 9500 feet on a standard day and at 6800 feet on a

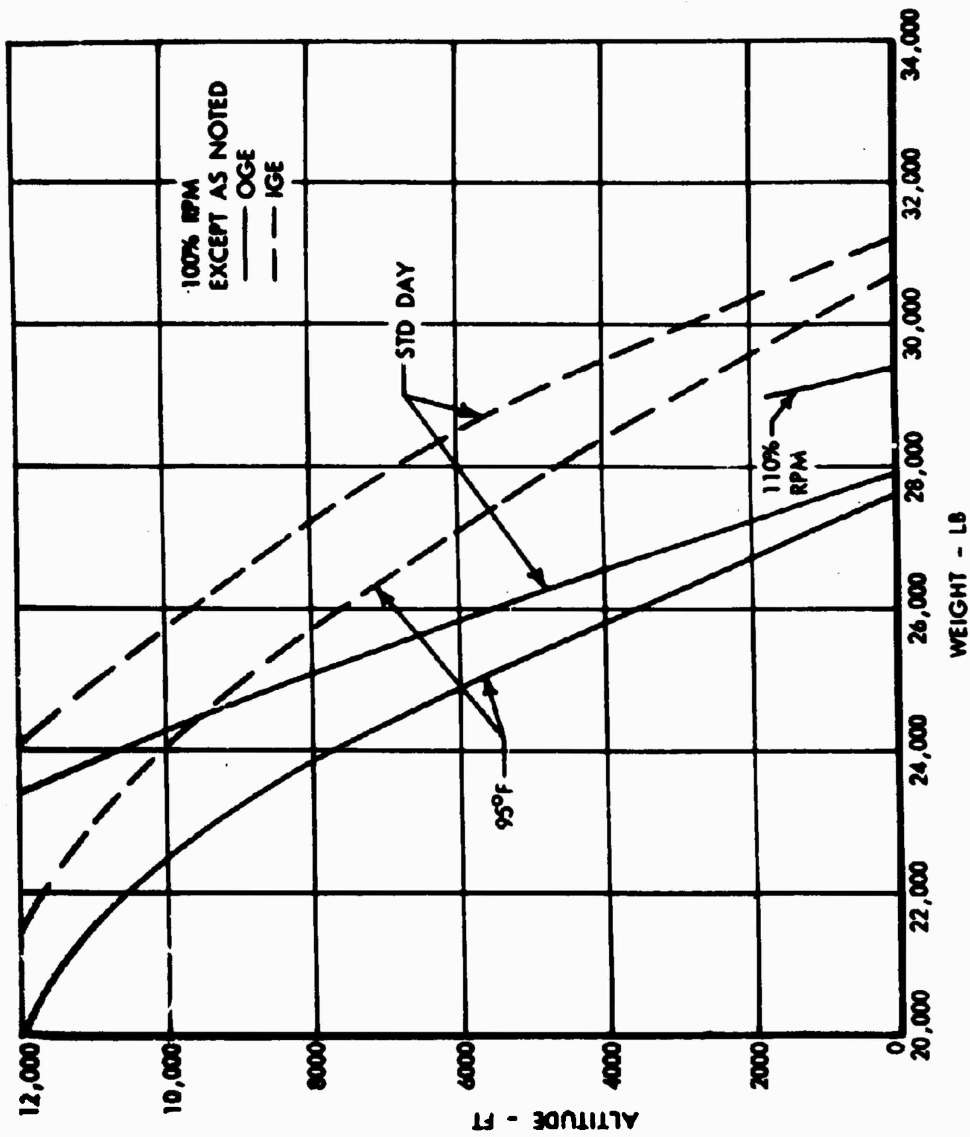


Figure 19. Hover Ceiling.

95°F day. The effect of varying tip speed on the gross weight which can be hovered at sea level within the transmission torque limits is shown in Figure 20. This shows that a 10-percent increase in rotor speed results in a 7-percent increase in allowable hover weight.

Vertical Rate of Climb

The required engine shaft horsepower as a function of vertical rate of climb is shown on Figure 21, for the design gross weight of 24,500 pounds. It may be seen that at the maximum torque limit of the transmission, the vertical rate of climb is 2000 feet per minute at sea level.

FORWARD FLIGHT

Parasite Drag

The requirements which apply to forward flight performance are:

- The lift-to-drag ratio based on total engine power must be at least 10.
- The maximum speed at sea level must be at least 300 knots, with 400 knots desired.

The analysis of the performance in light of these two requirements requires an accurate estimation of the minimum parasite drag in the airplane mode.

The estimation procedure used for minimum parasite drag is based on the use of wetted areas and suitable skin friction coefficients which have been verified by flight test results of comparable aircraft. Because of the uncertainty of Reynolds number corrections, small-scale wind tunnel results are used only to measure the drag of the "bluff body" components on the aircraft or to evaluate the drag effect of changes in the "wetted area" components. Table IV shows the wetted area, the estimated skin friction coefficient, and the product in equivalent flat plate area for all of the components of the CRA. For comparison, the skin friction coefficients which have produced satisfactory correlation on the Constellation (C-121) and the Hercules (C-130) are tabulated. The performance analysis of the CRA has been based on the total of the estimated column.

A last-minute wind tunnel test was done to measure the effect on drag of the partially exposed blades as contrasted to the drag with full doors and with no doors which had been measured during the first wind tunnel tests.

Since the change was both a bluff body change and a change to wetted area components, the measured increment in drag from the full door configuration is considered to be valid. These tests showed that the drag penalty of the partially exposed blades in equivalent flat plate area was 0.5 square foot at zero lift and 0.25 square foot at the attitude for

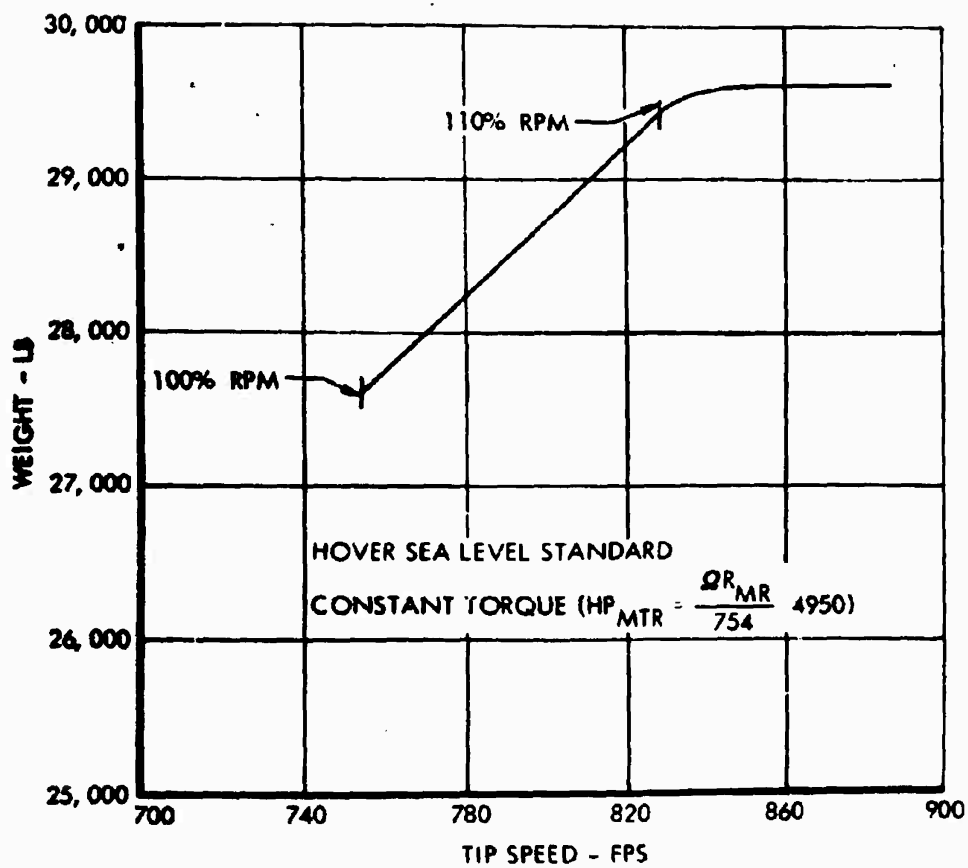


Figure 20. Effect of Tip Speed on Sea Level Hover .

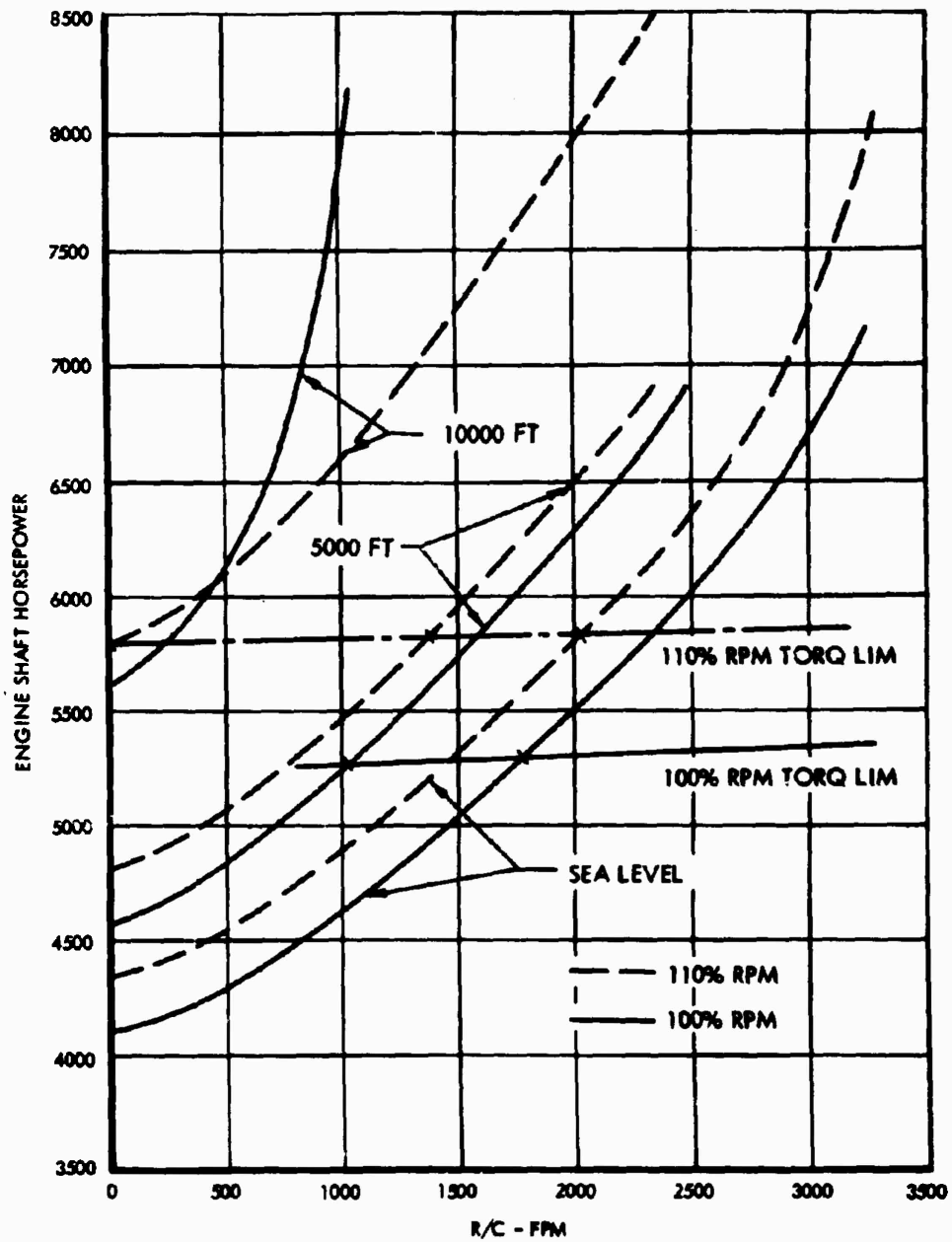


Figure 21. Power Required for Vertical Climb.

TABLE IV. ESTIMATION OF MINIMUM DRAG						
Configuration	Component	Skin Friction Coefficient, C_{Df}			CRA	
		Constellation (1049G)	C-130	(Estimated)	S_F	C_{Df} (Estimated)
Airplane	Wing	0.00350	0.00375	0.0038	445	1.69
	Fuselage	0.00370	0.00460	0.00425	1270	5.40
	Tail	0.00350	0.00310	0.00400	250	1.00
	Nacelles	0.00780	0.00480	0.00500	185	0.92
	TOTAL OF SKIN FRICTION					
	COMPONENTS					
	Tail Rotor					
	Partially Exposed Blades	0.00370	0.00432	0.00419	2150	9.01
						0.70
	TOTAL AIRPLANE					1.50*
Helicopter						11.21
	Wing					
	Fuselage					1.69
	Tail					5.40
	Nacelles					1.00
	Tail Rotor					0.92
	Main Rotor and Doors					0.70
						10.00
	TOTAL HELICOPTER					21.21
*Measured as 0.5 square foot during last-minute wind tunnel tests						

maximum lift-to-drag ratio. These values compare to the estimated value of 1.5 square feet in Table IV which has been used throughout the performance analysis. Thus, all of the performance estimations in the airplane mode are conservative.

Figure 22 shows how the estimated drag of the CRA compares to other subsonic airplanes. It may be seen that its aerodynamic cleanliness puts it in the same class as the C-54 and the C-130.

At high speeds, a compressibility correction must be applied to the drag coefficient. Figure 23 shows the corrections which have been used for the CRA. They were based on the material presented in Reference 8.

The variation of parasite drag as a function of lift coefficient has been tailored to favor the requirement for a maximum lift to drag ratio based on total power of at least 10. The wind tunnel model was constructed with wing airfoil sections identical to the C-130; i.e., NASA 63A 318 at the root and NASA 63A 412 at the tip. The variation of the increment of parasite drag coefficient, C_{D_p} , as measured on the wind tunnel model, is shown as a function of lift coefficient in Figure 24. This curve has its lowest point at a lift coefficient of 0.25. The lift coefficient corresponding to maximum lift-to-drag ratio is approximately 0.9, and at this point the value of C_{D_p} is 0.058. To obtain the required lift-to-drag ratio with the minimum of configuration changes, the final design of the wing has higher camber than was tested in the wind tunnel. The airfoils which have been selected are the NASA 63A 518 at the root and the NASA 63A 712 at the tip. With these airfoils, the C_{D_p} variation with lift coefficient is shown in Figure 24. It may be seen that the bottom of the curve has been shifted toward the value of lift coefficient at which the maximum lift-to-drag ratio is obtained. It should be noted that this amount of camber slightly penalized the high-speed capabilities of the aircraft by adding drag at the low lift coefficients corresponding to high speeds.

Total Drag

The total drag of the airplane is the sum of the parasite and the induced drag, where the induced drag coefficient, C_{D_i} , is given by the equation

$$C_{D_i} = \frac{C_L^2}{\pi AR}$$

This term has been added to the parasite drag coefficients in Figure 24, and the results are shown in Figure 25 for both flap-up and flap-down conditions. These curves have been used for the calculations of airplane performance.

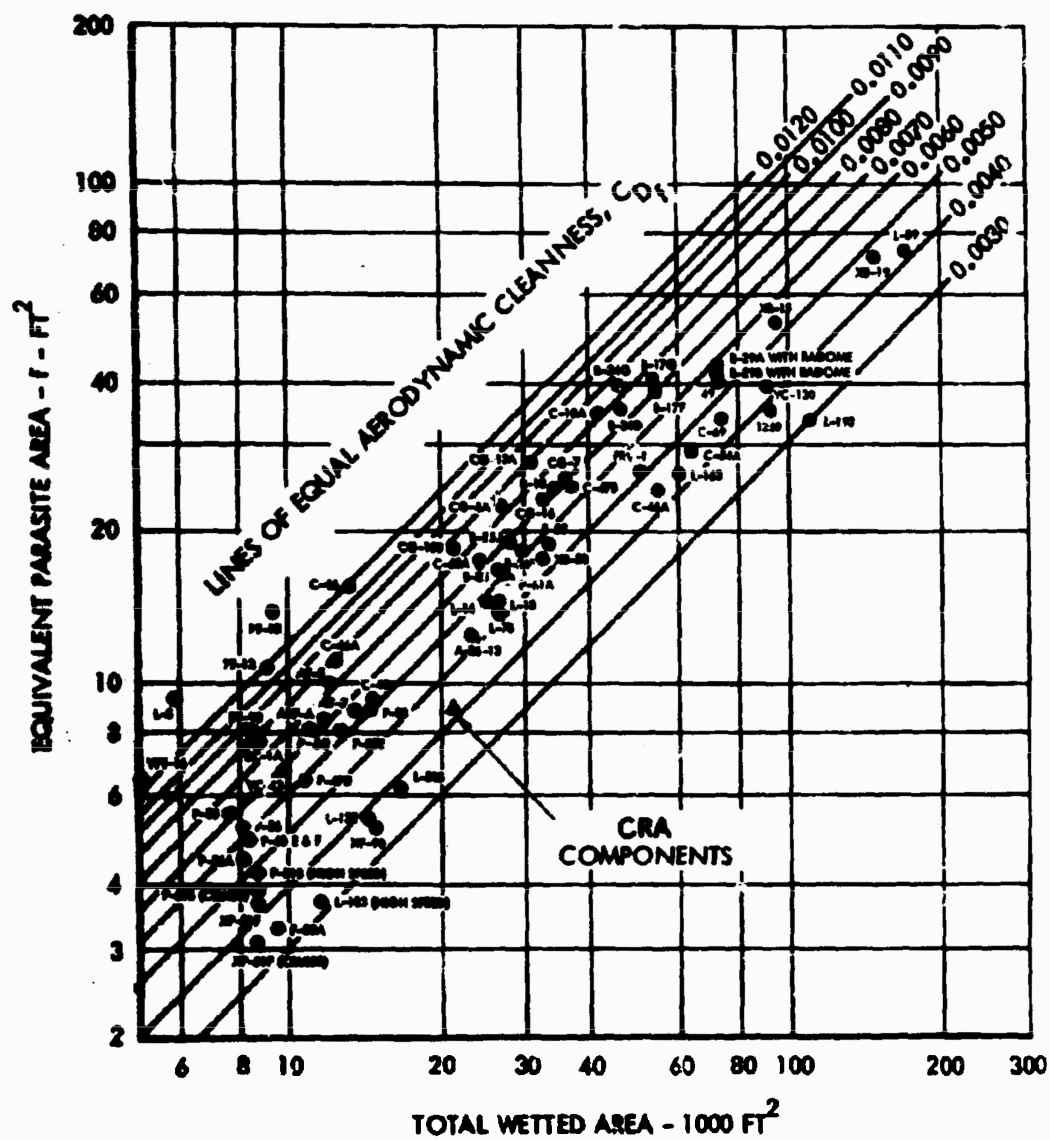


Figure 22. Equivalent Parasite Area of Complete Airplanes .

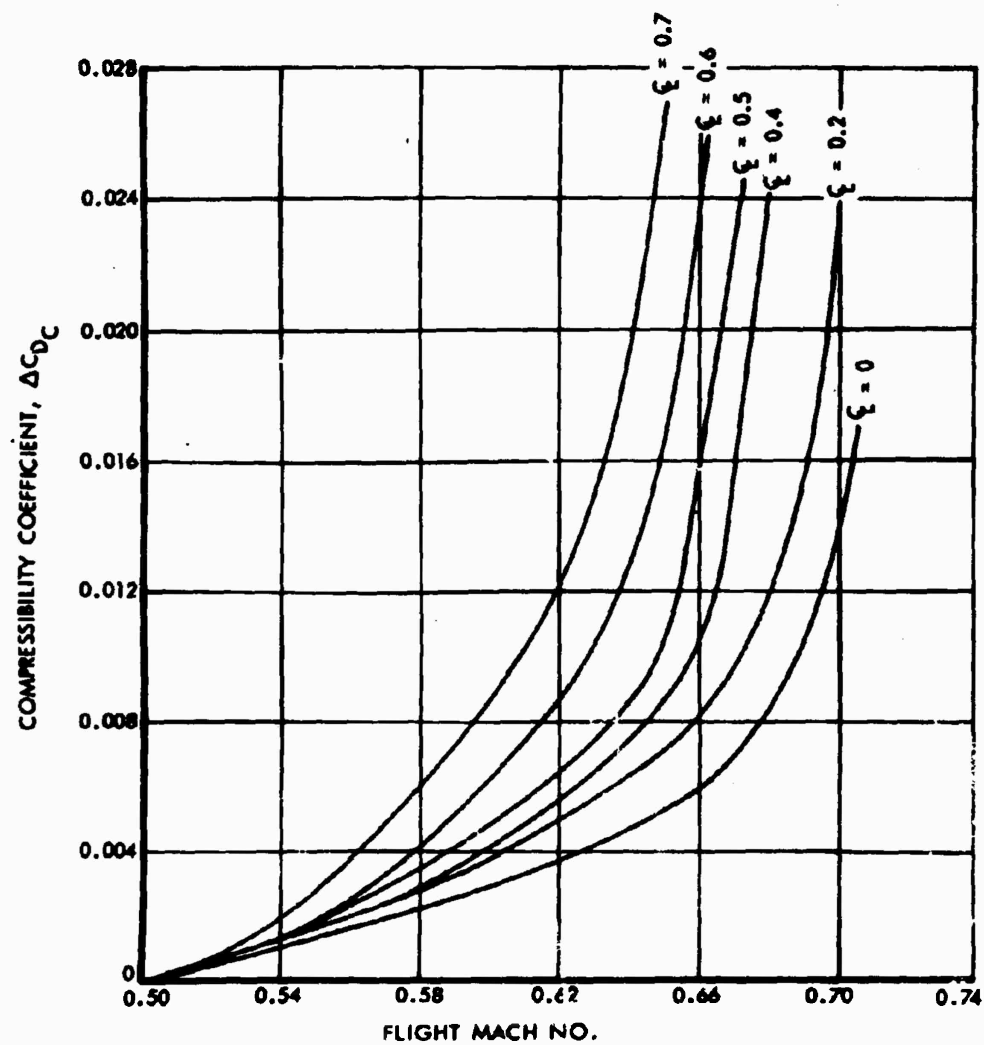


Figure 23. Airplane Compressibility Correction.

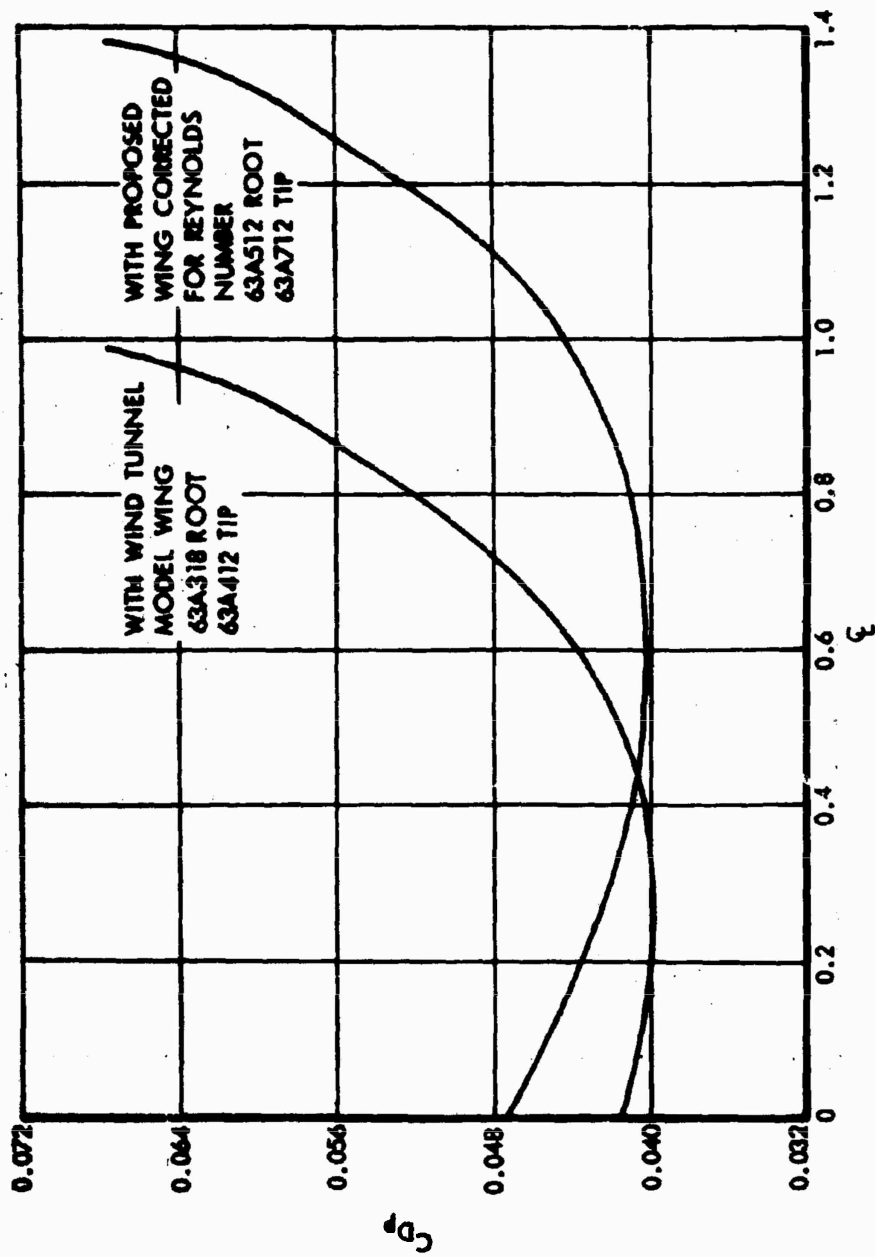


Figure 24. Parasite Drag Variation.

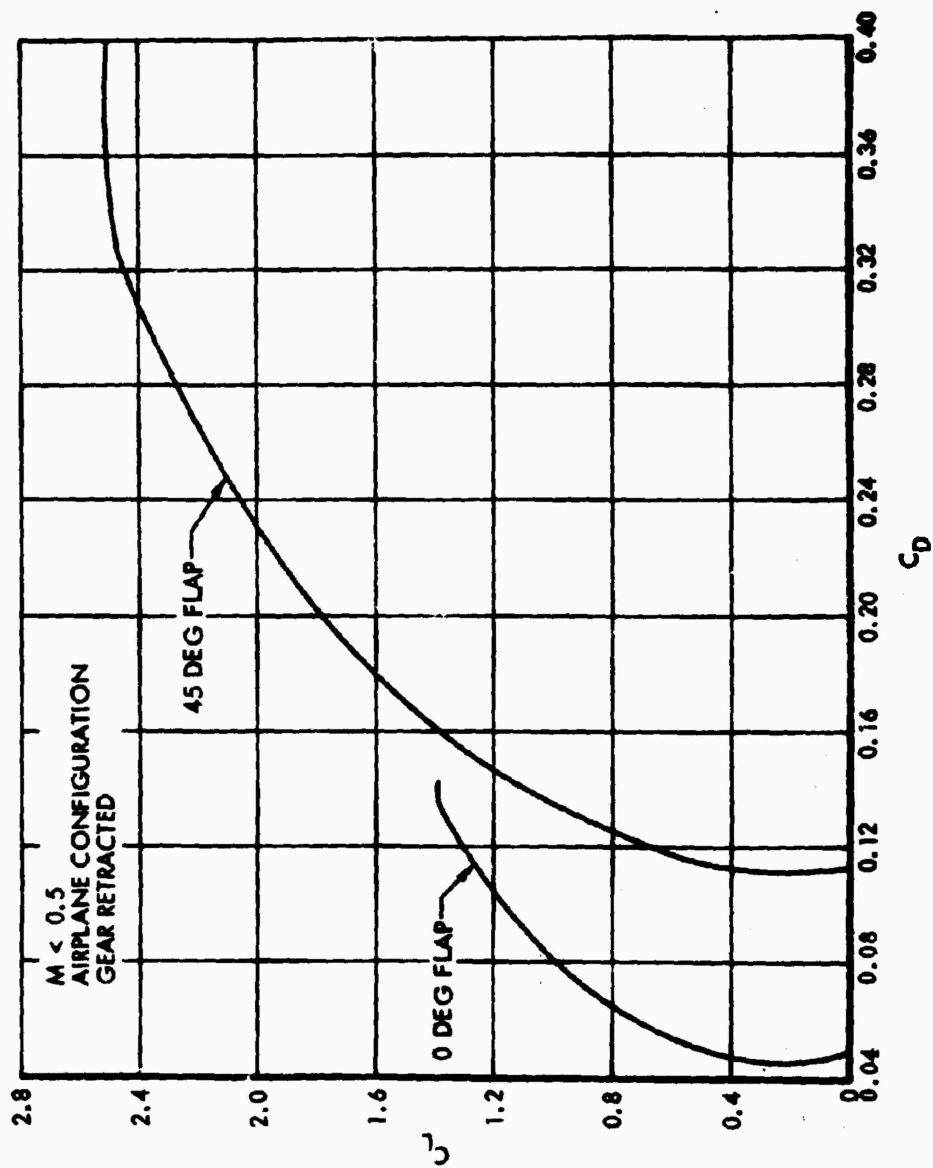


Figure 25. Total Drag Coefficients .

Propeller Performance

The propeller performance has been computed using a digital computer program. Figure 26 shows the relationship between propeller thrust and power for speeds between hover and 400 knots at sea level. Comparable performance for an altitude of 10,000 feet is shown in Figure 27.

Power Required

Computation of power required in the helicopter mode has been made using a digital computer program for compound helicopter performance and trim. This program computes the required main rotor and tail rotor power and the propeller thrust for a given set of flight conditions. To obtain the total engine power, the propeller power from plots such as Figure 26 and the transmission and accessory losses from Table III are added to the main rotor and tail rotor powers computed by the program.

In the airplane mode, the propeller thrust required is equal to the drag. The drag coefficients in Figure 25 have been used to calculate the propeller thrust required for level flight at several gross weights. The propeller power corresponding to the required thrust has been obtained from plots such as Figure 26, and the losses from Table III have been added to give the total engine shaft power as a function of forward speed and gross weight. Figure 28 shows the total engine power for both the helicopter and airplane modes with flaps up, and Figure 29 shows the total engine power for flaps down.

At speeds below the transition speed, the wing and rotor share the lift as shown in Figure 30.

Maximum Lift-to-Drag Ratio

The maximum lift-to-drag ratio at the design gross weight based on total power may be obtained from Figure 28 by reading the power and velocity for which the line from the origin is tangent to the power curve for 24,500 pounds. The lift to drag ratio is

$$\frac{L}{D} = \frac{(24,500)}{\frac{(550)(\text{H.P.})}{V}}$$

The line of tangent at 175 knots and 1270 horsepower. For this condition, the lift-to-drag ratio is 10.4.

Maximum Speed

The power available as a function of forward speed is superimposed on the power-required curves. The intersection of the two types of curves is at

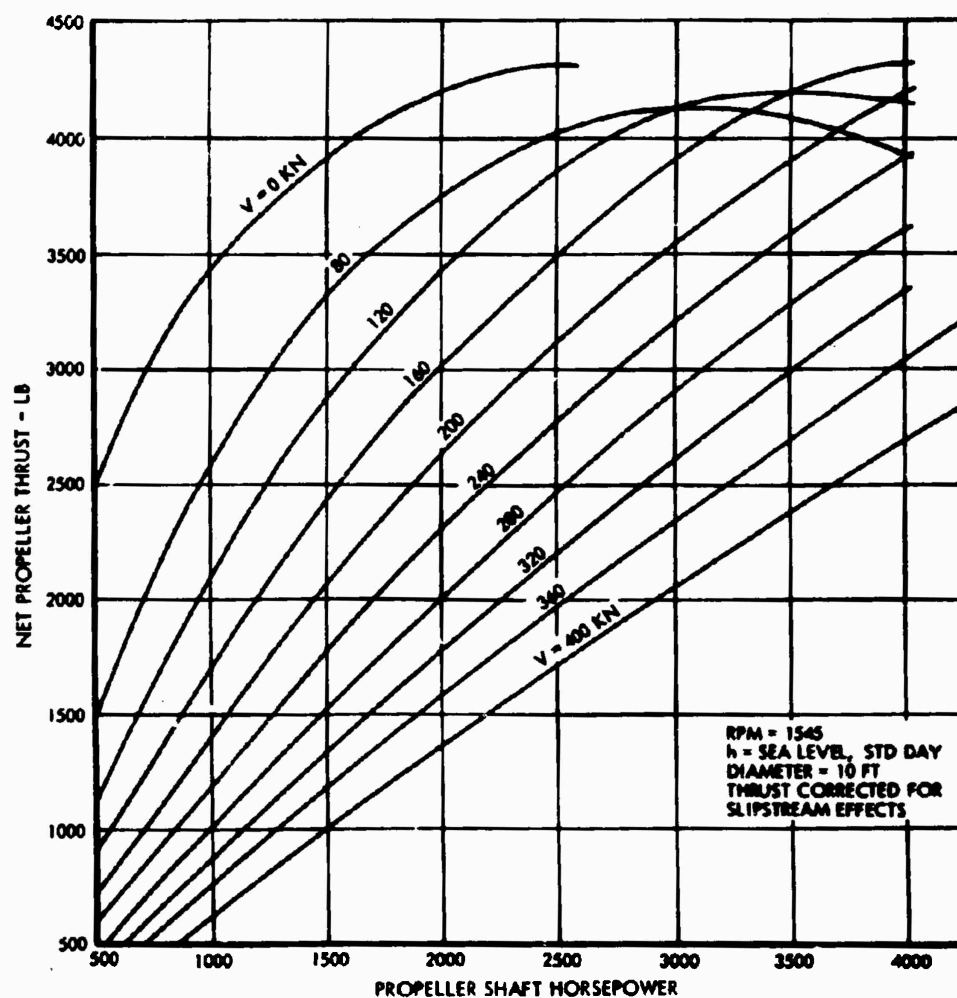


Figure 26. Propeller Power at Sea Level.

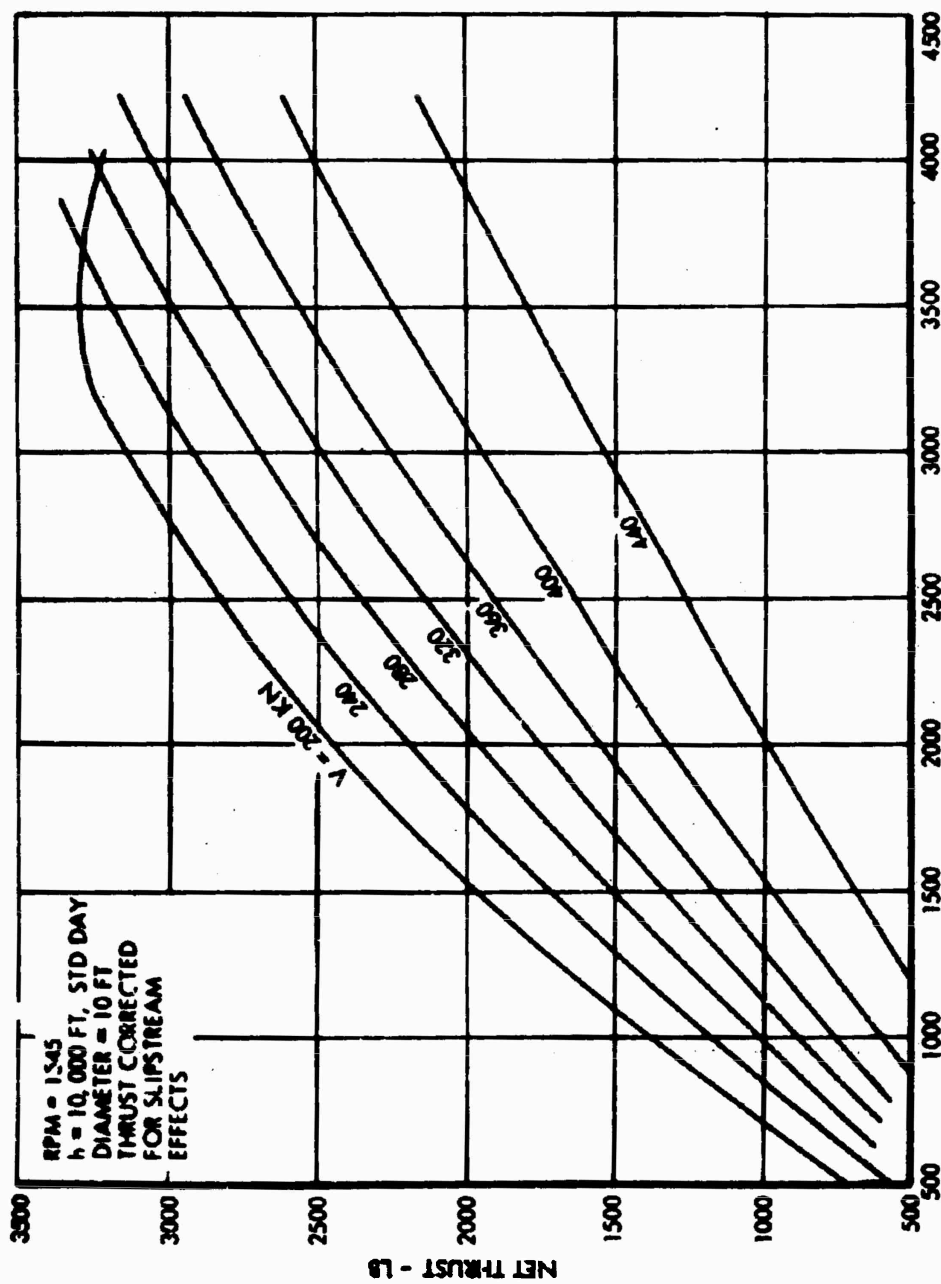


Figure 27. Propeller Power at 10,000 Feet.

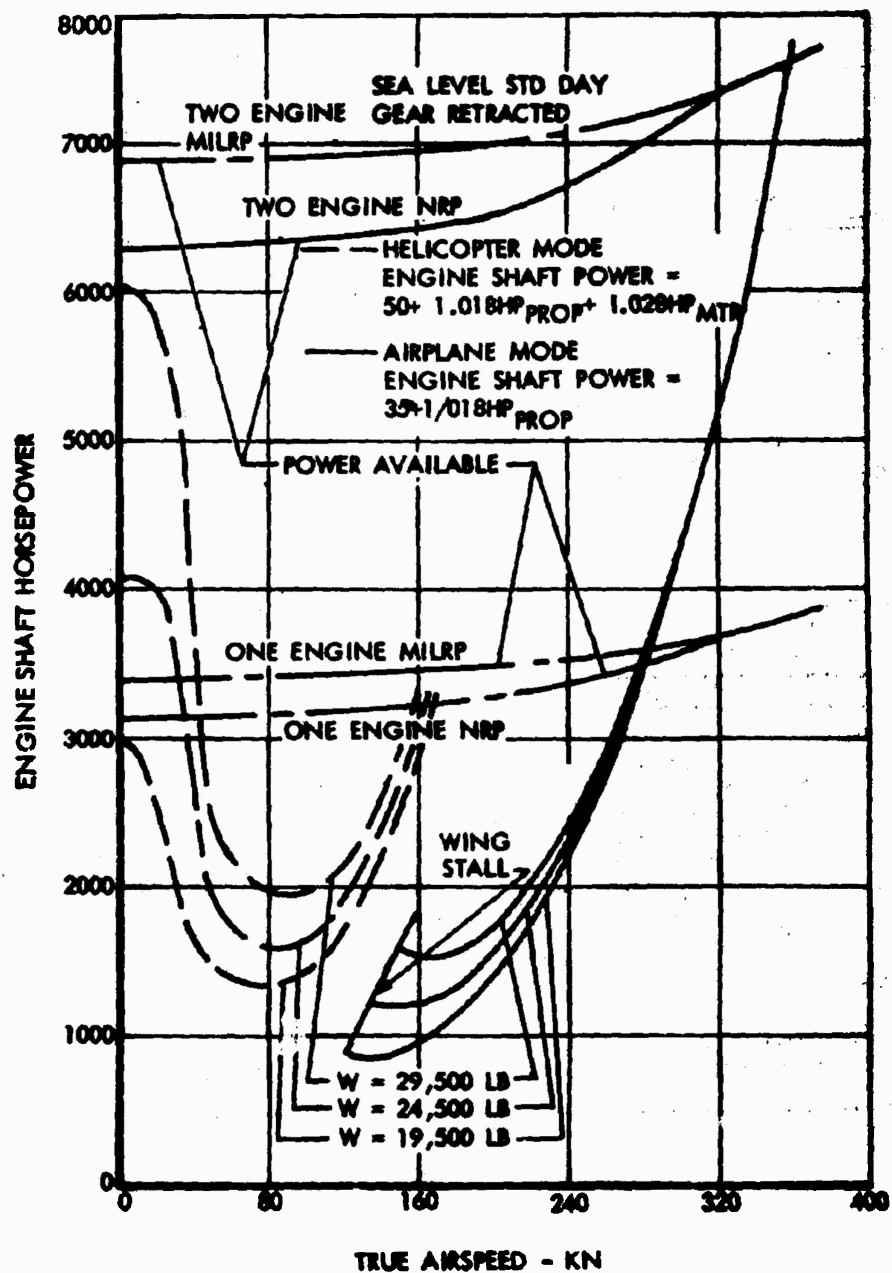


Figure 28. Power Required for Forward Flight, Flaps Up.

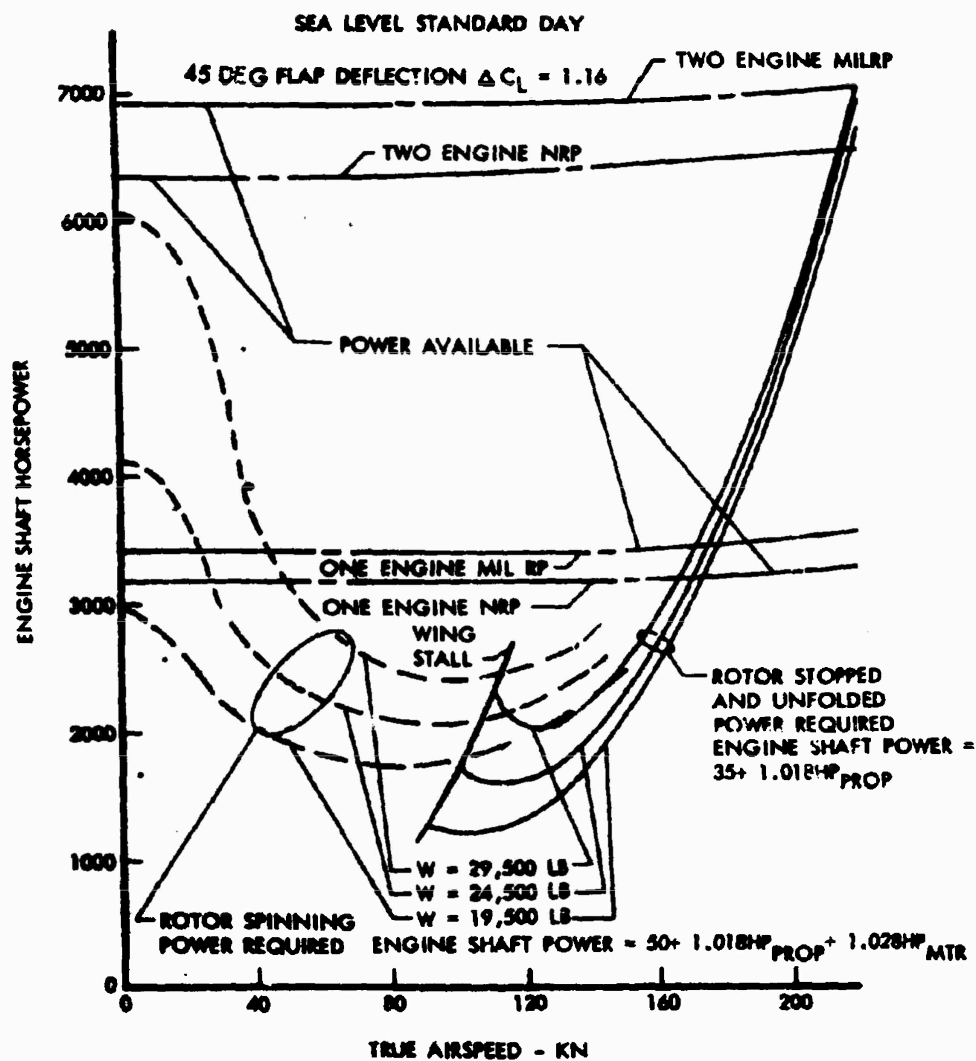


Figure 29. Power Required for Forward Flight, Flaps Down.

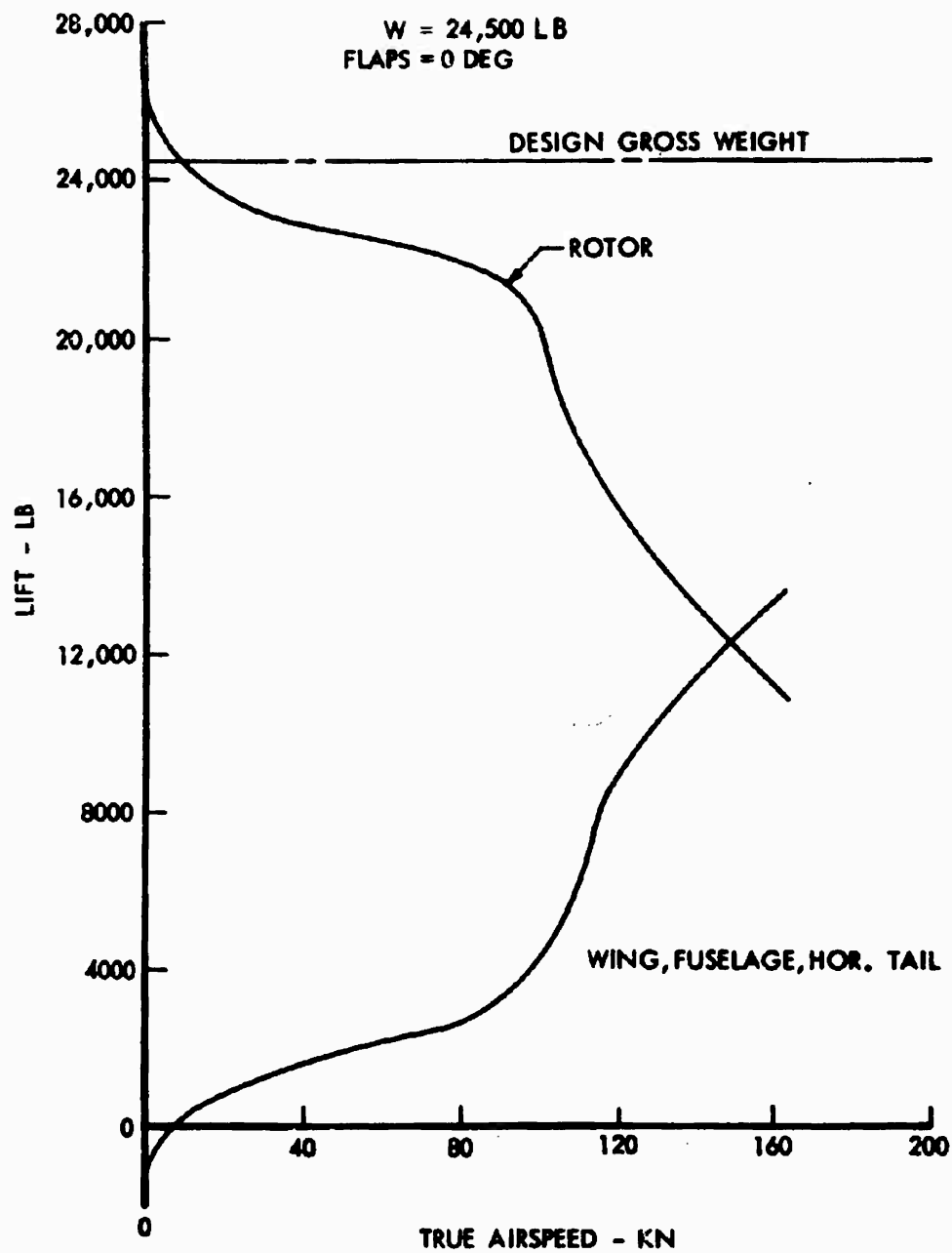


Figure 30. Lift Sharing Between Wing and Rotor .

the maximum speed. Figure 31 shows the maximum speed as a function of altitude. It may be seen that at sea level at the design gross weight of 24,500 pounds, the maximum speed is 358 knots.

Climb Performance

The maximum rate of climb has been computed in both the airplane and the helicopter modes. The maximum rates are plotted on Figure 32 as a function of gross weight for both modes. It may be seen that at the design gross weight of 24,500 pounds, the CL-945 can climb at 4330 fpm as an airplane.

Specific Range

The specific range in terms of nautical miles per pound of fuel as a function of forward speed and gross weight, for both one- and two-engine operation, is shown in Figure 33 for sea level, in Figure 34 for 10,000 feet, and in Figure 35 for 20,000 feet.

Specific Endurance

Specific endurance in terms of hours per pound of fuel as a function of forward speed and gross weight for both one- and two-engine operation is shown in Figure 36 for sea level.

Airport Performance

Landing Distance - As a helicopter, the CRA is capable of making vertical power-on landings at sea level at all gross weights up to 31,200 pounds, which is the hovering gross weight in ground effect as shown in Figure 19.

As an airplane, the CRA can make normal landings with the blades folded and stowed. The landing performance in the airplane mode is computed in accordance with the definitions of Military Specification MIL-C-5011A. The approach speeds and touchdown speeds correspond to $1.2 V_S$ and $1.1 V_S$, respectively. For research application, standard wheel brakes are provided as auxiliary test equipment, and the braking distance is determined with the use of a braking coefficient of 0.30 as defined by MIL-C-5011A.

The CRA is designed to land at weights up to 24,500 pounds, at which the total distance over 50 feet is 4800 feet with a touchdown speed of 112 knots. A plot of landing distance as a function of gross weight is shown in Figure 37.

Takeoff Distance - The CRA takes off in the airplane mode with a flap setting of 20 degrees with the engines operating at a thrust level corresponding to one-half that available at the full takeoff rating. The lift-off speed and the speed at the 50-foot height are chosen in accordance with the definitions of MIL-C-5011A as $1.1 V_S$ and $1.2 V_S$, respectively.

Under these conditions, for standard day operation at the design takeoff weight of 24,500 pounds, the lift-off speed is 126 knots and the distance to clear 50 feet is 6700 feet. The takeoff distance as a function of gross weight is presented in Figure 38.

MISSION ANALYSIS

Payload - Range

The specific range curves of Figures 34 through 36 have been used to compute the fuel required as a function of range at the optimum speed and altitude. From this calculation, the allowable payload was found as a function of range and plotted on Figure 39 for both one- and two-engine operation. It may be seen that for a takeoff gross weight of 24,500 pounds and two engines, the maximum range with no payload and auxiliary tanks is 1500 nautical miles; with full internal fuel and a 3000-pound payload, it is 600 nautical miles.

Ferry Range

The specific range curves of Figures 34 through 36 have been used to find the optimum altitude as a function of gross weight for maximum specific range. The results of this investigation are shown in Figure 40. The envelope of the curves on this figure is the optimum altitude as a function of gross weight. From the envelope, the range for several gross weights was computed and is plotted in Figure 41. At the ferry takeoff gross weight of 30,000 pounds, the CRA can take off with 10,910 pounds of fuel, and the ferry range with two engines is 2600 nautical miles with 10 percent reserves.

Payload - Endurance

The specific endurance curves of Figure 36 have been used to calculate fuel required as a function of endurance. These calculations were then used to plot the payload-endurance curve at sea level in Figure 42. It may be seen that the maximum endurance at the design gross weight of 24,500 pounds with one engine is 3.3 hours with full internal fuel; it is 6.8 hours with auxiliary fuel.

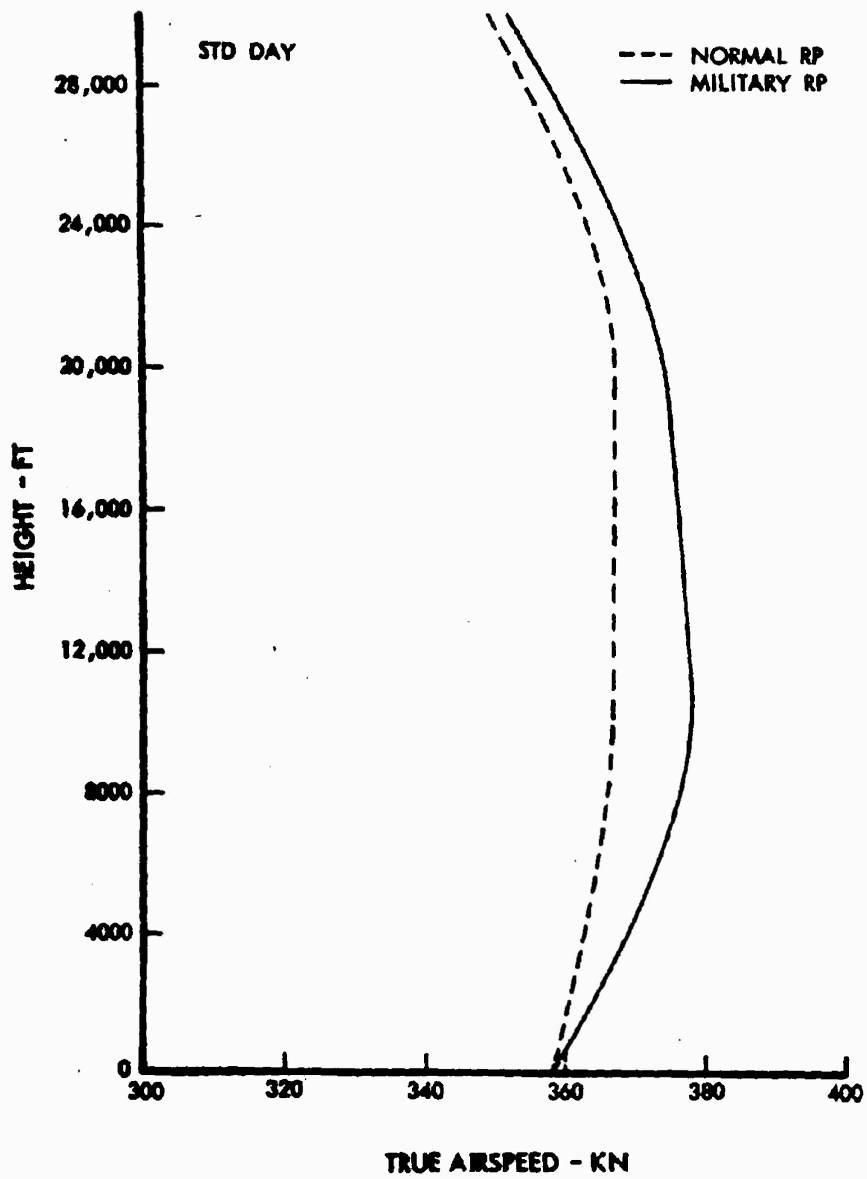


Figure 31. Maximum Speed as a Function of Altitude.

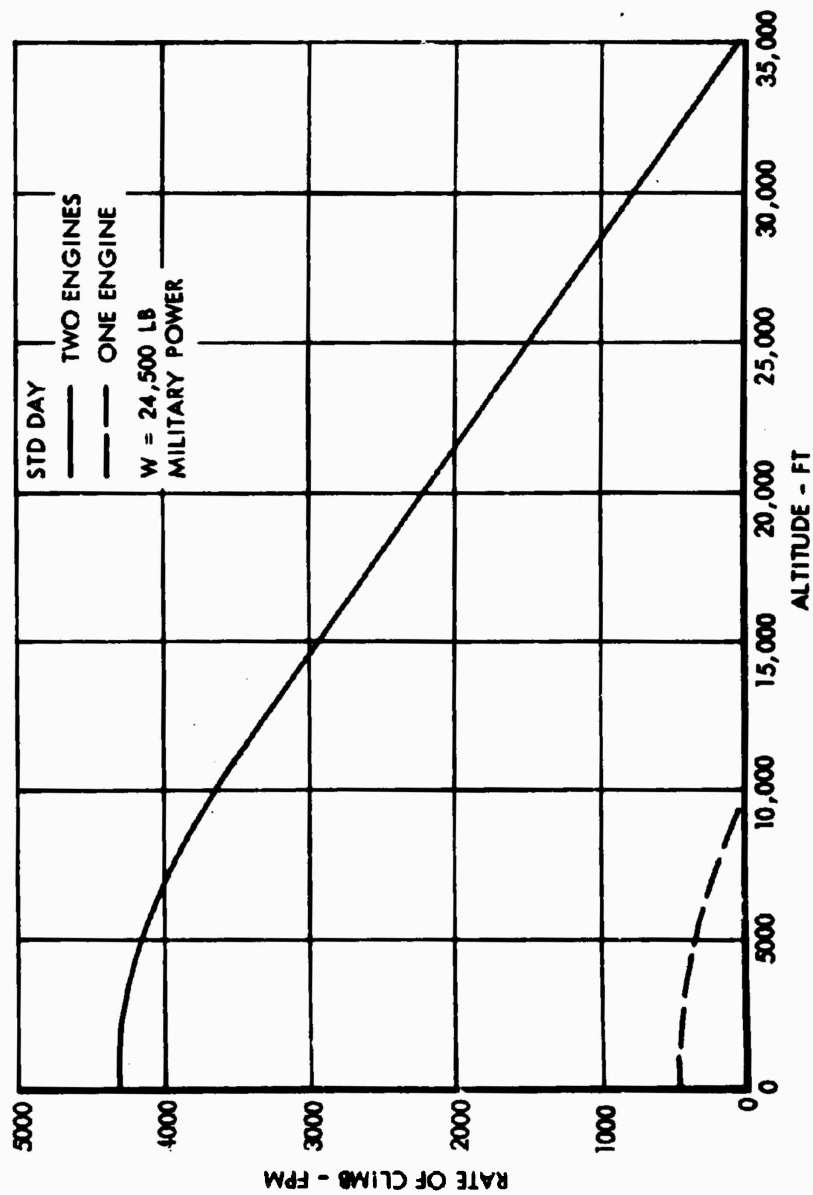


Figure 32. Maximum Rates of Climb.

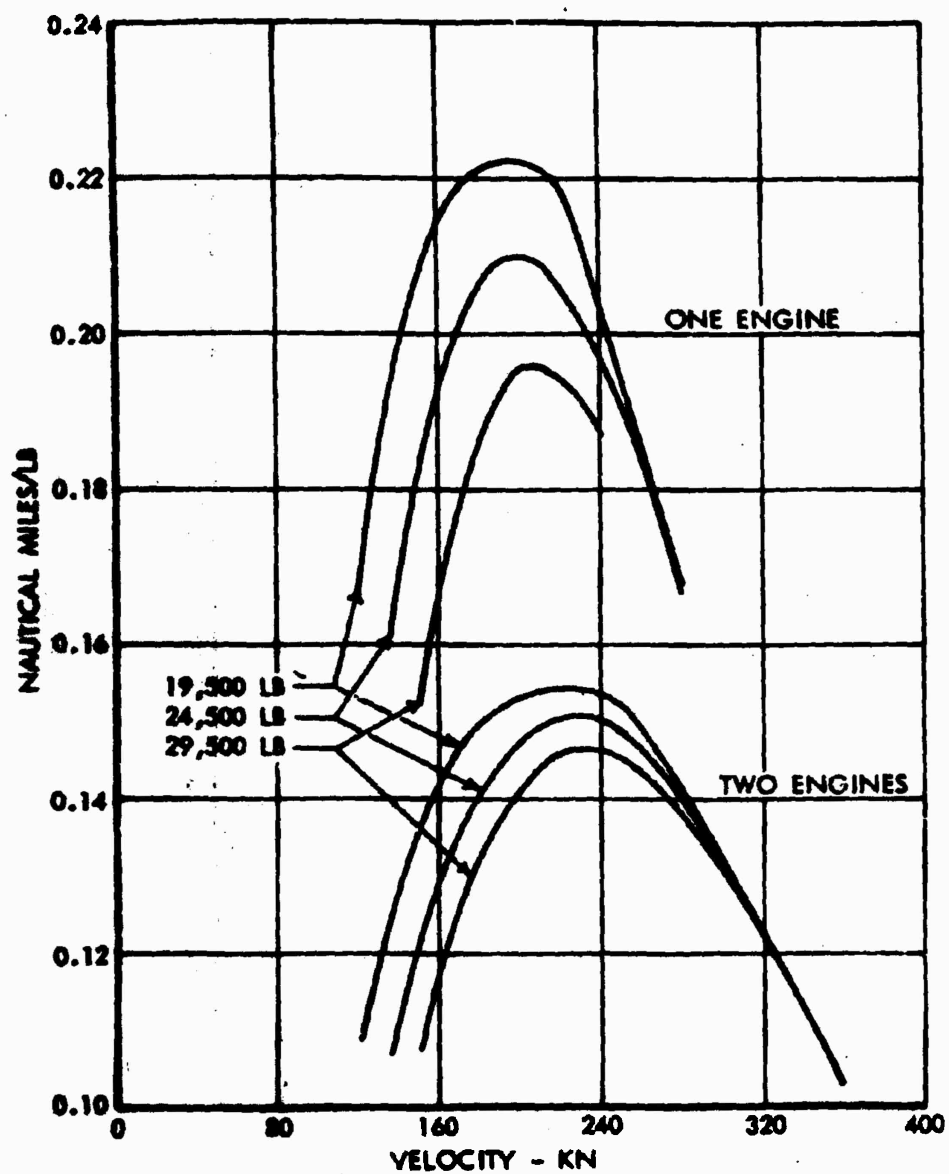


Figure 33. Specific Range at Sea Level.

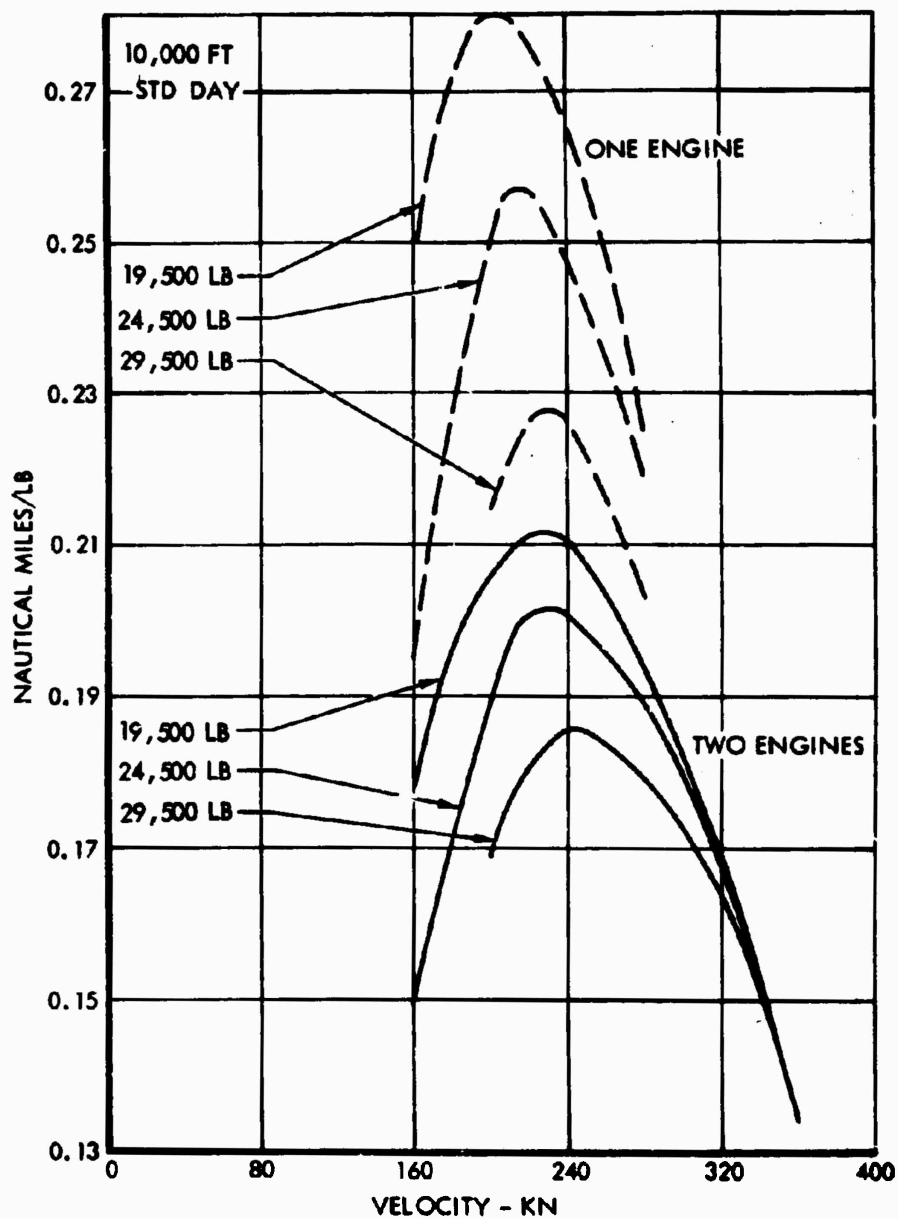


Figure 34. Specific Range at 10,000 Feet .

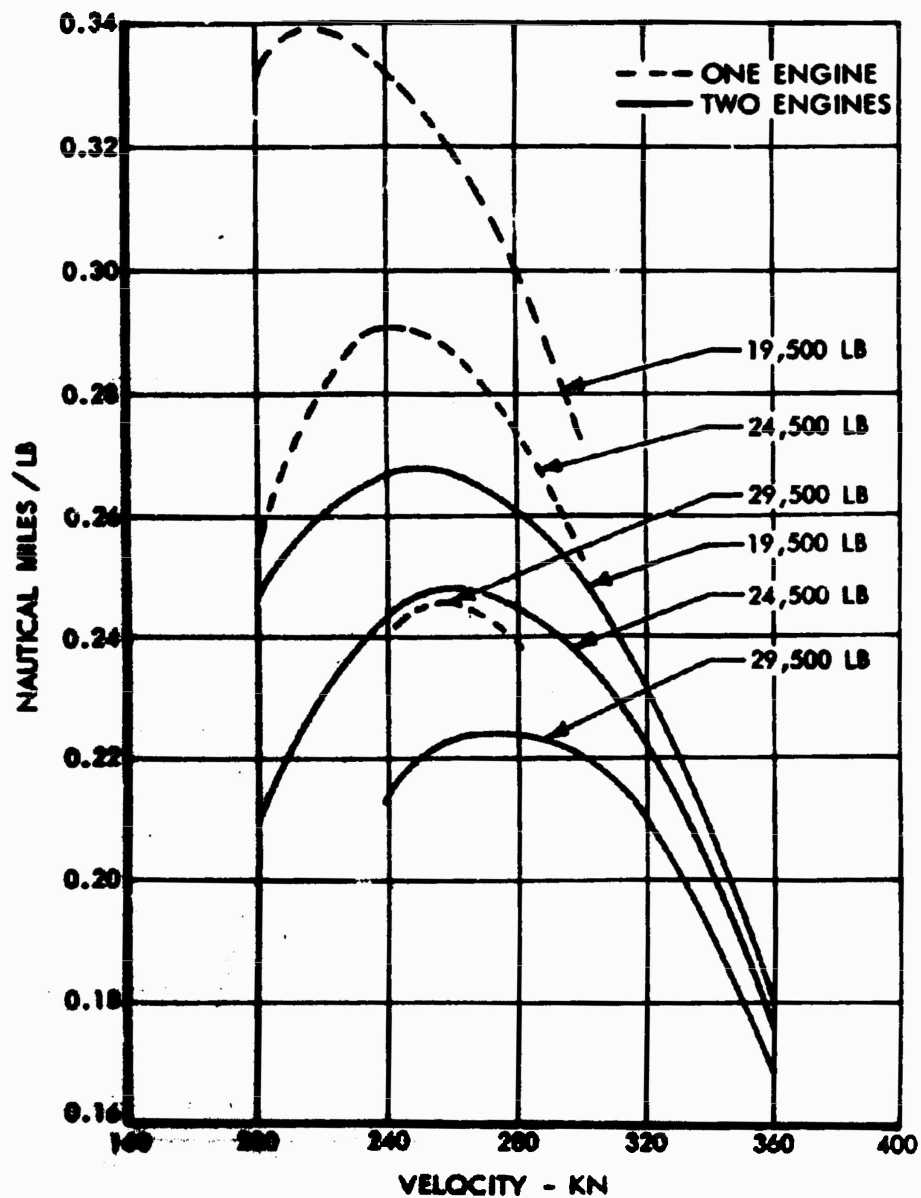


Figure 35. Specific Range at 20,000 Feet .

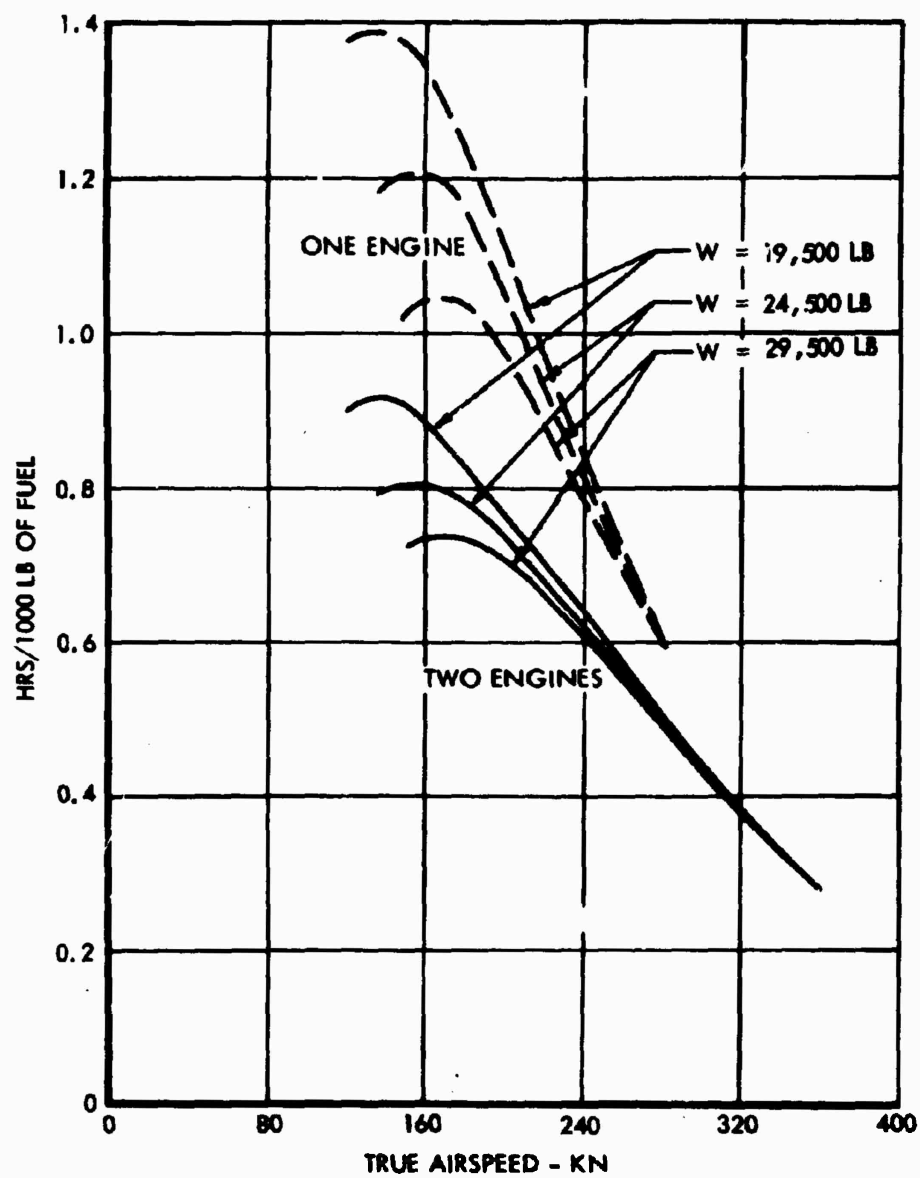


Figure 36. Specific Endurance at Sea Level .

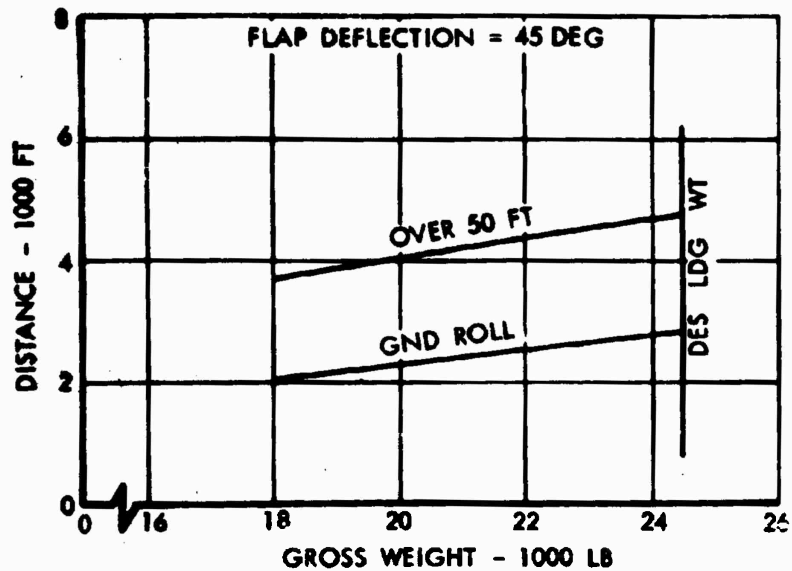


Figure 37. Landing Distance.

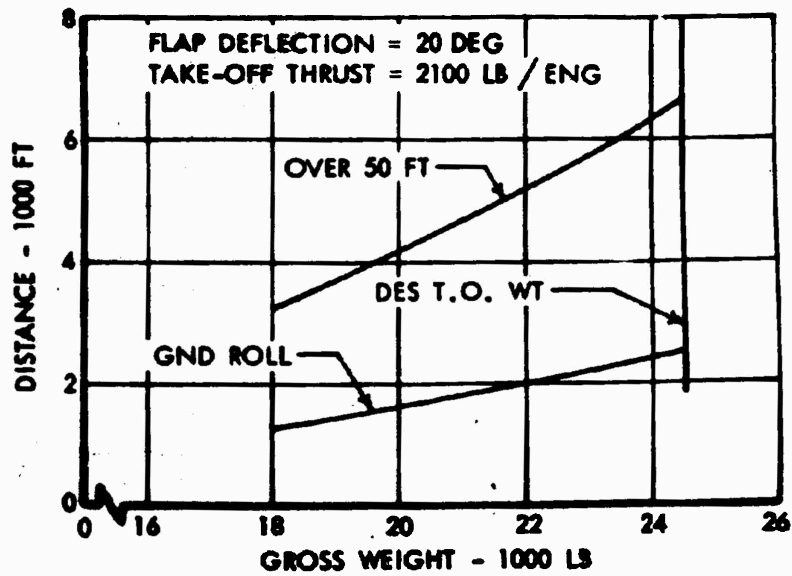


Figure 38. Takeoff Distance.

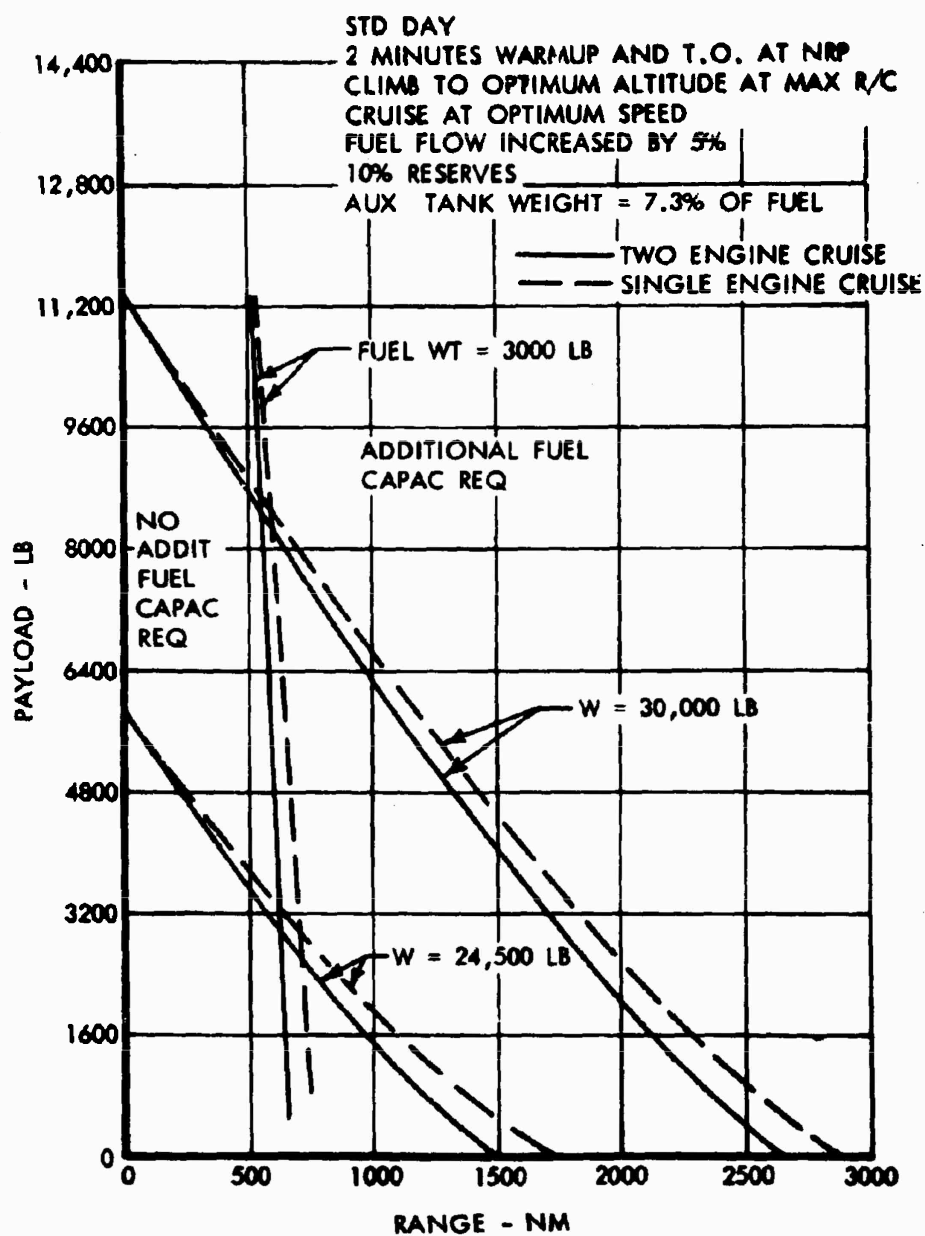


Figure 39. Payload - Range.

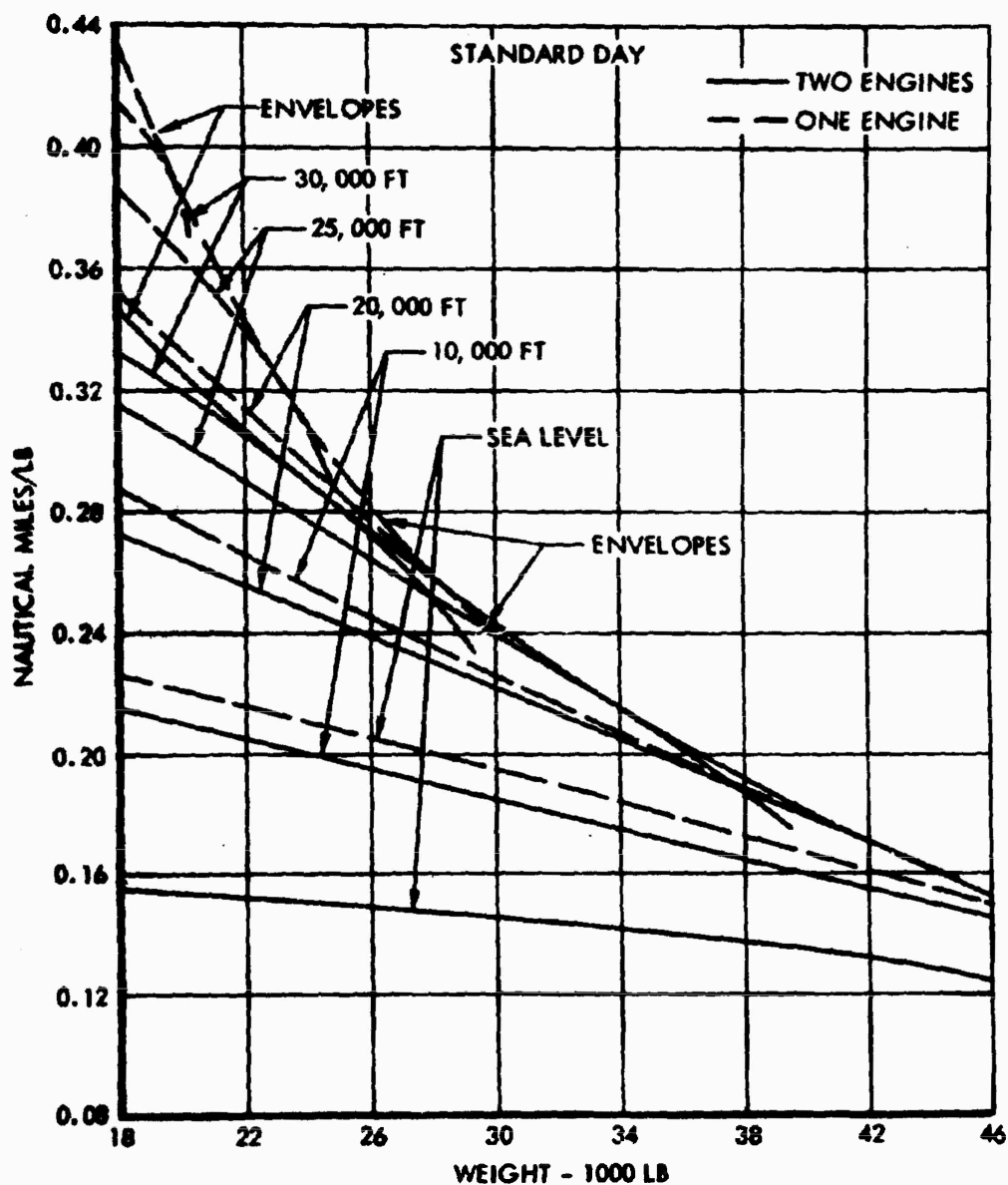


Figure 40. Altitude Effect on Specific Range.

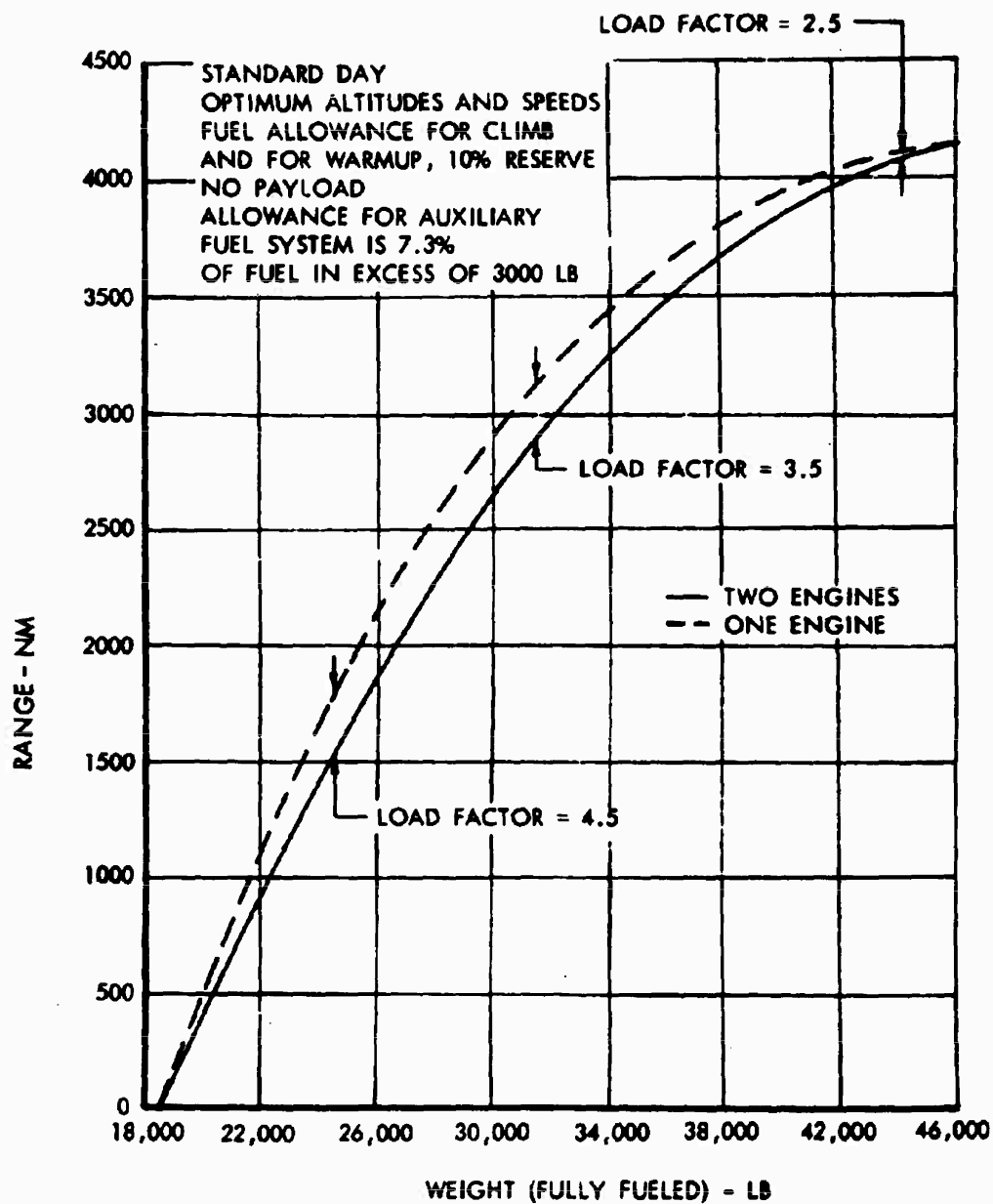


Figure 41. Range as a Function of Takeoff Weight.

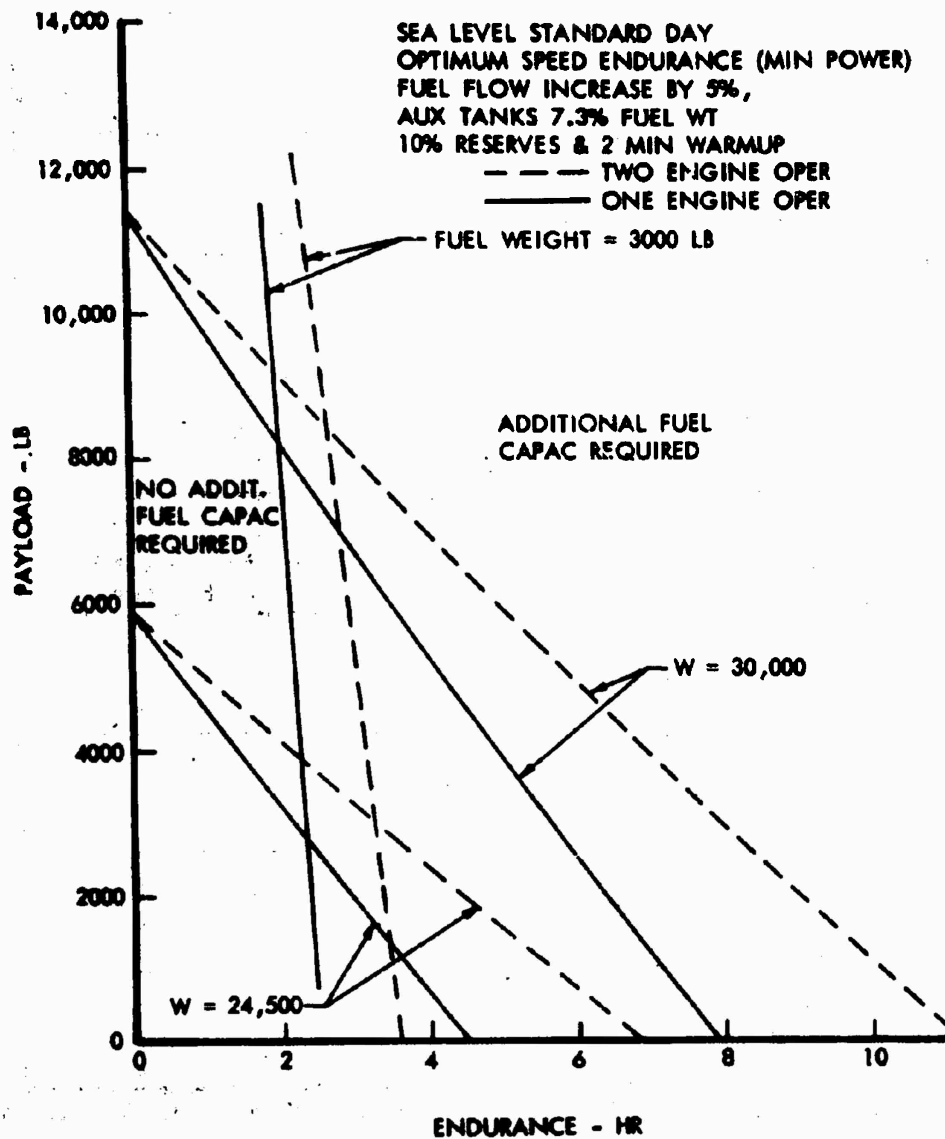


Figure 42. Payload - Endurance .

PART 3
PROPULSION

SECTION 5
POWER PLANT INSTALLATION

The power plant installation includes the engine air induction system, fuel system, mounting system, oil system, control system, fire protection system, starting system, compartment cooling, exhaust system, and cowling. Each system is discussed in subsequent paragraphs. An engine installation drawing is shown in Figure 43.

It was determined early in the studies of the Composite Research Aircraft that two engines would be used to provide multiengine safety. As a result, the aircraft can cruise in airplane mode at normal gross weight, with one engine shut down for cruise economy, and can hover in ground effect in helicopter mode, with one engine inoperative.

Consideration of the type of engine to be used led to the conclusion that a turboshaft engine would be most practicable for the research vehicle. Turbojet engines have been used in their primary mode for forward flight, and the exhaust gases have then been diverted to power tip-driven fans. Such a system could drive the main rotor through an external turbine, but no such propulsion system is presently available. Turboshaft engines offer a simple, proven, efficient means of diverting power to the various propulsive units.

A survey of shaft engines produced five existing or funded candidate engines which meet the performance and availability requirements of the aircraft. A trade-off analysis study was performed from which the T64-GE-16 engine was determined to be the optimum engine to meet the requirements of the CRA. The prime advantages of the T64 engine are the superior aircraft range and endurance which it affords, relative to the other four engines, and its planned existence in the Army inventory system for the Advanced Aerial Fire Support System (AH-56A) compound vehicle.

Location of the engines on the wings rather than in the fuselage was decided on the basis of a study which showed wing mounting to be superior. The results of this study are discussed in detail in a separate trade-off analysis study.

MAIN ENGINES

The research aircraft is powered by two T64-GE-16 free-turbine, turboshaft engines mounted under the wings. The maximum envelope dimensions of the engine are approximately 27 inches by 29 inches, and 58 inches in length between the inlet and exhaust flanges. Its dry weight is 696 pounds. It

has a sea level (SL) standard day military rating of 3,435 shaft horsepower (shp) at a specific fuel consumption of 0.480 pound per shaft horsepower per hour, and a 6,000-foot, 95°F maximum 10-minute rating of 2,650 shaft horsepower at 0.493 specific fuel consumption.

Table V shows uninstalled engine data for various operating conditions.

The output shaft to the gearbox, including torquemeter, is procured separately from the engine, since the T64-GE-16 engine does not include an output shaft. Mounting pads are provided on the front and mid-frames of the basic power unit.

AIR INDUCTION SYSTEM

The location of the cross-shafting and associated gearboxes precludes the use of a single top inlet. The engine airflow is taken aboard through twin ram inlets located on each side of the nacelle; the air then flows through a pair of short diffusers, and dumps into a plenum located ahead of the engine inlet. A boundary-layer diverter is located on the inside edge of the ram inlet, in order to prevent ingestion of the spinner-boundary layer.

TABLE V. T64 UNINSTALLED ENGINE DATA			
Condition	Altitude/ Temperature	Shaft hp	Specific Fuel Consumption lb/shp/hr
Military Ram Pwr, at 385 Knots	SL/59°F	3760	0.439
Mil. Pwr, Static	SL/59°F	3435	0.480
Norm. Pwr, Static	SL/59°F	3230	0.485
90% Normal, Static	SL/59°F	2905	0.493
75% Normal, Static	SL/59°F	2420	0.514
Max. Power, Static (10 minutes)	6000 ft/95°F	2650	0.493
Mil. Pwr, Static	6000 ft/95°F	2470	0.499

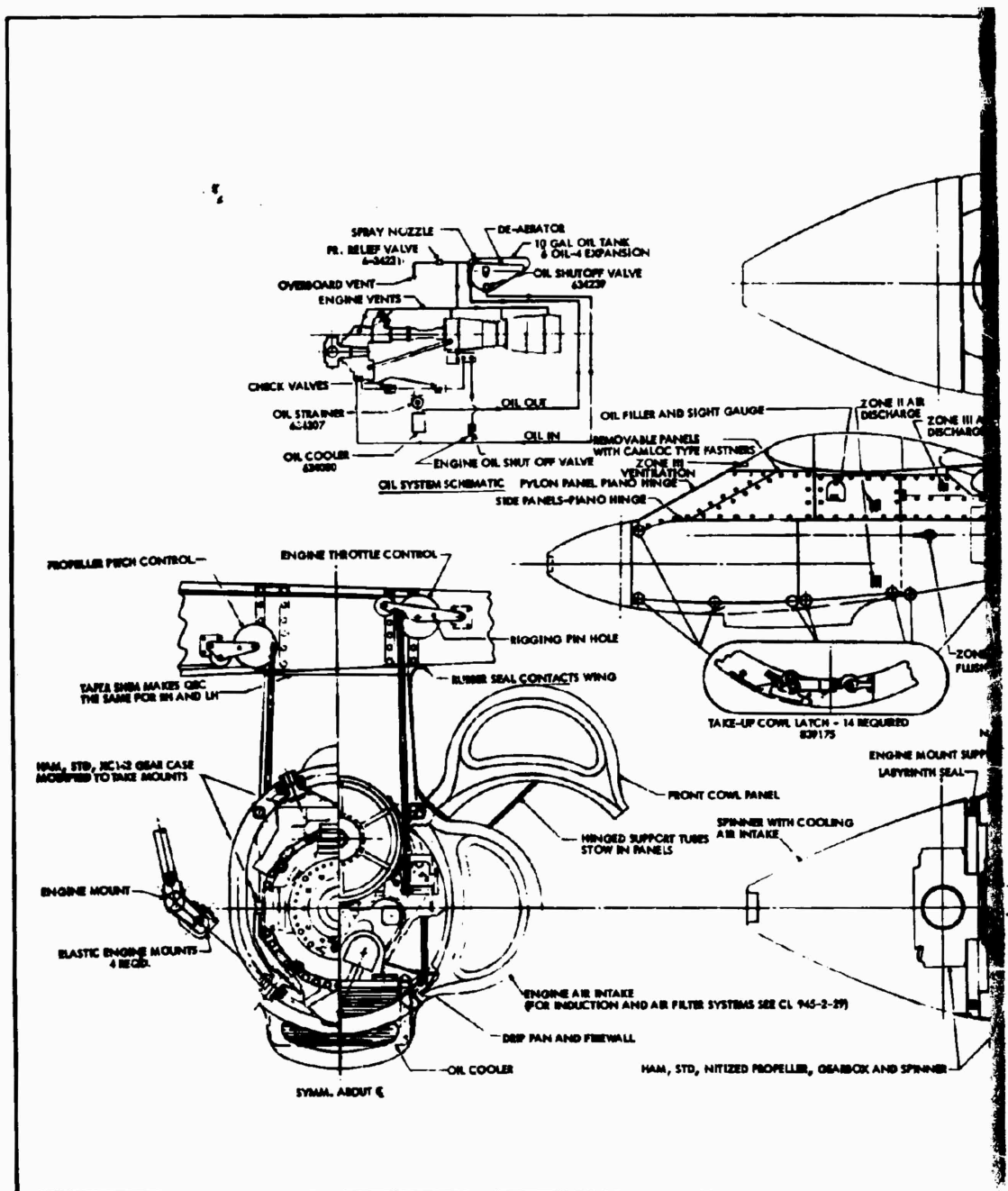
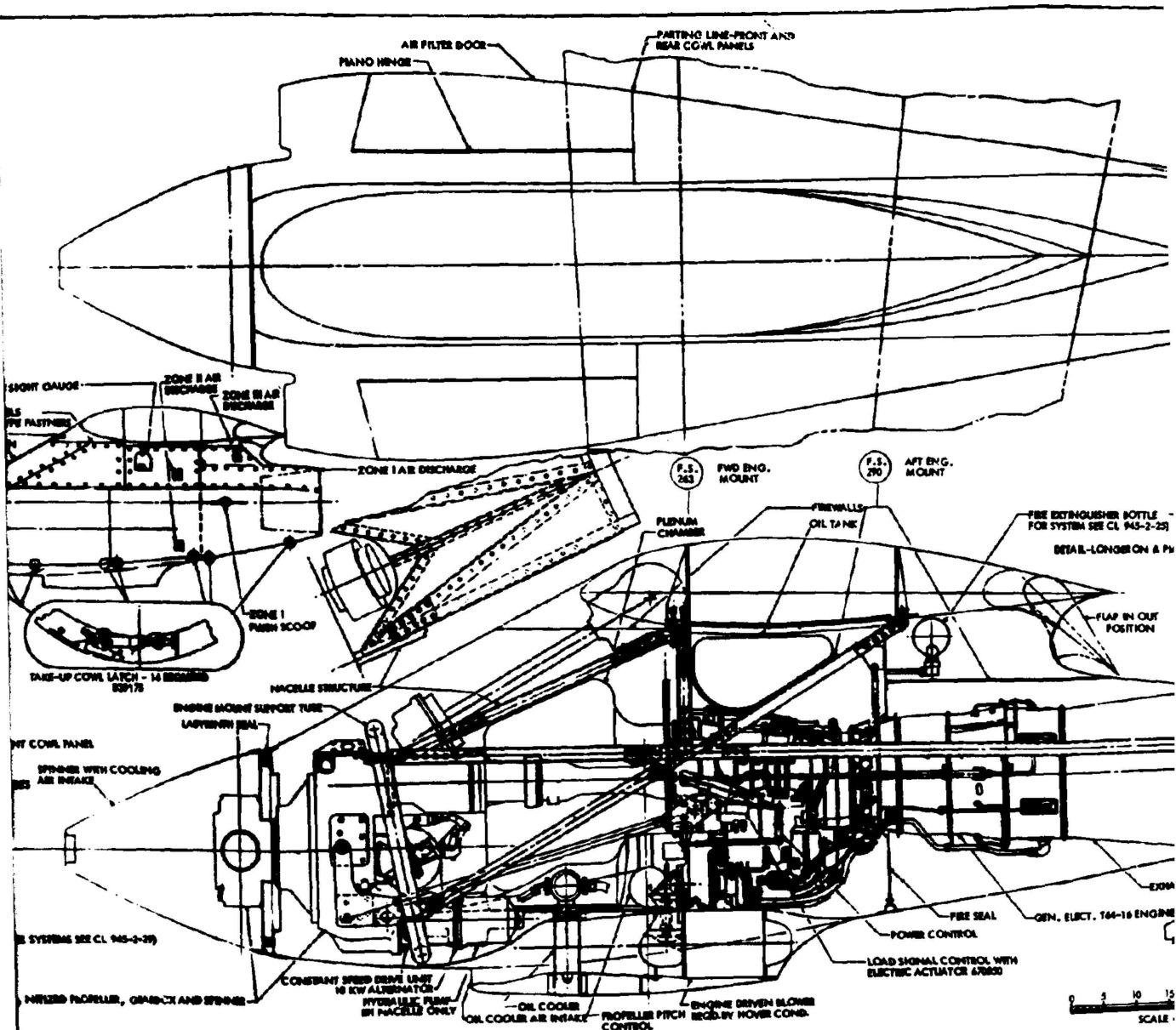


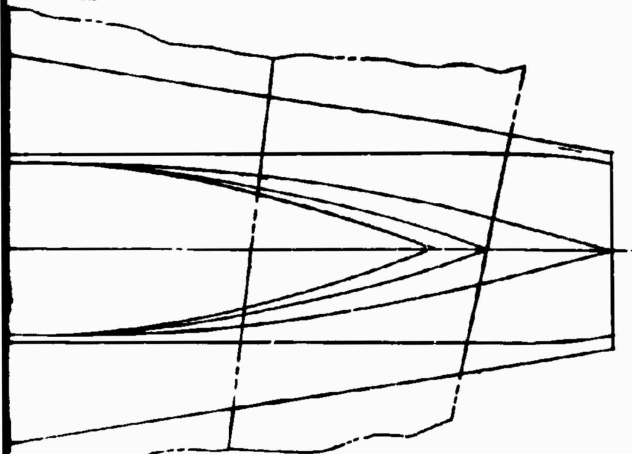
Figure 43. Powerplant Installation with Related Systems.



systems.

B

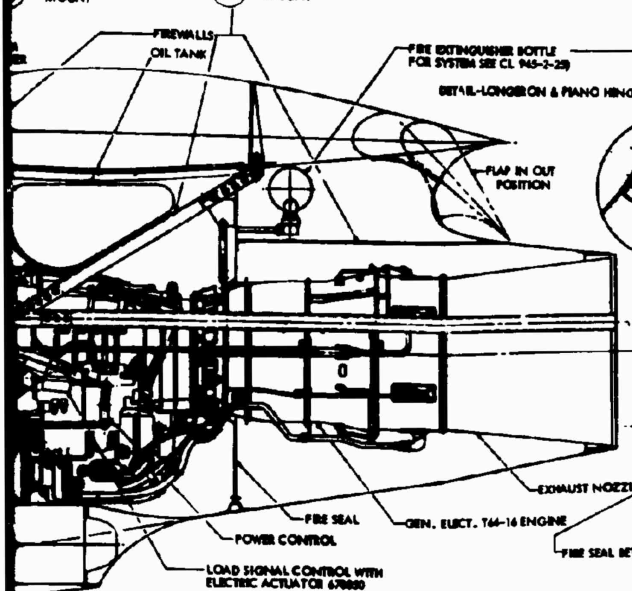
HING LINE-FRONT AND
COWL PANELS



FWD ENG.
MOUNT

F.S.
270

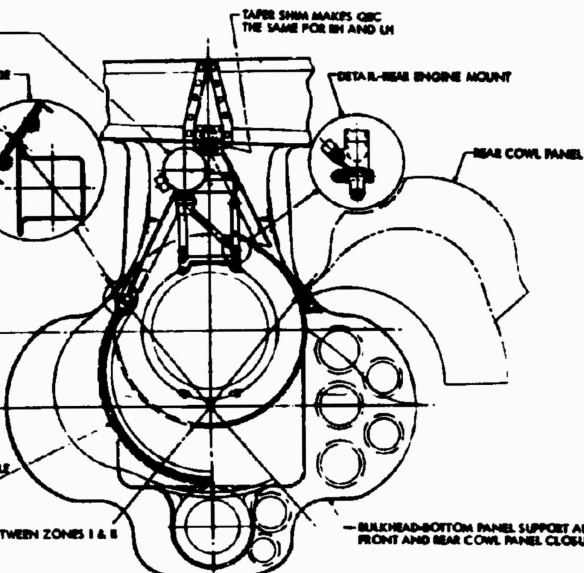
AFT ENG.
MOUNT



ENGINE DRIVEN BLOWER
BY NOVEL COND.

0 5 10 15 20 25 30
SCALE - INCHES

TAPER SHIM MAKES QRC
THE SAME FOR IN AND LH



SYMM. ABOUT C

Page Intentionally Left Blank

Inlet Design

The requirement that the aircraft be capable of sustained operation in the hover mode as well as in the high-speed cruise mode dictates an inlet which has good performance at both points. This is accomplished by providing a ram inlet with an elliptical inner lip, designated as an 18E configuration in Reference 9, which provides high recovery at the static and low-speed conditions. The cruise condition performance is maintained at a high level by designing the external contour of the duct lip and forward portion of the nacelle so that the engine airflow requirements are satisfied without (1) operating in the vicinity of the critical Mach number, at which point the flow may become sonic over the outside of the nacelle with an attendant drag penalty, or (2) operating in the vicinity of the critical (minimum) velocity ratio, below which the spinner flow separates and the inlet performance deteriorates. The configuration selected for this installation is designated as NACA 1-75-30, according to the data of Reference 10. This configuration has a critical Mach number of 0.685 and a critical velocity ratio of 0.44, which provides adequate margin at the cruise condition of $M_0 = 0.545$ at a velocity ratio of 0.474.

Propeller Spinner and Cuffs

The propeller spinner used on the CRA is a modified cone which prevents high, local surface velocities and attendant boundary-layer separation. Considerable test data are available showing the improvement in pressure recovery gained with this spinner in lieu of an NACA-1 series spinner. The design of this spinner contributes heavily to the insensitivity of the inlet lip loss with yaw angle for low velocity ratios.

The propeller blades are fitted with cuffs to improve the engine inlet and oil cooler total pressure recoveries at low speeds. Tests conducted on 0.37 scale-model propeller cuffs and flight tests conducted on full-scale cuffs indicate that an inlet total pressure rise of at least 1 percent can be expected at all speeds up to 350 knots. The exact amount of rise to be expected is dependent on the particular cuff, blade, and inlet design.

Inlet Protection

The two research vehicles will be operated from prepared surfaces and are not considered to require inlet protection against the ingestion of foreign objects for the basic research mission; hence, the simple induction system described previously under Air Induction System is used.

With the view that future use of the aircraft may entail operation in dusty or unprepared areas, the design provides for an alternative induction system arrangement, using filters in the auxiliary air flow path. In this system, filters and hydraulically operated doors in the ram duct and filter air flow paths provide for full filtration of all air when

hovering in ground effect, and for ram duct flow only in forward flight. For the 6,000-foot, 95°F hover out-of-ground-effect (OGE) condition, both flow paths would be opened for maximum induction system recovery. The weight increment incurred by the use of this system would be 80 pounds per aircraft.

FUEL SYSTEMS

Fuel Storage

Fuel, amounting to approximately 496 gallons, is stored in two integral tanks, one in each wing box beam, as shown in Figure 44. Should fuel leak into the pylon area, it is drained overboard. The nacelle structure over the hot section is made liquid and vapor-tight, to guard against the remote possibility of fuel penetration from the wing lower surface. Water drain valves are located at the low point of each tank, and drain passages are provided as required.

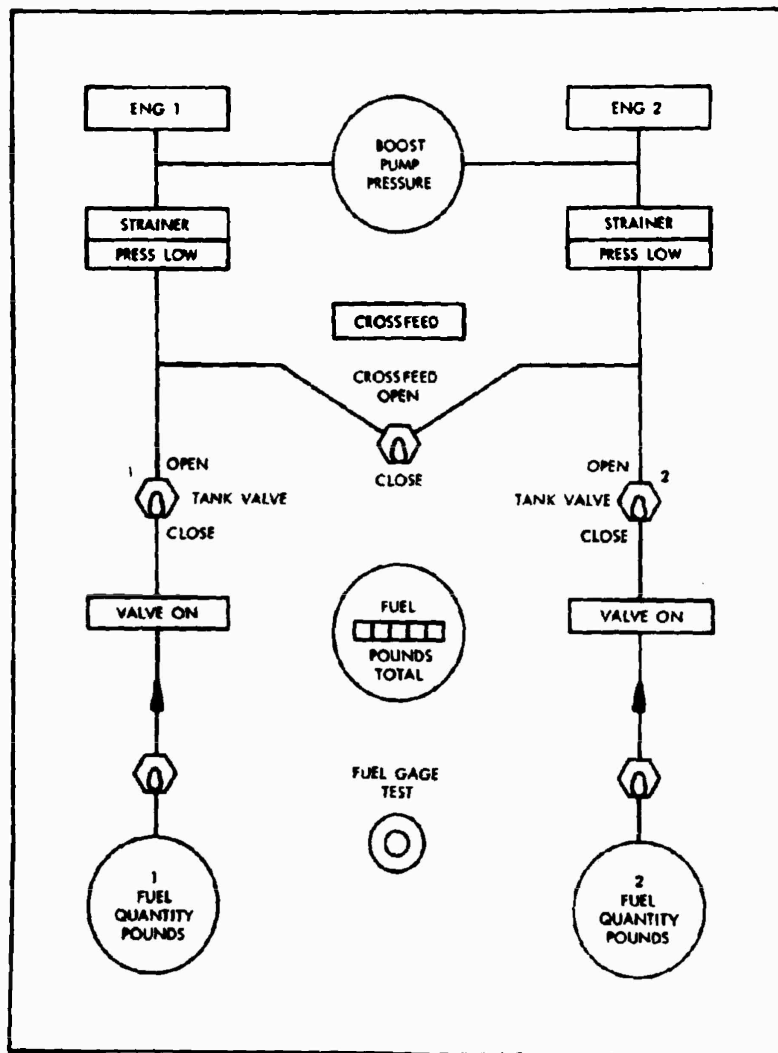
Engine Feed

During normal operation, each engine is supplied with fuel from its corresponding wing tank, as shown in Figure 44. Fuel is fed through the tank-mounted boost pump, located in the surge box at the tank inboard aft corner. In the event of boost pump malfunction, the fuel flows by gravity through a separate bypass. A dual check valve is installed near the outlet of each boost pump, so that fuel cannot be fed back into the tank through either the bypass or the fuel pump impeller.

In addition to the normal engine feed system, a crossfeed system is installed so that both engines can be fed from one tank. As shown in Figure 44, a system of valves is provided to permit shutting off either tank and routing fuel to the opposite engine. These are ac-motor-operated shutoff valves. However, the firewall emergency shutoff valve in each engine supply line is cable-operated from the flight station.

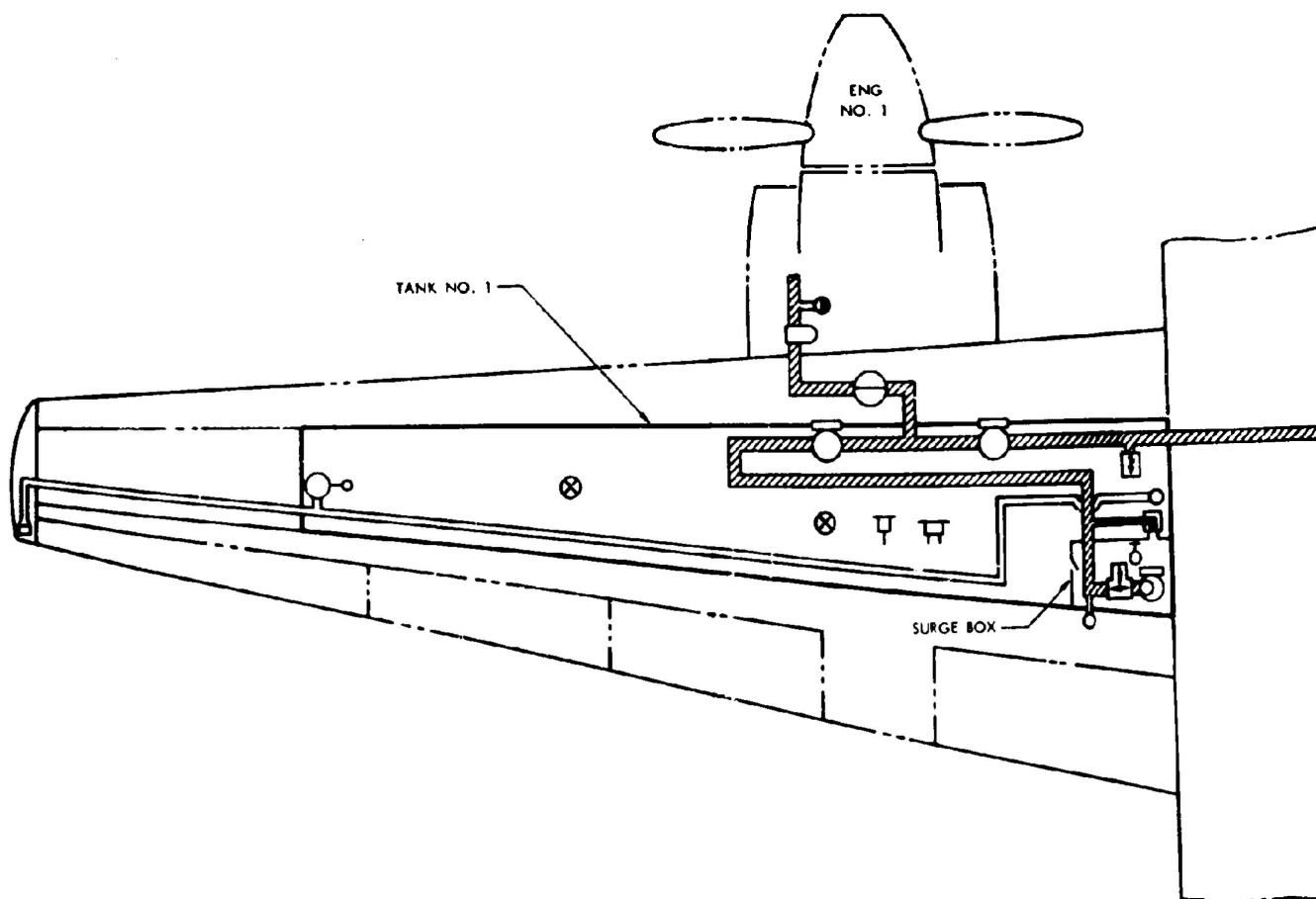
Signal lights are incorporated into the motor-operated valves to indicate satisfactory operation. The lights on the fuel management panel at the flight station (Figure 44) are on when the valves are in transit to either open or closed position; they are off when the selected position is reached. Gages are provided to permit observation of the fuel quantity in each tank, and to totalize the fuel quantity aboard the airplane. A Lucite rod sight-gage for visual determination of fuel quantity, designed to be withdrawn through the wing lower surface, is installed in each tank.

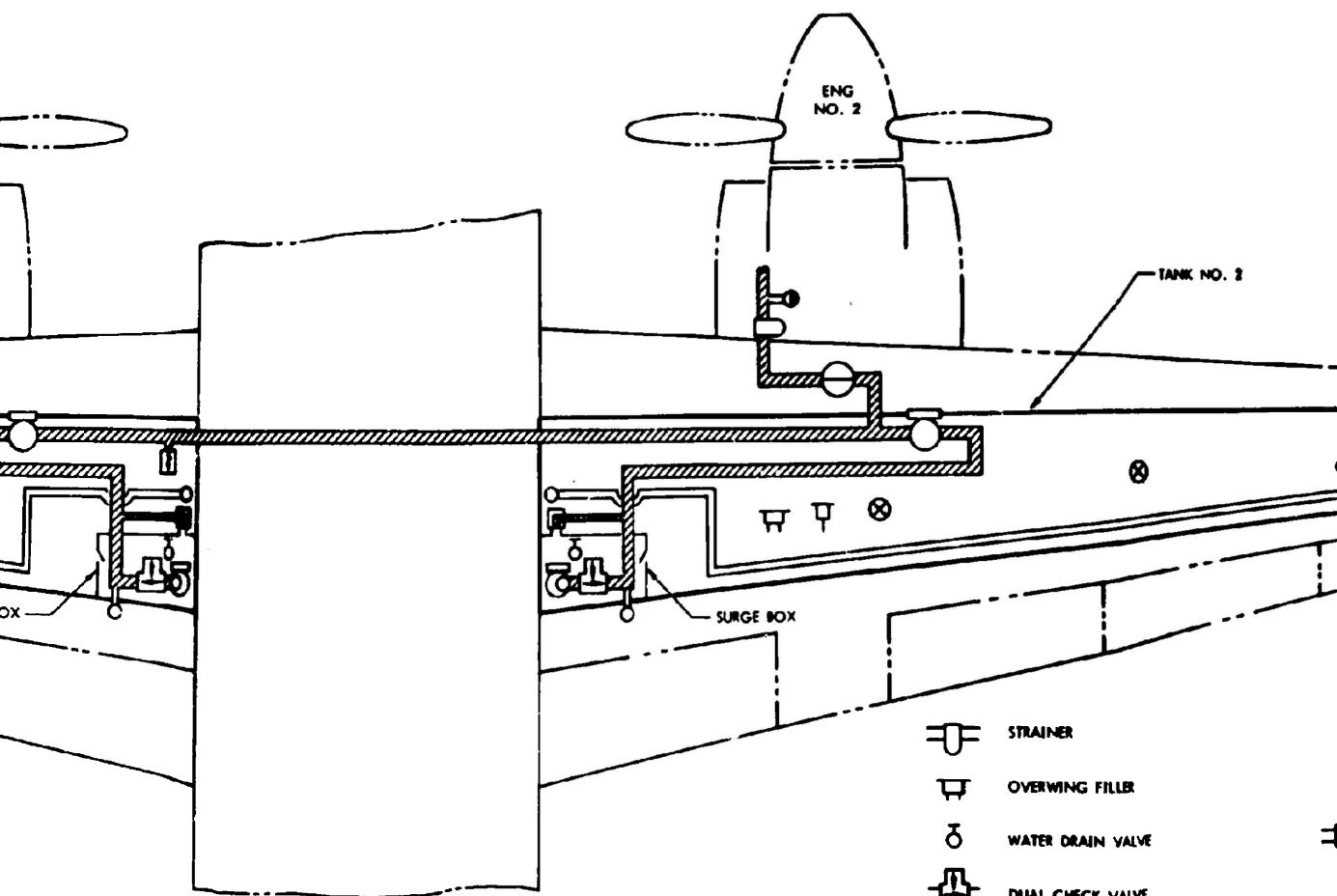
Thermal relief valves are incorporated into the motor-operated valves to permit thermal expansion of any trapped fuel. The main thermal relief valve is located in the cross-ship manifold, and it relieves into one of the feed tanks.








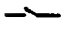




FUEL MANAGEMENT CONTROL PANEL

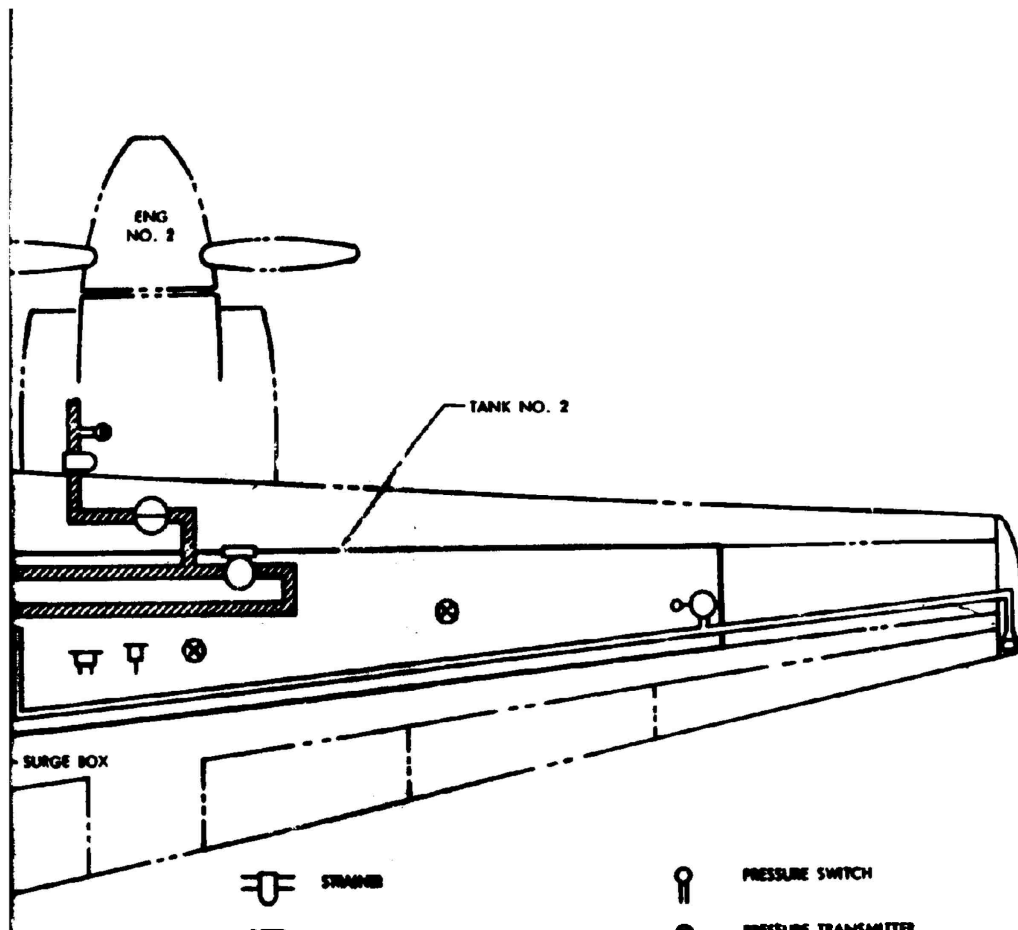
Figure 44. Fuel System Schematic.















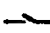








-  STRAINER
-  OVERWING FILLER
-  WATER DRAIN VALVE
-  DUAL CHECK VALVE
-  AC MOTOR-OPERATED SHUTOFF VALVE
-  MANUAL SHUTOFF VALVE
-  EJECTOR PUMP
-  FLAPPER CHECK VALVE
-  AC BOOST PUMP
-  FLOAT-OPERATED VENT VALVE

7



	STRAINER		PRESSURE SWITCH
	OVERRIDING FILLER		PRESSURE TRANSMITTER
	WATER DRAIN VALVE		THERMAL RELIEF VALVE
	DUAL CHECK VALVE		FLAME ARRESTOR AND VENT EXIT
	AC MOTOR-OPERATED SHUTOFF VALVE		FUEL QUANTITY TRANSMITTER
	MANUAL SHUTOFF VALVE		SIGHT GAGE
	EJECTOR PUMP		ENGINE FEED LINE
	FLAPPER CHECK VALVE		VENT LINE
	AC BOOST PUMP		EJECTOR PRIMARY LINE
	FLOAT-OPERATED VENT VALVE		

C

D

A pressure transmitter is located in each engine feed line so that the proper operation of each tank-mounted boost pump can be ascertained prior to takeoff. Fuel pressure switches, one in each pump discharge line, also operate indicator lights on the fuel management panel to warn of low line pressure with boost pump switches in the "on" position. Strainer lights are provided to indicate impending bypass of the 200-mesh fuel strainer that is installed ahead of each engine fuel pump inlet.

To assure maximum fuel availability in the feed tank, an ejector pump picks up fuel at the wing low point in the inboard end, for delivery to the surge box. The ejector pump uses available boost pump flow, which is tapped off from the main feed line as shown in Figure 44. With the pressure available, only a small quantity of ejector primary fuel is required to pump fuel to the surge box at the rate consumed by the engine.

The boost pumps are each sized to deliver the maximum cruise fuel flow to both engines. The feed line to each engine is sized to provide takeoff fuel flow at the required engine inlet pressure without boost pump assistance, from sea level to 6,000 feet. The cross-feed and direct-feed lines are also capable of supplying cruise fuel flow to the opposite engine at its required inlet pressure, without boost pump assistance, from sea level to 15,000 feet (maximum required operational altitude).

Refueling

Because of the small tank capacity, only gravity fueling is provided. Pressure fueling is considered unnecessary since, with the tank quantity involved, a major portion of the fueling time would be consumed in gaining access to the fueling adapter and in moving the hose and nozzle to and from the fueling location.

Gravity fillers are located in the upper wing surface, one per tank. The filler openings are covered with flush caps, each of which is secured by chain to the wing structure. Because the wing tanks are relatively shallow, deflectors are used to prevent fuel sprayback and spillage onto the wing surfaces at the maximum filling rates.

Defueling

Gravity defueling is not provided within the fuel tank. Defueling of each tank, however, can be accomplished by disconnecting the feed line at the engine inlet and attaching the line to a suitable hose for discharge to a storage tank. Fuel can be withdrawn from one engine feed line by opening the cross-feed valve as well as the tank valves and the emergency shutoff valve. Operation of the tank-mounted boost pumps is not required, unless a higher defueling rate than that available by gravity is required.

Venting

A vent line is routed from each tank upper inboard end to the vent exit at the wing tip on the lower surface aft of the rear beam. An additional vent tap, with float vent valve, is located at the outboard end of the tank. This keeps the vent opening in the tank air space for all airplane attitudes. The vent exit is a flush static opening. A flame arrestor is installed at the vent exit to prevent flashback from any ignition source.

ENGINE MOUNT SYSTEM

The engine and propeller gearbox assembly is supported by a truss attached to the front and rear wing spars. A mount ring which supports the gearbox is attached to the front of the truss at four points, and the engine has two rear truss attach points over the engine center of gravity. Redundancy is provided in the system, in that no single failure will result in loss of ability to withstand limit load. The engine and gearbox are interconnected to create one structural assembly by a torque tube and two struts.

LUBRICATION SYSTEMS

The propulsion lubrication system includes three separate oil systems: two engine and propeller gearbox oil systems, one in each nacelle, and the main transmission oil system. The main transmission oil system is discussed in detail in Section 6. The engine and propeller gearbox oil system for each nacelle is schematically shown in Figure 45. The design objectives of the engine lubrication system are established by the technical requirements of the engine-propeller lubrication system and are in general accordance with Section D 1-4 of the Handbook of Instruction for Aircraft Designers (HIAD).

The engine-propeller gearbox lubrication system consists of engine pressure and scavenge pumps, gearbox pressure and scavenge pumps, an oil strainer, an oil cooler, and an oil tank. Oil is drawn from the tank by the pressure pumps and is fed to the parallel engine and gearbox lubrication systems respectively. The propeller gearbox circuit supplies pressure oil to the power transfer gearbox, which transmits power to the cross-shaft in the wing leading edge. A drain line scavenges this gearbox, by gravity, to the propeller gearbox sump. The scavenge pump outflows from the engine and gearbox sumps are joined together at the strainer and then flow through the oil strainer and oil cooler to the tank. At the tank return, the oil is discharged onto a sloped shelf for deaeration. An engine-driven blower draws air from the atmosphere through the cooler and discharges overboard under the nacelle.

In the event of an engine shutdown, an engine oil shutoff valve is actuated which isolates the engine oil system from the gearbox lubrication.

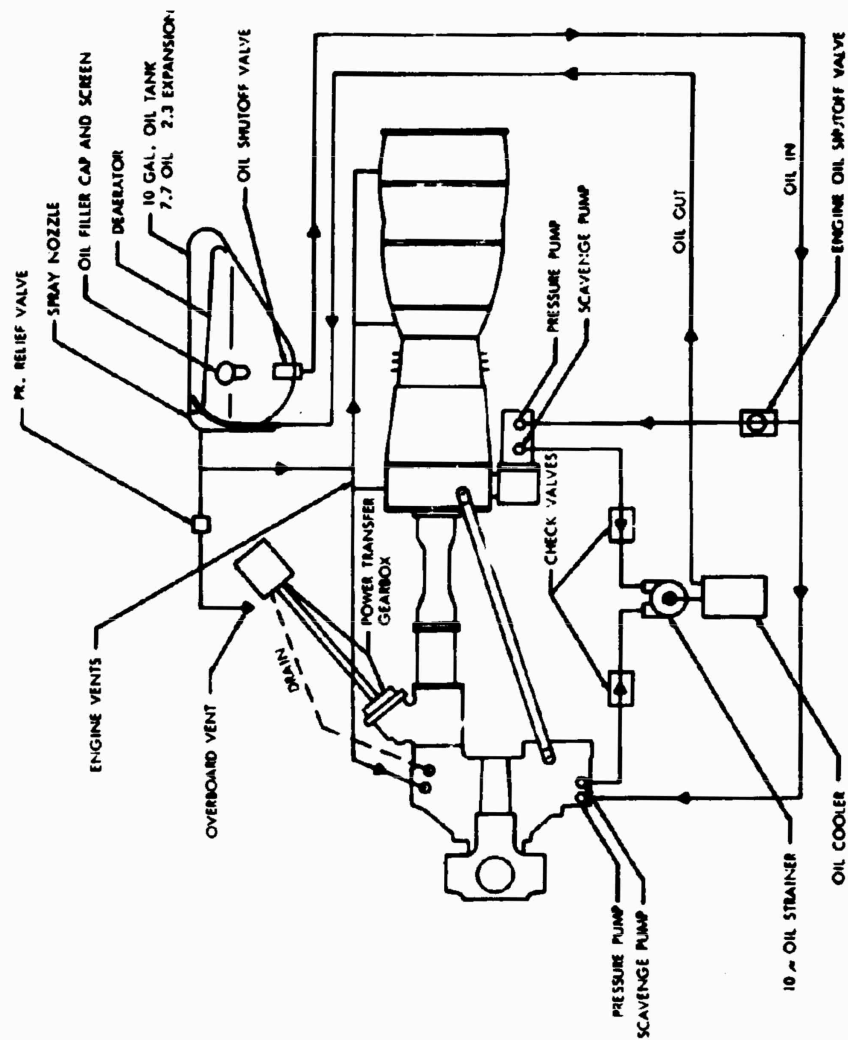


Figure 45. Engine and Propeller Gearbox Oil System Schematic .

system. A check valve is located upstream from the engine-gearbox scavenge oil junction to prevent gearbox scavenge oil from entering the engine lubrication system. A check valve is also located upstream from the scavenge oil junction in the gearbox scavenge line.

Oil Tank

The oil tank contains 7.7 gallons of MIL-L-7808E oil, with 30 percent expansion space for aeration, resulting in a total tank volume of 10.0 gallons. Assuming a flow rate of 24.55 gallons per minute (5.80 to the engine lubrication system and 18.75 to the propeller gearbox), the estimated total heat rejection of 3310 Btu per minute allows an approximate temperature rise of 35°F. The oil circulation rate is 3.18 cycles per minute, allowing a tank dwell time of approximately 19 seconds.

When the oil returns to the tank, it is sprayed upon a deaerating surface and flows into the tank sump. Air vapors from this surface plus the accumulated oil vapors are then vented back to the engine and gearbox or overboard, as shown in Figure 45. In the event that this overboard vent becomes clogged, a pressure relief valve actuates and relieves the tank pressure.

The oil tank is equipped with a transparent sight gage and an oil filler cap and screen. Both of these are located on the upper side of the engine pod.

System Components

The engine and propeller gearboxes are equipped with pressure and scavenge pumps. Each scavenge pump is equipped with a chip detector which indicates to the pilot the presence of metallic particles in the oil. The oil strainer is a 10-micron strainer.

All lines, fittings, and clamps are designed in accordance with HIAD, Section D 1-4. Lines which penetrate a fire zone are insulated and are capable of withstanding 2000°F for a period of 5 minutes. All lines can be completely drained and are sized for acceptable pressure drops. Drain valves are located at the low points in the oil tank, strainer, oil cooler, and each scavenge sump.

For instrumentation, each propeller gearbox has cockpit warning lights for chip detection, low oil pressure, and high oil temperature. In addition, dual reading gages for oil temperature and pressure are provided in the cockpit instrumentation for the engines and for the propeller gearboxes.

Oil Cooler

The oil-to-air heat exchanger is located in the scavenge system as shown in Figure 45. The cooler was sized to cool the oil to 200°F maximum. The cooling air is supplied by a modified off-the-shelf fan, driven from the engine accessory gearbox. The fan is designed to supply air at 2,740 cubic feet per minute at 100°F, with a total pressure rise of 8 inches of water. The air flows through the cooler air intake, the oil cooler, and the fan, and is ducted overboard. The cooling air inlet scoop, having an inlet area of approximately 60 square inches, is located on the lower surface of the nacelles. The inlet lip configuration is designed for the high-speed cruise condition, and the fan is sized to provide the pressure rise required to account for the inlet loss, the oil cooler pressure drop, and the exit loss at the hover condition. If an engine is shut down for cruise economy, the propeller and gearbox continue to be driven by the cross-shaft, and gearbox oil cooling is accomplished by ram air. Under these circumstances, the total heat rejection rate in the cooler is approximately 2,060 Btu per minute.

POWERPLANT CONTROL SYSTEM

Operating Characteristics

The dual nature of the Composite Research Aircraft requires that the engine control system provide positive engine control in helicopter mode and in airplane mode; further, the system must provide for a smooth transition from one mode to the other, without control discontinuity or uncontrolled power surges.

Pilot power and speed selection of the T64-GE-16 engine is made through a rotatable input shaft on the engine fuel control, which is termed the power control shaft. A schematic showing engine events related to power control shaft angle is presented in Figure 46. Engine shutoff is at the 0-degree position, starting is in the range of 0 to 30 degrees, and ground idle is at 33 degrees. The range from 33 to 75 degrees provides for gas generator condition control from minimum power to maximum power at power turbine speeds at or below a 100-percent power turbine speed of 13,600 rpm. The range from 75 to 120 degrees provides a power turbine governor speedsetting range, within which the power turbine will govern at constant speeds while the power output may vary. Since the power turbine governor has an inherent droop characteristic, a second governor shaft, concentric with the power control shaft, is provided for droop compensation. The second shaft, termed a load signal shaft, may be connected to the load control lever (collective lever, etc.) for automatic droop compensation, or it may be pilot-operated by a "beeper" switch. Thus, the engine control system provides for what has become rather conventional engine control for a turbine-powered helicopter. In addition, by deactivating the power turbine governor simultaneously with

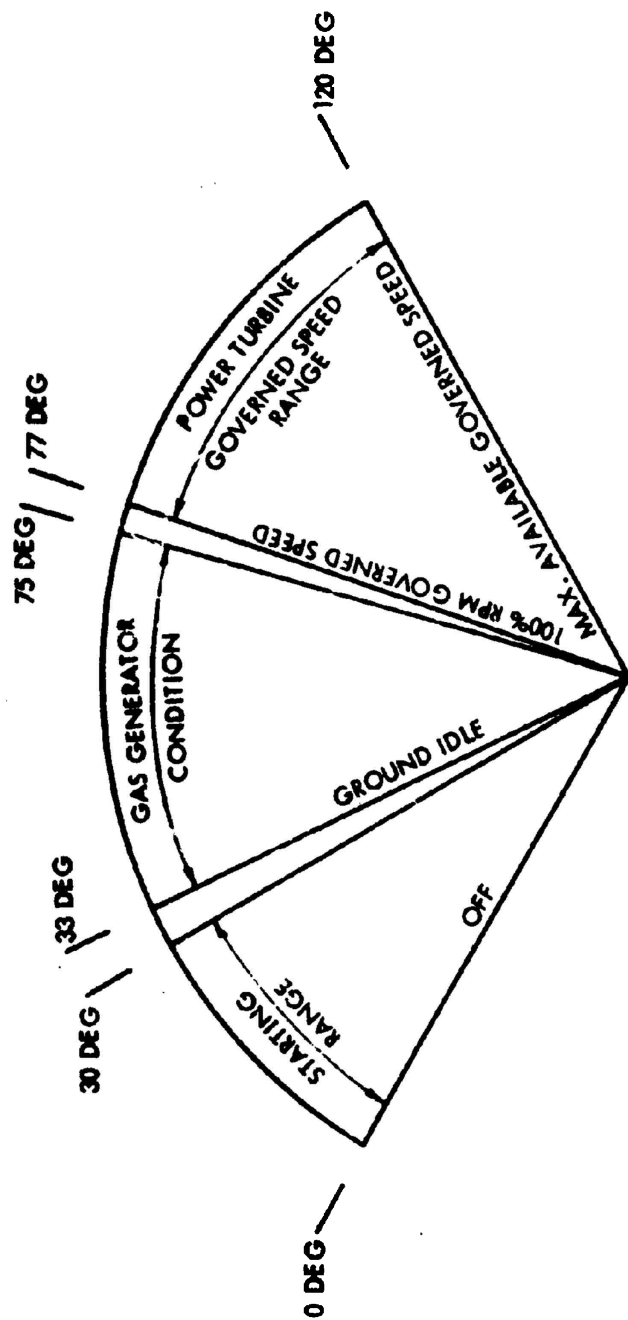


Figure 46. Engine Power and Speed Control Schematic.

the activation of a propeller governor, the governing method may be switched; the power control shaft range of 33 to 75 degrees then provides conventional engine control for a turbine-powered airplane having propeller speed control. Since the power turbine governor receives its speed sensing signal from an airframe-supplied speed signal shaft or cable, the governor may be deactivated by incorporation of a very small clutch in the speed signal cable. This is the system employed in the CRA engine control system.

Engine control devices at the crew station, shown in Figure 47, consist of a power lever for each engine, with a total range of movement corresponding to approximately 77 degrees of rotation of the governor power-control shaft; a propeller pitch-control lever for manual control of each propeller; and a propeller-governing wheel. Power control shaft rotation above the 77-degree point is not required in this installation, since only one constant turbine output speed is required. The propeller pitch control lever range of movement is from zero thrust setting, through a manual pitch-control range, to an extreme forward, detented feather position. The propeller-governing wheel provides an off position and a marked range for selection of governed propeller speed. When the propeller-governing wheel is advanced to any propeller-governing position, the small clutch in the speed signal cable to the engine governor is simultaneously disengaged, and the power turbine governor is deactivated. Propeller speed control is then automatically maintained by the single master propeller governor, and power is pilot-controlled with the power lever. Conversion from power turbine governing to propeller governing, and vice-versa, is accomplished smoothly and in a completely controlled manner by a simple technique.

Control During Starting and Normal Shutdown

For engine starting, the propeller pitch-control levers are at zero thrust and the propeller-governing wheel is in the off position. For normal engine shutdown, the power levers are simply moved to the stop position.

Helicopter Mode

During helicopter operation, the propeller pitch-control levers are in the zero thrust position and propeller governing is off. The power levers are advanced to the maximum forward position, corresponding to approximately 77 degrees of rotation of the engine fuel control input shafts. This simultaneously sets the power turbine speed governors to maintain 100-percent main rotor speed automatically; it also sets the gas producer governors for maximum power availability. The helicopter rotor speed is then maintained at 100 percent at all collective lever positions, with the exception of the effects of power turbine governor droop. Since the governors do have an approximate 10-percent speed droop between 0- and 100-percent power, two "beeper" switches are provided on the collective lever grip for pilot correction of engine speed as the power demand is changed.

Conversion

In the conversion from one flight mode to another, the method of governing engine output speed must also be converted. In converting from helicopter to airplane mode, propeller pitch is increased gradually, with the manually operated, propeller pitch control levers and the main rotor pitch gradually reduced with the collective lever, until the aircraft reaches a speed at which it is wing-supported and the main rotor pitch is zero. During this time, the power turbine governors continue to maintain 100-percent speed, with minor "beeper" switch corrections, and the propeller governor is in the off position. When the conversion speed is reached, the propeller pitch is held constant and the power lever settings are reduced until a slight drop in engine output speed is observed; then the power levers are advanced just enough to regain the speed loss. At this point, the power level of the gas generators exactly matches the power absorption of the propellers at the 100-percent speed of the power turbine. The propeller-governing wheel is then moved rapidly from the off position to the maximum, 100-percent setting. This places the propeller governor in operation and simultaneously declutches the speed signal feedback cables to the power turbine governors, thus deactivating the power turbine governors. No significant change of available power, engine speed, or power absorption has occurred during this operation. All airplane speed and power changes are now accomplished by manual control of the power levers, with the propeller governor automatically varying propeller pitch to maintain 100 percent power turbine speed. Lower governed engine speeds are available by moving the propeller governor setting toward the off position until the desired speed is reached. The main rotor may then be slowed, braked, folded, and stowed.

During airplane flight, both propellers are governed by a single master governor since, being interconnected, they must have synchronized governing for purposes of load sharing. Conversion from airplane to helicopter control is begun by adjusting the power lever settings until the conversion speed is reached, and the propeller pitch control levers are placed in approximately the correct positions corresponding to the actual propeller pitch at this point. An operational aircraft would be equipped with propeller pitch control indicators so that the manual pitch control levers could be precisely set prior to the governing conversion. For the research aircraft, it is considered safe to set the manual pitch control approximately. The main rotor is then unstowed and unfolded, and the propeller-governor wheel is then rapidly turned to the off position. This deactivates the propeller governor, simultaneously activating the power turbine governors, and the power levers are advanced to their maximum positions. At this time, due to the previous approximate setting of the propeller pitch control levers, corrective pitch adjustments may be necessary. This is considered satisfactory, since only aircraft speed is affected. The main rotor is then started, and during this period further propeller pitch control adjustment is required to offset rotor drag. When the rotor is at 100-percent speed, rotor pitch is gradually

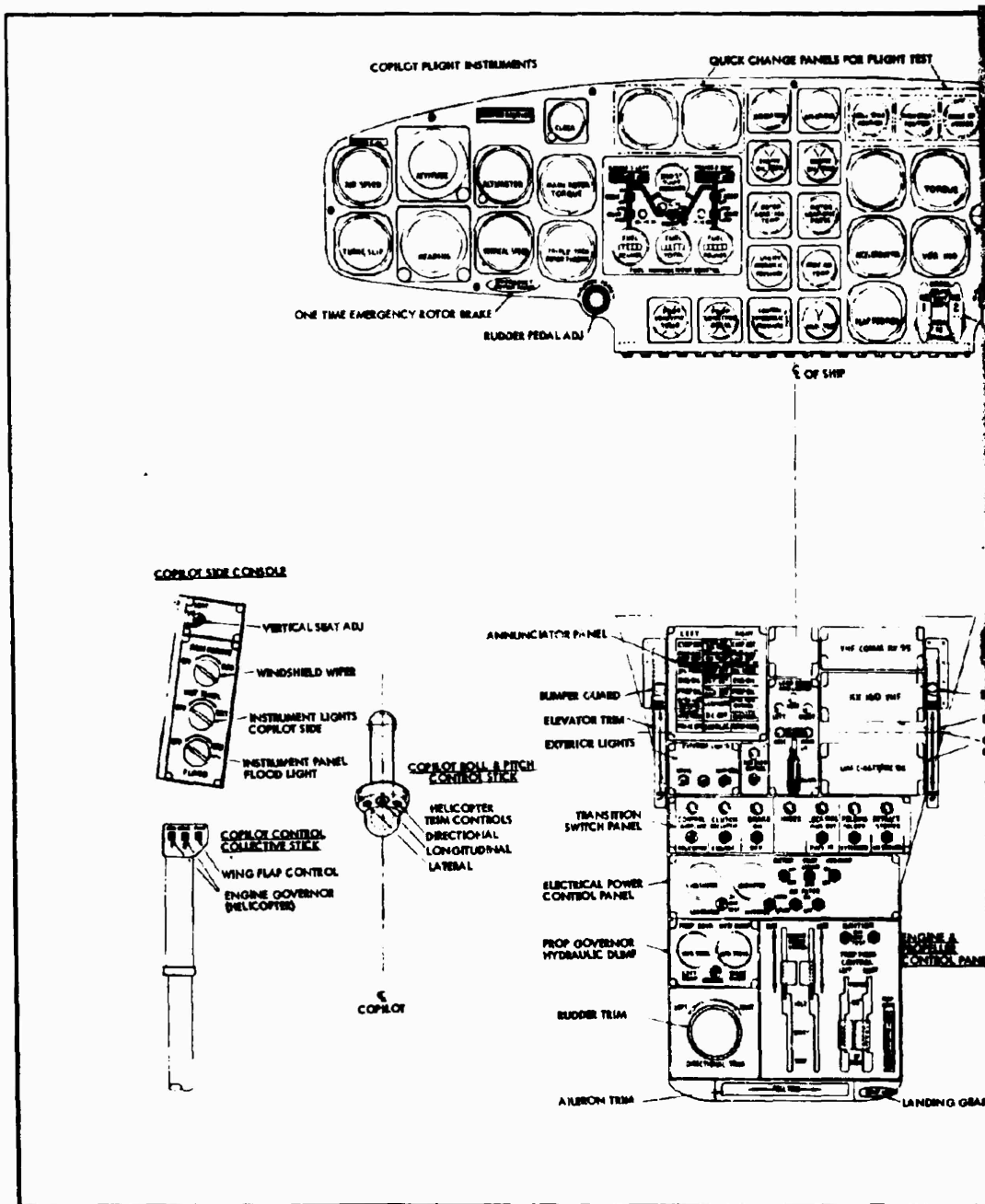
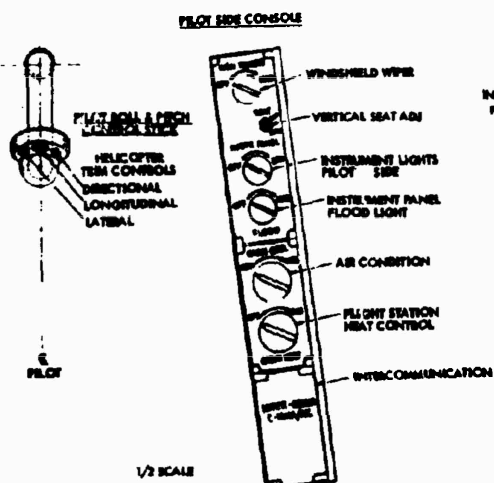
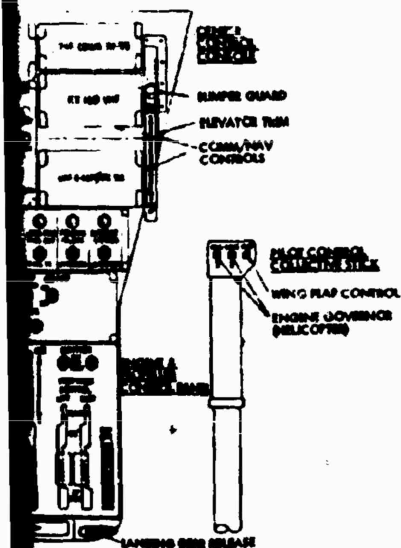
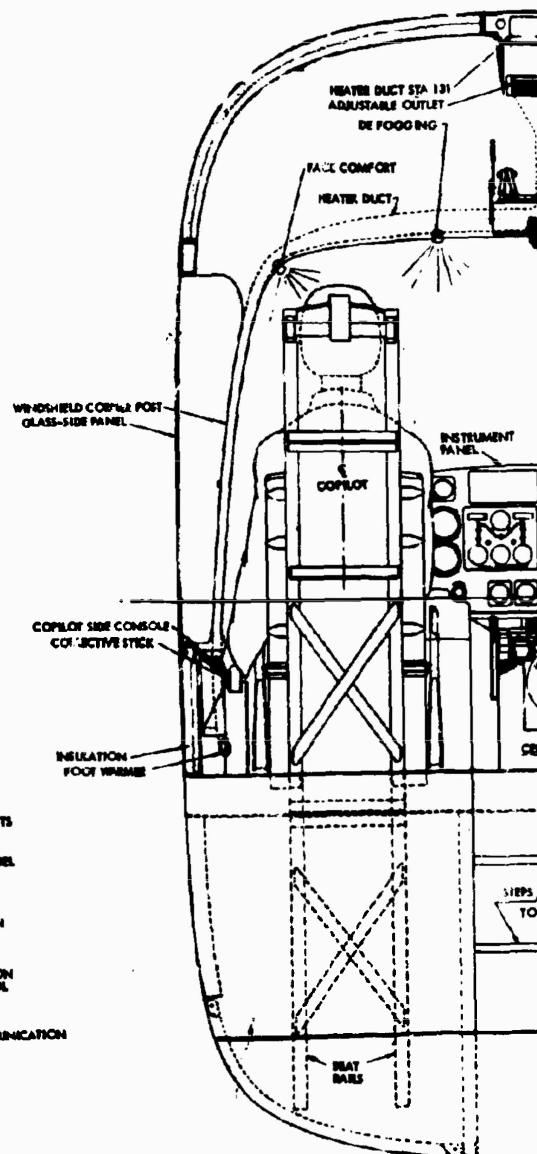
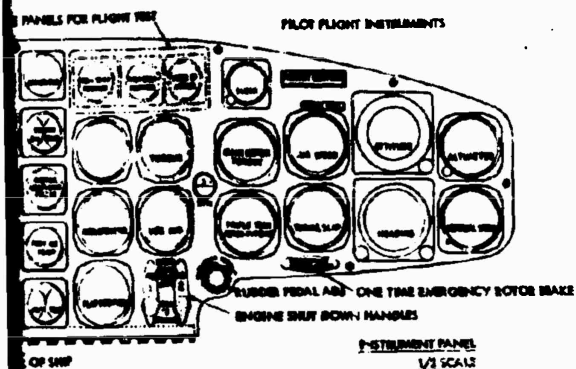


Figure 47. Flight Station Instrumentation.



B

Page Intentionally Left Blank

Increased and propeller pitch is gradually decreased, until the aircraft is supported by the rotor and the propellers are at zero thrust. All engine control is then accomplished by the helicopter control method described previously.

Airplane Mode

In airplane mode, propeller speed governing is used, the power turbine governor is deactivated, and aircraft speed and power are controlled manually with the power levers. For ground-starting as an airplane, the start may be accomplished with the propeller-governor either on or off, and the propeller pitch control levers must be at zero thrust setting. After the engine has started, and with the power levers initially in ground idle position, taxi speed may be controlled either with propeller governing and the power levers, or with power turbine governing and combined use of the propeller pitch control levers and the power levers. For takeoff and landing in this mode, propeller governing is used, and power is manually controlled by using the power levers.

FIRE PREVENTION

The engine nacelle is divided into three basic fire protection zones by a combination of titanium firewalls as shown in Figure 48. Zone I is the zone containing the burner, turbine, and tailpipe of the engine. Engine skin temperatures in this zone range from about 850°F to about 1250°F during normal operation. Any combustor burn-through would also occur in this zone. This zone contains only integral steel oil lines from the rear bearing; therefore, although combustor burn-through can occur, a fire caused by flammable fluid leakage is extremely unlikely in this zone. If a fire were to occur, it would be of low intensity.

Zone II contains the engine compressor, gearbox, and accessories. This zone contains many sources of fuel and oil leakage. There is a 20 kilovolt-ampere alternator on the left-hand engine, but none on the right-hand engine. The single alternator is cooled with air ducted from the oil cooler intake scoop, which precludes fuel/air vapors entering the alternator and becoming ignited. There are no dc generators or other pieces of electrical equipment, in either nacelle, which could cause ignition. There is rotating machinery in Zone II, such as the gearbox and the accessories, which is subject to overheating, bearing failures, case rubbing, seizure, etc., and which can cause overheating to such an extent that fuel or oil and air vapors could become ignited. However, the possibility of such failures is remote. When failures of this type do occur, they frequently are violent and result in broken fuel or oil lines or reservoirs, thus simultaneously creating both the source of ignition and flammable fluid leakage. In addition to these sources of ignition, the engine skin temperature in this zone (under all normal operating conditions) ranges up to 800°F. This is in excess of the turbine fuel minimum autoignition temperature, so there is a possibility of ignition

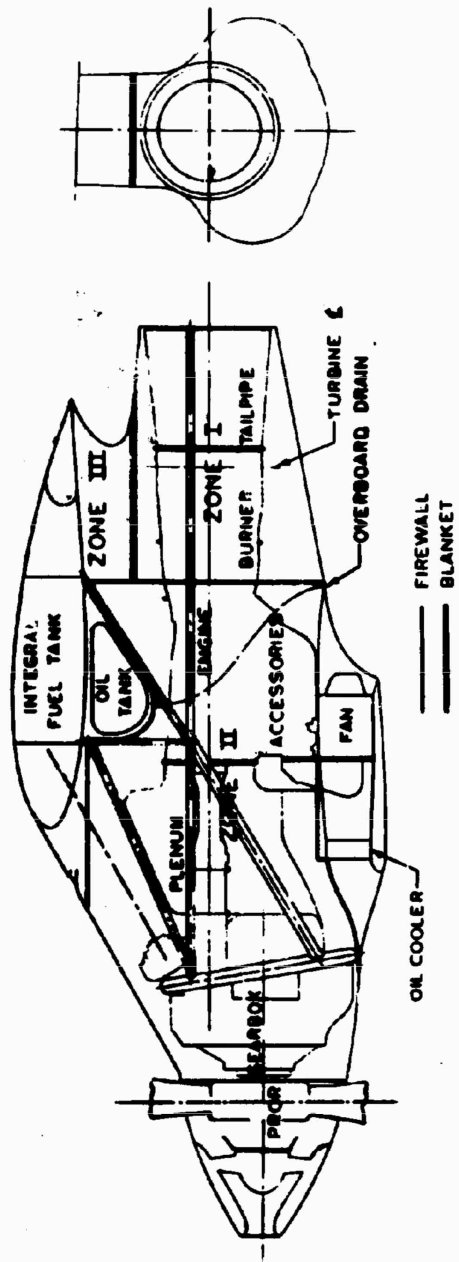


Figure 48. Engine Compartmentation Schematic.

from this source. All flammable fluid sources of leakage could be shrouded and drained overboard, but this is considered to be impractical.

Zone III is the region above the Zone I and II top firewalls. Zone III is subject to accumulations of fuel and oil from leaks in the integral fuel tank in the wing, the oil tank, and various fuel and oil fittings. To carry away such accumulations, the top firewall system is liquid-tight, and drains are provided at all low spots.

To prevent the accumulation of combustible vapors, all three zones are purged with ventilating (or cooling) air, providing at least three changes of air per minute. The cooling air provisions for Zones I and II are discussed later, under Engine Compartment Cooling. Zone III is ventilated by air entering a ram scoop in the leading edge of the pylon, just below the wing. This air passes between the wing and the top firewall system and exits through louvers on the sides of Zone III near the trailing edge of the pylon.

A heat-insulating blanket is provided on the bottom side of the Zone I top firewall. This blanket shields the firewall from engine hot section radiation and thereby prevents the firewall from getting hot enough to ignite fuel which may drop on it from a leak in the integral fuel tank aft bulkhead.

FIRE DETECTION

Effective corrective action in the event of a fire is largely dependent on early detection and rapid actuation of protective devices. Zone I contains only a minute source of flammable fluid leakage, making the possibility of fire in this zone remote. Engine combustor burn-through can occur, however, and in such a case the engine should be shut down. To detect an overheat in Zone I, a three-segment continuous fire detector element, conforming to MIL-Spec D-7006B, is installed around the engine in the middle of the cooling air passage, slightly aft of the engine exhaust flange. One segment is attached to each of the two cowl panels, and one segment is attached to the structure around the top of the engine. These segments are connected in series, and are set sufficiently high, so that false warnings will not occur in normal operation. An amber light on the pilot's panel is turned on to indicate overheat.

One section of continuous detector element is installed on each side of the nacelle in Zone II. These two systems are connected to a red light on the pilot's panel. Therefore, the pilot can determine if there is an overheat (amber light for Zone I) or a fire (red light for Zone II) and take appropriate corrective action; such as reducing power, shutting the engine down, only, or shutting the engine down and actuating the fire extinguishing system.

FIRE EXTINGUISHMENT

A one-shot fire extinguishment capability is provided for each engine by a bromotrifluoromethane (CF₃Br) system. The agent containers (one for each engine) are located in Zone III. Each bottle contains 2-1/2 pounds of the agent, which is enough to flood Zone II. Both the Zone II cooling air inlets in the spinners and the alternator cooling air inlet on the left engine are equipped with shutoff provisions so that Zone II on either engine can be sealed off, retaining the agent in this zone for some time after agent release.

Engine shutdown and ventilating air shutoff are accomplished by pulling an emergency handle in the cockpit. A separate switch, under the handle, is pressed for agent release. The agent containers are equipped with thermal discharge provisions and discharge indication, both of which are accessible to inspection from the ground.

FIRE CONTAINMENT

The spread of fire from zone to zone within the nacelle is inhibited by a network of titanium firewalls conforming to Federal Aviation Regulations 25 and 29. Zone II is in front of Zone I and below Zone III. The cowling on Zone II is titanium down to the longeron, which will prevent fire burning out of this zone, except below the longeron. During forward flight, fire issuing from Zone II through a burned-out lower cowl will impinge on the Zone I cowling, but it is prevented from burning into this zone because the Zone I cowling is titanium all around. During an autorotation landing, fire from Zone II is prevented from burning into Zone III because the zone is skinned with titanium. The titanium skin on Zone II extends far enough below the wing that fire, issuing from Zone II during an autorotation landing, is prevented from damaging the wing or causing explosion of fuel vapors in the integral tanks.

INSTRUMENTATION SYSTEM

Power plant instrumentation for the research aircraft is reduced to the types and quantities necessary to accomplish the research mission safely and adequately. However, the basic design would not preclude the use of full instrumentation per military specifications and/or FAA regulations for an operational aircraft.

Figure 47 shows the arrangement of powerplant and drive system instrumentation.

STARTING SYSTEM

The two T64-GE-16 turboshaft powerplants on this vehicle are started by a variable-displacement, 3,000-psi, 17.2-gallons-per-minute (gpm)

hydraulic motor, mounted on the accessory gearcase of each engine. The starter motor, starter valve, and utility hydraulic pump package used in this system are identical to those used on the AH-56A. Ground connections, located in the nosewheel well, are provided to join the ground hydraulic power unit to the system for starting the Number 2 engine. The Number 1 engine is started from the utility hydraulic power package driven by the started engine.

ENGINE COMPARTMENT COOLING

The engine nacelles are divided into three compartments as shown in Figure 49. Air for Zone I is admitted through flush scoops near the forward end of the zone, and on either side of the nacelle. This air is discharged through an angular slot between the trailing edge of the cowl- ing and the engine exhaust diffuser discharge.

Cooling air for Zone II is provided by a ram scoop in the nose of each spinner and flows over the propeller hub and through a rotary shutoff valve into Zone II. After flowing through Zone II, this air is discharged through louvered openings on either side of each nacelle, near the top and bottom rear of the zone. During hover operations when there is no ram, air is drawn through the spinner and into Zone II by fan blades inside the spinner. The left engine drives a 20-kilovolt-ampere, air-cooled alter- nator, which incorporates an integral fan capable of pumping sufficient air for cooling under hover conditions.

INSTALLATION LOSS ANALYSIS

The effects of inlet and exhaust system losses, power extraction, and cooling-air drag have been considered in determining the engine per- formance. The presentation of the data is in general accordance with MIL-D-17984A (ASG)-1, and it includes installed-engine performance for the T64-GE-16 engine.

Discussion and Presentation of Inlet Loss Analysis Results

The inlet total pressure recovery is shown in Figure 50. As envisioned for operational aircraft, the inlet doors are interconnected with the landing gear. Takeoff and any operation in ground effect (IGE) would normally be performed with the landing gear down and with only the filtered air source open. When the landing gear is retracted, the ram air source is opened and the filtered air source is closed. An override is provided, however, so that when the aircraft is hovering at 6,000 feet, 95°F, out of ground effect (OGE), where engine performance is critical, both inlets can be opened, thereby resulting in a relatively high inlet total pressure recovery ratio.

The research aircraft has auxiliary doors to provide the same recovery at 6,000 feet, 95°F as the operational version of this aircraft. Since

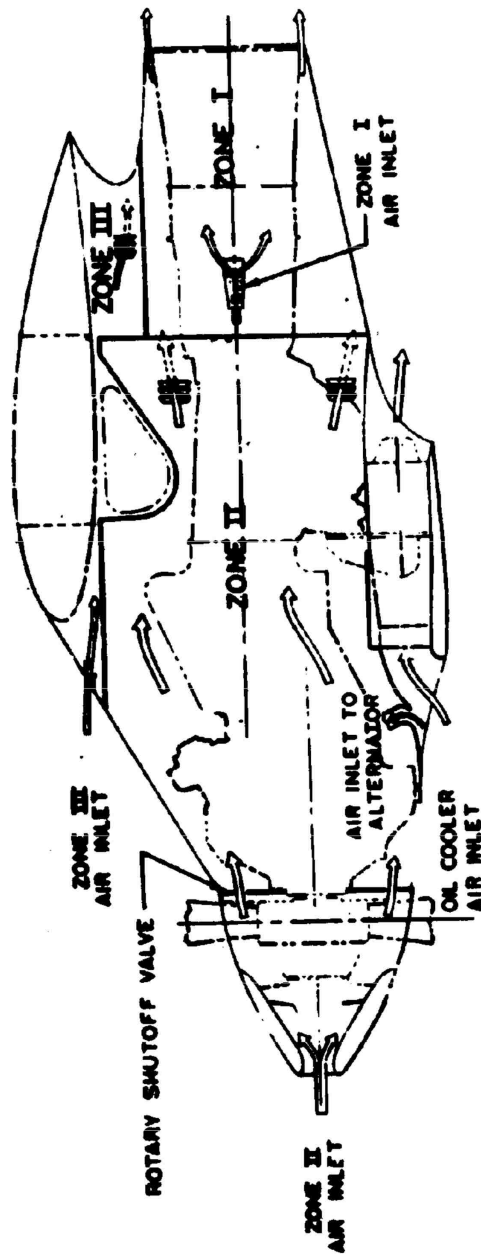


Figure 49. Engine Compartment Cooling Schematic.

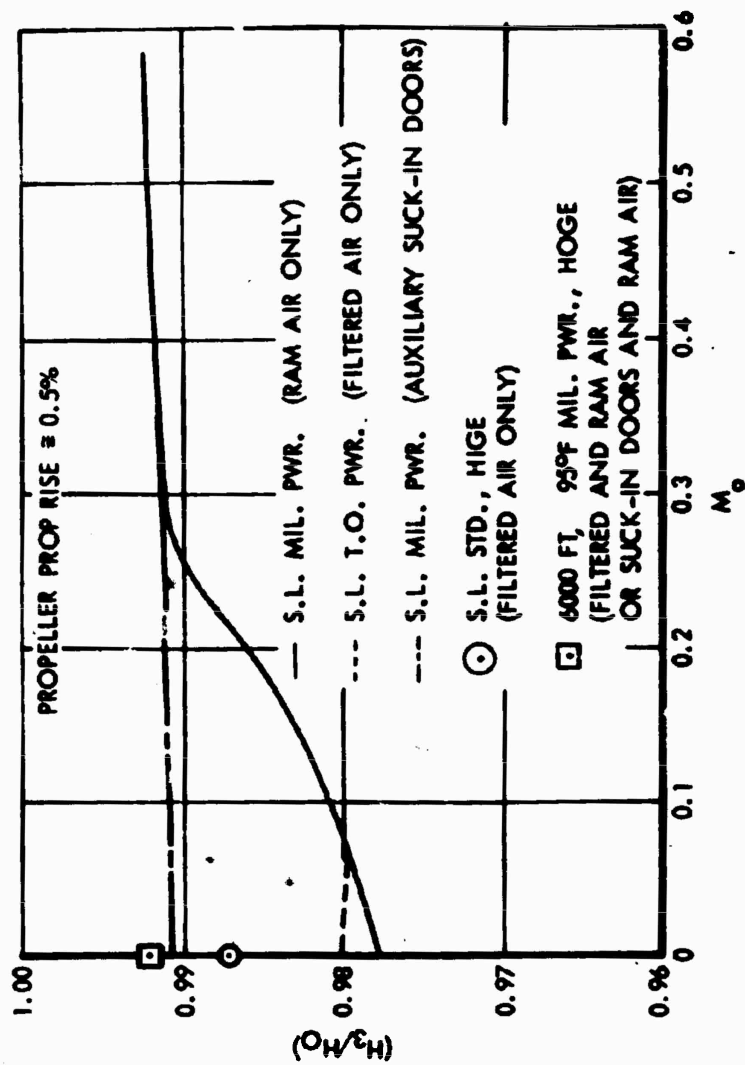


Figure 50. Estimated CBA Inlet Total Pressure Recovery.

these doors are spring-loaded suck-in doors, air source selection is not possible, and the sea-level takeoff inlet total pressure recovery ratio of this aircraft is higher than that of operational aircraft. Of course, any dust in the air may be ingested with this system.

Exhaust Duct and Exhaust Ejector Analysis

The exhaust system arrangement is shown in Figure 51. The exhaust gas diffuses from the engine flange (Area = 2.04 ft²) to the exhaust face (Area = 3.12 ft²) with an equivalent conical diffuser angle of 11.4 degrees. The exhaust gas also pumps cooling air through the hot section (Zone I) which contains the combustor, turbine, and tailpipe.

Exhaust Duct Analysis

The exhaust nozzle shown in Figure 51 is identical to that on which the engine manufacturer based engine performance; therefore, the exhaust system effect is already included in the specification performance.

Exhaust Ejector Performance

The exhaust nozzle and cowling constitute a zero-length ejector to pump ventilating air through Zone I. At least three air changes per minute are required to ventilate Zone I adequately. Experience indicates that the zero-length ejector will provide adequate Zone I ventilation.

Losses Due to Power Extraction

Accessory power extraction is tabulated in Table VI for three critical flight conditions. Power available to the propeller, main rotor, and tail rotor was predicated on power path efficiencies of 98.2 percent to each propeller, 97.2 percent to the main rotor, and 97.2 percent to the tail rotor. These efficiencies account for drive system losses. The sum of these gear losses and the accessory power extraction was subtracted from the engine installed shaft horsepower to obtain the power on which aircraft performance was based.

Miscellaneous

The recovery ratios shown in Figure 50 include an estimated propeller cuff pressure rise of approximately one-half percent over the entire flight Mach number range.

Cooling Air Drag

The cooling air required for oil cooling is pumped by a fan. Since the fan pressure rise, plus heat addition, converts some of the extracted horsepower already accounted for to thrust, the difference between this thrust and the ram drag is considered to be insignificant. For Zone I, II, and III cooling air drag, this combined drag is of an order of magnitude of 2 pounds, allowing at least 10 changes of air per minute

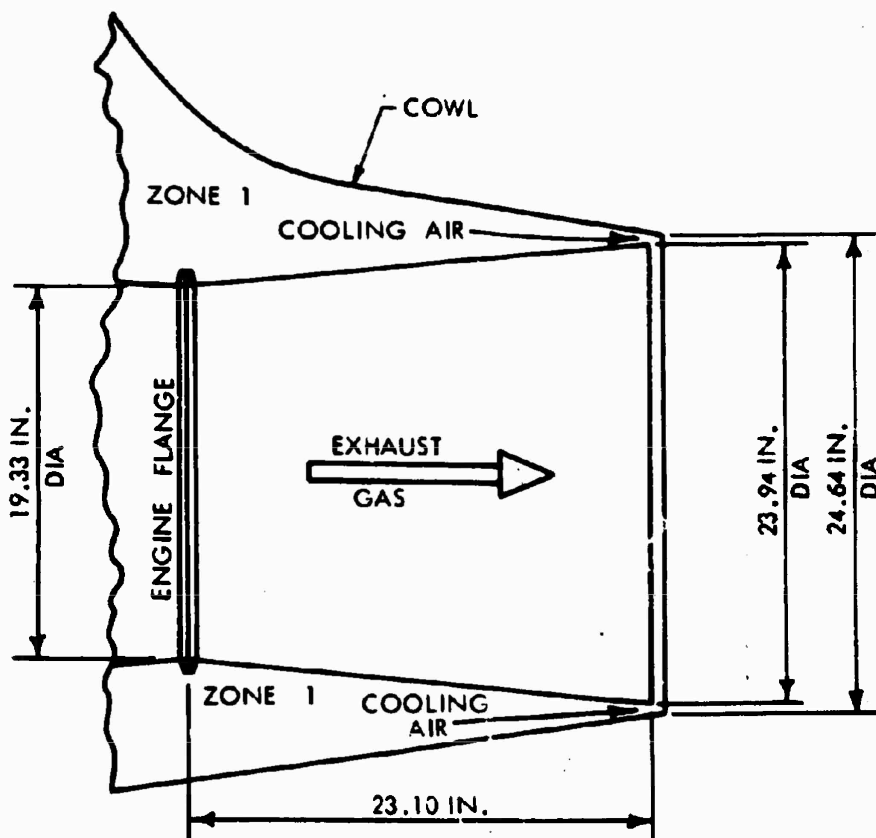


Figure 51. Exhaust System Arrangement.

TABLE VI. LOSSES DUE TO POWER EXTRACTION*				
Component	Sea Level Std. Day $V_o = 0$ Knots	Sea Level Std. Day $V_o = 385$ Knots	6,000 Ft, 95°F $V_o = 0$ Knots	
Drive System Losses	250	140	250	
Accessories:				
Lubrication	5	5	5	
Transmission Cooling	15	15	15	
Engine and Gearbox Cooling	10	10	10	
Electrical	15	15	15	
Hydraulic	15	15	15	
*Only 10 horsepower is extracted from the engine accessory drives, and only 10 horsepower is accounted for in Table V.				

through each zone. Therefore, the CRA engine performance is not corrected for cooling air drag. For a further discussion of the cooling system, refer to the previous paragraphs on Engine Compartment Cooling.

Overall Effect Upon Engine Installation Performance of Various Installation Losses

Installed engine performance for various altitudes, speeds, and power settings is presented in Figures 52 through 64.

ALTITUDE = 0. FT

□ - MILITARY POWER

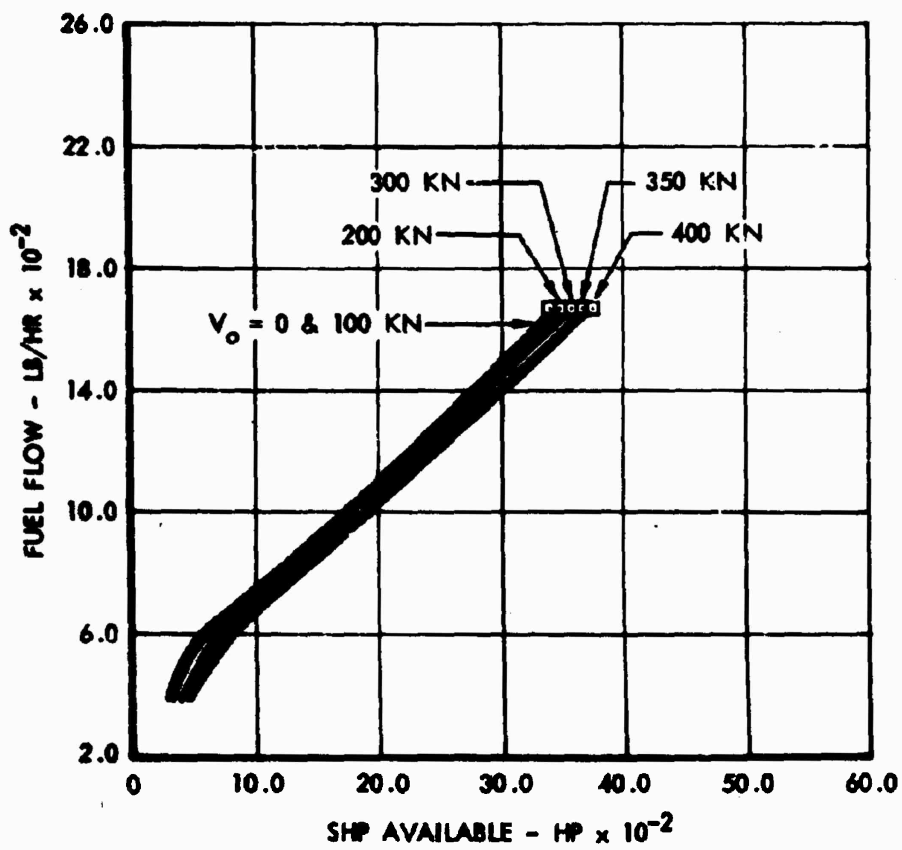


Figure 52. T64-GE-16 Installed Performance, Sea Level.

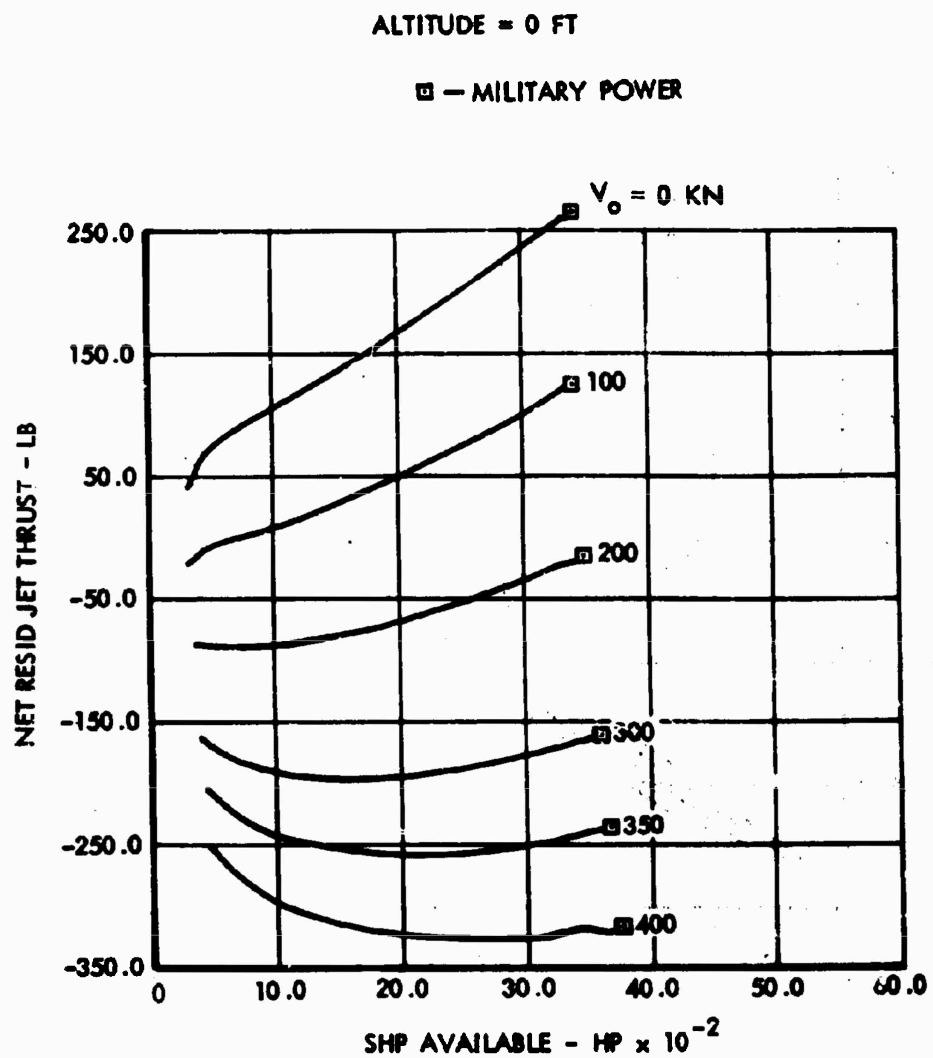


Figure 53. T64-GE-16 Installed Performance, Sea Level.

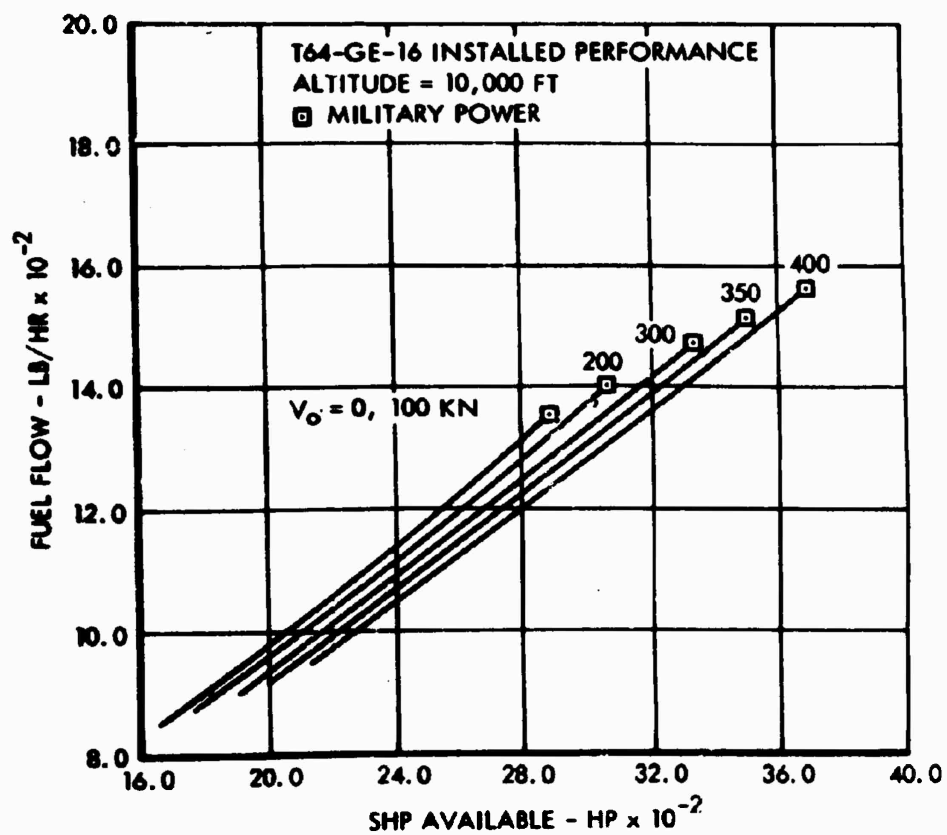


Figure 54. T64-GE-16 Installed Performance, 10,000 Feet.

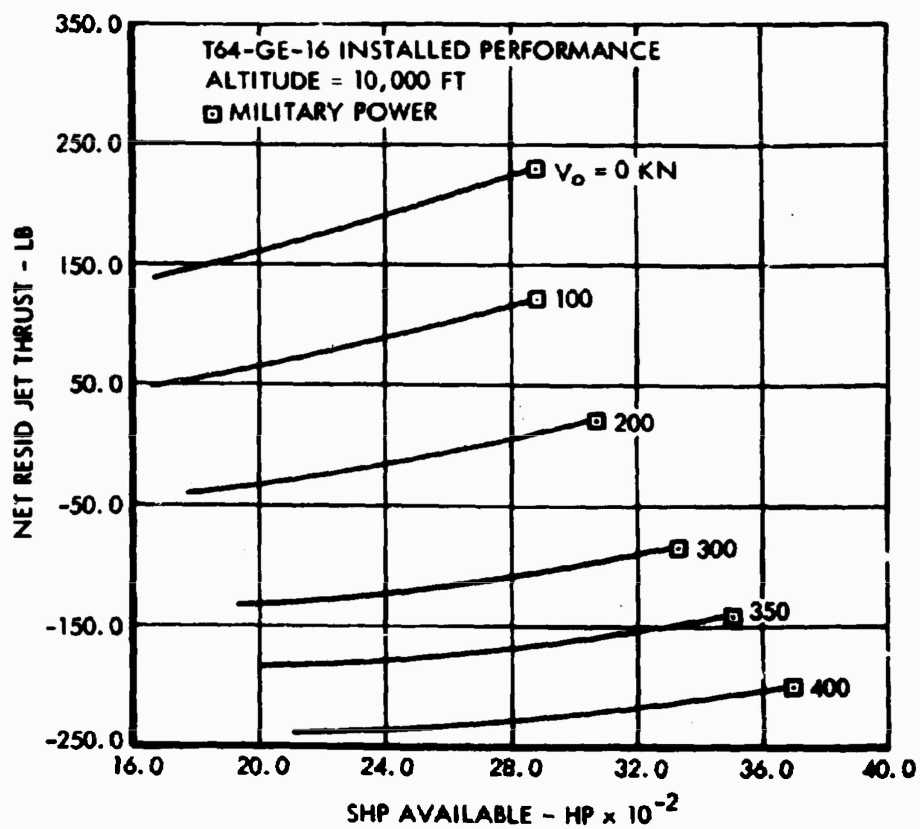


Figure 55. T64-GE-16 Installed Performance, 10,000 Feet.

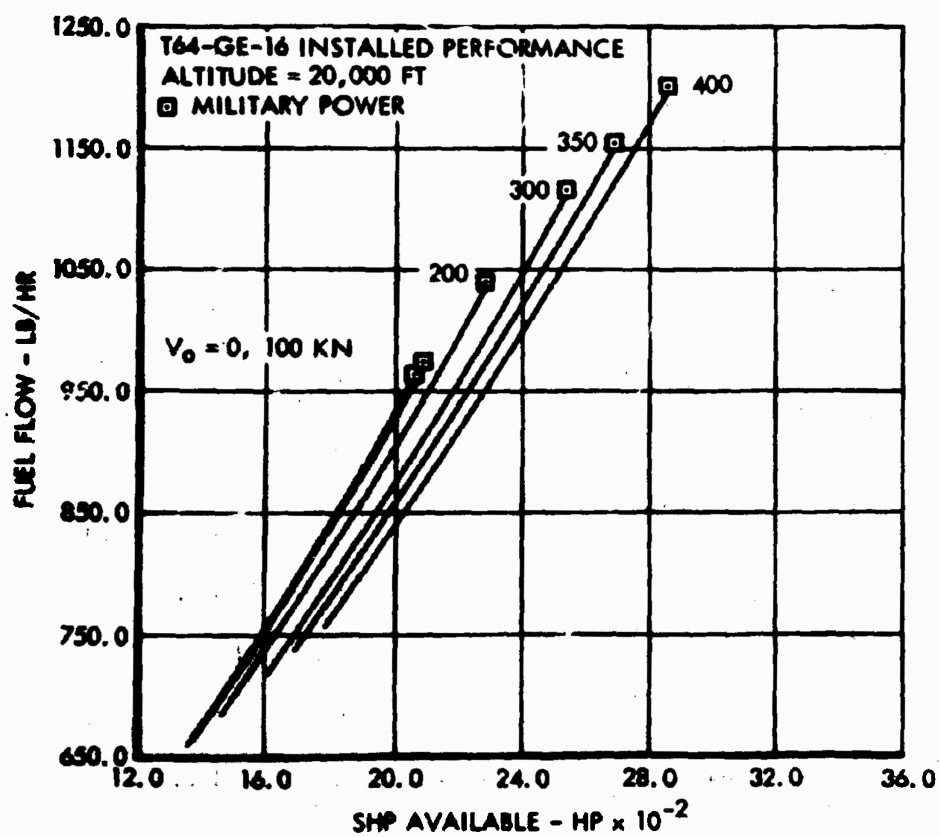


Figure 56. T64-GE-16 Installed Performance, 20,000 Feet.

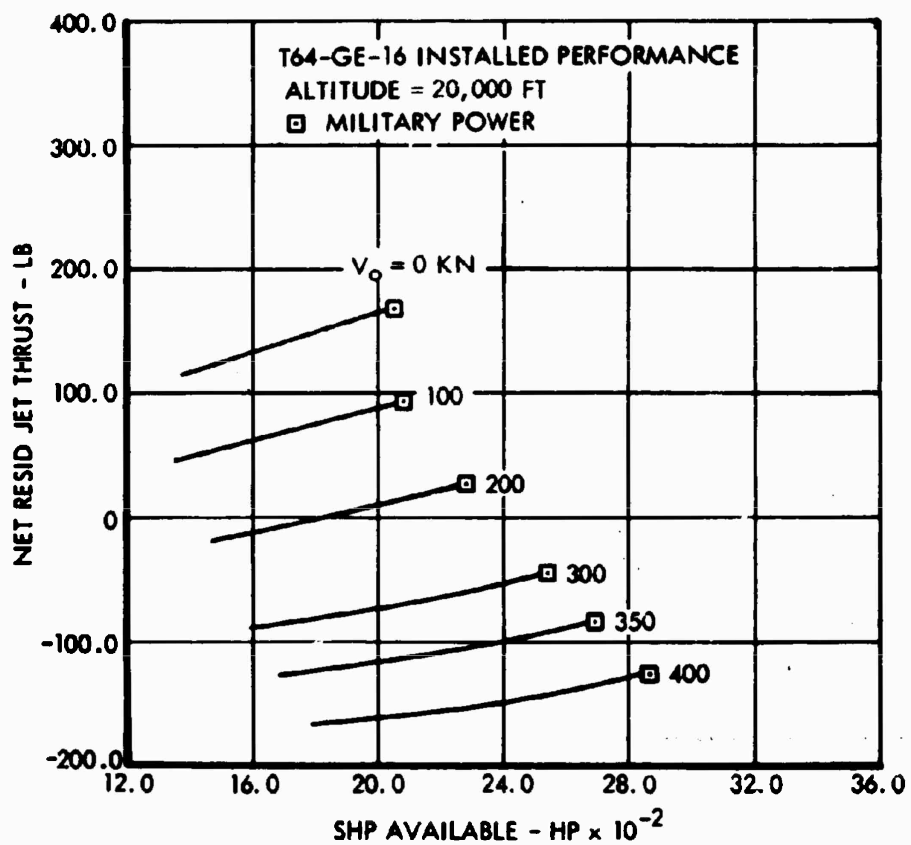


Figure 57. T64-GE-16 Installed Performance, 20,000 Feet.

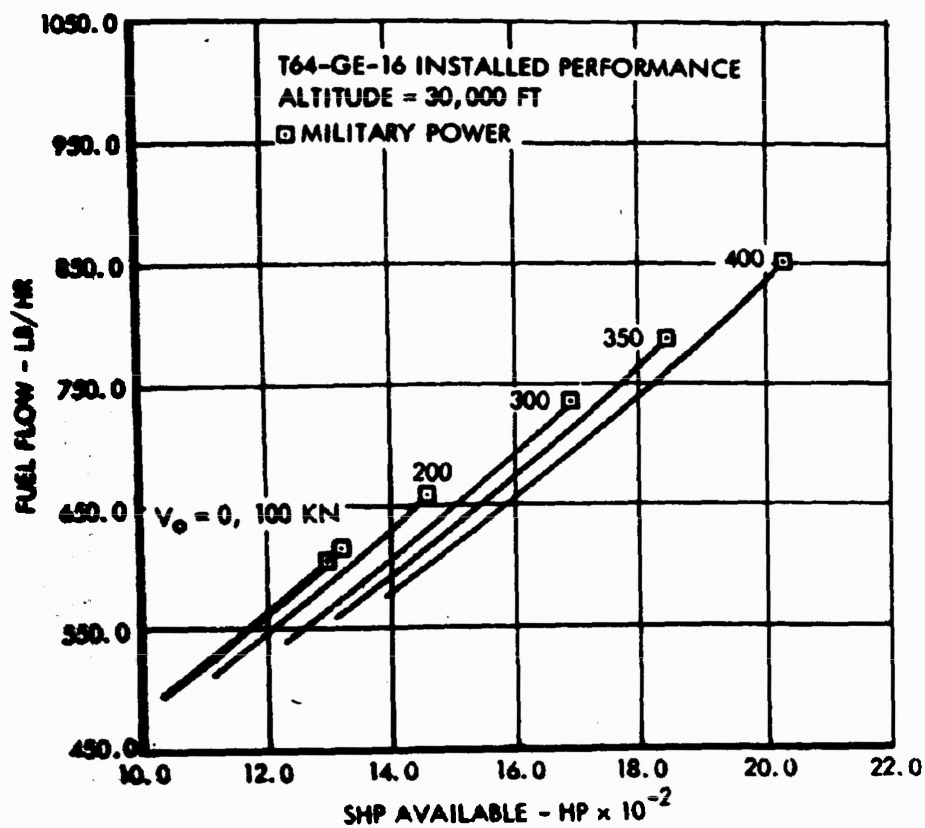


Figure 58. T64-GE-16 Installed Performance, 30,000 Feet.

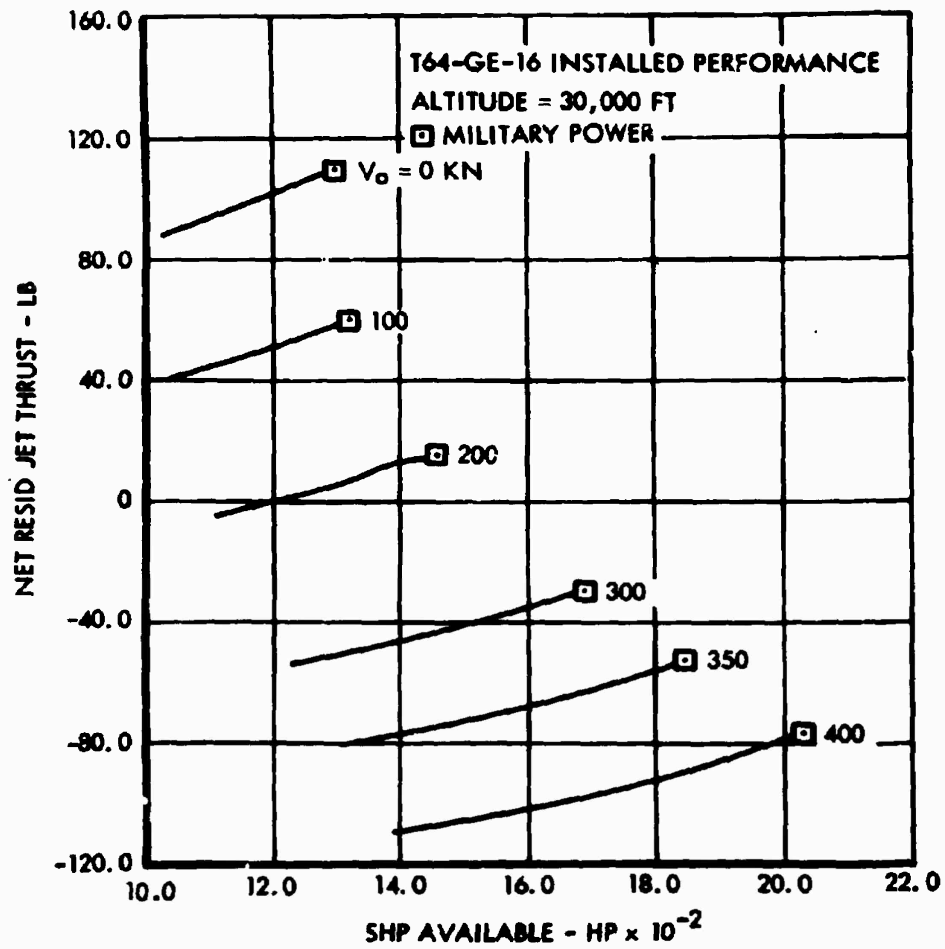


Figure 59. T64-GE-16 Installed Performance, 30,000 Feet.

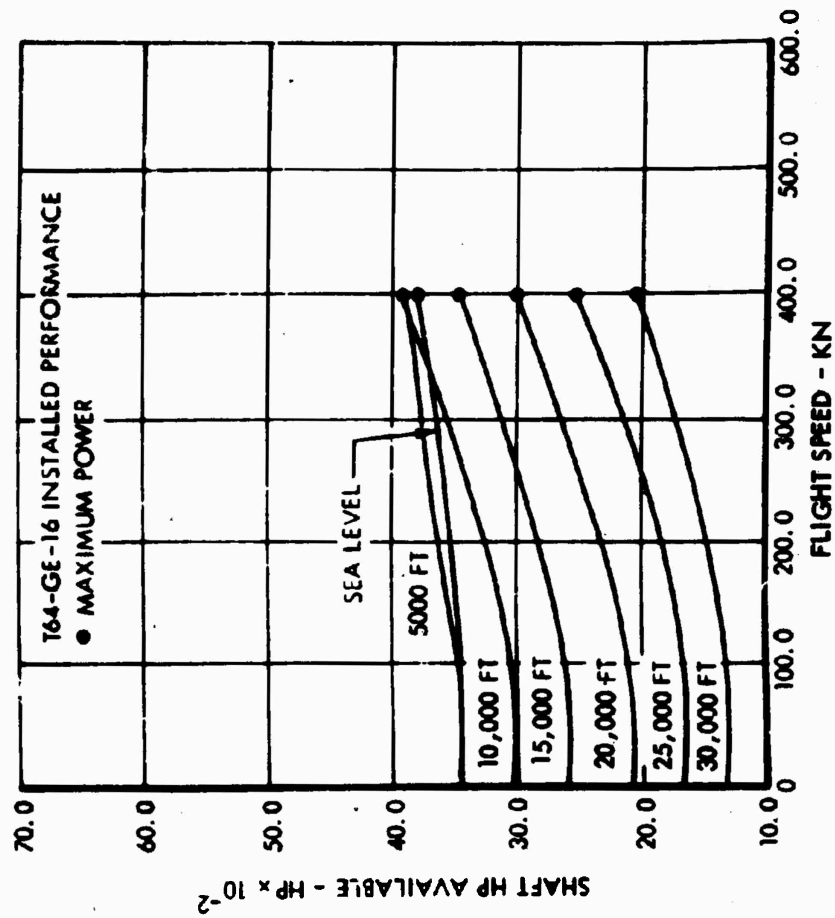


Figure 60. T64-GE-16 Installed Performance, Maximum Power.

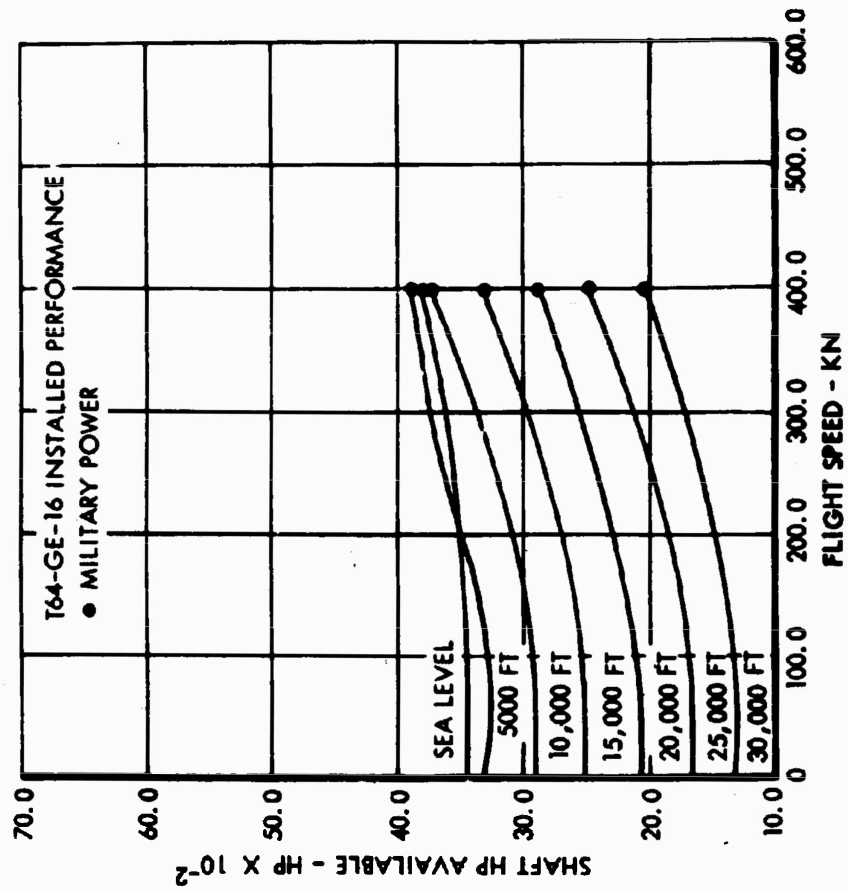


Figure 61. T64-GE-16 Installed Performance, Military Power.

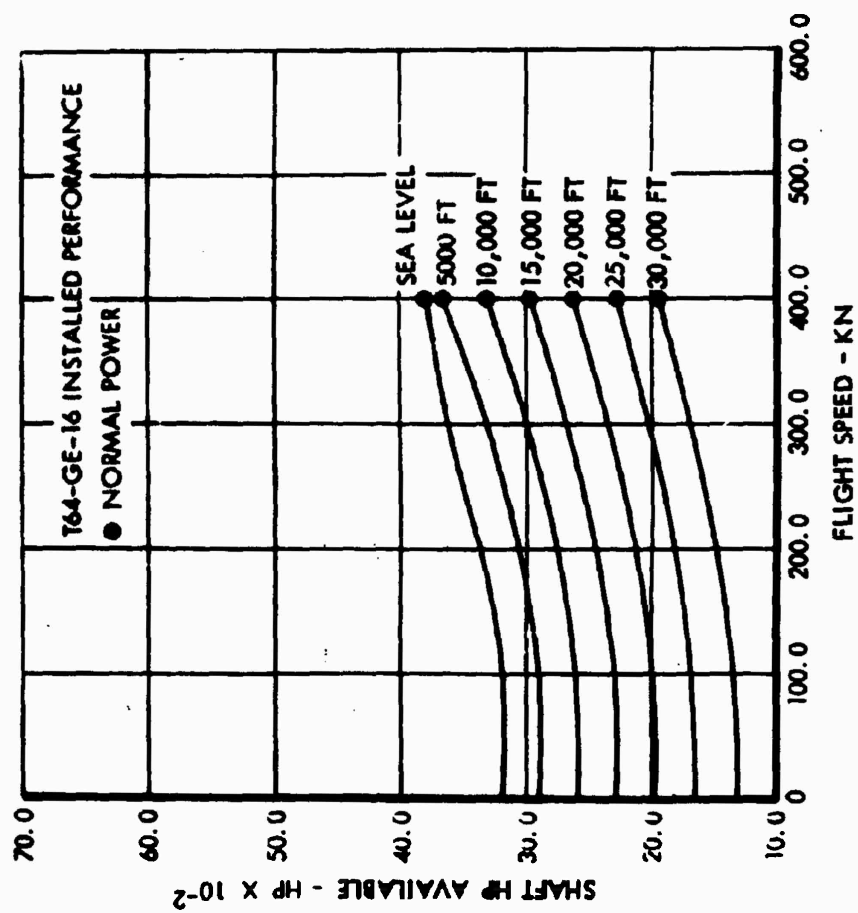


Figure 62. T64-GE-16 Installed Performance, Normal Power.

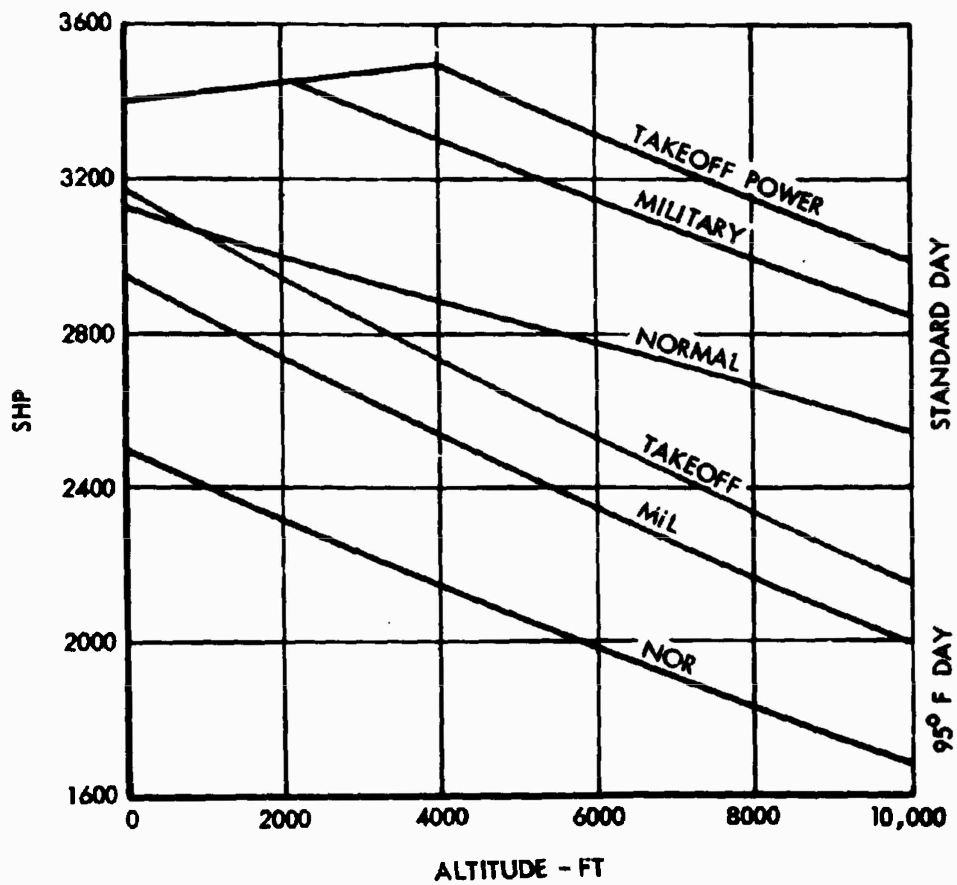


Figure 63. T64-GE-16 Installed Performance,
Hover in Ground Effect.

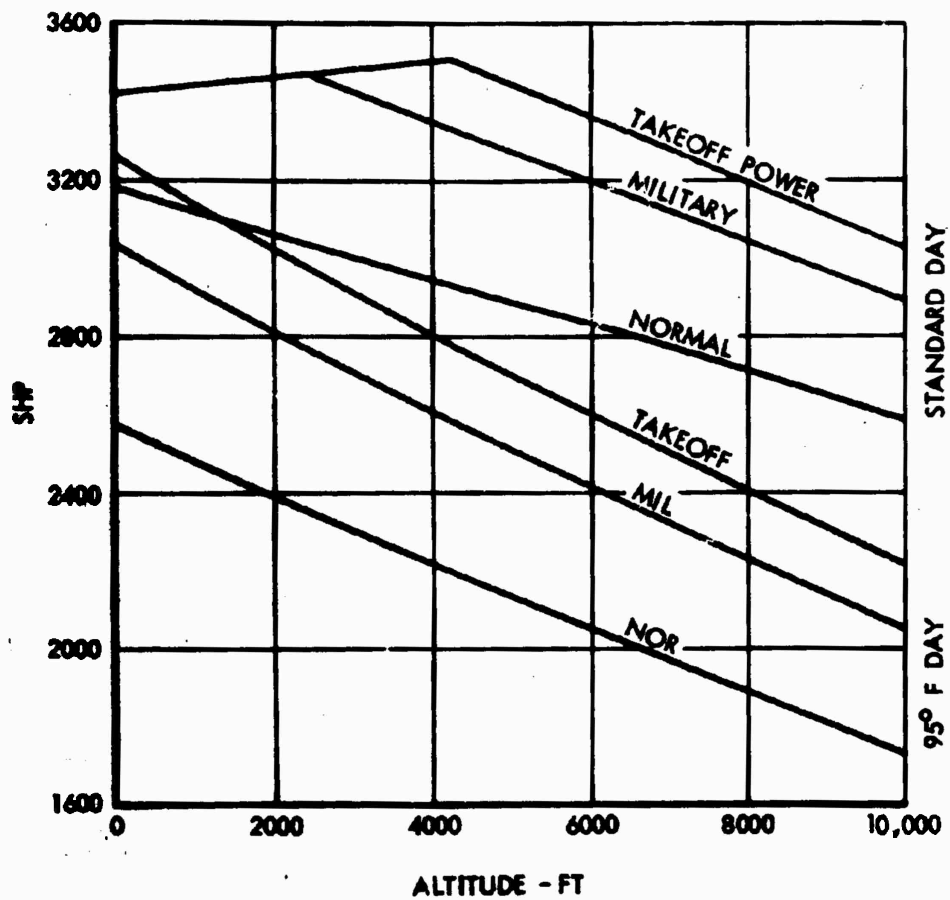


Figure 64. T64-GE-16 Installed Performance,
Hover out of Ground Effect.

SECTION 6
POWER TRANSMISSION SYSTEMS

DESIGN REQUIREMENTS

The power transmission system is designed in general accordance with the guidelines defined by specifications MIL-A-8860 through MIL A-8870 (ASG), and in conjunction with specifications MIL S-8698, MIL-T 5955B, and MIL-T-8679, as appropriate.

CAPABILITY AND PURPOSE

The transmission system is designed to satisfy these functional requirements:

- To transmit power from the wing-mounted engines to the aircraft propulsion systems, the forward thrust and the vertical lift system
- To provide proper supporting structure while the main rotor system is either stowed or extended
- To provide wing cross-shafting to interconnect the two propellers mechanically, to guard against asymmetric thrust due to an engine-out situation
- To provide either fixed-wing or VTOL propulsion capability

SPECIAL FEATURES

The power transmission system as designed for the Composite Research Aircraft is based on these features:

- Instant and automatic disengagement of an engine upon loss of power
- 3,600-hour aircraft service life on nonreplaceable components (i.e., gearing, shafting, and housings)
- 1,200-hour minimum operating time between overhaul requirements for bearings, couplings, clutches, and rotor brake
- 10 to 15 percent growth potential of engine without major development of drive system
- Lighter weight vertical lift system as a result of large shutdown time during fixed-wing mode of operation

- Compact main transmission capable of stowing/extending main rotor without interfering with cargo space
- Maximum use of available previously qualified components, where applicable, for cost and time savings

GENERAL DESCRIPTION

System Description

The power transmission system is a mechanical drive system transmitting the power from the wing-mounted engines to the aircraft propulsion systems, the forward thrust system (propellers), and the vertical lift system (main and tail rotors). Figure 65 shows the general arrangement of the power transmission system. The power transmission system ratings are shown in Table VII.

The arrangement of the power transmission system conforms with the aircraft's configuration and performance requirements. The design of the system's components has been selected from trade-off studies for maximum performance, efficiency, and reliability and minimum weight.

The system's arrangement provides for shutting down and reactivating the vertical lift system without interrupting the operation of the forward thrust system. Flight range and safety are improved by mechanically interconnecting the propeller transmissions and by an overrunning clutch at the engine output shaft. With one engine shut down, the other engine can drive both propellers in the forward thrust system and also the rotors in the vertical lift system.

A flight safety feature is the decoupler in the cross shaft between the propeller transmissions. In case of a propeller or gearbox malfunction, or a nacelle fire, actuation of the decoupler divorces the propeller transmission from the power transmission system.

The interfaces between the system components are designed for individual removal of components. Access is provided for servicing and maintenance.

The main components in the power transmission system are the engine/propeller transmission, the main rotor transmission, the tail rotor drive intermediate gearbox, and the tail rotor gearbox. Included in the power transmission system is the shafting between the components; the shaft bearings, supports, and couplings; the vertical lift system disengaging clutch; the rotor brake; the drives for the aircraft systems' accessories; and the lubrication systems.

The power path from the engines to the propulsion systems is as follows: The engine power output shaft drives through an overrunning clutch into the

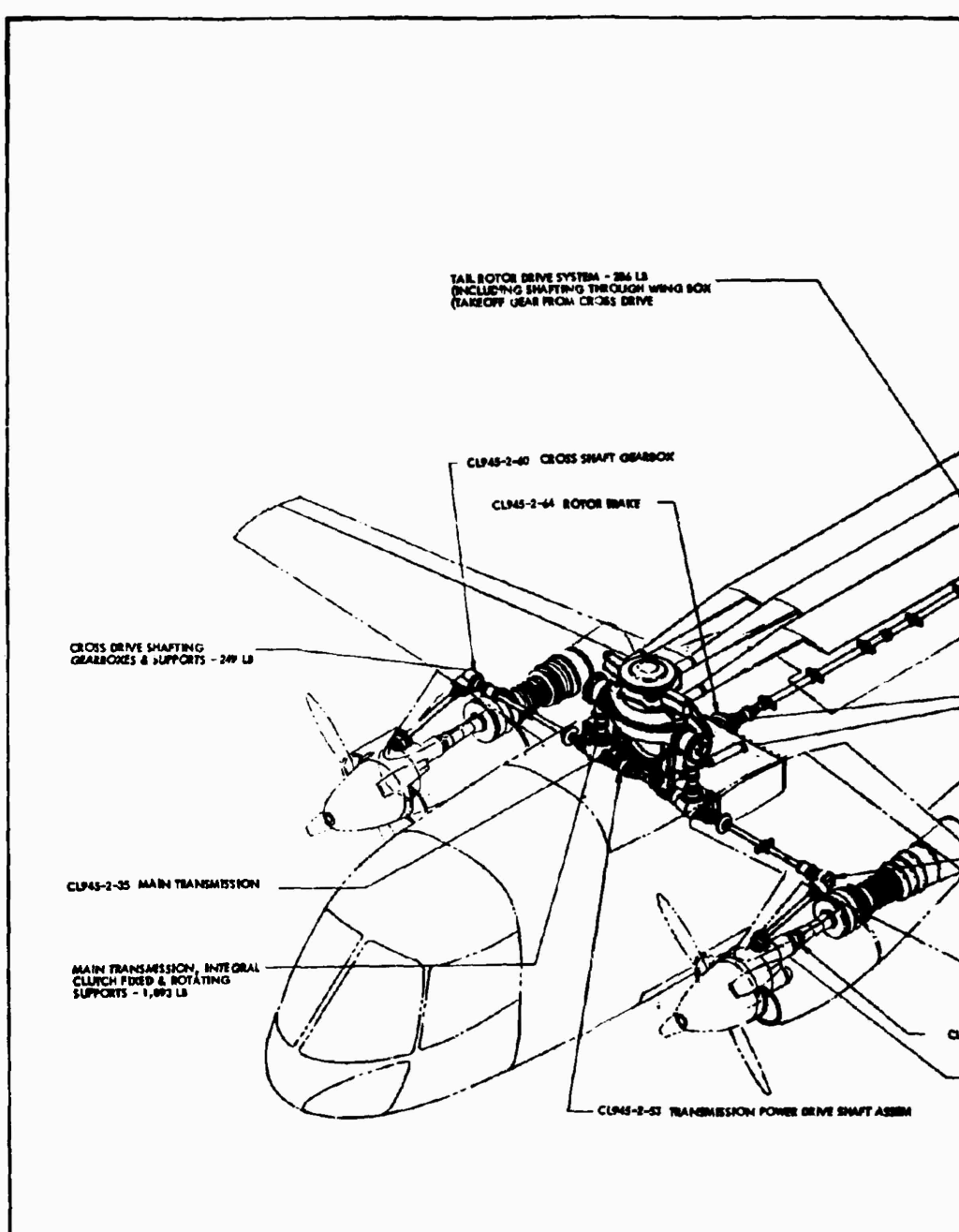
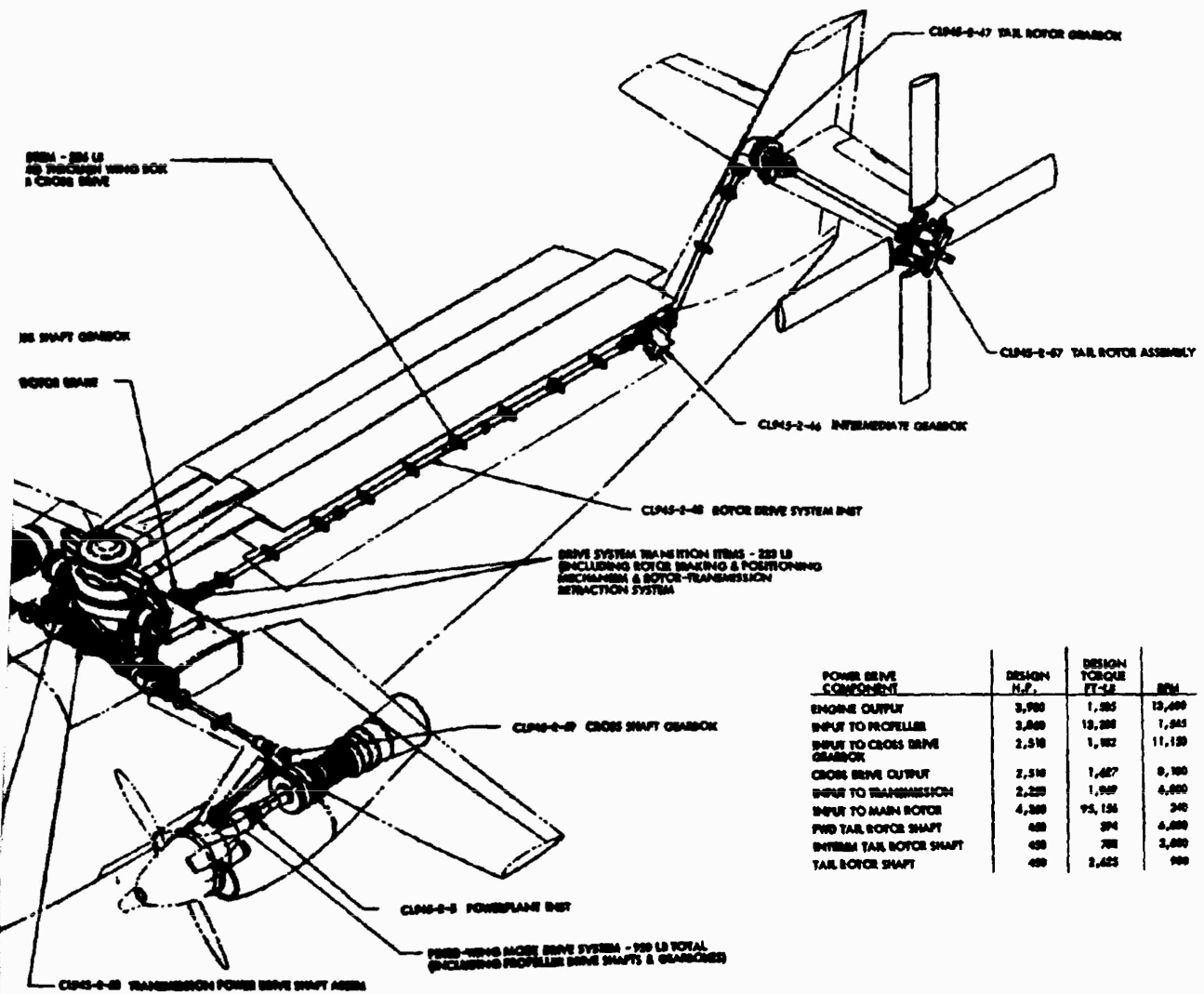


Figure 65. Power Drive System Arrangement.



Arrangement.

A

B

TABLE VII. POWER TRANSMISSION SYSTEM RATINGS					
Gearbox	Figure No.	Input Design Shp		rpm	
		Steady	Max.	(Normal)	
Engine/Propeller Transmission	2	3,900	4,875	Input	= 13,600
				Prep	= 1,545
				X-Shaft Extension	= 11,150
Wing Angle Gearbox	47	2,510	3,760	X-Shaft Extension	= 11,150
				X-Shaft	= 8,100
Main Rotor Transmission	49	4,500	5,625	Input	= 6,000
				Main Rotor	= 240
				Tail Rotor Drive	= 6,000
Intermediate Tail Rotor Drive Gearbox	51	450	600	Input	= 6,000
				Output	= 3,000
Tail Rotor Gearbox	52	450	600	Input	= 3,000
				Output	= 900

propeller transmission. This transmission contains two power paths, one to the propeller and one to the engine cross shaft. The cross shaft runs laterally through the wing and main rotor transmission to the engine propeller transmission on the opposite wing. A clutch in the main rotor transmission engages the cross shaft for power transmittal to the main and tail rotors. A power train within the main transmission drives the main rotor and the tail rotor drive shaft and accessory gearbox. The tail rotor drive shaft runs aft in the fuselage, through the intermediate gearbox and tail rotor gearbox, to the tail rotor.

Power System - Transmissions

Engine/Propeller Transmission

The engine/propeller transmission proposed for use on the CRA is a modified version of the propeller transmission used on the XC-142A V/STOL experimental aircraft.

Two added mount pads are located near the top of the gearbox as shown in Figure 43, one on each side located 20 degrees radially from the vertical center. Internal lubrication system changes necessary to provide adequate lubrication for all elements and to provide scavenging in the inverted position will be incorporated.

The modification to provide for driving the extension shaft to the wing gearbox consists of external mounting of a pair of bevel gears driven off the input to the gearbox. The relationship of the extension shaft to the engine-propeller gearbox and the wing gearbox is shown in Figure 43 also.

A comparison of the design factors of the present XC-142A gearbox and the gearbox as modified for the CRA vehicle is as follows:

	<u>XC-142A</u>	<u>Lockheed CRA Modification</u>
Engine rpm	13,600	13,600
Engine hp assumed	3,850	3,900
1st stage ratio	2.79	2.79
1st stage torque	1,490 ft-lb	1,509 ft-lb
2nd stage ratio	3.96	3.17
2nd stage hp	3,420	3,900
2nd stage rpm (output)	1,232	1,545
2nd stage torque (out)	14,550 ft-lb	13,300 ft-lb

The engine/propeller transmission will have a common lubrication system, designed to use MIL-L-7808 oil or equivalent, and will provide

sufficient capacity to lubricate the engine, the main gearbox, the adapter gearbox overrunning clutch assembly, and the wing gearbox.

Bevel Gearbox

The bevel gearbox, which drives the extension shaft to the wing gearbox, is mounted directly to the gearbox, and it supports the overrunning clutch assembly which is driven by the engine shaft. Torque is transmitted by a pair of spiral bevel gears which reduce the speed from 13,600 rpm engine output speed to 11,150 rpm of the extension shaft. The pinion gear shaft is splined to the shaft between the overrunning clutch and the propeller gearbox. Both pinion and gear have teeth integral with their shafts, and they are straddle-mounted in a common housing between radial roller bearings and duplex angular contact bearing sets.

Extension Shaft

The extension quill shaft from the bevel gearbox to the wing gearbox is mounted in splines at both ends; it is capable of accommodating the expected maximum misalignment of the two gearboxes and of transmitting the design torque to the wing box. In order to provide for shaft disassembly without disturbing the gearboxes, a short section of shaft near the lower end is made removable. A protective housing for the shaft serves also as a scavenge oil return path, and it is equipped with a flexible boot at each end to provide structural separation and access for shaft disassembly. The shaft mean diameter of 3.4 inches and the length of 30 inches provide a critical speed margin greater than 2.0.

Wing Angle Gearbox

A spiral bevel-mesh gearbox is located at the junction of the wing cross shaft and the drive centerline from the propeller transmissions.

The left-hand assembly includes provisions for driving and mounting the standby hydraulic pump.

The gears and bearings are supplied with lubricating oil provided from their respective propeller transmission main pressure systems. The wing gearbox oil flow is based on an estimated oil heat rejection of 526 Btu per minute. Assuming a maximum oil temperature rise of 40°F, the required oil flow rate is approximately 3.4 gallons per minute. The extension shaft protective housing is used as an oil drainage path. The metal housing is fitted with a boot at each end, and adequate drain holes are provided in the bearing retainer castings at each end of the housing to accommodate the 3.4-gallon-per-minute flow.

The wing angle gearbox is directly mounted to the structure that supports the propeller, transmission, and engine system, thereby ensuring

sufficient alignment to permit the use of a simple quill shaft drive from the propeller transmission.

A curvic coupling is used to connect to the cross shaft, which is, in turn, provided with flexible points to accommodate both axial and angular mismatch between the angle boxes and the lower main rotor transmission.

Main Rotor Transmission

The main rotor transmission assembly is the part of the power transmission system that combines the power from the two engines, transmits the power to the main and tail rotors, supports the main rotor, and transfers the main rotor forces to the aircraft fuselage. The transmission housing is divided into three pin-jointed subassemblies, and it folds around the pin joints when stowing the rotor. The transmission contains the engine power clutches for engaging and disengaging engine power when changing to and from helicopter and airplane modes, the rotor brake, and the drives for accessories required for the main rotor control and operation. Main rotor control and blade-folding components (actuators, swash plate, control rods, main rotor control gyro drive) are located on, and form an integral part of, the transmission assembly.

Figure 65 shows the main rotor transmission and the location in the aircraft fuselage.

The basic transmission assembly is divided into three major subassemblies: the lower transmission assembly, the lift truss assembly, and the upper transmission assembly. The lower transmission assembly is mounted in the fuselage on the forward side of the wing beam. The lift truss assembly is joined to the lower transmission assembly by trunnions (lower trunnion) concentric with the cross shaft. The upper transmission assembly is joined to the lift truss by trunnions (upper trunnion) parallel to the lower trunnion. Figure 66 shows the transmission envelope.

The trunnion-jointed, three-piece transmission assembly folds when the rotor is stowed. In the process of folding, the lift truss rotates about the lower trunnion, translating the rotor and upper transmission forward and down into the fuselage. During this translation, the upper transmission and rotor rotate backward around the upper trunnion joint, keeping the folded rotor blades parallel to the fuselage and positioned for stowage in the fuselage.

Power from the engine power cross shaft to the main rotor must cross over the two transmission trunnion joints. These joints rotate when the rotor is being stowed. To transfer power across the joints, a set of right-angle spiral bevel gears is used at each joint. The rotative motion at the joint causes one bevel gear to roll on the mating gear, the mating gear turning on its center.

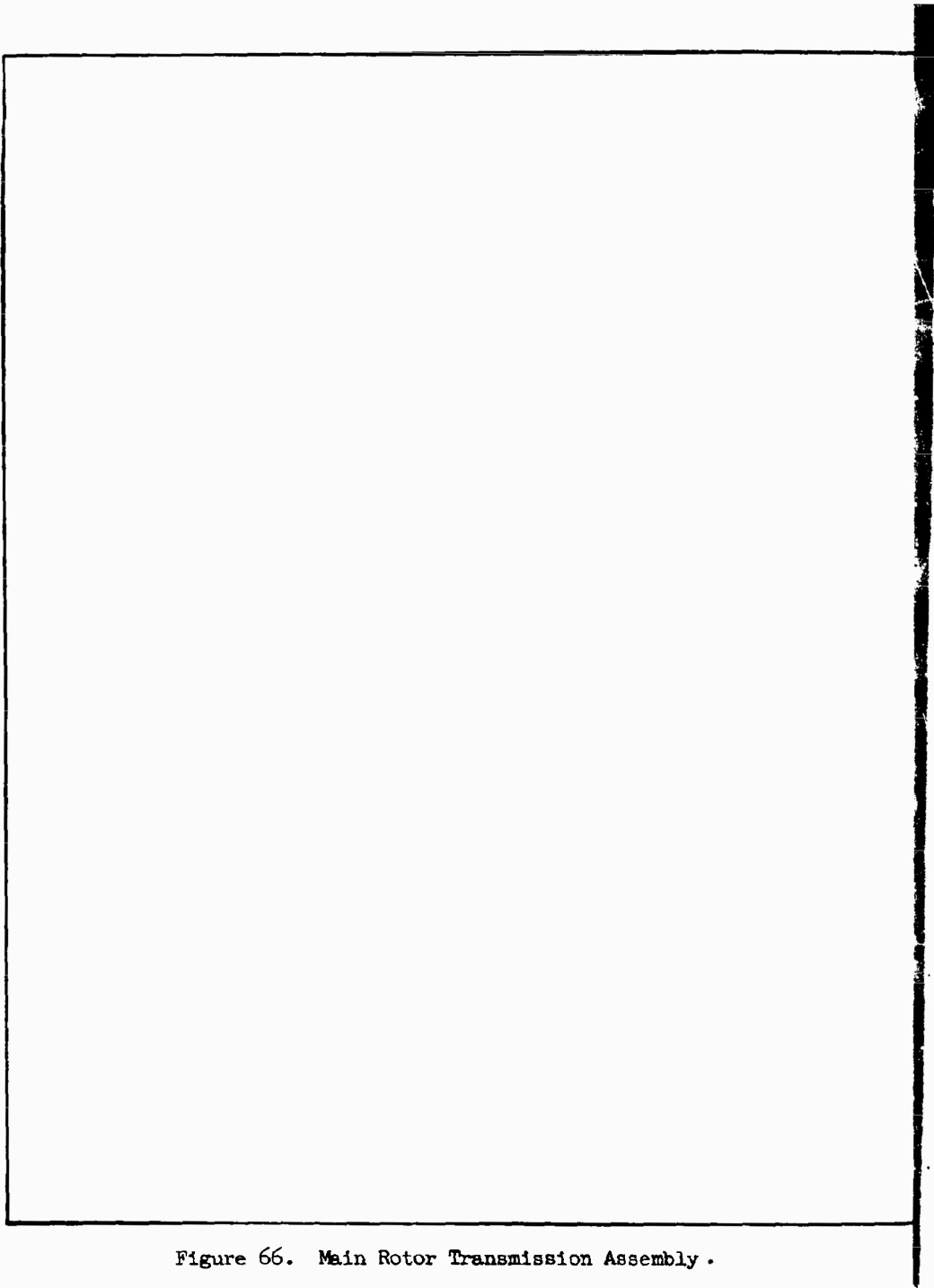
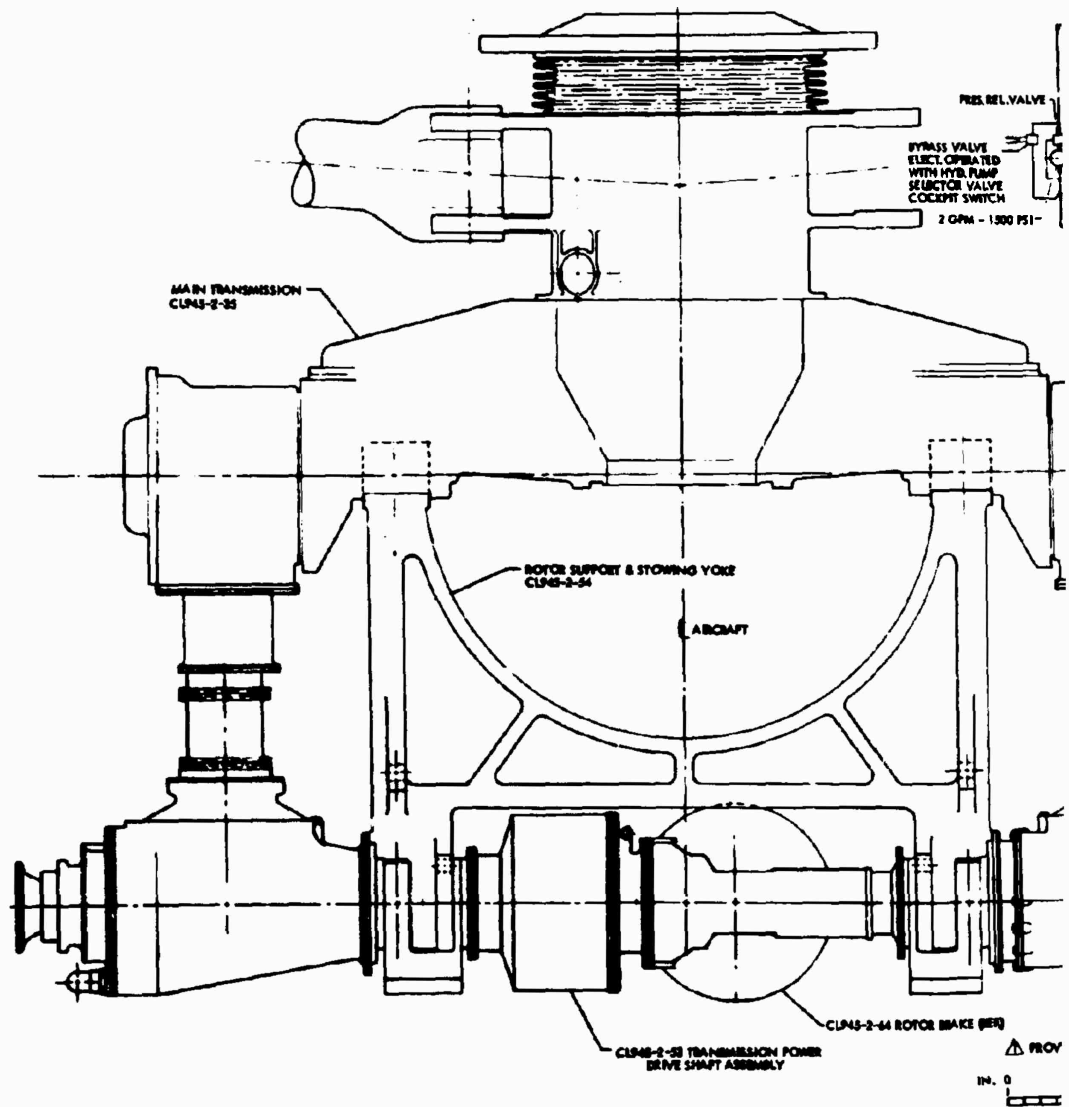
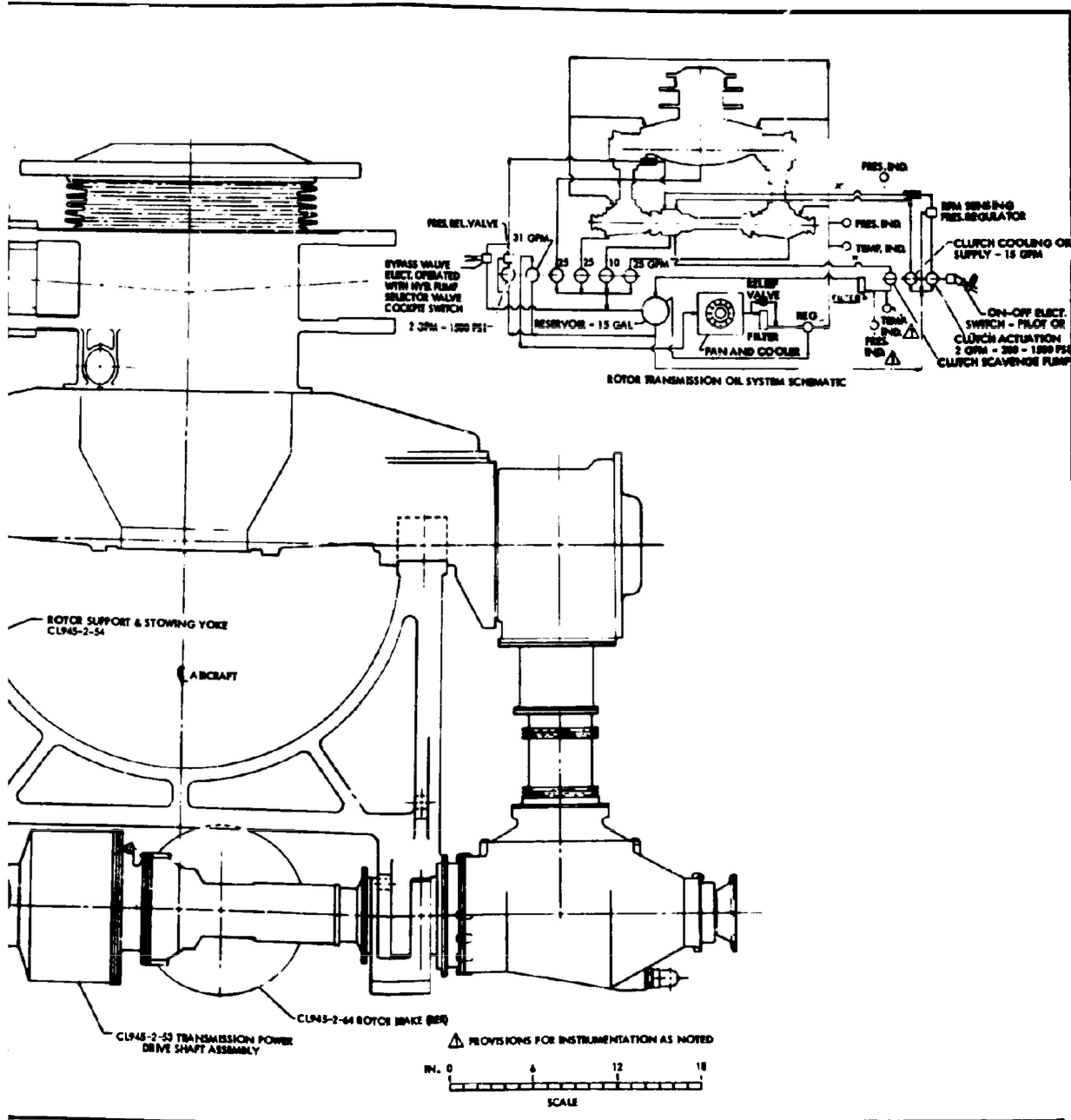


Figure 66. Main Rotor Transmission Assembly .



assembly .



Page Intentionally Left Blank

The power gear train within the transmission assembly is shown by the power transmission schematic, Figure 65.

The engine power cross shaft, running laterally in the nose of the wing, mechanically interconnects the engine power output shafts and combines engine power. This cross shaft passes through the lower transmission assembly, wherein hydraulically operated clutches engage the cross shaft. Dual power paths, laterally disposed, are used to transmit power to the upper transmission assembly, one-half rotor power in each path, and a clutch for each path. The speed reduction ratios in the transmission assembly are: total ratio from cross shaft to main rotor, 33.7; 1st bevel gear ratio, 1.35; 2nd bevel gear ratio, 1.60; 3rd bevel gear ratio, 1.45; spur gear stage, 3.53; and planetary gear stage, 3.00.

The tail rotor drive shaft is driven by a right-angle spiral bevel gearbox in the lower transmission assembly, with the drive pinion in the right-hand dual power path from the clutch to the upper transmission assembly. The driven gear drives through the wing beam to an accessory gearbox located on the aft side of the beam, and through the accessory box to the tail rotor drive shaft. The rotor brake is located on the accessory box output shaft. The tail rotor shaft coupling is a flexible diaphragm coupling.

The accessories mounted on, and driven by, the accessory gearbox are: transmission lubrication pressure and scavenging pumps; clutch actuating pumps; hydraulic pump for rotor flight controls; rotor tachometer generators; and rotor detent mechanism. The drive for the lubrication system oil cooler blower is located on the right-hand side of the lower transmission assembly, and it drives forward to the blower.

The power clutch between the engine cross shaft and the main transmission contains two complete clutch sections, one for each of the dual power paths to the upper transmission assembly. The clutches are hydraulically actuated, oil-cooled, axial wet clutches, with one sintered bronze disc in each clutch section. The clutch hydraulic system is combined with the transmission lubrication system, and they utilize a common oil tank. A separate pressure pump and a separate scavenge pump circulate cooling oil through the clutch when engaging the rotor power train; the scavenge pump discharges through a filter to the oil tank. The operation of the power clutch system is described in the Main Rotor Clutch paragraphs, which follow.

The lubrication system is a pressure system with oil spray nozzles at the gear meshes. A complete description of the system is given later, under the Lubrication System heading.

The bearings for all rotating gears and shafting are ball and roller bearings. The material of the bearing races and rolling elements is

specially processed steel for extra cleanliness and increased life. The material of the rolling element separators is silver-plated, heat-treated steel for extra strength and durability.

The gear material is case-hardened steel. The housing material is cast magnesium.

The rotor brake is a two-button disc type, with a master hydraulic cylinder for actuation.

Intermediate Gearbox

The intermediate gearbox transfers power from the wing shaft power takeoff to the tail rotor gearbox during the helicopter mode. Straddle-mounted spiral bevel gears with a 17:33 ratio are used to make an angular change and to reverse direction in the tail rotor drive shaft system. All housings are magnesium castings with steel bearing liners. The weight of the gearbox is approximately 55.6 pounds.

The gearbox is lubricated by means of a gear pump driven by a splined adapter on the output gear shaft. Oil is scavenged from the sump area and directed through a filter screen to the gear mesh and pinion shaft bearings. All remaining bearings are splash lubricated. The gearbox is cooled by directing air over and around the outer gearbox housings.

Tail Rotor Gearbox

During the helicopter mode, the tail rotor gearbox transfers power from the wing-shaft power takeoff, through the intermediate gearbox, to the tail rotor. Straddle-mounted spiral bevel gears, with a 16:55 ratio, are used to make a 90-degree angular change in the tail rotor drive shaft system. All housings are magnesium castings with steel-bearing liners. Duplication of details is used wherever possible. The weight of the gearbox is approximately 69.0 pounds.

The gearbox is lubricated by means of a gear pump driven by a set of 75:33 ratio spur gears off the output gear shaft. Oil is directed through a filter screen to both gear meshes and the output gear shaft bearings. All other bearings are splash lubricated. The gearbox is cooled in the same manner as the intermediate gearbox, with the tail rotor pulling additional air over the housing areas.

Main Rotor Clutch

The main rotor clutch is an integral component of the inboard main rotor drive cross-shaft transmission. The clutch is engaged by driving two pistons inward against a radial extension of the cross shaft. Each piston is torsionally coupled to a main rotor transmission drive bevel gear.

Description

The pistons are single-acting and coil-spring-biased toward the disengaged position. The piston is driven by a high-pressure lubricating oil supply, delivered through a carbon-ring, sealed, transfer spool between the piston shaft and outer casing. The piston friction surface has a direct deposition-sintered, bronze coating, contacting a plain, steel-bearing plate which, in turn, is coupled to the cross shaft.

Cooling oil is brought through the outer casing and directed to the back faces of the bearing plates. A network of axial feed ports of circumferential distribution passages and of radial grooving transports the cooling oil to the high-temperature areas of the contacting surfaces.

Operation

Clutch engagement is initiated by diverting fluid power from the high-pressure hydraulic system to a hydraulic motor which drives a three-element, lubricating oil pump. One element supplies cooling oil to the clutch at a rate of 15 gallons per minute at nominal pressure. Another element provides pressure oil to the piston actuation parts at a flow rate of 2 gallons-per-minute. Initial actuating oil pressure will be 200 psi; it will then be modulated to the steady-state pressure by a control valve which will monitor actuation-pressure based on rotor speed, so that the generated clutch heat load to the cooling oil will tend to be uniform throughout the engagement cycle. The third element of the oil pump will provide scavenging of the cross-shaft transmission assembly during the clutch engagement transient.

After the clutch is engaged, the supply of piston actuation oil will be furnished by a pump element located in the rotor transmission lubricating oil pump assembly, which is driven by the tail rotor drive shaft. At this point, the hydraulic motor will automatically stop driving the three-element pump. The cooling oil flow is not required when the clutch is fully engaged or disengaged and has no slip, and the scavenging function is provided by the basic transmission scavenging system.

Heat Load Requirements

Allowing for a rotor acceleration from zero speed to synchronous speed at 100-percent rotor speed, the energy dissipation in the clutch, due to the momentum transfer, is approximately 5,000 Btu. In addition, aerodynamic drag resistance during the acceleration is expected to add 1,000 Btu of clutch heat, resulting in a total of 6,000 Btu, or a design point of 3,000 Btu per clutch.

Clutch Type Selection

An external (dry) clutch is somewhat simpler to design and install, but the foregoing oil cooling results in an appreciable weight increase in the clutch in order to provide enough mass of metal to absorb the clutch heat rejection and transfer it to external cooling air. In contrast, building the clutch as an integral component of the main transmission, as is proposed here, facilitates oil cooling of the clutch, so that virtually all the clutch heat can be transferred to the oil system, resulting in lower weight and in reduction of thermally induced stresses.

The design engagement time strongly influences the size of the clutch. As the engagement time decreases, the time rate of heat loading increases, thereby requiring greater cooling-oil flow and increased heat transfer effectiveness to the cooling oil. Beyond a reasonable point, it becomes difficult to provide increased heat transfer to the oil without increasing the physical size of the clutch, and the balance of the heat load must be absorbed by the clutch metal. To ensure against possible clutch problems in the development phase of the rotor drive system, the design normal engagement time has been set at a nominally conservative value of 45 seconds. The clutch size should easily accommodate the 15 gallons-per-minute cooling-oil flow rate, which would then require a heat transfer effectiveness capable of raising the oil temperature about 40°F.

Steady Operation

Assuming that system vibration will prevent the attainment of an idealized static condition, the clutch is designed to transfer 125 percent of rated torque to the rotor, with a coefficient of friction of only 0.035. The required piston operating pressure is approximately 1,600 psi, of which approximately 400 psi is developed by the rotating column effect within the piston chamber. The nominal external oil supply pressure will be approximately 1,200 psi; however, lubrication system components are to be designed to increase this pressure to 2,000 psi for growth and contingency considerations.

Disengagement

Each piston chamber cavity is provided with an 0.030-inch-diameter continuous bleed hole near the outside diameter of the chamber. The clutch is disengaged by stopping the makeup oil flow to the piston chamber, thereby allowing the piston bias springs to pull the piston away from the cross-shaft driving surfaces.

Rotor Brake

The rotor brake is an air-cooled disc brake with two diametrically opposite, hydraulically actuated buttons. The buttons are self-adjusting, and the button displacement is the same for new or worn linings. The

brake is located on the tail rotor drive shaft, adjacent to the accessory gearbox, aft of the wing beam. Brake hydraulic pressure is supplied by the flight system's hydraulic pump, a valve modulating the pressure.

The brake is applied after the main rotor power clutch is released and rotor speed decays to 50 percent of normal speed (120 rpm). Full braking force is used until rotor speed decreases to 10 percent of normal speed (24 rpm). At this speed, the rotor brake pressure modulating valve operates in conjunction with the rotor detent mechanism to stop the rotor at the azimuth position required for blade folding. Full rotor brake pressure is applied when the rotor is at the desired position. The rotor hub stop is then engaged and the rotor brake pressure is released.

The rotor brake is sized for stopping the rotor system in 10 seconds for normal operation and in 4 seconds for emergency operation.

Tail Rotor Drive Shafting

The tail rotor shaft system consists of shafting, diaphragm couplings, bearing supports, ball spline coupling, intermediate gearbox, tail rotor gearbox, and tail rotor assembly and bearing support.

The tail rotor drive shaft, between the hydraulic accessory gearbox and the intermediate gearbox, is installed in three sections. A ball-spline coupling is mounted directly behind the first diaphragm coupling to absorb any axial movement. A single shaft is used between the intermediate and tail rotor gearboxes with a center bearing support. A diaphragm coupling joins the shaft to each gearbox by means of fixed curvic joints. To provide for angular misalignment, a slip spline is provided at the tail rotor gearbox to absorb axial movement.

A single shaft also connects the tail rotor gearbox and the tail rotor assembly. It is connected to the tail rotor gearbox with a diaphragm coupling and a fixed curvic joint to provide for angular misalignment. A slip spline is employed at the tail rotor bearing support to permit axial movement.

The tail rotor bearing support has an oil reservoir, filler plug, sight-level gage, and magnetic drain plug. The ball-spline coupling and the shaft bearings are grease lubricated. A minimum of 1,200 hours is required between servicing. Lubrication and description of the tail rotor and intermediate gearboxes are discussed later, in the Tail Rotor Drive System Lubrication paragraph.

DESIGN CRITERIA - TRANSMISSION SYSTEM

Structural Criteria

The following general structural criteria, in conjunction with the appropriate structural factors as defined in MIL-S-8698, are utilized for the transmission system.

External Loading Criteria

The following external loading criteria, as applied to the transmission system by the main rotor, tail rotor, and tail rotor/main propeller, are used:

- Maximum thrust
- Maximum gyroscopic forces in yaw, pitch, and roll combinations for normal rpm and for 116-percent rpm conditions
- Maximum moments in yaw, pitch, and roll combinations for normal rpm and for 116-percent rpm conditions

Inertia Load Factors

The inertia load factors for the various components of the power transmission system during flight, landing, and crash conditions are utilized to determine critical design conditions.

Drive System Criteria

Components comprising the power train are subject to the following design conditions or combinations thereof:

- Maximum design steady torque
- Maximum design transient torque
- Speed power spectrum, as applicable
- Starting and stopping loads
- Handling loads

Special Considerations

Listed below are the special considerations applicable to the power transmission system design:

- A dynamic factor of 1.25 is used in the engine/propeller, wing cross-shafting, and main rotor drive systems for the transient torque conditions.
- A dynamic factor of 1.33 is used in the tail rotor system for the transient torque conditions.
- Because of the high rpm values encountered, the cyclic stresses of all shafting and gearing during normal operation, coupled with the steady-state stresses, are kept below the notched fatigue strength of the material.

Dynamics Criteria

The following dynamics criteria, based upon experience at Lockheed and as defined in MIL-S-8692, are utilized for the transmission system:

- Drive shafting resonance is separated from any multiple of the product of the rotor/propeller speeds and the number of blades, with a minimum margin of 25 percent.
- The shafting critical whirling speeds are located at least 25 percent above the maximum operating range (normal rpm x 1.2 x 1.25).
- The system has a torsional natural frequency of at least 3 cycles per second.
- The drive system and the governing system of the powerplant are compatible.
- Failure in any one portion of the drive system will not cause resonance conditions in the remaining portions of the drive system.
- The coupling of the drive system to the airframe structure will not result in excessive vibration in either the drive system or the airframe.
- Transient torques due to normal engine accelerations and loads due to gusts will not produce excessive torque loads or oscillations.

Limit Torque/Shp Summary

The limit torque/shp values, as summarized on the following page, are noted in Table VIII. Starting and stopping torque conditions are not considered to be critical and were not included in the summary.

Power-Time Design Spectrum

The 1200-hour power-time design spectrum for the Composite Research Aircraft is shown in Table IX. This spectrum is derived primarily from data presented in the following external loads and power distribution paragraphs, and it is utilized as a basis for designing bearings in the transmission system.

DESIGN LOADS - TRANSMISSION SYSTEM

There are two principal sources of loads acting on the power train: the engine torque, and the external loads from the rotors and propeller. In addition to the principal loads, the power train is subjected to secondary loads arising from vibrations, misalignments, and deflections. These loads are considered in the analysis, and they are combined when this produces a more critical condition for both ultimate and fatigue conditions.

TABLE VIII. LIMIT TORQUE/SHAFT HORSEPOWER (SHP) SUMMARY - TRANSMITTER SYSTEM					
	Design Condition	shp	rpm	Torque (ft-lb)	Duration Note
Engine Output	Steady State	3900	13,600	1,520	3600 Hrs 1
	Transient Torque	-	-	1,900	5 Min 2
	Transient Overspeed	3900	17,000	1,215	15 Min 3
Propeller Drive	Steady State	3860	1,545	13,200	3600 Hrs 1
	Transient Torque	-	-	16,500	5 Min 2
	Transient Overspeed	3860	1,925	10,550	15 Min 3
Wing Gearbox Cross Shaft	Steady State	2550	8,000	1,675	3600 Hrs 1
	Transient Torque	-	-	2,095	5 Min 2
	Transient Overspeed	2550	10,000	1,340	15 Min 3
Main Rotor Drive	Steady State	4500	240	98,500	3600 Hrs 1
	Transient Torque	-	-	123,000	5 Min 2
	Transient Overspeed	4500	300	78,800	15 Min 3
Tail Rotor Drive System (Input to Tail Rotor System)	Steady State	450	6,900	394	3600 Hrs 1
	Transient Torque	-	-	524	5 Min 4
	Transient Overspeed	450	7,500	315	15 Min 3
Notes:					
1. System is designed to withstand the steady design shp at 110 percent rpm continuously					
2. Represents design limit torque and is equal to 1.25 times the mean torque for maximum continuous power					
3. Represents design steady shp at 125 percent rpm					
4. Represents design limit torque and is equal to 1.33 times the steady torque					

TABLE IX. CRA TRANSMISSION SYSTEM - 1200-HOUR POWER-TIME DESIGN SPECTRUM (CONSTANT RPM)										
Condition	Time		Eng rpm	System Shaft Horsepower (shp)				Rotor	Tail Rotor	Remarks
	%	hr		Engine	Prop	Access- series				
Hover	5	60		2625	75			4500	450	
$V_{20K} - V_{140K}$	5	60		1875	550			2250	225	$V_{140} = \text{Transition}$
$V_{140K} - V_{250K}$	10	120		1280	1230					
V_{cruise}	40	480		1280	1230					$V_{\text{cruise}} = 225 \text{ knots}$
$V_{250K} - V_{350K}$	10	120		3100	3050					
V_{max}	10	120		3860	3830					$V_H = 380 \text{ knots}$
Climb	6	72		2625 3860	75 3830			4500	450	HR <u>A/C Condition</u> 5C <u>VTOL Mode</u> 22 Fixed Wing
Steady Descent	4	48		1400	75			2250	225	
Maneuvers	5	60		2625 3100	75 3050			4500	450	HR <u>A/C Condition</u> 30 <u>VTOL Mode</u> 30 Fixed Wing (V_{350})
Start/Takeoff Landing	5	60		0-2625	0-75			0-4500	0-450	
	100	1200								

External Tail Rotor Loads

Figures 67 and 68 define the tail rotor loads for the normal hover conditions.

Power Distribution

The power distribution criteria as utilized for design of the CRA transmission system loads are presented in this section (see Table X and Figures 69, 70, and 71).

Shaft Horsepower/Torque Design Input Power

The CRA power transmission system has been structurally designed to accommodate an installed engine output capability at the following conditions:

59°F, Sea Level

Shaft horsepower = 3900
Torque = 1520 ft-lb (steady)
Output shaft rpm = 13,600 (normal rated)
Output shaft rpm = 17,000 (maximum)

95°F, 6,000 Feet

Shaft horsepower = 2650
Torque = 1020 ft-lb (steady)
Output shaft rpm = 13,600 (normal rated)
Output shaft rpm = 17,000 (maximum)

Shaft Horsepower Distribution

Table X defines the structural design shaft horsepower distribution for both the helicopter and fixed-wing modes.

Supercritical Operation

As an alternative configuration, a super-critical shaft installation has been considered for the tail drive shaft. This configuration would have a damped elastic bearing located 21 inches from each end of the 345-inch-long shaft and would operate between the seventh and eighth critical modes. Computer results, using the program described in the preceding paragraph, indicate that with damping at the bearing of 1 lb/in./sec and a bearing support stiffness of 100 lb/in., the shaft could operate at all critical speeds safely. This type of drive has been used successfully on the Breguet aircraft, and it has advantages such as elimination of the large number of bearings required and the relaxation of balance requirements.

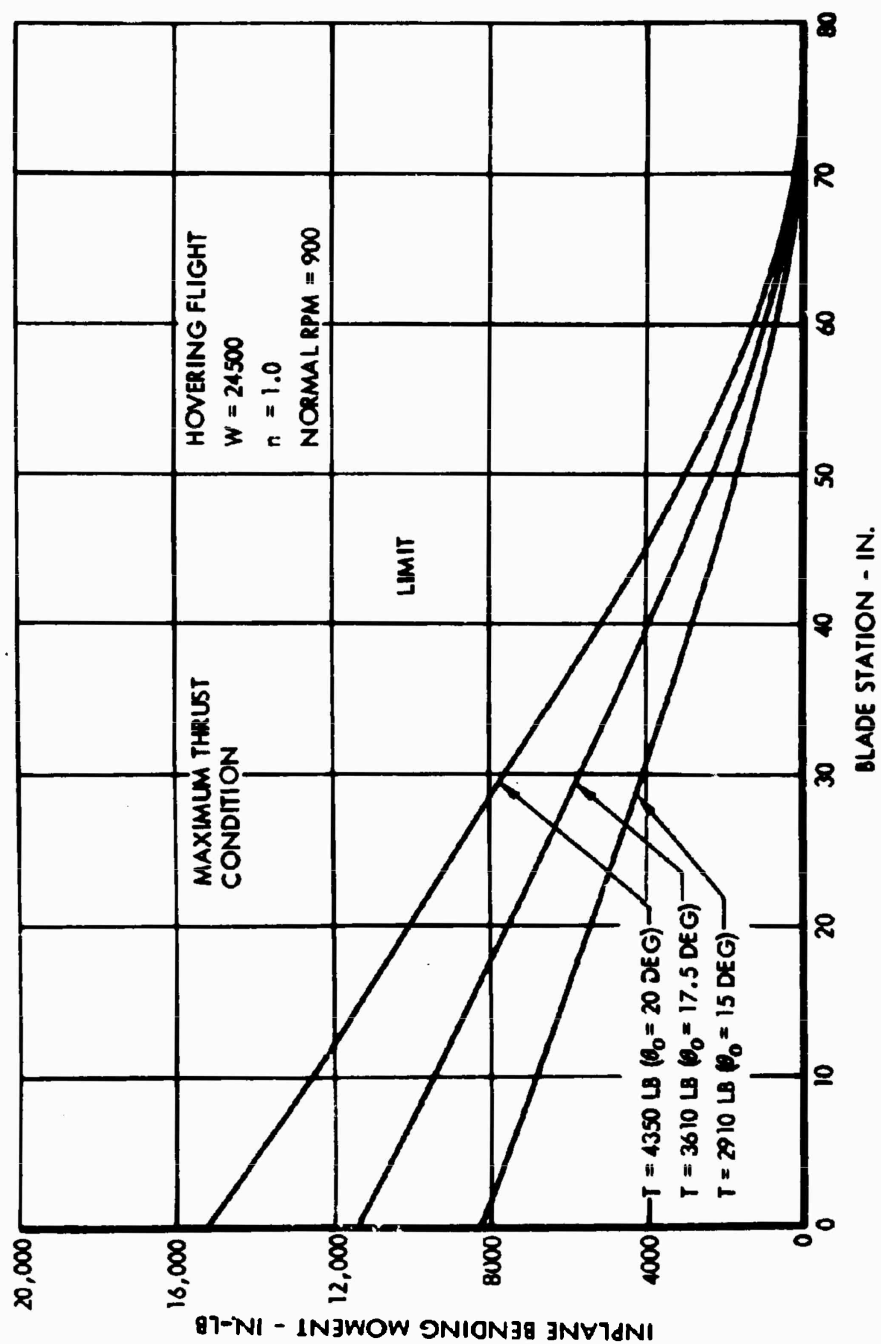


Figure 67. Tail Rotor In-plane Bending Moment-Maximum Thrust.

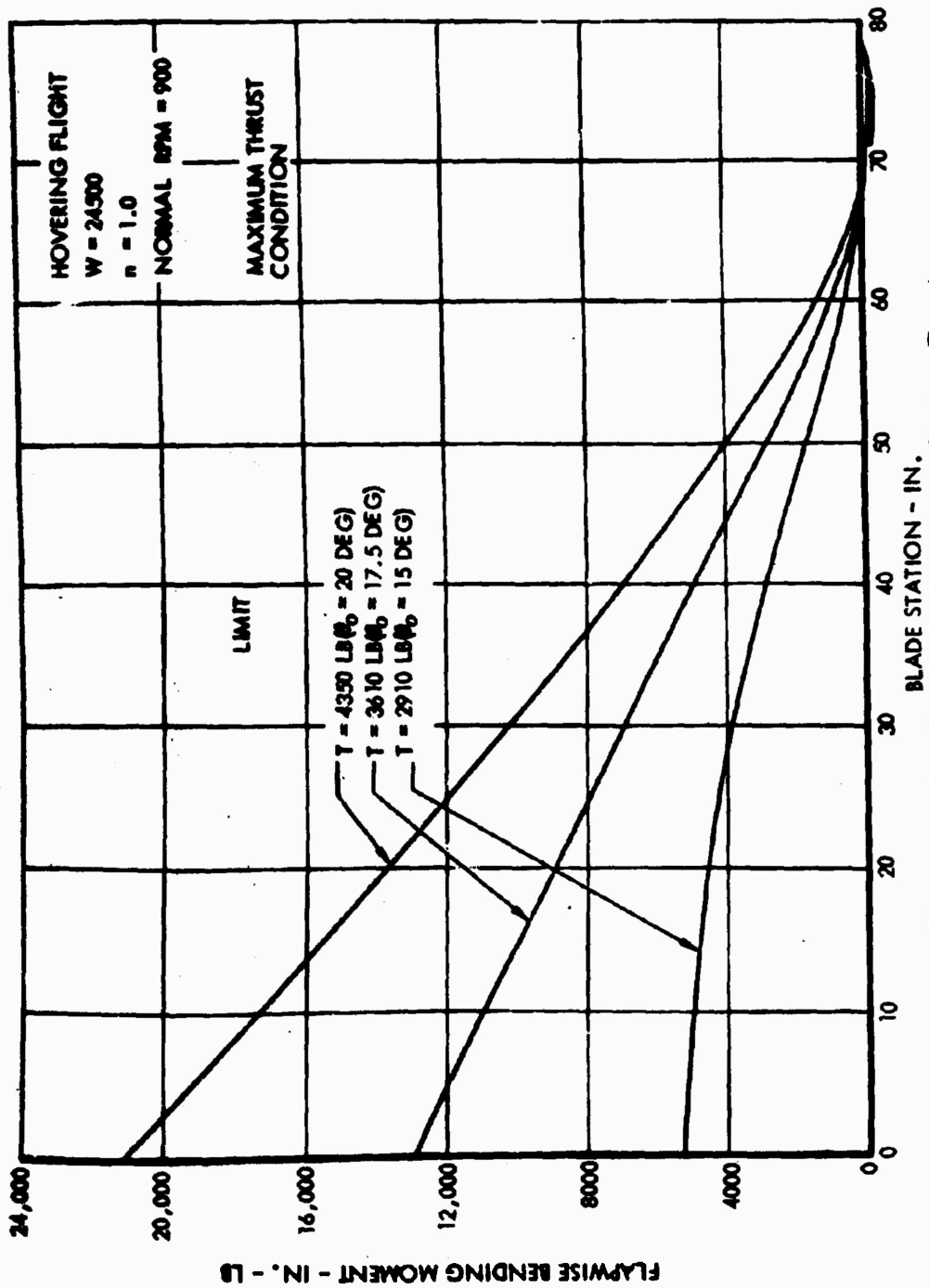


Figure 68. Tail Rotor Flapwise Bending Moment-Maximum Thrust.

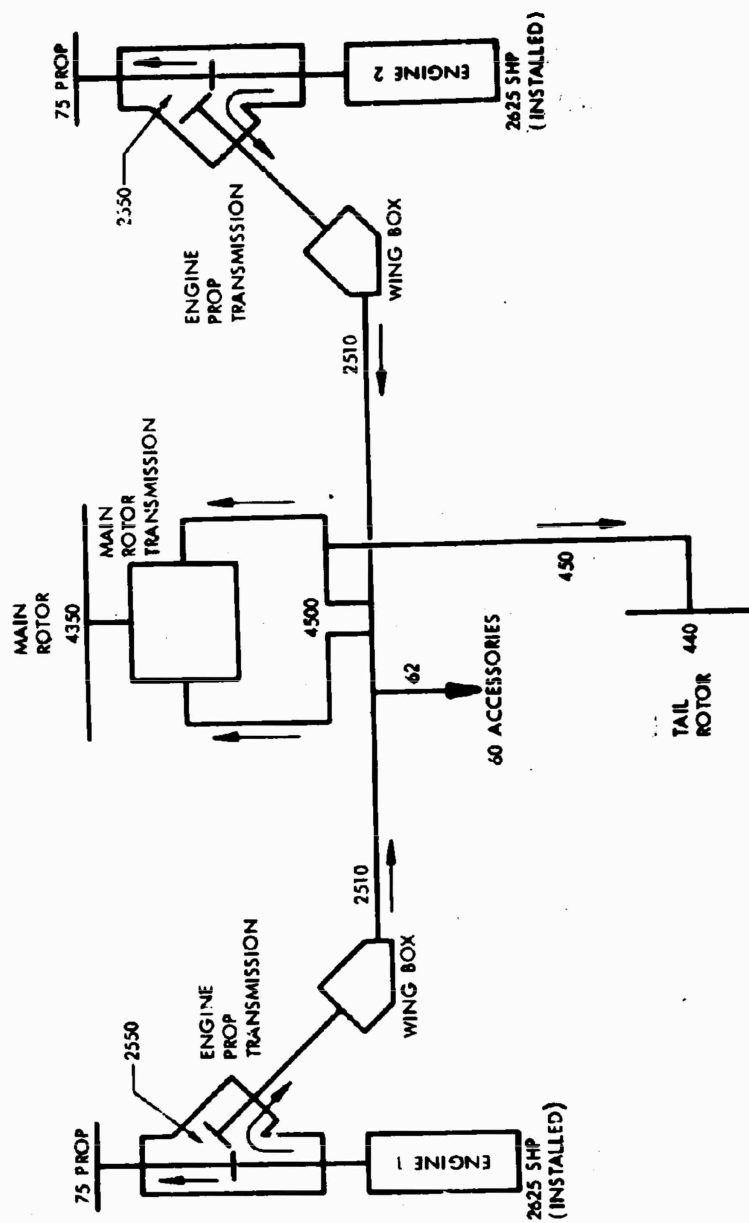
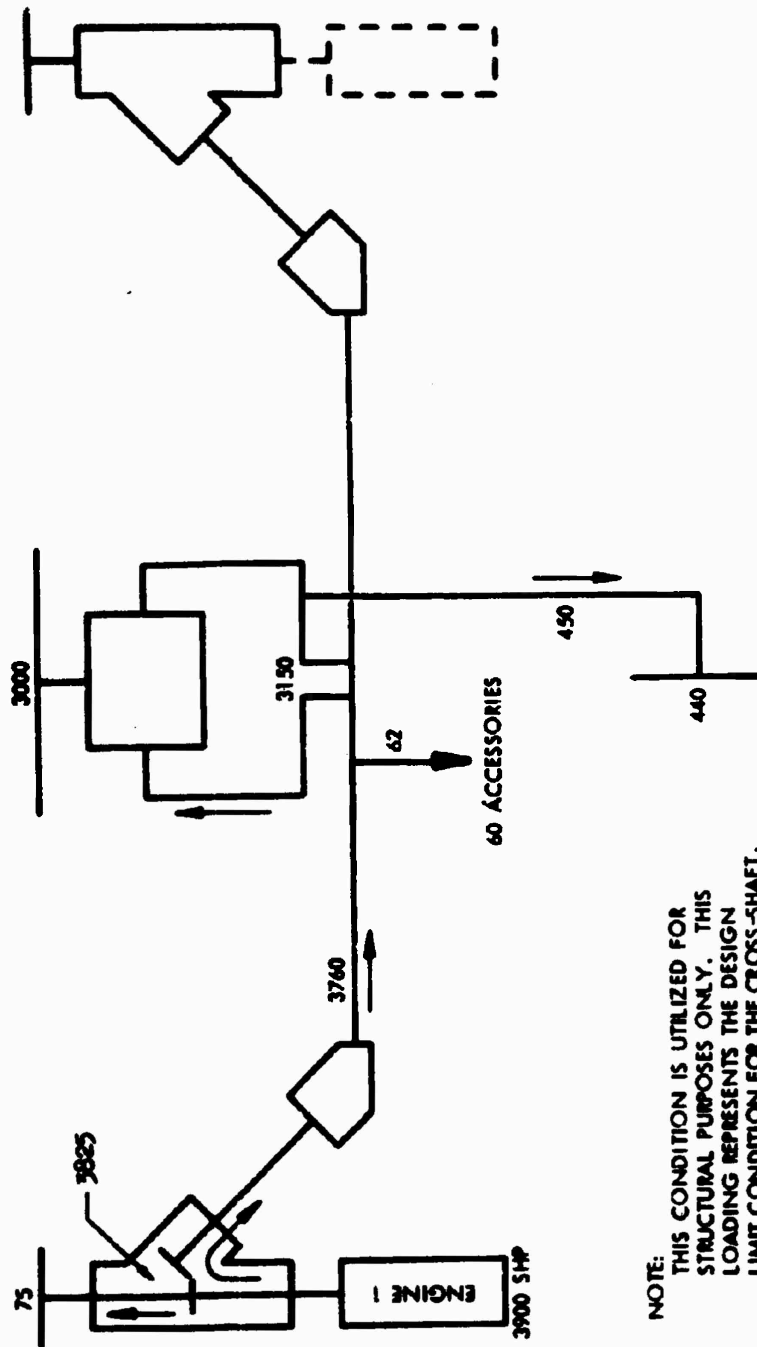


Figure 69. Power Transmitted, Hover/VTOL Mode.



NOTE:
THIS CONDITION IS UTILIZED FOR
STRUCTURAL PURPOSES ONLY. THIS
LOADING REPRESENTS THE DESIGN
LIMIT CONDITION FOR THE CROSS-SHAFT.

Figure 70. Power Transmitted, Hover/VTOL Mode - Emergency .

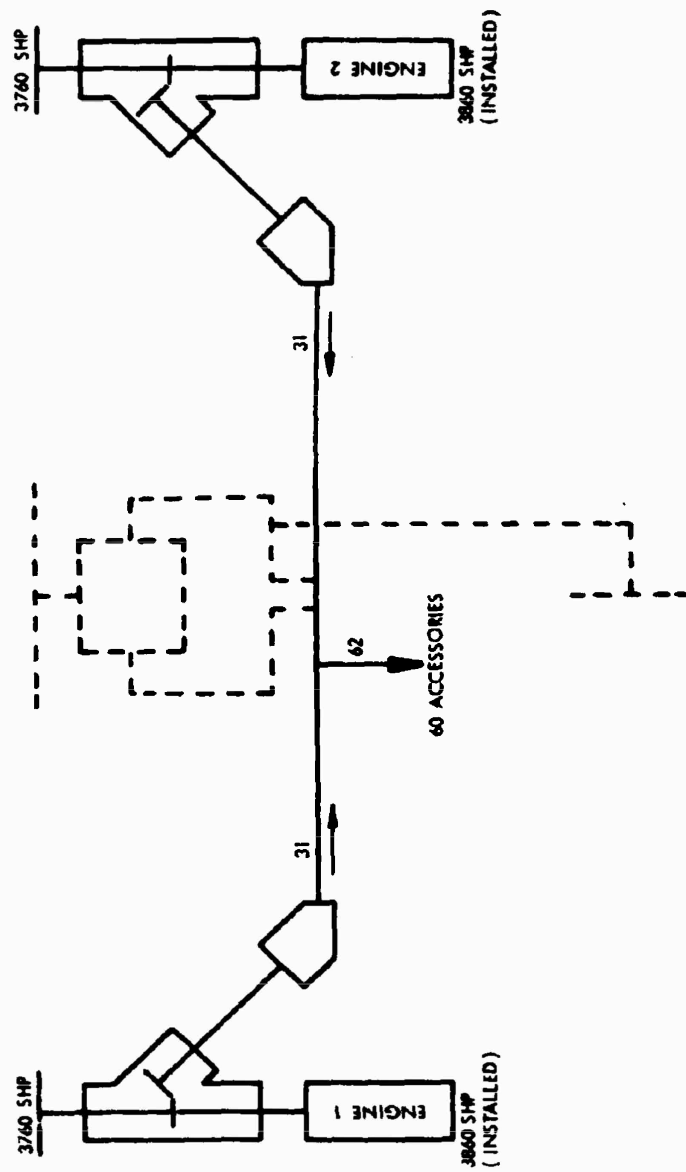


Figure 71. Power Transmitted, Fixed-Wing Mode.

TABLE X. SHAFT HORSEPOWER (SHP) DISTRIBUTION			
Component	Helicopter		Fixed Wing
	Hover Sea Level (SL) Std Day	Hover 6,000 ft at 95°F	SL Std Day
Main Rotor	4350	4350	0
Tail Rotor	440	440	0
Two Propellers	150	150	7520
Drive System Losses	250	250	140
Accessories			
Lubrication	5	5	5
Transmission Cooling	15	15	15
Electrical	15	15	15
Hydraulic	15	15	15

Engine Control Stability

An estimate of the stability of the engine and fuel control system, when it is connected to the mechanical rotor drive system, has been made by comparing the CRA drive system with that of the AH-56A, which is known to be stable. Since the natural frequencies of the CRA drive system are equal to or greater than those of the AH-56A, and since the effective mass of the system relative to the engine is greater than for the AH-56A, it is concluded that the system has a better stability margin than the AH-56A. A more detailed analysis will be performed in the detail design stage.

LUBRICATION SYSTEM

Main Transmission Lubrication System

The main transmission lubrication system consists of an engagement system and a sustained-operation system. Each of these two systems is in turn composed of an oil pressure supply system and an oil scavenge system. The overall system is shown schematically in Figure 72.

The engagement system is driven by a hydraulic motor, prior to starting the rotor. This system contains three pumps as shown in Figure 72.

The engagement system hydraulic motor receives hydraulic oil, under pressure, from the main aircraft hydraulic system. Hydraulic oil to the motor is controlled by an electric dump valve actuated by a three-position switch on the pilot's panel.

The sustained-operation lubrication system contains two pressure pumps and four scavenge pumps. These pumps are all driven by the output side of the main rotor drive. When the rotor is stationary, the pumps are inoperative. When the rotor is brought up to operating speed, however, the pumps perform all transmission lubrication functions.

Tail Rotor Drive System Lubrication

The tail rotor drive system consists of two gearboxes: one at the base of the fin, which changes the direction; and one at the base of the horizontal stabilizer, which changes the direction and speed. The lubricating features of these two gearboxes are similar. The gears run in an oil bath, and a pump is provided in each gearbox to assure positive lubrication.

Each box is vented and equipped with a filler neck and sight gage. The sumps are fitted with magnetic chip detectors. Cooling is provided by convection and radiation.

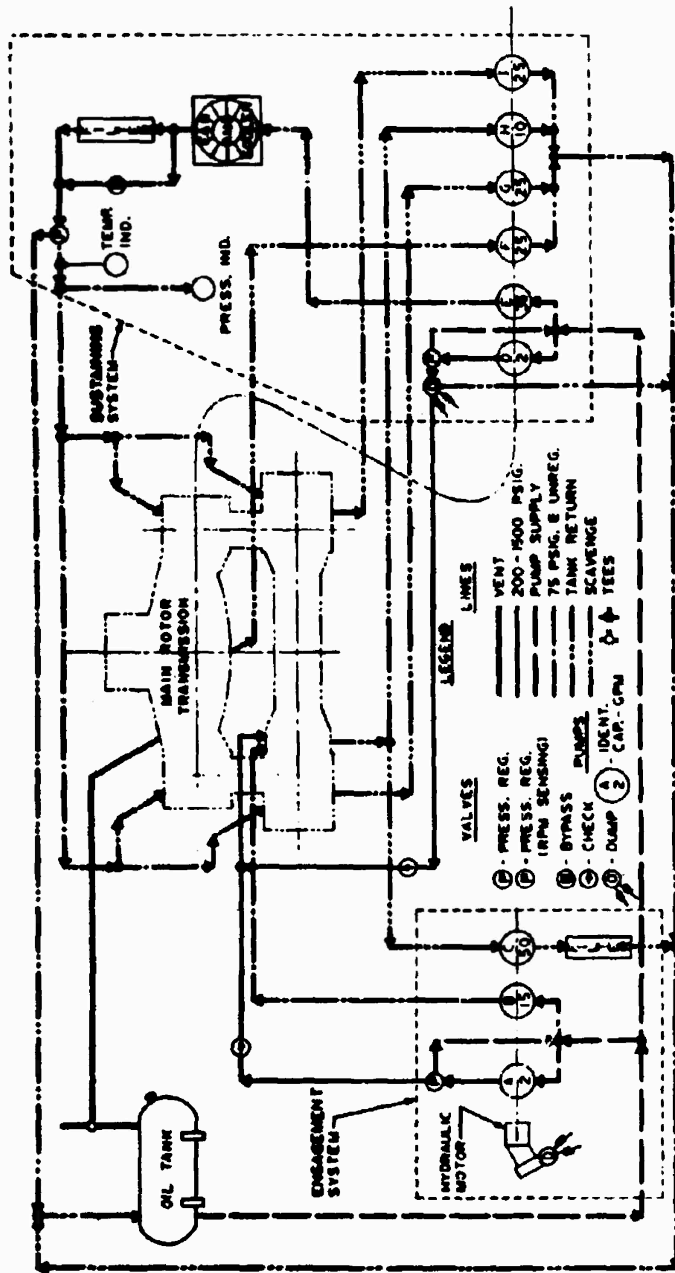


Figure 72. Main Transmission Oil System Schematic.

SECTION 7
VERTICAL LIFT SYSTEM

MAIN ROTOR

In the evaluation of the rotor design, the initial selection of rotor diameter was influenced by the desire to minimize the stowage problem, by using the smallest possible diameter. The study ground rule of 10-pounds-per-square-foot maximum disc loading led to an initial selection of 56 feet as the rotor diameter.

A limited parametric study was then performed to optimize solidity and tip speed. Holding constant rotor diameter, solidity (σ) and tip speed (V_t) were varied. Beginning with an assumed gross weight, main rotor horsepower and rpm were calculated. Then the weight of the main rotor and main transmission could be calculated. Several iterations were required in order to converge on a final gross weight and horsepower required for each combination of σ and V_t .

Three different assumptions were made as to the effect, on the remaining empty weight, of variations in gross weight due to changes in rotor and main transmission weight. The results of the three assumptions were plotted. Comparison of the plots showed that while the variation of remaining empty weight was very important to the absolute values of horsepower required and gross weight, the trends of horsepower and gross weight variation with σ and V_t were largely independent of the assumption. Consequently, this simplified parametric study could be used with confidence to select a best combination of σ and V_t , although it could not be used to predict absolute values of horsepower and gross weight. One of these plots is presented in Figure 73.

With the objective of minimizing both gross weight and horsepower required, the plots were studied to select a best combination of σ and V_t . Solidities above 0.09 involved some difficulty in stowing the blades in the fuselage because of the higher blade chord. With this in mind, a σ of 0.085 and a V_t of 750 feet per second were selected.

A parallel study showed that a divergence speed above 165 knots could be obtained for any of the σ and V_t combinations of interest, by the proper selection of blade root thickness and spanwise thickness taper. Later in the evaluation of the design, it became evident that the horsepower requirements of a 56-foot rotor were not compatible with available powerplants. The rotor diameter was increased to 60 feet. Divergent speed was held above 165 knots by increasing the blade root thickness. It was not necessary to repeat the σ and V_t optimization study, as it was essentially a rotor figure of merit or profile power optimization, and the change in diameter was principally a change in induced power.

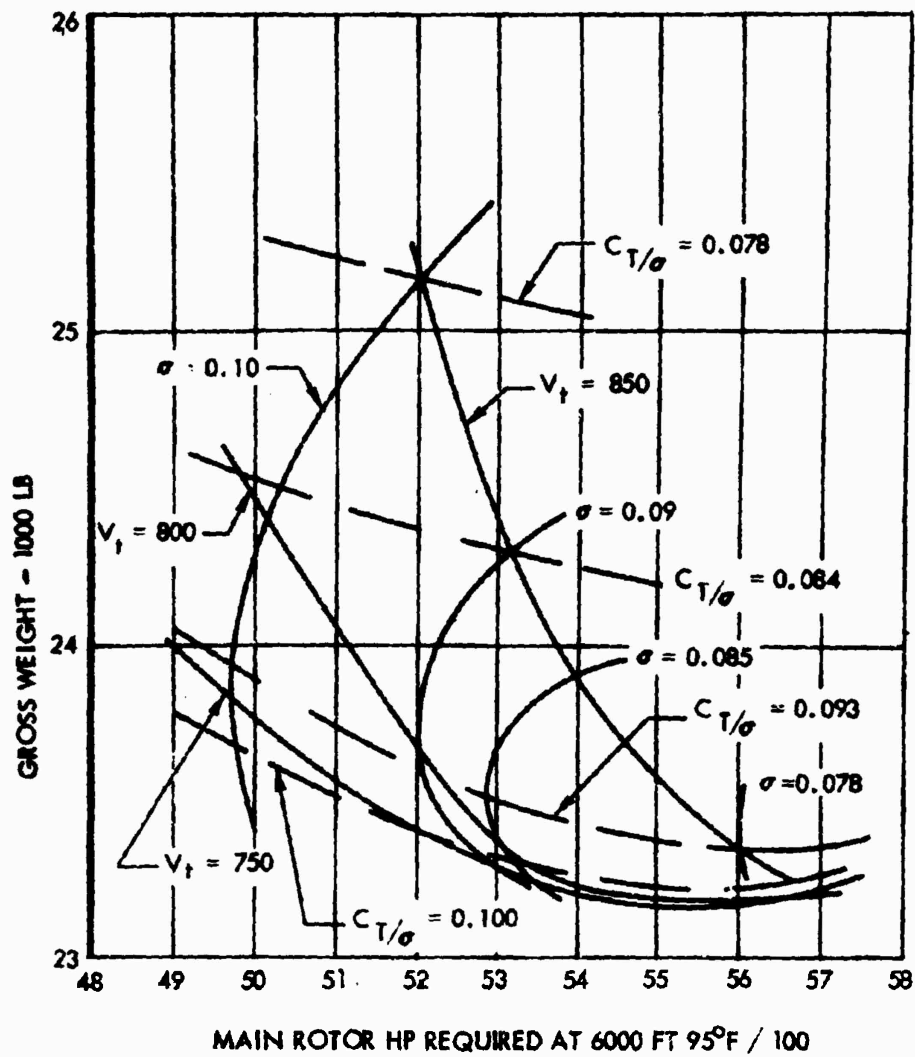


Figure 73. Rotor V_t and σ Optimization Map.

The final configuration resulting from this analysis is a three-blade rotor incorporating the features of the gyro-controlled rigid rotor, as well as the design details of the rotor stopping and blade folding development mode. This 33-foot-diameter stopped rotor was tested successfully in the NASA-Ames 40-foot by 80-foot wind tunnel, and will subsequently be tested in flight. The basic structural, dynamic, aerodynamic, and control characteristics, which were proven during this investigation, have been retained and are incorporated in the CRA main rotor design.

Rotor Blades

There are two fundamental considerations in the design of the CRA rotor blades. The first is that when the rotor is slowed down or stopped in flight, centrifugal forces no longer act to stiffen the blades. In this case, the blade strength and dynamic properties must permit blade divergent speeds of the stopped rotor under gust conditions that satisfy allowable velocity requirements. The second consideration is a relaxation of normal rotary-wing requirements in that maximum flight speeds as a helicopter are not necessary. Problems associated with high Mach tip-speed ratios and retreating blade stall are considerably reduced by the unloading of the main rotor and by the relatively low speeds required by transition.

For many years, it has been customary to design blades for convenience of manufacture, resulting in rotor blades having uniform mass stiffness distributions. As a result, the second mode natural-flapping frequency has been near the 3-per-revolution forcing function. However, the design of this blade is such that the second flapwise frequency is well above the 3-per-revolution function without resorting to anti-node weights. The relation between the blade natural frequencies and excitation frequencies is shown in Figure 74. The selected natural frequencies for the significant modes of blade motion fall between major excitations, thus avoiding resonance effects. Another feature of this rotor design is that the rotor energy is sufficiently high that no tip weights are required for autorotative flare.

The main rotor blade is shown in Figure 75. The blade has a constant 32-inch chord and a linear taper in thickness from an NACA 63A 021 section at 20 percent of radius, to an NACA 63A 010 section at the tip. The leading edge spar is one continuous piece of stainless steel from the spindle to the blade tip. This method of construction eliminates major structural joints in the blade.

Outboard of Station 110, the spar is opened at the rear and a doubling channel is added to close the D section. The enclosed area is filled from the spindle to Station 270 with polyurethane foam. This foam has a density of 8 pounds per cubic foot. Outboard of Station 270, the spar is hollow. The aft portion of the blade contour is filled with aluminum alloy honeycomb. The trailing edge is laminated of four 0.010-inch stainless steel strips. An outer skin of 0.010-inch stainless steel covers the

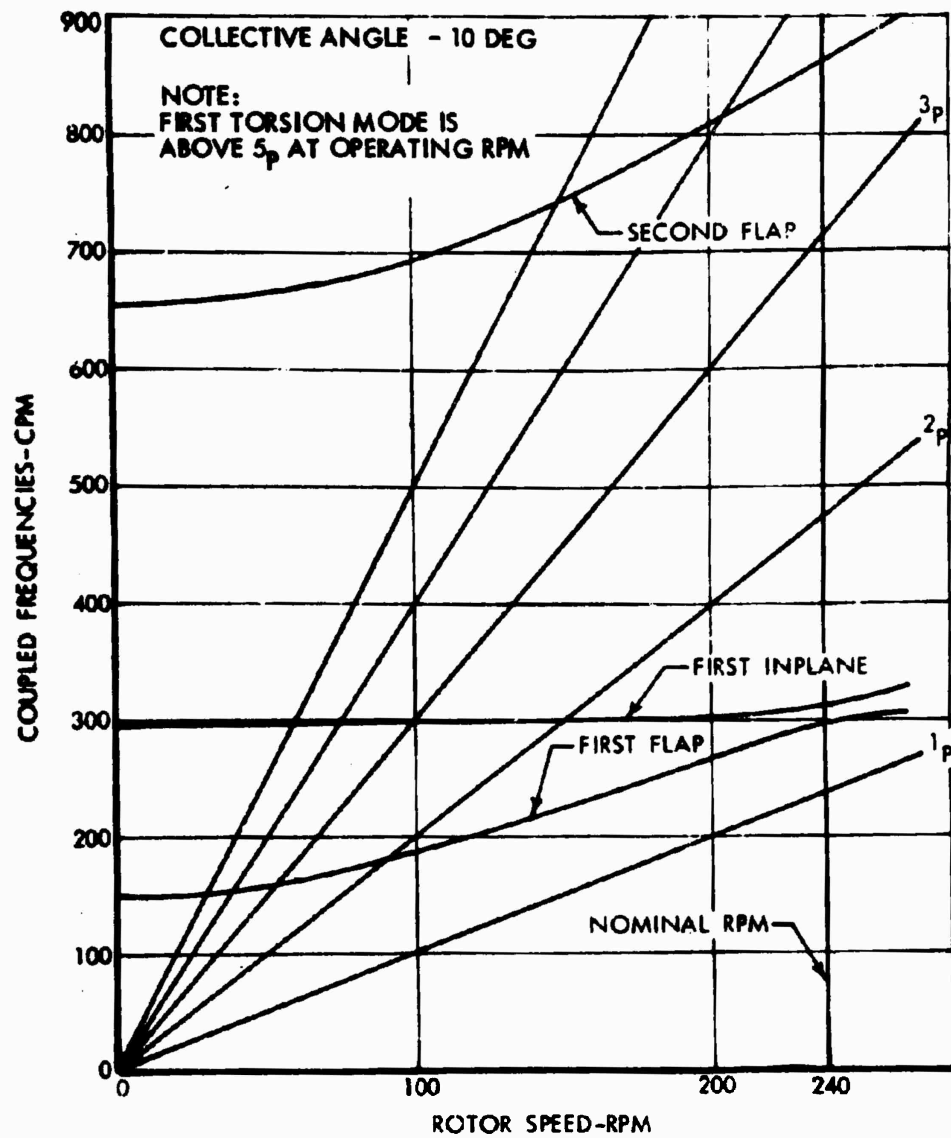


Figure 74. Main Rotor Blade Coupled Frequency Spectrum.

entire blade structure. The blade is balanced about the quarter chord point from Station 180 to Station 360 by locating a stainless steel balance strip against the inside leading edge of the D spar. This strip is safety-secured with monel rivets near the blade tip. An abrasion shield of 0.050-inch polyurethane is provided for the leading edge area from Station 240 to Station 360. The root and tip closure ribs are stainless steel and form the caps to areas which can be filled with ballast for finish blade balancing.

The spindle portion of the spar, which constitutes the inner shaft for the feathering needle bearings, is threaded on the inboard end for the blade retention fixture. This fixture also retains the pitch horn, which is splined to the spindle. The proposed rotor design contains only two structural joints per blade, and one of these joints is coincidental with the feathering bearings.

The rotor hub structure is a one-piece, tubular shaped, alloy steel member. It has a 15-inch inside diameter at the upper end and is reduced to a 9-inch inside diameter at the lower end. There, it is attached to the rotor drive transmission. This permits the control swash plate and pitch control linkage to be mounted integral to the rotor hub. The gyro-drive gearbox and swash plate mounts are supported from the upper surface of the hub as shown in Figure 66. A flexible oil seal boot is attached to the top of the hub to allow the gyro to tilt or precess and also to accommodate vertical motion resulting from collective pitch changes. The three-blade, pitch change, bellcrank bearing supports are integral with the hub tube structure. These bearings also contain rotary oil seals. The lower end of the hub interfaces with the transmission at a set of bearings and spline fittings that drive the rotor. An annular flange, located on the hub, interfaces with the upper end of the transmission to form an oil-seal face, and it serves to strengthen the hub at the bellcrank bearings. This flange also has a local extending lug that mates with the stopped rotor positioning or index pin, which is hydraulically extended up from the transmission case. The control system components located inside the hub are lubricated by the same oil-circulating system that supplies the transmission. An oil pan, located at the bottom of the transmission, also serves as a mounting pad for all of the hydraulic actuators.

Accessibility

Access to the control system components located within the hub is achieved by simply removing the gyro and seal boot at the top of the hub, removing the pins at the three gyro control rods, and then removing the gyro gearbox. The control support unit and central housing can be lifted out of the hub, exposing the blade pitch bellcranks and the blade-folding hydraulic fittings. The lower transmission cover, or oil sump, has a cover plate at the bottom to permit access to the swash plate input control linkages. All five hydraulic control actuators are face-mounted to the lower transmission case for easy removal. The rotor indexing lock-pin cylinder is an integral

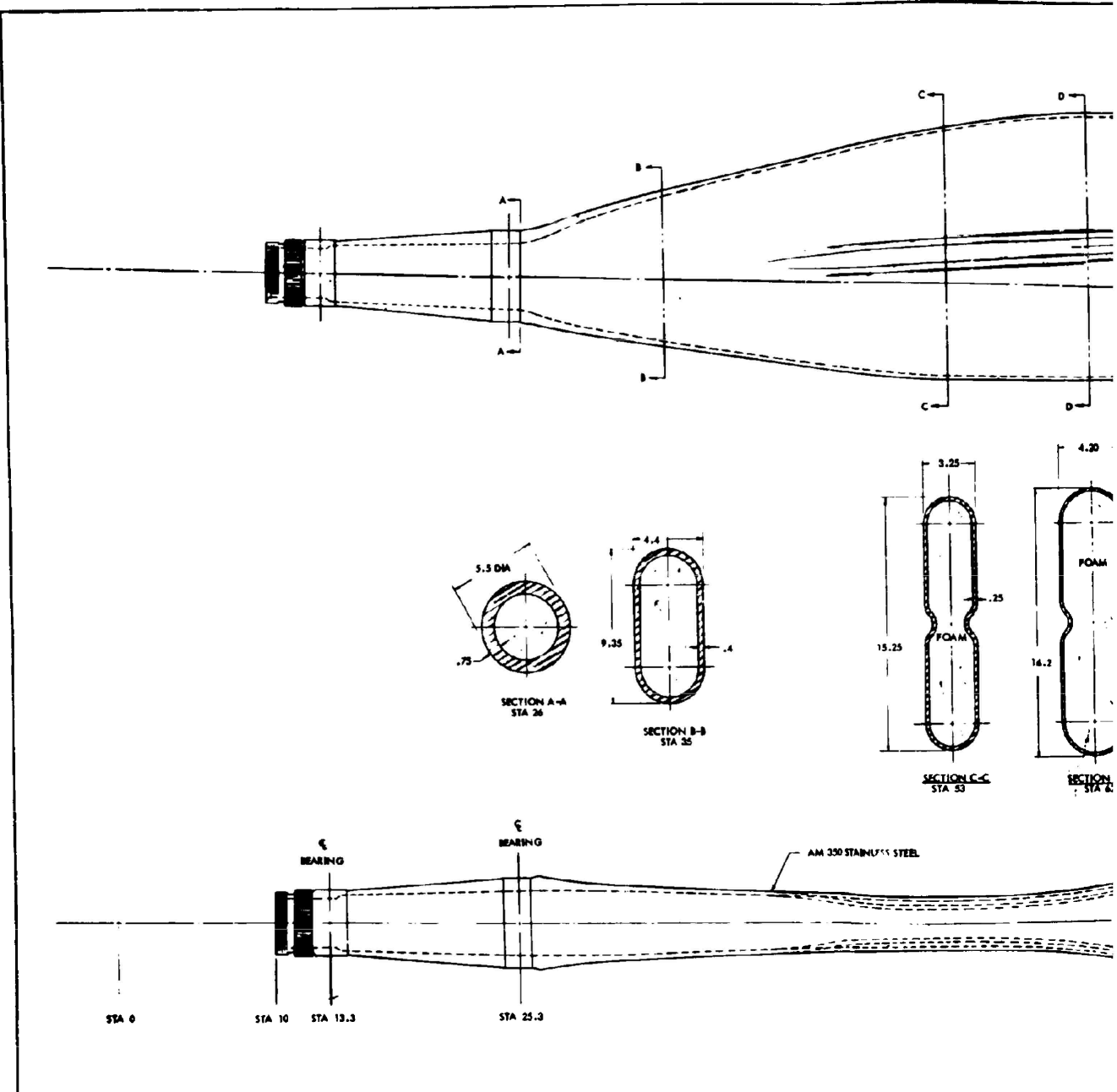
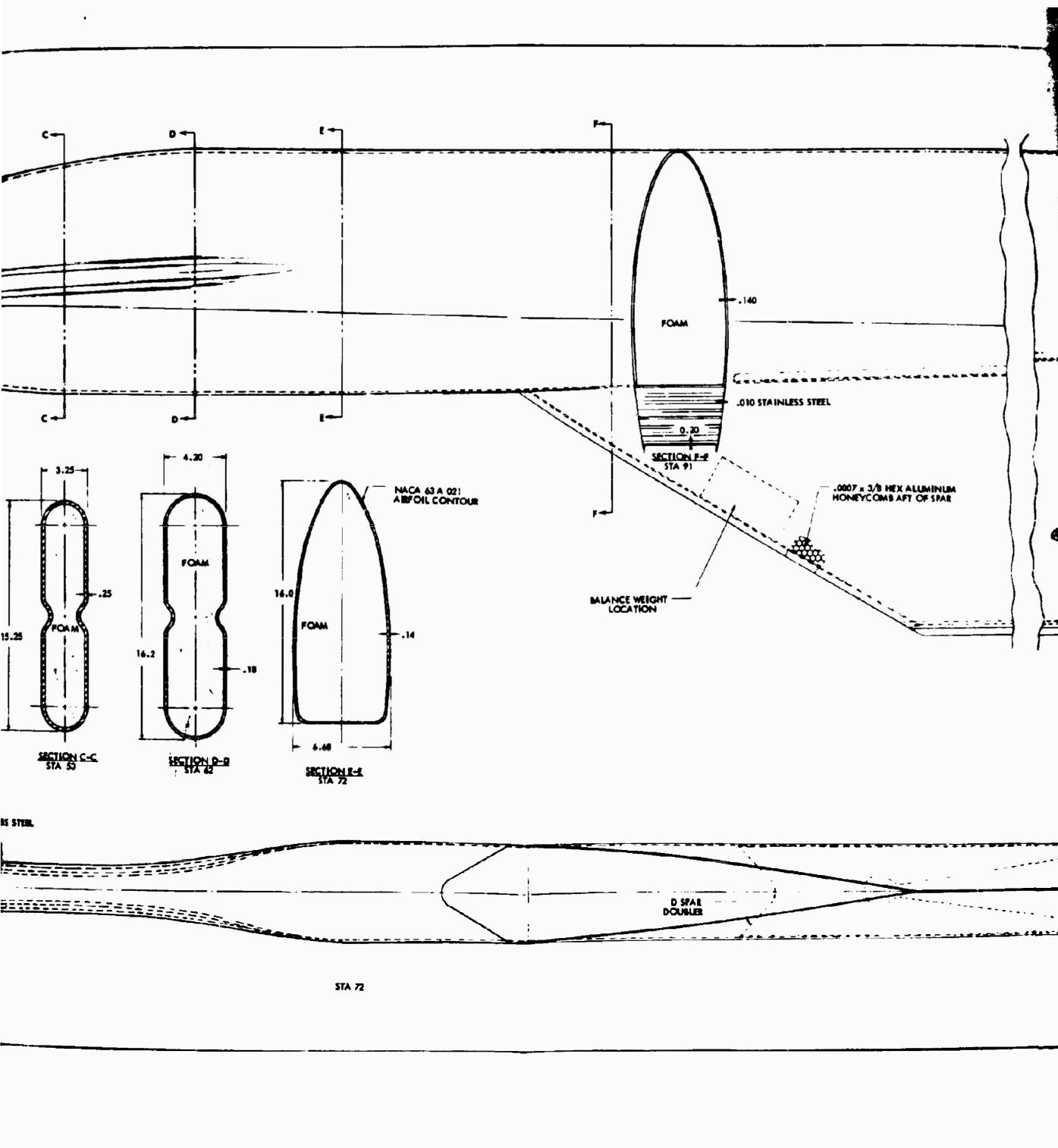
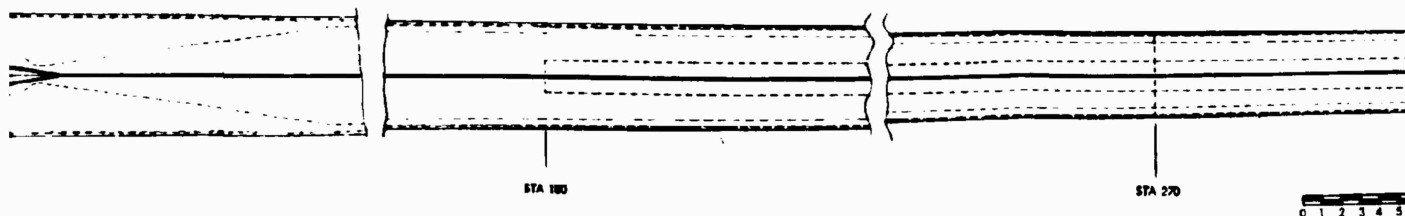
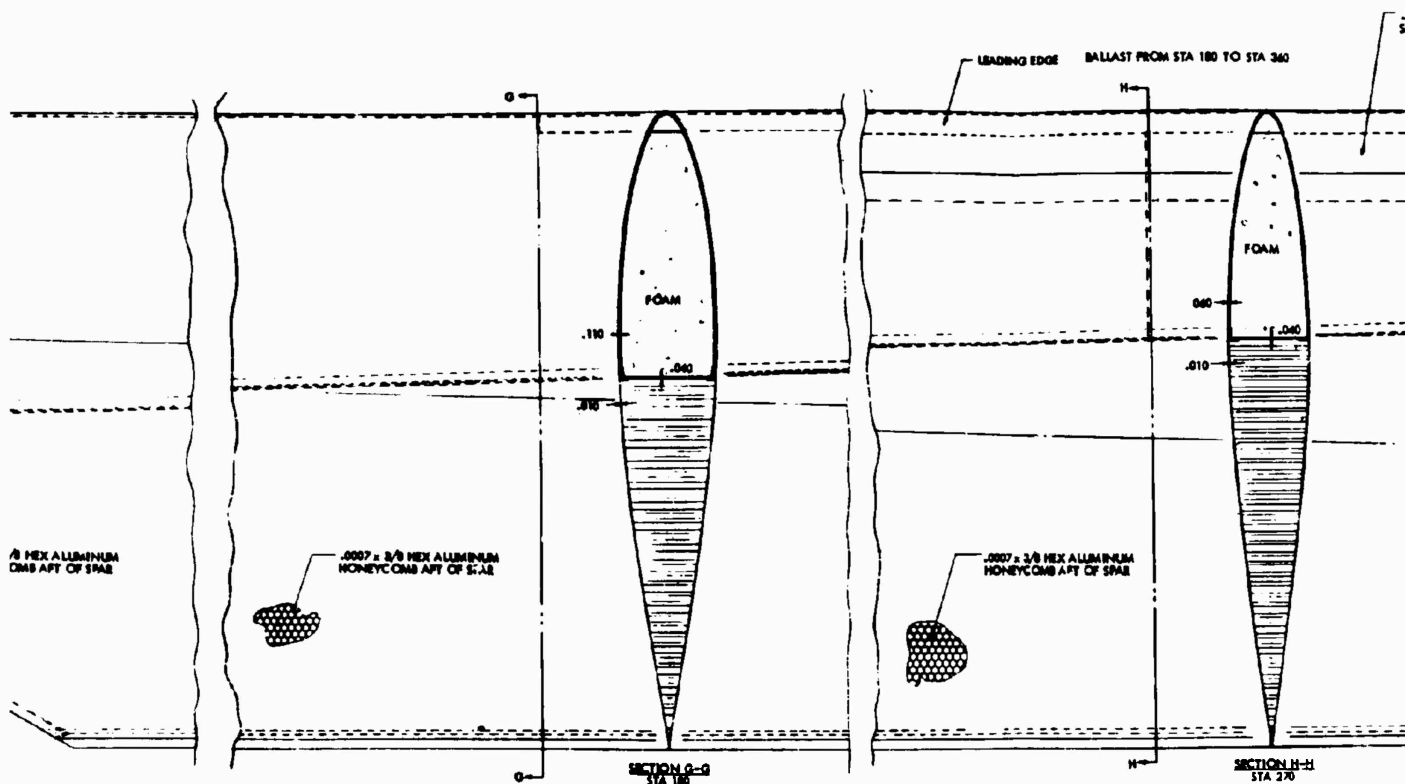
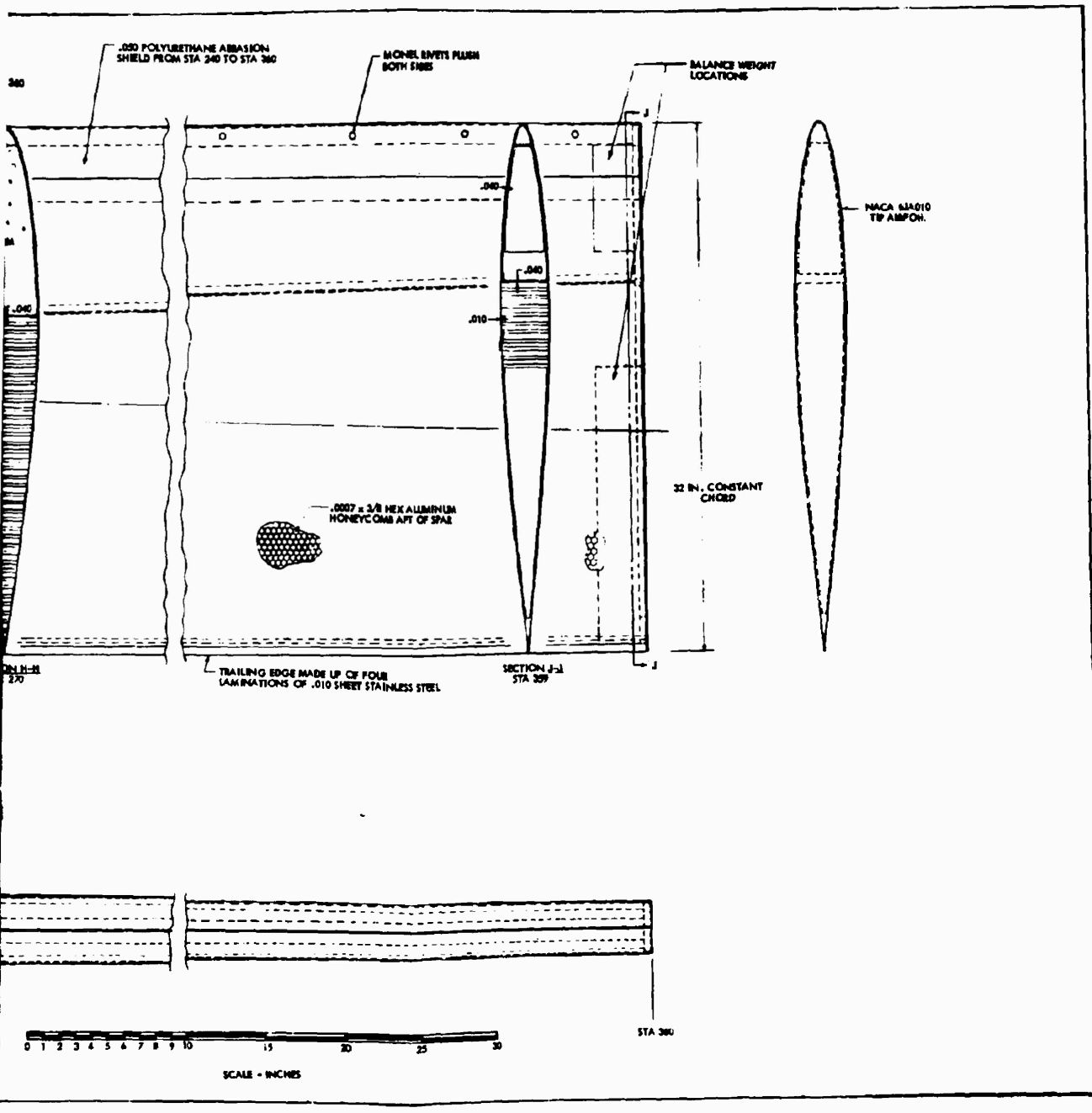


Figure 75. Rotor Blade Assembly.







Page Intentionally Left Blank

part of the transmission, and it would require breaking into part of the case for servicing. All other rotor system components are exposed for access with the rotor extended, and no special tools or equipment are needed for servicing.

ROTOR FOLDING AND STOWING SYSTEM

The stowed rotor concept calls for a vertical lift system that is deactivated for vehicle operation as a conventional high-speed fixed-wing aircraft. The vertical lift system configuration selected as a result of this study is a three-bladed, high-speed, gyro-controlled rigid rotor that is stopped in flight and rotationally indexed with a master blade in the aft or 360 degree position. The right and left blades are then rotated about clevis pins in the blade cuffs, folding aft to the blade-nested position. The complete rotor upper transmission, hub, and blade system is then pivoted on its support arms so as to lower it into a long compartment on top of the fuselage. Forward doors completely cover the retracted rotor hub assembly so as to present an aerodynamically clean configuration, as shown in Figure 2.

Various alternate configurations were considered, such as stopping the rotor in flight and attempting to reduce its drag by positioning the blades or by extending various fairings up from the fuselage to reduce aerodynamic drag. In each case, either the aerodynamic loads or the drag on the blades and fairings at high speed become untenable, or the characteristics when operated as a helicopter become unacceptable.

Since the fundamental purpose of the CRA is to achieve high-speed flight with a vehicle having helicopter characteristics, the configuration with the main rotor system completely stowed was carefully evaluated relative to the added complexity and weight of the articulated rotor support, control, and drive system with respect to the critical effect on vehicle drag ratios. With a rotor that is simply stopped, and the blades folded, the vehicle lift-to-drag ratio is about 7.5. With the same rotor stowed in an open compartment on top of the fuselage with the forward portion of the compartment and rotor hub completely covered with faired doors, the lift-to-drag ratio is slightly more than 10.0, in keeping with the aircraft requirements. This configuration will allow a potential of increased speeds in the future, and it is the configuration selected.

The number of blades used in the main rotor has been studied, and the three-bladed system appears to be optimum when rotor mechanical dynamics (three blades are polar symmetrical), solidity requirements, and the blade-folding geometry are considered. The main rotor folding system is shown in Figure 76.

The sequence for transfer from a helicopter mode to a high-speed fixed-wing airplane mode of flight is as follows:

- Take-off as a helicopter.
- Increased forward speed to 145 knots by gradually decreasing rotor collective pitch to zero and increasing propeller thrust.
- Declutch the drive to the main and tail rotors.
- Slow down, brake, stop, and position-index the main rotor.
- Fold the right and left blades aft to a nested position. (The blade collective pitch angle is changed from 0 degrees to +23 degrees as the blades near the nested position.)
- Retract the rotor system and close the door fairing.
- Increase speed for airplane flight mode.

The reverse sequence is used to return to the helicopter mode, and the system is fully reversible in either direction. For a more detailed description of the transition sequence, see Sections 15 and 16, Hydraulic and Mechanical Systems. In this system, positive control of the blade pitch angles is maintained throughout the folding and stowing operation by locating the blade-fold hinge at the axis of the blade horn push-pull rod.

The rotor hub and folding mechanism is shown in Figure 76. The central rotor hub is an integral part of the upper rotor mast, and it consists of two flanges which accept the blade retention pins. The blade folding mechanism consists of a hydraulic rotary actuator, a cable system, cable drums, and special blade retention pins for the folding blades. Each blade cuff is retained by two pins which are located so that the centripetal force applied to the cuff lies between them, making load reversal quite infrequent.

Folding and Unfolding System

The folding mechanism is located entirely in the upper rotor mast and blade cuff areas. This apparatus, shown in Figure 76, consists of a drive actuator, a cable system, cable drums, and two retracting-blade retention pins with locks. All motion is actuated hydraulically.

The drive is a rotary-hydraulic actuator. This system is safety-pressure relieved so that, when operating, it will attenuate very large aerodynamic loads resulting from gusts.

Cable drums are located on the cuffs of each of the folding blades and on the actuator assembly. These drums are sectors of circles, as the maximum rotation that any of them sees is less than 130 degrees. The drums on each of the blade cuffs have grooves for eight cables: four to fold the blade and four to unfold it. Fittings are provided to hold each cable end to the drums. The actuator drum has grooves for sixteen cable

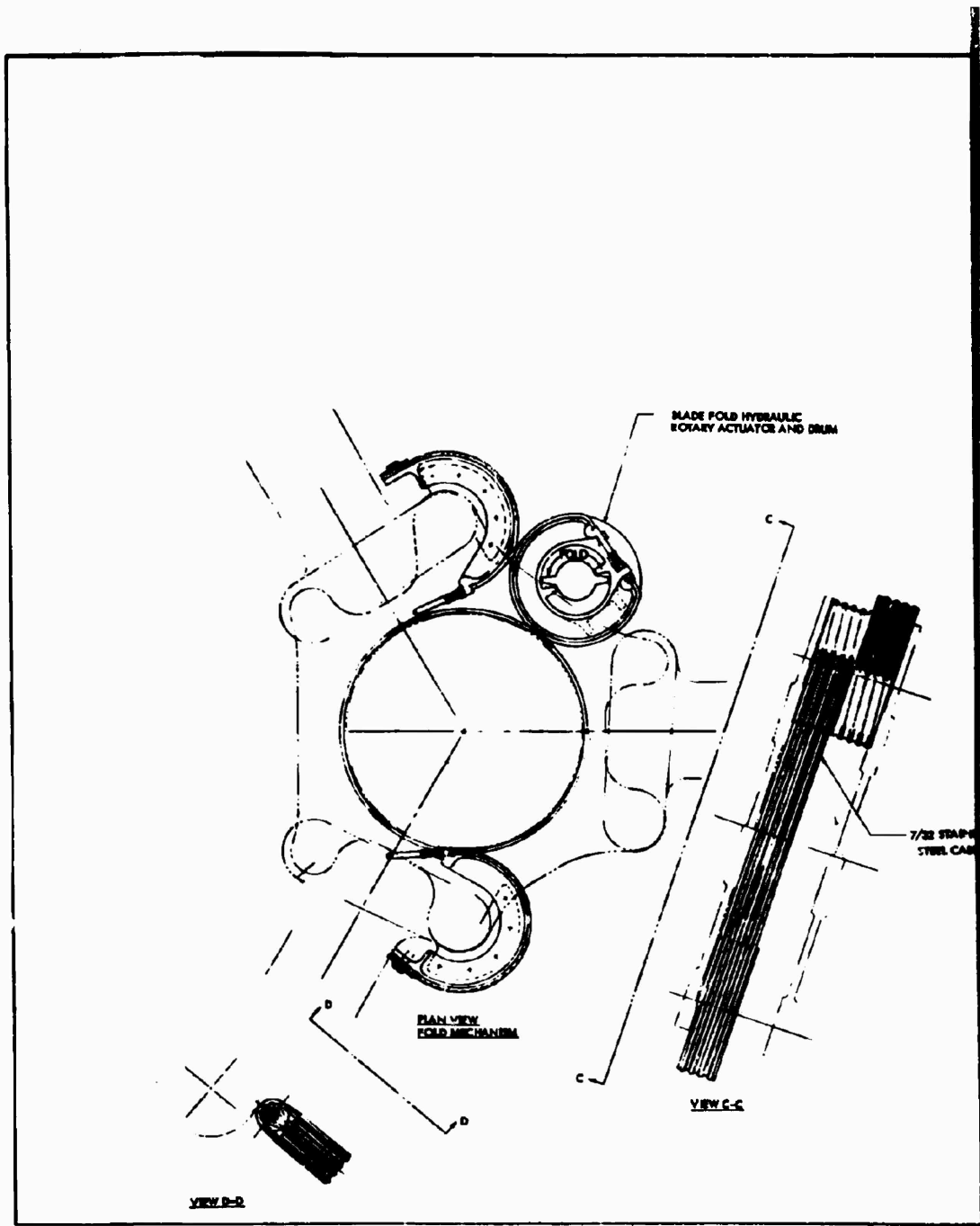
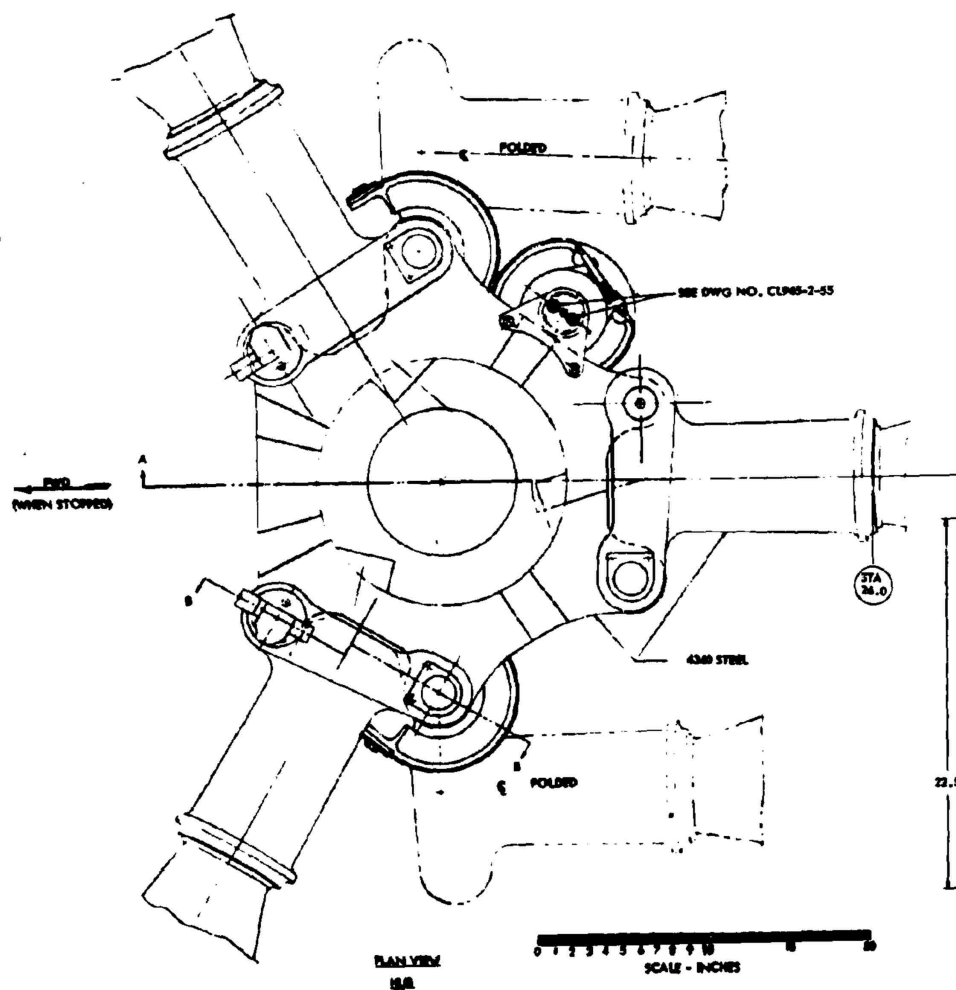
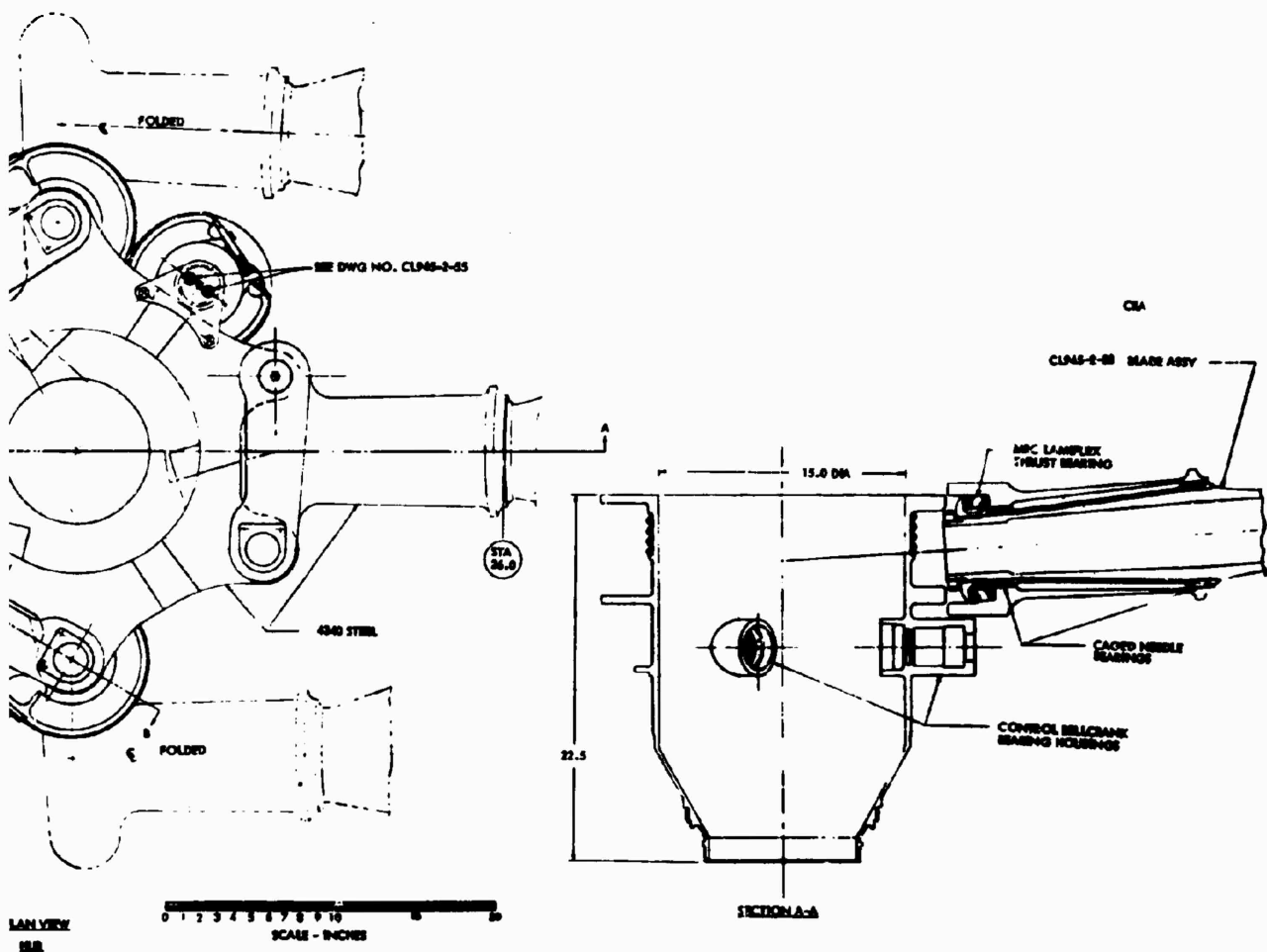


Figure 76. Main Rotor Hub and Blade-Folding Mechanism.



mechanism.



Page Intentionally Left Blank

strands, and it has flat areas and lugs for locating adjustment fittings. This cable and drum folding arrangement makes only four separate lengths of cable act as sixteen individually adjustable tension members, to provide simplicity and redundancy simultaneously.

The cables are 7/32-inch-diameter stainless steel. Each separate cable begins with an adjustable fitting at the blade cuff and runs to the actuator drum, where it passes through a stop and another threaded adjustment fitting, and then goes back to the cuff drum. It then passes around a fixture, returns to the actuator drum, goes through another adjustment fitting and another lug, and then returns to an end fitting at the cuff drums. There are two of these cables for each blade; but since they are each doubled over, there are actually four independent strands pulling on each blade for folding or unfolding. This system is fail-safe in that two of these strands can safely carry normal folding or unfolding loads.

The stowed rotor hub is enclosed with a set of doors. These doors extend to just aft of the rear beam, where the exposed rotor blades continue aft to just forward of the vertical tail. The doors part at the vehicle centerline and are double-hinged when open as shown in Figure 77. The doors are connected by links to the transmission lift truss so that the doors are opened or closed automatically when the transmission is moved. The aft portion of the top of the fuselage is contoured to support the nested blades and to provide an aerodynamic fairing at the aft end of the stowed blades.

The sequence of, and time required for, each operation to stow or extend the rotor are as follows:

Stop Rotor and Stow

Declutch main rotor to brake activation time	20 seconds
Brake action to stop and index rotor	15 seconds
Rotor blades folded	8 seconds
Rotor, hub, and transmission stowed and forward doors closed	8 seconds
Total	51 seconds

Extend and Start Rotor

Unstow rotor	8 seconds
Unfold blades	8 seconds
Clutch	45 seconds
Total	61 seconds

ANTI-TORQUE ROTOR

Counteraction of torque generated by the main rotor is required during helicopter mode flight. It is gradually reduced as the vehicle approaches transition velocities where the main rotor collective pitch is reduced to zero. Vehicle yaw control is gradually transferred to the vehicle's conventional rudder control surface at the same time. These requirements can be met with a variety of devices that are well within the state of the art and are reasonably efficient. However, after a study of the good and bad features of each concept, a conventional tail rotor configuration was selected as the best compromise of design features.

In spite of the complexity of the power-driven train associated with the conventional tail rotor configuration, the advantages of development status and similarity to other flight systems make it the more desirable design.

The size and design specifications for the selected tail rotor system were chosen to optimize the following parameters:

- Controllability and stability through all phases of flight
- Power required
- System weight
- Development requirements
- Aerodynamic drag during high-speed flight

Some of the restraints or desirable requirements of the tail rotor design are as follows:

- The maximum diameter is limited by a desire to have sufficient ground clearance for a 13.5-degree landing flare-angle clearance
- Clearance with main rotor and the length of the tail required
- Blade stiffness to meet divergence speed requirements
- Tip speeds using gear ratios such that when the main rotor is stopped, one blade of the tail rotor will automatically point forward
- Simplicity of locking the flapping axis of the rotor during stopped-rotor high-speed flight

The final selection of tail rotor specifications is as follows:

- | | |
|-----------------------|------------|
| ● Tail rotor diameter | 13.50 feet |
| ● Number of blades | 4 |

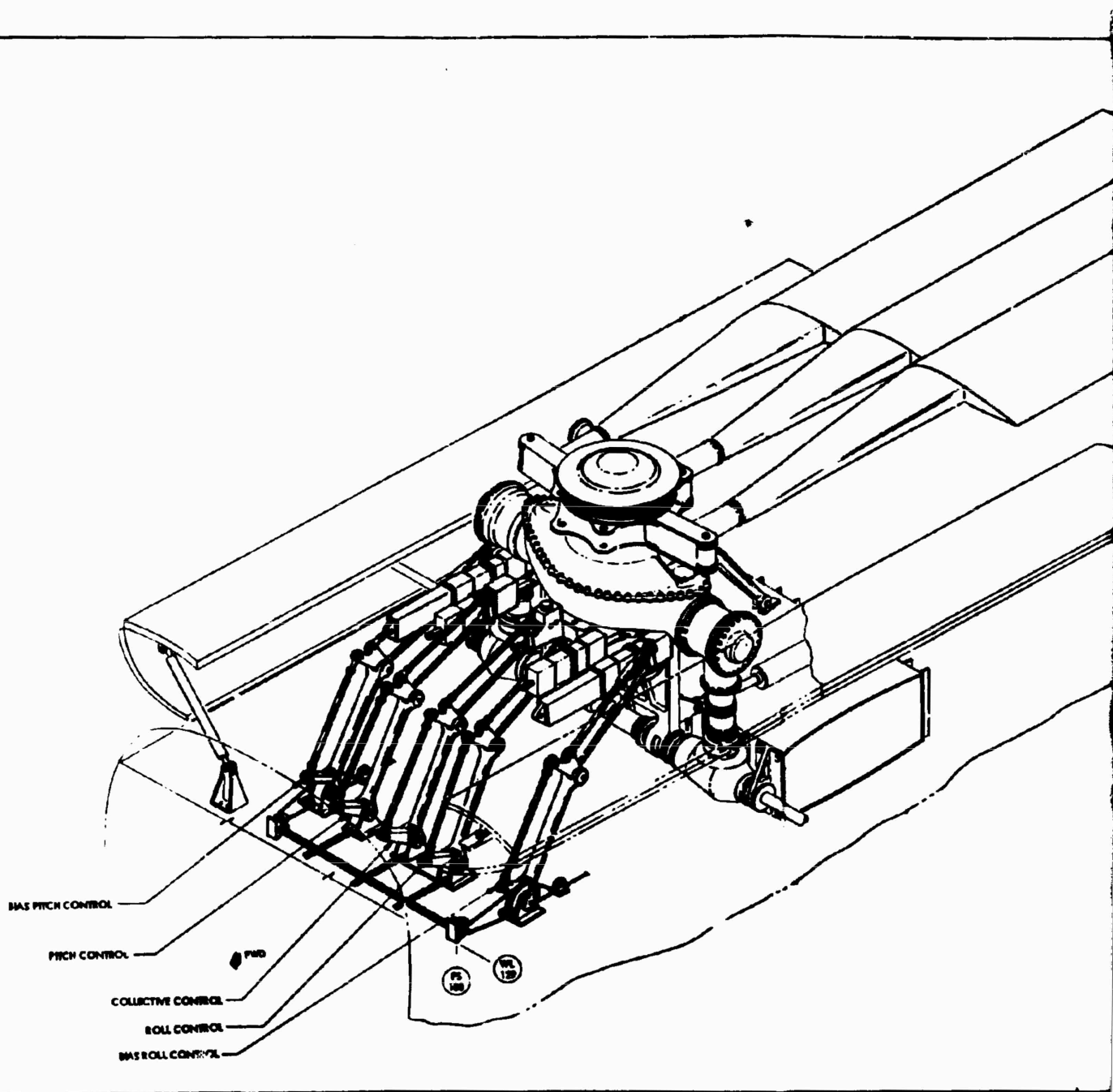
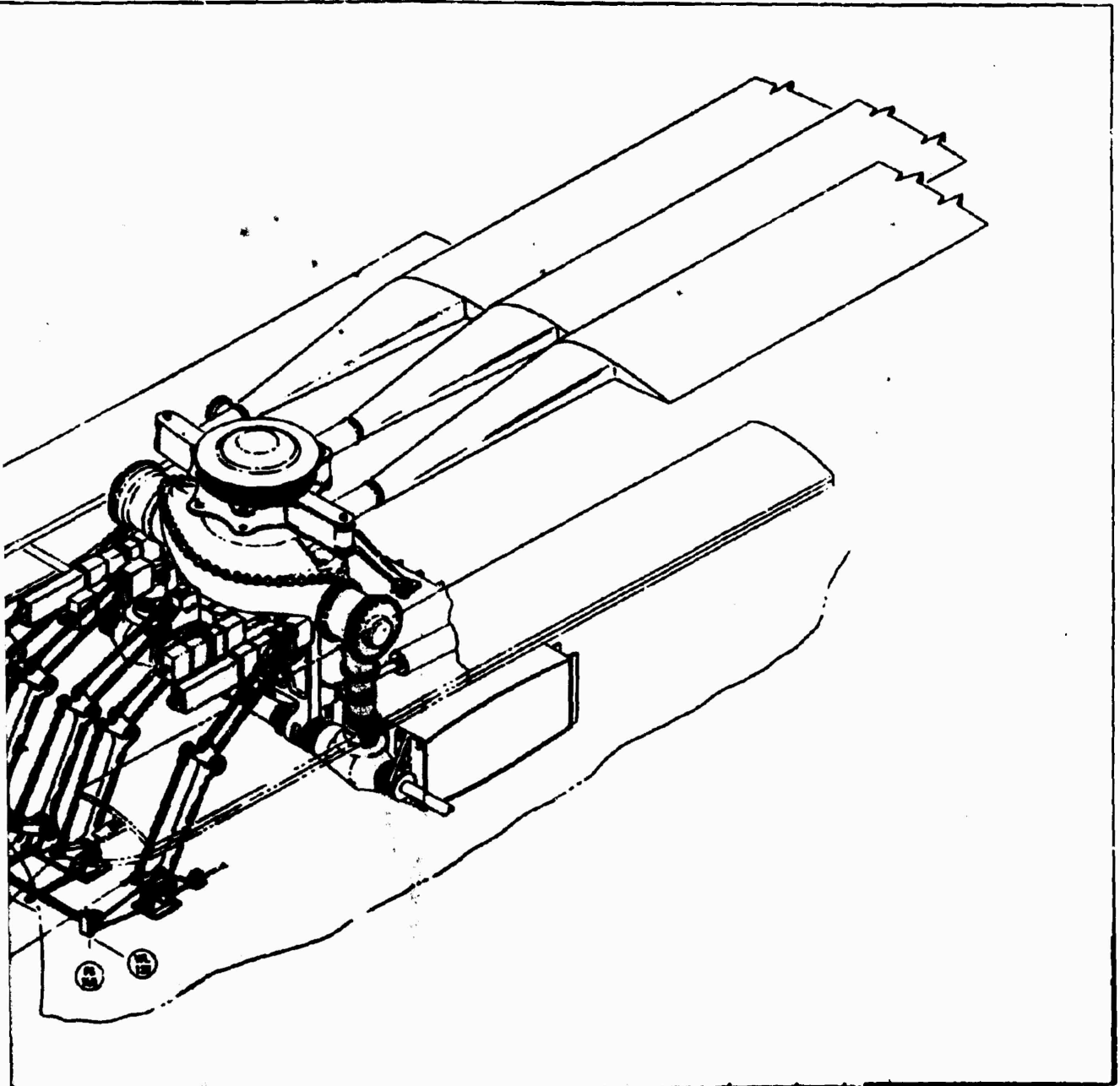


Figure 77. Main Rotor Controls Arrangement.



Controls Arrangement.

A

B

• Tip speed	636 feet per second
• Design rpm	900
• Tail rotor disc area	143 square feet
• Solidity	0.251
• Blade chord	16 inches, constant
• Blade twist	0 degrees

Tail Rotor

The trade-off studies conducted to find the optimum tail rotor geometry indicated that the necessary control power for the critical condition (hover out of ground effect at 6,000 feet, 95°F) could be obtained with a minimum horsepower and weight, with a 13.5-foot-diameter four-bladed rotor of 0.251 solidity.

The final selection of a tip speed of 636 feet per second was the result of choosing a gearing ratio which allowed the tail rotor blades to remain aligned fore and aft when the main rotor blades are folded, main rotor speed being the governing factor.

The planform of the rotor blades was selected to be of constant chord, 16.0 inches wide. The thickness ratio was fixed at 0.10 chord at the tip of the blade, linearly increasing to a virtual 0.25 chord at the rotor center of rotation. This thickness distribution gives desirable aerodynamic characteristics and also adequate beam depth in the inboard portions of the blade.

The geometric blade twist was made zero degrees.

The four blades are arranged with their feathering axis located at 37 percent of the chord from the leading edge. Both sweep and coning angles are zero.

A rotor configuration comprised of a universally mounted hub with provisions for locking the hub to the driving shaft was found to satisfy the requirements, as shown in Figure 78.

Tail Rotor Accessories and Controls

The operation of the vehicle with the rotors stopped requires some means to assure that the tail rotor remains fixed and in a specific position to prevent aeroelastic divergence. The gearing ratio through the drive system was selected so that, when the main rotor is stopped and folded, the tail rotor blades are oriented one pair fore and aft and the other pair vertically.

The positive locking of the tail rotor is achieved by the action of a set of flyweights mounted on the rotor shaft. When the rotational speed of the rotor falls below a given value, the flyweights are forced, under the action of springs, to return to a position which prevents the tilting of the rotor plane relative to the driving shaft. The fixity provided to the rotor, combined with the elastic properties of the rotor itself and supporting structure, assures a system which will not diverge aeroelastically. For operation in the helicopter flight mode, a system providing collective pitch control is installed.

- Kinematically, the arrangement of the control linkage is set to produce an effective delta-three angle of 45 degrees, the pitch arm connection being forward of the blade pitch axis.

Directional Control

The pilot and copilot are provided with conventional directional control pedals which are interconnected.

A trim and feel mechanism is connected to the linkage near the transfer mechanism. This consists of a double-acting centering and feel spring and an elastic trim actuator. It provides pedal centering, artificial feel, and trim.

Page Intentionally Left Blank

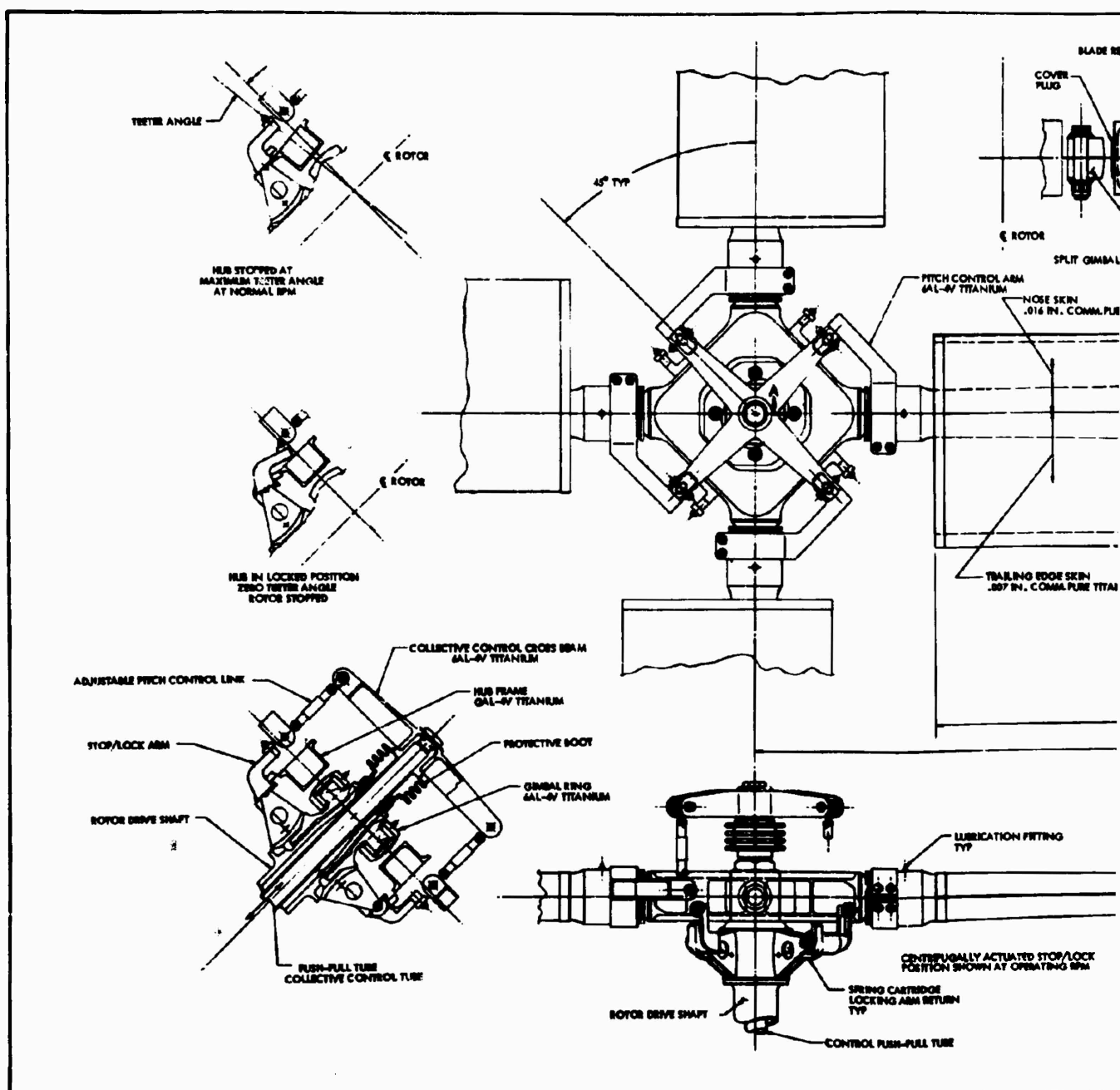
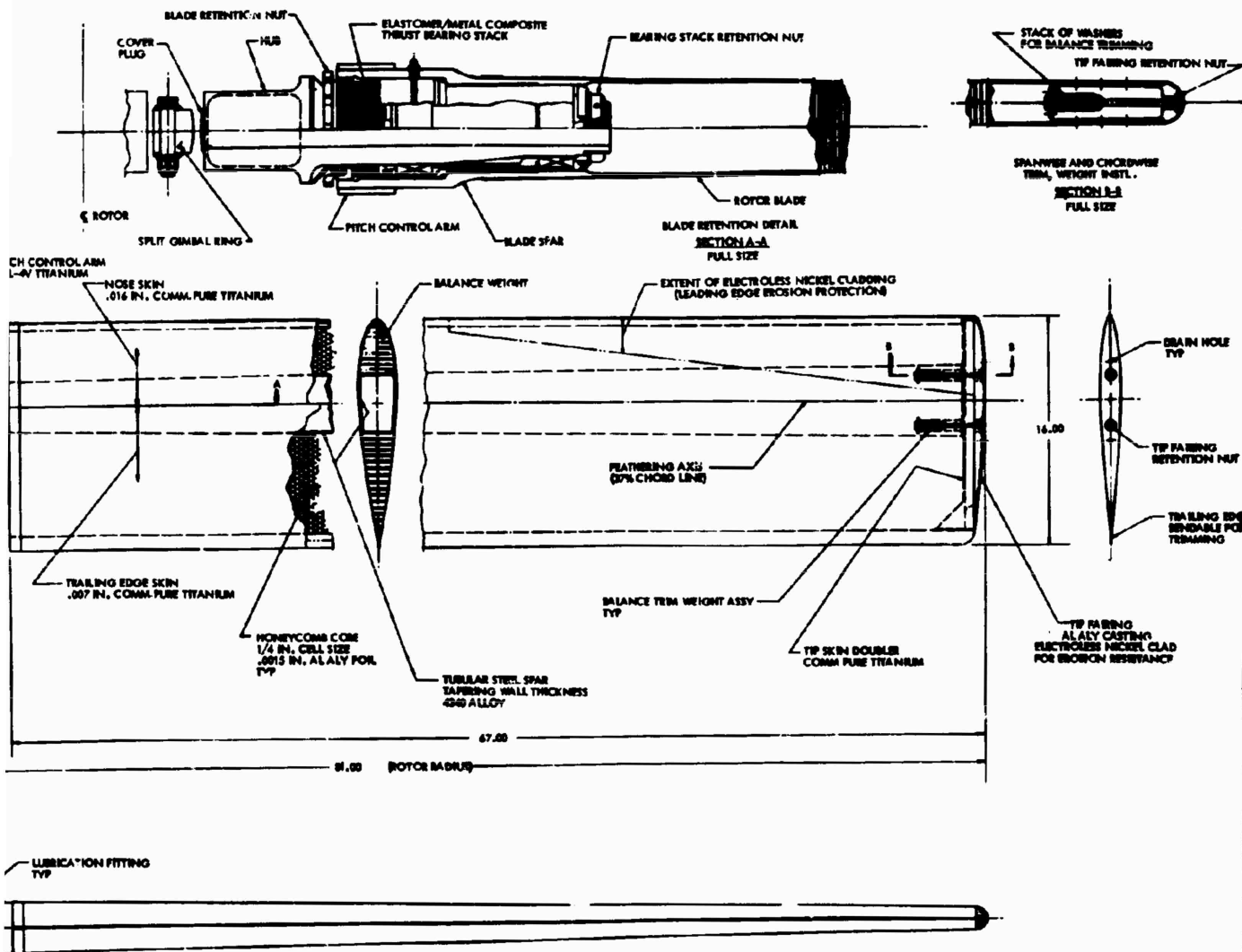


Figure 78. Tail Rotor Assembly.



INFLUENTIALLY ACTUATED STOP/LOCK
 TON SHOWN AT OPERATING RPM

OR
 RETURN

TURN

4. BLADE SECTION CONTOUR BASED ON:
 NASA 6818 AT TIP
 NASA 6822 AT ROTOR C
 (INTERMEDIATE SECTIONS ARE LINEARLY INTERPOLATED)
 3. BLADE GEOMETRIC TWIST IS ZERO DEGREES
 2. ROTOR IS SHOWN WITH BLADES WITH ZERO COL-
 LECTIVE PITCH ANGLE AND HUB AT ZERO TITEL POSITION
 1. LOCKING DEVICE IS SHOWN IN THE RELEASE MODE
 EXCEPT WHERE OTHERWISE NOTED
- NOTES:

Page Intentionally Left Blank

SECTION 8
FORWARD THRUST SYSTEM

The forward-thrust system (propellers, gearboxes, and propeller controls) must satisfy the following design requirements:

- A diameter of 10 feet is required to satisfy the forward-thrust requirement and still provide adequate tip clearance.
- The gearboxes must be interconnected to provide maximum engine-out safety.

A survey of the field reveals that the XC-142 gearbox is the only one presently available which could be applied to the CRA program.

Hamilton-Standard advises that a new gear ratio, a revised lubrication system for inverted operation, a cross-shaft drive modification, and two new mounts can be added to the present XC-142 gearbox within the allotted time span. This gearbox, therefore, has been considered for application to the CRA as an alternative to the design of a new gearbox.

The XC-142 gearbox and four-bladed propeller hub are integral, and modification to incorporate only three blades, if desired, would be extensive. The CRA, therefore, also incorporates four blades. Available propeller blade designs include optimized blades built on an AH-56A propeller core, or modified AH-56A propeller blades. The XC-142 propeller cannot be considered because its diameter is far too great for application to the CRA. The AH-56A blades are designed for a lower speed range than the CRA, and the propeller efficiency with AH-56A blades would be about 10 percent lower than it would be with blades specifically designed to provide optimum performance. Hamilton Standard advises that new design blades can be made available within the allotted time span; therefore, the CRA incorporates new design optimized blades.

A propeller control system currently available which could be adapted to the CRA is the XC-142 control system, which is manufactured by Ling-Temco-Vought (LTV). This firm has agreed to supply unmodified control system components, but modification costs and timing are not presently available. In addition, Hamilton Standard has available the control system for the X-22 aircraft and a modified X-22 propeller control system could be made available for the CRA within the allowable time span.

PROPELLER BLADES

The proposed propeller blades are a steel-core, foam-filled fiber glass shell design with a steel, integral ball-race shank. The diameter is

10 feet, and the blades have an activity factor of 120 and an integrated design lift coefficient (C_{L_i}) of 0.33, resulting in a maximum efficiency of approximately 88 percent.

Steel-core fiber glass shell blades have been found to be very durable in damage-resistance tests. Leading-edge reinforcements, such as plating, can improve the damage, corrosion, and erosion resistance of these blades to better than that of steel or aluminum blades. Severe stone nicks and scratches in steel and aluminum blades cause stress concentrations, from which dangerous fatigue cracks can start if these defects are not removed. The fibers in fiber glass construction act as crack stoppers when severe nicks occur. Therefore, fatigue cracks resulting in blade failure are confined to the steel core, which is protected from nicks and scratches, rendering the possibility of such failure much more remote than for steel or aluminum blades.

HUB AND GEARBOX

The propeller hub and gearbox proposed for the CRA comprise a single integrated assembly. This assembly is currently used on the XC-142 experimental VTOL aircraft. The XC-142 gearbox is fully qualified and has accumulated 800 hours of flight test use with an excellent service record.

The hub is designed and constructed in such a manner that the blades and pitch change mechanism can be removed as subassemblies, greatly facilitating propeller maintainability. The XC-142 pitch-change actuator is included with the hub and gearbox assembly.

PART 4
WEIGHT AND BALANCE

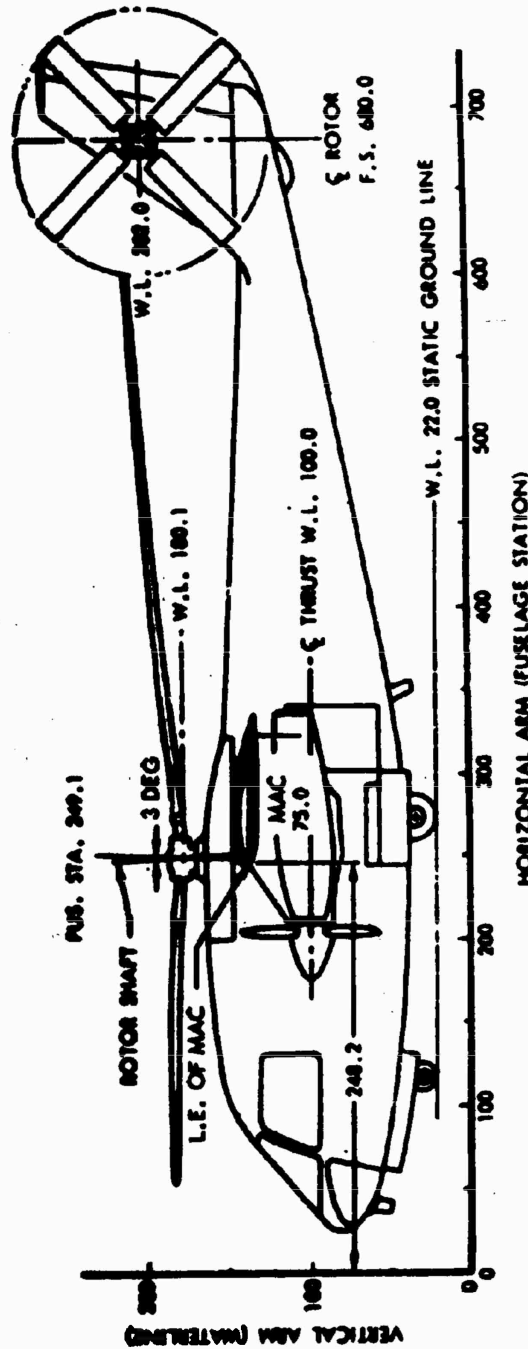
SECTION 9
ESTIMATED WEIGHT REPORT

This section contains an estimated weight report prepared in accordance with MIL-W-25140 (ASG). The weight data shown in Figures 79 and 80 are representative of the Model CRA optimum vehicle only, and no allowance is made for the use of off-the-shelf equipment where the use of such equipment would involve a weight penalty. Also not included are optional installations such as the engine air induction filter system or special installations for use during the test program such as ejection seats or test instrumentation.

Since the weight allowances specified in the contract have been used for avionics, armor, auxiliary power unit, and furnishings and equipment, detailed weight and balance data for these groups are not included.

The composite aircraft operates in two distinct modes of flight (helicopter and airplane), and its balance characteristics must be such that structural and stability limits will be observed during both modes and during transition from one mode to the other. Retraction of the rotor causes a rearward movement of the center of gravity of about 5 inches at 23,000 pounds gross weight, and this determines the location of the wing. Landing gear retraction causes only a very minor forward movement of center of gravity. (See Tables XI, XII, XIII, XIV and XV.)

The center-of-gravity travel diagram (Figure 81) shows that the center-of-gravity envelope for each mode of operation is well within the appropriate limits. Good flexibility in the location of the payload within the cargo compartment is apparent. For example, half of the total design payload may be placed in the forward half of the compartment with none in the rear half. The equivalent composite location of smaller or greater quantities allows for considerable latitude in the placement of various payloads. No fuel management is required, and operation will be within the envelopes shown with one or two crew members.



CENTER-OF-GRAVITY LIMITS FOR THE HELICOPTER MODE ARE AS FOLLOWS AND VARY LINEARLY BETWEEN WEIGHTS SHOWN. THESE LIMITS ARE EQUIVALENT TO $\pm 175,000$ INCH-POUNDS SHAFT MOMENT.

GROSS WEIGHT (LB)	C.G. LIMIT (FUS. STA.) FWD AFT
18,000	242.5 261.9
20,000	243.4 260.9
22,000	244.2 260.1
24,000	244.9 259.5
26,000	245.5 258.9

CENTER-OF-GRAVITY LIMITS FOR THE FIXED-WING AIRPLANE MODE ARE 10.0 PERCENT MAC FORWARD LIMIT AND 25.0 PERCENT MAC LIMIT.

Figure 79. Dimensional Data for Reference Axes.

MIL-STD-451 PART 1
NAME
DATE

ROTORCRAFT
SUMMARY WEIGHT STATEMENT
WEIGHT EMPTY

PAGE
MODEL
REPORT

1						
2	ROTOR GROUP					2156
3	BLADE ASSEMBLY				1490	
4	HUB				258	
5	FOLDING AND BLADE RETENTION					
6		RETENTION			288	
7		LEAD LAG				
8		PITCH				
9		FOLDING			114	
10	WING GROUP					1540
11	WING PANELS-BASIC STRUCTURE					
12	CENTER SECTION-BASIC STRUCTURE				259	
13	INTERMEDIATE PANEL-BASIC STRUCTURE					
14	OUTER PANEL-BASIC STRUCTURE-INCL TIPS	7 LBS			1033	
15	SECONDARY STRUCT-INCL FOLD MECH	LBS			34	
16	AILERONS - INCL BALANCE WTS	9 LBS			32	
17	FLAPS					
18	-TRAILING EDGE				182	
19	-LEADING EDGE					
20	SLATS					
21	SPOILERS					
22						
23	TAIL GROUP					611
24	TAIL ROTOR				196	
25	- BLADES			128		
26	- HUB & STABILIZER			68		
27	STABILIZER - BASIC STRUCTURE				141	
28	FINS - BASIC STRUCTURE - INCL DORSAL	LBS			129	
29	SECONDARY STRUCTURE - STABILIZER AND FINS				8	
30	ELEVATOR - INCL BALANCE WEIGHT	19 LBS			67	
31	RUDDER - INCL BALANCE WEIGHT	24 LBS			70	
32						
33	BODY GROUP					3046
34	FUSELAGE OR HULL - BASIC STRUCTURE				2055	
35	BOOMS - BASIC STRUCTURE					
36	SECONDARY STRUCTURE - FUSELAGE OR HULL				646	
37	- BOOMS					
38	- DOORS, PANELS & MISC				345	
39						
40						
41	SLIGHTING GEAR - LAND TYPE					889
42	LOCATION	ROLLING	STRUCT	CONTROLS		
43		ASSEMBLY				
44						
45	MAIN	198	469	76	743	
46	NOSE	26	107	13	146	
47						
48						
49						
50	SLIGHTING GEAR GROUP - WATER TYPE					
51	LOCATION	FLOATS	STRUTS	CONTROLS		
52						
53						
54						
55						
56						
57						

* WHEELS, BRAKES, TIRES, TUBES AND AIR

Figure 80. Summary Weight Statement.

NAME
NAME
DATE

ROTORCRAFT
SUMMARY WEIGHT STATEMENT
WEIGHT EMPTY

**PAGE
MODEL
REPORT**

1	2	3	4	5	6	7	8	9	10	11	12	13	14	15	16	17	18	19	20	21	22	23	24	25	26	27	28	29	30	31	32	33	34	35	36	37	38	39	40	41	42	43	44	45	46	47	48	49	50	51	52	53	54	55	56	57	58	59	60	61	62	63	64	65	66	67	68	69	70	71	72	73	74	75	76	77	78	79	80	81	82	83	84	85	86	87	88	89	90	91	92	93	94	95	96	97	98	99	100
1	2	3	4	5	6	7	8	9	10	11	12	13	14	15	16	17	18	19	20	21	22	23	24	25	26	27	28	29	30	31	32	33	34	35	36	37	38	39	40	41	42	43	44	45	46	47	48	49	50	51	52	53	54	55	56	57	58	59	60	61	62	63	64	65	66	67	68	69	70	71	72	73	74	75	76	77	78	79	80	81	82	83	84	85	86	87	88	89	90	91	92	93	94	95	96	97	98	99	100
1	2	3	4	5	6	7	8	9	10	11	12	13	14	15	16	17	18	19	20	21	22	23	24	25	26	27	28	29	30	31	32	33	34	35	36	37	38	39	40	41	42	43	44	45	46	47	48	49	50	51	52	53	54	55	56	57	58	59	60	61	62	63	64	65	66	67	68	69	70	71	72	73	74	75	76	77	78	79	80	81	82	83	84	85	86	87	88	89	90	91	92	93	94	95	96	97	98	99	100
1	2	3	4	5	6	7	8	9	10	11	12	13	14	15	16	17	18	19	20	21	22	23	24	25	26	27	28	29	30	31	32	33	34	35	36	37	38	39	40	41	42	43	44	45	46	47	48	49	50	51	52	53	54	55	56	57	58	59	60	61	62	63	64	65	66	67	68	69	70	71	72	73	74	75	76	77	78	79	80	81	82	83	84	85	86	87	88	89	90	91	92	93	94	95	96	97	98	99	100
1	2	3	4	5	6	7	8	9	10	11	12	13	14	15	16	17	18	19	20	21	22	23	24	25	26	27	28	29	30	31	32	33	34	35	36	37	38	39	40	41	42	43	44	45	46	47	48	49	50	51	52	53	54	55	56	57	58	59	60	61	62	63	64	65	66	67	68	69	70	71	72	73	74	75	76	77	78	79	80	81	82	83	84	85	86	87	88	89	90	91	92	93	94	95	96	97	98	99	100
1	2	3	4	5	6	7	8	9	10	11	12	13	14	15	16	17	18	19	20	21	22	23	24	25	26	27	28	29	30	31	32	33	34	35	36	37	38	39	40	41	42	43	44	45	46	47	48	49	50	51	52	53	54	55	56	57	58	59	60	61	62	63	64	65	66	67	68	69	70	71	72	73	74	75	76	77	78	79	80	81	82	83	84	85	86	87	88	89	90	91	92	93	94	95	96	97	98	99	100
1	2	3	4	5	6	7	8	9	10	11	12	13	14	15	16	17	18	19	20	21	22	23	24	25	26	27	28	29	30	31	32	33	34	35	36	37	38	39	40	41	42	43	44	45	46	47	48	49	50	51	52	53	54	55	56	57	58	59	60	61	62	63	64	65	66	67	68	69	70	71	72	73	74	75	76	77	78	79	80	81	82	83	84	85	86	87	88	89	90	91	92	93	94	95	96	97	98	99	100
1	2	3	4	5	6	7	8	9	10	11	12	13	14	15	16	17	18	19	20	21	22	23	24	25	26	27	28	29	30	31	32	33	34	35	36	37	38	39	40	41	42	43	44	45	46	47	48	49	50	51	52	53	54	55	56	57	58	59	60	61	62	63	64	65	66	67	68	69	70	71	72	73	74	75	76	77	78	79	80	81	82	83	84	85	86	87	88	89	90	91	92	93	94	95	96	97	98	99	100
1	2	3	4	5	6	7	8	9	10	11	12	13	14	15	16	17	18	19	20	21	22	23	24	25	26	27	28	29	30	31	32	33	34	35	36	37	38	39	40	41	42	43	44	45	46	47	48	49	50	51	52	53	54	55	56	57	58	59	60	61	62	63	64	65	66	67	68	69	70	71	72	73	74	75	76	77	78	79	80	81	82	83	84	85	86	87	88	89	90	91	92	93	94	95	96	97	98	99	100
1	2	3	4	5	6	7	8	9	10	11	12	13	14	15	16	17	18	19	20	21	22	23	24	25	26	27	28	29	30	31	32	33	34	35	36	37	38	39	40	41	42	43	44	45	46	47	48	49	50	51	52	53	54	55	56	57	58	59	60	61	62	63	64	65	66	67	68	69	70	71	72	73	74	75	76	77	78	79	80	81	82	83	84	85	86	87	88	89	90	91	92	93	94	95	96	97	98	99	100
1	2	3	4	5	6	7	8	9	10	11	12	13	14	15	16	17	18	19	20	21	22	23	24	25	26	27	28	29	30	31	32	33	34	35	36	37	38	39	40	41	42	43	44	45	46	47	48	49	50	51	52	53	54	55	56	57	58	59	60	61	62	63	64	65	66	67	68	69	70	71	72	73	74	75	76	77	78	79	80	81	82	83	84	85	86	87	88	89	90	91	92	93	94	95	96	97	98	99	100
1	2	3	4	5	6	7	8	9	10	11	12	13	14	15	16	17	18	19	20	21	22	23	24	25	26	27	28	29	30	31	32	33	34	35	36	37	38	39	40	41	42	43	44	45	46	47	48	49	50	51	52	53	54	55	56	57	58	59	60	61	62	63	64	65	66	67	68	69	70	71	72	73	74	75	76	77	78	79	80	81	82	83	84	85	86	87	88	89	90	91	92	93	94	95	96	97	98	99	100
1	2	3	4	5	6	7	8	9	10	11	12	13	14	15	16	17	18	19	20	21	22	23	24	25	26	27	28	29	30	31	32	33	34	35	36	37	38	39	40	41	42	43	44	45	46	47	48	49	50	51	52	53	54	55	56	57	58	59	60	61	62	63	64	65	66	67	68	69	70	71	72	73	74	75	76	77	78	79	80	81	82	83	84	85	86	87	88	89	90	91	92	93	94	95	96	97	98	99	100
1	2	3	4	5	6	7	8	9	10	11	12	13	14	15	16	17	18	19	20	21	22	23	24	25	26	27	28	29	30	31	32	33	34	35	36	37	38	39	40	41	42	43	44	45	46	47	48	49	50	51	52	53	54	55	56	57	58	59	60	61	62	63	64	65	66	67	68	69	70	71	72	73	74	75	76	77	78	79	80	81	82	83	84	85	86	87	88	89	90	91	92	93	94	95	96	97	98	99	100
1	2	3	4	5	6	7	8	9	10	11	12	13	14	15	16	17	18	19	20	21	22	23	24	25	26	27	28	29	30	31	32	33	34	35	36	37	38	39	40	41	42	43	44	45	46	47	48	49	50	51	52	53	54	55	56	57	58	59	60	61	62	63	64	65	66	67	68	69	70	71	72	73	74	75	76	77	78	79	80	81	82	83	84	85	86	87	88	89	90	91	92	93	94	95	96	97	98	99	100
1	2	3	4	5	6	7	8	9	10	11	12	13	14	15	16	17	18	19	20	21	22	23	24	25	26	27	28	29	30	31	32	33	34	35	36	37	38	39	40	41	42	43	44	45	46	47	48	49	50	51	52	53	54	55	56	57	58	59	60	61	62	63	64	65	66	67	68	69	70	71	72	73	74	75	76	77	78	79	80	81	82	83	84	85	86	87	88	89	90	91	92	93	94	95	96	97	98	99	100
1	2	3	4	5	6	7	8	9	10	11	12	13	14	15	16	17	18	19	20	21	22	23	24	25	26	27	28	29	30	31	32	33	34	35	36	37	38	39	40	41	42	43	44	45	46	47	48	49	50	51	52	53	54	55	56	57	58	59	60	61	62	63	64	65	66	67	68	69	70	71	72	73	74	75	76	77	78	79	80	81	82	83	84	85	86	87	88	89	90	91	92	93	94	95	96	97	98	99	100
1	2	3	4	5	6	7	8	9	10	11	12	13	14	15	16	17	18	19	20	21	22	23	24	25	26	27	28	29	30	31	32	33	34	35	36	37	38	39	40	41	42	43	44	45	46	47	48	49	50	51	52	53	54	55	56	57	58	59	60	61	62	63	64	65	66	67	68	69	70	71	72	73	74	75	76	77	78	79	80																				

Figure 80. Summary Weight Statement. (Continued)

MIL-STD-451 PART 1
NAME
DATE

ROTORCRAFT
SUMMARY WEIGHT STATEMENT
WEIGHT EMPTY

PAGE
MODEL
REPORT

1					
2					
3					
4	INSTRUMENT AND NAVIGATIONAL EQUIPMENT GROUP				178
5	INSTRUMENTS				
6	NAVIGATIONAL EQUIPMENT				
7					
8					
9	HYDRAULIC AND PNEUMATIC GROUP				181
10	HYDRAULIC				
11	PNEUMATIC				
12					
13					
14	ELECTRICAL GROUP				524
15	A C SYSTEM				
16	D C SYSTEM				
17					
18					
19	ELECTRONICS GROUP				900
20	EQUIPMENT				
21	INSTALLATION				
22					
23					
24	ARMAMENT GROUP - INCL GUNFIRE PROTECTION		300 LBS		300
25					
26	FURNISHINGS AND EQUIPMENT GROUP				262
27	ACCOMMODATIONS FOR PERSONNEL				
28	MISCELLANEOUS EQUIPMENT X INCL		LBS BALLAST		
29	FURNISHINGS				
30	EMERGENCY EQUIPMENT				
31					
32					
33					
34	AIR CONDITIONING AND ANTI-ICING EQUIPMENT				55
35	AIR CONDITIONING				
36	ANTI-ICING				
37					
38					
39	PHOTOGRAPHIC GROUP				
40	EQUIPMENT				
41	INSTALLATION				
42					
43	AUXILIARY GEAR GROUP				
44	AIRCRAFT HANDLING GEAR				
45	LOAD HANDLING GEAR				
46	ATO GEAR				
47					
48					
49					
50					
51					
52					
53					
54	MANUFACTURING VARIATION				
55					
56					
57	TOTAL WEIGHT EMPTY - PAGES 2, 3 AND 4				17961

Figure 80. Summary Weight Statement. (Continued)

NIL-STD-451 PART 1
NAME
DATE

SUMMARY WEIGHT STATEMENT
USEFUL LOAD GROSS WEIGHT

PAGE
MODEL
REPORT

LOAD CONDITION		DESIGN			
		GROSS WT			
1	SCREEN - NO. 2				400
2	PASSENGERS - NO.				
3	SPIN	LOCATION	TYPE	GALS	3020
4	UNUSABLE			26	
5	INTERNAL	WING	JT-1	462	3000
6					
7					
8	EXTERNAL				
9					
10					
11	BOMB BAY				
12					
13					
14					
15	WILL				119
16	UNUSABLE				
17	ENGINE				
18					
19					
20	WARRAGE				
21	WARRAGE				3000
22					
23	ARMAMENT				
24	WING-LOCATION	TYPE	QUANTITY	CALIBRE	
25					
26					
27					
28	ARM				
29					
30	BOMB INSTL.				
31	BOMBS				
32	TORPEDO INSTL.				
33	TORPEDOS				
34	ROCKET INSTL.				
35	ROCKETS				
36	EQUIPMENT-TECHNICS				
37	-PHOTOGRAPHIC				
38					
39	-COMM				
40					
41	-MISCELLANEOUS				
42					
43	USEFUL LOAD				6539
44	GROSS WEIGHTS - PAGES 2-3				
45	* IF NOT SPECIFIED AS WEIGHT EMPTY ** FIXED, FLEXIBLE, ETC.				

Figure 80. Summary Weight Statement. (Continued)

MIL-STD-491 PART 1
NAME
DATE

SUMMARY WEIGHT STATEMENT
DIMENSIONAL STRUCTURAL DATA
ROTORCRAFT

PAGE
MODEL
REPORT

1	LENGTH - OVERALL OPERATING	= 72 FT. 7 IN.	X	BLADES FOLDED	61 FT. 6 IN.		
2	GENERAL DATA			BOOM	FUS	MAC	CABIN
3	LENGTH - MAXIMUM FEET				57.4		
4	DEPTH - MAXIMUM FEET				10.4		
5	WIDTH - MAXIMUM FEET				6.8		
6	WETTED AREA TOTAL-SQ. FT.				1271		
7	WETTED AREA GLASS						
8	WING TAIL & FLOOR DATA			WING	H TAIL	V TAIL	FLOOR
9	GROSS AREA - SQUARE FEET			279	58	64	
10	WEIGHT/GROSS AREA - POUNDS PER SQUARE FEET			5.52	3.53	3.28	
11	SPAN - FEET			50	15	10.75	
12	FOLDED SPAN - FEET						
13	THEORETICAL ROOT CHORD - INCHES			107	55	107	
14	MAXIMUM THICKNESS - INCHES			19.26	9.90	19.26	
15	CHORD AT PLANFORM BREAK - INCHES						
16	MAXIMUM THICKNESS - INCHES						
17	THEORETICAL TIP CHORD - INCHES			27	37	36	
18	MAXIMUM THICKNESS - INCHES			3.24	6.60	4.32	
19	DORSAL AREA INCLUDED IN FUSELAGE			50 FT	TAIL		SQ FT
20	TAIL LENGTH 25% MAC WING TO 25% MAC HORIZONTAL TAIL				33.91		FEET
21	AREA - SQ FT PER ROTORCRAFT FLAPS	42.4		AILERONS	12.5		SPOILERS
22		SLATS		WING LE			WING TP
23	ROTOR DATA - TYPE -						RIGID
24		X	MAIN ROTOR	XX	TAIL ROTOR		
25	FROM CL ROTATION - INCHES	90.0	ROOT	30.0	TIP	14.0	ROOT
26	CHORD - INCHES		32.0		32.0		18.0
27	THICKNESS - INCHES		6.41		3.20		3.60
28						MAIN-FWD	MAIN-AFT
29	BLADE RADIUS - FEET				30.0		TAIL
30	NUMBER BLADES				3		4
31	BLADE AREA-TOTAL-OUTBOARD	0	INCHES RADIUS		240		36
32	DISC AREA - TOTAL SWEEP	2830	SQUARE FEET - OVERLAP				SQUARE FEET
33	TIP SPEED AT DESIGN LIMIT ROTOR-SPEED-POWER-FT/SEC				830		
34	DESIGN FACTOR USED BY CONTRACTOR				1.10		
35	LOCATION FROM HORIZONTAL REF DATUM		INCHES (MAIN	249.1)	(TAIL	680.0)	
36	PRESSURE JET & BLADE SECTION AREA FOR DUCT						
37	TIP JET THRUST						BEAR***
38	POWER TRANSMISSION DATA		(AIRPLANE MODE		HP	RPM	RATIO
39	MAX POWER - MILITARY - 2 ENG.		HELICOPTER MODE		1870	13600	56.67:1
40	QUALITY GEAR TYPE**		TRICYCLE		4350		MAIN-AFT AUX-FWD
41	GEAR LENGTH - USED EXTND CL AXLE TO CL TRUNNION						
42	DECO TRAVEL - FULL EXTENDED TO COMPRESSED		INCHES			10.0	8.0
43	WHEEL SIZE AND NUMBER REQUIRED					(2) 28-9	(1) 22-6.0
44	FUEL AND OIL SYSTEM		LOCATION NO. TANKS	****	BAL NO. TANKS	****	BAL
45					UNPRCTD		PROTECTD
46	FUEL - BUTLY IN				496		
47	FUEL - EXTERNAL						
48	LUBRICATING SYSTEM		NACELLES	2	20		
49	HYDRAULIC SYSTEM						
50	STRUCTURAL DATA - CONDITION				FUEL IN DESIGN	STRESS	WELL AND
51					WINGS-L	GROSS WINGROSS W	ULT LP
52	FLIGHT			3000	24500	24500	4,506.75
53	LANDING			3000	24500	24500	2,822.82
54	% DESIGN LOAD - HLL.	WING	0	FWD RTH	100	AFT RTH	
55	% DESIGN LOAD - APT.		100		0		
56	TYPE OF POWER TRANSMISSION - GEARED -						
57							

* PARALLEL TO CL & CL ROTORCRAFT *** BEAR RATIO-ENG TO ROTOR
 ** CROSS OUT NON-APPLICABLE TYPE **** TOTAL USEABLE CAPACITY
 ***** REFER TO PARA. 9.1.1.3-ITEMS 6-33 & 6-34 *** EXCESSIVE FUELING OFFER ***
 Figure 80. Summary Weight Statement. (Continued)

TABLE XI. WEIGHT AND BALANCE SUMMARY

	Weight (lb)	Center of Gravity	
		Horizontal Arm (in.)	Vertical Arm (in.)
Weight Empty - Gear Down	17,961	257.0	122.8
Gross Weight			
Helicopter Mode - Gear Down	24,500	257.1	119.7
Airplane Mode - Gear Down	24,500	261.9	115.1
Extreme Fwd C.G. Condition			
Helicopter Mode - Gear Up	20,000	250.4	119.9
Airplane Mode - Gear Up	20,000	256.2	114.4
Extreme Aft C.G. Condition			
Helicopter Mode - Gear Down	21,300	258.8	124.6
Airplane Mode - Gear Down	21,300	264.2	119.4

TABLE XII. GROUP WEIGHT AND BALANCE SUMMARY

Item	Weight (lb)	Horizontal Arm (in.)	Vertical Arm (in.)
Rotor Group	2150	249.1	180.1
Wing Group	1540	284.1	136.0
Tail Group	611	682.6	198.7
Body Group	3046	249.2	92.4
Lighting Gear Group	889	246.4	47.1
Flight Controls Group	1010	273.4	141.0
Nacelle Group	804	266.8	108.4
Propulsion Group	5361	267.4	124.8
Auxiliary Power Plant	150	45.0	80.0
*Instruments Group	178	138.6	109.2
*Hydraulics Group	181	240.0	116.5
*Electrical Group	524	114.2	90.8
Electronics Group	900	106.0	113.0
Armament Group	300	164.0	103.0
*Furnishings & Equipment Group	262	144.3	102.7
*Air Conditioning Group	55	110.0	122.7
WEIGHT EMPTY, GEAR DOWN AND ROTOR EXTENDED	17961	257.0	122.8
CONTRACT WEIGHT ALLOWANCES:			
Electronics	900		
Armor	300		
Auxiliary Power Plant	150		
*Furnishings & Equipment	1200		

TABLE XII. GROSS WEIGHT BALANCE			
Item	Weight (lb)	Horizontal Arm (in.)	Vertical Arm (in.)
HELICOPTER MODE			
Weight Empty - Gear Down	17,961	257.0	122.8
Pilot	200	100.0	100.0
Copilot	200	100.0	100.0
Oil - Including Unusable	119	268.3	122.0
Unusable Fuel	20	266.0	136.0
Payload	3,000	256.0	86.0
Fuel	3,000	279.4	137.0
Gross Weight - Gear Down	24,500	257.1	119.7
Gear Retraction (Table VII)			
Gross Weight - Gear Up	24,500	257.0	119.9
AIRPLANE MODE			
Gross Weight (Helicopter) - Gear Down	24,500	257.1	119.7
Rotor Retraction (Table VIII)			
Gross Weight - Rotor Stowed	24,500	261.9	115.1
Gear Retraction (Table VII)			
Gross Weight - Rotor Stowed and Gear Up	24,500	261.7	115.4

TABLE XIV. EXTREME FORWARD CENTER-OF-GRAVITY CONDITION

Item	Weight (lb)	Horizontal Arm (in.)	Vertical Arm (in.)
HELICOPTER MODE			
Weight Empty - Gear Down	17,961	257.0	122.8
Pilot	200	100.0	100.0
Copilot	200	100.0	100.0
Oil - Including Unusable	119	268.3	122.0
Unusable Fuel	20	266.0	136.0
Payload - Forward Cargo Compt.	1,500	211.5	86.0
Extreme Forward C.G. - Gear Down	20,000	250.5	119.6
Gear Retraction (Table VII)			
Extreme Forward C.G. - Gear Up	20,000	250.4	119.9
AIRPLANE MODE			
Extreme Fwd. C.G. (Helicopter) - Gear Down	20,000	250.5	119.6
Rotor Retraction (Table VIII)			
Extreme Fwd. C.G. - Rotor Stowed	20,000	256.3	114.1
Gear Retraction (Table VII)			
Extreme Fwd. C.G. - Rotor Stowed and Gear Up	20,000	256.2	114.4

TABLE XV. EXTREME AFT CENTER-OF-GRAVITY CONDITION			
Item	Weight (lb)	Horizontal Arm (in.)	Vertical Arm (in.)
HELICOPTER MODE			
Weight Empty - Gear Down	17,961	257.0	122.8
Pilot	200	100.0	100.0
Oil - Including Unusable	119	268.3	122.0
Unusable Fuel	20	266.0	136.0
Fuel	3,000	279.4	137.0
Extreme Aft C.G. - Gear Down	21,300	258.8	124.6
Gear Retraction (Table VII)			
Extreme Aft C.G. - Gear Up	21,300	258.6	124.9
AIRPLANE MODE			
Extreme Aft C.G. - Gear Down	21,300	285.3	124.6
Rotor Retraction (Table VIII)			
Extreme Aft C.G. - Rotor Stowed	21,300	264.2	119.4
Gear Retraction (Table VII)			
Extreme Aft C.G. - Rotor Stowed and Gear Up	21,300	264.1	119.7

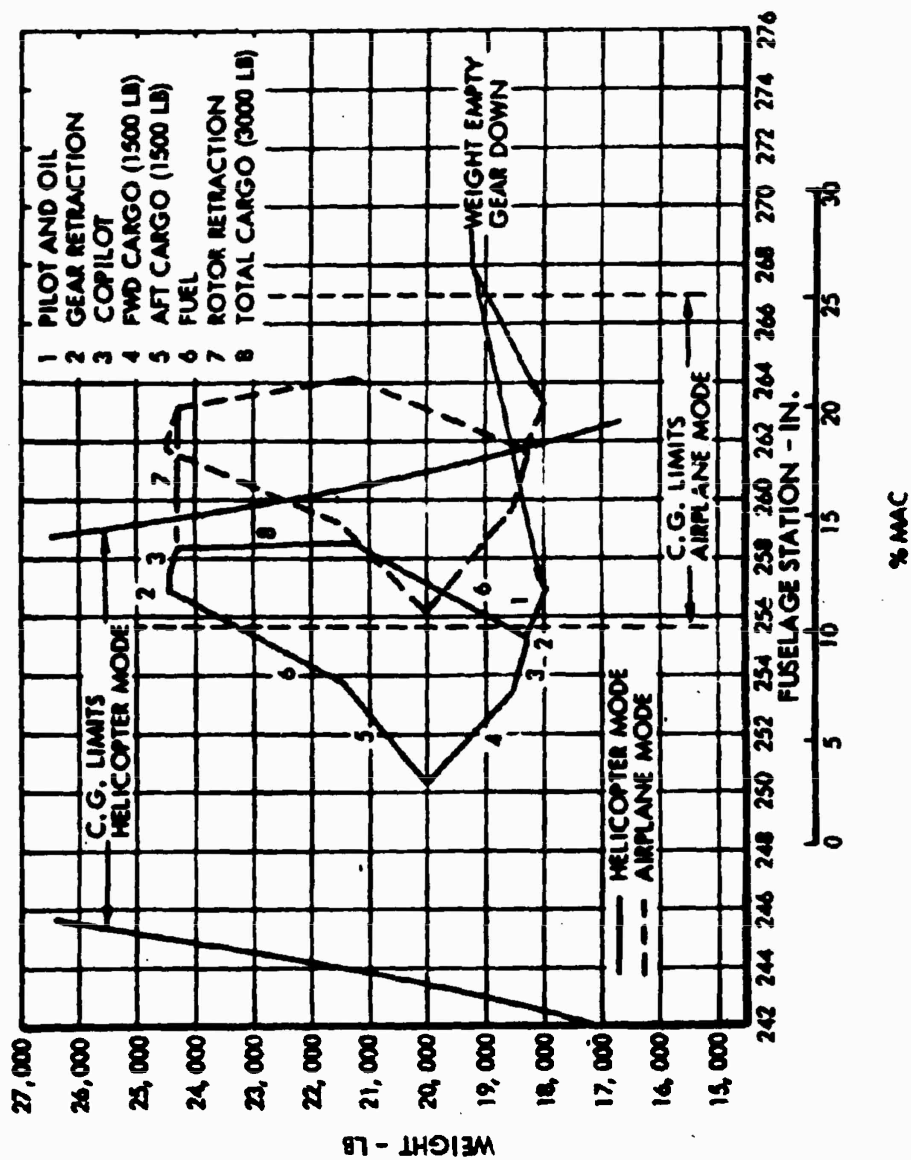


Figure 81. Center-of-Gravity Travel Diagram.

SECTION 10
SUPPLEMENTARY WEIGHT DATA

VARIATIONS FROM OPTIMUM DESIGN

The weight effects of certain variations in the optimum design configuration are shown in Table XVI. These include alternate design criteria, alternate components, optional installations, and certain installations required for the test program only.

EQUIPMENT WEIGHT ALLOWANCES

The weight allowances for equipment as specified in the work statement of the contract were used for derivation of the empty weight for the optimum design configuration.

TABLE XVI. WEIGHT VARIATIONS FROM OPTIMUM DESIGN CONFIGURATION	
Item	Weight Change (lb)
Increases in Weight Empty	
Nose Landing Gear - C-140 dual-wheel design in lieu of single-wheel alternate design	+ 68
Crew Seats - downward ejection in lieu of non- ejection installation	+213
Air Induction Filter System	+ 80
Decreases in Weight Empty	
Wing - 40-foot span in lieu of 50-foot span	-145
Reduced Load Factor - design limit load factor for fixed-wing mode reduced from 4.5 to 3.0	- 92

PART 5
STABILITY, CONTROL, AND FLYING QUALITIES

SECTION 11
FLIGHT CONTROL SYSTEMS

The primary flight control systems enable the pilots to control the aircraft in all the modes of flight using the same cockpit controls. These controls are of the same types as those used by other helicopters and airplanes. Maximum safety and reliability are obtained through the use of dual separated mechanical systems and dual tandem hydraulic actuators. Power for the actuators is provided by two physically separated hydraulic systems. Each system is powered by a pump driven off the main propulsion drive shaft. Either system is adequate to control the aircraft. In the airplane mode, the pitch of both propellers is controlled by a single propeller governor. In the helicopter mode, the propeller pitch is controlled manually with two levers on the center console.

When the aircraft is flown in the helicopter mode, the airplane controls are deactivated, and the operation is the same as that for other helicopters.

Deactivation of the airplane controls reduces the breakout friction forces to a level suitable for helicopter flight.

At the beginning of a transition, after the aircraft has been brought to the transition speed and attitude and trimmed there, the controls are transferred from helicopter mode to airplane mode. This involves activating the airplane controls and deactivating the helicopter controls. The helicopter controls are deactivated to remove the artificial feel from the controls for airplane flight. This also makes the airplane controls independent of hydraulic pressure. The mechanism used for transferring the controls gradually shifts over the controls from one mode to the other so that the transition is made smoothly and without discontinuity. This mechanism can be replaced with another mechanism which operates the helicopter controls and the airplane controls simultaneously so that this configuration can be evaluated. For the research vehicles, the transition from flight in the helicopter mode to flight in the airplane mode and vice versa has been broken down into a number of separately controlled steps to facilitate the recording of flight test data. It is expected that an operational aircraft would be designed so that this transition would be controlled automatically and result from a single pilot input. Then the rotor is stopped, the blades are folded, and the rotor is stowed.

After the transition, the aircraft is flown in the same manner as a fixed-wing airplane with type I mechanical controls and aerodynamic balances.

The pilot's and copilot's control sticks operate the longitudinal and lateral controls for both modes of flight. The rudder pedals operate the directional controls for both modes of flight. The collective levers are used only for vertical control in the helicopter mode.

Because of the downward ejection escape system, the pilot's control sticks are mounted on four bar linkages which give the required stick movement without a true pivot. The linkages include push-pull rods which are spring-loaded to shorten themselves and thus pull the sticks forward out of the pilot's way. This action is initiated by cables attached to the "D" rings of the seats. These cables release latches which normally maintain the rods at full length.

ROTARY-WING FLIGHT CONTROL SYSTEM

In the helicopter mode, the propeller blades are in the zero thrust position, and the aircraft is controlled in the same way as other helicopters. Below the transition speed, forward flight can be accomplished with the rotor, and maneuvers can be accomplished in the same manner as for other helicopters. The pilot also has the choice of using the propellers to obtain thrust for forward flight.

The pilot's procedure for entering autorotation is dependent upon the speed at which power failure occurs. At speeds up to 100 knots, transition to autorotation is similar to that of other helicopters.

At speeds between 100 and 140 knots, the propellers can be used to extract energy from the passing airstream and thus minimize rotor speed decay. Decreasing the propeller pitch accomplishes this.

The mechanism used for transferring the cyclic and directional controls from the helicopter mode to the airplane mode consists of a linkage with a single input and two outputs. When the shifting mechanism is in the helicopter position, the helicopter output responds to any input, and the airplane output remains fixed. As the shifting mechanism is moved by an electric actuator from the helicopter position to the airplane position, the helicopter output motion decreases and the airplane output motion increases proportionately.

When the shifting mechanism is in the airplane position, the airplane output responds completely to any input, and the helicopter output remains fixed. When shifting from the airplane controls to helicopter controls, the reverse is true. At no time is either set of controls disconnected from the cockpit. Provisions will be made in the research vehicles so that these mechanisms can be replaced by other mechanisms that will allow both the helicopter controls and the airplane controls to be operated simultaneously. When the aircraft is parked, the controls are transferred into the helicopter mode, and the mechanisms act as control surface locks.

The same mechanism is used in the collective control system, but in that application it has two inputs and one output. The pilot's input is used for flight in the helicopter mode. An electric actuator is used for the other input. It provides the correct amount of collective control movement to allow the blades to overlap when folded.

HELICOPTER CONTROLS

Main Rotor Controls

The cyclic control system is similar to the control systems on other rigid-rotor helicopters. The pilot's cyclic stick controls the rotor blade pitch through a control gyro. This gyro is mounted in the rotor hub above the blades. It is driven at 6600 rpm by a two-stage planetary gear train from the main shaft. The high speed at which the gyro runs increases its effectiveness, so that it can be lighter in weight and smaller in size.

The hydraulic actuators are all located on the lower part of the transmission housing. Since the rotor retracts into the fuselage, the control linkages provide for this movement.

To establish an understanding of the operation of the cyclic control system, it is appropriate to outline the sequence of events which occur following a pilot input:

- Assume that the pilot pushes the cyclic stick forward one inch.
- The valve on the boost cylinder is displaced and the boost cylinder compresses the longitudinal spring to apply a rolling moment to the swash plate.
- The rolling moment is transferred to the gyro swash plate through the parallel linkage and causes the control gyro to develop a precession rate in the nose-down direction. The gyro displacement is not hindered by the spring in the lateral control system because the force in the lateral compensating actuator balances the effect of the spring.
- Displacement of the gyro with respect to the rotor shaft produces a cyclic feathering of the blades about their feathering axes with the blade pitch decreased on the right side and increased on the left side.
- The cyclic pitch produced by the gyro displacement causes the rotor blades to flap down in the 180-degree azimuth position and up in the 0-degree azimuth position.

- A nose-down hub moment is developed by the rotor flapping which accelerates the helicopter nose-down until the airframe rate of pitch is equal to the rate of precession of the gyro.
- When the aircraft has pitched nose-down to the attitude the pilot desires, he then returns the control stick to neutral, thus relieving the servo load on the gyro and stopping its rate of precession.
- As the gyro ceases to precess, the vehicle ceases to pitch and remains in a nose-down attitude while it accelerates into forward flight.
- A reversal of the process will bring the aircraft back to hover.

The cyclic systems are provided with feel springs at the stick and trim systems between the boost cylinder and the swash plate. The trim systems consist of springs attached to linear electromechanical actuators which are controlled by switches on the cyclic stick. With these systems, the pilot can balance any moments applied to the gyro by blade bending moments acting through the forward blade sweep. The trim systems are effective with boost on or off.

The collective pitch system consists of conventional collective pitch sticks for both the pilot and the copilot. These sticks operate a dual hydraulic actuator which raises and lowers the swash plate and gyro in a collective mode. The linkages between the collective sticks and the actuator are duplicated, and the hydraulic actuator is operated from two separate transmission-mounted hydraulic pumps. An adjustable friction device and a feel-spring cartridge are included to provide optimum feel characteristics in the system.

Directional Control

The directional control system consists of adjustable rudder pedals for both the pilot and the copilot, a dual hydraulic actuator at the tail rotor, and linkage for moving the tail rotor blades in collective pitch. The linkage between the pedals and actuator is duplicated, and the actuator is operated by two separate transmission-mounted hydraulic pumps. The trim and feel system on the pedals is similar to that on the cyclic stick.

FIXED-WING FLIGHT CONTROL SYSTEM

In the airplane mode, the main rotor is stopped and stowed, and the aircraft is controlled in the same manner as a conventional fixed-wing airplane.

Longitudinal Control System

Longitudinal control is provided by a stick in the cockpit and a positive mechanical system which controls an aerodynamically balanced elevator. The system incorporates a 12-pound downspring to provide free control stability at the aft center-of-gravity limit. The aerodynamic balance consists of a round nose balance and a 1:1 geared trailing edge tab. The geared tab is also used as a trim tab. The trim tab is a mechanically adjustable tab which holds a given setting by friction. The horizontal stabilizer has two incidences: a zero incidence for all flights in the airplane mode except landing, where a 6-degree nose-down position can be selected.

Lateral Control System

Lateral control is provided by a stick in the cockpit and a positive mechanical system which controls an aerodynamically balanced aileron. The aerodynamic balance is a Frise-type balance which is designed so that it provides a favorable yawing moment when the ailerons are deflected. The ailerons are equipped with a trim tab which is mechanically adjustable and holds a given setting by friction.

Directional Control System

Directional control is provided by rudder pedals and a positive mechanical system which controls a rudder. The rudder does not require an aerodynamic balance. Trim is provided by a trim tab on the rudder which is mechanically adjustable and holds a given setting by friction.

TRANSITION CONTROLS

At the beginning of a transition, after the aircraft has been accelerated to transition speed and level attitude and has been trimmed, the controls are transferred gradually from helicopter mode to airplane mode. This involves activating the airplane controls and deactivating the helicopter controls.

The mechanism used for transferring the cyclic controls from the helicopter mode to the airplane mode consists of a linkage with a single input and two outputs. When the shifting mechanism is in the helicopter position, the helicopter output responds to any input, and the airplane output remains fixed. As the shifting mechanism is moved by an electric actuator from the helicopter position to the airplane position, the helicopter output motion decreases and the airplane output motion increases proportionately. When the shifting mechanism is in the airplane position, the airplane output responds completely to any input, and the helicopter output remains fixed. When shifting from the airplane controls to helicopter controls, the reverse is true. At no time is either set of controls disconnected from the cockpit.

The same mechanism is used in the collective control system, but in this application it has two inputs and one output. The pilot's input is used for flight in the helicopter mode. An electric actuator is used for the other input. It provides the correct amount of collective control movement to allow the blades to overlap when folded.

Wing Flap Control System

The wing flaps extend or retract at a fixed rate in response to three-position, momentary-contact switches located on the collective levers. An asymmetry detection system is provided to sense any asymmetrical condition in the flaps and to light a warning light in the cockpit.

Rotor Stopping Control System

When transition speed has been reached, when the aircraft flight controls have been changed from helicopter mode to airplane mode, and when the rotor system has been declutched from the engines and allowed to slow to 50 percent of speed, the rotor may be stopped by engaging the rotor-stopping control system. The stopping system is engaged by operating the brake switch located on the center console in the cockpit to the "Brake On" position. After the switch has been operated, the rotor system is automatically controlled to stop the rotor at the precise position necessary to permit folding of the blades.

As the main rotor speed decreases and as the gyro loses its effectiveness to control the feathering angle of the rotor blades, two rotor blade pitch bias actuators, which normally act as gyro nutation dampers, become increasingly effective to control blade feathering angles.

Rotor Blade Pitch Bias System

The bias actuators are controlled by an aerodynamic vane located on the left wing tip of the aircraft. The vane is connected to the bias actuators by a system of levers, links, and cables, and is held in a mid-stroke position. The bias actuators hold the rotor blades at zero pitch. If the aircraft encounters a gust while the rotor is decelerating, accelerating, or stopped, the vane senses the adverse airflow and automatically causes the bias actuators to change rotor blade pitch in the proper direction to reduce the rotor blade load. In the helicopter mode, the rotor blade pitch bias actuators act as gyro nutation dampers.

PROPELLER CONTROLS

Forward thrust is provided by two propellers located on nacelles on the wings and interconnected by the cross shaft. The propeller pitch can be controlled manually or it can be controlled automatically by the propeller governor. Two levers are located on the right side of the center console for controlling propeller pitch. These are used for taxiing the aircraft,

for accelerating from hover to transition speed, and for decelerating from transition speed.

A control wheel is located on the extreme right side of the center console for controlling the propeller governor. A single propeller governor controls the speed by adjusting the pitch of both propellers to fit the power level established for the engines and the forward speed of the aircraft. Advancing the control wheel from the "Off" position activates the propeller governor and deactivates the engine governors.

Propeller governing is used for flight in the airplane mode and for taking off and landing as an airplane. At the same time that the propeller governor is activated, a low-pitch stop is engaged in each propeller to keep it from going into flat pitch during flight in the airplane mode.

The propeller control levers are connected to the propeller control by cable systems. The output of the propeller governor is carried through a separate torque tube to each propeller control mechanism.

SECTION 12

STABILITY AND CONTROL ANALYSIS

This section contains the analytical work which is used to substantiate the compliance of the CRA with all pertinent stability and control requirements. The discussion of the compliance with specific requirements is presented in the Compliance With Requirements part of this section.

HELICOPTER MODE

Longitudinal Characteristics

Longitudinal Static Stability

The longitudinal static stability of a helicopter from the pilot's standpoint is measured by the change of stick position and stick force required to change forward speed. The stick position will change as a function of forward speed for two reasons: (1) it is related to the gyro position which is related to the cyclic pitch required to trim, and (2) it is related to the forces required to balance out external moments acting on the gyro.

The longitudinal stick position for the CRA as a function of forward speed, center-of-gravity position, and flight condition has been computed using the outputs of the IBM computer trim program for cyclic pitch and feedback moments and the geometry of the control system. The results of these calculations are shown on Figure 82. The stick force gradient which was used to calculate the force is 2 pounds per inch. Note that Figure 82 shows that the stick position and force are stable in both the helicopter regime and the compound aircraft regime.

Longitudinal Dynamic Stability

The dynamic stability of the CRA has been analyzed with an analog computer which solves the equations of motion of the helicopter and the control gyro. The computer has been used to generate time histories of the response of the aircraft following control inputs and simulated gust disturbances.

The equations of motion which are used in the analog computer and the methods of evaluating the coefficients of the equations are presented in Reference 11.

A systematic study of the response of the CRA to control step and pulse inputs has been made. Figures 83 through 85 show time history responses to longitudinal step control inputs at 0 and 80 knots. Figure 86 shows a corresponding response to a 1-inch, 1/2-second, longitudinal control pulse.

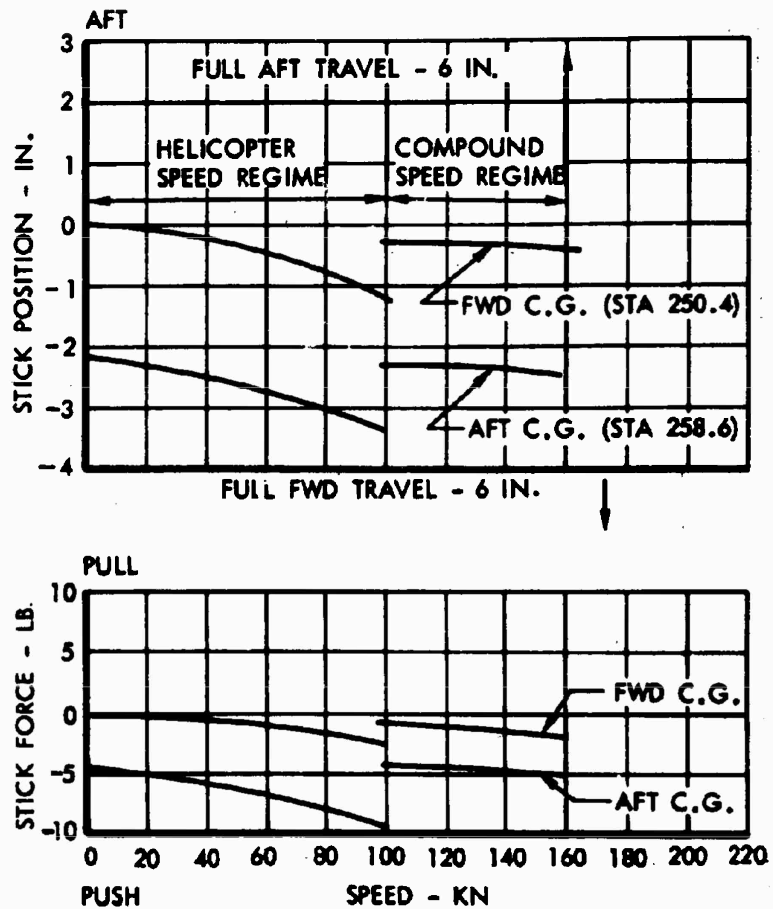


Figure 82. Longitudinal Stick Force and Position Vs. Speed - Helicopter Mode.

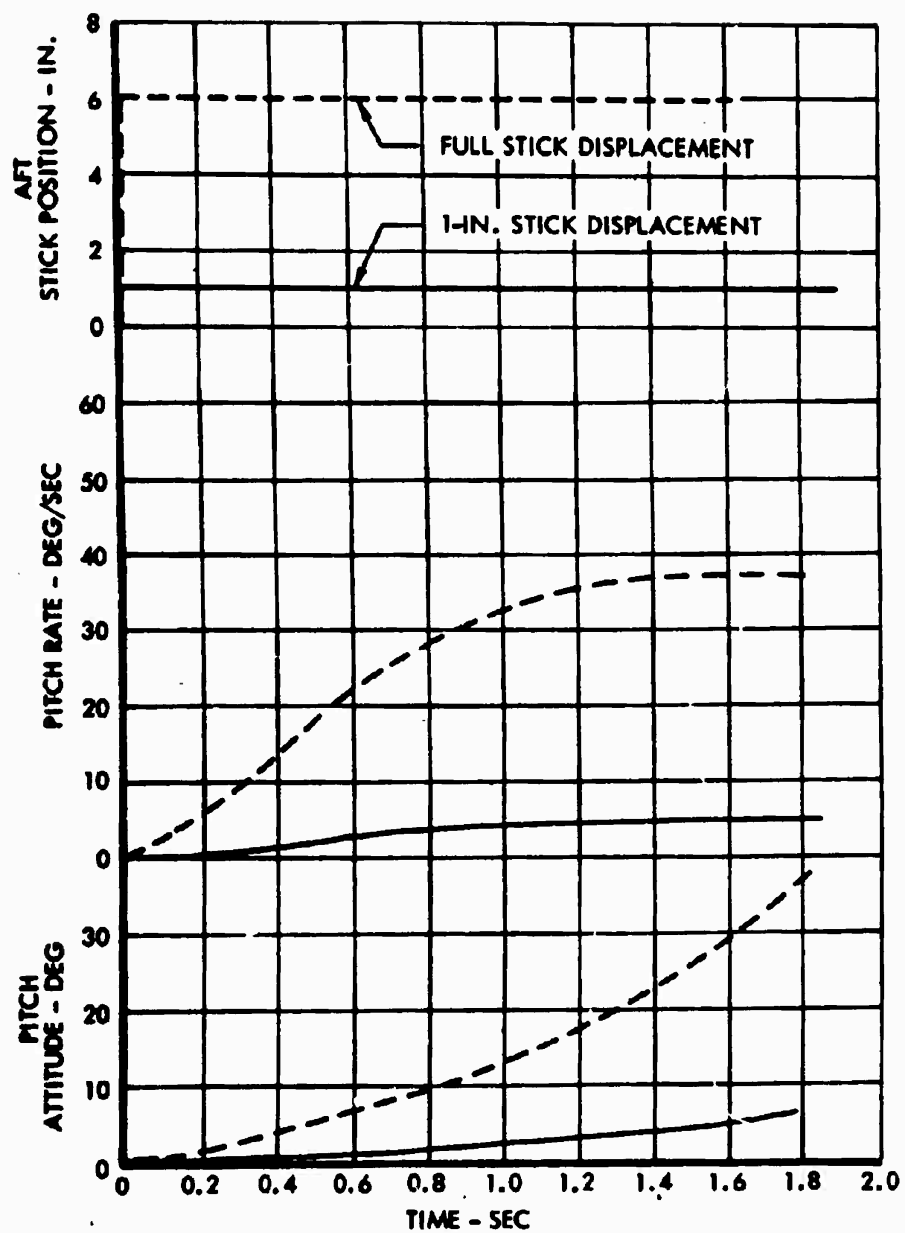


Figure 83. Response to Longitudinal Step Inputs in Hover.

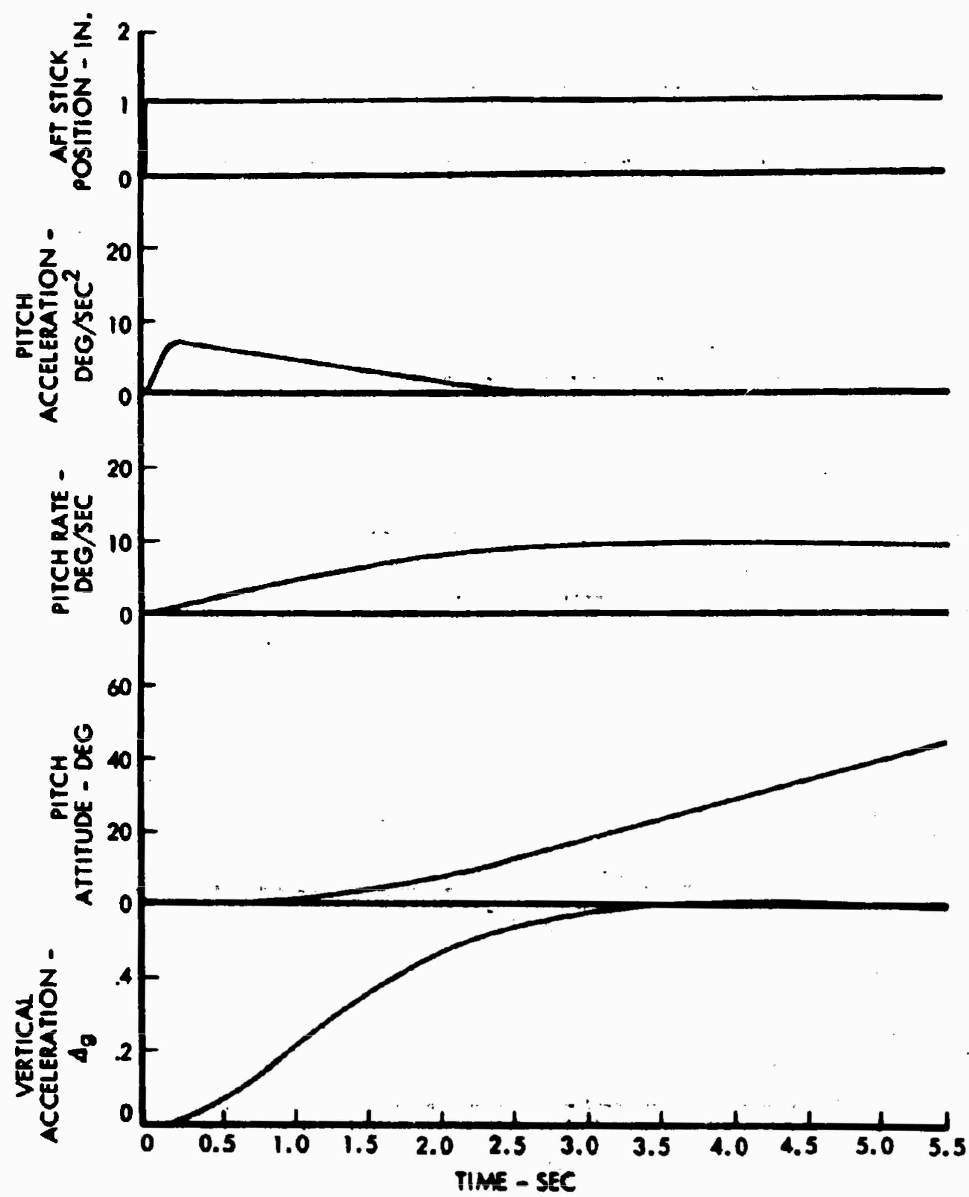


Figure 84. Response to a 1-Inch Longitudinal Step Input, 80 Knots, Aft Center of Gravity.

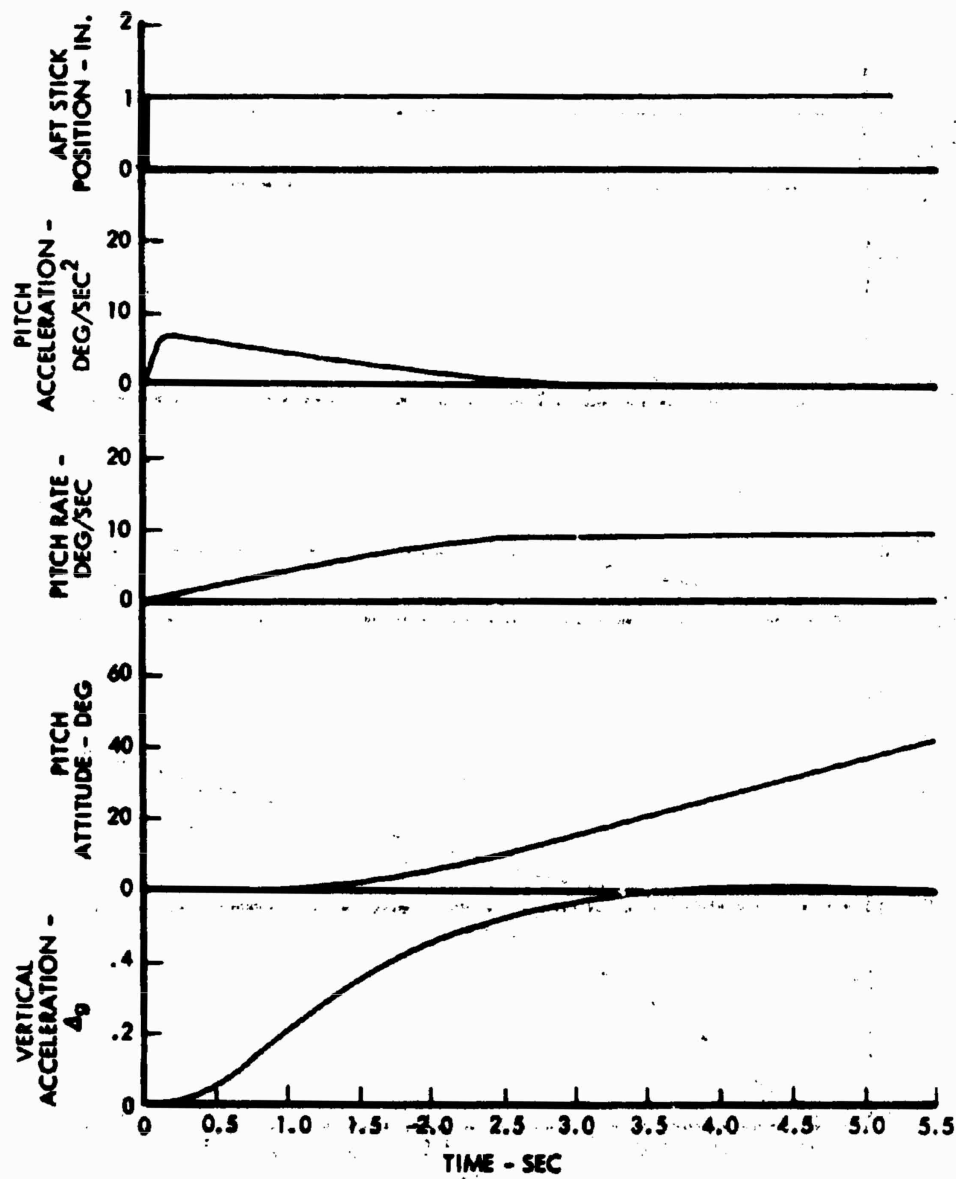


Figure 85. Response to a 1-Inch Longitudinal Step Input, 80 Knots, Forward Center of Gravity.

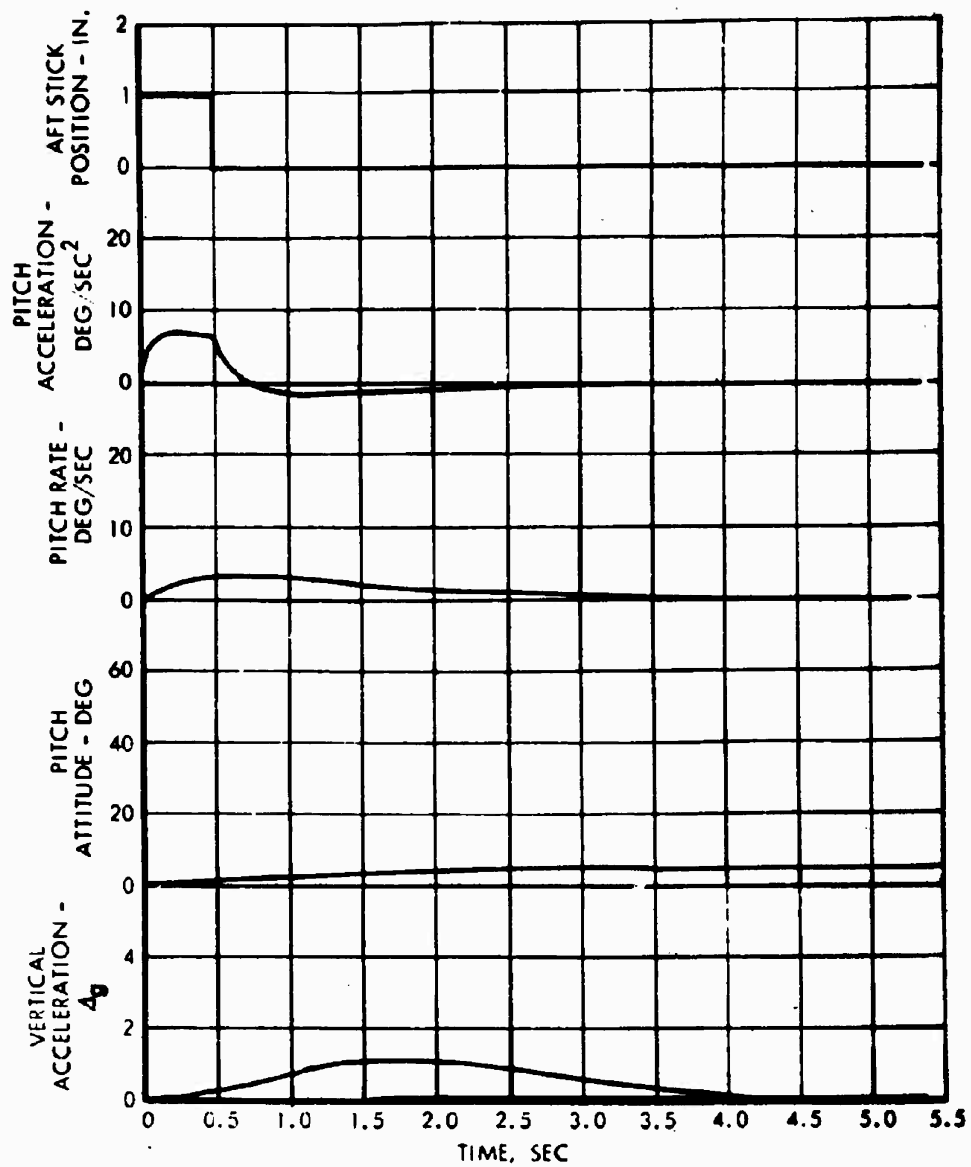


Figure 86. Response to a 1-Inch Longitudinal Pulse Input at 80 Knots,

A study of the analog computer traces of Figures 84 and 85 shows that there is little difference in the characteristics of the responses as a function of center-of-gravity position. This lack of difference is the result of the fact that the longitudinal and lateral dynamics of rigid-rotor helicopters are primarily influenced by the rotor stiffness, the gyro characteristics, and the moment of inertia of the fuselage and only secondarily by the changes in forces acting on the vehicle.

Longitudinal Control Power and Damping in Hover

The control power and damping in hover can be approximated from a consideration of the gyro and the forces which act on it. The control system is essentially a rate system; but the blade sweep forward generates a feedback moment on the gyro, as explained in the controls description, which changes its characteristics to a pseudo-displacement system. This fact can be used to calculate the rotor moment generated by a 1-inch stick displacement with the rotor shaft fixed in space. For the CRA, the gyro rolling moment is 166 foot-pounds per inch of fore and aft stick displacement.

The damping can be derived by noting that, at the condition for a steady pitch, the rate of pitch is equal to the rate of precession of the gyro and that the precession rate of the gyro is produced by the rotor moment acting through the blade sweep forward. For the CRA, the damping in pitch is -31,500 foot-pounds/radian/second.

The calculated values and the requirements for control power and damping from MIL-H-8501A can be plotted on the stability map of M_H/I and C/I of Figure 85.

For the CRA at the overload gross weight of 28,800 pounds, the requirement of paragraph 3.2.13 of MIL-H-8501A is 1.61 degrees of pitch in the first second following a 1-inch longitudinal stick displacement. This requirement can be incorporated in an expression between control power and damping by solving a one-degree-of-freedom system which results in the equation for pitch displacement of

$$\Theta = \frac{M}{I} \left[\tau + \frac{1}{\frac{C}{I}} \left(e^{-\frac{C}{I} \tau} - 1 \right) \right] \quad (1)$$

For $\Theta = 1.61$ degrees, the corresponding plot of M/I vs C/I is shown on Figure 87. The requirement for C/I is based on paragraph 3.2.14 of MIL-H-8501A. For the overload weight of 28,800 pounds, the requirement is -20,550 foot-pounds/radian/second. This has been divided by the inertia in pitch and plotted on Figure 87. The actual control

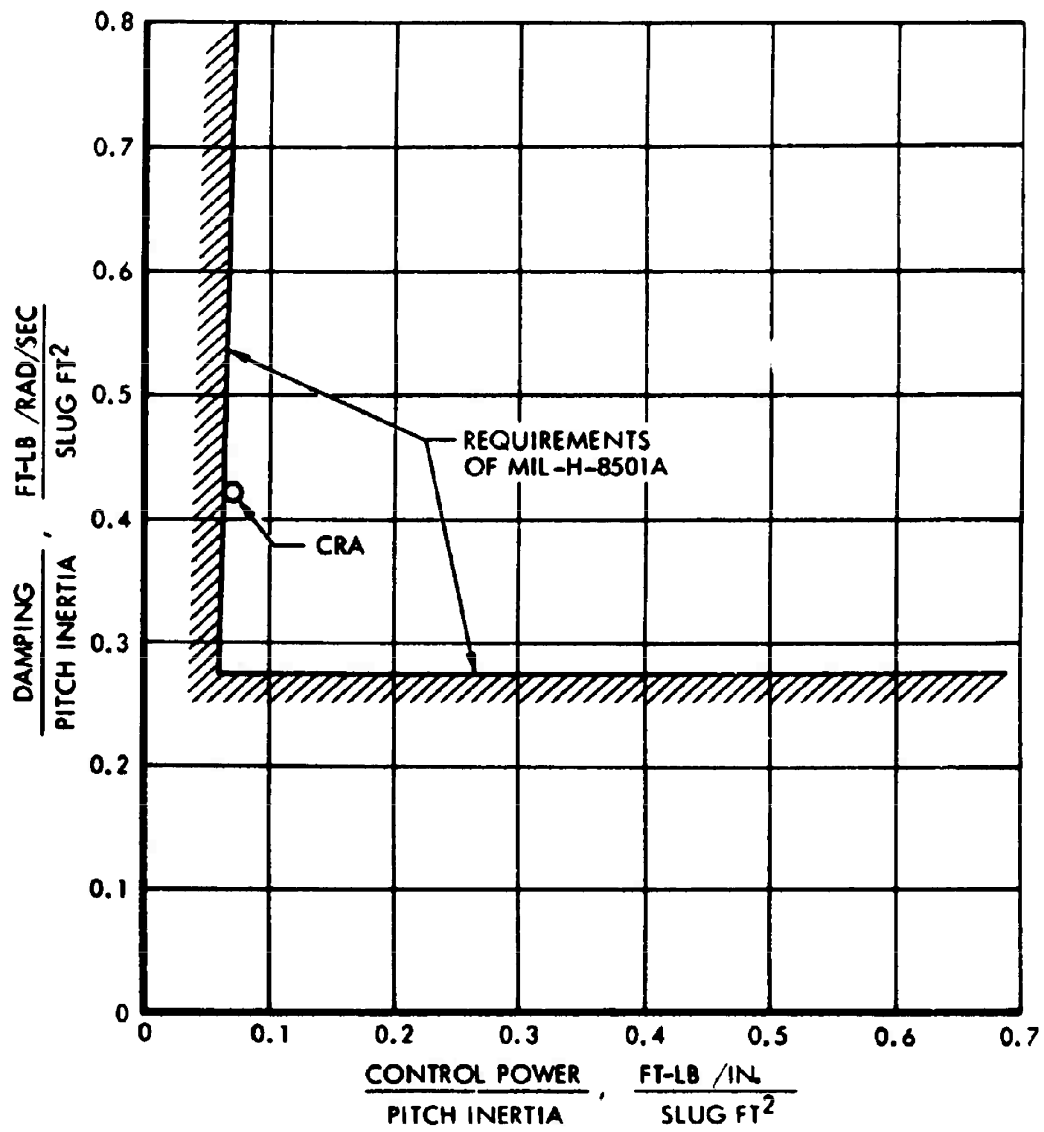


Figure 87. Control Power and Damping in Pitch - Helicopter Mode.

power of the CRA produces the capability of a displacement of 2.3 degrees in the first second as shown on Figure 83. It may be seen from Figure 87 that the CRA satisfies the MIL-Spec requirements.

Longitudinal Trim Capability

The longitudinal trim system has been designed to balance an external gyro moment of 1000 foot-pounds. The highest center-of-gravity offset shown in Figure 81 results in a pitching moment, M_H , of 17,000 foot-pounds. This results in a gyro moment of only 611 foot-pounds. Thus, the trim system can balance moments due to the highest operational center-of-gravity offsets and have a large margin for aerodynamic moments acting on the helicopter.

Maneuvering Stability

The longitudinal maneuvering stability as measured as stick force per g has been calculated by adding the bob-weight effect of 9 pounds/g to the force generated by the feel springs per g. The latter contribution was found from the analog results for one-inch step control inputs of Figures 84 and 85 for the fore and aft center-of-gravity positions by the following equation:

$$\frac{\Delta F}{g} = \frac{2}{g_{MAX}} \quad (2)$$

Figure 88 shows the results of this study.

Lateral Characteristics

Lateral Stick Position as a Function of Sideslip Angle

The lateral stick position in forward flight has been computed by a procedure similar to that used for the longitudinal case. The effect of sideslip is to rotate the cyclic pitch orientation in the direction of the flight path and to produce a rolling moment due to wing dihedral. These effects have been used to compute the lateral stick position plotted in Figure 89. Figure 90 shows the dihedral effect as measured in the wind tunnel.

Response to Lateral Control Input

The analog computer was used to investigate the response to lateral control step and pulse inputs. Figures 91 and 92 show the response to step inputs at hover and at 80 knots. As in the case of the response to longitudinal inputs, there is little difference in the responses as a function of speed. Figure 92 shows that there is little yaw for the first 2 seconds of a rolling maneuver. Figure 93 shows that the response to a roll pulse in forward flight is highly damped.

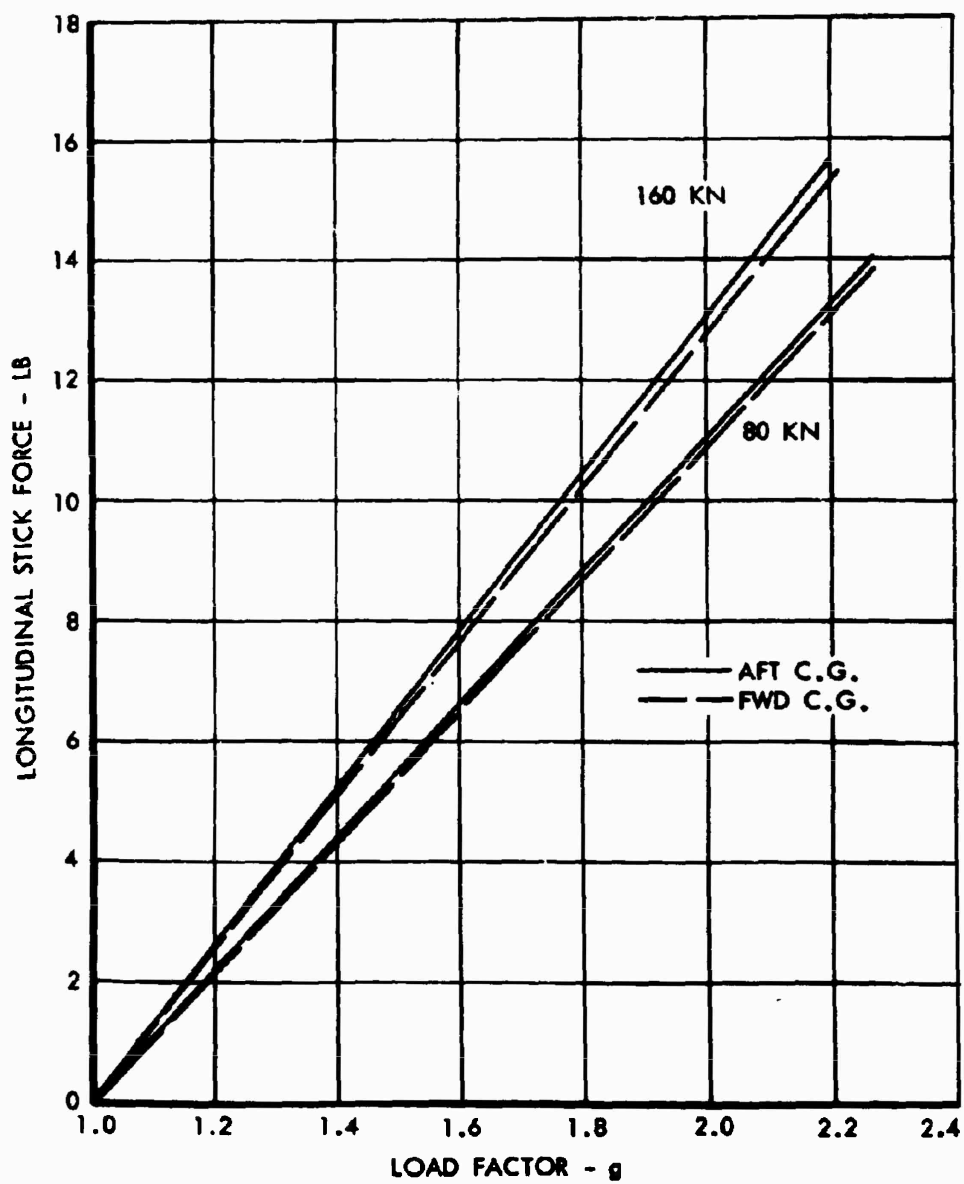


Figure 88. Maneuvering Stability - Helicopter Mode.

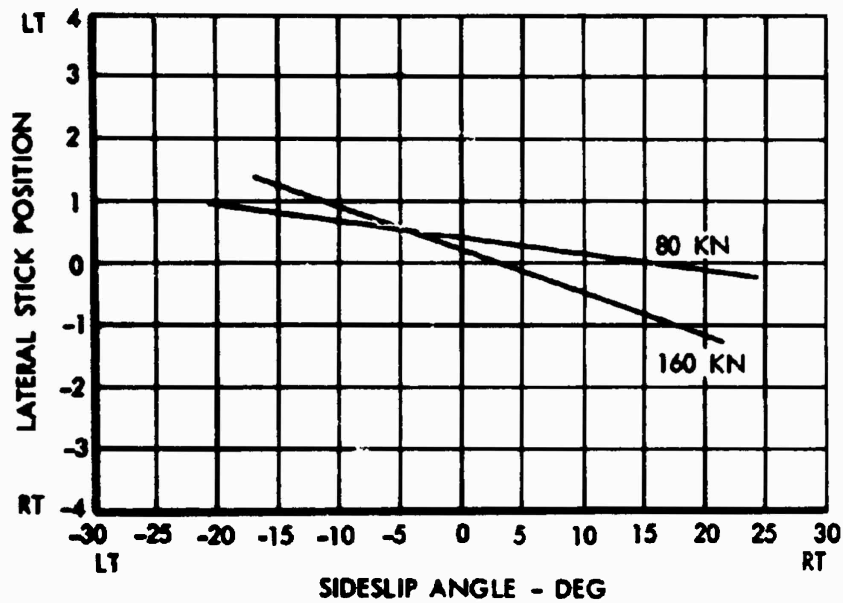


Figure 89. Lateral Stick Position Vs. Sideslip Angle-Helicopter Mode.

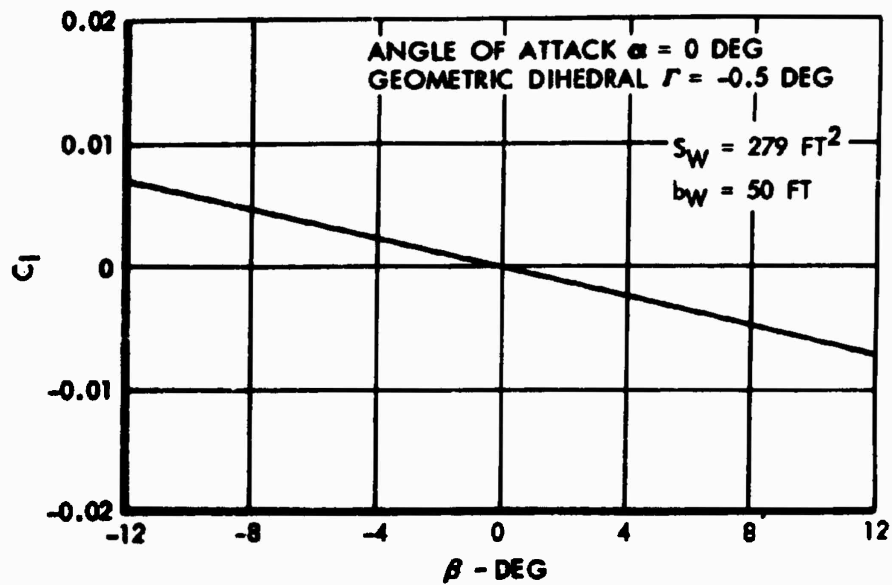


Figure 90. Rolling Moment Coefficient Vs. Sideslip Angle.

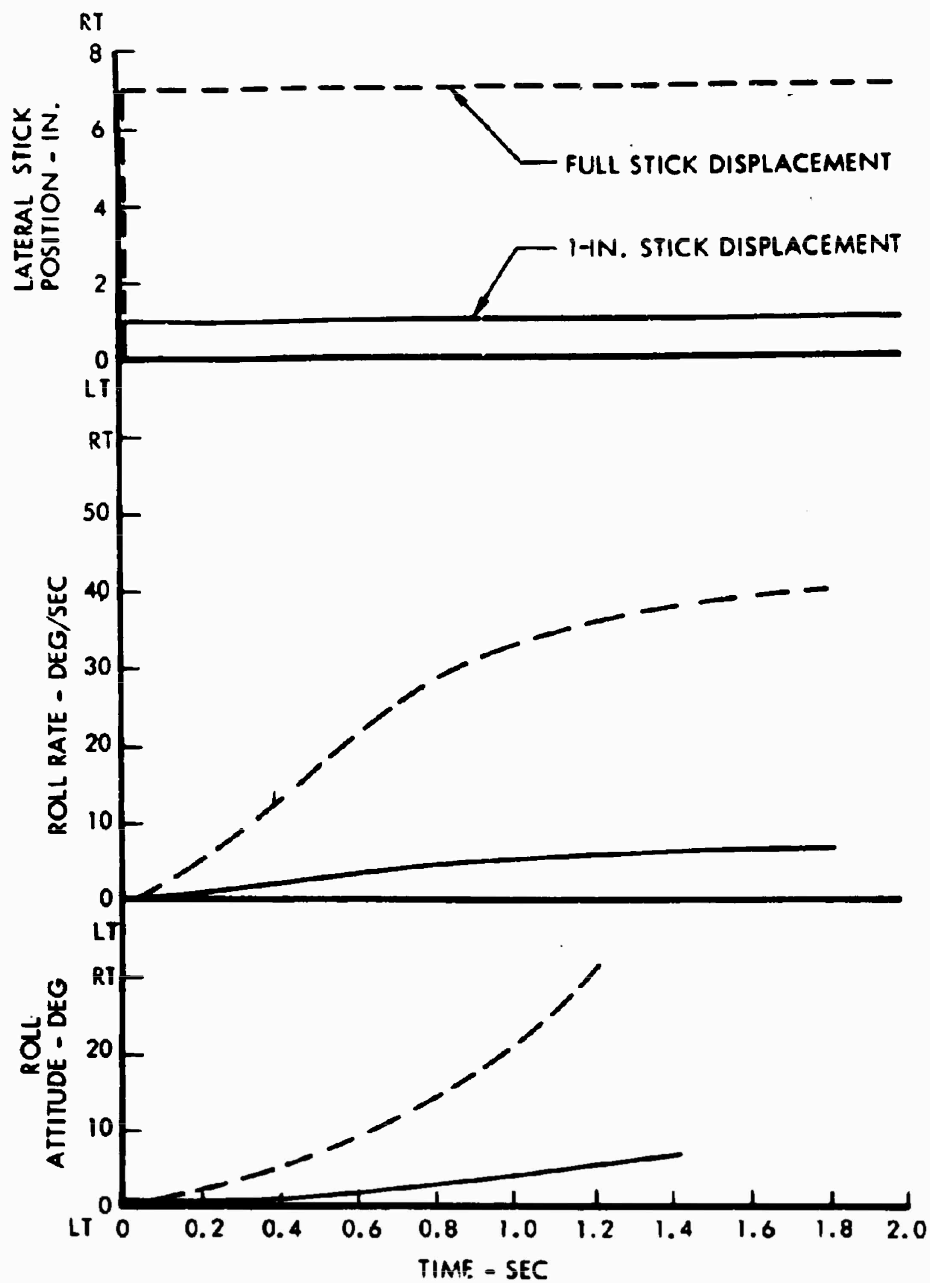


Figure 91. Response to Lateral Step Inputs in Hover.

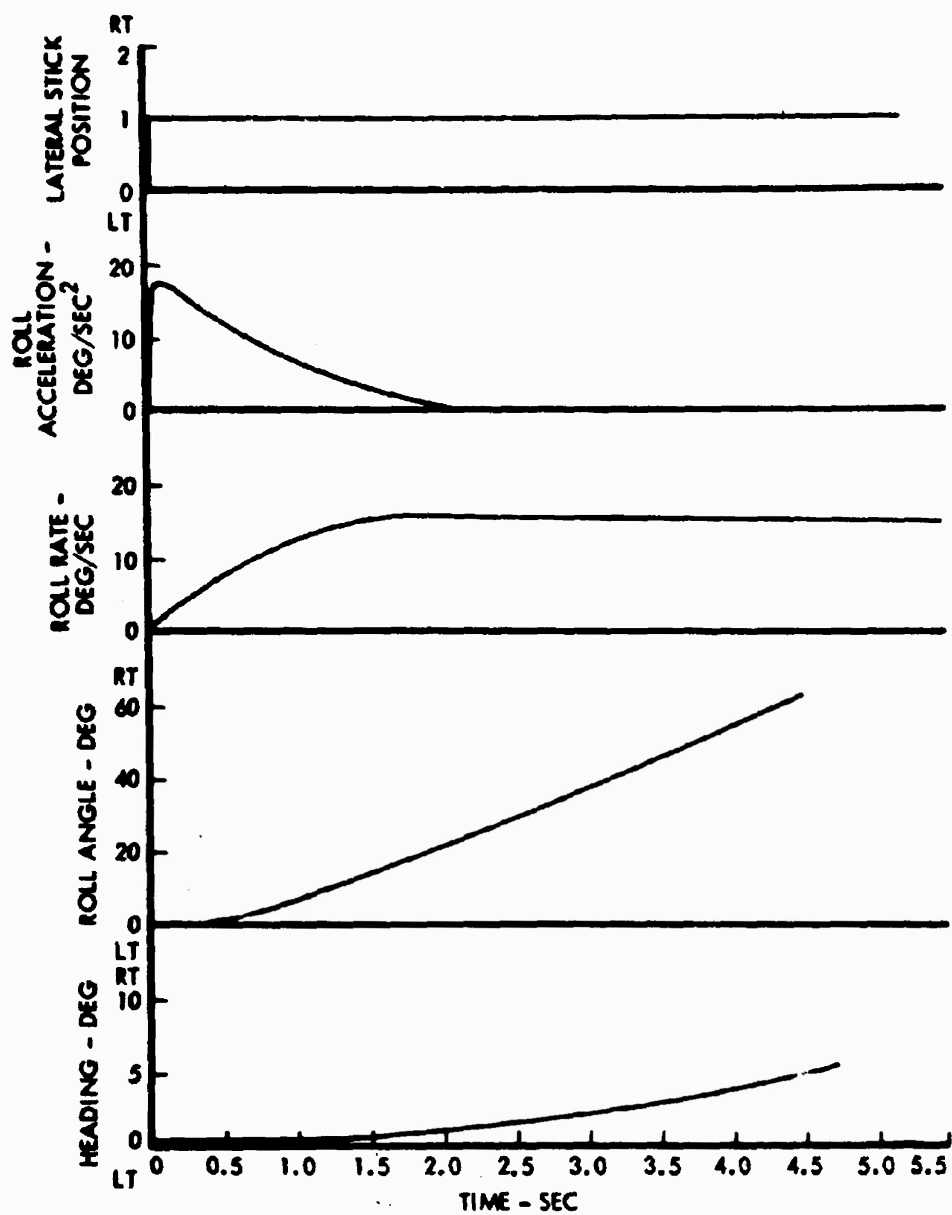


Figure 92. Response to a 1-Inch Lateral Step Input, 80 Knots.

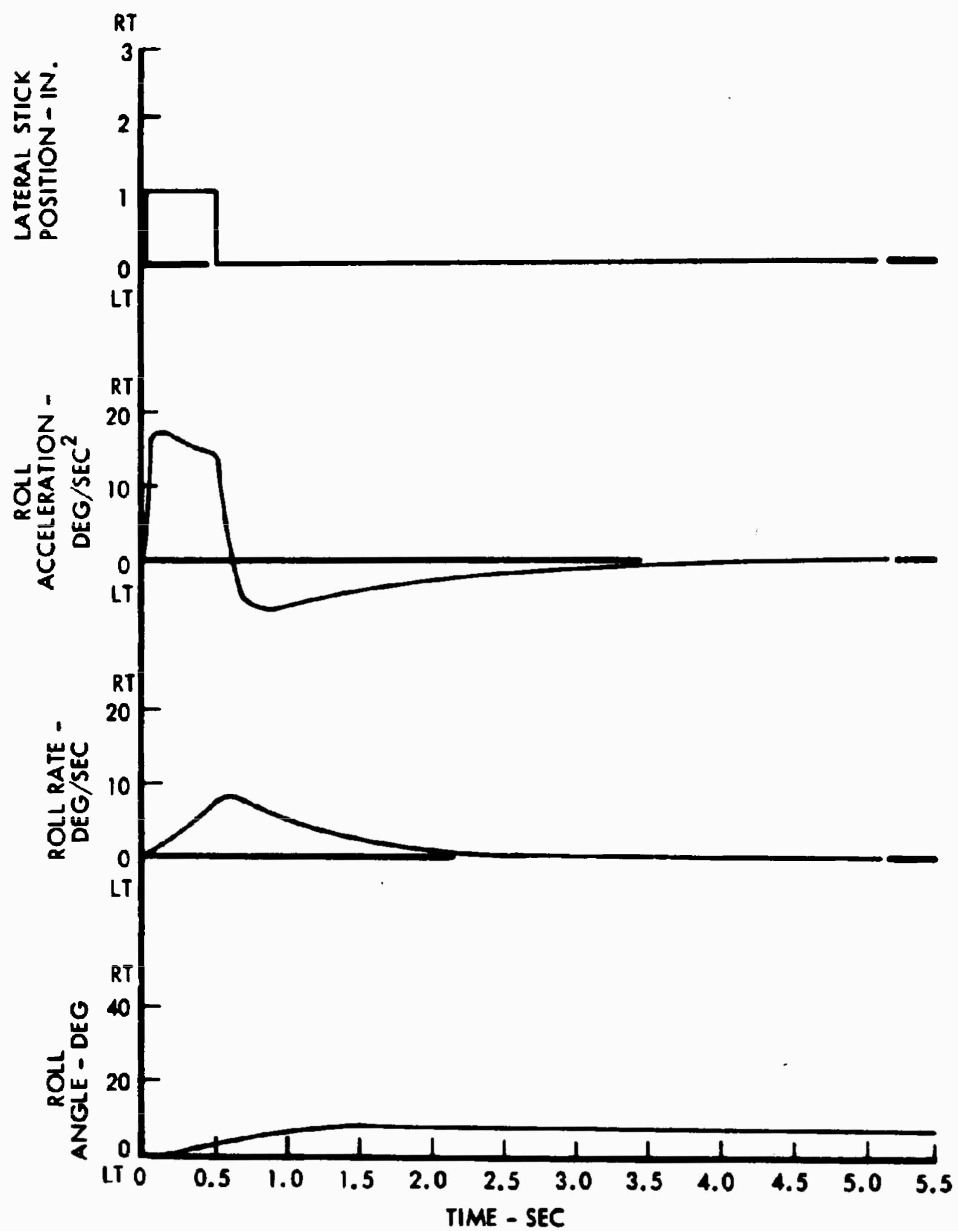


Figure 93. Response to a 1-Inch Lateral Pulse Input, 80 Knots.

Lateral Control Power and Damping in Hover

The analysis of lateral control power and damping in hover is identical to the longitudinal analysis. The lateral damping due to the rotor and gyro is identical to the longitudinal damping or -31,500 foot-pounds/radian/second. This compares to a requirement of -25,600 foot-pounds/radian/second based on the requirements of MIL-H-8501A. The lateral control power is 1.58 times the longitudinal control power, since the control system is designed to produce 262 foot-pounds of moment on the gyro for 1 inch of lateral stick input compared to 166 foot-pounds for 1 inch of longitudinal stick input. Thus, the lateral control moment is $1.58 \times 52,400$ or 82,600 foot-pounds per inch of stick displacement.

The damping and control power in roll have been plotted on the stability map of Figure 94 along with the MIL-Spec requirements. It may be seen that the CRA exceeds the requirements. For this case, the requirement for roll displacement in the first half second is 0.97 degree, but the CRA has the capability of 1.6 degrees in the first half second.

Directional Characteristics

Pedal Position and Force as a Function of Speed

The pedal position is directly related to the tail rotor collective pitch through a mechanical linkage. The tail rotor collective pitch is one of the outputs of the digital computer performance and trim program. Figure 95 shows the pedal position as a function of speed.

Pedal Position and Force as a Function of Sideslip Angle

The directional stability of the CRA was measured during the wind tunnel tests described in Reference 1. These results are plotted in Figure 96 and have been used to determine the tail rotor collective pitch required to trim in sideslip at various speeds. A plot of the results is presented in Figure 97.

Sideward Flight

In sideward flight, the tail rotor must produce enough thrust to balance the aerodynamic moment on the fuselage as well as the main rotor torque. The fuselage moment on the CRA in sideward flight has been estimated by replacing the fuselage side elevation by a simpler one made up of flat-plate rectangles and trapezoids, and summing the moment due to each by integration.

Using a simplified side view, the expression for the fuselage yawing moment is

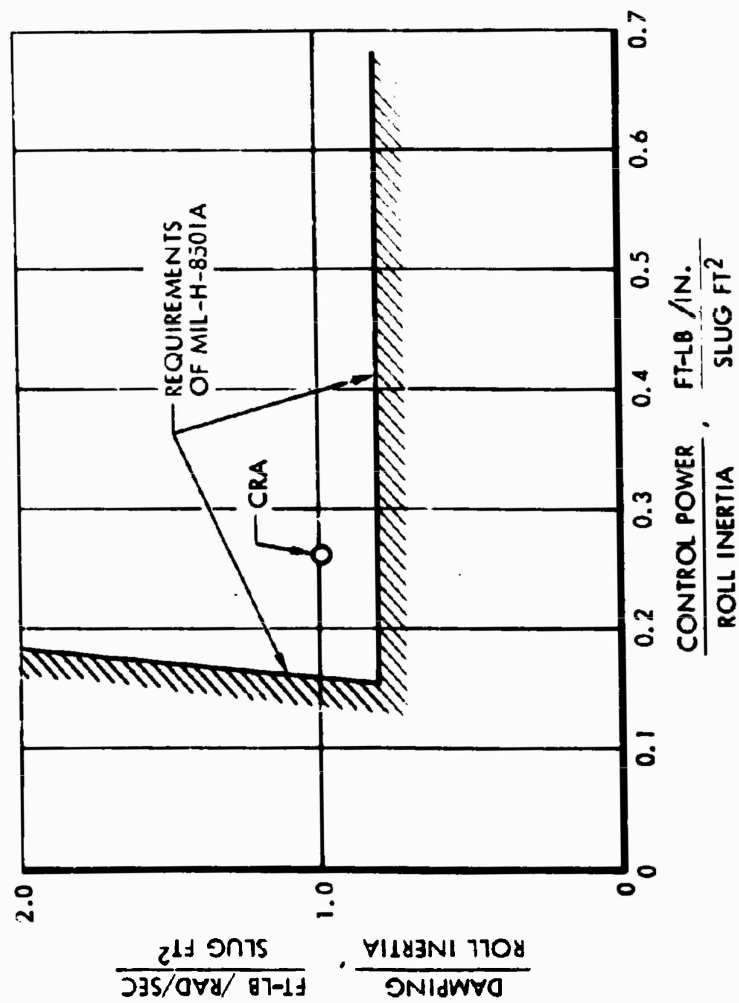


Figure 94. Control Power and Damping in Roll - Helicopter Mode.

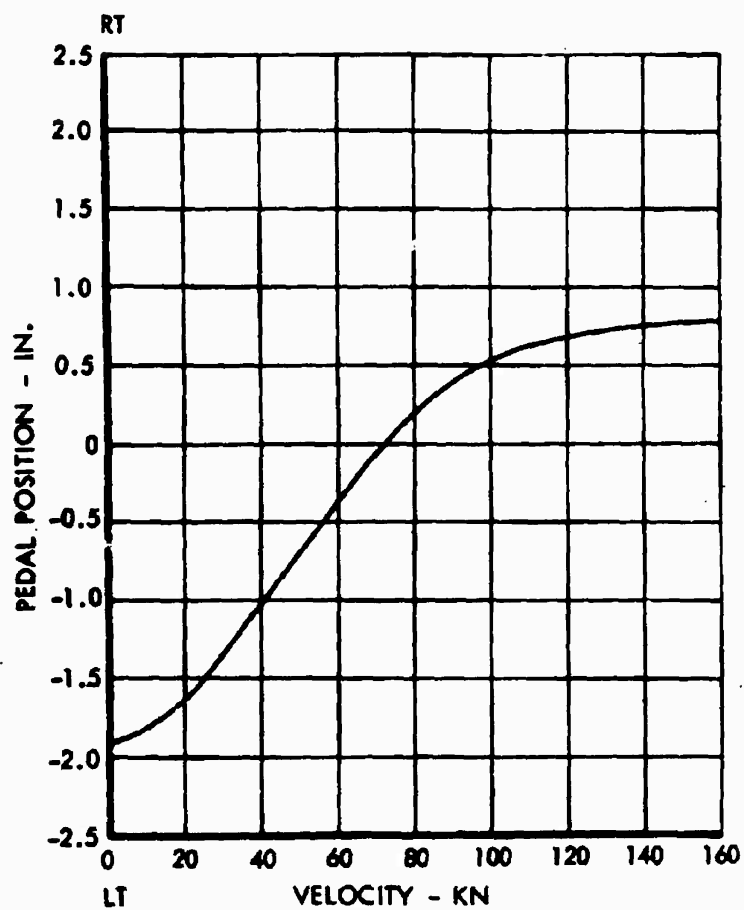


Figure 95. Pedal Position Vs. Velocity - Helicopter Mode.

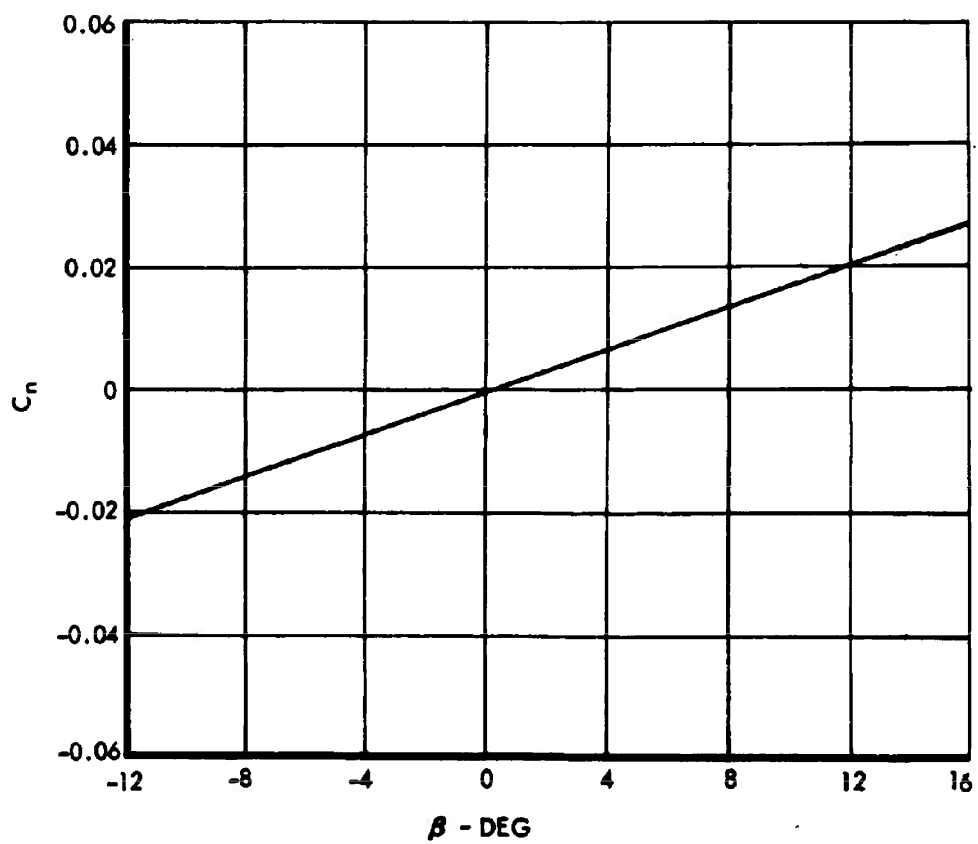


Figure 96. Yawing Moment Coefficient Vs. Sideslip Angle.

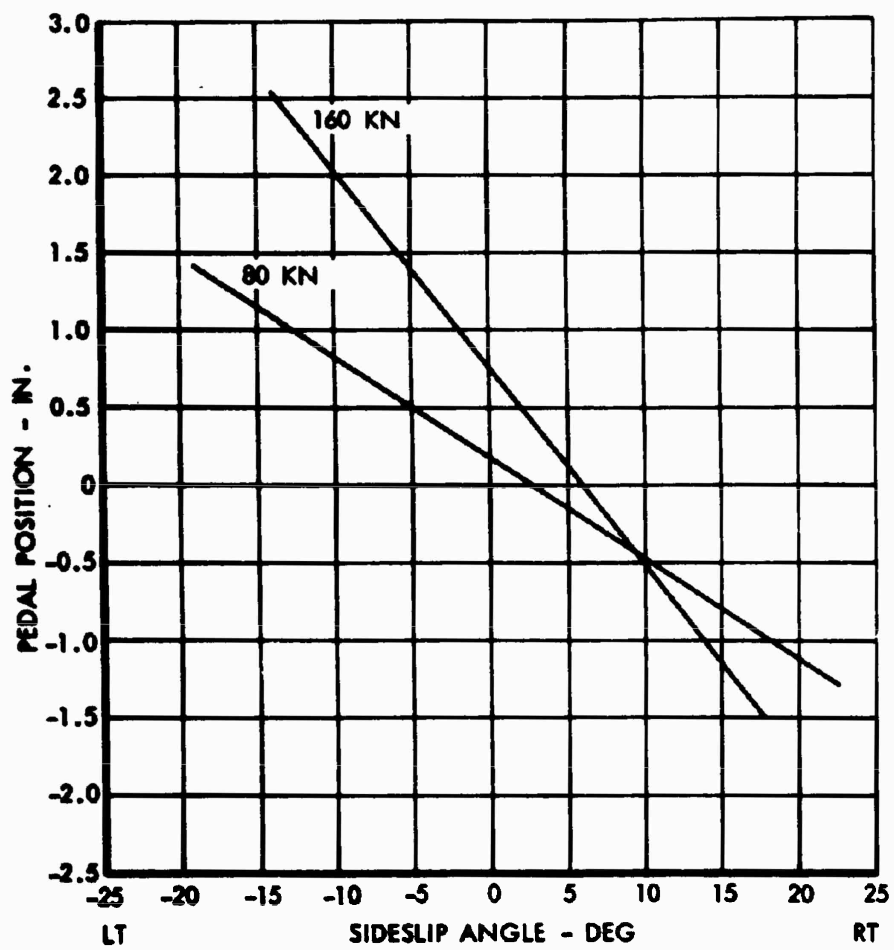


Figure 97. Pedal Position Vs. Sideslip Angle - Helicopter Mode.

$$N_T = C_D q \left[- \int_0^{16} 10.4 \ell d\ell + \int_0^{4.25} 10.4 \ell d\ell + \int_{4.25}^{10.3} (11.5 - .26\ell) \ell d\ell + \int_{10.3}^{32} (11.7 - .274\ell) \ell d\ell + 68(36.4) \right] \quad (3)$$

Using a drag coefficient of 1.0, the moment is

$$N_T = 4286q \quad (4)$$

The thrust required of the tail rotor in sideward flight is

$$T_{TR} = \frac{Q + 4286q}{\ell_{TR}} \quad (5)$$

The torque, Q , of the main rotor has been calculated and is shown as a function of velocity in Figure 98. Figure 99 shows the thrust capability of the tail rotor at its maximum collective pitch setting of 26° as a function of sideward flight velocity, along with the thrust required of it. It may be seen that a sideward velocity of 60 knots can be achieved.

Hovering Turns

Hovering turns over a spot in calm air or in winds may be studied by use of the single-degree-of-freedom equation for yawing motions:

$$N_{initial} = I_z \ddot{\psi} + \frac{\partial N}{\partial \psi} \dot{\psi} \quad (6)$$

The solution for a pedal kick from initial equilibrium is

$$\psi = \frac{N_{initial}}{-\frac{\partial N}{\partial \psi}} \left\{ t - \frac{I_z}{\frac{\partial N}{\partial \psi}} \left[e^{\frac{\frac{\partial N}{\partial \psi}}{I_z} t} - 1 \right] \right\} \quad (7)$$

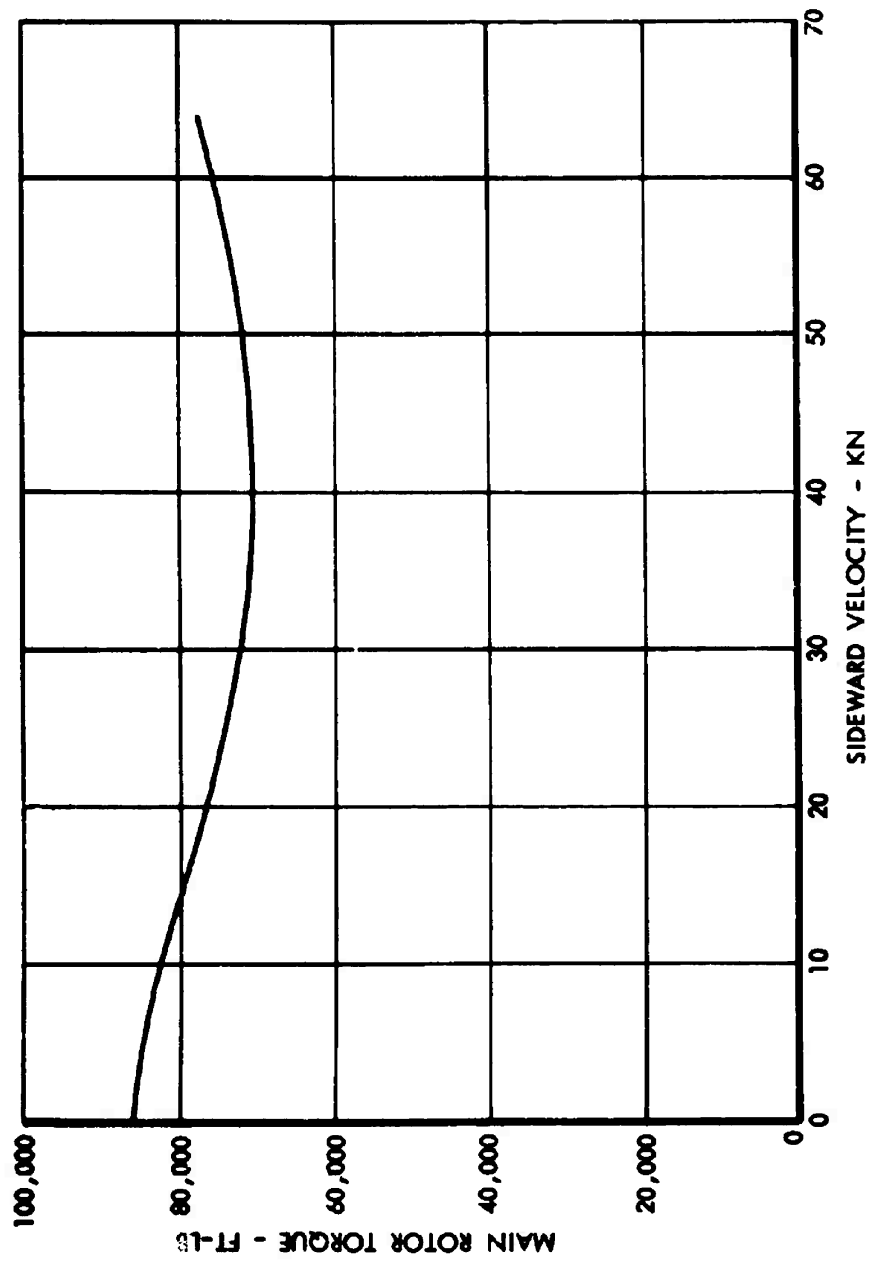


Figure 98. Main Rotor Torque Vs. Sideward Velocity.

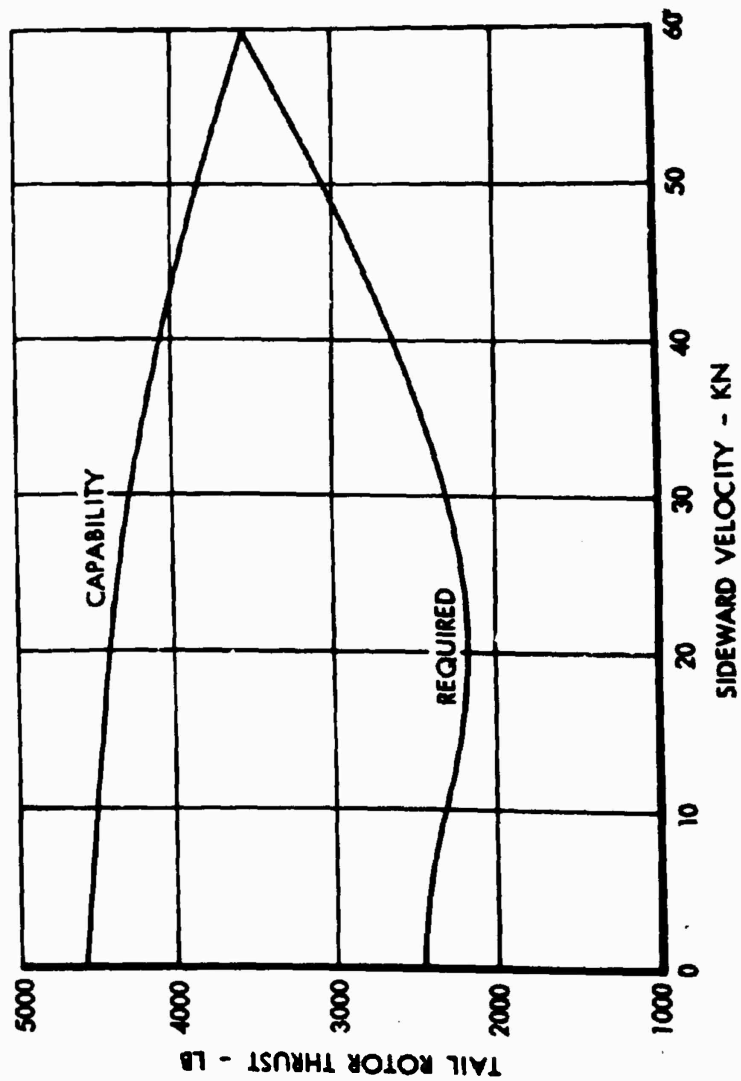


Figure 99. Tail Rotor Capability and Requirement in Sideward Flight.

where $\partial N / \partial \dot{\psi}$ is the damping in yaw due to both the fuselage and the tail rotor. The tail rotor's contribution was found by using the Hovering and Vertical Flight Computer Program to calculate tail rotor thrust over a range of sideward flight velocities for fixed values of collective pitch. The values of tail rotor thrust so obtained were plotted against sideward flight velocity. The slope of this curve is $\partial T_{TR} / \partial V$, which determined the tail rotor yaw damping:

$$\left(\frac{\partial N}{\partial \dot{\psi}} \right)_{TR} = l_T^2 \frac{\partial T}{\partial V} \quad (8)$$

The tail rotor damping is -25,060 foot-pounds/radian/second.

The contribution of the fuselage and vertical tail was calculated using the simplified fuselage side view. The general equation for the yawing moment of the fuselage and tail in sideward flight with concurrent yawing is

$$\begin{aligned} N_f = & -\frac{1}{2} \rho C_D \frac{(v_s + \dot{\psi} l)}{|v_s + \dot{\psi} l|} \int_{\frac{1}{2} \left(\left| \frac{v}{\dot{\psi}} \right| - \frac{v}{\dot{\psi}} \right)}^{l_{fwd}} h_{fwd} (v_s + \dot{\psi} l)^2 l dl \\ & - \frac{1}{2} \rho C_D \frac{(v_s + \dot{\psi} l)}{|v_s + \dot{\psi} l|} \int_C^{\frac{1}{2} \left(\left| \frac{v}{\dot{\psi}} \right| - \frac{v}{\dot{\psi}} \right)} h_{fwd} (v_s + \dot{\psi} l)^2 l dl \\ & + \frac{1}{2} \rho C_D \frac{(v_s - \dot{\psi} l)}{|v_s - \dot{\psi} l|} \int_C^{\frac{1}{2} \left(\left| \frac{v}{\dot{\psi}} \right| + \frac{v}{\dot{\psi}} \right)} h_{aft} (v_s - \dot{\psi} l)^2 l dl \\ & + \frac{1}{2} \rho C_D \frac{(v_s - \dot{\psi} l)}{|v_s - \dot{\psi} l|} \int_{\frac{1}{2} \left(\left| \frac{v}{\dot{\psi}} \right| + \frac{v}{\dot{\psi}} \right)}^{l_{aft}} h_{aft} (v_s - \dot{\psi} l)^2 l dl \end{aligned} \quad (9)$$

where V_s is the sideward flight velocity or equivalent wind velocity during hovering. In still air ($V_s = 0$), only the first and fourth integrals exist, since there is no l region between 0 and $V_s/\dot{\psi}$. In this case, for the particular simplified fuselage sideview described above,

$$\begin{aligned}
 N_1 &= -\frac{1}{2} \rho C_D \frac{\dot{\psi}}{|\dot{\psi}|} \int_0^{16} 10.4 \dot{\psi}^2 l^3 \, dl \\
 &= -\frac{1}{2} \rho C_D \frac{\dot{\psi}}{|\dot{\psi}|} \int_0^{4.25} 10.4 \dot{\psi}^2 l^3 \, dl \\
 &= -\frac{1}{2} \rho C_D \frac{\dot{\psi}}{|\dot{\psi}|} \int_{4.25}^{10.3} (11.5 - 0.26l) \dot{\psi}^2 l^3 \, dl \\
 &= -\frac{1}{2} \rho C_D \frac{\dot{\psi}}{|\dot{\psi}|} \int_{10.3}^{32} (11.7 - 0.274l) \dot{\psi}^2 l^3 \, dl \\
 &= -\frac{1}{2} \rho C_D \frac{\dot{\psi}}{|\dot{\psi}|} (34.0)^3 (0.8)
 \end{aligned} \tag{10}$$

This equation reduces to

$$N_1 = -5006 \dot{\psi}^2 \tag{11}$$

so that the yaw damping of the fuselage and vertical tail is

$$\frac{\partial N_1}{\partial \dot{\psi}} = -10,012 \dot{\psi} \tag{12}$$

To obtain a conservative solution, this is evaluated at $\dot{\psi} = 0.5$ radian/second

$$\frac{\partial N_f}{\partial \psi} = -5006 \text{ foot-pounds/radian/second} \quad (13)$$

Thus, the total yaw damping in hover is -30,066 foot-pounds/radian/second. The yawing moment created by a sudden displacement of the rudder pedals is given by

$$N_{\text{initial}} = l_{\text{TR}} \left(\frac{\partial T_{\text{TR}}}{\partial \theta_o} \frac{\partial \theta_o}{\partial x_p} x_p \right) \quad (14)$$

The pedal gearing in the CRA is such that $\partial \theta_o / \partial x_p = 6.14$ degrees/inch.

The value of $\partial T_{\text{TR}} / \partial \theta_o$ obtained from the computer data mentioned earlier is 258 pounds/degree. Using these values, the yawing moment caused by a 1-inch pedal displacement was determined to be 56,200 foot-pounds. When this yawing moment and the yaw damping are substituted into the equation for ψ , the fuselage yaw angle 1 second after the pedal kick is found to be 5.0 degrees at an overload gross weight of 28,800 pounds ($I_z = 98,716$ slug-ft²). At a minimum flight weight of 18,400 pounds ($I_z = 91,400$ slug-ft²), the corresponding yaw angle is 16.0 degrees. For the case of the normal gross weight, the requirement of paragraph 3.3.5 of MIL-H-8501A specifies a displacement of 3.7 degrees at the end of the first second.

In Figure 99, it can be seen that the tail rotor is capable of creating a thrust of 2100 pounds, which produces a yawing moment of 74,500 foot-pounds, over and above the amount necessary to balance all moments while hovering in still air at an overload gross weight of 28,800 pounds. A full pedal displacement in hover will result in an initial yawing moment of like amount. The corresponding yaw displacement after 1 second is 19.6 degrees, and the requirement from MIL-H-8501A is 11.1 degrees.

The yawing displacement for full pedal control inputs while hovering in a 35-knot wind may be obtained by the same procedure as above.

In this case, since V (35 knots; i.e., 59.1 ft/sec) is always greater than $\dot{\psi}$ (max $0.5 \times 36.4 = 18.2$ ft/sec), only the first and third integrals exist (or the second and fourth if V is minus). For the particular simplified fuselage noted earlier,

$$\begin{aligned}
N_f = & -\frac{1}{2} \rho C_D \int_0^{16} 10.4(59.1 + \dot{\psi} l)^2 l dl \\
& + \frac{1}{2} \rho C_D \int_0^{4.25} 10.4(59.1 - \dot{\psi} l)^2 l dl \\
& + \frac{1}{2} \rho C_D \int_{4.25}^{10.3} (11.5 - 0.26)(59.1 - \dot{\psi} l)^2 l dl \\
& + \frac{1}{2} \rho C_D \int_{10.3}^{32} (11.7 - 0.274)(59.1 - \dot{\psi} l)^2 l dl \\
& + \frac{1}{2} \rho C_D (59.1 - 34.6\dot{\psi})^2 (34.6)(68)
\end{aligned} \tag{15}$$

This equation reduces to

$$N_f = 16846 - 21454\dot{\psi} + 4602\dot{\psi}^2 \tag{16}$$

from which the yaw damping is

$$\frac{\partial N_f}{\partial \dot{\psi}} = -21,454 + 9204\dot{\psi} \tag{17}$$

Evaluated at $\dot{\psi} = 0.5$ rad/sec, the fuselage yaw damping is

$$\frac{\partial N_f}{\partial \dot{\psi}} = -16,852 \text{ ft-lb/rad/sec} \tag{18}$$

The total damping, including the contribution of the tail rotor, is

$$\frac{\partial N}{\partial \psi} = -41,912 \text{ ft-lb/rad/sec} \quad (19)$$

From Figure 99, the tail rotor thrust margin available at 35 knots is 1750 pounds. This is equivalent to a yawing moment of 62,000 ft-lb, and the resulting yaw displacement after one second is 15.7 degrees. The requirement for this condition from paragraph 3.3.6 of MIL-H-8501A is 3.7 degrees.

Response to Directional Control Inputs

The analog computer was used to study the response to pedal step and pulse inputs. Figure 100 shows response to a 1-inch step input.

Autorotation Characteristics

Entry Into Autorotation

The rotor speed decay characteristics are analyzed in this section to establish conformity with the requirement that it shall be possible to make a safe transition to autorotation following a complete power failure.

In hover, the rotor deceleration, $d\Omega/dt$, can be given in terms of the initial torque, Q_1 , and a time varying torque, $\Delta Q(t)$, as follows:

$$\frac{d\Omega}{dt} = \frac{-[Q_1 + \Delta Q(t)]}{I} \quad (20)$$

The time-varying portion of the torque can be evaluated by expanding the torque in terms of the torque coefficient and the rotor speed which are the pertinent parameters. This gives

$$\Delta Q(t) = \left(\frac{\partial Q}{\partial C_Q} \right) \left(\frac{\partial C_Q}{\partial \Omega} \right) \Delta \Omega + \left(\frac{\partial Q}{\partial \Omega} \right) \Delta \Omega \quad (21)$$

The assumption is made that the change in rotor speed, $\Delta \Omega$, is linear with time. For time periods of less than two seconds, this assumption has been found to be valid. Thus,

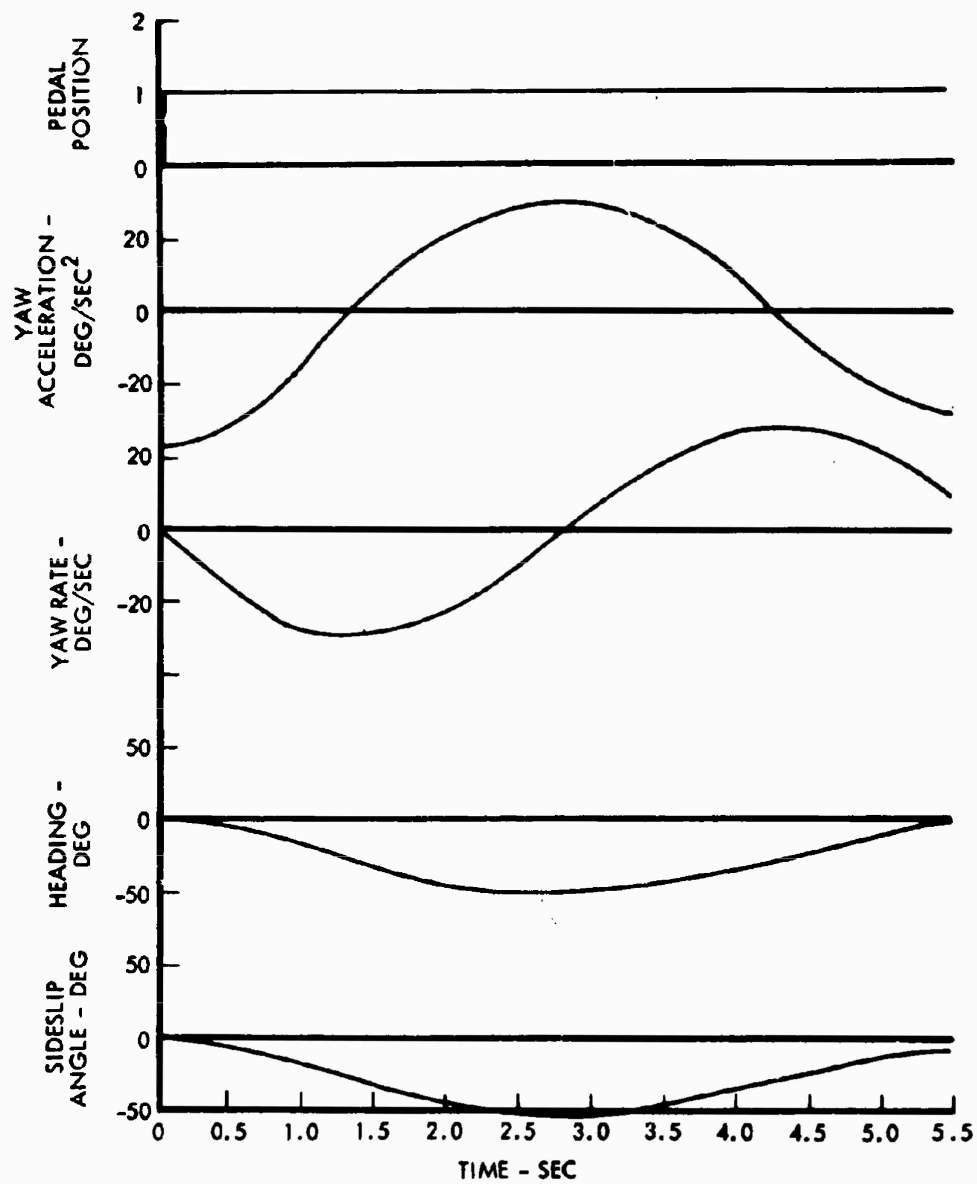


Figure 100. Response to a 1-Inch Directional Input, 80 Knots, Aft Center of Gravity.

$$\Delta\Omega = \left(\frac{d\Omega}{dt} \right) t \quad (22)$$

Combining Equations (20), (21), and (22) results in the following expression for rotor speed:

$$\Omega_2 = \Omega_1 \left\{ 1 - \frac{Q_1}{I\Omega_1 K} \left[\ln(1 + Kt) \right] \right\} \quad (23)$$

where

$$K = \frac{\left[\frac{\partial Q}{\partial C_Q} \frac{\partial C_Q}{\partial \Omega} + \frac{\partial Q}{\partial \Omega} \right]}{I} \quad (24)$$

For the purposes of evaluating the parameter K, it can be assumed that C_Q remains essentially constant. This implies a constant collective pitch angle and constant induced velocity. Therefore,

$$K \approx \frac{\frac{\partial Q}{\partial \Omega}}{I} \approx \frac{2Q_1}{I\Omega_1} \quad (25)$$

It is noted that the parameter $Q_1/I\Omega_1$ can be given in terms of the equivalent power as $HP550/1\Omega_1^2$. This permits the use of the more readily available engine horsepower data. Equation (23) for rotor speed decay can now be given as

$$\Omega_2 = \Omega_1 \left\{ 1 - 1/2 \ln \left[1 + \frac{2HP550}{I\Omega_1^2} t \right] \right\} \quad (26)$$

where I is the equivalent system moment of inertia of the main rotor, the tail rotor, and the propellers.

The rotor speed decay using Equation (26) has been determined for a gross weight of 24,500 pounds, and the results are shown in Figure 101.

The minimum safe tip speed of 467 fps is plotted in Figure 101. This is the tip speed corresponding to a mean blade lift coefficient of 1.1 at a load factor of unity. Tip speeds below this limit would result in blade stall and preclude the possibility of regaining rotor speed with collective pitch reduction.

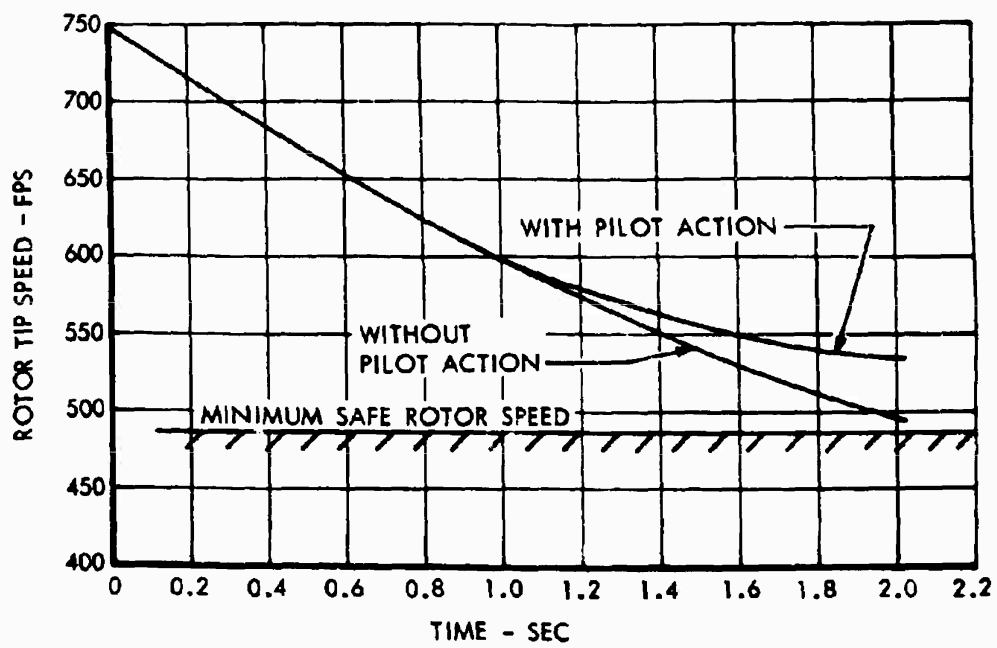


Figure 101. Time History of Rotor Speed
Following Engine Failure in Hover.

Figure 101 also shows the effect of reducing the collective pitch to its minimum value during the time between the first and second second.

In forward flight, the rotor speed decay following a power failure is determined by a method based primarily on a consideration of the energy equation, which can be written in differential form as

$$I\Omega \frac{d\Omega}{dt} = - (Q\Omega)_1 - \Delta(Q\Omega) \quad (27)$$

where $(Q\Omega)_1$ represents the initial power and $\Delta(Q\Omega)$ represents the time-varying power increment due to changes in the torque and rotor speed and the introduction of power from the propellers. The power increment is separated into the main contributing sources as follows:

$$\Delta(Q\Omega) = \Delta(Q\Omega)_R + \Delta(Q\Omega)_f - \Delta(Q\Omega)_{pp} \quad (28)$$

where

$\Delta(Q\Omega)_R$ = Rotor power required at power failure

$\Delta(Q\Omega)_f$ = Power due to drag

$\Delta(Q\Omega)_{pp}$ = Power extracted by the propellers from the airstream and introduced into the main rotor system.

Each of the above terms is expanded in terms of the basic flight parameters as follows:

$$\Delta(Q\Omega)_R = \frac{\partial(Q\Omega)}{\partial\Omega} \Delta\Omega + \frac{\partial(Q\Omega)_R}{\partial C_{Q_R}} \Delta C_{Q_R} \quad (29)$$

$$\Delta(Q\Omega)_f = \frac{\partial(DV)}{\partial V} \Delta V \quad (30)$$

$$\Delta(Q\Omega)_{pp} = (Q\Omega)_{pp} + \frac{\partial(Q\Omega)_{pp}}{\partial\Omega} \Delta\Omega + -\frac{\partial(Q\Omega)_{pp}}{\partial V} \Delta V \quad (31)$$

The changes in rotor speed, $\Delta\Omega$, and forward speed, ΔV , are estimated in terms of the parameters $d\Omega/dt$ and dV/dt as follows:

$$\Delta\Omega = \left(\frac{d\Omega}{dt}\right) t \quad (32)$$

$$\Delta V = \left(\frac{dV}{dt}\right) t = - \left(\frac{D}{W}\right) g t \quad (33)$$

where time, t , is considered to start at time of failure. It is assumed that the rotor torque coefficient, C_{Q_R} , remains constant so that

$$\Delta C_{Q_R} = 0 \quad (34)$$

With the above assumptions, the equation for $d\Omega/dt$ resolves into the following form:

$$\frac{d\Omega}{dt} = - \bar{Q} \left[\frac{A - Bt}{1 + Ct} \right] \quad (35)$$

which is readily integrated to give the rotor speed as a function of time as

$$\Omega_2 = \Omega_1 \left\{ 1 - \bar{Q} \left[\left(\frac{A}{C} + \frac{B}{C^2} \right) \ln(1 + Ct) - \frac{B}{C} t \right] \right\} \quad (36)$$

The parameters to be identified and evaluated for the above expression are as follows:

$$A = (K_V - K_{PP}) \quad (37)$$

$$B = (K_V - K_{PV}) \quad (38)$$

$$C = (k_R - k_{pp}) \quad (39)$$

$$\bar{Q} = \frac{(Q \Omega)_1}{1 \Omega_1^2} \quad (40)$$

$$K_v = \frac{\frac{\partial(DV)}{\partial v} \left(\frac{D}{W}\right)_g}{(Q_1 \Omega_1)} \quad (41)$$

$$K_{pv} = \frac{\frac{\partial(Q \Omega)_{pp}}{\partial v} \left(\frac{D}{W}\right)_g}{(Q_1 \Omega_1)} \quad (42)$$

$$K_{pp} = \frac{(Q \Omega)_{pp}}{(Q_1 \Omega_1)} \quad (43)$$

$$k_{pp} = \frac{\frac{\partial(Q \Omega)_{pp}}{\partial \Omega}}{1 \Omega_1} \quad (44)$$

$$k_R = \frac{\frac{\partial(Q \Omega)_R}{\partial \Omega}}{1 \Omega_1} \quad (45)$$

To evaluate the above parameters, it is necessary to develop expressions for the derivatives

$$\frac{\partial(DV)}{\partial v}, \frac{\partial(Q \Omega)_{pp}}{\partial v}, \frac{\partial(Q \Omega)_{pp}}{\partial \Omega} \text{ and } \frac{\partial(Q \Omega)_R}{\partial \Omega}$$

in terms of known quantities. To do this, the following additional expressions are introduced:

$$DV = \frac{p}{2} A \pi v^3 \quad (46)$$

$$(Q\Omega)_R = C_{Q_R} \rho A (\Omega R)^3 \quad (47)$$

$$(Q\Omega)_{pp} = C_{Q_{pp}} \rho^2 \pi \eta^3 D^5 \quad (48)$$

$$\eta = \frac{\Omega R}{2\pi} \quad (49)$$

$$J = \frac{V}{\eta D} \quad (50)$$

It is noted that the propeller derivatives depend on $C_{Q_{pp}}$ which can be evaluated from the propeller charts in Reference 13 as a function of the advance ratio J . An empirical equation for $C_{Q_{pp}}$ has been derived from this data as

$$C_{Q_{pp}} \approx 0.022 \left[1.5 - \frac{1}{J} \right] \quad (51)$$

With the above relationships, the following derivatives can be obtained:

$$\frac{\partial(DV)}{\partial V} = 3 \frac{\rho}{2} A \pi \eta^2 = \frac{3(DV)}{V_1} \quad (52)$$

$$\frac{\partial(Q\Omega)_R}{\partial \Omega} = 3 C_{Q_R} \rho A (\Omega R)^2 = \frac{3(Q\Omega)_1}{\Omega_1} \quad (53)$$

$$\frac{\partial(Q\Omega)_{pp}}{\partial V} = \frac{\partial C_{Q_{pp}}}{\partial J} \frac{\partial J}{\partial V} \rho^2 \pi \eta^3 D^5 \quad (54)$$

$$= \frac{(Q\Omega)_{pp}}{\left[1.5 - \frac{1}{J} \right]} \left(\frac{11}{V_1} \right) \left(\frac{\Omega 1}{V_1} \right) \quad (55)$$

$$\frac{\partial(Q \Omega)_{PP}}{\partial \Omega} = \frac{\partial Q_{PP}}{\partial J} \frac{\partial J}{\partial \eta} \frac{1}{2\pi} \frac{\Omega^2}{\Omega} (\rho 2\pi \eta^3 D^5) \quad (56)$$

$$= \frac{-(Q \Omega)_{PP}}{\left[.5 - \frac{1}{J}\right]} \left(\frac{11}{V_1}\right) \quad (57)$$

Expressions for the required parameters in the integrated form of the equation for the rotor speed are now summarized as follows:

$$K_V = \frac{3 \text{ HP}_f}{\text{HP}_1} \left(\frac{D}{W}\right) \frac{g}{V_1} \quad (58)$$

$$K_{PP}^V = \frac{\text{HP}_{PP}}{\text{HP}_1} \left[\frac{1}{\left(.5 - \frac{1}{J}\right)} \right] \frac{11}{V_1} \Omega_1 \left(\frac{D}{W}\right) \frac{g}{V_1} \quad (59)$$

$$K_R = \frac{3 \text{ HP}_R 550}{I \Omega_1^2} \quad (60)$$

$$K_{PP} = \frac{\text{HP}_{PP} \times 550}{I \Omega_1^2} \left[3 - \frac{1}{\left(.5 - \frac{1}{J}\right)} \right] \frac{11}{V_1} \Omega_1 \quad (61)$$

To account for a delay time before changing pitch of the propellers, the propeller terms should be kept at zero. At the instant that propeller pitch is changed (to extract power from the airstream), the rotor speed decay can be computed using the prevailing conditions as the initial conditions and with the propeller terms included.

The rotor speed following a power failure at 140 knots has been calculated from Equation (36) for the case of no pilot action for two seconds and for the case in which the pilot reduces propeller pitch to the windmill setting of 20 degrees in the period between the first and second second. The resulting time histories are plotted on Figure 102.

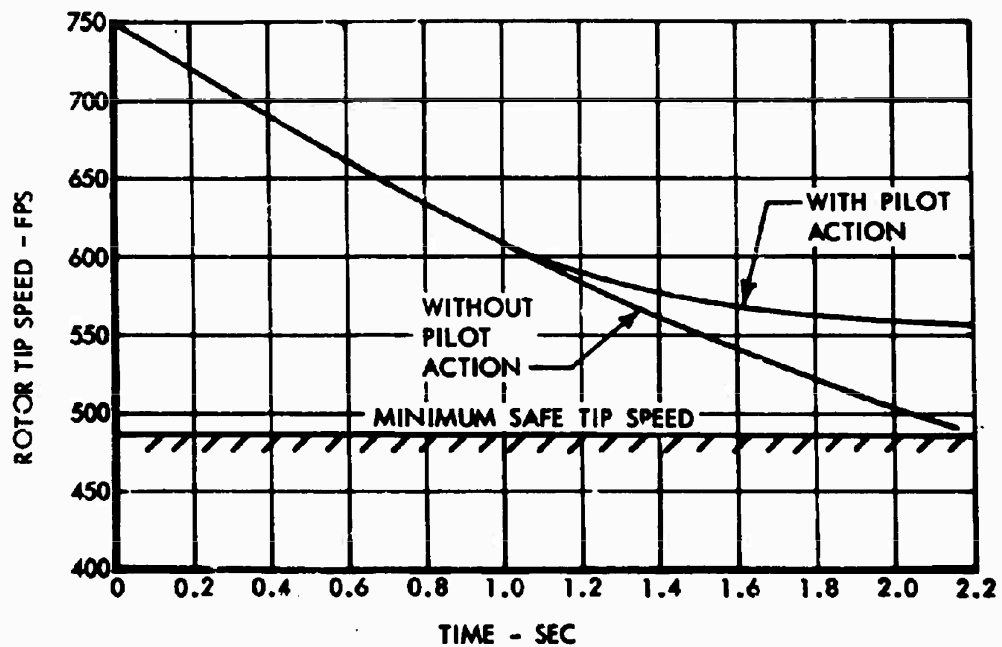


Figure 102. Time History of Rotor Speed Following Engine Failure at 140 Knots.

Steady Autorotation

The rate of descent in autorotation has been computed by a variation of the performance and trim program which solves for trim conditions with zero rotor torque. The rate of descent in steady autorotation as a function of speed is shown in Figure 103. It may be seen that the CRA at its design gross weight has a minimum rate of descent of approximately 1970 feet per minute at a forward speed of 80 knots.

Height-Velocity Diagram - Helicopter Mode

The flight conditions which preclude a safe autorotative landing are defined by a typical height-velocity diagram. The key points on which the construction of this diagram is based are (1) the high hover point, (2) the low hover point, and (3) the critical velocity. The height-velocity diagram for the CRA has been determined by methods developed in Reference 14, the results of which are plotted in Figure 104.

Height-Velocity Diagram - Airplane Mode

Following complete power failure in the airplane mode, the CRA has the capability of unstowing, extending, and bringing the rotor to operating rotor speed in order to make a landing in autorotation. The unstowing and extending are done with hydraulic power from pumps driven by windmilling propellers. The time required for these two operations is 16 seconds. The rotor will be brought up to speed by clutching it into the cross shaft and absorbing power from the windmilling propellers. At a speed of 140 knots, a power level of 133 horsepower per propeller can be transmitted from the propellers into the rotor. Resulting time to bring the rotor up to its operating speed of 25 radians per second is 36 seconds.

Thus, a total of 52 seconds is required to unstow, extend, and bring the rotor up to speed.

Assuming that a glide speed of 140 knots is maintained and that the flaps are down, the rate of descent may be estimated from the power required to maintain level flight in this condition: 2000 horsepower. From energy considerations, the rate of descent is 45 feet per second.

In the time of 52 seconds required, the aircraft will lose 2330 feet of altitude.

In cases in which the aircraft is at less than 2330 feet but at speeds higher than 140 knots, the aircraft can be climbed by trading the kinetic energy of forward flight for altitude.

Figure 104 shows that at speeds above 268 knots, the capability exists to climb to 2330 feet, from which altitude a transition to the autogyro mode is possible.

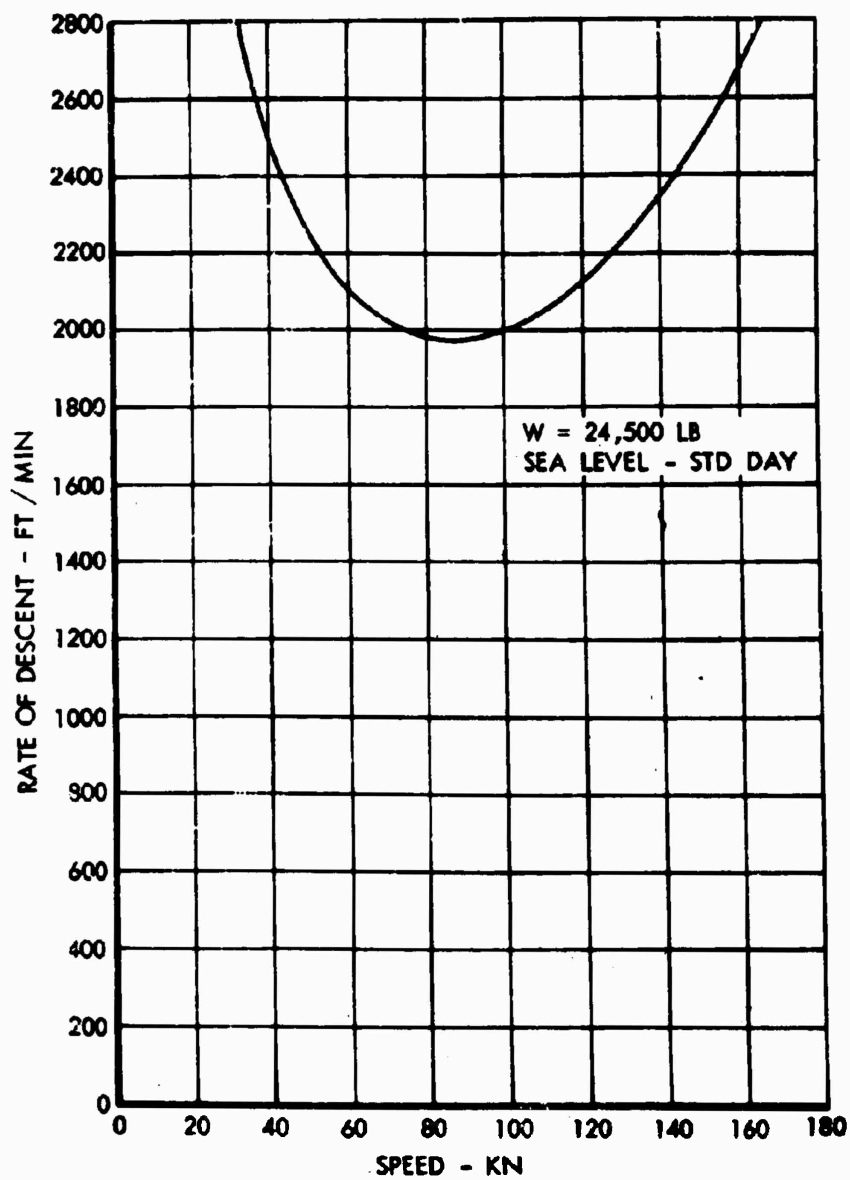


Figure 103. Rate of Descent in Steady Autorotation.

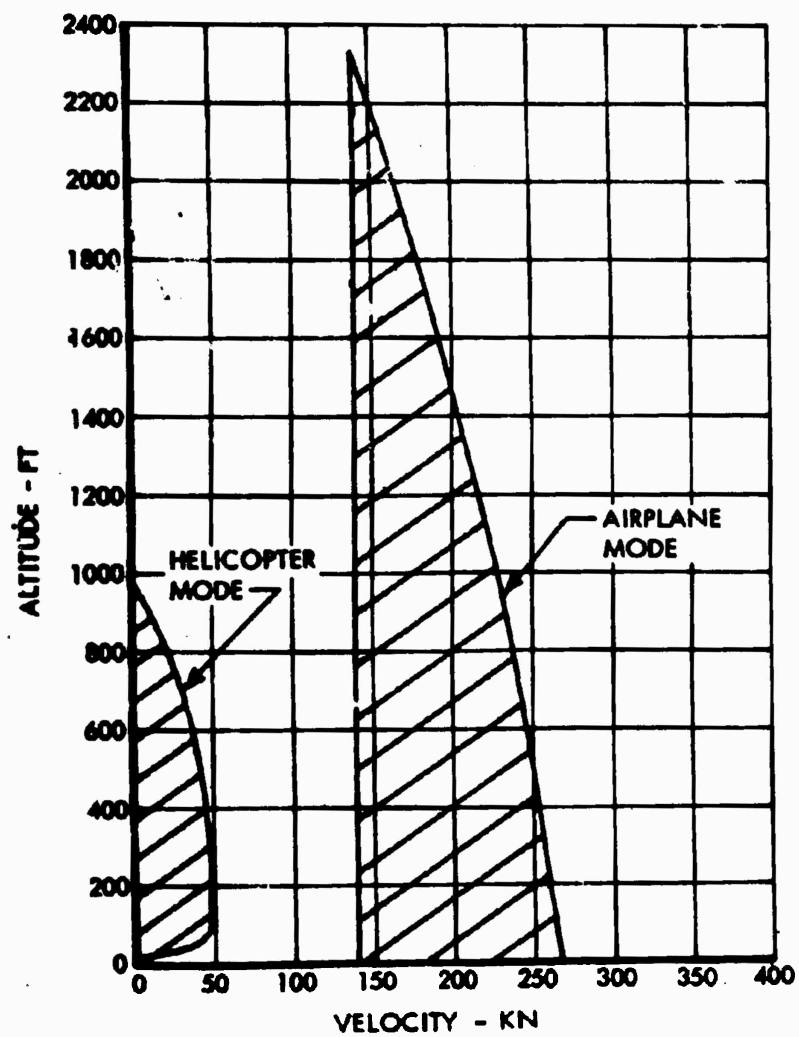


Figure 104. Height-Velocity Curves for Landing in Autorotation.

FIXED-WING MODE

Wind Tunnel Data

Low-speed wind tunnel tests of a configuration similar to the CRA were conducted to provide a basis for the estimation of the stability and control characteristics. The results of these tests are described in detail in Reference 1.

The final configuration differs somewhat from the early wind tunnel model primarily because of design changes required to assure the attainment of the required lift-to-drag ratio. These changes included the use of greater wing span to reduce the drag due to lift, and the choice of increased wing camber to minimize the parasite drag in the higher lift coefficient range. Other changes which improve the aerodynamic characteristics include increased flap span and elimination of the flap cutout to provide greater effectiveness, and increased fuselage length resulting from the choice of larger diameters for the main rotor and tail rotor. The basic wind tunnel results are modified, to reflect these changes, by standard aerodynamic methods which are described in the succeeding section.

Longitudinal Characteristics

Lift

The lift data presented in Figure 105 were obtained by correcting the wind tunnel data for aspect ratio, wing incidence, and flap geometry. Reference 15 was used to correct the wing lift curve slope for aspect ratio. Reference 16 was used to estimate the increase in trailing edge single slotted flap effectiveness.

Figure 106 is presented as validation of the method used for the calculation of flap effectiveness for the CRA. The estimated flap lift increment for the wind tunnel configuration, when added to the flaps-up test data, is seen to yield results which are conservative with respect to those achieved in the tunnel. Since identical methods were used to estimate the characteristics of the improved flaps, it is anticipated that some conservatism remains in the final flaps-down data of Figure 105. The estimated flap effectiveness was obtained by estimating the incremental lift due to flap deflection at $\alpha_A = 0$ and assuming the same lift curve slope as the flaps-up wind tunnel data.

It should be noted that the wind tunnel data for the flapped configuration were obtained with the fixed rotor installed on the model, which appreciably increases the lift curve slope ($\Delta C_{L_{\sigma_{rotor}}} \approx 0.059$). Lift data with flaps down and rotor off were not obtained during this test series.

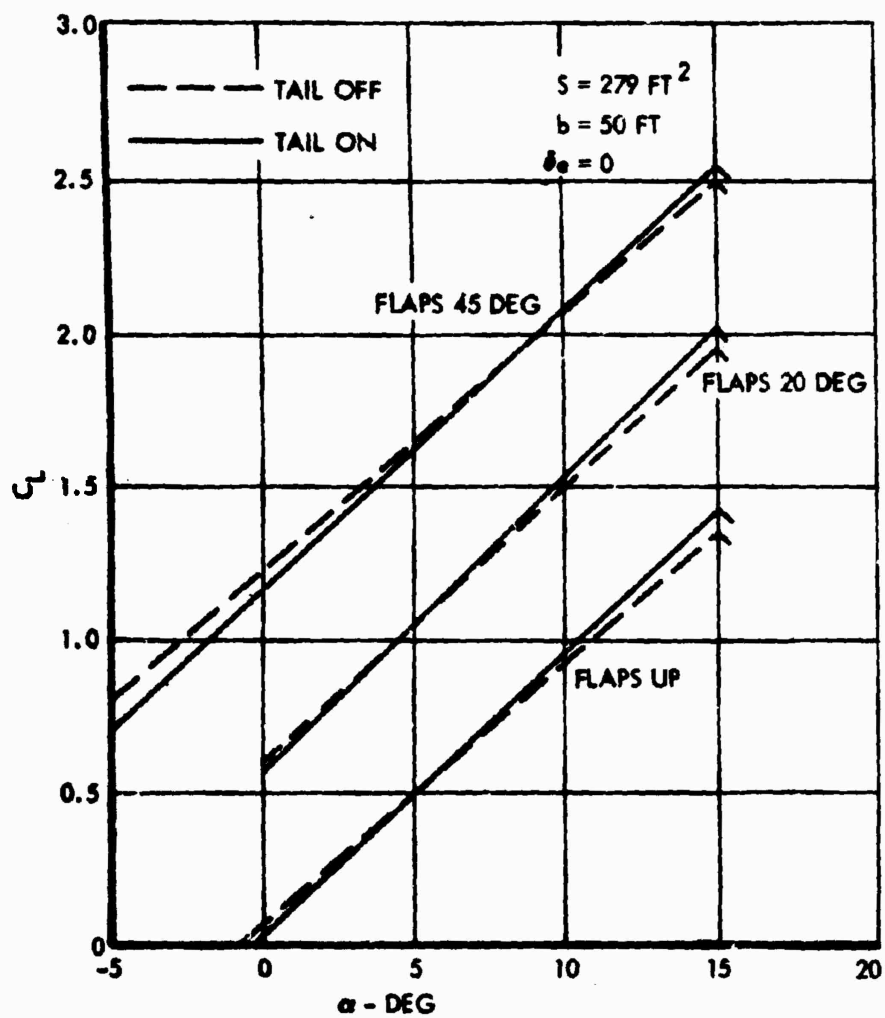


Figure 105. Lift Curve - $\delta_F = 0^\circ, 20^\circ, 45^\circ$.

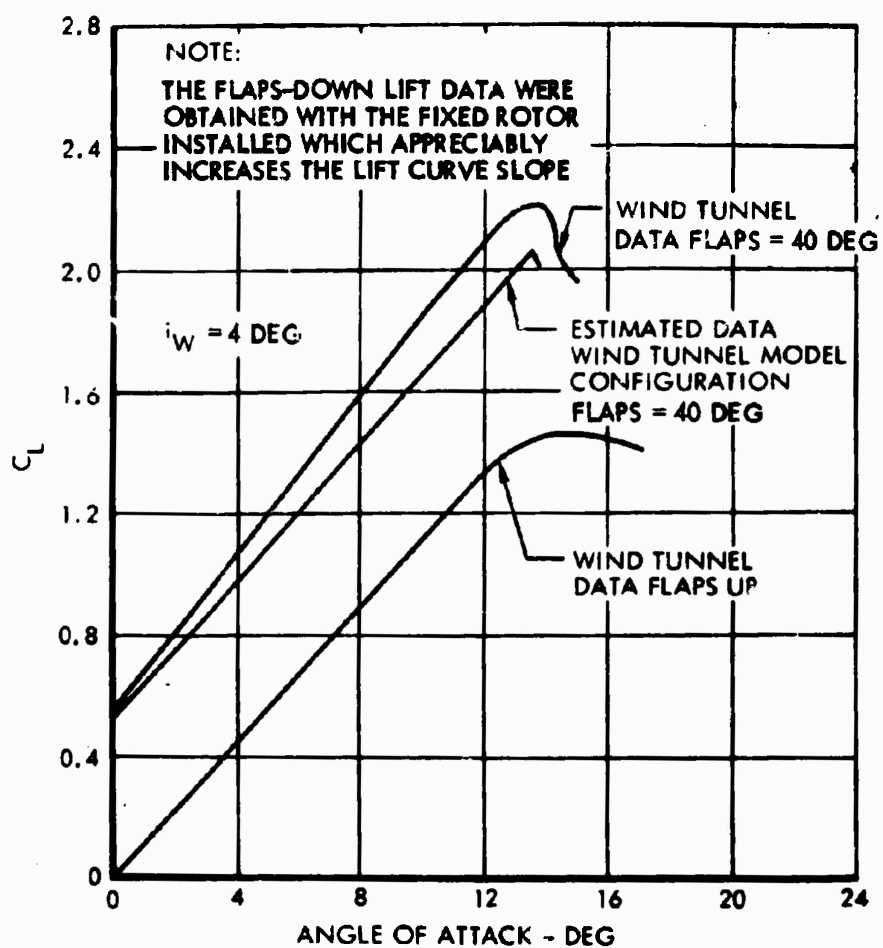


Figure 106. Comparison of Wind Tunnel with Estimated Flap Lift Data.

Pitching Moment

The tail-off pitching moment data presented in Figure 107 were obtained by adding an estimated incremental lift and pitching moment due to flap deflection to the wind tunnel tail-off, flaps-up data.

The elevator deflection required to trim to $C_{L_{max}}$ out of ground effect is shown as a function of center-of-gravity position in Figure 108. Adequate power for trim is available throughout the center-of-gravity range.

Power Effects

The added lift due to power is presented in Figure 109 for the approach and landing flap deflection and in Figure 110 for the takeoff flap deflection.

The pitching moment due to power is presented in Figure 111 for the 45-degree flap deflection and in Figure 112 for the 20-degree flap deflection.

Elevator Hinge-Moments

Longitudinal control forces are generated by the elevator hinge-moments through a mechanical control system linking the control stick with the elevator hinge-line. The elevator aerodynamic balance consists of a 29-percent elevator chord round-nosed balance and a 25-percent chord 1:1 geared tab. The control system incorporates a 6-pound downspring on the stick, and the elevator has a mass unbalance of 6 pounds, which gives a total of 12 pounds of downspring effect. This force will not be felt under normal ground operation, since the pilot will be using helicopter controls; it will be felt only during ground operation at low speed in the airplane mode.

References 19 through 22 were used to design the elevator aerodynamic balance to limit the longitudinal control forces to the values specified by MIL-F-8785(ASG). The estimated hinge-moment coefficients were +0.0005 for $C_{h_{\alpha}}$ and -0.0016 for $C_{h_{\delta_e}}$.

Static Longitudinal Stability

Stick force per "g" is used to evaluate the flying qualities of an airplane in maneuvering flight. This gradient varies directly with center-of-gravity position, being heavier at the forward c.g.'s and lighter at the aft c.g.'s.

The results of the analysis which are presented in Figure 113 show that, throughout the operating center-of-gravity range, the CRA exhibits positive stick-free static stability with stick force per "g" characteristics well within the allowable limits.

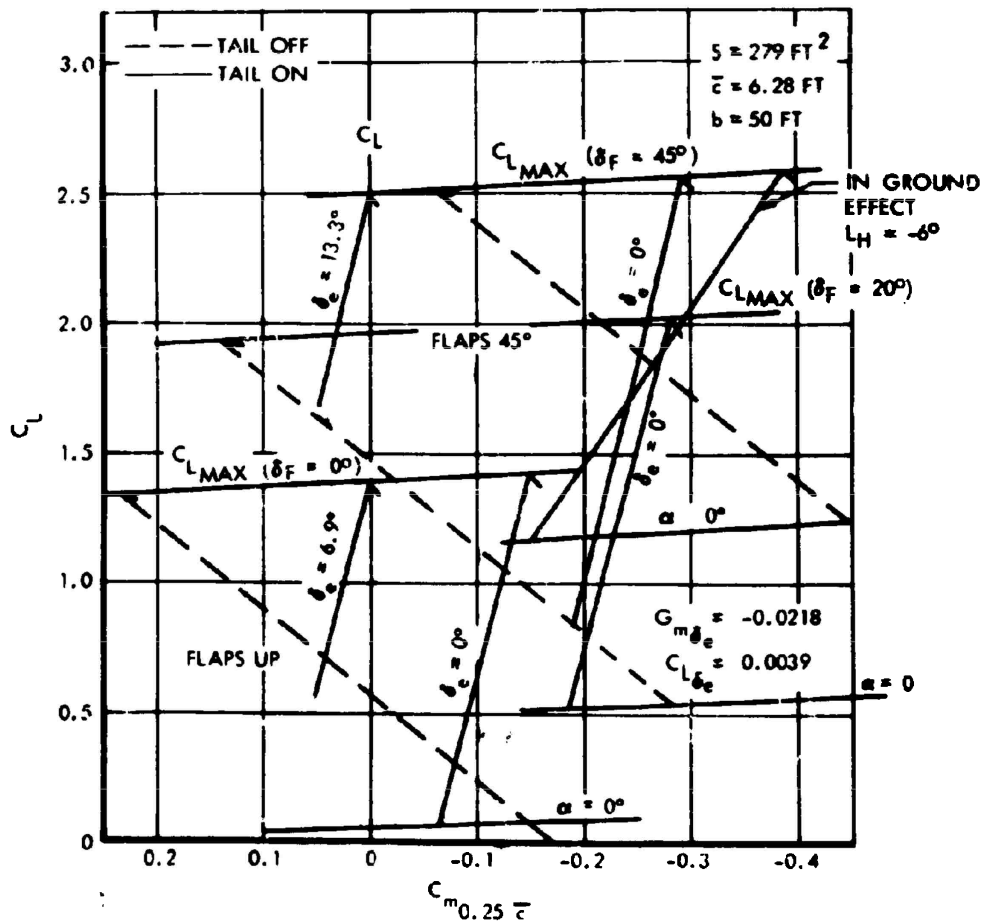


Figure 107. Static Stick-Fixed Stability.

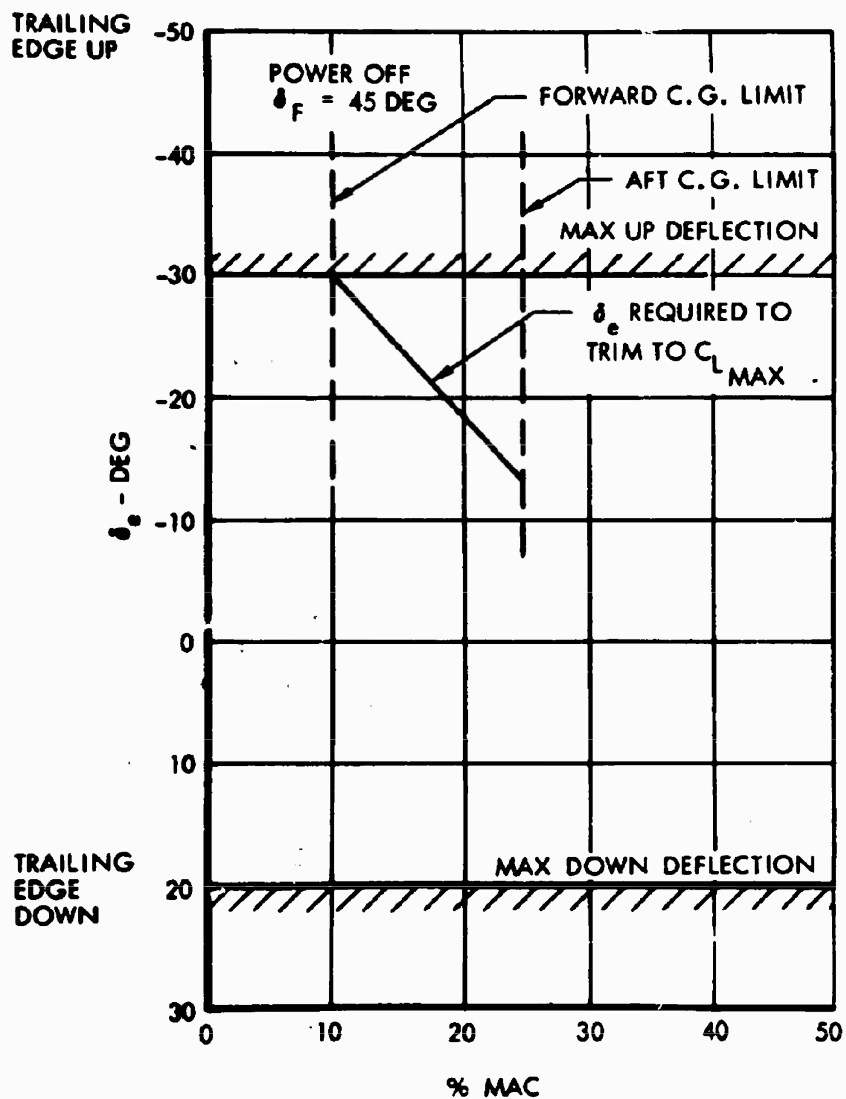


Figure 108. Elevator Required to Trim $C_{L \text{ max}}$.

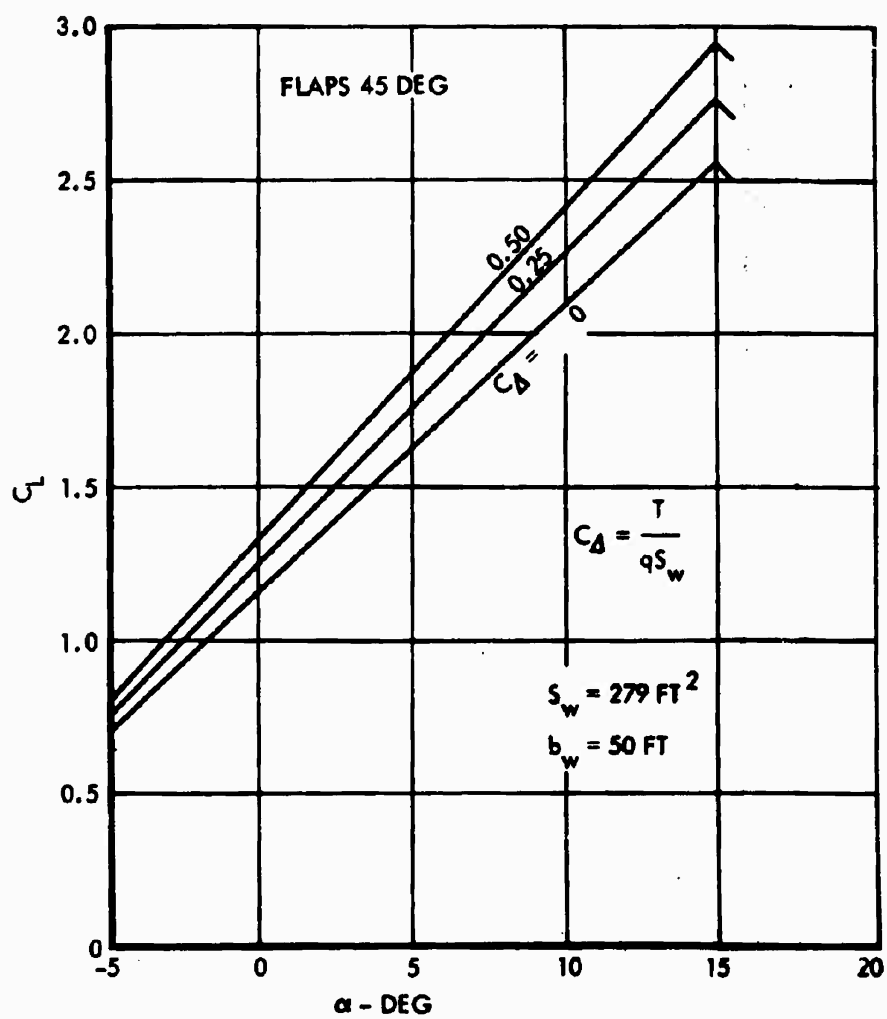


Figure 109. Power-On Lift Curve - $\delta_F = 45^\circ$.

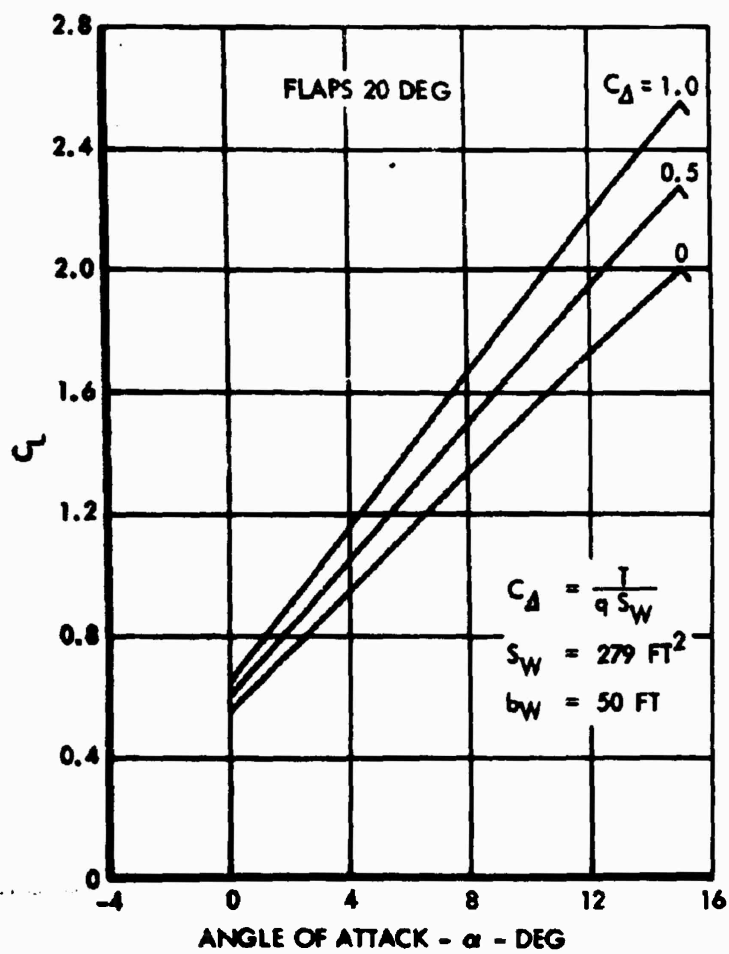


Figure 110. Power-On Lift Curve - $\delta_F = 20^\circ$.

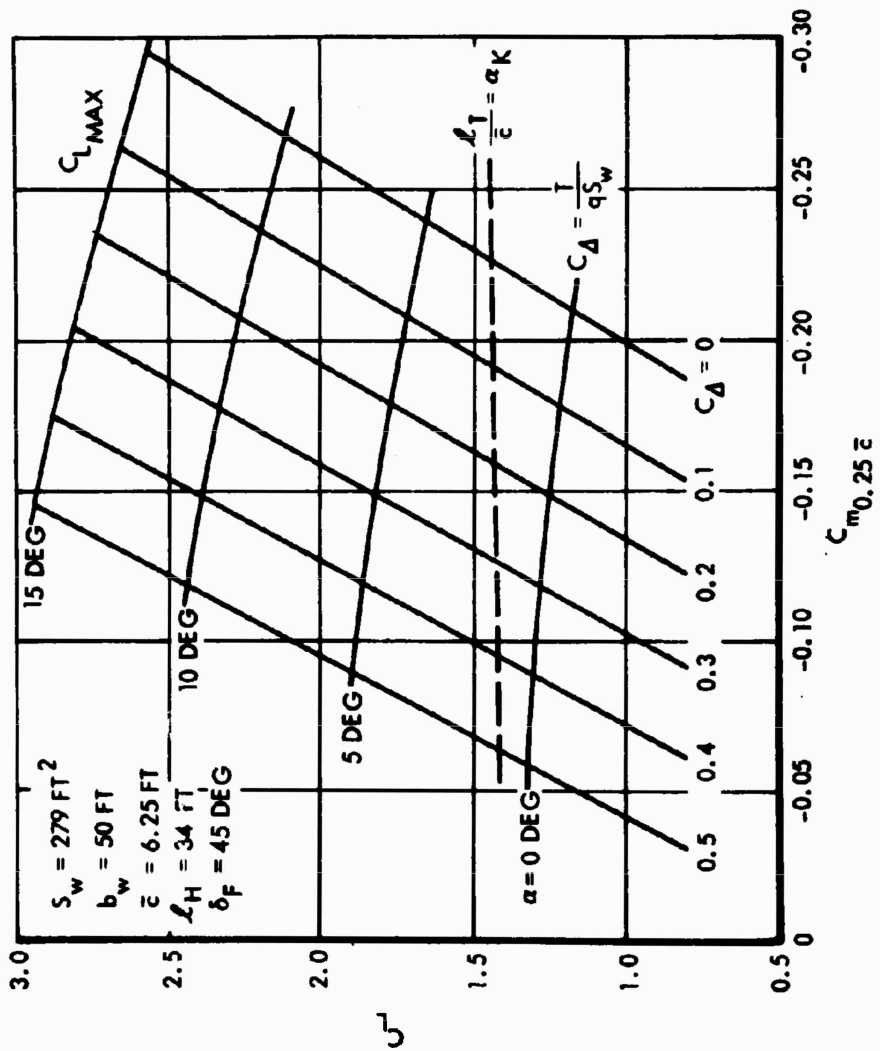


Figure 111. Power-On Pitching Moment - $\delta_F = 45^\circ$.

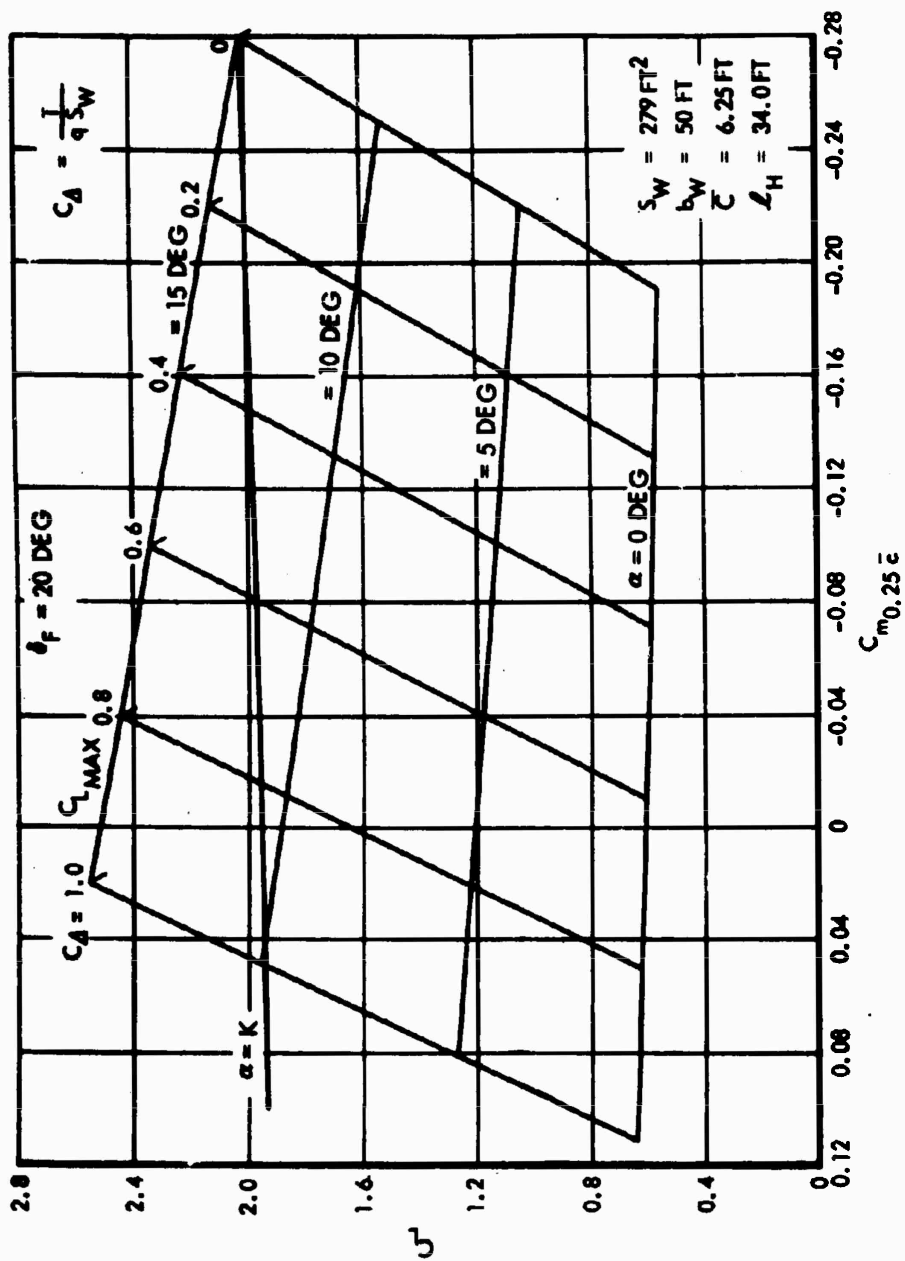


Figure 112. Power-On Pitching Moment - $\delta_F = 20^\circ$.

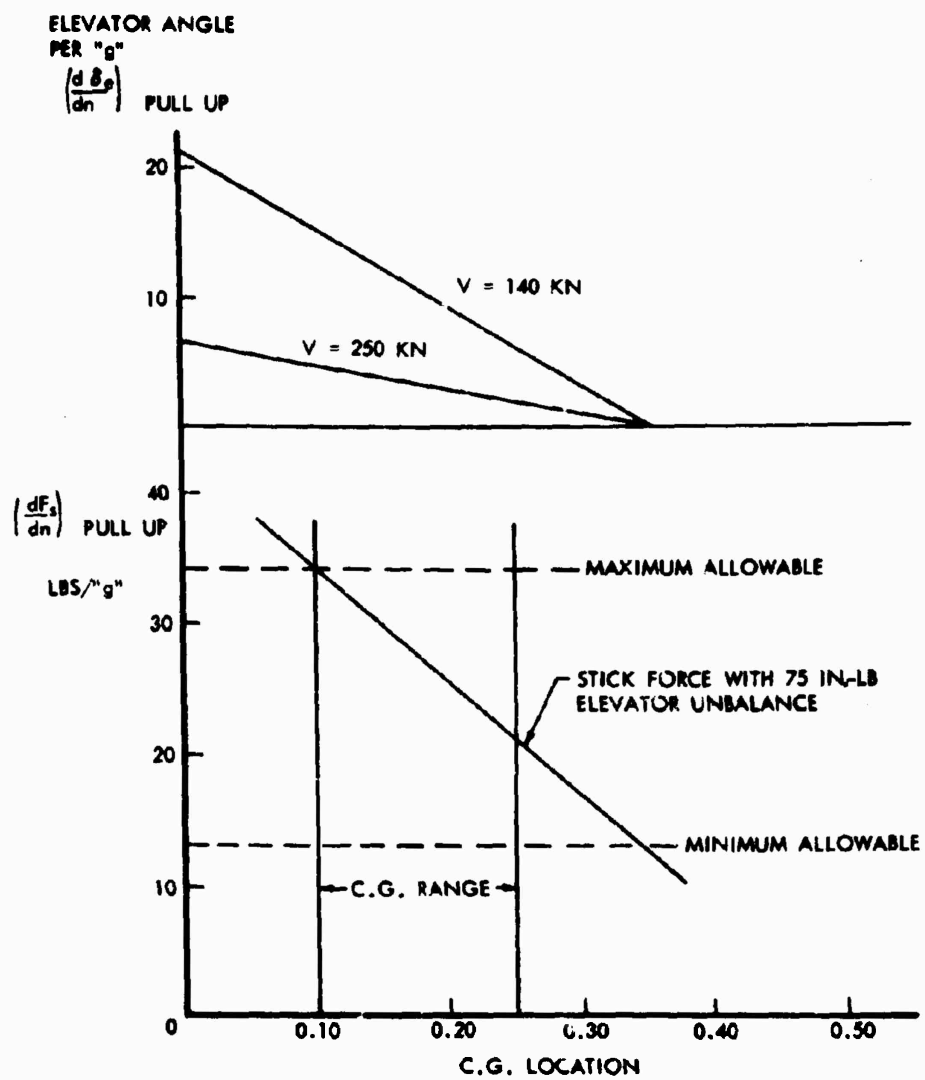


Figure 113. Stick Force per g in Pull-Up.

For desirable flying qualities, it is necessary that the pilot be required to apply pull forces on the stick for flight at speeds below the trim speed and push forces for flight at speeds above the trim speed. The variation of elevator angle and stick force with speed is shown in Figures 114 through 118 for several conditions of trim and power setting at the critical center-of-gravity position. The CRA is seen to exhibit positive stability both stick fixed and stick free under all conditions.

The slope F_s versus V varies with center of gravity, the slope becoming more stable as the center of gravity is moved forward. The most aft center-of-gravity position is, therefore, the most critical. The gradient of stick force versus speed, dF_s/dV , plays a major role in determining the pilot's feel of the airplane, i.e., the pilot's concept of the airplane's stability. A large gradient will tend to keep the airplane flying at constant speed and will resist the influence of disturbances toward changing speed. It will also enable the pilot to trim the airplane easily and will not require pilot attention to hold the given trim speed.

Table XVII presents a tabulation of the stick-fixed neutral point and the stick-free neutral point and shows that the stick-free neutral point is aft of the stick-fixed neutral point for the critical flight conditions at the aft c.g. limit.

TABLE XVII. NEUTRAL POINTS						
Condition	Weight (lb)	Flaps (deg)	Power	V_{TRIM} (Kt)	$\left(\frac{dC_m}{dC_L}\right)_{FIXED}$	$\left(\frac{dC_m}{dC_L}\right)_{FREE}$
Transition	24,500	45	Off	140	-0.061	-0.115
Transition	24,500	45	Power for Level Flight	140	-0.020	-0.074
Takeoff	24,500	20	Off	140	-0.061	-0.115
Takeoff	24,500	20	Takeoff	140	-0.001	-0.055
Cruise	24,500	0	Level Flight	250	-0.061	-0.115
Max. Speed	24,500	0	Level Flight	400	-0.061	-0.115

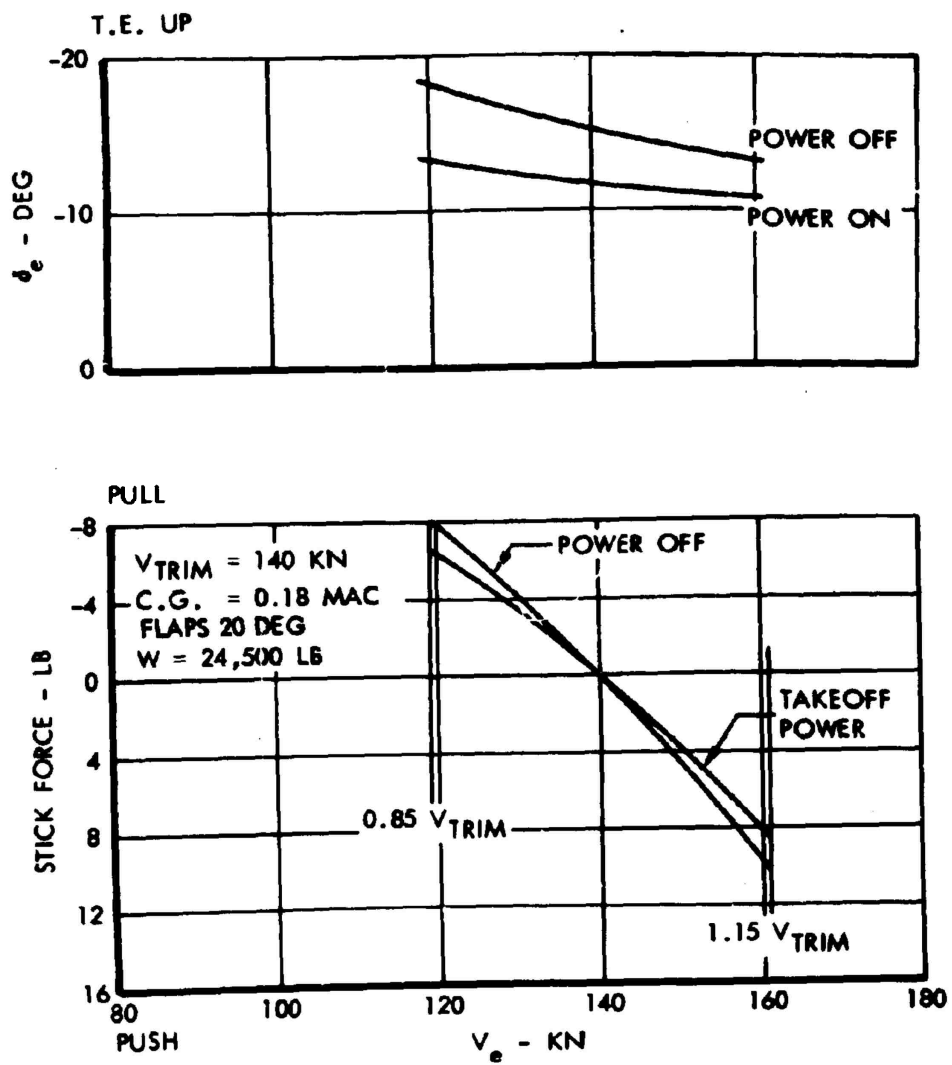


Figure 114. Stick Force Gradient in Unaccelerated Flight (Takeoff).

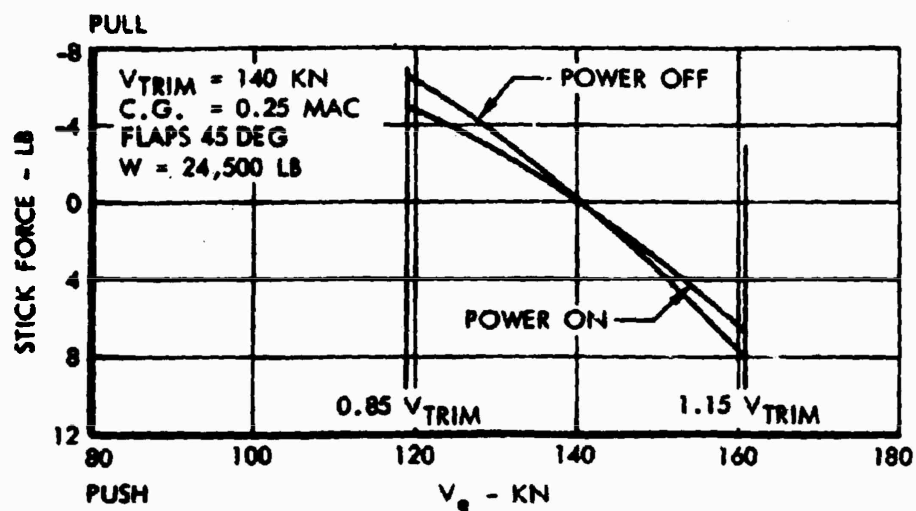
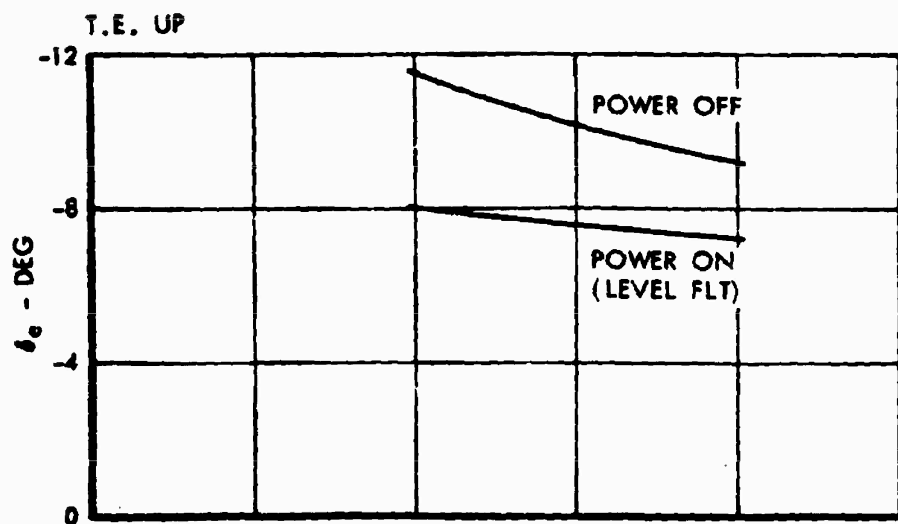


Figure 115. Stick Force Gradient in Unaccelerated Flight (Transition).

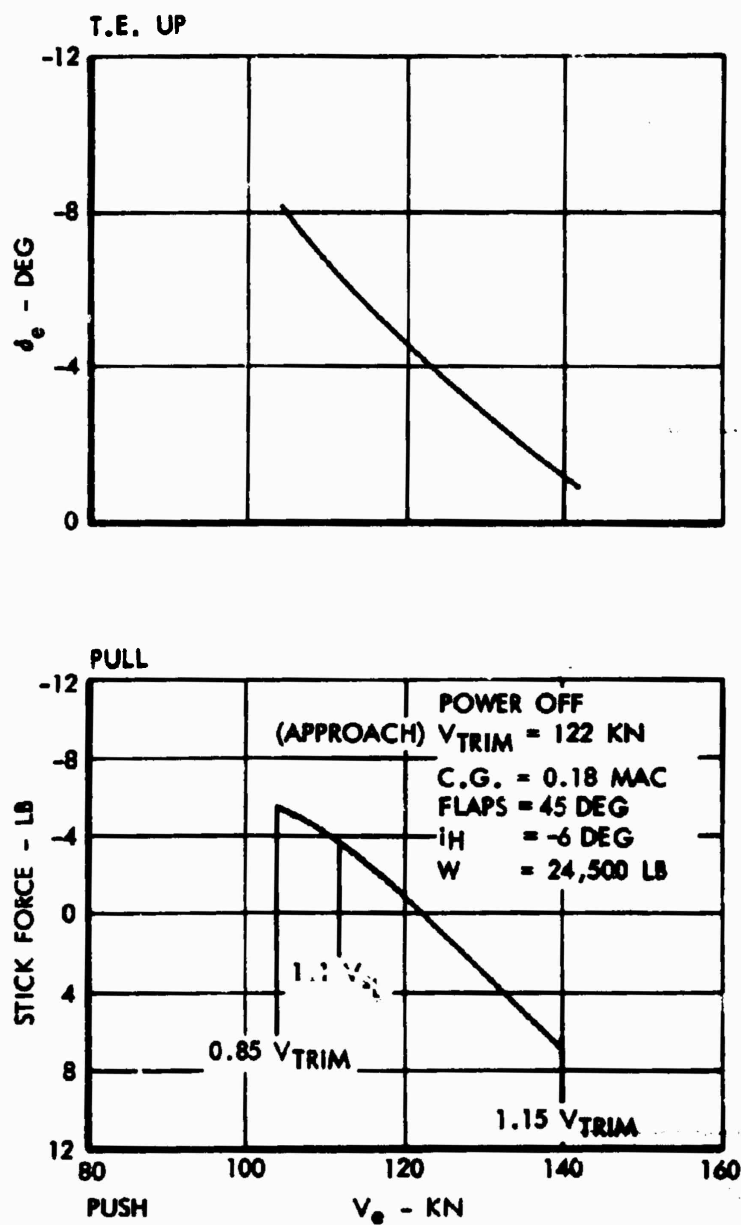


Figure 116. Stick Force Gradient in Unaccelerated Flight (Approach).

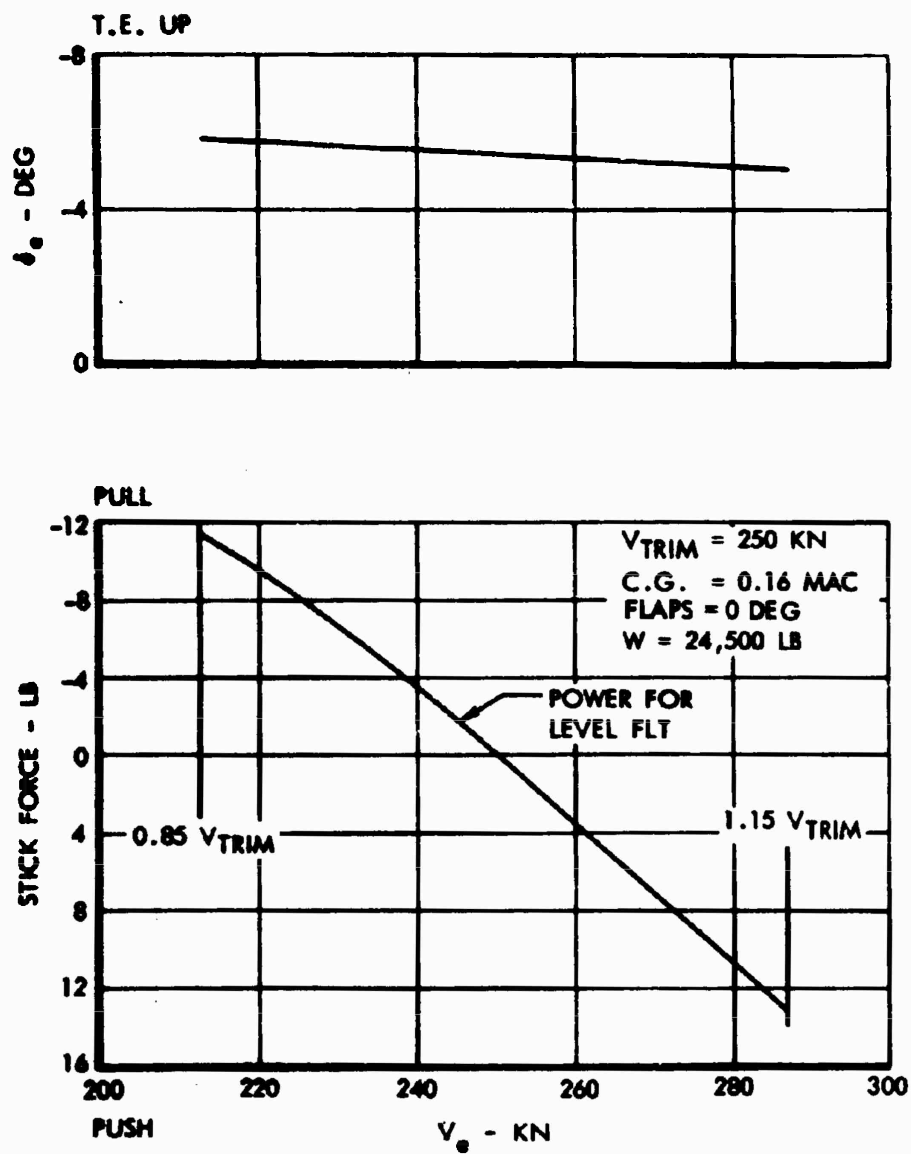


Figure 117. Stick Force Gradient in Unaccelerated Flight (Cruise).

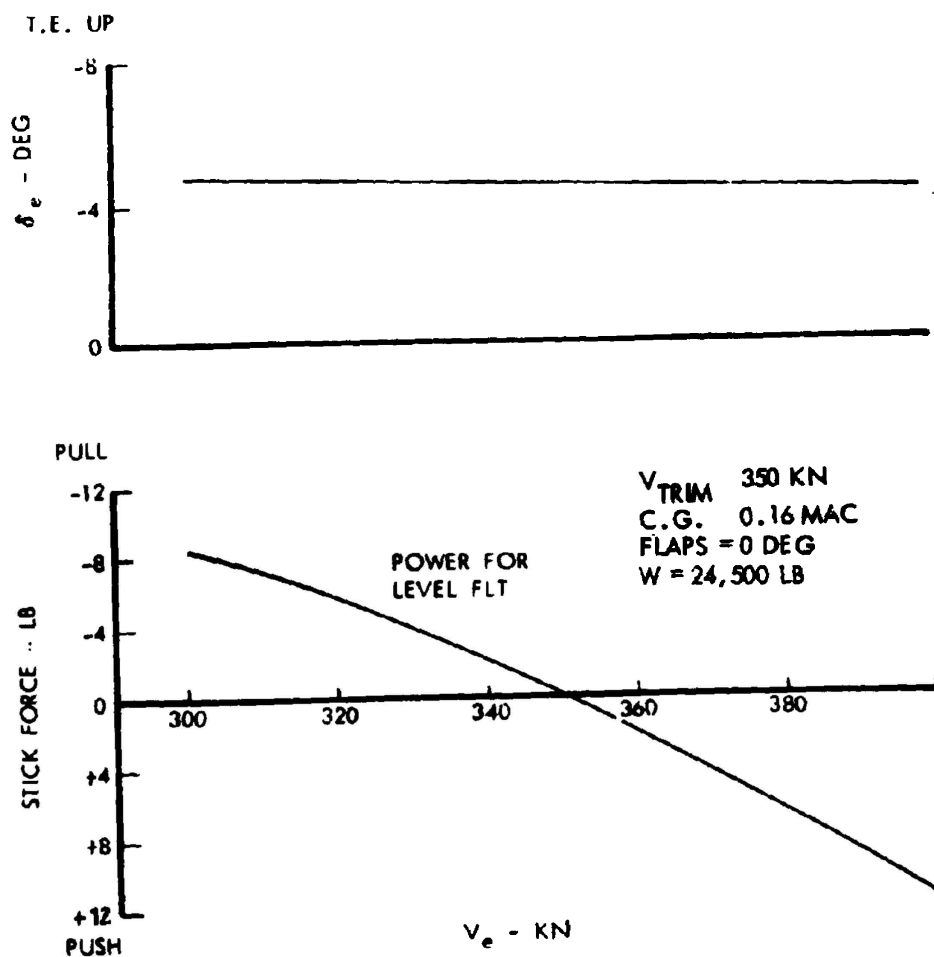


Figure 118. Stick Force Gradient in Unaccelerated Flight (Maximum Speed).

Trim During Transition - Helicopter to Airplane Mode

Prior to beginning the transition, the pilot will establish steady flight at the transition speed with the rotor unloaded and with the pitching moments on the aircraft trimmed so that no balancing moments are required from the rotor. At this point, the control system is shifted from helicopter controls to airplane controls with the system previously described. Since the aircraft was in trim prior to the control shift, it will remain in trim after the shift, and no stick ~~motion will be required. The next step is to declutch the rotor from~~ the drive system. While the rotor is being decelerated, the rotor drag will remain essentially constant so that no change in longitudinal trim will occur. The application of the rotor brake at 100 rpm will require the use of the rudder to trim directionally. For full brake application, which will stop the rotor in 15 seconds, the applied torque, Q , is

$$Q = \frac{I\Omega}{15}$$

where

$$I = 13,000 \text{ slug-ft}^2$$

and Ω (at 100 rpm) = 10.4.

The resultant torque is 9,000 foot-pounds. At the minimum speed of 120 knots, a 3.4-degree rudder deflection and a pedal displacement of 0.73 inch is required to balance this torque. When the rotor stops, the rudder can be centered. The drag of the stopped rotor is essentially the same as an unloaded but rotating rotor, so that no longitudinal trim change will occur with rotor stopping.

The wing tunnel tests of the 33-foot stopped rotor showed that folding the blades increased the rotor drag approximately 50 percent. The rotor hub and blades have an equivalent flat-plate area of 8 square feet, and the increase in flat-plate area is 4 square feet, which at 120 knots will produce a nose-up pitching moment of 980 foot-pounds. Blade folding also moves the center of gravity back 4.5 inches, which at the design gross weight represents an additional nose-up pitching moment of 9200 foot-pounds. The total change in pitching moment can be trimmed out with an elevator deflection of only -5.4 degrees.

Retracting the rotor and closing the doors over the hub results in a drag reduction and a corresponding nose-down pitching moment representing the removal of 12 square feet of flat-plate area at an arm of 5 feet. This change in moment requires a +1.6-degree change in elevator deflection.

When the flaps are retracted and the aircraft is accelerated to 180 knots, a nose-down moment is produced which requires a +1.5-degree change in elevator deflection.

Figure 119 shows the time history of elevator and rudder deflections required during the various phases of the transition.

Trim During Transition - Airplane to Helicopter Mode

The transition from the airplane to the helicopter mode is almost the reverse of the transition just discussed. The aircraft will be trimmed out at about 180 knots. The extension of the flaps and the deceleration to the transition speed will occur simultaneously with the corresponding trim change of -1.5 degrees of elevator deflection. The unstowing and extension of the blades will require 16 seconds and will produce the trim changes discussed in the previous section. The rotor will be started with a clutch, which will bring the rotor up to full speed in 45 seconds. The clutch can generate a torque at the main rotor of 6700 foot-pounds. A rudder deflection of -2.5 degrees is required to balance this torque. Figure 120 shows the time history of the control deflections during the transition from airplane to helicopter mode.

Dynamic Stability

The longitudinal dynamic stability characteristics were computed by means of the 5-D Maneuver and Dynamic Modes Program adapted to three degrees of freedom. This stability and control program extracts roots and determines transfer functions of the longitudinal and lateral-directional equations of motion. The input is common to all functions and includes aircraft descriptive geometry, the usual aerodynamic parameters which can be linearly dependent on angle of attack, yaw, inertia characteristics, engine gyroscopic moments, thrust characteristics dependent on speed and altitude, and three axis primary control parameters.

The longitudinal load portion assembles the three equations of motion and the control describing functions and extracts the roots from the characteristic matrix. The various longitudinal mode characteristics such as natural and damped frequencies and periods, damping parameters describing the short period and phugoid, and other associated time constants are obtained.

The lateral-directional modes portion is very similar to the longitudinal portion. The three basic equations of motion together with roll and yaw control functions are assembled and the roots are extracted. The lateral-directional modes such as Dutch roll, spiral and roll subsidence, and their descriptive frequency and damping characteristics are obtained.

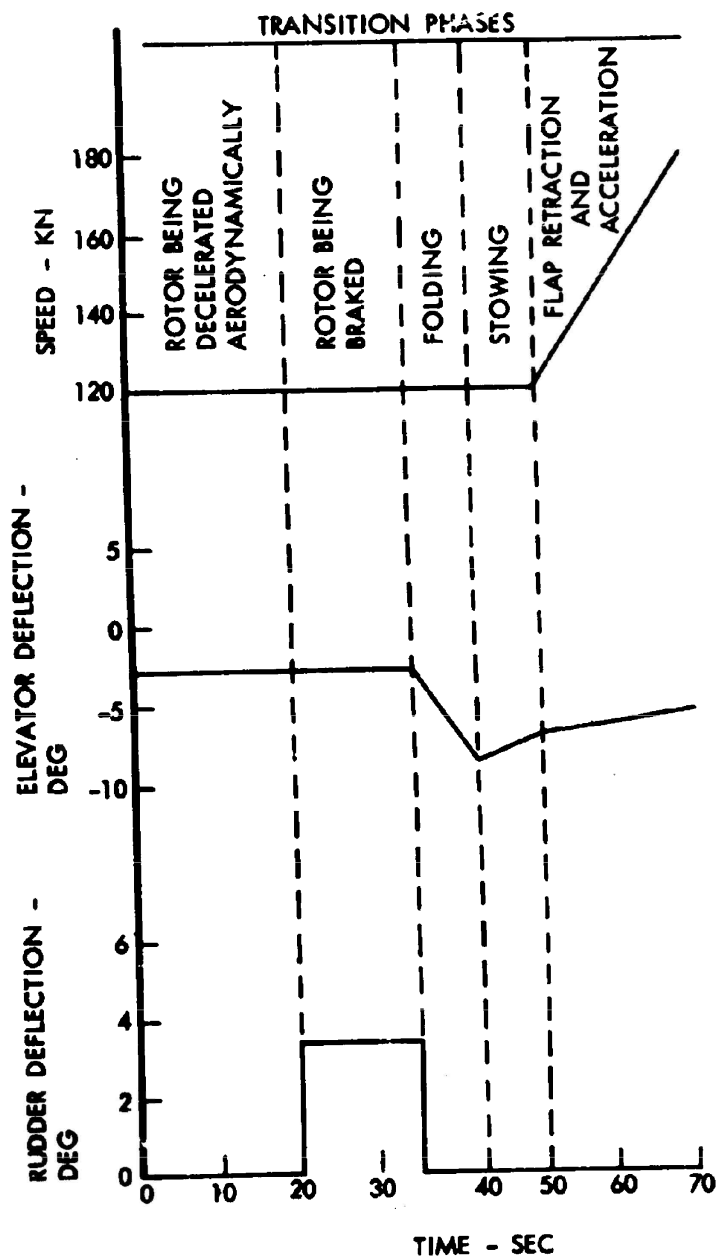


Figure 119. Time History of Control Motions During Transition from Helicopter to Airplane Mode.

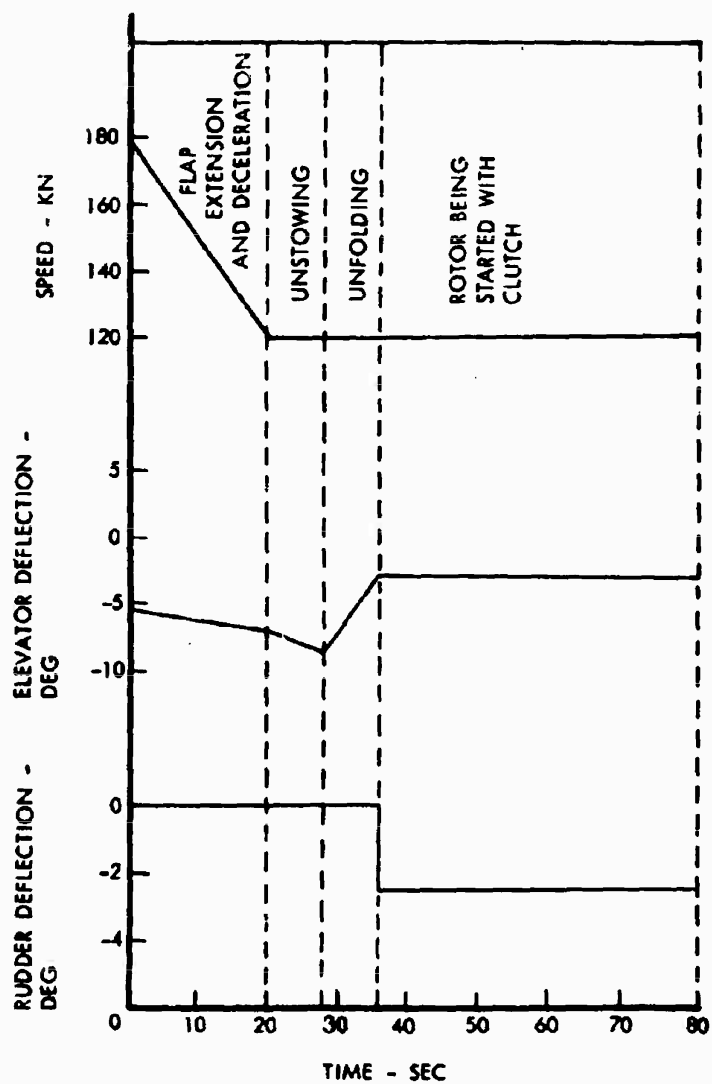


Figure 120. Time History of Control Motions During Transition from Airplane to Helicopter Mode.

The analysis was restricted to incompressible flow, rigid airframe, and fixed control conditions. An average gross weight of 23,000 pounds and a c.g. location at 18.5 percent MAC were held constant for all flight conditions. This corresponds to design gross weight less half-fuel and average c.g. travel. The representative flight conditions considered are power approach, transition, flap placard speed, cruise speed, and maximum speed.

The longitudinal dynamic stability derivatives are listed in Table XVIII for the representative flight conditions. The values for C_L and CD_{CL} were obtained from the lift curve and drag polar, based on wind tunnel test data. The static stability derivative Cm_{CL} was also taken from these data with account taken of the change in reference c.g. location.

The change in drag coefficient due to Mach number (CD_M) was utilized to effectively account for thrust effects due to the propellers, since the program used accounted only for jet engines. In this adaptation

$$C_{D_M} = - \frac{C_{X_u}}{M}$$

The term C_{X_u} is computed from page 149 of Reference 23, with the assumption that

$$\left(\frac{\partial T}{\partial u} \right)_0 = - \frac{T}{u_0}$$

This finally reduces to

$$C_{D_M} = \frac{3 C_D}{M}$$

for propeller-driven airplanes.

The pitching rate derivatives, Cm_q and $Cm_{\dot{\alpha}}$, are primarily due to the effect of the horizontal stabilizer. These are computed on the basis shown in Section 10-4 of Reference 19. Thus,

$$C_{m_q} = - 2(1.1) C_{L_{\alpha_H}} \frac{q_H}{q_0} \frac{S_H}{S_w} \left(\frac{l_H}{c_w} + \frac{\Delta X}{c_w} \right)^2 \quad (62)$$

$$C_{m_{\dot{\alpha}}} = \frac{C_{m_q}}{1.1} \frac{d\epsilon}{d\alpha_A}$$

The factor 1.1 accounts for basic wing and body contributions at a quarter-chord c.g. location. A correction for wing damping contribution is obtained from Reference 24 for a c.g. location away from the quarter chord. For the reference c.g. of this analysis, this correction amounts to only 5 percent of that computed by the preceding equations.

The results of the computed longitudinal dynamic stability characteristics are presented in Table XVIII and Figure 121. The long-period motion is damped in all cases and has a period always greater than one-half minute. Time to damp to 1/10 amplitude is plotted against oscillation period for the short-period motion in Figure 121, which shows that the short-period characteristics are satisfactory for all flight conditions.

Stability During Transition

The crucial phase in transition flight from a longitudinal stability standpoint is in the stopped and unfolded rotor position. If aerodynamic lift is sustained by the stopped blades, large destabilizing moments can result. The use of a very large horizontal tail surface for stabilization under this condition is uneconomical from the standpoints of weight and drag and is made unnecessary by the use of the rotor blade pitch bias system, which senses angle-of-attack changes with an angle-of-attack vane and puts in the correct amount of cyclic pitch to eliminate rotor pitching moments. This system is constructed to follow the linear schedule shown in Figure 122. This figure is based on results of the wind tunnel tests referred to above. These values correspond to zero rotor lift. The residual pitching moment requires only one-half degree elevator deflection to trim.

Longitudinal Trim Change Conditions

Deviations from trim are most important within the area of airfield operations. From an elevator control handling standpoint, rapid changes in flap deflection or throttle setting may require significant stick force to maintain the desired flight path. The pertinent flight conditions have been analyzed for the CRA, and the results are presented in Table XIX. The conditions are numbered in accord with Table XXVIII of MIL-F-8785(ASG). The effects of c.g. shift due to changes in landing gear position are negligible. The other items cited in MIL-F-8785(ASG) do not apply.

Lateral-Directional Characteristics

Directional Stability

The tail-off yawing moment coefficient data presented in Figure 123 were obtained from wind tunnel test data and referred to the increased values of wing area and wing span.

The directional stability contribution of the vertical tail and the rudder effectiveness (presented in Figure 123) were computed for the final configuration vertical tail using the sidewash and dynamic pressure from wind tunnel test data.

TABLE XVIII. LONGITUDINAL DYNAMIC STABILITY DERIVATIVES						
Flight Condition	Power Approach	Transi- tion	Flap	Placard Speed	Cruise Speed	Max. Speed
Flaps (deg)	45	45	45	0	0	0
Speed (kts)	130	140	175	175	250	385
Altitude	Sea Level					
Weight (lb)	23,000					
X _{c.g.} (% MAC)	18.5					
I _{yy} slug-ft ²	81,172					
CL _{α} (1/deg)	0.091					
C _{m\dot{q}} (1/rad)	-0.620					
C _{m$\dot{\alpha}$} (1/rad)	-0.186					
C _{m\ddot{C}_L}	-0.126					
C _{D\dot{C}_L}	0.110	0.083	0.055	0.080	0.032	0
C _{D\ddot{M}}	2.82	2.34	1.67	0.77	0.37	0.22
*Phugoid Period (sec)	36	39	49	49	70	113
*Phugoid is convergent.						

Side Force

The tail-off side force data presented in Figure 124 were obtained from wind tunnel test data and referred to the increased values of wing area and wing span. The contribution of the vertical tail was corrected for vertical tail geometry.

TABLE XIX. ELEVATOR STICK FORCE DUE TO SUDDEN DEVIATIONS FROM LONGITUDINAL TRIM										
W = 23,000 Lb, Gear Up c.g. at 16.4% MAC Gear Down c.g. at 16.8% MAC										
Condi- tion No.	Altitude	Speed		Gear	Flaps (deg)	Power	Config Change	Parameter Held Constant	Change in Elevator Angle (deg)	Req'd. Stick Force (lb)
		V/V _s (Config)	Knots							
2	Sea Level	1.4 (G)	185	Down	0	PLF	45° Flaps	Altitude	-3.7	14.6 (Pull)
3	Sea Level	1.4 (G)	138	Down	45	PLF	Idle Power	Speed	-1.0	1.6 (Pull)
4	Sea Level	1.15 (L)	114	Down	45	PLF	Takeoff Power	Altitude	+1.5	1.2 (Push)
6	Sea Level	1.5 (TO)	164	Up	20	Take- off	0° Flaps	Rate of Climb	+3.9	0.9 (Push)
	Sea Level	1.4 (L)	164	Up	45	PLF	0° Flaps	Altitude	+1.4	6.0 (Pull)

FLAGS - FLAPS 45 DEG

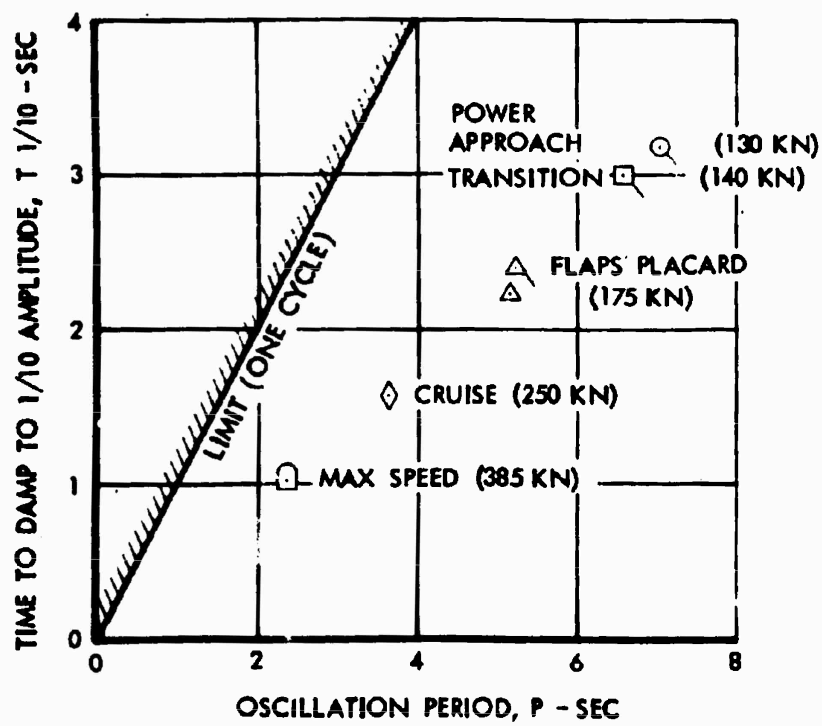


Figure 121. Longitudinal Short-Period Damping.

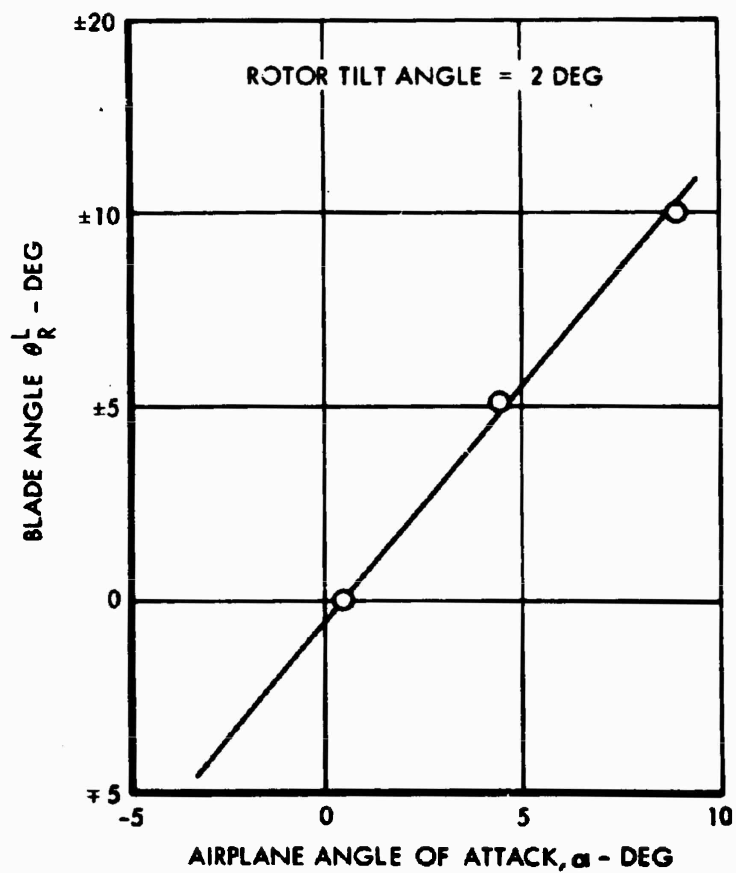


Figure 122. Stopped-Rotor Blade Angle Schedule for Maintaining Zero Rotor Load.

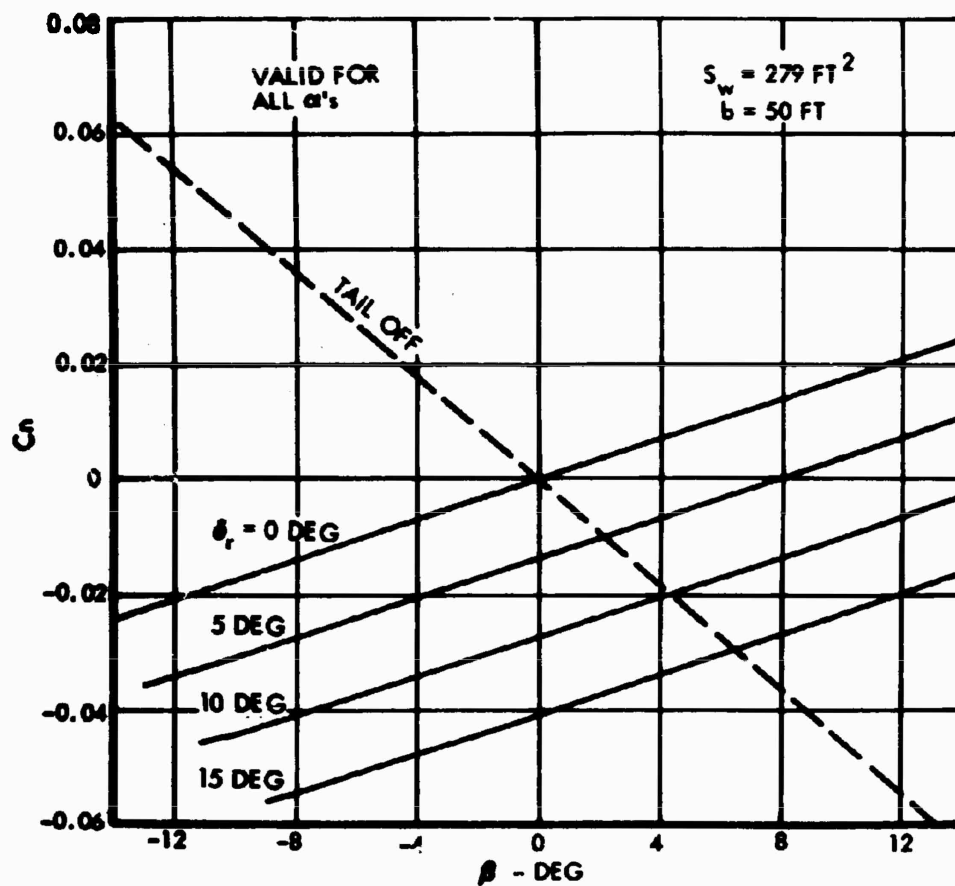


Figure 123. Yawing Moment Coefficient Versus Sideslip Angle (Flaps Up and Down).

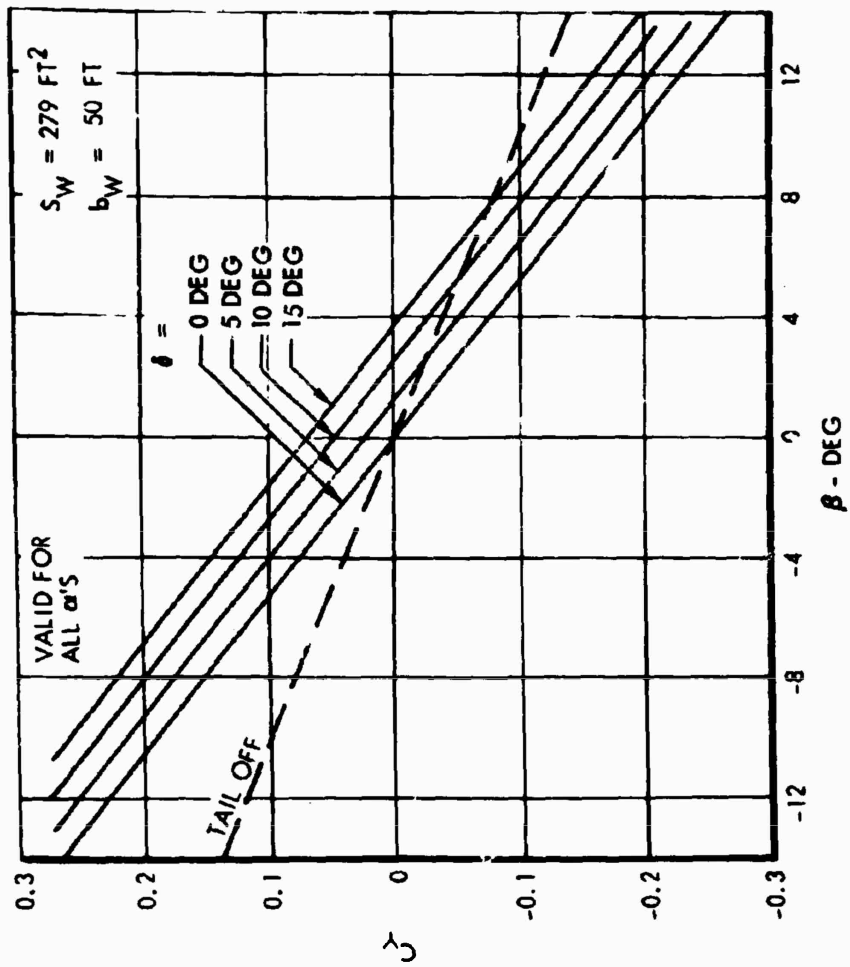


Figure 124. Side Force Coefficient Vs. Sideslip Angle (Flaps Up and Down).

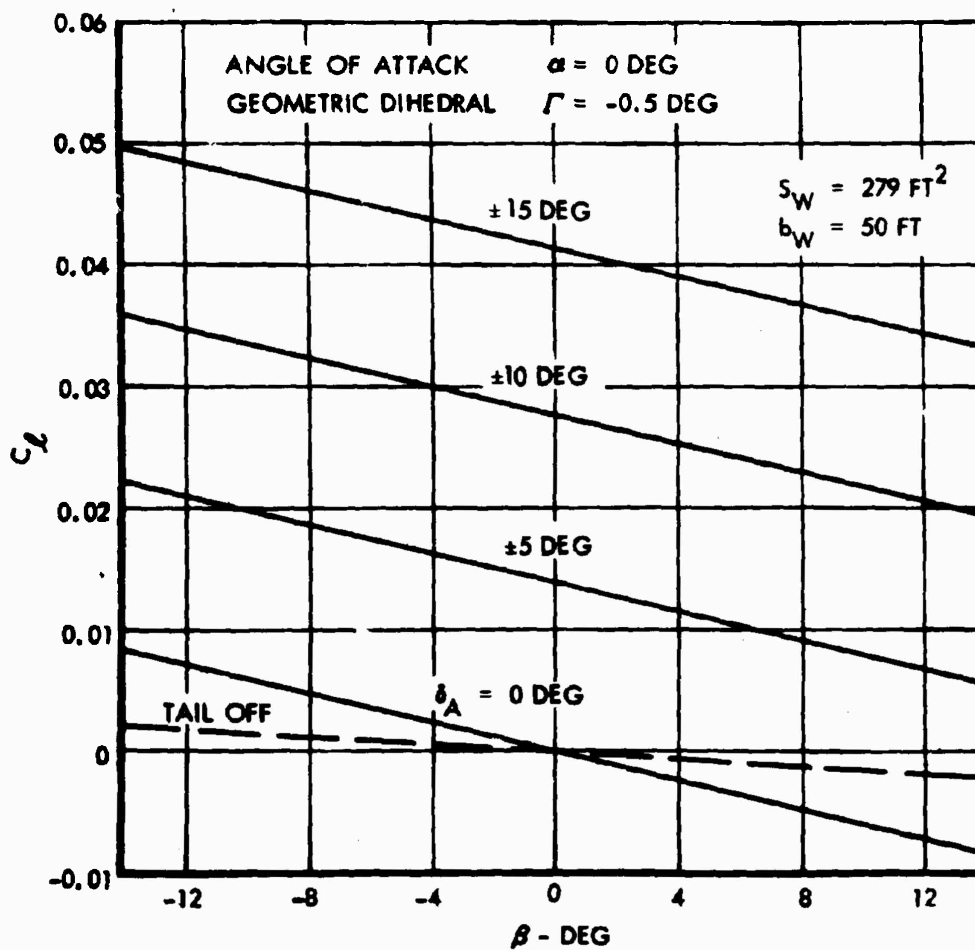


Figure 125. Rolling Moment Coefficient Vs. Sideslip Angle (Flaps Up and Down).

$S_W = 279 \text{ FT}^2$
 $b_W = 50 \text{ FT}$
 GEOMETRIC DIHEDRAL $\Gamma = -0.5 \text{ DEG}$

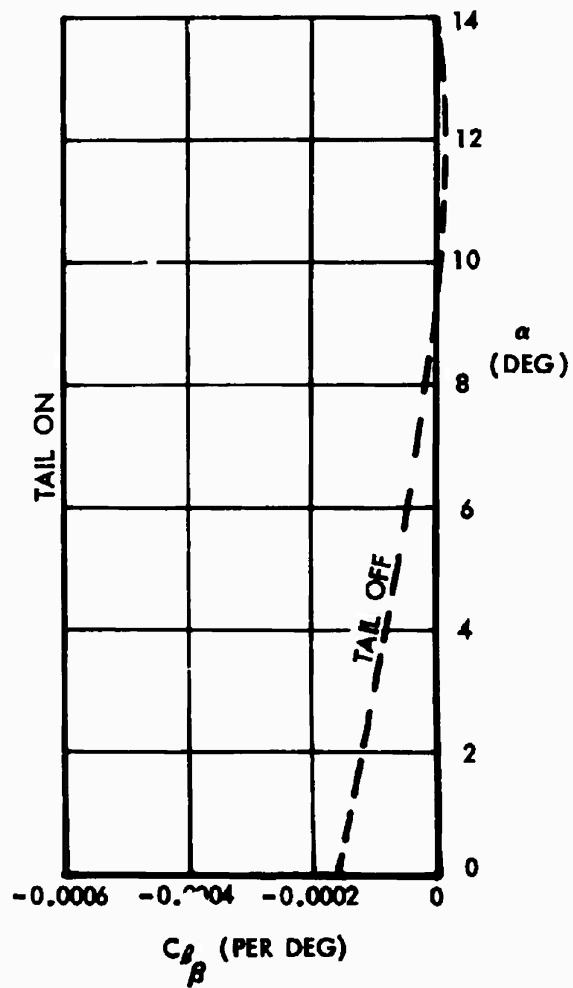


Figure 126. Dihedral Effect (Flaps Up and Down).

Dihedral Effect

The tail-off dihedral effect ($C_{l\beta}$) presented in Figures 125 and 126 was obtained from wind tunnel test data corrected for wing geometry. The contribution of the vertical tail was corrected for vertical tail geometry and wing geometry.

The ratio of $C_{l\beta}$ to $C_{n\beta}$ should be approximately -0.50 or less for good Dutch roll characteristics. The wind tunnel model which had no geometric dihedral indicated a value of $C_{l\beta}/C_{n\beta} = 0.75$. To assure satisfactory Dutch roll characteristics, the CRA wing will incorporate a negative dihedral of 0.5 degree, which reduces $C_{l\beta}$ to -0.00060. This effect is included in the data of Figure 125 and in all subsequent analyses.

The value of $C_{l\delta_a}$ shown in Figures 125 and 127 was obtained from wind tunnel data and corrected for wing geometry.

Maximum Roll Rates

The roll requirements in MIL-F-8785(ASG) are in terms of $(Pb/2V)_M$. The specification requires 0.07 over the speed range up to 300 knots. Since

$$(Pb/2V)_M = \frac{C_{l\delta_a} \delta_{aM}}{C_{l_p}}$$

the value of $(Pb/2V)_M$ is independent of speed. The maximum aileron deflection of ± 11 degrees was determined by the $(Pb/2V)_M$ requirement.

A single-degree-of-freedom time history at transition speed (140 knots) presented in Figure 128 shows that the average $Pb/2V$ over the first 30 degrees of bank angle is 0.040, which is a satisfactory roll rate.

Aileron and Rudder Hinge Moment

Lateral control is provided by a Frise-type aileron. The balance was chosen to limit the lateral control forces to specification values. The C_b/C_a is approximately 30 percent. The hinge-moment coefficient data presented in Figure 129 were obtained from References 21 and 25.

The rudder hinge-moment coefficients are -0.0005 and -0.0074 for $C_{h\alpha}$ and $C_{h\delta}$ respectively without a nose balance. These values provide rudder pedal forces that are within the specification limits.

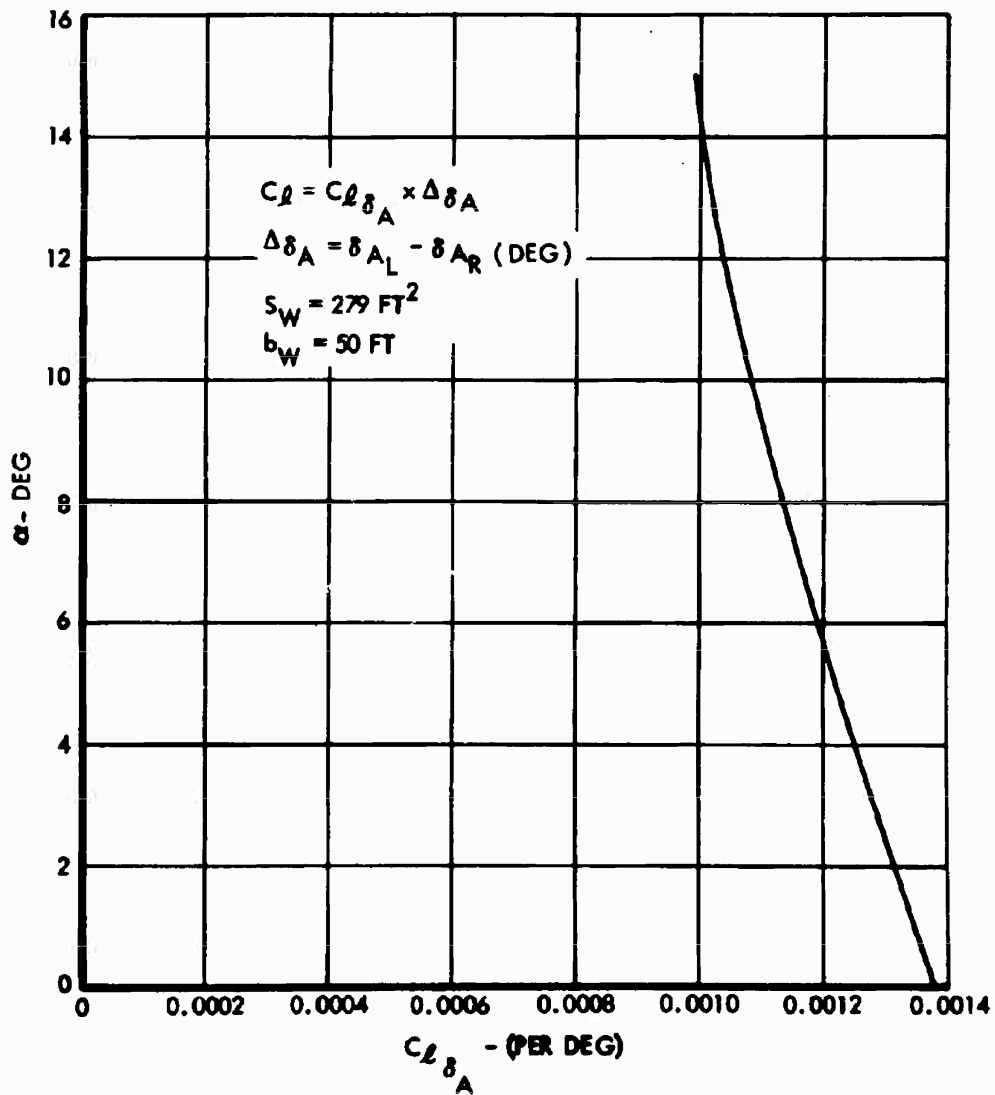


Figure 127. Aileron Effectiveness.

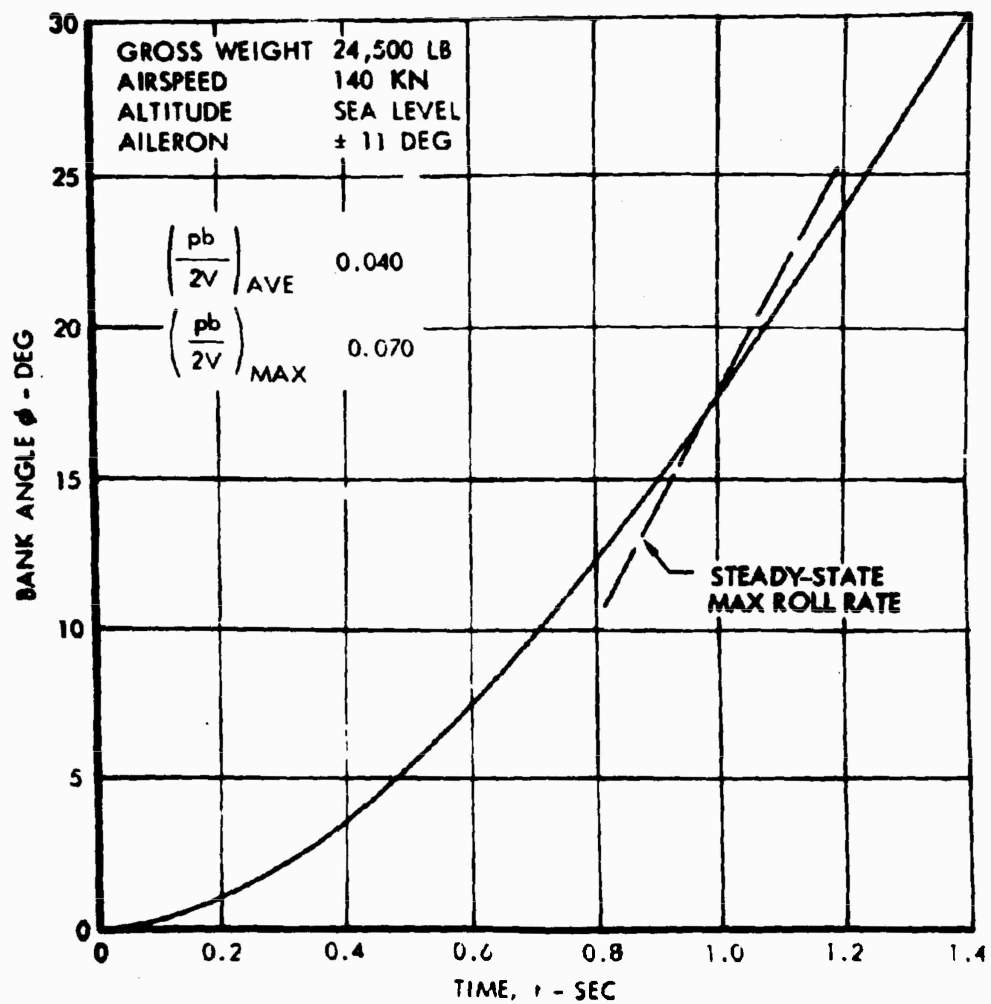


Figure 128. Bank Angle Time History at Transition Speed.

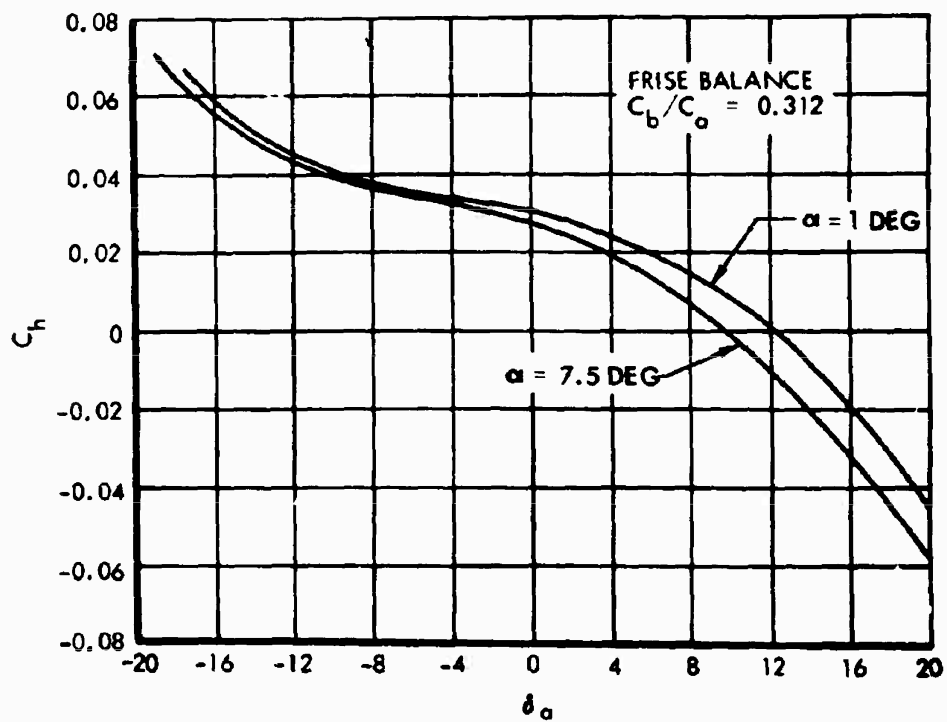


Figure 129. Aileron Hinge Moment Coefficient.

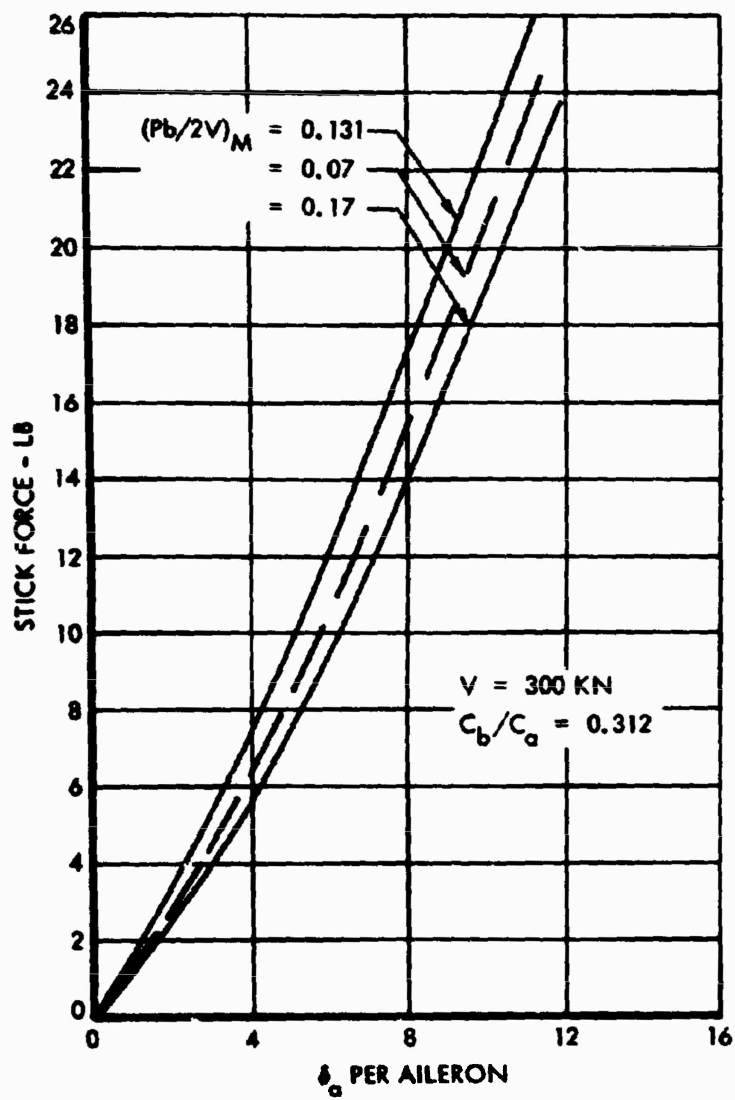


Figure 130. Aileron Stick Force.

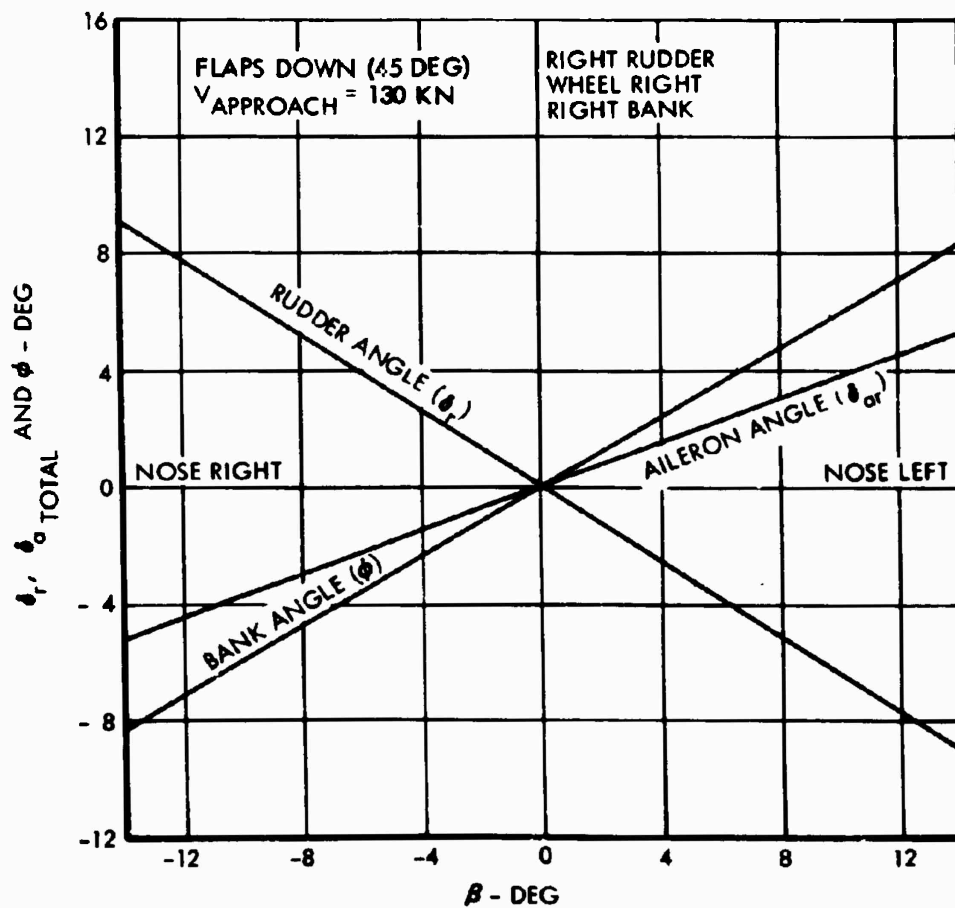


Figure 131. Characteristics in Steady-State Sideslip (Approach).

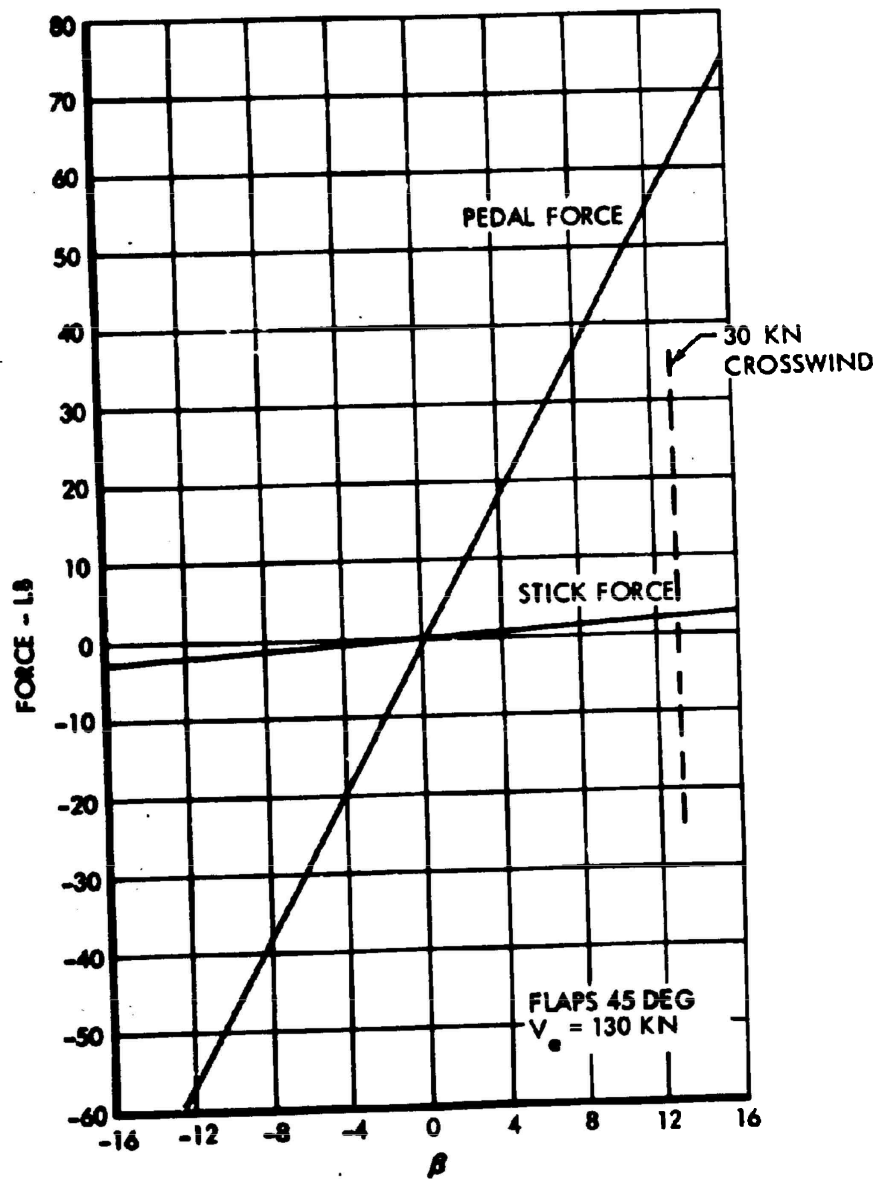


Figure 132. Control Forces in Straight Yawed Flight (Approach).

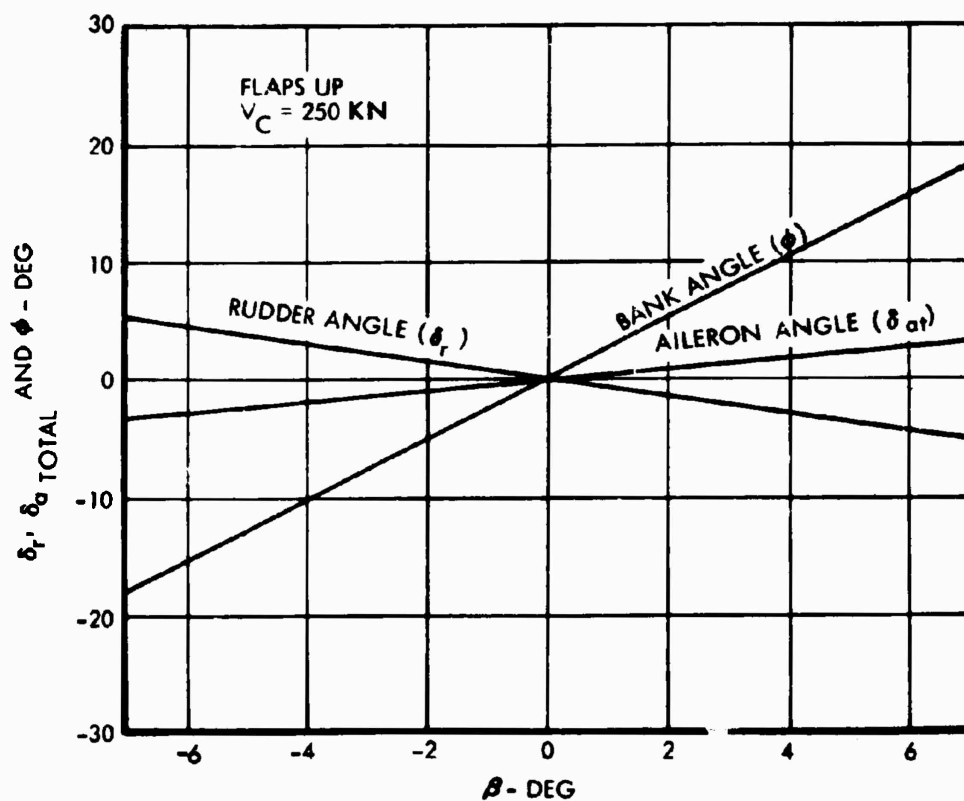


Figure 133. Characteristics in Steady-State Sideslip (Cruise).

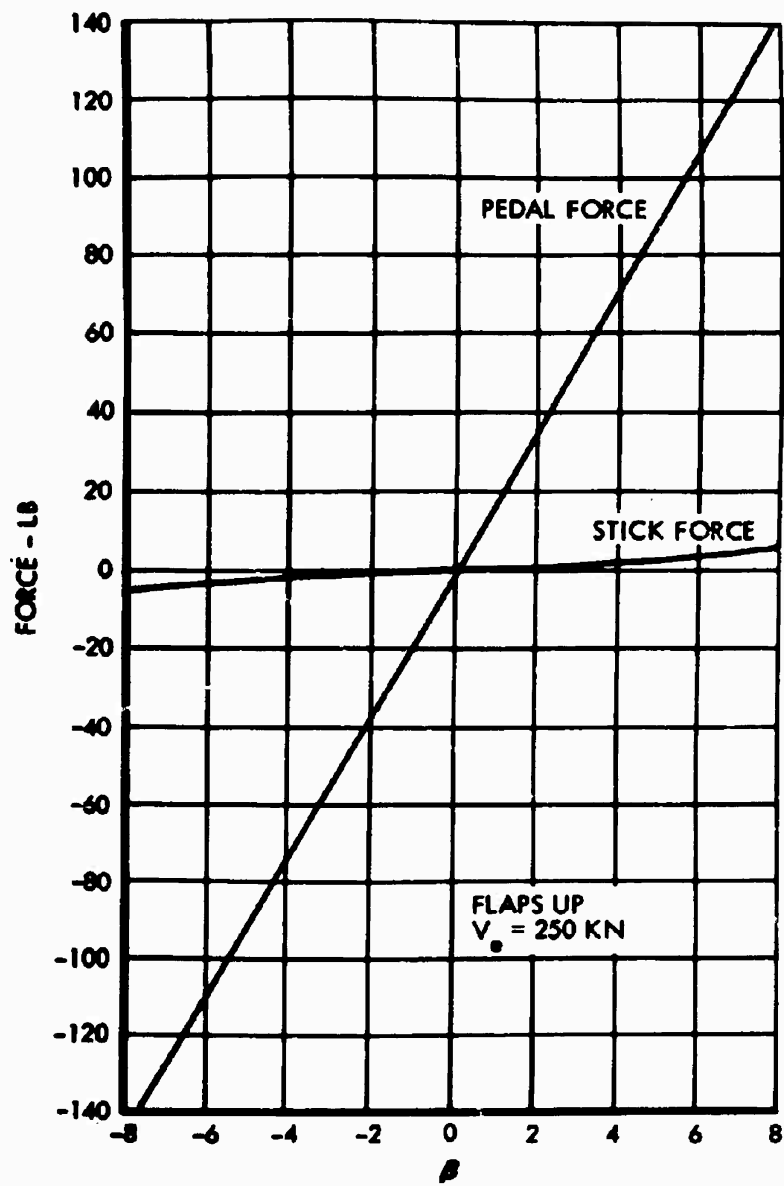


Figure 134. Control Forces in Straight Yawed Flight (Cruise).

Aileron Stick Forces

Figure 130 presents lateral control stick forces for maximum aileron deflection rolls at 300 knots. MIL-F-8785(ASG) requires a $(P_b/2V)_M = 0.07$ at all speeds up to 300 knots with a lateral control force of 25 pounds or less. The lateral control force will be less at lower speeds.

Steady-State Sideslips

The characteristics in steady-state sideslips are shown in Figures 131 through 134 for power approach and cruise flight conditions. MIL-F-8785(ASG) requires crosswind landing capability with a 30-knot crosswind with pedal forces less than 180 pounds. The 30-knot crosswind at 130 knots requires a sideslip capability of 13 degrees. Figures 131 and 132 show that a sideslip angle of 13 degrees can be obtained with a rudder deflection of approximately 8.5 degrees with a pedal force of 65 pounds, which is well within the specification requirement. There is no specific specification requirement for sideslip capability at cruise speeds. Figures 133 and 134 show that sufficient sideslip is available with moderate values of rudder pedal force.

Lateral-Directional Dynamic Stability

The lateral-directional dynamic stability characteristics were derived from the computer program described above. The same basic assumptions and representative flight conditions were also used. The lateral-directional derivatives used in this study are listed in Table XX. The sideslip-dependent derivatives ($C_{Y\beta}$, $C_{n\beta}$, $C_{l\beta}$) were taken from the wind tunnel test data.

The roll-rate derivatives (C_{Yp} , C_{np} , C_{lp}) were computed by methods outlined in Reference 21. C_{Yp} relates directly to lift coefficient. C_{np} is further complicated by c.g. location and flap deflection. The term C_{lp} is basically a function of wing geometry and is essentially constant over the flight regime.

The yaw-rate derivatives (C_{Yr} , C_{nr} , C_{lr}) were computed by methods shown in References 19, 23 and 24. The derivative C_{Yr} is due chiefly to the vertical stabilizer. C_{nr} is computed in a manner similar to $C_{m\dot{\alpha}}$. The wing has a powerful effect in this term. Lift coefficient and flap deflection are the factors affecting the value of C_{lr} .

The results of the lateral-directional dynamic stability computations are shown in Table XX and Figure 135 for the representative flight conditions. The time to double bank angle, in a divergent spiral, is listed in Table XX. The Dutch roll mode is graphically expressed in Figure 135. The inverse of cycles to damp to one-half amplitude is plotted against the rolling parameter, $(|\phi/V_e|)$.

TABLE XX. LATERAL-DIRECTIONAL DYNAMIC STABILITY DERIVATIVES

Flight Condition	Power Approach	Transi- tion	Flap	Placard Speed	Cruise	Max. Speed
Flaps (deg)	45	45	45	0	0	0
Speed (kt)	130	140	175	175	250	385
Altitude	Sea Level					
Weight (lb)	23,000					
$X_{c.g.}$ (% MAC)	18.5					
I_{xx} (slug-ft ²)	25,362					
I_{zz} (slug-ft ²)	98,716					
$C_{Y\beta}$ (1/deg)	-0.019					
$C_{n\beta}$ (1/deg)	0.00175					
$C_{l\beta}$ (1/deg)	-0.00060					
C_{Yp} (1/rad)	-0.348	-0.300	-0.240	-0.180	-0.089	-0.037
C_{np} (1/rad)	-0.157	-0.133	-0.102	-0.072	-0.024	-0.003
C_{lp} (1/rad)	-0.44					
C_{Yr} (1/rad)	0.661					
C_{nr} (1/rad)	-0.128	-0.104	-0.082	-0.045	-0.025	-0.021
C_{lr} (1/rad)	0.378	0.334	0.279	0.225	0.141	0.040
Spiral, time to double bank angle (sec)	8.7	9.8	13.3	15.7	32.0	187.7

<u>SYMBOL</u>	<u>CONDITION</u>	<u>SPEED (KN)</u>
○	APPROACH	130
□	TRANSITION	140
△	FLAPS PLAC'D	175
◇	CRUISE	250
◻	MAX SPEED	385
FLAGS	(FLAPS 45 DEG)	

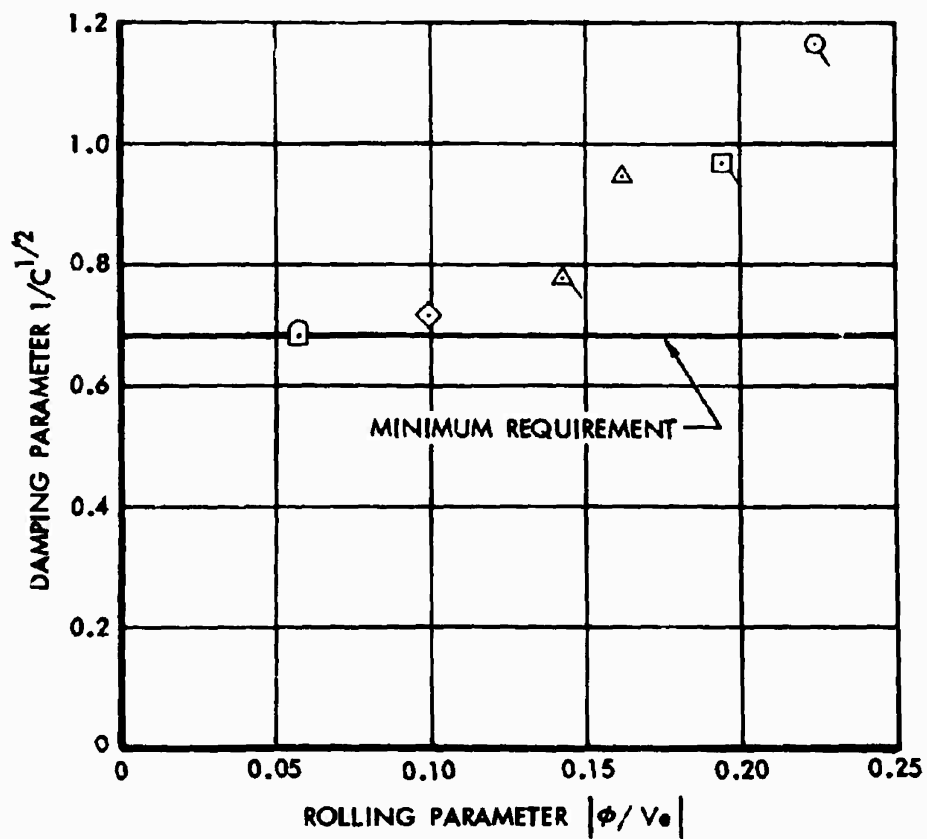


Figure 135. Dutch Roll Characteristics.

PART 6
STRUCTURES

SECTION 13
STRUCTURAL DESIGN CRITERIA

DESIGN ROTOR SPEEDS

The range of main rotor speeds for structural design are listed in Table XXI. The normal rotor speed of 240 rpm is based on the performance requirements for hover. The maximum and minimum values give a reasonable tolerance beyond the range for which the governor is set; the limit value is essentially 5 percent above the maximum value and represents the rotor speed which must be flight demonstrated in order that the design maximum may be designated the placard speed. The power-off values are selected to give as wide a range of speeds as possible so that the pilot, when confronted with the autorotation mode, has enough latitude to permit retrimming the vehicle. Also, a further limitation is imposed: at maximum rotor speed and forward speed, the Mach number of the advancing blade should not exceed 1.0. At the transition speed of 140 knots, this value is $M = 0.998$.

The minimum rotor speed at which the vehicle can attain 1.0g on the rotor is shown as a function of gross weight on Figure 136.

TABLE XXI. DESIGN ROTOR SPEEDS				
	RPM	Angular Velocity (Rad/Sec)	Tip Speed (FPS)	M_{t_a}
Normal Rotor Speed	240	25.1	753	0.886
Power On				
Design Minimum	227	23.7	712	0.850
Design Maximum	252	26.3	788	0.920
Limit Rotor Speed	265	27.7	830	0.955
Power Off				
Design Minimum	201	21.0	630	0.777
Design Maximum	263	27.5	825	0.950
Limit Rotor Speed	279	29.2	875	0.998
Note: M_{t_a} is the tip Mach number of the advancing blade at a forward speed of 140 knots at sea level.				

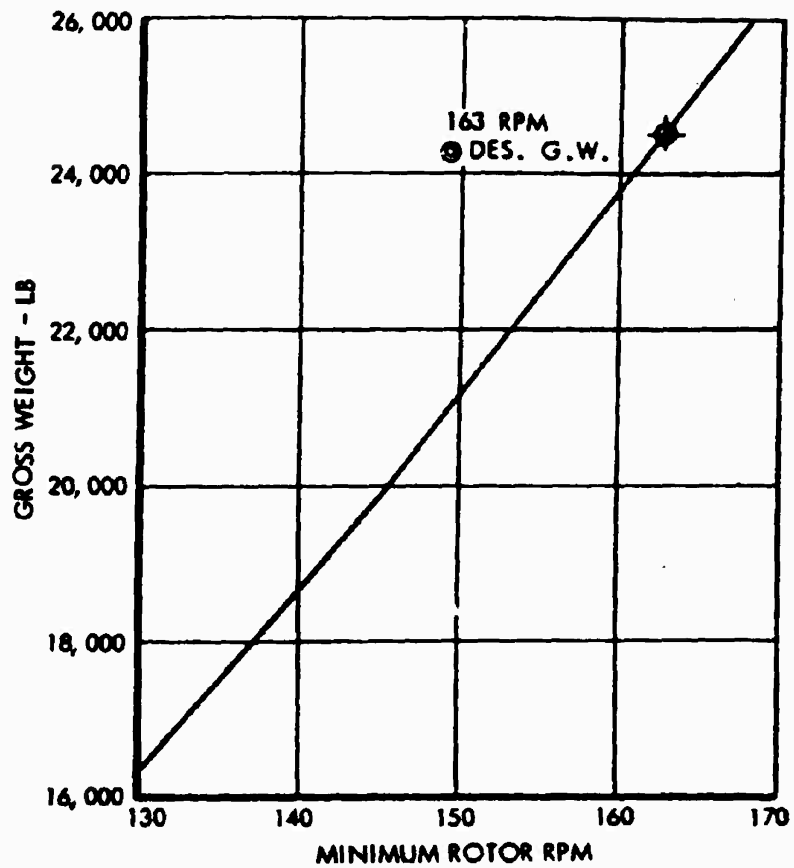


Figure 136. Minimum Rotor Speed Vs. Gross Weight for 1.0 g Flight.

DESIGN LIMIT FLIGHT MANEUVER LOAD FACTORS

Requirements

The limit flight maneuver load factors for the basic design gross weight are

- + 3.0g and -0.5g (helicopter mode)
- + 4.5g to dive speed
- 1.0g to V_H then varying to 0 at V_L } (Fixed-wing mode)

These load factors are applicable to the basic design gross weight or maximum design gross weight. For gross weight above this design weight, the load factor is determined based on the design value of nW being constant; however, for the ferry mission, the limit maneuver load factor is +2.5g. The V-n diagram for flight in the fixed-wing mode is given in Figure 137.

Figure 138 shows some experimental values of the maximum two-dimensional lift coefficient versus Mach number for a 12-percent thick airfoil. By curve-fitting techniques, an expression for $C_{L_{max}}$ is obtained. This expression and the corresponding curve are also shown in this figure. For a blade whose thickness ratio varies linearly along the span, the use of the thickness ratio at 0.75 radius gives satisfactory results for loads determination. The value of 12-percent is a reasonable choice for the main rotor blade of the CRA.

Figure 139 shows the calculated value of n_{max} and the structural design envelope at the design gross weight for various rotor speeds at sea level conditions. Load factors at higher altitudes are less than those for sea level.

Division of Load Between Rotor and Vehicle-Less-Rotor

Both the main rotor and the vehicle-less-rotor contribute to the total lift in the compound mode. The vehicle-less-rotor, having the configuration of a fixed-wing aircraft, will develop lift as a function of forward speed and angle of attack. The rotor will develop lift as a function of collective pitch setting and angle of attack of the rotor disc. Acting in parallel, the total lift is effectively that of the two lifting components. Figure 140 shows this division of lift at 1.0g.

The discussion under "Transition Speed Range" states the range of transition speeds for the optimized performance of the vehicle as 120 to 140 KEAS. A maximum value of 160 KEAS is also given as an overspeed to permit recovery from stall at the minimum transition speed. For purposes of structural design, the transition speed range is assumed to be from 140 to 160 KEAS.

At the transition speed chosen for a given flight plan, the collective pitch is reduced linearly from its maximum value of 100 KEAS to zero at the speed at which the rotor is stopped. For normal operation, this collective pitch

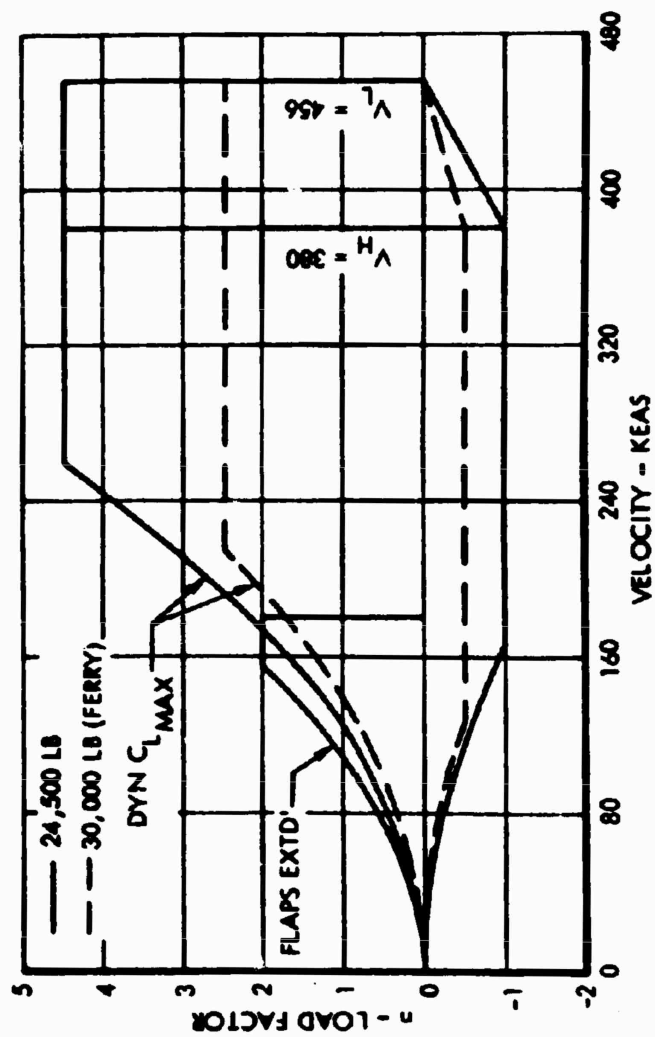


Figure 137. V-n Diagram - Fixed-Wing Mode.

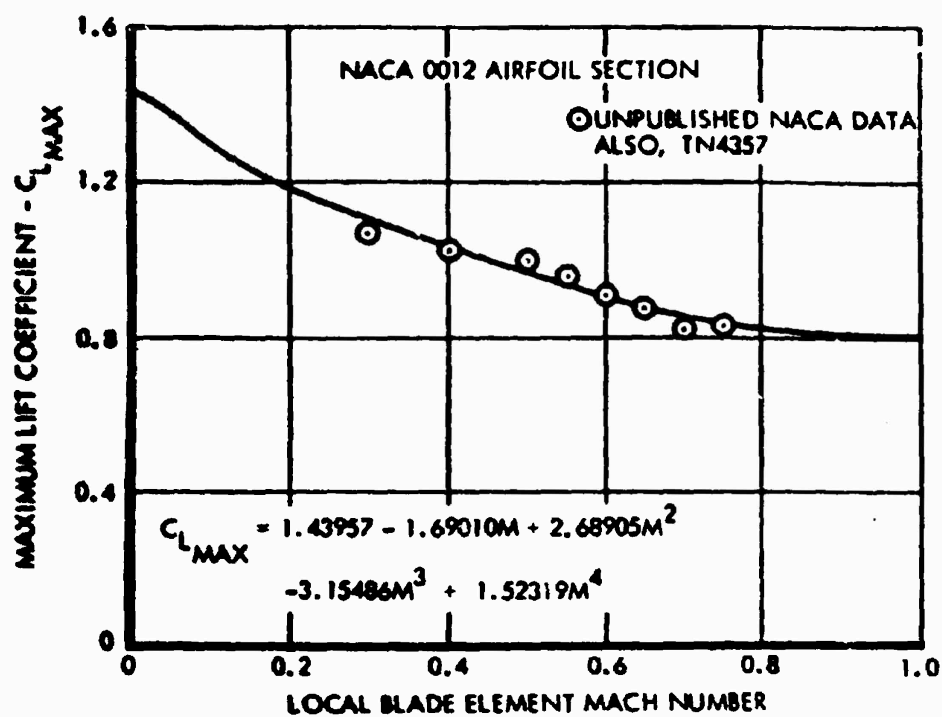


Figure 138. Variation of Section Maximum Lift Coefficient with Mach Number.

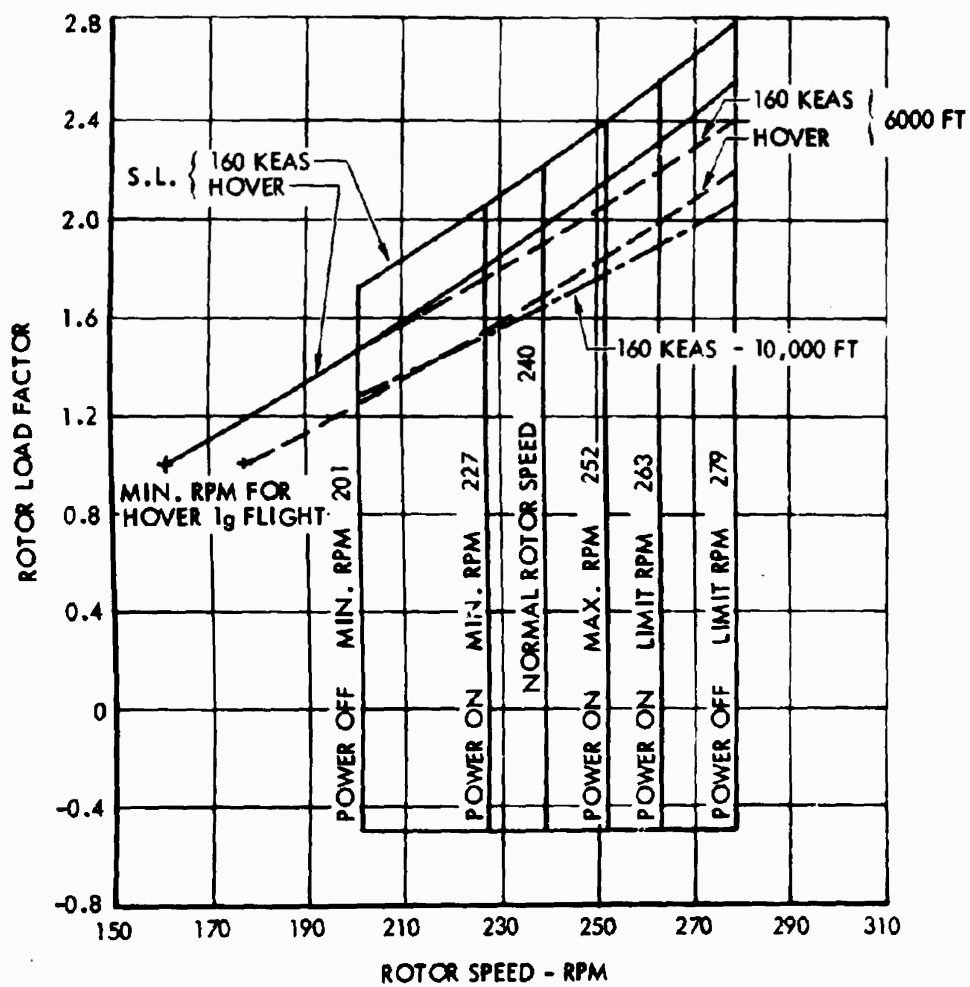


Figure 139. Maximum Rotor Load Factor Vs. Rotor RPM.

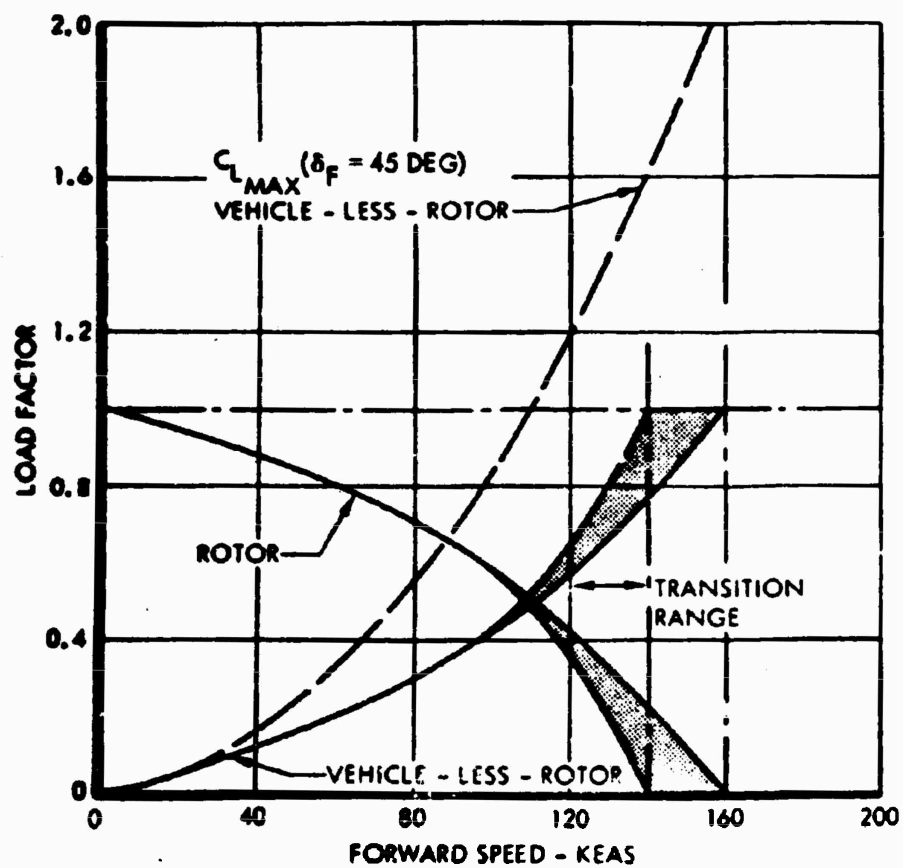


Figure 140. Division of Lift Between Rotor and Vehicle Less Rotor - 1.0 g.

change is shown in Figure 141 as the two lines emanating from the common point at 100 KEAS and decreasing linearly to zero at the minimum and normal transition speeds. For establishing the strength level, the programmed collective pitch change is assumed to reduce to zero at 140 to 160 KEAS as shown in the shaded area in the figure. This selection of the collective pitch variation with speed results in higher rotor loads than will be experienced in normal operation. The curves (e.g., Figures 140 and 142, etc.) which reflect the collective range are based on that chosen for structural design. At the minimum value of collective pitch between 140 and 160 KEAS, the rotor is completely unloaded and the wing and control surfaces have taken over the functions of lift and trim respectively.

The division of load between both major lifting components is obtained for 1.0g flight by trimming the vehicle at various speeds in the compound mode such that the combination of collective and cyclic pitch results in a c.g. acceleration of 1.0g. The collective pitch is kept at the maximum value consistent with the vehicle angle of attack necessary to develop the airload on the wing. For maneuvering flight, the collective pitch is increased to its maximum value at that speed; the angle of attack is then increased to the extent necessary to attain the desired load factor at the center of gravity. The V-n diagram for flight in the compound mode is shown in Figure 142.

Unsymmetrical Flight Load Factors

The design unsymmetrical load factors are those specified in References 26 and 27.

- a. The lateral maneuvering load factors are $0.8 n_{\max}$ and zero. In the compound mode, the maximum positive load factor is 0.8 of the values shown in Figure 140 corresponding to the forward speed and rotor rpm for the condition under consideration.
- b. The directional maneuvering load factor is 1.0 at all speeds from hover to V_L .

DESIGN GUST LOAD FACTORS

The design gust load factors are determined for the requirements of Reference 26 for the compound mode and Reference 27 for the fixed-wing mode. In the compound mode, the discrete gust intensity is 50 fps. As a fixed-wing aircraft, the gust intensities are:

<u>Velocity - knots</u>	<u>Gust Intensity - fps</u>
214	66
380	50
456	25

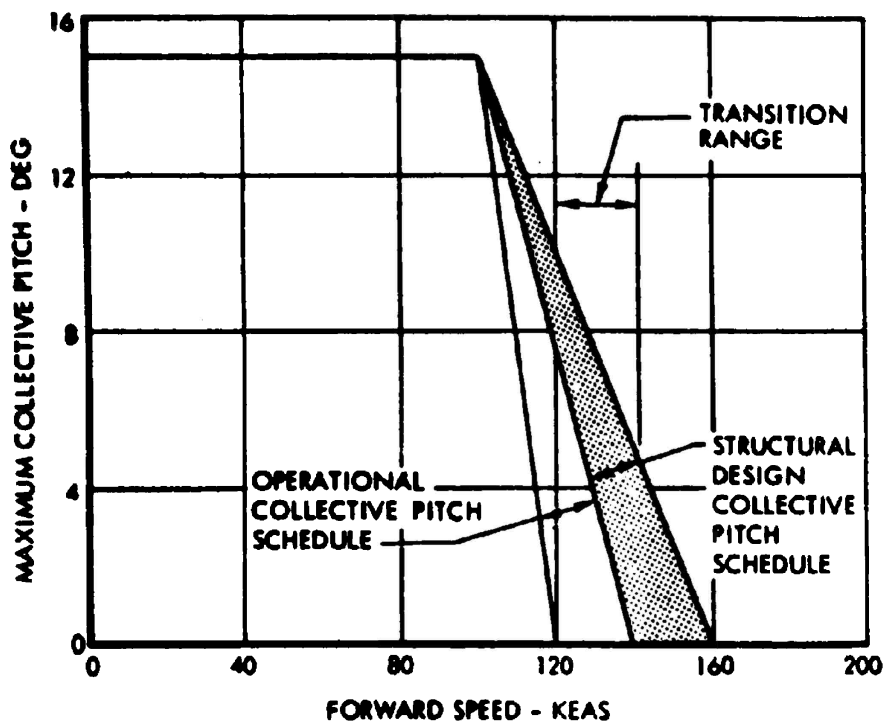


Figure 141. Maximum Collective Pitch Vs. Forward Speed.

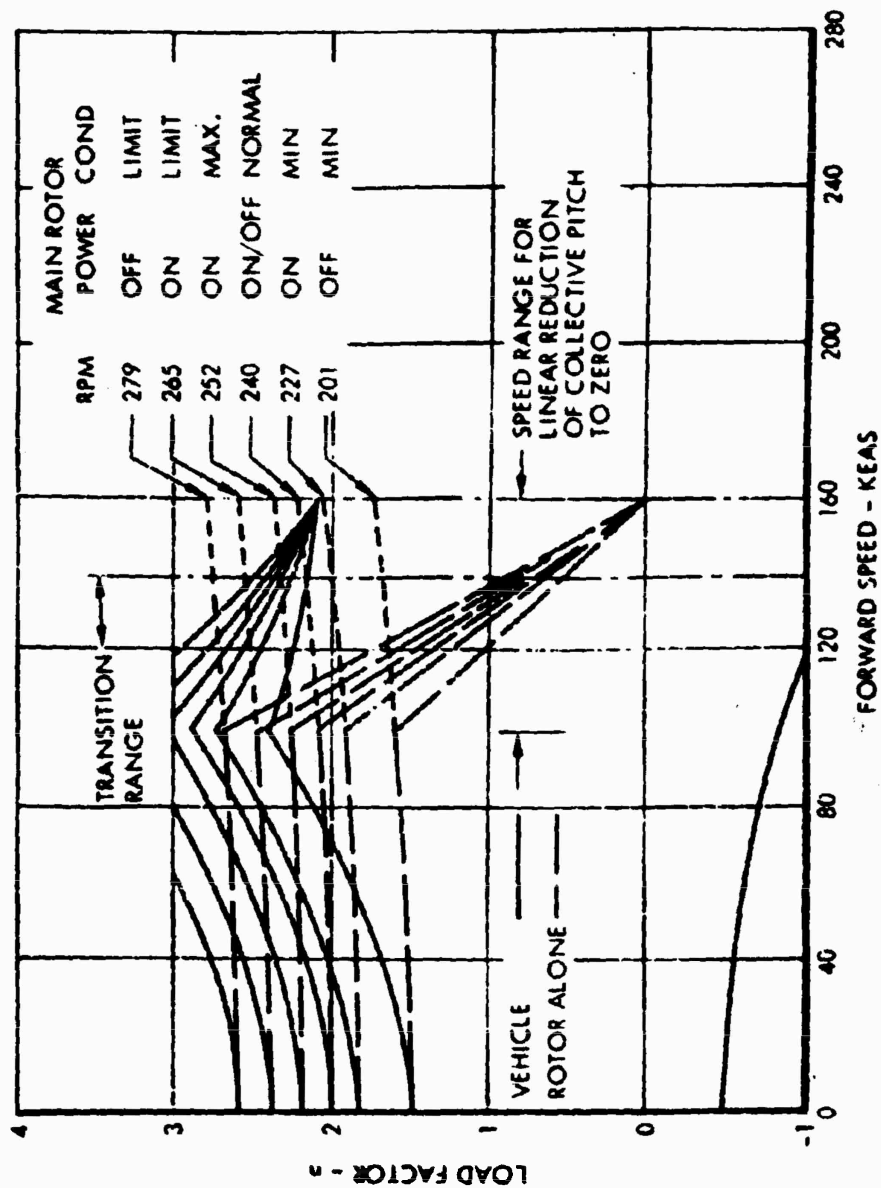


Figure 142. V-n Diagram - Compound Mode.

Main Rotor Gust Load Factor

The incremental gust load factor on the rotor, assuming a gust alleviation factor of unity, is obtained from Figures 143 and 144 using the relationships

$$\begin{aligned}\Delta\mu &= \frac{50}{\Omega R} \\ \Delta\alpha_{\text{rad}} &= \frac{\Delta\mu}{\mu} \\ \Delta n &= \Delta C_t \frac{[\pi R^2 \rho (\Omega R)^2]}{W}\end{aligned}$$

Vehicle Less Rotor Load Factor

The incremental gust load factor for the vehicle less rotor is obtained for the speeds and gust intensities noted in Table XXII, using the relationship

$$\Delta n = \frac{K U V C_{La}}{498 W/S}$$

The value of the gust alleviation factor, K, is obtained from

$$\begin{aligned}K &= \frac{0.88\mu}{5.3 + \mu} \\ \mu &= \frac{2 W/S}{g c m \rho}\end{aligned}$$

Table XXIII presents the load factors.

Symmetrical Flight

The requirements for symmetrical flight maneuvers are those of Reference 26 and Reference 27 for the compound and the fixed-wing modes respectively.

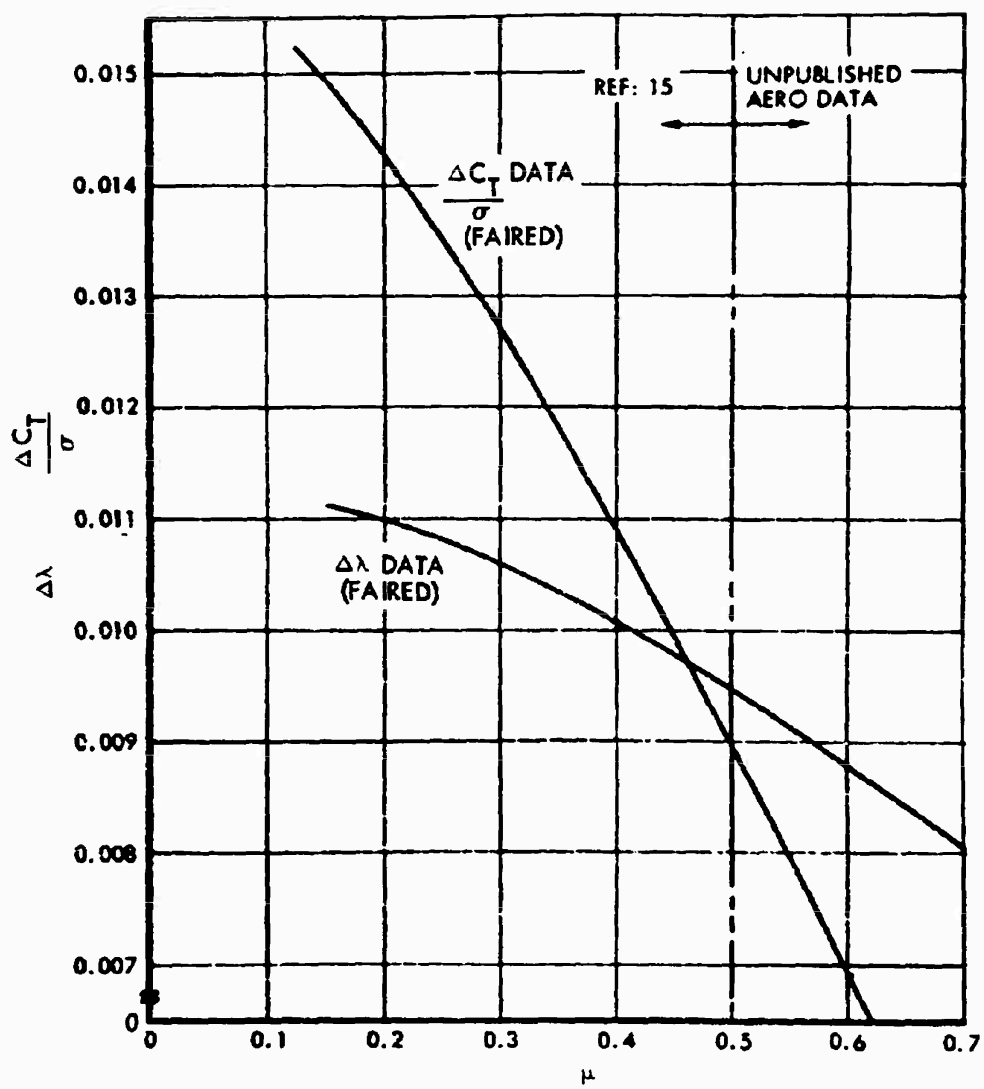


Figure 143. $\Delta C_T/\sigma$ and $\Delta\lambda$ per 1° Collective Pitch Vs. Advance Ratio.

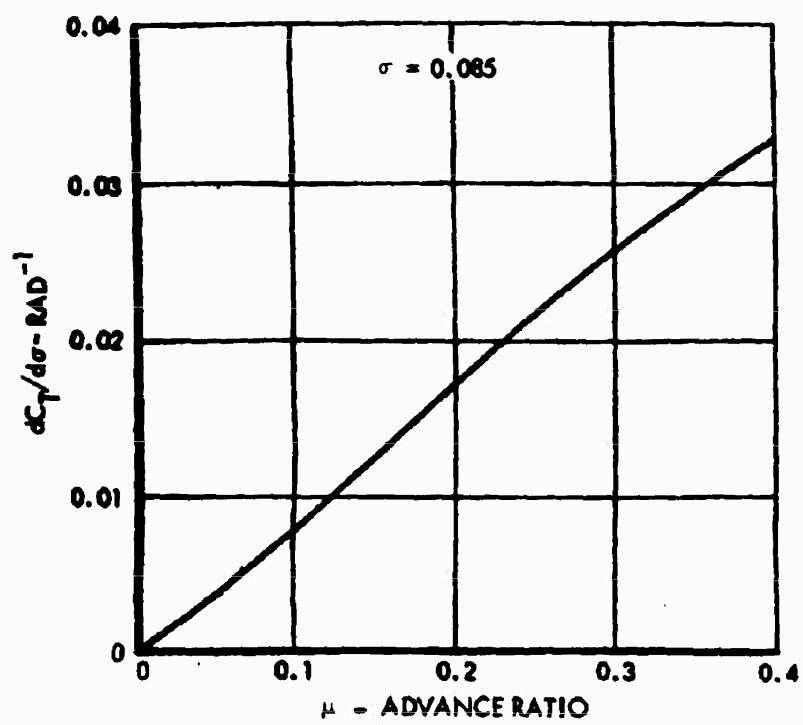


Figure 144. $dC_T/d\sigma$ Vs. Advance Ratio.

TABLE XXII. GUST INCREMENTAL LOAD FACTOR - MAIN ROTOR		
V_{KEAS}	Δn	
	Tip Speed: 753	875
20	0.77	0.89
40	0.82	0.94
60	0.86	0.99
80	0.89	1.02
100	0.91	1.05
120	0.91	1.06
140	0.90	1.06
160	0.88	1.05

TABLE XXIII. GUST INCREMENTAL LOAD FACTOR - VEHICLE LESS ROTOR		
V_{KEAS}	U_{fps}	Δn
214	66	1.42
380	50	2.60
456	25	1.56

Compound Mode. Four basic flight conditions are considered:

- a. Maximum Speed Condition. This is a 1.0g condition, the speed being the limit speed in the forward, rearward, and sideward directions. The rotor speeds considered are: (1) limit, power on (263 rpm) and (2) design minimum, power on (227 rpm).

- b. Symmetrical Dive and Pullout. For these maneuvers, the control surfaces are moved at the maximum rate established for the output of the powered control system to the displacement which results in the design load factor, followed by a linear return of the control surfaces at the same maximum rate to that required for level flight. The rotor speeds considered are the same as those for the maximum speed condition. The forward speeds are 160 KEAS and any lower speeds that result in critical loads on any part of the vehicle.
- c. Vertical Takeoff (Ground Takeoff). The collective pitch is changed from minimum to maximum angle at the maximum rate established for the output of the powered control system and held until the maximum attainable load factor is reached. The rotor speed is the limit, power-on value of 263 rpm.
- d. Autorotational Flight and Dive Pullout. These conditions are similar to item (b), above, except for:
 - 1. The forward speeds are 160 KEAS and that for minimum rate of descent.
 - 2. The rotor speeds are those for power off.
 - Limit -- 279 rpm
 - Design Minimum -- 201 rpm

Fixed-Wing Mode

The symmetrical flight conditions are those of Reference 27, the pitching maneuvers being those for the prescribed pitching acceleration.

Unsymmetrical Flight

The requirements of References 26 and 27 are applicable without deviation.

Compound Mode - (Rolling Pullout)

- a. Forward Speed. The forward airspeed is 160 KEAS and any lower speed that results in critical loads.
- b. Rotor Speed. The rotor speeds considered are
 - 1. Limit, power on (263 rpm).
 - 2. Design minimum, power on (227 rpm).
- c. The rate of roll is the maximum attainable rate when the pitch settings of the main and tail rotor blades and the ailerons and rudder are moved at the maximum rate established for the output of the powered control system.

- d. The normal load factors are $0.8 n_{\max}$ and 0.
- e. The maximum rate of roll and the maximum normal load factor are considered to occur simultaneously.
- f. The directional control is considered to be:
 - 1. Maintained in its neutral position.
 - 2. Displaced in the direction of recovery at the maximum rate established for the output of the power control system.

Compound Mode

The requirements of Paragraph 3.2.3.2 of Reference 26 are applicable with the exception that the tail rotor collective pitch and the rudder are displaced at the maximum rate established for the output of the power control system to the maximum deflection as limited by stops or by the maximum system output.

- a. Speed. V_L in forward or sideward flight, or any lesser speed which might produce critical loads in any component.
- b. Rotor Speed. Limit rotor speed, power on (263 rpm).
- c. The control displacement is maintained until the maximum angle of sideslip is developed and then returned to neutral at the same rate as specified above.

For autorotational flight, the same criteria are applicable except that the rotor rpm is 279.

Fixed-Wing Mode

The unsymmetrical flight conditions of Reference 27 are applicable except that, in lieu of the engine failure requirement (which cannot result in unsymmetrical thrust because of the positive interconnection of the propellers through the transmission system), a propeller pitch control malfunction is substituted. With such a malfunction, the propeller will automatically feather.

DESIGN LANDING CONDITIONS

The landing requirements specifically detailed in Paragraph 2.1.1g of the Statement of Work which forms a part of the Contract (Reference 30) are: "Landing gear shall be designed for applicable VTOL landing conditions specified in MIL-S-8698(ASG). The Contractor shall investigate the landing gear capabilities for emergency landing in the fixed wing mode on standard runway."

The CRA is, therefore, designed to the landing criteria for helicopters (Reference 26) and for airplanes (Reference 31), the criteria of the latter specification being used as a guide to establish the capabilities of the vehicle in the fixed-wing mode.

The nose landing gear of the C-140 has been found to be adaptable to the CRA. Figure 145 gives the load factor-stroke curves from which the nose gear load factor of 1.67 is read at the maximum stroke of 12 inches.

Design Landing Conditions - Helicopter Mode

Sinking Speed

The limit sinking speed is 8 feet per second in combination with $2W/3$ rotor lift. This sinking speed is applicable to the basic design gross weight.

Reserve Energy Requirement

The structure shall not fail when the initial contact with the ground occurs at a sinking speed of $8\sqrt{1.5}$ or 9.8 feet per second.

Landing Load Conditions

The requirements of Chapter 2 and 3 of Reference 32 apply as modified by Paragraphs 3.4.5, 3.4.5.1, 3.4.5.2 and 3.4.5.3 of Reference 26, and by the following:

- a. Those landing conditions resulting in unbalanced moments about the center of gravity will be put into equilibrium by rotational inertia forces on the vehicle and by moments introduced in the rotor hub based on the compliance rate of the rigid rotor.
- b. Landing gear loads and the resulting vehicle response are determined for both level and sloping terrain landings, the maximum slope being 15 degrees. For sloping terrain landings, the vehicle is assumed to be oriented so that its longitudinal axis is normal to the direction of the slope.
- c. For landings on level terrain, the loads are obtained for the critical translational speeds parallel to the ground, from zero to the maximum design values in the forward, aft, or side directions.
- d. For landing on the 15-degree slope, the translational velocity of the vehicle is assumed to be zero.

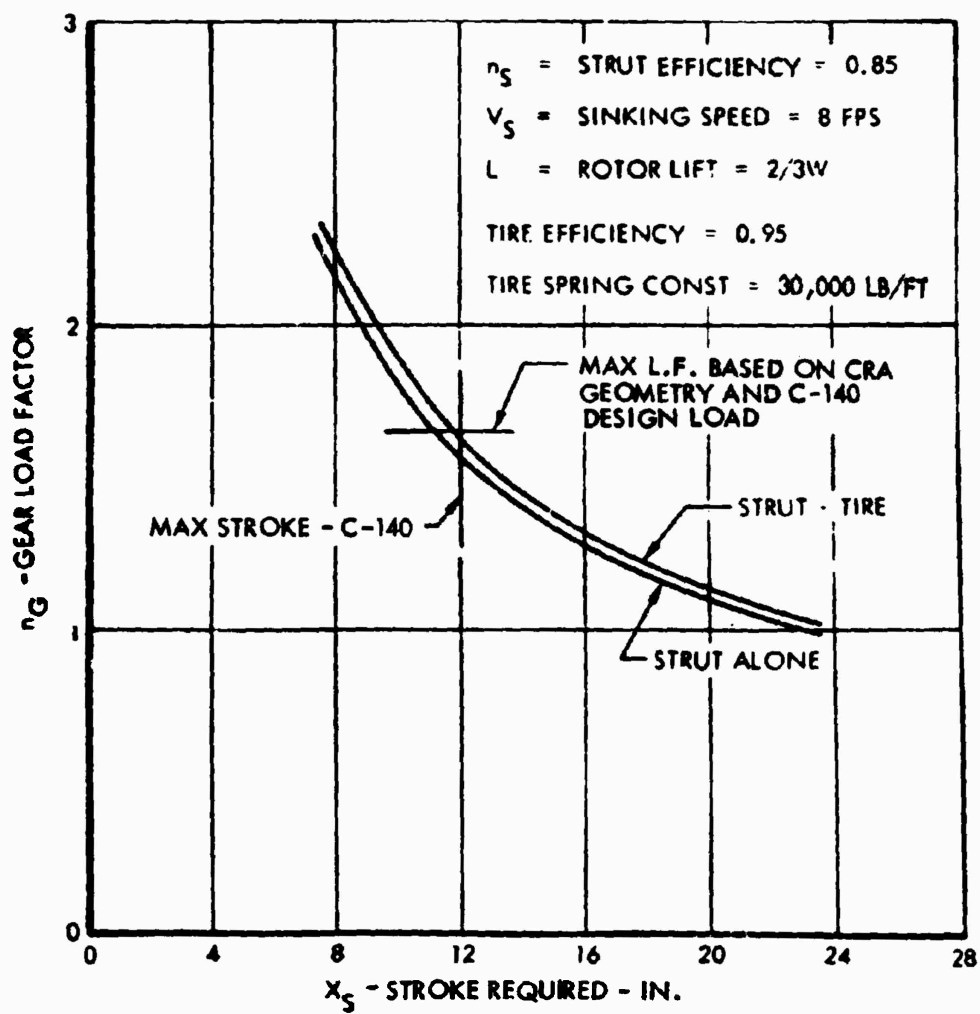


Figure 145. Nose Landing Gear Load Factor Vs. Strut Stroke.

Design Landing Conditions - Fixed-Wing Mode

Sinking Speed

The landing gear capability for landing in the fixed-wing mode is based on the strength level established for the helicopter. This capability is determined by equating the total energy to be absorbed for the helicopter mode to that for the fixed-wing mode. For this calculation, it is assumed that the orifice is optimized to give the same load factors for both the hydraulic and the air peak and that this peak load factor determined for landing as a helicopter will not be exceeded when landing as an airplane. The equation for landing gear energy balance is

$$P_{V_{\max}} \eta_s x_s = \frac{V^2}{2g} - \frac{\eta_t K_t x_t^2}{2} + (W - L)(x_s + x_t)$$

where

$P_{V_{\max}}$ = maximum vertical load developed in landing

V = vertical velocity at ground contact, fps

η_t = tire efficiency (to account for nonlinearity of tire deflection curve)

K_t = tire spring constant, lb/ft

x_t = tire deflection, ft

W = landing weight, lb

L = wing or rotor lift at ground contact, lb

x_s = strut stroke, ft

η_s = strut efficiency

Since the landing gear load factor may be expressed as

$$n_{LG} = P_{V_{\max}} / W$$

the energy expression may be rewritten in terms of n_{LG} ,

$$n_{LG} = \frac{\frac{V^2}{2g} - \frac{\eta_t K_t x_t^2}{2W} + (1 - \frac{L}{W})(x_s + x_t)}{\eta_s x_s}$$

Equating the landing gear load factors for the helicopter and the fixed-wing modes and assuming that the tire energy remains effectively unchanged, we obtain the following expression for the sinking speed in the fixed-wing mode:

$$\frac{\frac{64}{2g} \frac{\eta_t K_t x_t^2}{2W} + (1-\frac{2}{3})(x_{sH} + x_t)}{x_{sH}} = \frac{\frac{V^2}{2g} \frac{\eta_t K_t x_t^2}{2W} + (1-1)(x_{sF} + x_t)}{x_{sF}}$$

where x_{sH} = strut deflection for the helicopter mode, and x_{sF} = strut deflection in the fixed-wing mode

for

$$\begin{aligned} x_{sH} &= 1 \text{ ft} \\ x_t &= 1/3 \text{ ft} \\ \eta_t &= 0.95 \\ K_t &= 30,000 \text{ lb/ft} \\ V^2 &= 88.37 x_{sF} + 4.25 \end{aligned}$$

This is plotted in Figure 146.

DESIGN TAXI AND TAKEOFF CONDITIONS

The taxi and takeoff criteria for the CRA are those of References 26 and 31 for the helicopter and the fixed-wing modes of flight. Reference 26, in turn, refers these requirements to Reference 32, which is similar to the fixed-wing criteria of Reference 31. Thus, only one of these specifications need be used for this phase of the criteria and loads determination. The following conditions are investigated:

- a. Two-wheel braked roll
- b. Three-wheel braked roll
- c. Unsymmetrical braking
- d. Reverse braking
- e. Turning
- f. Pivoting
- g. Taxiing

Under normal conditions, with the main rotor deployed and rotating, sufficient lift can be generated to reduce the gear loads in turning, pivoting, and taxiing sufficiently to make analysis unnecessary. However, the requirement for taxi and takeoff in the fixed-wing mode necessitates consideration of all the above conditions.

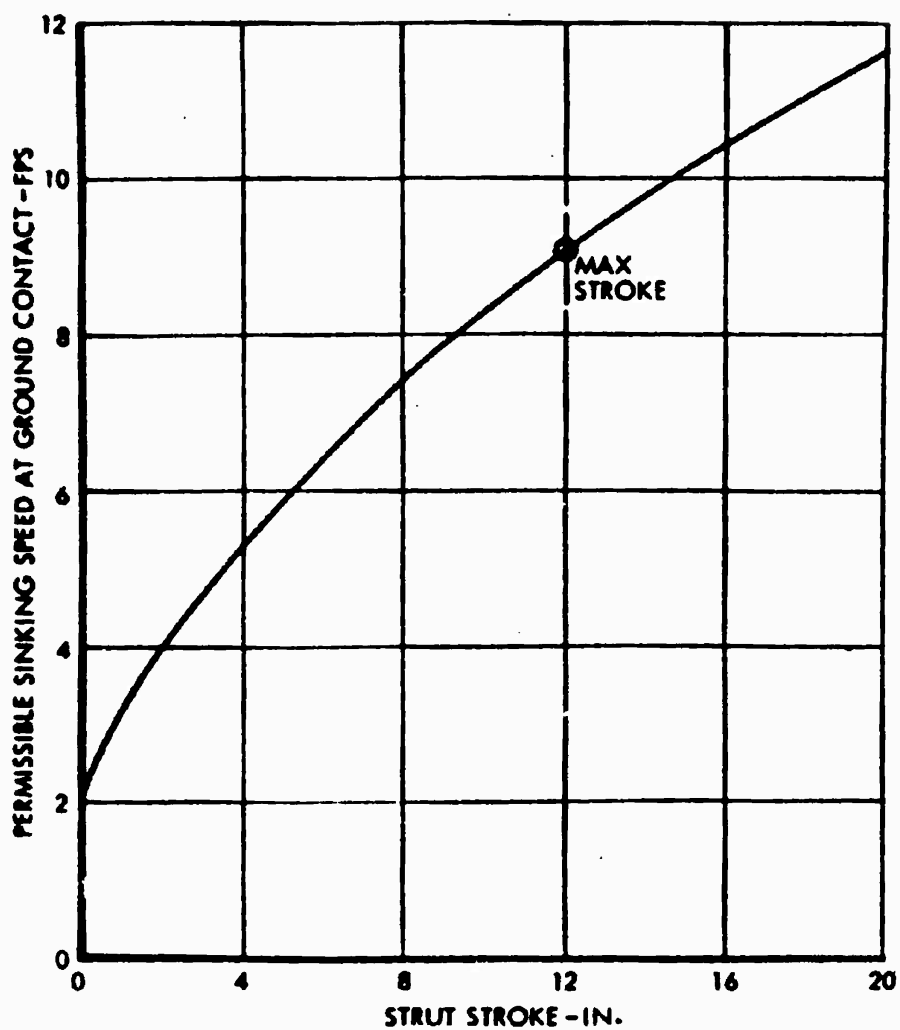


Figure 146. Landing Gear Capability - Fixed-Wing Mode.

Takeoff from sloping terrain is in accordance with a programmed sequence in which the pilot first applies collective pitch to obtain a lift of at least $W/3$, followed by cyclic control input to bring the vehicle to a level attitude. The collective pitch is then increased and the cyclic pitch reduced to maintain the level attitude as the uphill gear load is reduced to zero and the vehicle becomes airborne. It is assumed that the vehicle is oriented so that its longitudinal axis is normal to the direction of the slope. The CRA is designed to the requirements for takeoff from a 15-degree slope.

The maximum hub moment for this condition occurs at the instant that the downhill landing gear just clears the ground.

This condition applies to the helicopter mode; takeoff in the fixed-wing mode shall be conducted on level terrain.

MAIN ROTOR STRUCTURAL REQUIREMENTS

The main rotor is designed to the following specific requirements:

- a. The main rotor structure is designed to withstand the critical flight, landing, and takeoff loads, the criteria for which are presented under "Flight Conditions" and "Ground Loading Conditions."
- b. The hub, blades, blade attachments, and blade controls which are subject to alternate stresses are designed to the fatigue requirements discussed in Section 3.
- c. The rotor assembly is designed to withstand, at all speeds from zero to the maximum transition speed, a design limit torque of 1.25 times the mean torque for maximum continuous power.
- d. The requirements for rotor acceleration are those of Paragraph 3.3.1 of Reference 26. The rotor acceleration loads are those developed by the application of 1.5 times the torque developed at the military power rating of the engine in 0.1 second. These loads are equally distributed to all blades of the rotor.
- e. The rotor assembly is designed to withstand the loads resulting from stopping the rotor at the transition speed.
- f. The blades and the hub attachments are considered to be subjected to atmospheric turbulence during the stopping and folding operation.

TAIL ROTOR STRUCTURAL REQUIREMENTS

In the helicopter and the compound modes of flight, the tail rotor supplies the necessary thrust to counteract the main rotor torque and to apply directional control forces for maneuvering.

The tail rotor thrust for antitorque control is determined for all speeds from hover to 160 KEAS. Similarly, increments of tail rotor thrust are obtained

throughout the helicopter and compound flight modes for directional control in yawing and rolling maneuvers.

The tail rotor is also designed to the requirement for an abrupt directional control displacement at all speeds from zero to 160 KEAS, including hovering.

The tail rotor system is designed for a transient torque surge of 1.33 (mean torque at military power).

At transition, the tail rotor is stopped with the blade collective pitch reduced to give zero thrust and minimum drag. In the fixed-wing mode, these blades act as auxiliary fins for which loads are obtained for all pertinent conditions.

POWER PLANT INSTALLATION

The power plant installation is considered to be composed of:

- a. Two wing-mounted nacelles, each containing the engine, propeller drive shaft, propeller, and gearbox for power drive to the rotors.
- b. The various drive shafts to the main and tail rotor.
- c. The various transmissions and housings.

Fail-safe and safe-life concepts are applied to the various components as required.

Engine Installation

The engine mounts and supporting structure are designed to the critical flight and ground loading conditions. The engine characteristics are given in Tables V and XXIV. The data in these tables are applied to each critical condition. The engine installation is also designed to the load factors listed under "Emergency Landing Conditions."

Propeller

- a. The propellers are designed to the maximum engine output as modified by the power required for accessory drive and system losses.
- b. Propeller normal forces resulting from deviation of the thrust axis from the relative wind (pitch and yaw) are determined, consideration being given to the inflow velocity as affected by main rotor downwash, wing upwash, and fuselage effects. These normal forces and associated hub moments are determined by use of an equation developed by Hamilton Standard which expresses these values in terms of inflow angle, speed, and propeller physical properties.

TABLE XXIV. ENGINE DATA FOR ENGINE MOUNT LOADS

Engine Weight Installed (With Residual Fuel)			705 lb
			FS 287
Engine C.G. Locations			WL 109
			BL ±108
Engine Output			
Rating	Military	Normal	
Duration	30 Minutes	Continuous	
Maximum Shaft Horsepower	3695	3230	
Torque for Rated Power and Speed	1326 Ft-Lb	1247 Ft-Lb	
Max. Gas Generator Speed-RPM (a)	18230	18010	
Rated Power Turbine Speed-RPM (b)	13600	13600	
Engine Rotor Moments of Inertia			
Power Turbine			0.357 Slug-Ft ²
Gas Generator			0.604 Slug-Ft ²
Engine Static Moments of Inertia (Estimated)			
Ixx			7.75 Slug-Ft ²
Iyy			47.60 Slug-Ft ²
Izz			49.17 Slug-Ft ²
Notes: (a) Maximum allowable transient gas generator overspeed limit is 18500 rpm for 10 seconds.			
(b) Maximum allowable continuous output speed for T64-GE-12/AAFSS engine is 17000 rpm.			
(c) The transient torque surge factor for design of the engine mount is 1.515 as cited in Paragraph 3.13.1 of the T64-GE-12 Engine Model Specification E1102.			

- c. Gyroscopic moments are determined for the maximum pitching and yawing velocities.

Transmissions

The various transmissions, containing the gear drives and distribution systems, are designed to the critical loadings in the shafting complex with consideration given to vibration attenuation and torque surge. The housings are also designed to the inertia loads from critical flight and ground loading conditions and those due to emergency loading. Safety devices are incorporated to preclude the remaining engine and/or main rotor from driving an engine which has failed. The transmission is so designed that the remaining engine can drive the propellers and rotors.

The main rotor transmission shall be designed for a maximum continuous power of 4350 hp.

WING DESIGN CRITERIA

The wing is designed to the requirements of Reference 27 for flight conditions (steady state and maneuvering) and for ground loading conditions (static and dynamic). These various flight and ground loading criteria are discussed under "Flight Conditions" and under "Ground Loading Conditions".

Since the fuel is carried in the wing, those conditions for which the minimum inertial relief results in the highest design loads are treated as minimum fuel conditions (10% fuel).

In the compound mode where the goal is to reach transition speed as quickly as possible, the high-lift (flaps down) configuration is used, the flaps being considered full down from takeoff through transition. For this flight regime, the lift on the wing and the control power of the ailerons increase with q , free-stream dynamic pressure, until, at transition speed, the wing assumes the full lift and roll control of the vehicle. Because of the partial effectiveness of the wing under these conditions, no critical loads will result.

FUSELAGE DESIGN CRITERIA

The fuselage is designed to the critical combination of airloads and inertia on the body together with the corresponding wing, main rotor, and empennage loads. Consideration is given to the cyclic aspects of the loads in accordance with the fatigue and fail-safe requirements.

Fuselage Forebody

The forebody is subjected to inertia loads both in flight at the design load factor of 4.5 and in dynamic landing. Flight airloads are considered in conjunction with the flight inertias. Pressure distribution on the windshields

is obtained as a function of α , β and q . For ground loading conditions, the nose gear load is introduced along with the fuselage inertia.

Fuselage Aftbody

The aftbody is subjected to the same type of air and inertia loadings as the forebody together with compatible loads from the empennage (horizontal and vertical surfaces and the tail rotor).

Fuselage Midbody

The midbody, for all design conditions, is completely balanced so that the local inertia and airloads, when added to the loads from the forebody, aftbody, wing, and main rotor, will result in equilibrium about the vehicle center of gravity.

EMPENNAGE DESIGN CRITERIA

Configuration

The CRA is designed to fly both as a compound helicopter and as a conventional fixed-wing airplane. Because of this dual configuration, the tail surfaces must be of the conventional type to permit control of the vehicle in the airplane mode. The left stabilizer must, in addition, support the antitorque tail rotor together with its drive and control mechanism.

A modified T-tail is used, the horizontal surfaces being attached to the fin at a location approximately 60 inches above the fuselage. The design loads on the left stabilizer and on the fin must, for this configuration, include not only their own individual loadings but also the loads imposed by the tail rotor and the horizontal tail respectively.

Tail Rotor

The design criteria for the tail rotor are specified in "Tail Rotor Structural Requirements". For purposes of empennage design, the critical loading conditions for the vertical and horizontal tail surfaces require consistent loads on all components affecting the design. Thus, complete sets of loads for all possible critical conditions are obtained. Tail rotor loads are therefore obtained not only for the maximum design values but for other conditions compatible with the design of the vertical and horizontal surfaces.

Horizontal Tail

Compound Mode

The total horizontal tail surface loads in the compound mode will not result in critical loading conditions because (1) the unbalanced pitching moments about the c.g. are partly carried by the rotor and (2) the maximum positive and negative maneuver load factors are less than in the fixed-wing mode.

However, loading in the compound mode must be examined to the extent that the input from the antitorque rotor affects the fixed surfaces. Rotor thrust, in-plane forces, gearbox torques, etc., consistent with a given flight condition shall be included in determining the net loading on the left stabilizer and on the fin.

Fixed-Wing Mode

In the fixed-wing mode, the stabilizer and elevator are designed to the requirements of the MIL-A-8860 series specifications. The effects of tail rotor inertia and blade airloads in the stopped and feathered position are considered in establishing the loading on the left stabilizer.

To account for aerodynamic stall or buffet, the horizontal tail load is distributed by multiplying the airloads on one side of the plane of symmetry by 1.5 and those on the other side by 0.5. This distribution is applicable for all flight conditions at or near the vehicle attitude for maximum lift coefficient. For all other flight conditions, these multiplying factors are 1.15 and 0.85.

The elevators are aerodynamically balanced. In accordance with paragraph 3.1.11 of Reference 27, the maximum torque on the surface is that resulting from neglecting the torque due to airloads forward of the hinge with the stipulation that this torque need not exceed that which can be supplied by the control system. It is assumed, therefore, that the available control system torque governs. The airloads on the surface are distributed to give the critical torque on the structure of the elevator consistent with the above.

Vertical Tail

Compound Mode

In the compound mode, the essential loads on the vertical tail are those due to the horizontal tail and tail rotor. The vertical tail surfaces are thus designed to the requirements of flight in the fixed-wing mode.

Fixed-Wing Mode

The requirements of MIL-A-8860 series specifications are applicable to the vertical tail surfaces when flying in the fixed-wing mode. For the design conditions, compatible loads from the horizontal tail surfaces, including loads on the stopped tail rotor, are applied at the stabilizer-fin junction.

The maximum torque on the rudder is that obtained from the control system. This is similar to the requirements for torque on the elevator as discussed above.

The spanwise airload distribution on the vertical tail surfaces reflects the end plating effect of the fuselage and the horizontal tail. Essentially, the distribution is two-dimensional between these surfaces.

CONTROL SYSTEM

The same primary control system in the pilot's compartment activates the conventional control surfaces for each mode of flight. A linkage is provided whereby the cockpit controls which operate the cyclic and collective pitch on the main rotor and the collective pitch of the tail rotor during compound flight are used to operate the fixed-wing movable control surfaces. This is accomplished at transition by moving the linkage in such a manner as to deactivate the helicopter controls and provide continuity of the pilot control motions to the fixed-wing movable surfaces: ailerons, elevator, and rudder.

The control system is designed to meet the requirements of Paragraph 3.5 of Reference 26 and Paragraph 3.7 of Reference 31 for the compound and the fixed-wing mode, respectively.

Compound Mode

Main Rotor Controls

Cyclic

Forward or aft 200 lb

Lateral 100 lb

Collective 150 lb

Tail Rotor Controls 300 lb

Fixed-Wing Mode

Longitudinal 200 lb

Lateral 100 lb

Directional (Pedal) 300 lb

Common Controls

Brake 300 lb

Crank, Wheel, Lever $\frac{(1 + R)}{3}$ 50 (Range: 50 - 150)

Twist Control 133 in.-lb

Dual Control Requirements

Seventy-five percent of the above loads shall be applied at each of the control stations simultaneously.

EMERGENCY LANDING REQUIREMENTS

Item: Hazardous to Personnel

Items in this category are those mass items which would be apt to injure personnel if they became loose in the event of a minor crash landing. These include such items as cockpit equipment, transmission housing, etc. The load factors are ULTIMATE and act in the combinations shown in Table XXV.

Seat Installations

In lieu of an applicable seat specification, the following ULTIMATE load factors shall apply. The specified load factors shall act separately.

Longitudinal load factor = 20g acting forward of all azimuths within 20 degrees of the longitudinal axis

Vertical load factor = 10g directed downward normal to the longitudinal axis.

FATIGUE LOADING CRITERIA

Intended Use of Vehicle

The approach to the subject of fatigue analysis of a new vehicle starts with careful consideration of the intended use of the vehicle. Since the CRA is basically a research vehicle, the flight and ground test program plans will outline the intended vehicle use. The Lockheed flight test program covers 50 hours of flying for each of two aircraft. A careful distribution of selected flight test missions over the remainder of the 200 hours, based on experience with previous development programs, completes the mission analysis.

TABLE XXV. EMERGENCY LANDING LOAD FACTORS		
n_x	n_y	n_z
-8.0	0	-1.5
+1.5	0	-1.5
0	± 1.5	-1.5
0	0	-4.5
0	0	+2.0

Examples of preflight missions are:

- Whirl tower test
- Tie-down test
- Preflight check
- Taxi in rotorcraft configuration
- Taxi in fixed-wing configuration

Examples of flight missions are:

- Preliminary rotorcraft test
- Preliminary fixed-wing test
- Transition rotorcraft/fixed-wing test
- Structural load measuring flight test
- Complete mission flight test program
- Ferry mission

An account of the number of events where ground-air-ground cycles occur is added for each mission.

Each mission is subsequently divided into specific loading conditions according to the time spent in these conditions and the number of occurrences. Finally, a condition list is compiled, listing the time and occurrences of each loading condition contained in all the missions.

Loading Conditions

Most of the loading conditions can generally be presented as static loading conditions, from which the structural loads and stresses in the components can be derived by conventional methods. Many loading events, however, can be analyzed only dynamically; for instance, landing conditions, pull-up maneuvers, and generally all transient maneuvers. For those loading conditions, it is necessary to consider the load distribution within the time span of the event. For some loading conditions, the flight test results show a relationship of loading with one of the flight parameters. For example, flapwise bending of the rotor blade increases with pitching acceleration. The available control power is directly related to the maximum pitching acceleration obtainable, and the pitching acceleration actually experienced is thus dependent on the control input of any of the pitching conditions. A probability distribution of pitching acceleration derived from publications on various aircraft maneuvers, shown in Figure 147, is used to evaluate the loads content of these conditions in the total flight time.

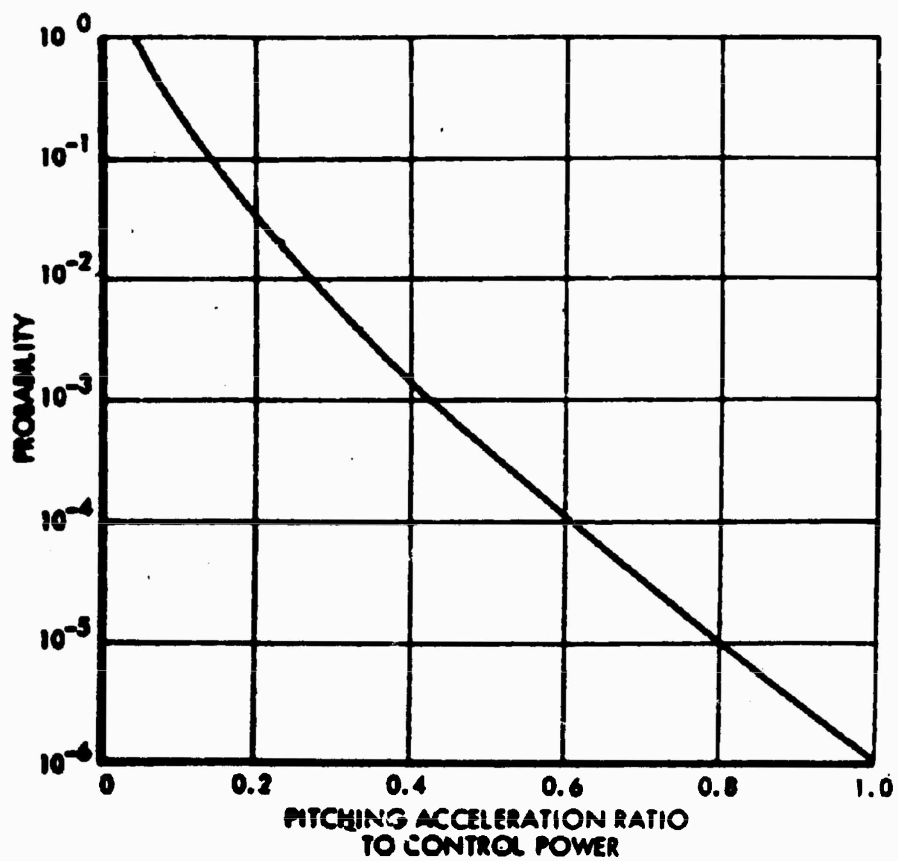


Figure 147. Probability Distribution of Events by Pitching Acceleration.

Consideration of the variations involved in defining the loading conditions according to the speed ranges, ranges in center of gravity, gross weight, rotor rpm, and so on, show a rapid expansion of the total number of loading conditions to be processed for the fatigue analysis.

The transition from rotorcraft to fixed-wing aircraft can be described by a number of individual loading conditions, which are expanded for such variables as the rotor rpm range from normal to stop and back to normal, the azimuth folding angle range, and the c.g. shift during folding and stowing.

A few more conditions are listed without their expansion in order to cover the scope of the subject more broadly. These are:

Ground Conditions

- Rotor on-off, on-idle-on
- Ground-air-ground cycles
- Maintenance runs
- Preflight check runs
- Taxi runs (including fixed-wing configuration)
- Takeoff and landing on a slope

Flight Conditions

- Autorotation, including maneuvers and landing
- Flare
- Left and right turns
- One-engine performance tests
- Flap extension and retraction tests
- Control reversals
- Sideward and rearward flight
- Acceleration tests throughout the speed range
- Descent with varied power setting

Many of the maneuvers in the rotorcraft configuration are accomplished with a combination of collective and cyclic control inputs. Hence, some distribution of time between these inputs must be established. This distribution

will probably be dependent on forward velocity. The same consideration applies to the lift distribution between rotor and wing.

The complete condition list will contain all loading conditions required to demonstrate the requirements of the design V-n diagram. The corresponding distribution of time and events will result from careful consideration of the flight test program.

Design Loading Spectra

The loading conditions discussed under "Loading Conditions" are used for structural load calculations for the various vehicle components. Considering the time spent at each event, the loads pertinent to each part are combined in a fatigue loading spectrum, which forms the basis for subsequent cumulative damage calculation of the component. Each part must be surveyed by analysis or visual inspection to determine those locations most susceptible to fatigue damage. Dependent on the specific structural function of the part, or the particular location of interest on the part, either a single load or stress or a combination of loads or stresses must be considered. A separation of mean and varying loads is always made. Consideration is also given to angular and phase relationship.

After some initial grouping, a pattern of better defined loading groups will emerge. A first grouping by load similarity may, for instance, combine most of the level flight conditions, including some of the less severe maneuvers (see Figure 148a). The second grouping may contain most of the more severe maneuvers (see Figure 148b). The maneuvers of extreme severity could be contained in a third grouping, as shown in Figure 148c.

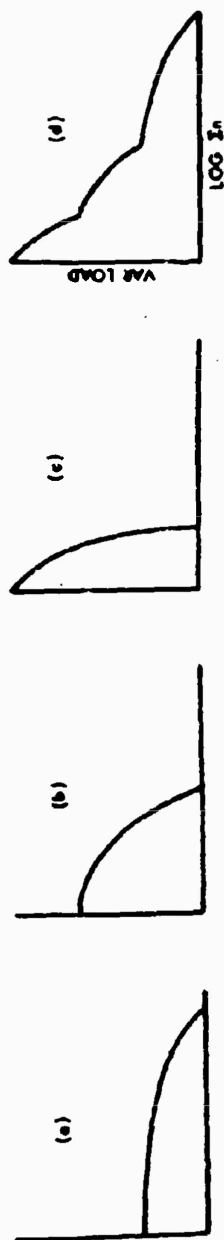
Figure 148d shows the combination into one spectrum for groups one, two, and three discussed above.

A mean load level may be entered for each of those spectra.

The previous discussion of simple spectra applies generally to those of more complex nature, where a multiple of loads and moments, and position of the part with respect to those loads, must be considered simultaneously. In such case, the spectrum is most conveniently presented in tabular form, as illustrated in Figure 148e, accompanied by a schematic presentation of mean and varying loads, shown in Figure 148f.

Structural Component Fatigue Analysis

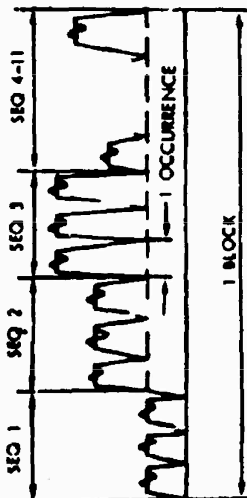
For the majority of the structural components, a formal fatigue analysis will be made, based on established S-N curves, and aided by experience gained from previously developed rotorcraft vehicles. The predicted life is based on Miner's Cumulative Damage Theory.



(a) EXAMPLE BLOCK SPECTRUM

SEQ	NO. OF OCCUR. PER BLOCK	NO. OF RPM PER OCCUR.	NO. OF RPM PER BLOCK	THRUST KIP	TORQUE IN-KIP	HUB MOMENT IN-KIP
1	200	1350	250,000	12.5	148	47
2	50	70	9,300	42	814	110
3	4	30	170	31	640	295
	100	23	2,500			186
	1000	60	60,000			110
4	90	8	770	25	376	200
	475	65	30,875			110
	335	60	26,800			58
5	560	15	47,500	16	194	110
	420	150	63,000			58
	1160	70	81,200			47
6	4	5250	21,000	12.5	148	186
	375	190	109,250			86
	110	2750	247,500			58
7	5	10	60	23	0	800
	26	30	600			110
	15	180	6,300			86
	20	40	2,800			47
8	1400	15	49,000	16	-150	295
	290	60	22,400			186
9	140	30	4,200	33	-341	295
	120	35	4,550			186
10	20	25	500	-9	276	55
11	140	9	900	-9	-341	47

(f) SCHEMATIC



PREDICTED LIFE: 60 BLOCKS
 - SUPPLEMENTED HUB MOMENT
 ONE OCCURRENCE IS DEFINED AS AN
 EXCURSION FROM:
 SEQ 1: THRUST - 0, TORQUE 0
 SEQ 2-11: THRUST 12.5 KIP, TORQUE - 148 IN-KIP
 TO THE VALUES LISTED IN TABLE (a).
 THESE VALUES ARE MAINTAINED FOR THE
 INDICATED NUMBER OF REVOLUTIONS.

Figure 148. Typical Fatigue Loading Spectrum Presentations.

SECTION 14
STRUCTURAL DESIGN LOADS

ROTOR DYNAMIC LOADS DETERMINATION

Forward Flight

Rotor loads in forward flight are computed using two digital computer programs. One of these programs is an airloads program used to obtain the distribution of airloads on the blade and to obtain trimmed conditions for the vehicle when required. The other program is used to find the dynamic response of the rotor system to these airloads. These programs can be used either separately or combined.

Airloads Program

Aerodynamic expressions for rotor thrust, torque, pitching and rolling moment, and forward and side force are developed, assuming that the blades are infinitely stiff. The program permits a choice of up to four of these resultant loads to be trimmed. In trimmed forward flight with power on, these will be forward force, vertical thrust, and pitching and rolling moments. An iteration procedure is used to find the control angles and attitude of the vehicle in the trimmed position.

The aerodynamic input determines the radial distribution of aerodynamic loads at the selected azimuth station and the azimuthal distribution, in harmonic form, at the selected radial stations. The blade loading at any radial station and azimuth position is obtained using the actual C_L and C_D data versus angle of attack and Mach number.

The output of this program consists of a harmonic analysis of airload distributions in the trimmed or given condition and a harmonic analysis of airloads due to blade flapwise, inplane, and torsional response.

Dynamic Response Program

The equilibrium position of the blade in the centrifugal force field under the steady-state part of the airloads is computed by an iteration procedure in which the nonlinear effects are included. The coupled response of the blade to the oscillatory part of the airloads is computed for each harmonic separately, using linearized equations based on the equilibrium position under steady load.

The oscillatory response of the blade is used to obtain the harmonic inertia forces (normal and parallel to the chord plane and moment in the plane of the blade elements). The inertia forces are added to the airloads, and the net flapwise and inplane bending moments and the net torsion due to the combined airloads and inertia loads are computed.

Correlation With Flight Test Data

Correlation with flight test data has indicated that loads can be obtained with sufficient accuracy using a linearized dynamic loads program. Iteration by means of feedback of the blade response into the airloads results in further refinement of the analysis.

These programs will be used to determine rotor loads in trimmed flight and during steady maneuvers. A modification of these programs will be used to determine the gust response.

Application of Programs to the CRA

For the 1.0 g conditions, the control inputs are derived from trimmed conditions for the vehicle. The distribution of lift between wing and rotor is shown in Figure 140.

The airloads on the blade account for a variation in inflow distribution related to lift distribution as well as for lift loss and for reverse flow effects in forward flight.

Conditions with maximum load factor on the rotor are obtained as follows:

In vertical flight, starting with 1.0 g trimmed condition (hover), the collective control angle is changed to its maximum value of 15 degrees.

In forward flight, starting with 1.0 g trimmed conditions, the angle of attack is increased to a point where both rotor and wing are stalled. The angle of attack of the rotor is taken at +15 degrees, and the resulting load distribution is computed.

The changes in collective angle or rotor angle of attack result in unbalanced roll and pitch moments. In the present preliminary analysis, these moments are dealt with using the following simplifying assumptions:

- a. The pitching moment of inertia of the rotor is negligible compared with the pitching moment of inertia of the vehicle minus rotor. As a result of this assumption, the unbalanced pitching moment acts on the vehicle minus rotor only, and no additional inertia forces on the rotor occur due to vehicle pitching acceleration.
- b. The rolling moment of inertia of the vehicle is negligible compared to the gyroscopic inertia of the rotor. As a result of this assumption, the unbalanced roll moment is reacted by gyroscopic forces on the rotor blades. These gyroscopic forces are due to angular velocity of the axis of rotation and are added to the airloads on the blade.

In the accelerated vertical flight conditions, the maximum rotor thrust is obtained using maximum collective angle of attack. This results in a condition in which the rotor rpm cannot be maintained with the available horsepower. Conservatively, it was assumed that 4,000 hp is available to drive the main rotor. This determines the torque applied to the rotor and the rate of deceleration of the rotor, $d\Omega/dt$. This deceleration results in inertia forces on the blade elements which are added to the airloads.

Stopped Rotor Loads

As the rotational speed of the main rotor approaches zero at the transition speed of the vehicle, the technique of analytically determining the forces acting on the blades differs from that used in the helicopter mode. The determination of stopped rotor blade loads for various azimuth positions at the transition speed requires the use of a digital computer program utilizing an iterative procedure to obtain the equilibrium position of the blades consistent with the blade aeroelastic characteristics.

The blade element loading is assumed to be comprised of two distinct types of aerodynamic loads resulting from the components of forward speed resolved normal and parallel to the blade span.

The local spanwise blade element angle of attack acted on by the velocity component parallel to the blade is assumed to be composed of the spanwise flexure slope, the resolution of the rotor angle of attack as a function of the blade azimuth position, the upflow angle due to the interference of the body on the free-stream velocity, and the upwash/downwash gradient due to wing lift. The aerodynamic load due to the component of velocity parallel to the blade span is obtained by considering the blade to be a low-aspect-ratio flat plate at the angle of attack as determined above.

The load is assumed to act at the 50-percent chord position, thus producing a nose-down feathering moment when the blade is located at azimuth positions between 90 degrees and 270 degrees.

The local blade element angle of attack acted on by the velocity component normal to the blade consists of the collective and cyclic pitch, the resolution component of the rotor angle of attack, the upflow angle due to body interference, the upwash/downwash gradient due to wing lift, and the torsional elastic effect. This loading is assumed to act at the 25-percent blade chord for the blade locations between rotor azimuth 0 degrees and 180 degrees and at 75-percent blade chord for rotor azimuth positions between 180 degrees and 360 degrees.

The aeroelastic equilibrium of the blade is established by an iterative process in which the local change in blade slope between two successive evaluations is compared. Equilibrium is assumed to exist when the change in slope is less than 0.0001 radian between successive evaluations.

This method for determining the loads in the blades when the rotor is brought to rest has been compared to test results obtained in the wind tunnel on an 8.24-foot-diameter model of a two-bladed rigid rotor (Reference 33) and on a 33.0-foot-diameter full-scale model of a three-bladed rigid rotor. The correlation with wind tunnel test data indicates that stopped rotor blade loads can be obtained with a good degree of consistency.

COMPONENT LOADS

The design loads on the following components are presented:

- Main Rotor
- Tail Rotor
- Wing
- Fuselage
- Empennage
- Nacelle
- Landing Gear
- Transmission
- Rotor Stowage Doors

These loads, except for the landing gear reserve energy drop conditions, are LIMIT and are representative of the critical design loading conditions.

Main Rotor Loads

Three sets of main rotor loads are presented. The first set constitutes the net loading on the blades resulting from flight in the helicopter/compound mode with the rotor turning at rates within its prescribed limits. The second group of loads comprises those occurring at transition with the rotor brought to rest (including very low speeds at which the centrifugal forces are negligible). The third gives the hub moment and blade loads associated with takeoff from a 15-degree slope.

Helicopter/Compound Mode

The blade mass and stiffness distribution used in the calculation of the blade response to the various loading conditions is given in Figure 149.

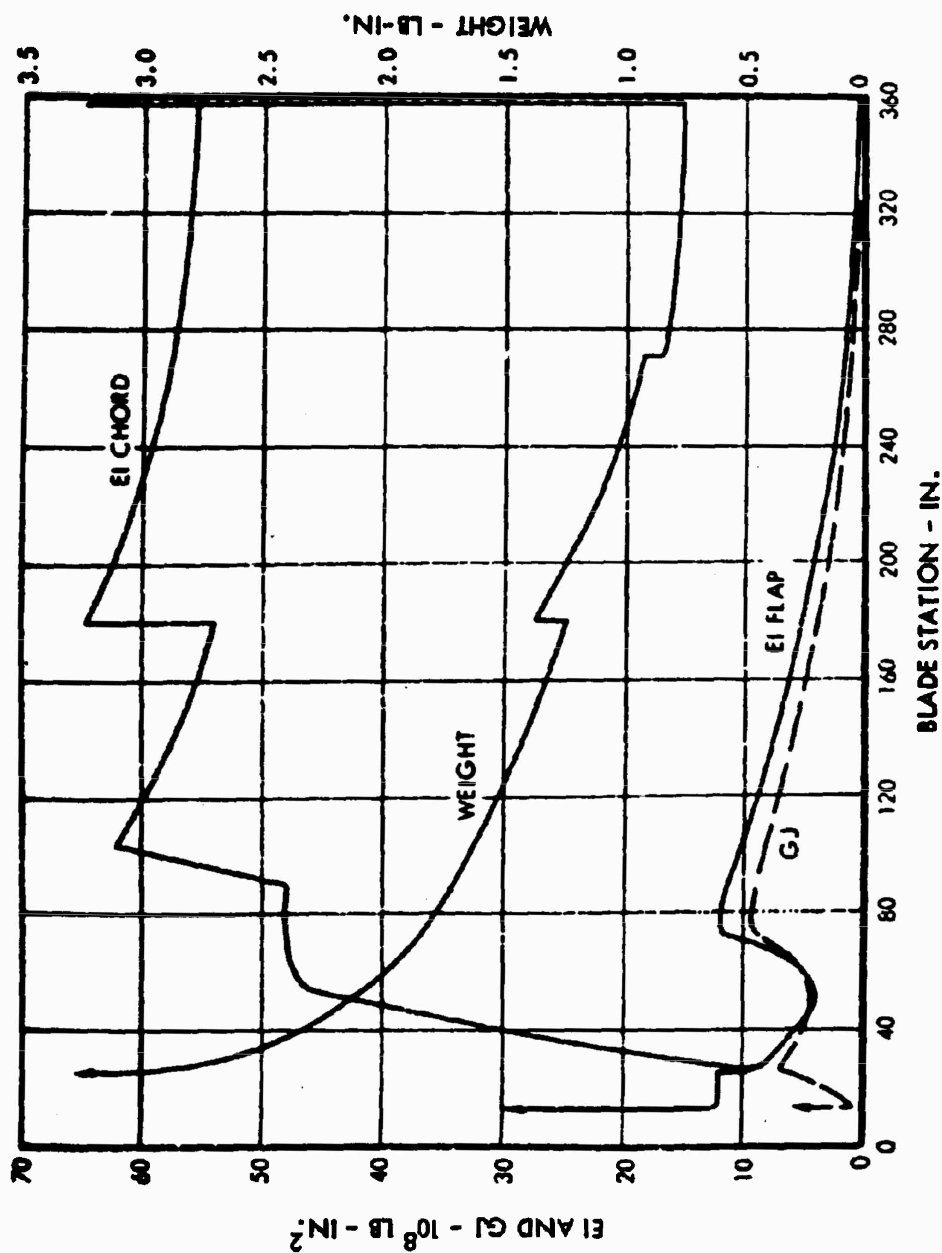


Figure 149. Main Rotor Mass and Stiffness Distribution.

The response of the blade to various harmonic inputs as shown in Figure 150 indicates that within the rpm range of interest, resonance will not occur. Centrifugal force versus blade station is given in Figure 151.

Figures 152 and 153 show typical flapwise and in-plane moments and torsion variation with blade azimuth position. Although these are shown for hover and 100 KEAS, they are similar for other conditions.

The following sets of curves (Figures 154 through 161) present steady values, maxima and minima of flapping and in-plane bending moments, and torsion for the design conditions at various load factors: 227 rpm, 239 rpm, and 265 rpm; 7.0-inch center-of-gravity offset; and the basic design weight of 24,500 pounds.

Stopped Rotor Loads

Flapwise and in-plane bending moments and torque (feathering moments) are presented for two transition speeds used for structural design (140 and 160 KEAS). These curves (Figure 162 through 167) are in parametric form to permit determination of the loads for a range of angles of attack and collective pitch. For transition, the value of collective pitch is zero and the corresponding angle of attack is approximately 2.5 degrees. However, to allow the pilot a reasonable tolerance in control system actuation and to evaluate the effect of gust on the blades (considered as incremental angles of attack), the collective pitch range is taken as 0 degrees to 4 degrees and the angle-of-attack range is taken as from 0 degrees to 10 degrees. By interpolative procedures, loads for any combination of these two angles may be obtained. The loads are determined at Blade Station 21.6.

Slope Terrain Takeoff

The rotor hub moments developed in takeoff from a 15-degree slope are obtained from the following expression, which accounts for rotor thrust, landing gear characteristics, and center of gravity offset:

$$R_H = L_H + M_H$$

$$R_H = \frac{12}{\left[1 + \frac{T}{K_\theta} (h + h_r)\right]} \left[h W \sin (\theta_s + \theta) \right. \\ \left. + \left(\frac{\ell_G}{2} + n \right) W \cos (\theta_s + \theta) - \frac{\ell_G}{2} T \right] + W \ell$$

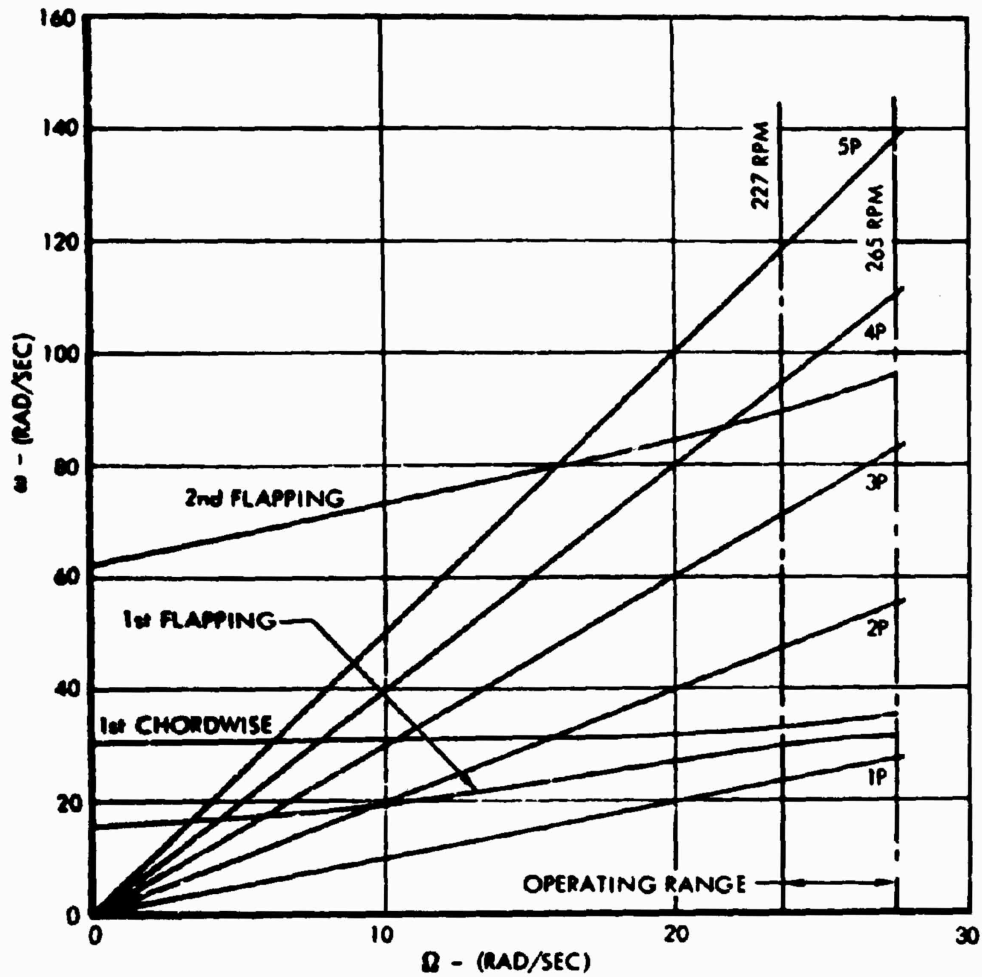


Figure 150. Main Rotor Coupled Blade Frequencies - $\theta = 0.15$ RAD.

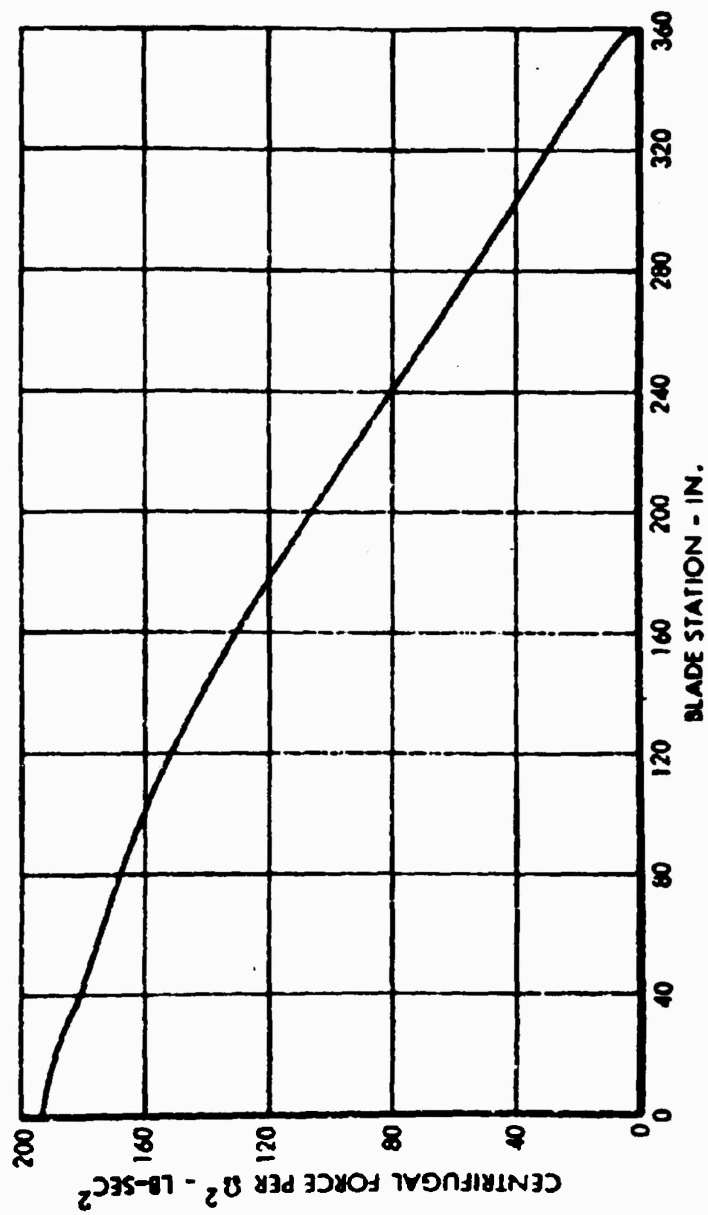


Figure 151. Main Rotor Centrifugal Force Per Ω^2 .

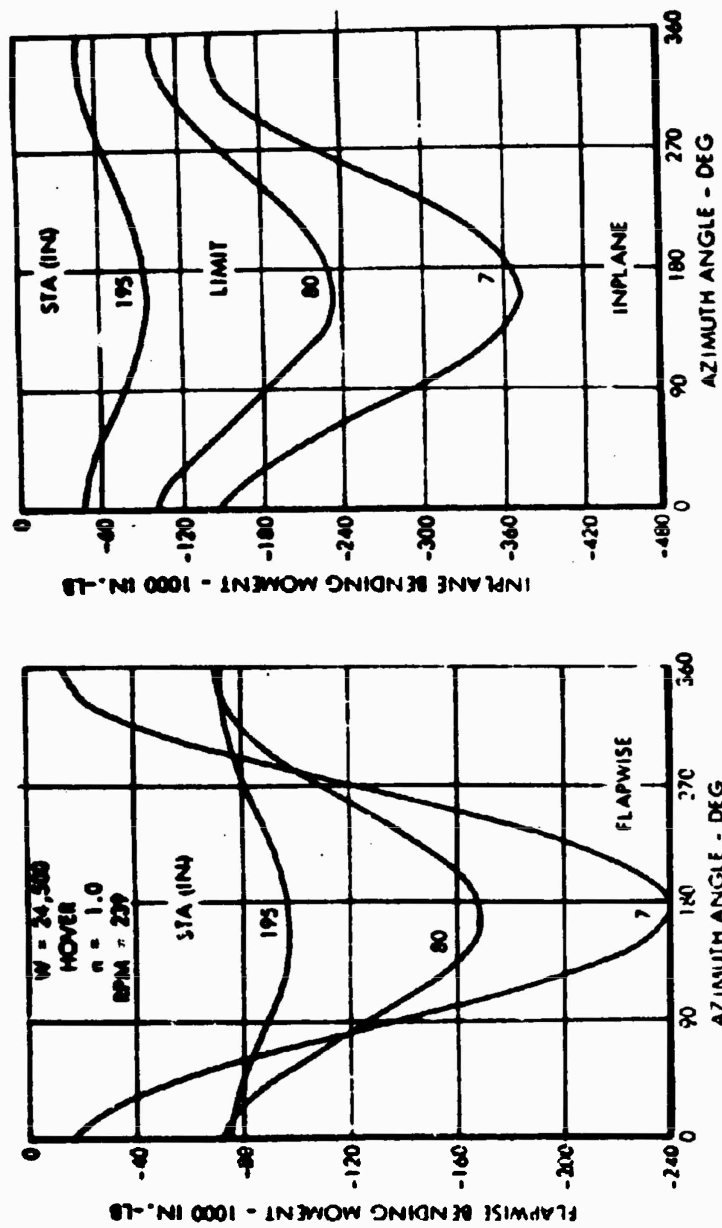


Figure 152. Main Rotor Bending Moments Vs. Azimuth Angle - Hover.

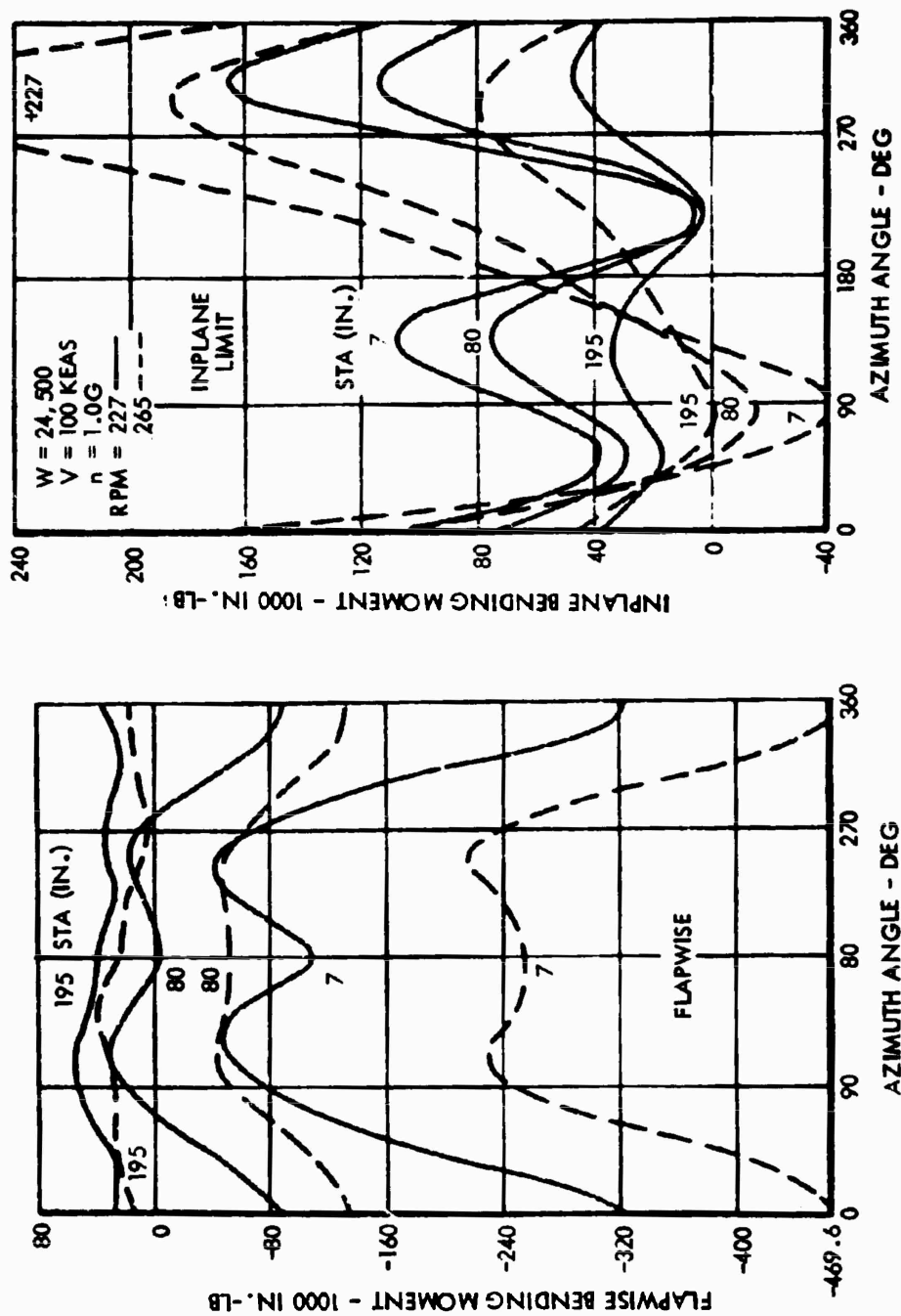


Figure 153. Main Rotor Bending Moments Vs. Azimuth Angle - V = 100 KEAS.

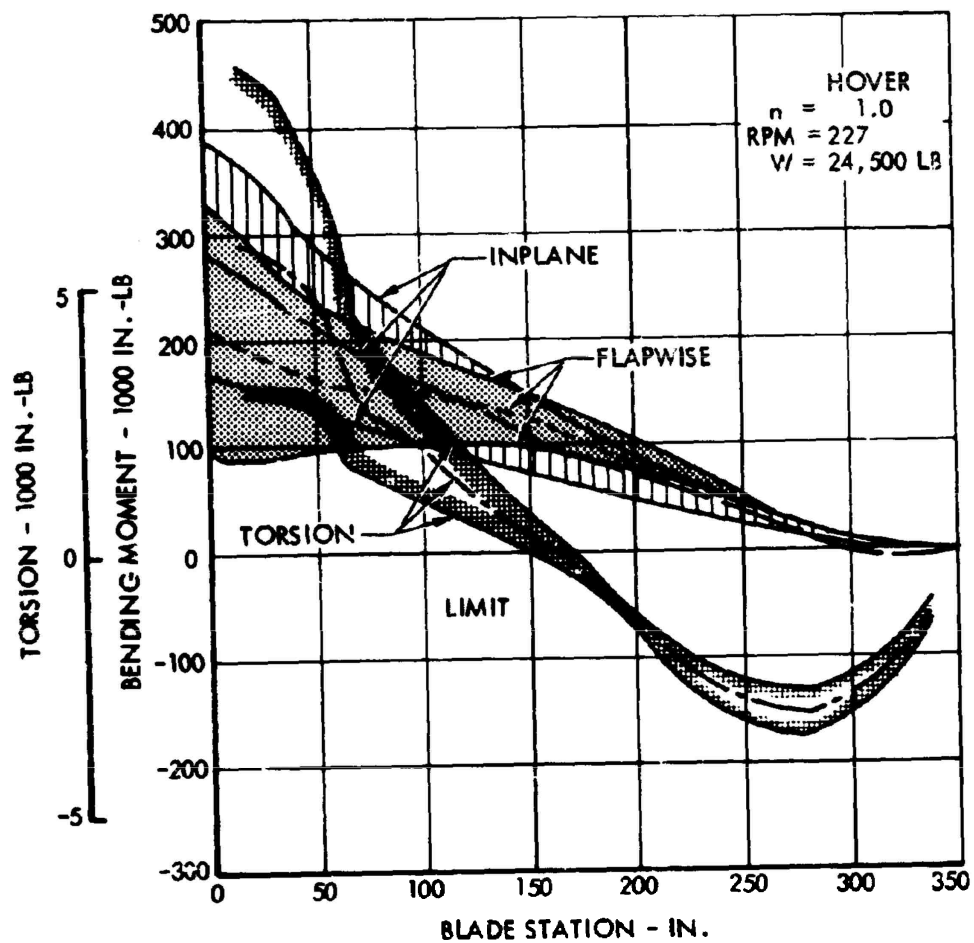


Figure 154. Main Rotor Bending Moments and Torsion -
 1.0 g, Hover, 227 RPM.

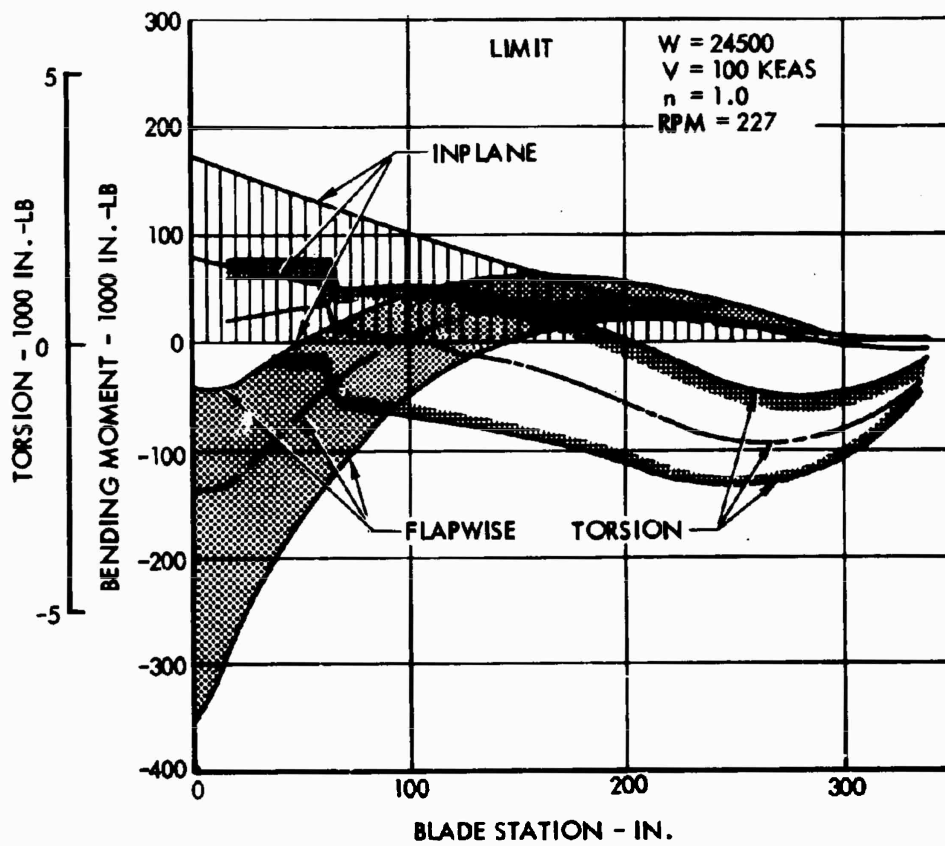


Figure 155. Main Rotor Bending Moments and Torsion - 1.0 g, V = 100 KEAS, 227 RPM.

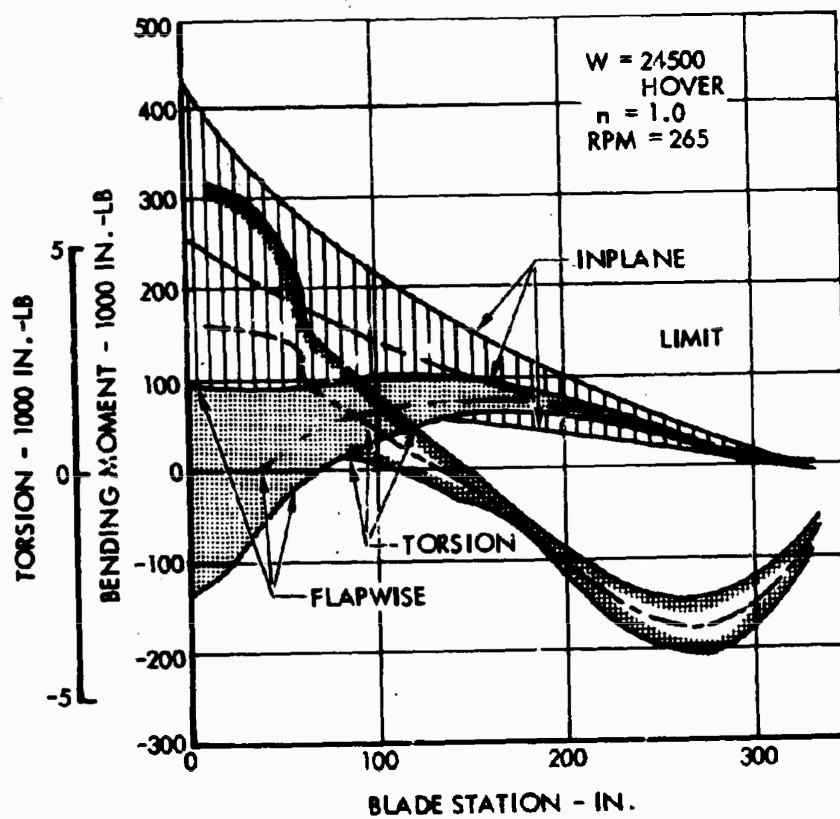


Figure 156. Main Rotor Bending Moments and Torsion - 1.0 g, Hover, 265 RPM.

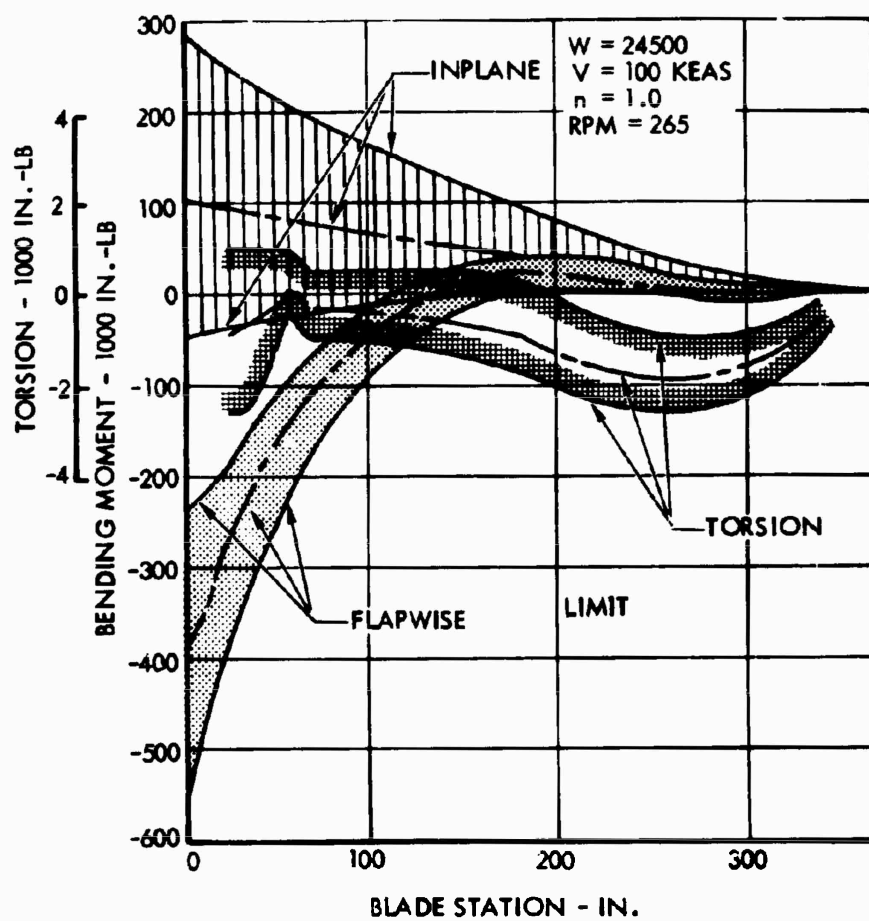


Figure 157. Main Rotor Bending Moments and Torsion - 1.0 g, V = 100 KEAS, 265 RPM.

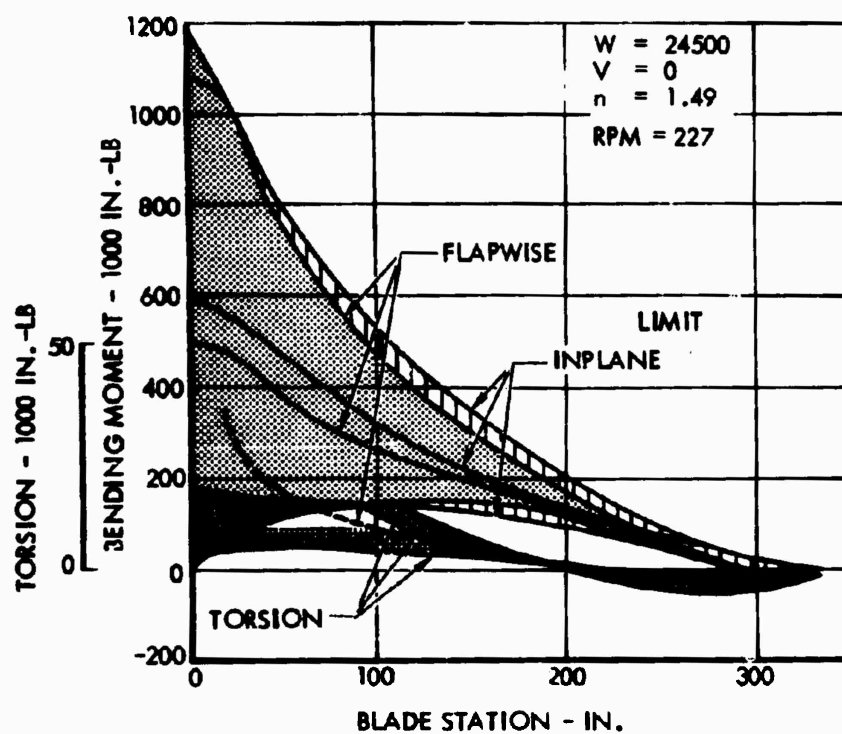


Figure 158. Main Rotor Bending Moments and Torsion - 1.49 g, Hover, 227 RPM.

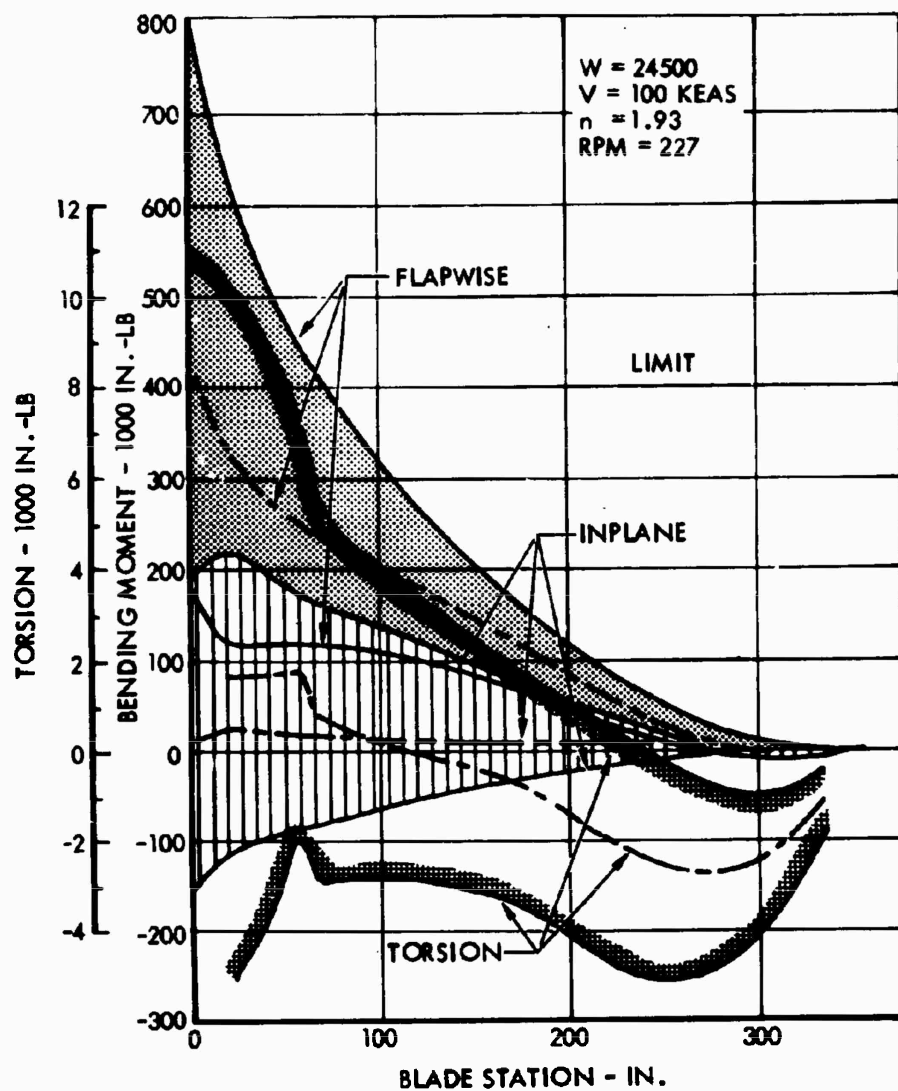


Figure 159. Main Rotor Bending Moments and Torsion - 1.93 g, V = 100 KEAS, 227 RPM.

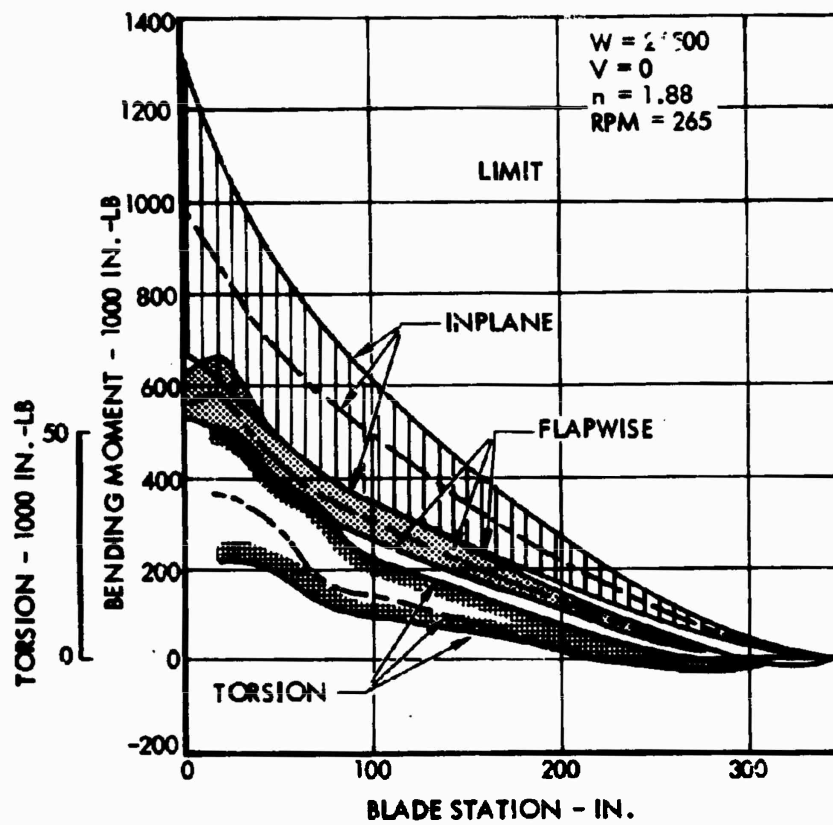


Figure 160. Main Rotor Bending Moments and Torsion - 1.88 g, Hover, 265 RPM.

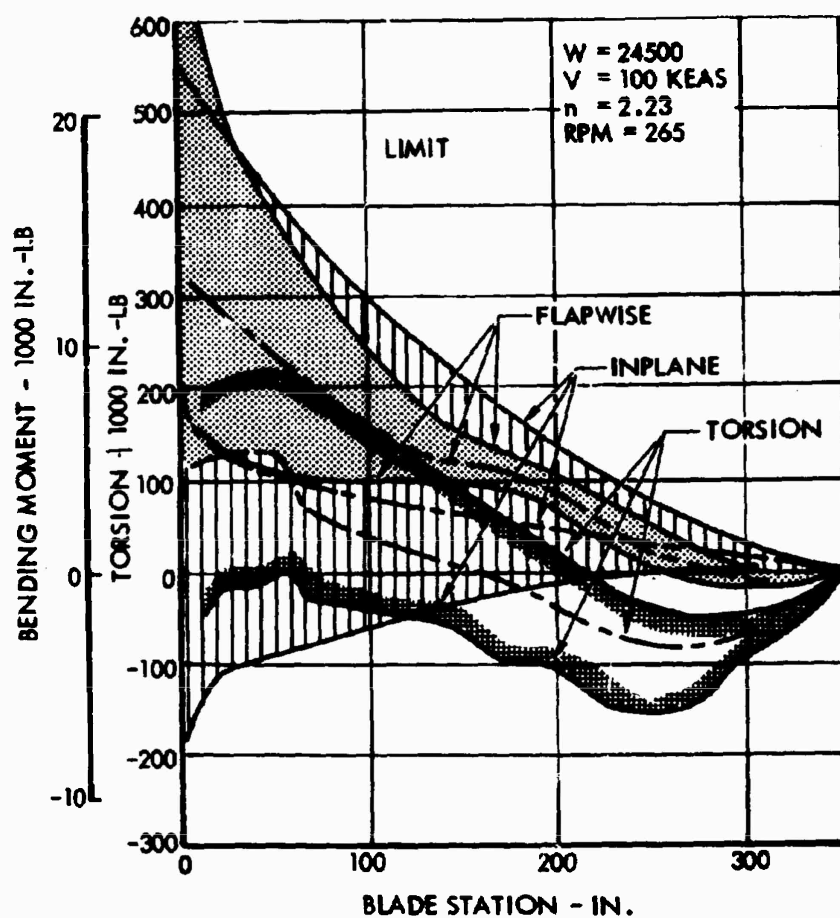


Figure 161. Main Rotor Bending Moments and Torsion - 2.23 g, V = 100 KEAS, 265 RPM.

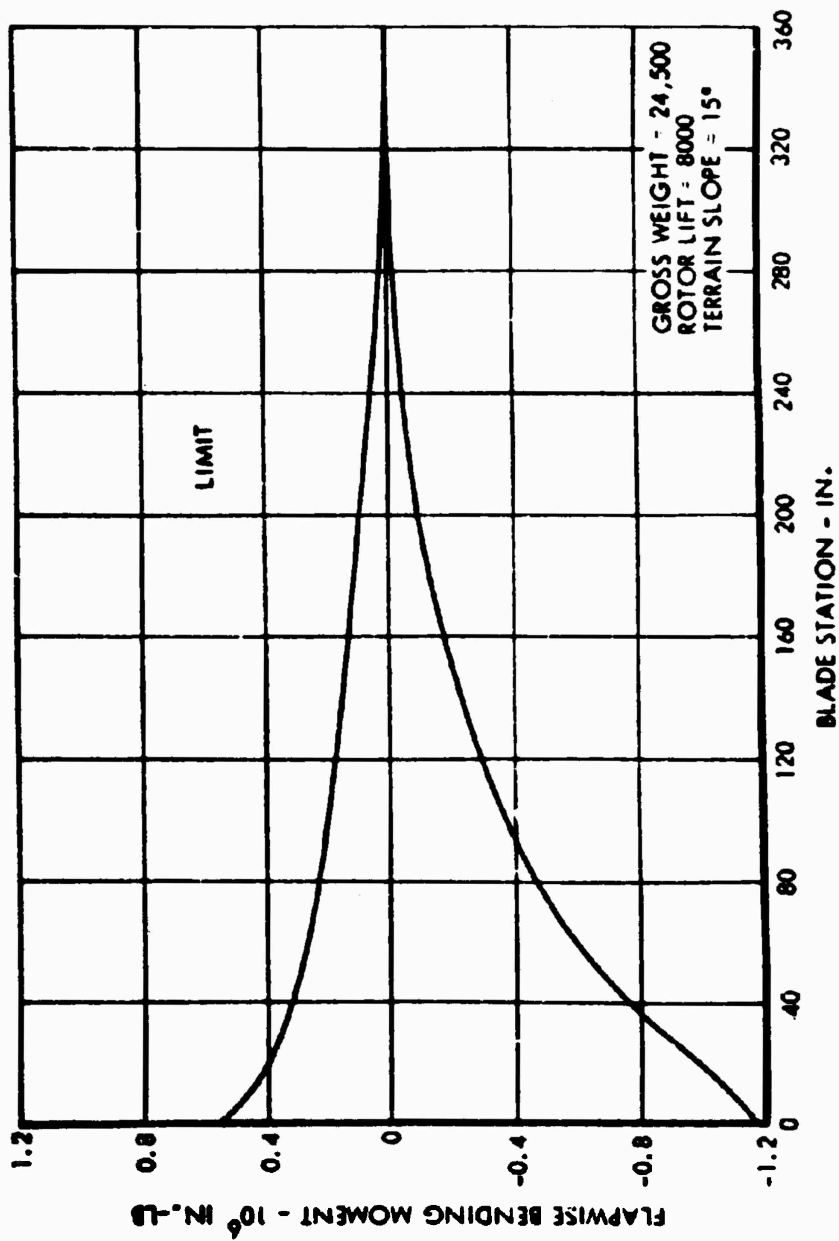


Figure 162. Main Rotor Flapwise Bending Moments - Slope Terrain Takeoff.

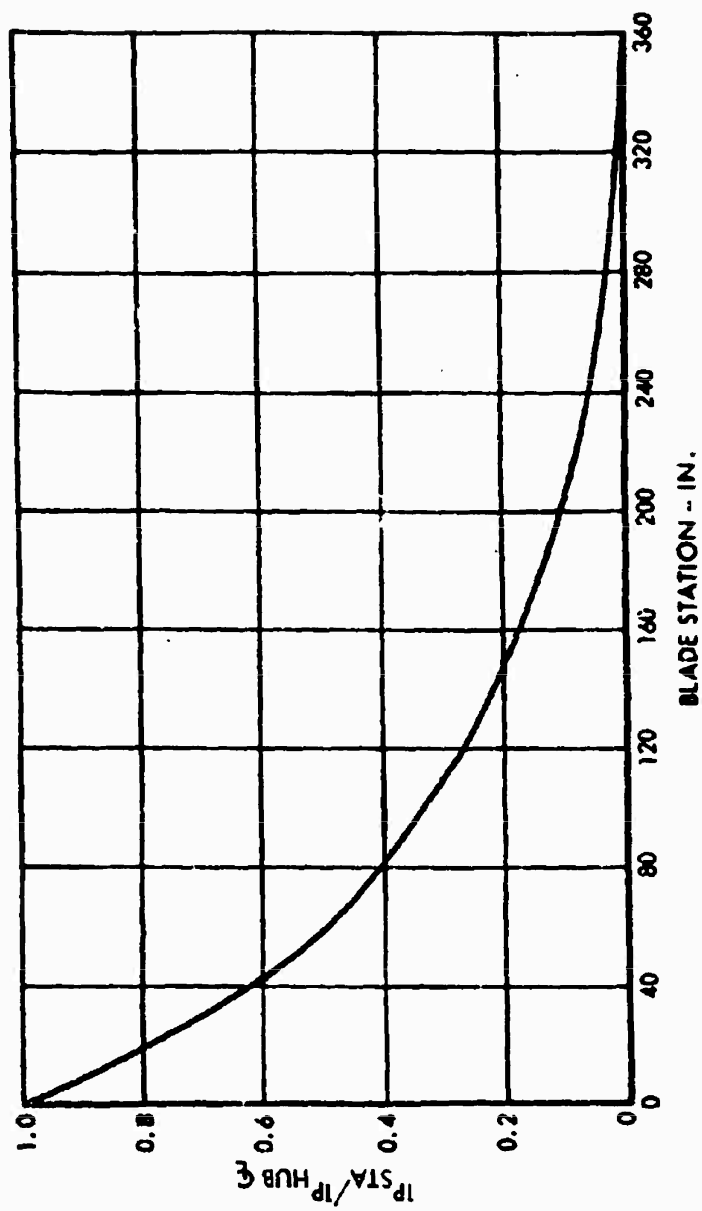


Figure 163. Main Rotor - 1st Mode Flapping Distribution Curve.

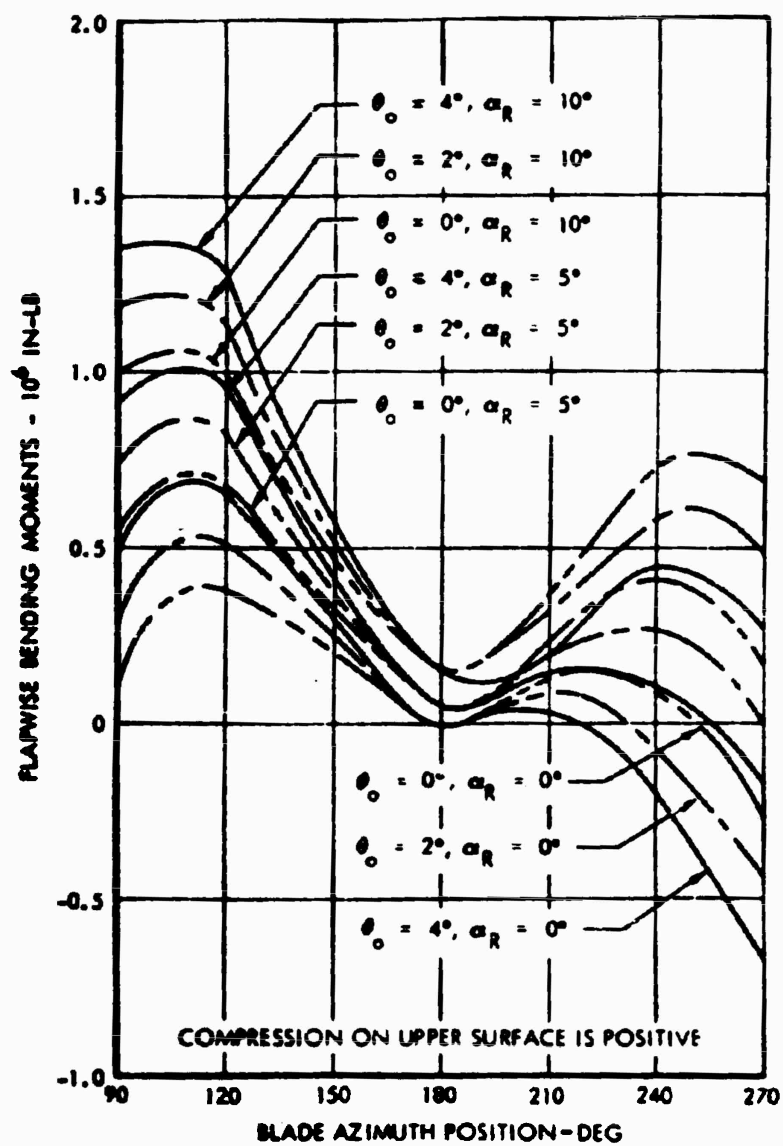


Figure 164. Main Rotor Flapwise Bending Moments - Rotor Stopped at $V = 140$ KEAS.

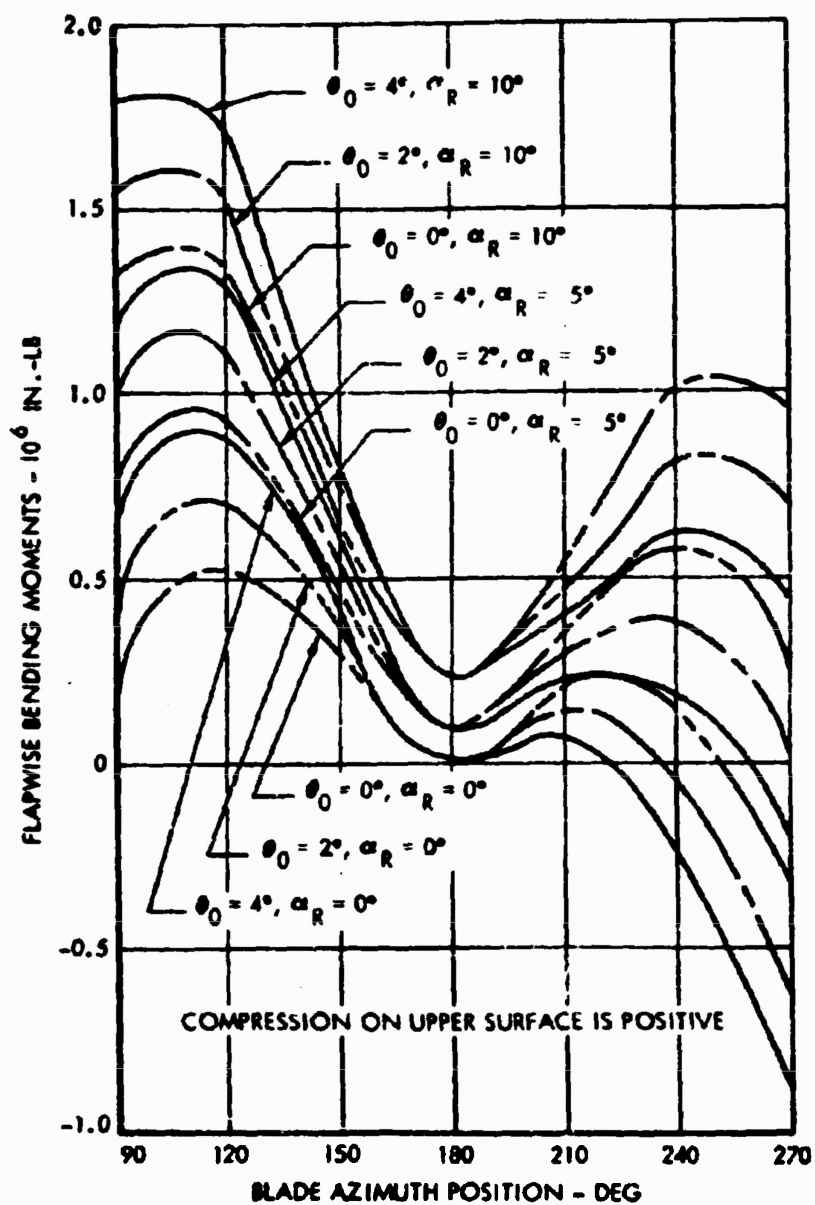


Figure 165. Main Rotor Flapwise Bending Moments - Rotor Stopped at $V = 160$ KEAS.

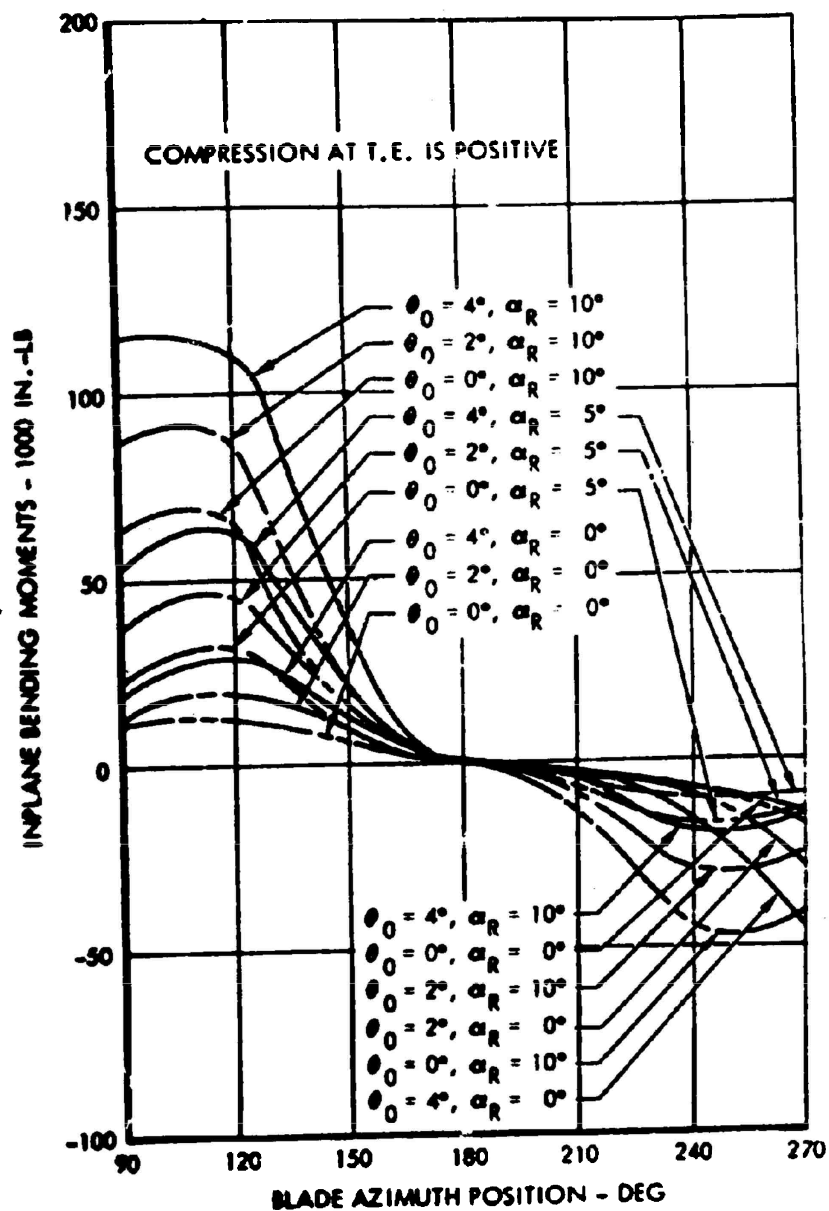


Figure 166. Main Rotor Inplane Bending Moments - Rotor Stopped at $V = 140$ KEAS.

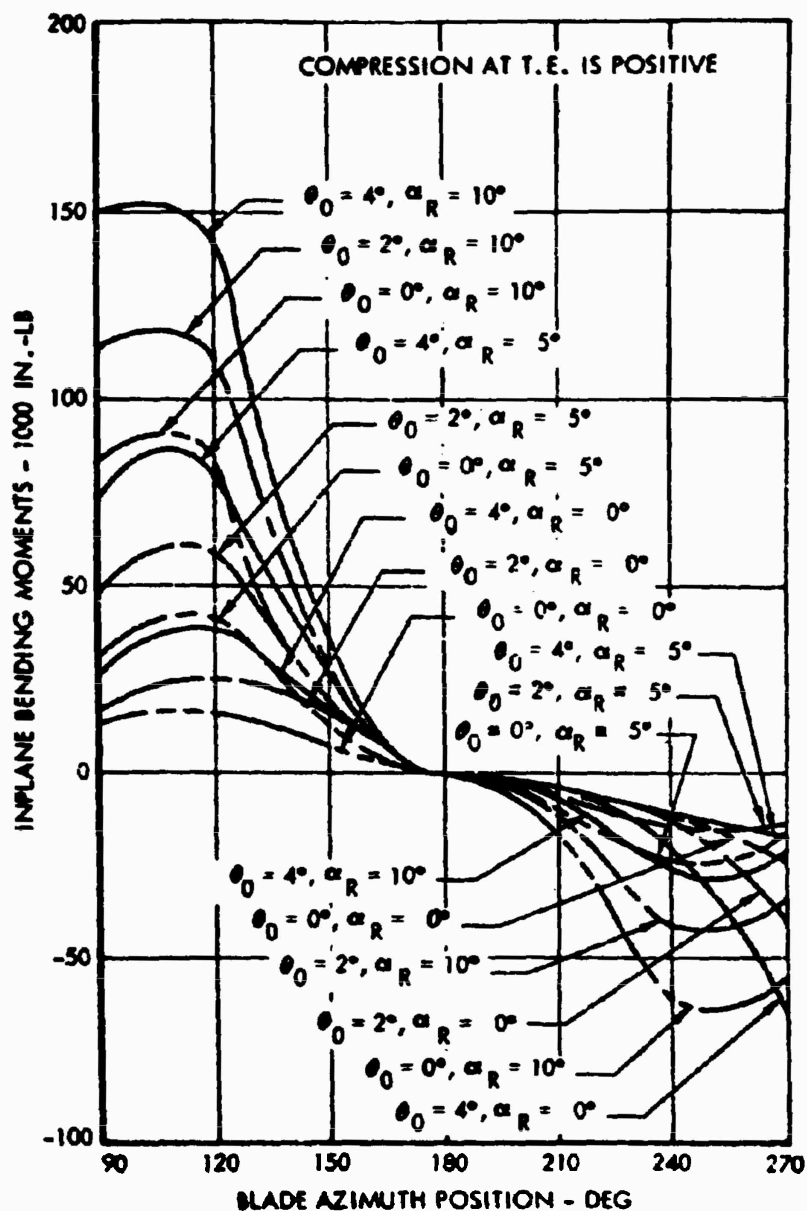


Figure 167. Main Rotor Inplane Bending Moments - Rotor Stopped at $V = 160$ KEAS.

where

- L_H = Rotor hub rolling moment (in.-lb)
- M_H = Rotor hub pitching moment (in.-lb)
- R_H = Maximum rotor hub moment (in.-lb)
- K_θ = Rotor stiffness = 1,775,360 ft-lb/radian
- T = Rotor lift/blade = 8167 lb
- W = Gross weight = 24,500 lb
- h = Distance between waterline through c.g. and ground line at the uphill main landing gear = 7.167 ft
- h_r = Distance between waterline through c.g. and rotor hub = 5 ft
- l = Longitudinal c.g. offset with respect to the rotor shaft = 0.608 ft
- l_g = Landing gear tread = 10 ft
- n = Lateral c.g. offset with respect to the rotor shaft = 0 feet
- θ = Angle formed by the attitude of the vehicle with the ground plane when the downhill main landing gear just clears the ground = -2.9 degrees
- θ_g = Angle of ground line with the horizontal = 15 degrees

Substitution of the values of the various terms into the equation results in a rotor hub moment of 1,301,500 in.-lb. The spanwise distribution of hub moment into the blades is shown in Figure 168. This distribution is accomplished by adding and subtracting, from the steady blade bending, two-thirds of the maximum hub moment times the first mode flapping distribution curve shown in Figure 169. The steady flapwise bending moments are based on a rotor lift of 8167 pounds/blade (one-third of the design gross weight).

Tail Rotor Loads

The tail rotor loads are shown in Figures 67, 68, 170 and 171. The spanwise distribution of inplane and flapping moments is shown for the conditions giving the highest loads: hovering flight at maximum thrust and hovering flight for overspeed. The curves are presented in parametric form for those values of collective pitch (or its equivalent: thrust).

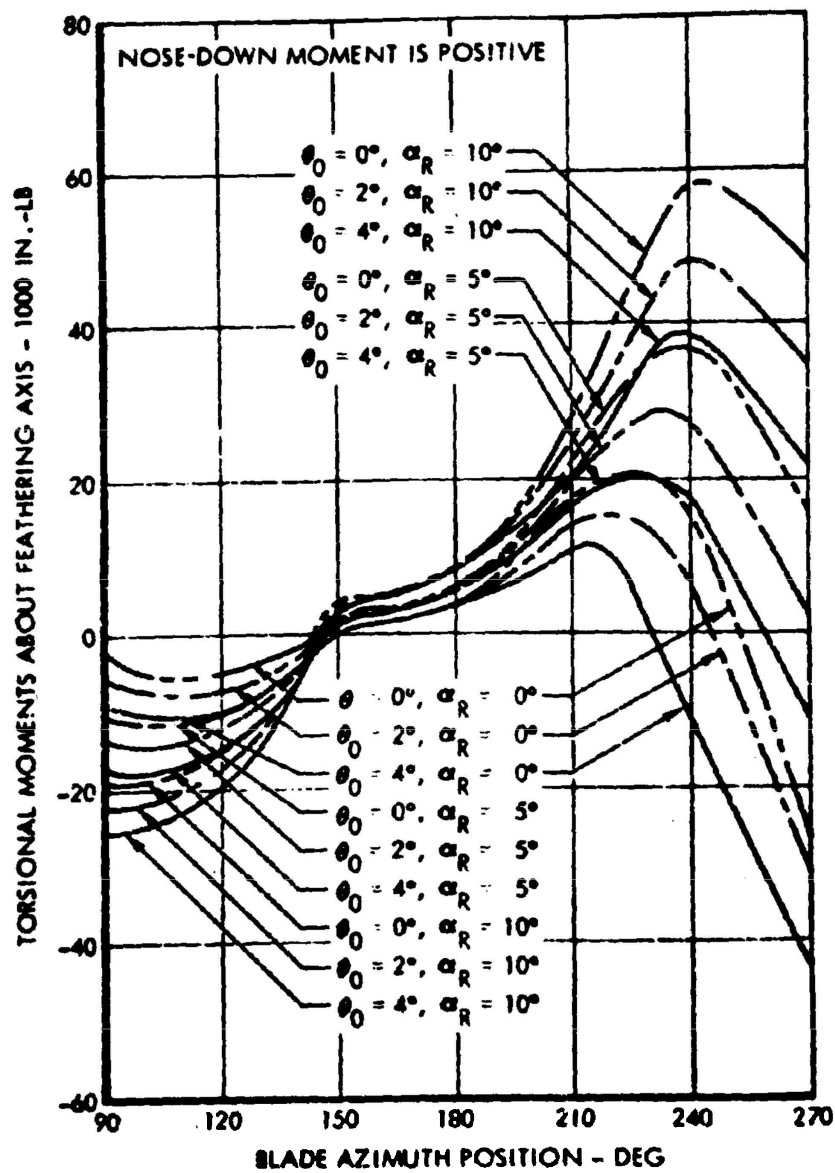


Figure 168. Main Rotor Feathering Moments -
Rotor Stopped at $V = 140$ KEAS.

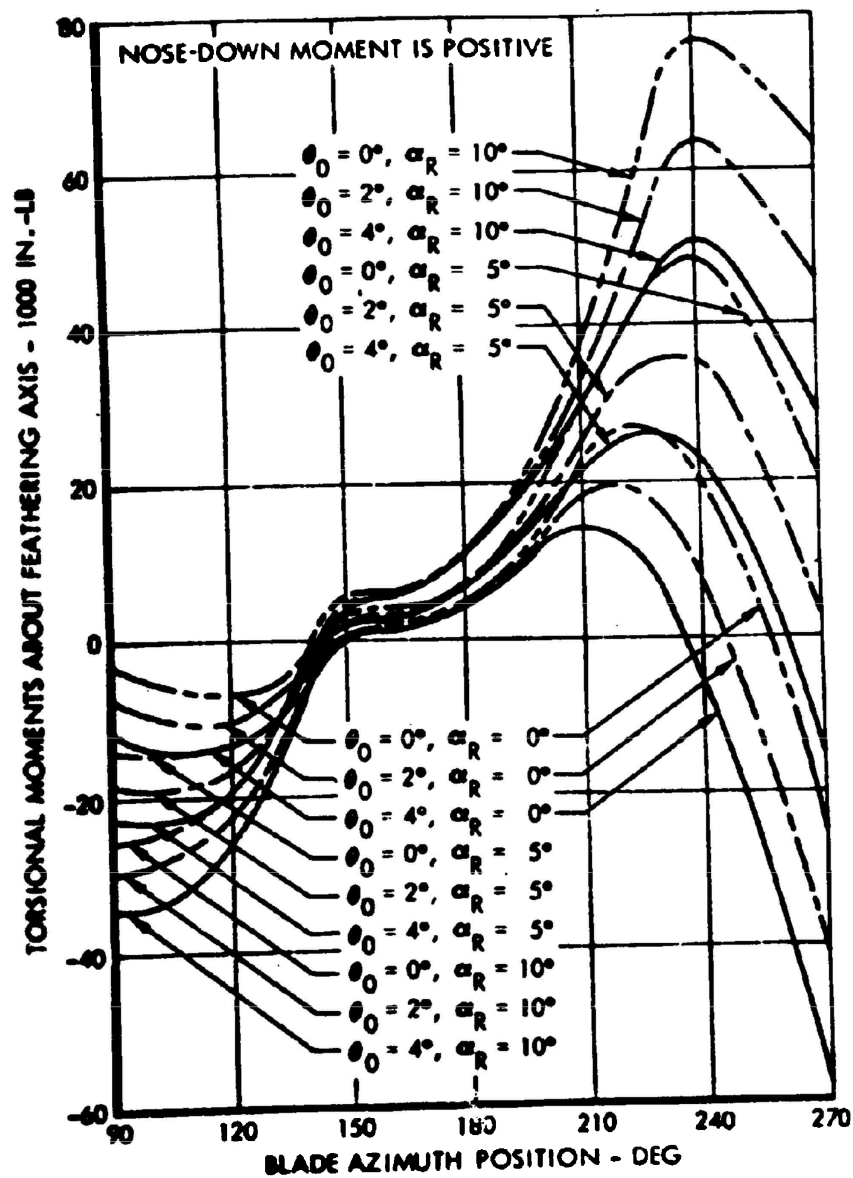


Figure 169. Main Rotor Feathering Moments - Rotor Stopped at $V = 160$ KEAS.

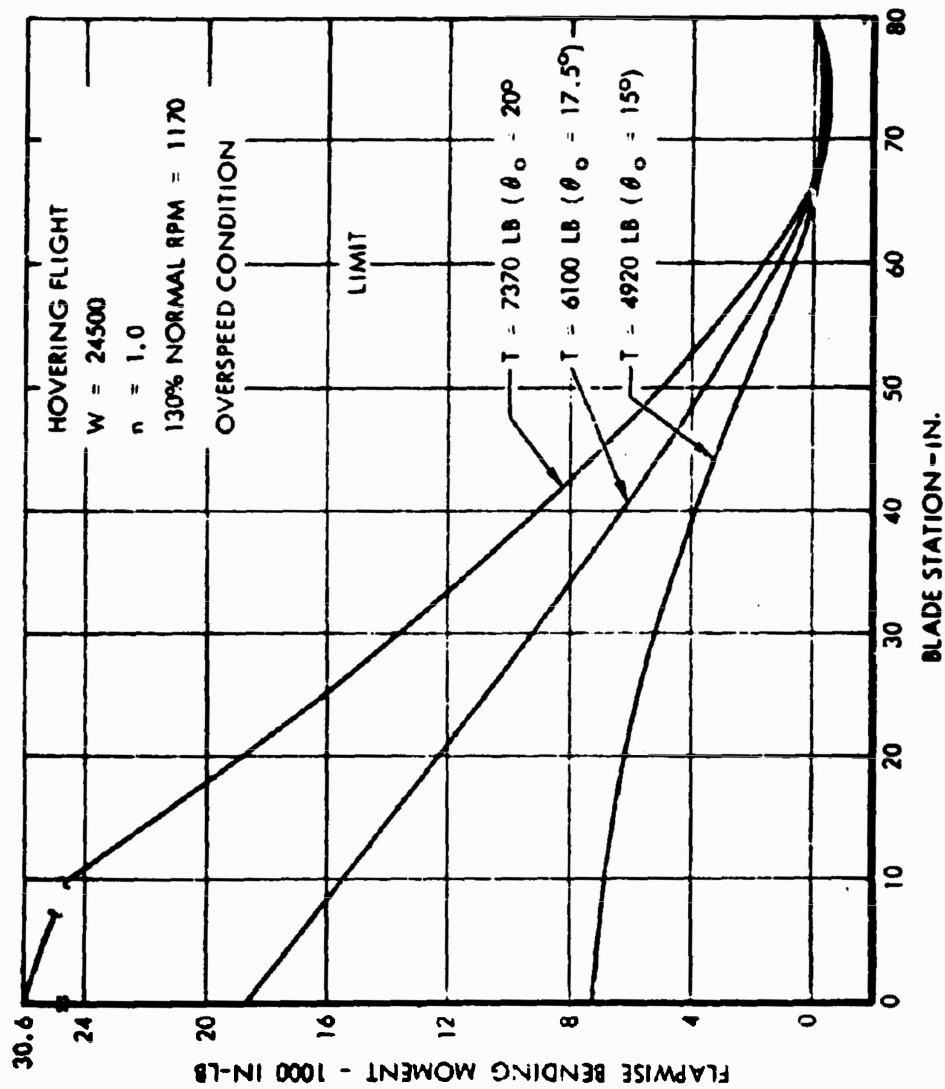


Figure 170. Tail Rotor Flapwise Bending Moment - Overspeed.

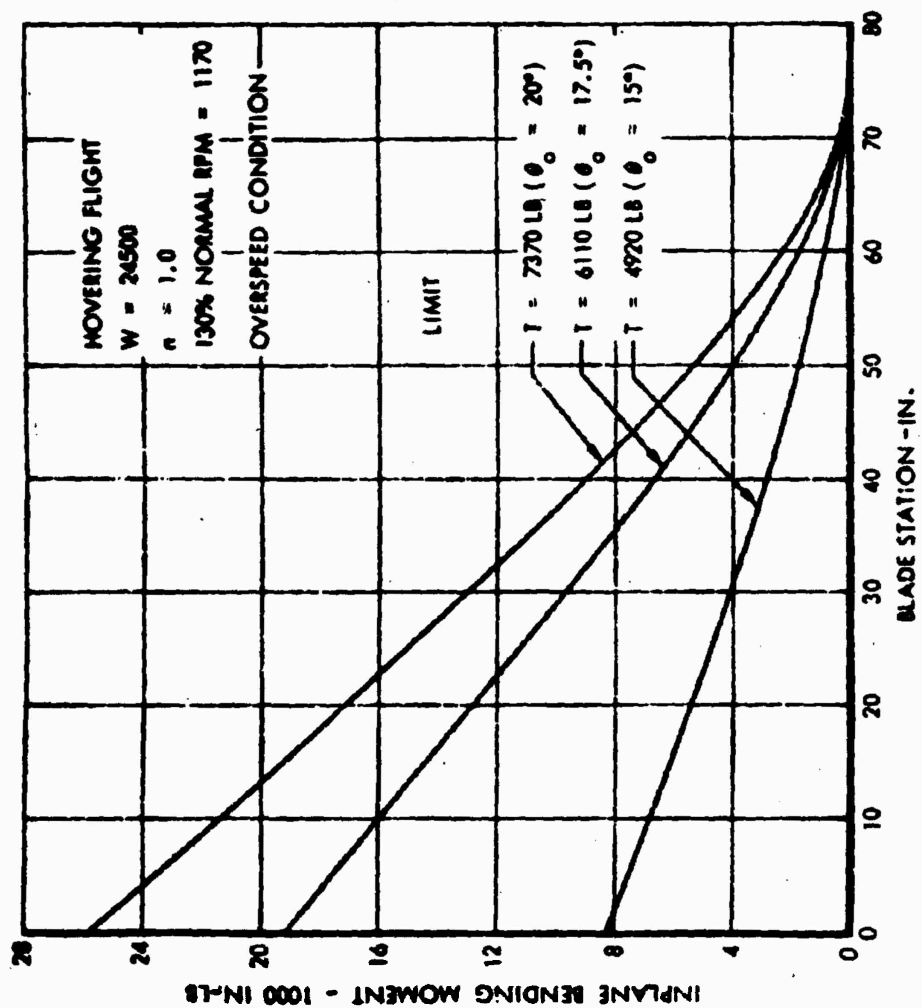


Figure 171. Tail Rotor Inplane Bending Moment - Overspeed.

PART 7
HYDRAULIC AND MECHANICAL SYSTEMS

SECTION 15
HYDRAULIC SYSTEM

Conventional 3000-psi hydraulic systems are used to take advantage of the reliable components that are available and to minimize development problems.

The power necessary for operation of the "helicopter mode" flight controls is provided by two completely separate hydraulic systems to assure the integrity and reliability of the controls. Hydraulic power is not required for operation of the "fixed-wing mode" flight control system.

The two hydraulic systems, designed substantially in accordance with Specifications MIL-H-5440D and SD-24-J (Figures 172 and 173), are independent actuating systems, since a failure in one system will not adversely affect the functioning of the other system.

The flight control hydraulic system consists of a hydraulic power package which, with a second pump, supplies hydraulic power to the roll, pitch, yaw and collective servo actuators, pitch-bias and roll-bias actuators, propeller-pitch actuators, and flap-drive motor. A 7.5-gpm-at-8200-rpm variable displacement pump in the power package powers the flight control system and is driven by the tail rotor accessory gearbox located at the rear beam of the wing.

The second 5.0-gpm-at-7000-rpm variable displacement pump in the flight control system augments the flow requirements for the propeller pitch actuators in both helicopter and airplane modes. The pump is located on the gearbox at the intersection of the pylon and cross shafting.

The power normally supplied by the hydraulic power source for the roll, pitch, and collective servo actuators, propeller-pitch actuator, pitch- and roll-bias actuators, and a second flap-drive motor. The utility system also furnishes hydraulic power to the landing gear system, engine-starting system, rotor-stopping control system, rotor blade shear pin positioning system, rotor blade folding system, and rotor transmission and forward doors positioning system.

The utility system is powered by an 18.5-gpm-at-700-rpm variable displacement pump in the hydraulic power package mounted on the No. 2 propeller gearbox.

The roll, pitch, and collective flight control servos, propeller-pitch actuators, and roll- and pitch-bias actuator systems can be powered by

either hydraulic system, thus providing the necessary system redundancy. The roll, pitch, and collective servo actuators are mounted on the rotor transmission housing and are controlled from the cockpit by the pilot. In the helicopter mode, the three servo actuators, through control linkages, change the rotor blade pitch angles. The propeller pitch actuators are located in the respective propeller hubs.

The yaw flight control servo actuator is powered by the flight control hydraulic system pressure only. The yaw servo actuator is mounted in the horizontal stabilizer and is controlled from the cockpit by the pilot. In the helicopter mode, the servo actuator, through control linkages, changes the tail rotor blade pitch angle.

The flap positioning is powered by either hydraulic system, thus providing redundant power to the hydraulic flap motors.

The rotor-stopping control and blade pitch-bias control are powered by the utility hydraulic system.

The rotor blade shear pin positioning system is powered by the utility hydraulic system.

The rotor blade folding system is powered by the utility hydraulic system.

The rotor transmission positioning system is powered by the utility hydraulic system.

Each of the engine-starting motors is powered by the utility hydraulic system for in-flight operation. In addition, the engine starter motor on the No. 2 engine may be driven on the ground from the ground hydraulic cart.

The landing gear system is powered by the utility hydraulic system.

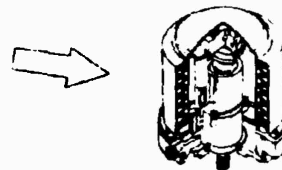
The propeller pitch positioning system is powered by redundant hydraulic system pressures.

The manual wheel brake system is powered by the rudder toe pedal force actuating the master brake cylinders on the rudder pedal linkage.

Operation of either the pilot's or the copilot's right or left rudder toe pedal relays hydraulic pressure to a left or a right main landing gear wheel transfer valve and through to the brake cylinders. Either the pilot or the copilot can steer the vehicle on the ground by applying the brakes on the right or left landing gear wheel.

Page Intentionally Left Blank

- ① ④ POWER PACKAGE INCLUDES
- PRESSURE PUMP
 - BELLOWS
 - RESERVOIR PISTON
 - RESERVOIR RELIEF
 - PRESSURIZED RESERVOIR
 - FILTER
 - FILTER BYPASS
 - LOADED FILTER INDICATOR
 - FLUID LEVEL INDICATOR
 - DISPLACEMENT ACTUATOR
 - COMPENSATOR
 - PRESSURE TRANSDUCER
 - CHECK VALVE
 - SOLENOID OPERATED BYPASS
 - HIGH PRESSURE RELIEF



⑤ NLG BSTR

⑥ NLG FLC

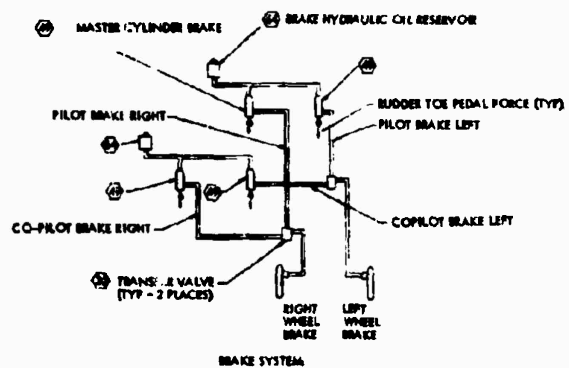
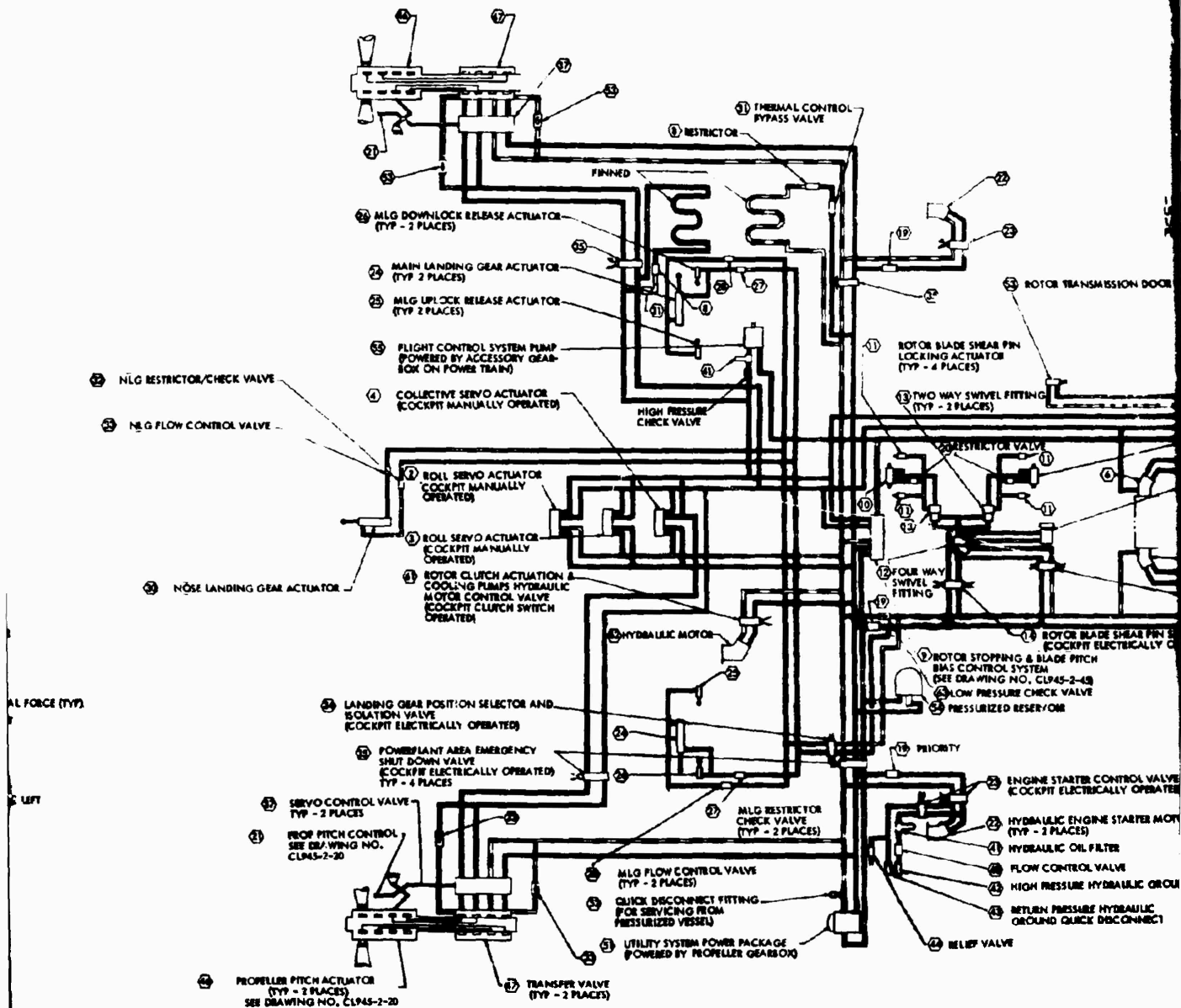
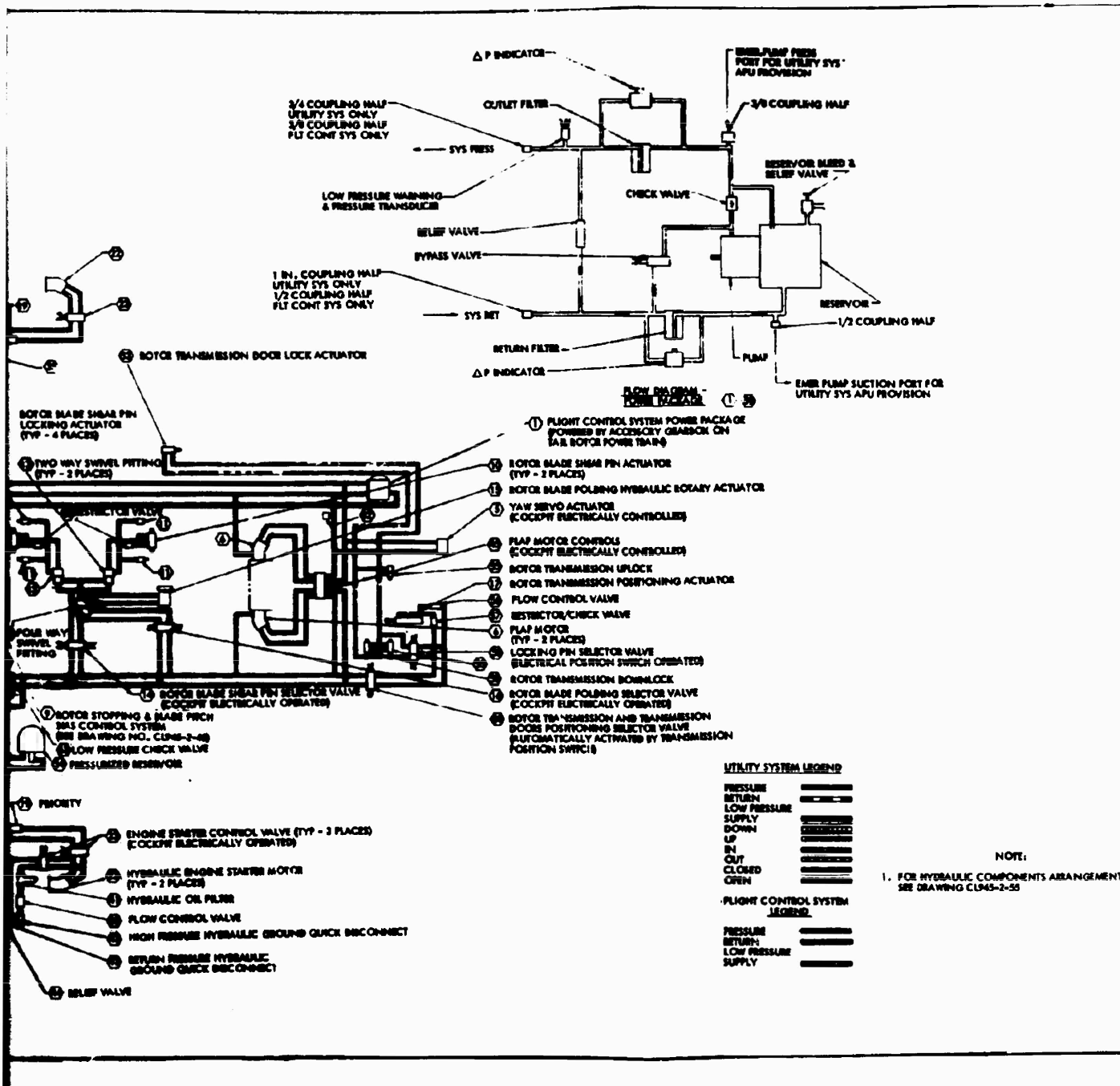


Figure 172. Hydraulic Systems Schematic.

A



B



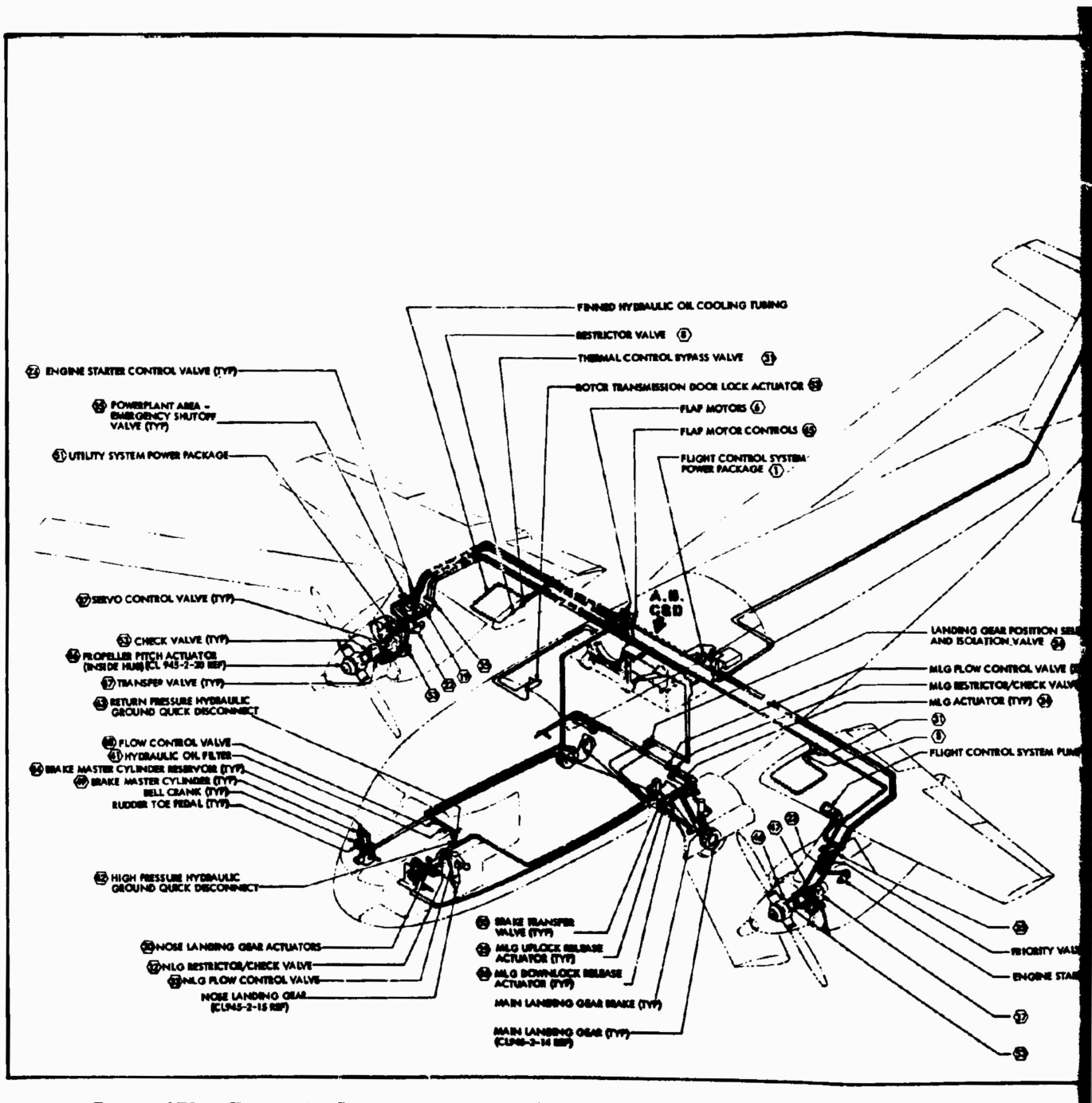
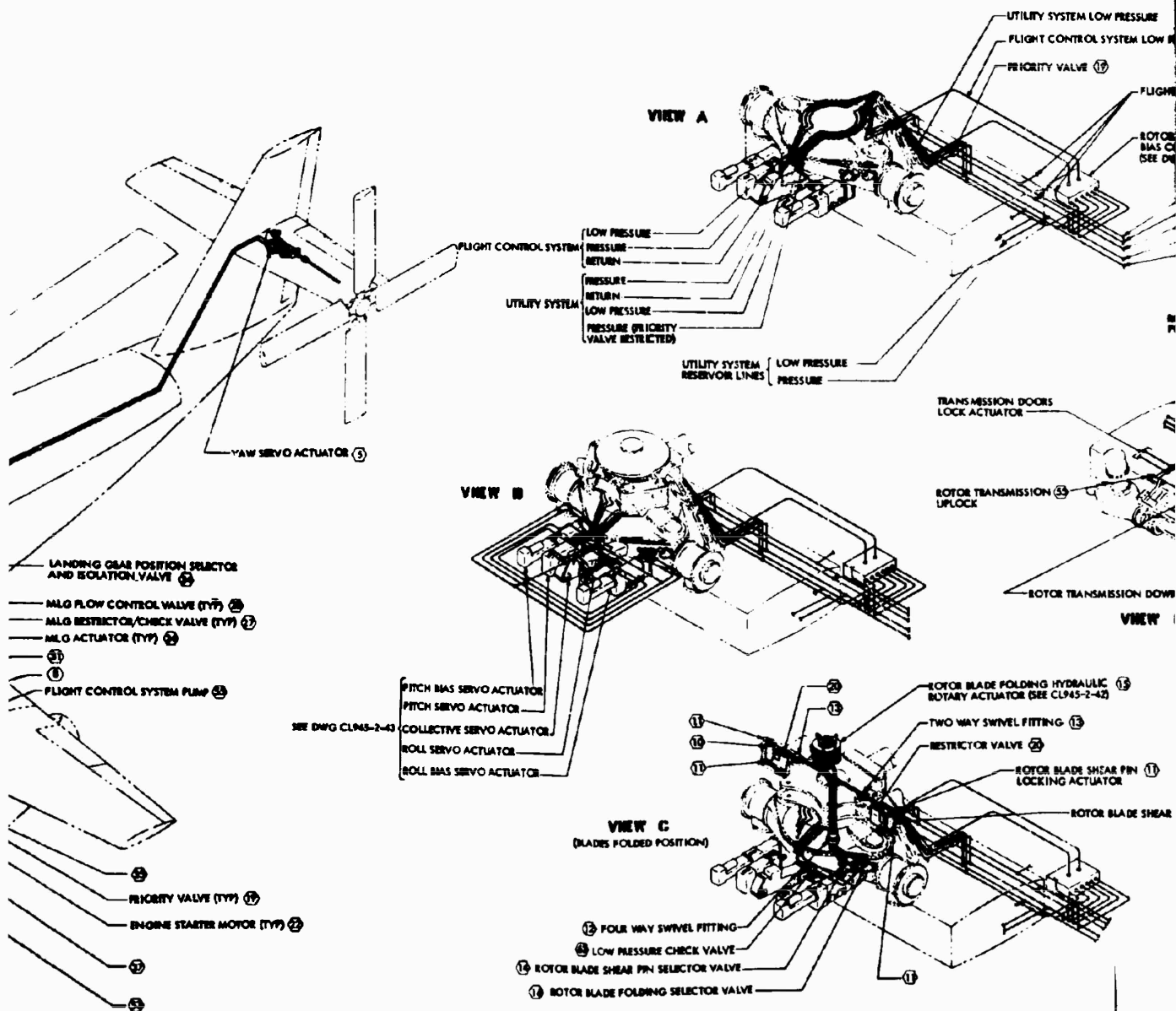
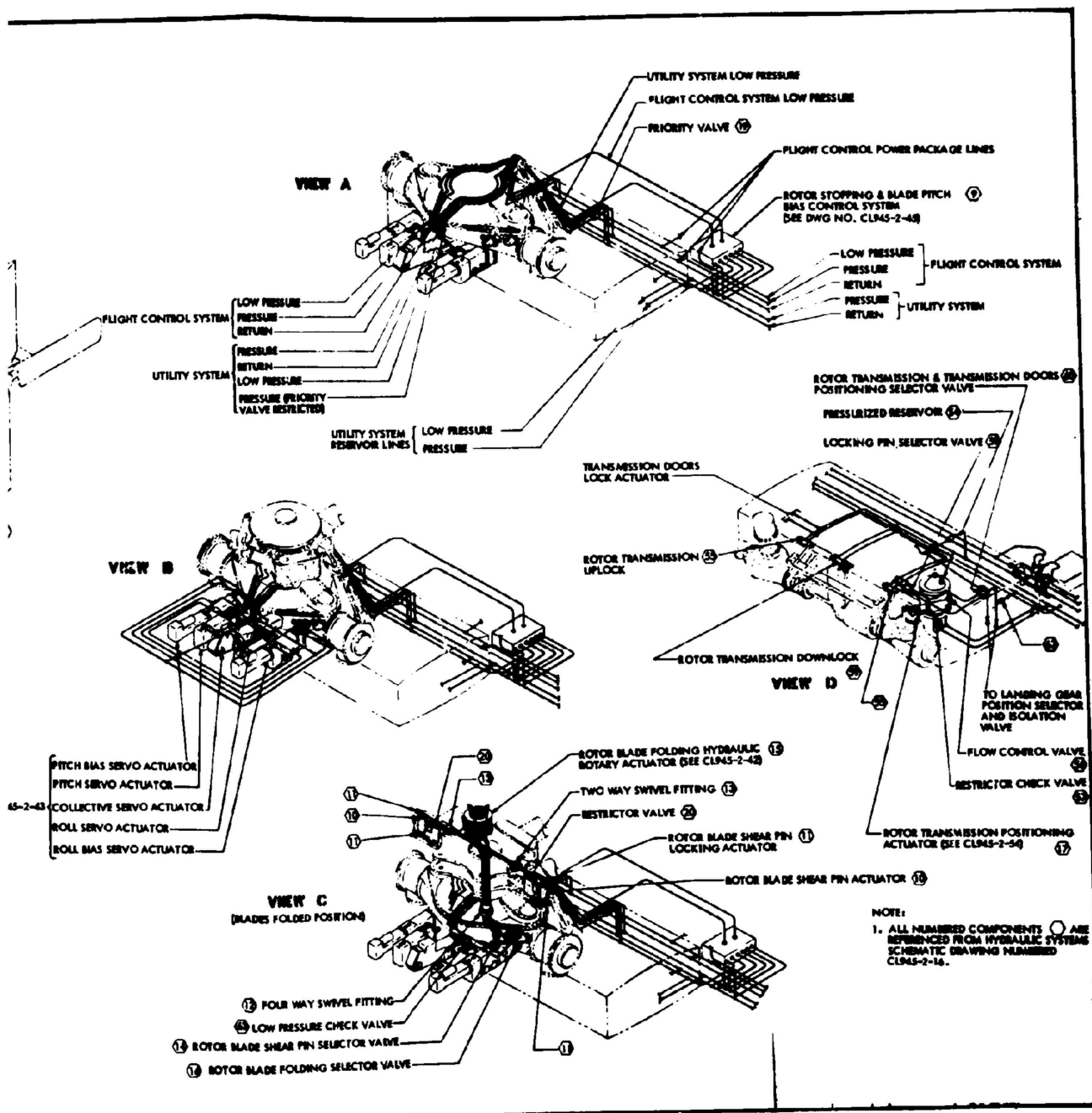


Figure 173. Hydraulic Systems Components Arrangement.



B



Page Intentionally Left Blank

SECTION 16

MECHANICAL SYSTEMS

LANDING GEAR

A tricycle arrangement was decided upon as the most suitable configuration for this type of vehicle. This arrangement provides for maximum stability during ground handling and for versatility in operation either in the helicopter mode or as a conventional airplane in the fixed-wing mode on standard runways. The landing gear operating cycle is accomplished in less than 10 seconds.

Operation

Control of the landing gear is normally exercised by the manual operation of a lever, terminated in a wheel-shaped knob, mounted on the center console. Operation of the gear through all ranges is as follows:

The landing gear control lever is held in the down position by a spring-loaded lock pin. This pin is removed from the lock position by an electrical solenoid, which is energized by a switch actuating to the closed position upon removal of the aircraft's weight from the gear. This allows the lever to be placed in the UP position, thereby actuating a switch which energizes a hydraulic control valve solenoid. The opening of this valve releases hydraulic power, which actuates the gear to the retracted position.

Three indicator lights are provided, one for each "leg," to indicate when the landing gear is down and locked. Two additional indicator lights are also provided, one for the nose gear and one for the main gear, which are illuminated if the gear is not fully retracted and correctly stowed.

Main Landing Gear

The main landing gear structure consists of a shock strut assembly mounting; a wheel, brake, and tire; a drag strut; a lateral strut supporting the top of the shock strut; a main structural leg; a retraction system; locking devices; a transverse I-beam connecting right and left gears; and closure doors. The gear assembly is a cantilever type, hydraulically operated, which retracts inward and upward to a position under the cargo compartment floor. The fuselage is not wide enough to retract the gear straight in, normal to the aircraft centerline. An unusual linkage system positions the wheels, when retracted, to an approximate tandem position. A manual emergency release system is provided for use in case of failure in the electrical or hydraulic systems. When retracted, each main gear is enclosed by doors.

Towing and jacking provisions are provided on the main landing gear shock-strut and leg assemblies. Shock-strut servicing fittings are located at

the top of the strut and are readily accessible. The MLG shock strut has a stroke of 10 inches, and it is designed for a limit sinking speeds of 8 fps. The complete gear is attached at four points on the fuselage and is removed as a unit. Right and left gears are identical. The shock strut utilizes a 28 x 9:00, 26-ply rating, pneumatic tire, mounted to a compatible brake and wheel assembly. The two gear actuating assembly units are identical, each side, and are removed as complete units. Actuation is through a splined shaft that slips into the main gear leg pivot shaft.

A coil spring in the head of the actuating cylinder forces the gear out to the locked-down position in emergency operations.

The two gear-up- and down-lock assemblies are identical, each side, and are removable as complete units. The unit is connected by a splined shaft to the main gear leg pivot shaft. The locks are of the latch type, spring-loaded through the hydraulic actuating cylinders. Due to the geometry of the gear, the wheels move toward each other when extension is started. Interference would result if gears were extended at equal rates. When operated by emergency manual extension, the left up lock is released; when the gear enters the down-locked position, a cable from the left down lock system releases the up lock on the right gear. With normal retraction and extension, interference of tires is eliminated by the incorporation of flow control valves and restricted check valves in the hydraulic system. An electrical switch is mounted on the antitorque scissors at the shock strut. The switch is connected to a solenoid on the gear control lever in the flight station. A pin locks the control until the shock strut is fully extended.

Nose Landing Gear

The basic nose landing gear, consisting of shock-strut assembly, drag linkage assembly, torque arm assemblies, and retraction actuator assembly, is identical to that used on the C-140 currently in production.

Since no steering is required on the CRA, the steering mechanism and related plumbing have been removed. In their place, a shimmy damper of the viscous type is attached to the shock-strut cylinder assembly and linked to the existing swivelled steering collar. To ensure proper functioning of the uplatch and downlatch mechanisms, particular care is given to maintaining the same retraction geometry as used on the C-140 in adapting the nose wheel to this application.

The gear is of the conventional type, consisting of a piston assembly operating in a cylinder under a pressure head of air and oil. In operation, oil is metered from one chamber to another through an orifice. Upon full extension of the piston, prior to gear retraction, alignment cams within the cylinder automatically center the piston and wheels with the wheel well. The wheels are supplied with 18 x 4.4-12-ply type VII tires which are readily available.

The uplatch and downlatch are both integrated with the drag link assembly. These latches are actuated by locating the hydraulic actuator cylinder in a manner to unlatch the gear from its down position upon the initial retraction of the cylinder just prior to retraction of the gear. Likewise, the uplatch is released just prior to gear extension by the initial extension of the hydraulic retraction actuator.

Gear-up and -down positions are signaled by micro-type electric switches appropriately arranged to open and close the required circuits. A rubber bumper is provided on the upper drag strut to absorb the shock of retraction against the structure.

PART 8
EMERGENCY SYSTEMS AND PROCEDURES

SECTION 17
EMERGENCY SYSTEMS

The crew escape system incorporated in the CRA specifically for emergency conditions consists of the flight-crew ejection seats and the emergency exits.

An extensive trade-off study has been conducted to determine the emergency egress system applicable to the CRA for the flight envelope of the research program, and to determine the feasibility of a zero-zero ejection seat. The principal areas of consideration for the study are:

- Available systems
- Applicability of system to different modes of flight
- Safety during evacuation
- Flight envelope for the research program
- Amount of flight test time in different modes
- Relative hazard associated with different modes
- System costs

EMERGENCY SYSTEM DETERMINATION

The basic flight envelope of the research program will be to takeoff and climb to conversion altitude in the helicopter mode; to convert to fixed-wing mode; to operate in the fixed-wing mode (at or above the conversion altitude); to convert to helicopter mode; and to descend and land in the helicopter mode. Additional flight testing and evaluation flights will be conducted outside of this basic envelope.

The aircraft operates both as a helicopter and as a conventional fixed-wing airplane. Therefore, existing upward ejection systems will not provide emergency egress throughout the flight regime of the research program. Consequently, the request, of the study contract Statement of Work, to provide a qualified zero-zero ejection seat cannot be satisfied in total. As a result, it is necessary to determine which emergency escape system will provide the flight crew with the maximum protection possible for the research program.

To permit a comprehensive evaluation of the problem, the following must be analyzed:

- Type and amount of flight testing, in the different modes, with a relative index of the hazard associated with the various conditions.
- Type of emergency egress systems applicable to the different modes

A tabulation of the various flight conditions with corresponding amount of flight time for each condition (based on a total test program of 100 hours) is shown in Table XXVI. The relative hazard index for these flight conditions is also shown in Table XXVI.

The determining factors for these data are summarized as follows:

- The CRA will operate in the fixed-wing mode for a total of 44.0 hours. Of this time, 36.2 hours will be above an altitude of 2,000 feet (with minimum altitude of 2,000 feet required for downward ejection). Therefore, the only conditions where ejection is not possible in the fixed-wing mode are during takeoff, landing, and climb or descent. The aircraft will be flown for 5.9 hours under these conditions, with the objective of demonstrating the takeoff and landing capabilities of the aircraft in the fixed-wing mode. This takeoff and landing demonstration will be accomplished after the aircraft has been flown at altitude in the fixed-wing mode, since initial takeoffs and landings will be accomplished in the helicopter mode. This manner of testing will provide detailed knowledge on handling characteristics of the aircraft.
- The CRA will be operated in the helicopter mode for a total of 36.0 hours, of which 21.6 hours will be above an altitude of 2,000 feet. As in the case of the fixed-wing mode, the conditions during which ejection is seriously compromised in the helicopter mode include taking off, landing, or climbing or descending for the range of altitudes from 0 to 2,000 feet. The aircraft will be flown 14.4 hours under these conditions. The initial investigation of the handling characteristics in the helicopter mode will be accomplished close to the ground, where an ejection system is not necessary, since the helicopter is capable of autorotational landing. An ejection system would not be effective for this type of flying, since the reaction time would not permit activation before the aircraft would contact the ground. The autorotational capability also applies to the helicopter regime for takeoff, landing, and climb or descent from 0 to 2,000 feet. Above 2,000 feet, either autorotational landing or downward ejection would be effective for emergency conditions.

TABLE XXVI. EMERGENCY EGRESS DATA

Mode	Condition	Height (Ft)	Speed (Knots)	Time (Hr)	Hazard Rating	Type of* Ejection
HELICOPTER	Hover-Taxi	0-50	up to 30	5.5	11.0	None
	Hover-Taxi	50-150	up to 30	1.0	2.0	None
	Forward Flight	0-150	30 to 160	1.8	3.6	None
	Forward Flight	150-2000	Hover to 160	1.8	3.6	None
	Climb	0-2000	30 to 160	1.7	2.0	None
	Normal	> 2000	Hover to 160	21.6	43.2	Down
	Approach	150-0	160-0	1.0	2.0	None
	Landing	0	30-0	0.5	1.0	None
	Autorotation	0 and up	0 to 160	1.8	3.6	None or Down
			Subtotal	36.0	72.0	
TRANSITION	Rotor Slowing	>2000	140	1.8	18	Down
	Rotor Stopped	>2000	140-160	5.0	50	Down & Up
	Rotor Folding	>2000	140-160	1.6	16	Down & Up
	Rotor Folded	>2000	140-160	5.0	50	Down & Up
	Rotor Stowing	>2000	140-160	1.6	16	Down & Up
	Extending Rotor	>2000	140-160	1.6	16	Down & Up
	Rotor Unfold	>2000	140-160	1.6	16	Down & Up
	Rotor Start	>2000	140-160	1.8	18	Down
			Subtotal	20.0	200	
AIRPLANE	Running	0	0	.5	.5	Up
	Takeoff	0-5000	0-V _{climb}	.5	.5	Up
	Climb	500-2000	V _{climb}	2.2	2.2	Up
	Normal	> 2000	V _{stall} -V _{max}	36.2	36.2	Down & Up
	Approach	< 2000	V _{approach}	2.7	2.7	Up
	Land	0	1.2 V _{stall}	.5	.5	Up
	Taxi	0	Taxi	1.4	1.4	Up
			Subtotal	44.0	44.0	
No. of flight hours when upward ejection is possible						= 50.4 hr
No. of flight hours when downward ejection is possible						= 77.8 hr
Time in most hazardous condition						= 20 hr
% of time downward ejection possible, during most hazardous condition						= 100%
*Based on existing, qualified ejection seat systems						

- Handling characteristics of the aircraft in the conversion between the helicopter and the fixed-wing mode have been explored in theory and in wind tunnel testing. Since operational experience is not available, a higher relative hazard index was assigned to the flights during conversion. All of the flight time (20.0 hours) will be accumulated at an altitude of 2,000 feet or above. As such, the downward ejection seat is effective throughout the complete conversion, while an upward ejection would not be effective for that portion during which the rotor system was engaged and turning.

For upward ejection, a rocket catapult ground-level escape system provides immediate escape from the CRA in the fixed-wing mode, at all altitudes and speeds within the range of this aircraft, and up to the transition point when the rotor system is engaged and turning for the transition mode, thereby partially satisfying the required zero-zero ejection. However, in the helicopter mode and in transition with the rotors turning, the upward ejection seat is not feasible without some means of clearing a path through the rotor blade plane. Blade removal is possible by employing shaped ballistic charges, but this would require an extensive development program to test the concept and to provide positive assurance that an accidental discharge could not happen. To complement an upward ejection system for the helicopter mode, an emergency escape hatch could be located through the lower section of the fuselage just aft of the flight station. This would provide a passage that would clear the rotors or propellers. This method is altitude limited.

The downward ejection seat, by the very nature of the system, has a minimum altitude limitation for activation. A large percentage of the flight test program, and all of the testing for the conversion between fixed-wing and helicopter mode, would be conducted above this minimum altitude. Downward ejection must be capable of clearing the aircraft at its maximum sink rate so that there is no involvement of parachute and aircraft. Parachute bailout has this same concern, plus the possibility of high g-forces restricting the movements of the crew.

Sideward ejection was investigated, based on the principle which pulls the occupant out of the seat and aircraft by a rocket catapult instead of ejecting the seat and occupant. This system would require considerable development for both the escape system and for clearing a passage through the aircraft structure.

The study concludes that downward ejection would provide the maximum protection for the crew during the critical research flight test program. It is recognized that downward ejection has not proved to be as satisfactory as upward ejection for operational high-performance aircraft. However, the circumstances associated with downward ejection in these aircraft are entirely different from those for a research program.

EMERGENCY ESCAPE - CREW

Both flight stations are equipped with a modified version of the downward ejection system. This system is capable of safe ejection for all modes of flight for the CRA above an altitude of 2,000 feet, and for the complete speed range. The seat is capable of downward ejection or downward free-fall. The arrangement of the cockpit section is shown in Figure 174.

System Description

The ejection seat system for both the pilot and the copilot consists of the seat, a fixed-rail assembly permanently attached to the aircraft, an escape hatch below the seat, and necessary controls for adjustment and ejection.

The metal bucket-type seat is mounted on the rails so that during ejection it will slide down the rails and clear the airplane. The seat incorporates a headrest, a thruster, a catapult, leg braces, feet retraction, cyclic stick stowage, a dual-strap inertia reel, seat belts, and arm retention webbing. The connections for the inertia reel and seat belt straps are compatible with the MA-2 Integrated Torso Harness Restraint System being used in the CRA.

Vertical seat adjustment is provided by an electric actuator mounted on the lower end of the catapult. The foot retraction and retention system consists of a reel assembly and cable with a ball lock assembly that attaches to the foot retainers. The reel assembly allows the pilot free movement about the cockpit and is actuated to the locked position by a cable attached to the leg guard. A manual system is installed to permit cutting of the foot-retraction cable without firing the seat. The action of the leg braces also initiates the cyclic stick stowage system which pulls the stick forward out of the ejection path. The "D" ring located on the front of the seat bucket is the control for ejection. The system provides an overtravel which releases the seat for free-fall in the event that the catapult fails to fire. By removing the free-fall disconnect safety pin, the action of the "D" ring will provide free-fall instead of catapult ejection. The catapult ejection sequencing is shown in Figure 175.

An escape hatch located directly below each seat is mechanically jettisoned in sequence with the ejection seat. The hatch consists of a frame formed to match the contour of the fuselage skin and the latching mechanism. A manual latch release permits release of the hatch without disturbing the seat.

Pilot-seat separation is accomplished by means of a gas-operated actuator and straps. The actuator is sequenced with the opening of the seat belts and the cutting of the foot-retaining cables. The action of the drum tightens the straps, forcibly separating the occupant from the seat. The parachute lanyard is activated by the occupant's leaving the seat.

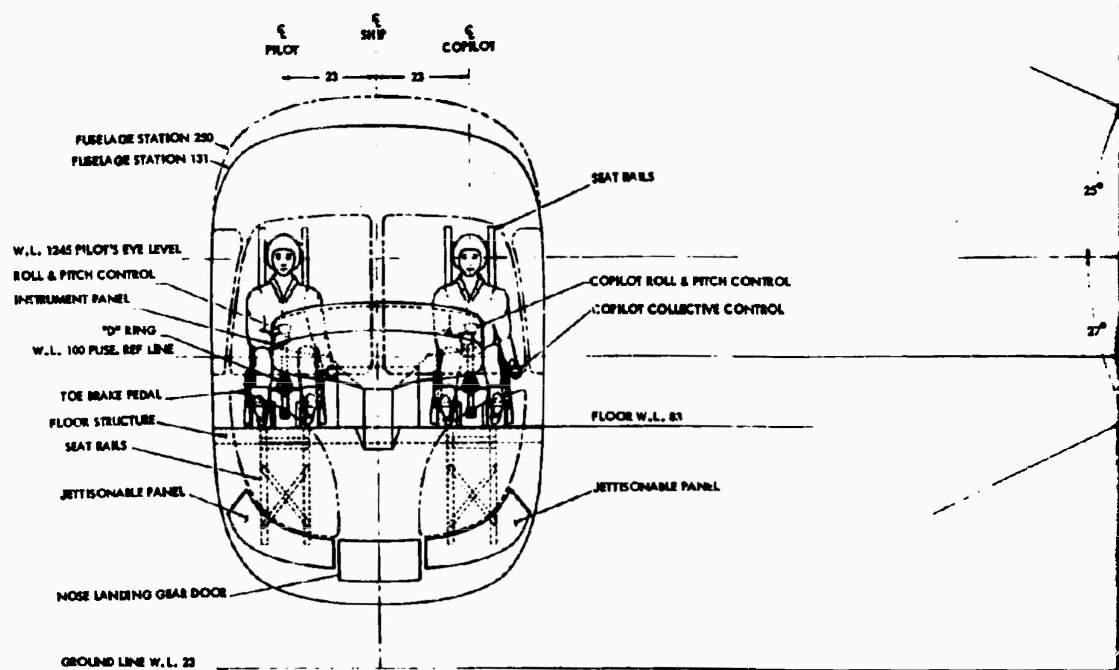
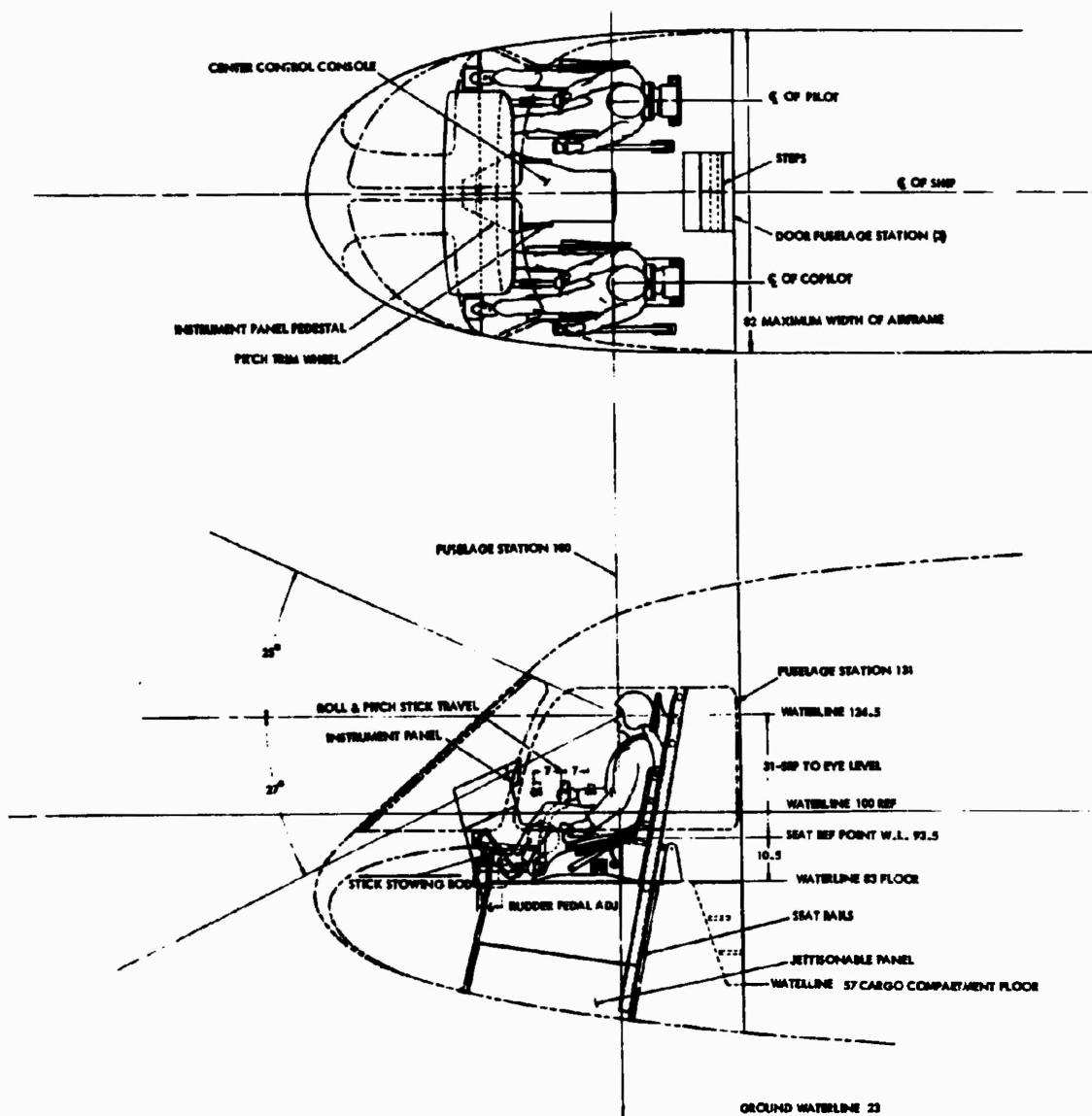


Figure 174. Flight Station Arrangement.



B

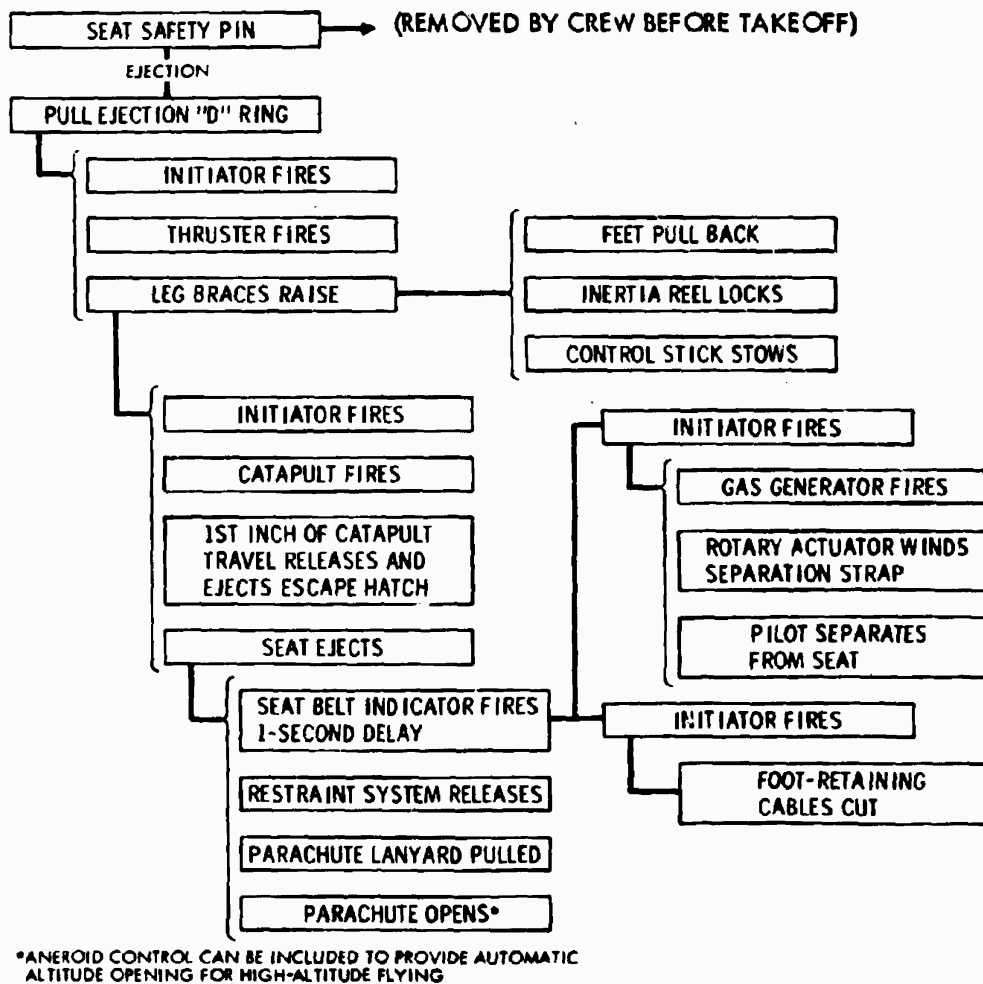


Figure 175. Ejection-Seat System Sequencing.

Each seat is activated by the action of its own "D" ring and can be ejected simultaneously or separately (the command seat can be delayed). A one-second delay is recommended to assure separation of each system. In addition to the ejection system, emergency exits are provided through the side panels of the canopy. The cargo compartment doors also serve as emergency exits.

The canopy side window panels, one on each side of the aircraft, are manually jettisonable through the operation of a handle connected to a series of attaching pins. Each handle is interconnected to an exterior flush-mounted handle for ground rescue. Boarding provisions are incorporated to permit easy and rapid access to the cockpit area by ground personnel. Rescue markings for the location and operation of the emergency exits are in accordance with MIL-A-25165. The size of the opening is 35 inches high by 52 inches wide, which exceeds the requirements of the HIAD.

The cargo compartment doors are located on both sides of the aircraft at the aft end of the cargo compartment. It is not envisioned that these doors will serve as emergency exits for the flight crew, but they will be used if additional crew members are employed during certain phases of the test program. These doors will be identified and marked as rescue openings for ground personnel.

Emergency Procedure - Helicopter Mode

The flight envelope of the CRA in the helicopter mode will be takeoff, climb to conversion altitude, descend from conversion altitude, and land. For any emergency occurring when the vehicle is in the helicopter mode for takeoff, landing, and climbing to an altitude of 2,000 feet, the emergency procedure will be to execute an autorotational landing. The pilot procedure for entering autorotation in the CRA, assuming loss of both engines, will depend upon the forward speed at which the failure occurs. At speeds up to approximately 100 knots, the CRA is essentially a helicopter and will be flown like one during the transition to autorotation. The CRA rotor has sufficient inertia so that, even at hover, the collective pitch reduction may be delayed 2 seconds without the speed decreasing to the point where the blades stall under lg flight conditions.

Near transition speeds, the technique for making the transition to autorotation in the CRA is quite different from that used with conventional helicopters. It also differs from compound helicopters powered by jet engines. The fundamental difference is that at high speeds, the propellers can be used to extract energy from the passing airstream and thus can be used to minimize main rotor speed decay (reference Figure 102). The pilot procedure is as follows:

- Following recognition of a power failure, the pilot simply decreases the propeller pitch to a 20-degree blade angle by twisting the propeller pitch control to the "autorotation detent." This places the propellers in a windmill state, allowing them to furnish power to the main rotor. It also produces a negative propeller thrust which helps to decelerate the aircraft.
- Simultaneously with the reduction of propeller pitch, the collective pitch to the main rotor is decreased to the autorotation value. For entries into autorotation at high speeds, the collective pitch setting will already be near the proper autorotation value, and little or no corrective action is required.
- Until the aircraft slows to 100 knots, the rotor speed is monitored with propeller pitch or alternatively by developing rotor load factors in descending turns. Increased propeller pitch reduces rotor rpm, and decreased pitch increases rotor rpm; increasing rotor load factor in turn also increases rotor speed.
- At a speed of 100 knots, the pilot controls rotor rpm with main rotor collective pitch and forward speed with cyclic pitch as he would in a conventional helicopter.
- The aircraft is brought to a steady autorotative state at a speed of 80 knots.

In the helicopter mode for flights above an altitude of 2,000 feet, the reaction by the flight crew to an emergency condition can be one of the following:

- Enter into an autorotational descent and landing
- Effect emergency stopping of the rotor system and fly as an airplane
- Eject.

The course of action to any one emergency would be at the discretion of the pilot. Normally in a flight research program, the pilot would make every effort possible to correct the emergency condition before leaving the aircraft. Since the aircraft has VTOL characteristics, the usual procedure would be to enter an autorotational descent unless the vehicle was completely out of control. In this case, the ejection system would be used, since most of the flight testing and all of the transition testing will be conducted above the minimum ejection altitude.

The braking system for the main rotor, under normal operating conditions, is designed to stop and index the rotor blades (master blade trailing aft with the other two blades at azimuth positions of 120 and 240 degrees)

within 35.0 seconds. The design of the brake system will permit a one-time emergency application which will stop the rotor in approximately 6 seconds. If the emergency were associated with the rotor system, an emergency rotor stop could be made and the aircraft could be landed in the fixed-wing mode.

Emergency Procedure - Fixed-Wing Mode

The CRA in the fixed-wing mode is capable of executing landing during emergency conditions, including the remote possibility of the loss of power from both engines. In the event of complete power failure in the airplane mode, the pilot has the option of gliding to a suitable emergency landing field as an airplane or of unfolding and starting the rotor in order to land in autorotation.

In order to unstow the rotor, a glide is established at 140 knots, the flaps are extended, and the propellers are brought up to full speed by operating them in the windmill state to ensure full hydraulic pressure from the hydraulic pumps which are mounted on the propeller gearboxes. The pilot will start the unstowing cycle by putting the "Retract" switch on the console in the "Unstow" position. This operation will take approximately 8 seconds. With the rotor raised out of the fuselage, the blades are unfolded by placing the "Fold" switch to the "Extend" position. The unfolding will require about 8 seconds. Since the propellers are turning the cross shaft, the rotor can be brought up to full speed by releasing the rotor brake and engaging the clutch, just as in a normal start with the windmilling propellers furnishing the required power. This step will require approximately 36 seconds. From this condition, the aircraft can make a normal autorotational landing. The total time between the establishment of the steady glide at 140 knots and the attainment of full rotor speed will be approximately 52 seconds. During this time, the rate of descent will be about 45 fps based on the power required to maintain level flight at 140 knots with flaps down. Thus, the aircraft will require an altitude of about 2330 feet to make the transition from the airplane mode to steady autorotation.

In case the power failure occurs at a speed above 140 knots and at less than 2330 feet, the excess kinetic energy of forward speed can be traded for altitude in a zoom maneuver. At speeds above 268 knots, a safe landing can be made even if the power failure occurs next to the ground.

SECTION 18
EMERGENCY PROCEDURES

The various operating systems of the CRA with respect to possible emergency conditions were analyzed. System malfunctions were considered with regard to their resulting impact on the operation of the aircraft and the corrective procedure available to the flight crew.

The following paragraphs cover the emergency procedures associated with the following systems:

- Main Rotor System
- Flight Controls
- Power Plant System
- Drive System

Emergency conditions were based on engineering research flight test criteria, with emphasis on the most hazardous areas. Contractor engineering pilot reactions to typical test emergency conditions were analyzed on the basis of past history and anticipated reaction to the CRA flight spectrum of testing.

MAIN ROTOR SYSTEM

The flight controls for the main rotor system incorporate dual systems, including dual hydraulics, to provide a fail-safe control system. This same concept applies to the flap drive controls. Therefore, there would have to be a dual failure to create an emergency as a function of these controls. As discussed under the hydraulic system, the aircraft in either mode is controllable in the event of a complete hydraulic failure.

The controls for the fixed-wing aerodynamic surfaces and the helicopter directional control do not incorporate dual systems. However, the loss of these controls would not result in an out-of-control condition of the aircraft. The fixed-wing aerodynamic surfaces are aerodynamically balanced, and the function of one surface, as applied to control of the aircraft, could be substituted for by the function of another surface. The loss of directional control will require corrective action, as explained in the discussion of the drive system. In this event, the flight should be terminated and the aircraft landed.

POWER PLANT SYSTEM

The aircraft is capable of maintaining level flight with one engine operating at the design gross weight of 24,500 pounds at the following speeds: up to 280 knots for the fixed-wing mode; down to 40 knots in the helicopter mode; at 140 knots during transition. Safe landing can be made in the event of a complete power failure for either the helicopter mode or the fixed-wing mode as previously discussed.

DRIVE SYSTEM

The emergency conditions associated with the drive system are:

- Main transmission chip detection
- Main transmission oil temperature
- Main transmission oil pressure
- Main transmission gear failure
- Intermediate gearbox gear failure
- Tail rotor drive system failure

All of the conditions listed, except the intermediate gearbox gear failure, pertain to the helicopter mode. The intermediate gearbox gear failure pertains to both the helicopter and the fixed-wing mode.

The main transmission and tail rotor gearbox magnetic chip detectors provide a means of detecting the presence of magnetic materials in the oil system and will give advance warning of gear or bearing failure. Warning lights in the cockpit are activated by the chip detectors. A chip detector warning is not cause to discontinue the test flight; but the condition should be investigated and necessary corrective action taken, or the condition should be noted prior to the next flight.

Indicators and warning lights are located in the instrument panel in the cockpit to monitor the main transmission oil temperature and pressure. If an indication is received from the warning light for either high-oil temperature or low-oil pressure, the power to the transmission should be reduced and a landing executed.

A gear failure in the main transmission is highly improbable if the oil temperature and pressure are properly maintained. In the event of a gear failure resulting in a jammed gear train, the shear section in the main rotor drive shaft will free the rotor and permit autorotational descent and landing.

In the event of an intermediate gearbox failure, the affected system can be disconnected from the drive system through the actuation of the emergency engine shutdown handle, which actuates the hydraulic decoupler. A one-engine landing would be made if the aircraft is in the fixed-wing mode, or a normal landing would be made if the aircraft is in the helicopter mode.

For a malfunction of the tail rotor drive or control, the procedure would be to reduce rotor torque and trim the aircraft by propeller thrust. A landing should be made as soon as possible.

PART 9
COCKPIT ARRANGEMENT

SECTION 19
GENERAL ARRANGEMENT

The general arrangement of the flight station for the aircraft is shown in Figure 174. The aircraft is designed for normal operation by a crew of two, and all normal flight test operations are accomplished from the flight station. The figure shows that the pilot will be seated on the right-hand side and the copilot on the left. Dual primary controls are provided for both crewmen so that the vehicle can be flown from either side. All other required controls, such as power, flight, and trim controls, are situated on the center console within easy reach of either crew member. An important feature of the CRA is that, by the flick of an electrical switch, the same controls may be used for both helicopter and airplane modes.

This composite vehicle presents a unique feature; i.e., with the pilot seated on the right side as a helicopter pilot and with the copilot seated on the left as an airplane pilot, the controls are so arranged that both will feel equally comfortable in a familiar environment.

The general principle used for display and control location was to provide each crewman with displayed information directly before him and with controls readily available to him. Communication control panels are grouped on the center console. Personal controls for heating, cooling, rain removal, and intra-crew communication are located on a small side console. The following paragraphs discuss anthropometric adequacy and general control-display arrangements.

PILOT VISIBILITY

The analysis of pilot visibility is shown in Figure 176. The principal emphasis was placed on the extent of the visual angles available for the pilot's maximum safety and ease of navigation. In addition, during helicopter landings and takeoffs, maximum visibility for safety is again required. Given these visibility requirements, the vehicle was provided with a large flat-wrapped windshield and side panel. The use of flat-wrapped development, along with the large curvature of the intersections, provided the most distortion-free vision of all formed glass. The addition of windows in the lower nose section (below the flight station floor) enables the pilot to have as much visibility as he would in the average helicopter.

Page Intentionally Left Blank

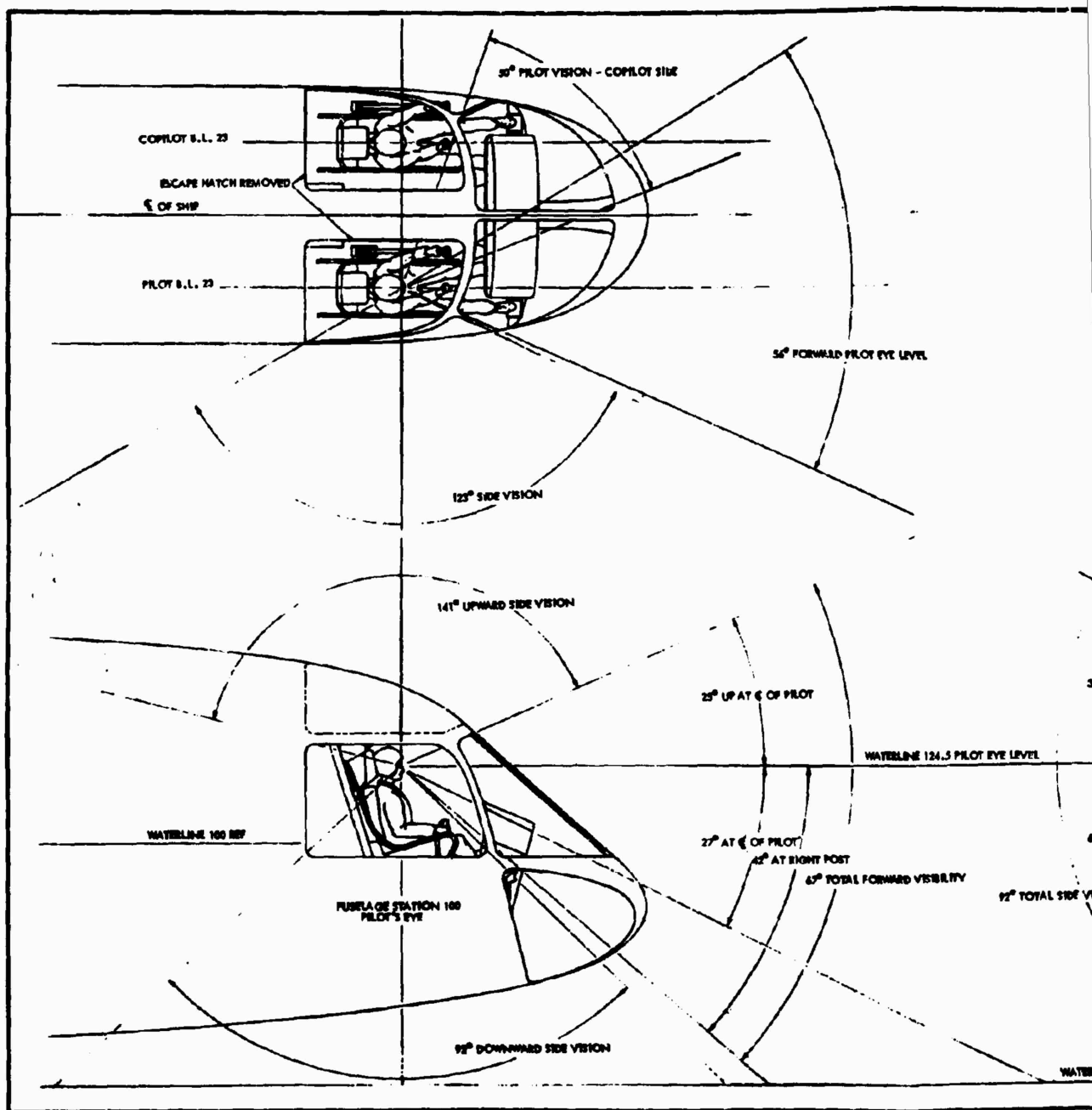
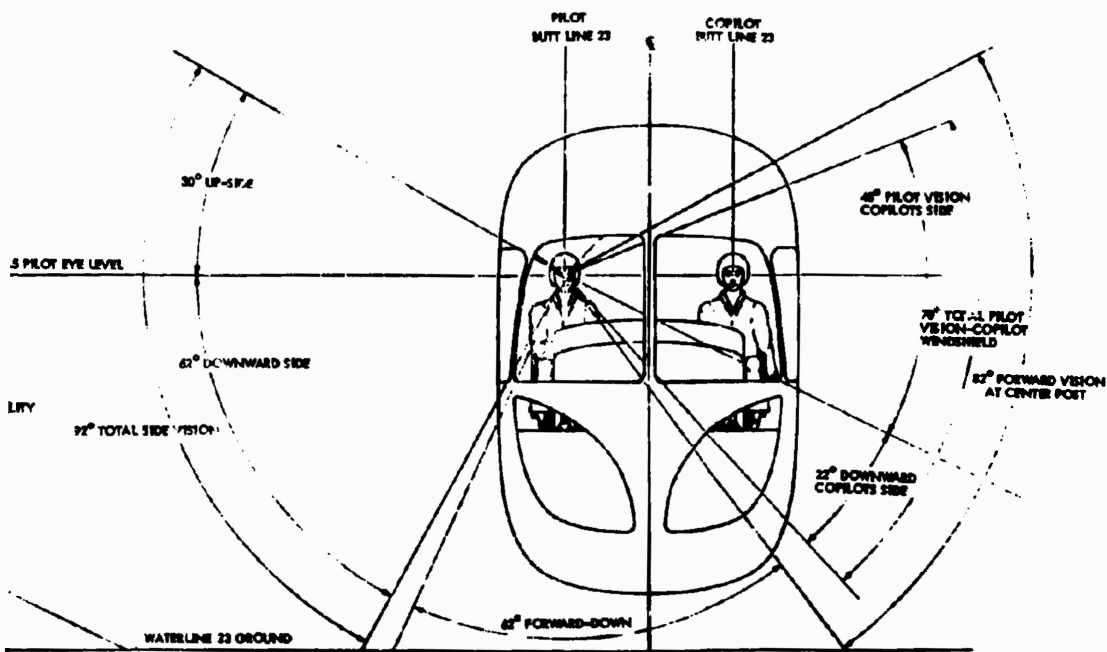


Figure 176. Flight Station Visibility Angles.



B

The intersection of the pilot's line-of-sight with the lower windshield was used to plot the shape of the instrument panel in order not to obstruct his vision. This is evident in the pictures of the mockup (Figure 177).

Every effort was made to provide maximum visibility. The seats were placed as far from the centerline of the aircraft as possible in order to place the crew members close to the side windows. The side windows play an important role, permitting an upward-viewing angle of 141 degrees, which enables the crew to check the rotor extension and blade indexing during transition from either helicopter or airplane flight modes.

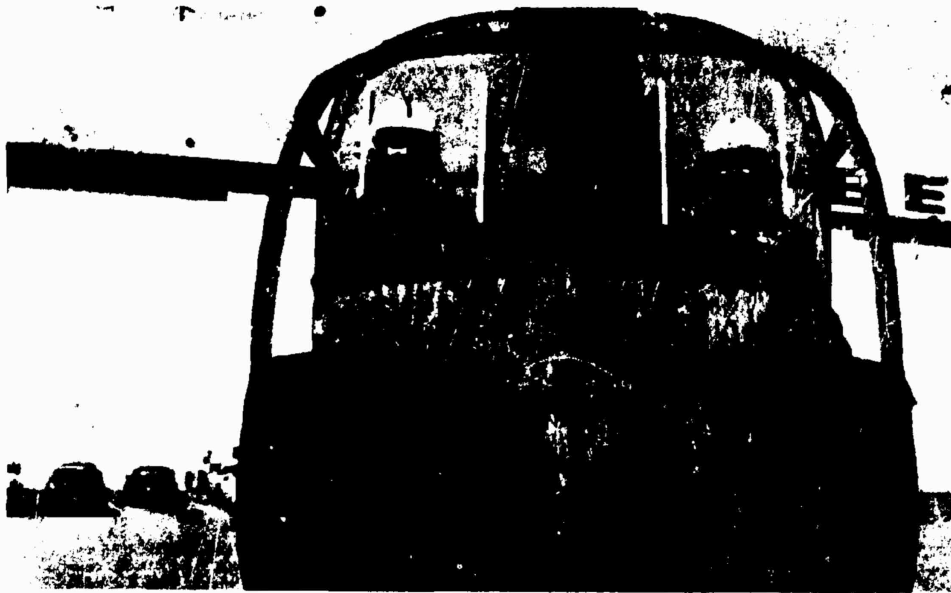


Figure 177. Mockup Visibility.

SECTION 20
FLIGHT STATION PROVISIONS

The flight station is separated from the mid-body or cargo compartment by a structural bulkhead located at Fuselage Station 131. Personnel access to the aircraft is by means of the cargo door and through the cargo compartment. Access to the flight station is through a door in the bulkhead.

The maximum width of the flight station is 82 inches, and the height at the entrance (from the flight station floor) is 6 feet 2 inches.

The design decisions relative to anthropometric adequacy are based on the criteria of MIL-STD-803A-1 (Human Engineering Design Criteria for Aerospace Systems and Equipment) and AS33575 (Dimensions, Basic, Cockpit, Helicopter). Reach distance to displays and controls conforms to the optimal manual area envelopes required for military aircraft.

INSTRUMENT PANEL

Figure 47 shows the overall picture of the instrumentation of the CRA vehicle. The main display is the instrument panel, which contains all the necessary flight and engine instruments for safe controlled flight. The details of this panel will be discussed in a following section.

Directly below the instrument panel and between the pilot and copilot is the center console, which contains the power and aircraft trim controls. It will be noted that this center console is slightly offset at the rear to provide better access to the pilot's seat. Above the center console, at the top of the windshield, a small overhead console is mounted. This console is hinged and remains in the up position until needed or serviced. Its basic purpose is to keep the emergency circuit breakers within easy reach of pilot or copilot.

The collective control lever is located at the left side of both the pilot and the copilot, and it has a small head containing three switches. Two of these switches control the prop governor during the helicopter mode. The remaining switch controls the flap. The control stick located at the C_L of the pilot contains the helicopter trim controls, which are deactivated when the vehicle is flown as an airplane. Small side consoles are included in the instrument panel layout and contain the personal controls of the crew.

Figure 178 gives a more detailed view of the actual instruments used. The "basic six" instruments are located in front of the pilot and are repeated on the copilot's side, so the vehicle can be flown and navigated from either seat. Engine displays are grouped in the center so that they can

be shared by both of the crew members. The two panels shown in phantom in the figure are for quick change during the first flight test phase.

The instrument panel is fully shock-mounted, and all instruments can be removed from the front of the panel. The panel is also hinged for easy maintenance. The center console, located between and within easy reach of both the pilot and the copilot, is shown in detail in Figure 179. With the exception of the trim controls on the collective and cyclic control sticks, all controls are located on this center console.

CONTROL-DISPLAY ARRANGEMENT

The general criteria used for arranging displays and controls were those of MIL-STD-25CB, "Cockpit Controls, Location and Actuation of, for Helicopters" (7 May 1964); MS33572, "Instrument, Pilot, Flight, Basic, Standard Arrangement for Helicopters"; MIL-STD-411B, "Aircrew Station Signals"; and MIL-STD-803A-1, "Human Engineering Design Criteria for Aerospace Systems and Equipment, Part 1, Aerospace System Ground Equipment".

Control Location

All controls of a like function are grouped together. Powerplant controls are numbered left to right and are arranged to correspond to the power plant with which they are associated. Controls are actuated in such a manner that conventional usage is the main actuating procedure (or actuation of controls in the same direction as the direction of flight). Provisions are made for cockpit instructions to be indicated in places where the information is relevant.

Displays Location

Wherever possible, displays are located along with applicable controls. As an example, the transition controls, which are used to convert from the helicopter to the airplane mode and vice versa, are located centrally on the center control console. The controls are arranged in sequence and are operated in sequence, either left to right to stow the rotor, or right to left to unstow the rotor. The displays showing the subsystem status are directly above their control, so the pilot will know exactly where he is in the sequence and, therefore, will be able to reverse the cycle at any point.

Displays which demand frequent monitoring or emergency action are located directly in front of the crew members. Displays which are infrequently monitored are located with the associated control, but not directly in front, to avoid distracting the pilot from more important information.

COPILOT FLIGHT INSTRUMENTS

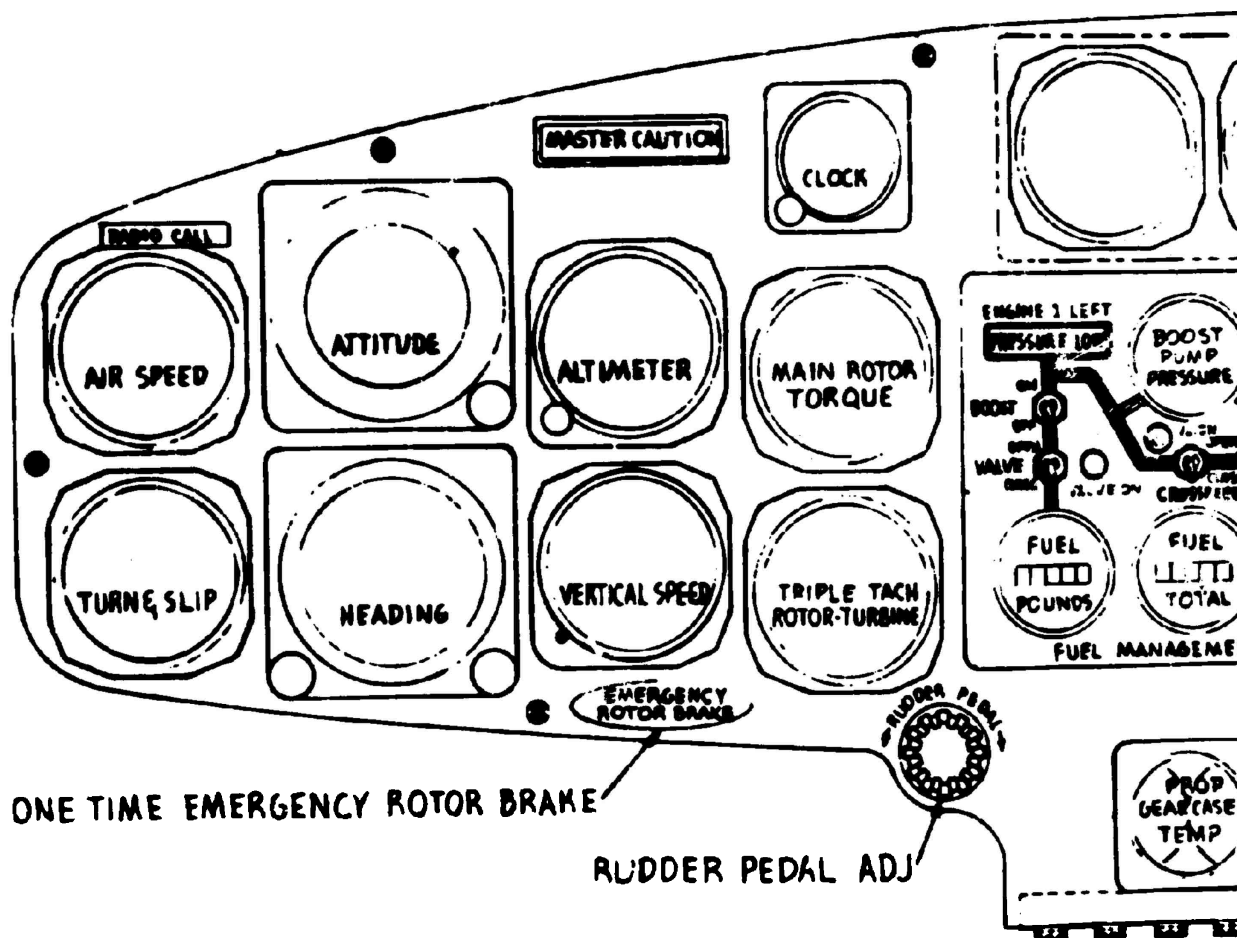
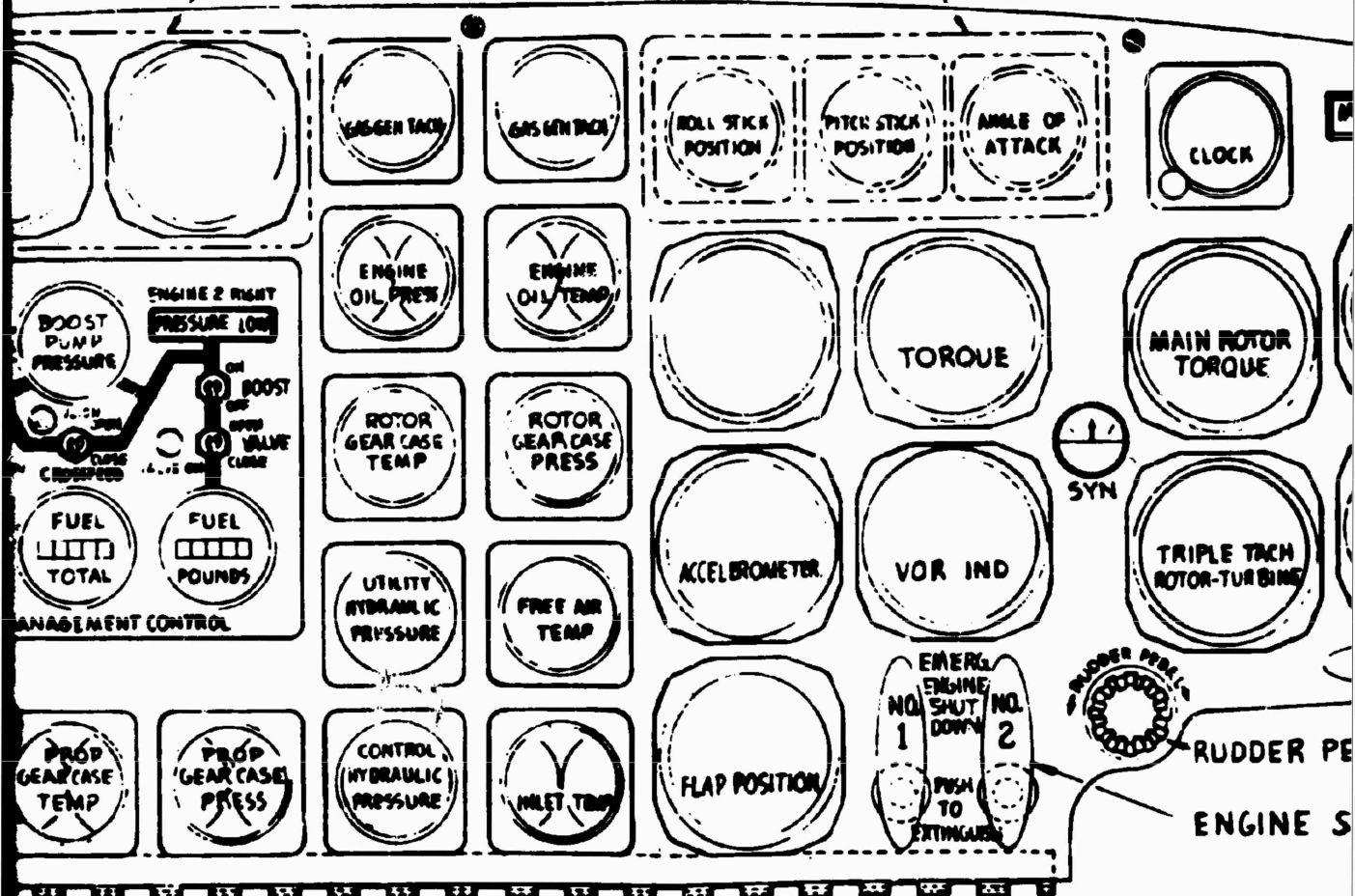


Figure 178. Instrument Panel.

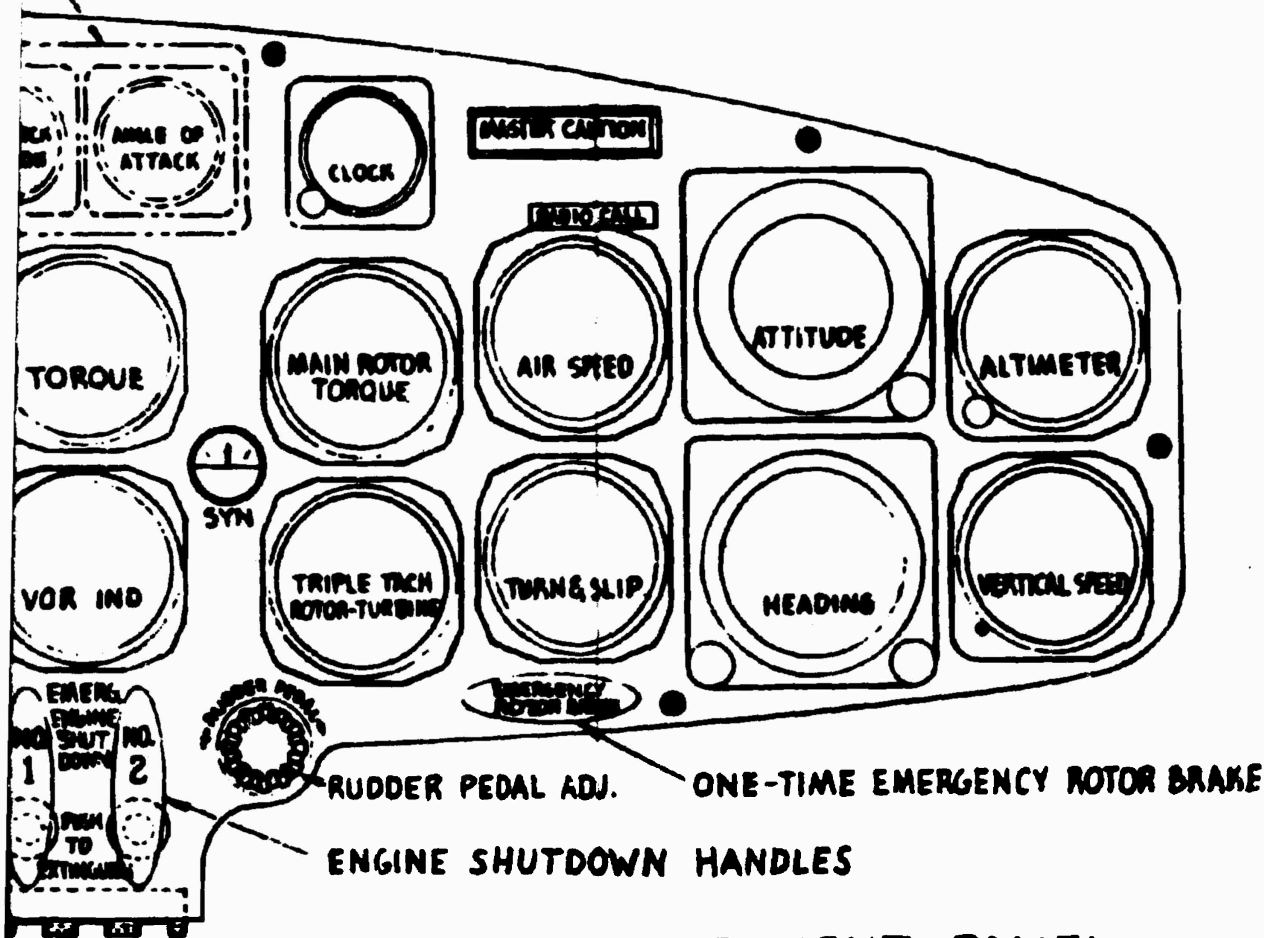
A

QUICK CHANGE PANELS FOR FLIGHT TEST



↑
OF SHIP

PILOT FLIGHT INSTRUMENTS



INSTRUMENT PANEL
1/2 SCALE

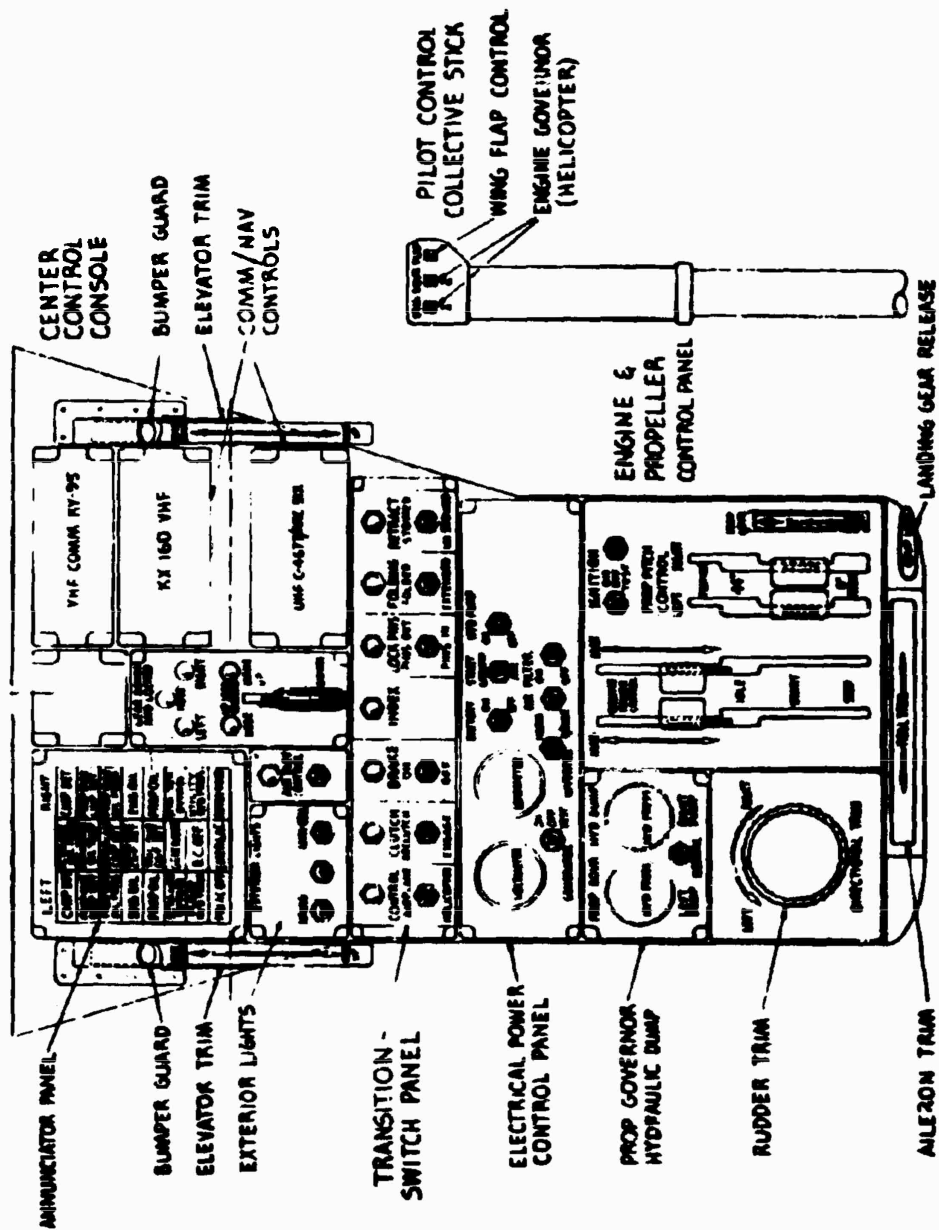


Figure 179. Center Control Console.

PART 10
AEROELASTICITY

SECTION 21
COMPOUND HELICOPTER FLIGHT

MAIN ROTOR AEROELASTIC STABILITY

The main rotor of the CRA is essentially a dynamically scaled enlargement of a 33-foot-diameter stopped-rotor system tested prior to November, 1964, Figures 180 and 181. Also see Reference 43. More recently, additional wind tunnel tests were conducted at the NASA 40-foot by 80-foot wind tunnel, Ames Aeronautical Laboratory, under Bureau of Naval Weapons Contract NOW 66-0246-f. (See Figure 182.)

Briefly, the 33-foot-diameter rotor system whirl tower tests were conducted for rotor rotational speeds varying from 0 to 400 revolutions per minute and thrust loadings varying from -500 to +7400 pounds, the latter representing a load factor of about 1.5. Induced fuselage rolling and pitching were varied from 0 to 32,000 inch-pounds. The rotor remained both stable and easily controllable during the entire course of whirl tower tests. There were no indications of marginal damping levels.

In the course of wind tunnel tests, the 33-foot stopped-rotor system was subjected to 54 start-and-stop sequences at various tunnel speeds up to 140 knots and at rotor angles of attack up to 12 degrees. These tests further bolstered the credibility of the stopped-folded-stowed rotor concept. Specific results obtained in the course of these tests are discussed in Section 22.

The basic dynamic characteristics of the CRA may be simply described in terms of a gyroscopic rotor, flexibly connected to the fuselage and slaved to a control gyroscope which receives feedback from the rotor and fuselage as well as control inputs from the pilot.

Several digital computer programs have been developed for the prediction of rotor stability levels as affected by rotational speed, collective blade angle, collective control stiffness, vehicle weight, and forward flight speed. One such program, comprising 229 degrees of freedom, is being used to analytically study the coupled cyclic and collective stability characteristics of the CRA. The fundamental importance of this program is that it accommodates dynamic coupling between cyclic and collective modes of the rotor and an anisotropic fuselage. With this large-order analytical description as the basis, investigations of various aeroelastic phenomena are conveniently accomplished by excerpting appropriate descriptions of a reduced order; that is, only those degrees of freedom which are necessary to adequately define a specific aeroelastic phenomenon are retained. In some cases, the order is further reduced by modalization. The modal shapes generally used for this purpose are those illustrated in Figure 183.



Figure 180. Whirl Tower Installation of
33-Foot-Diameter Stopped-Rotor Model.

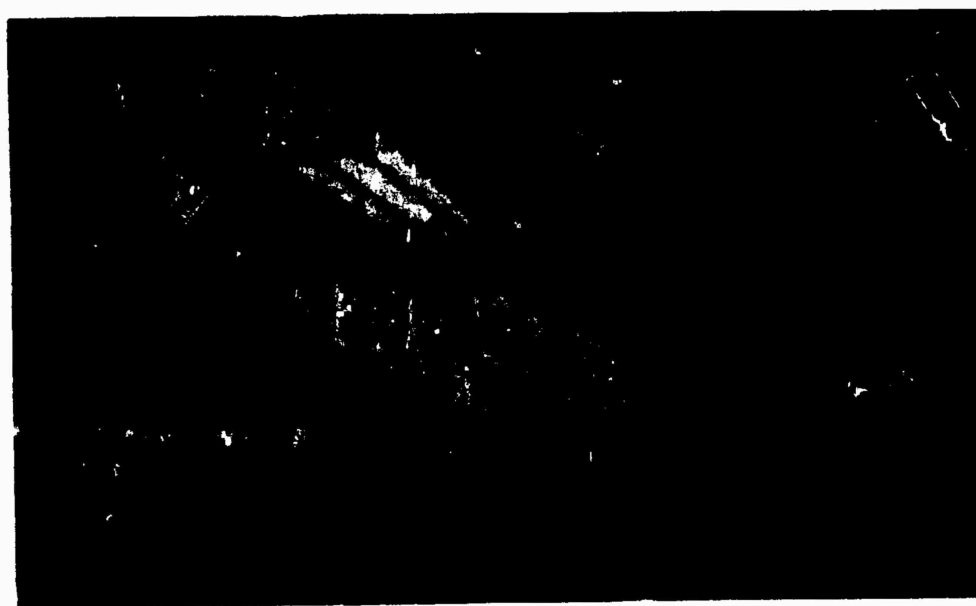
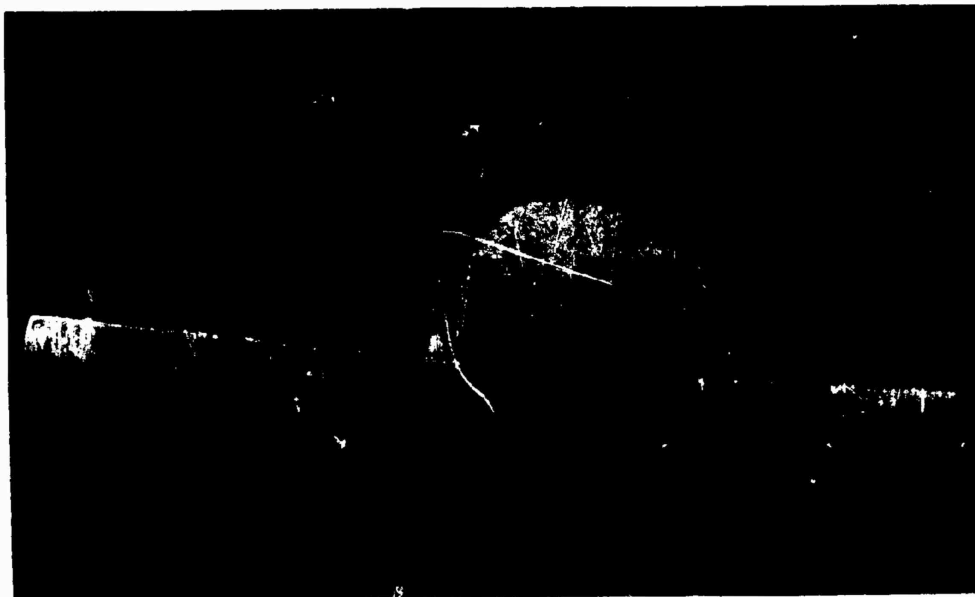


Figure 181. View of 33-Foot-Diameter Stopped-Rotor Model with Blades Folded.

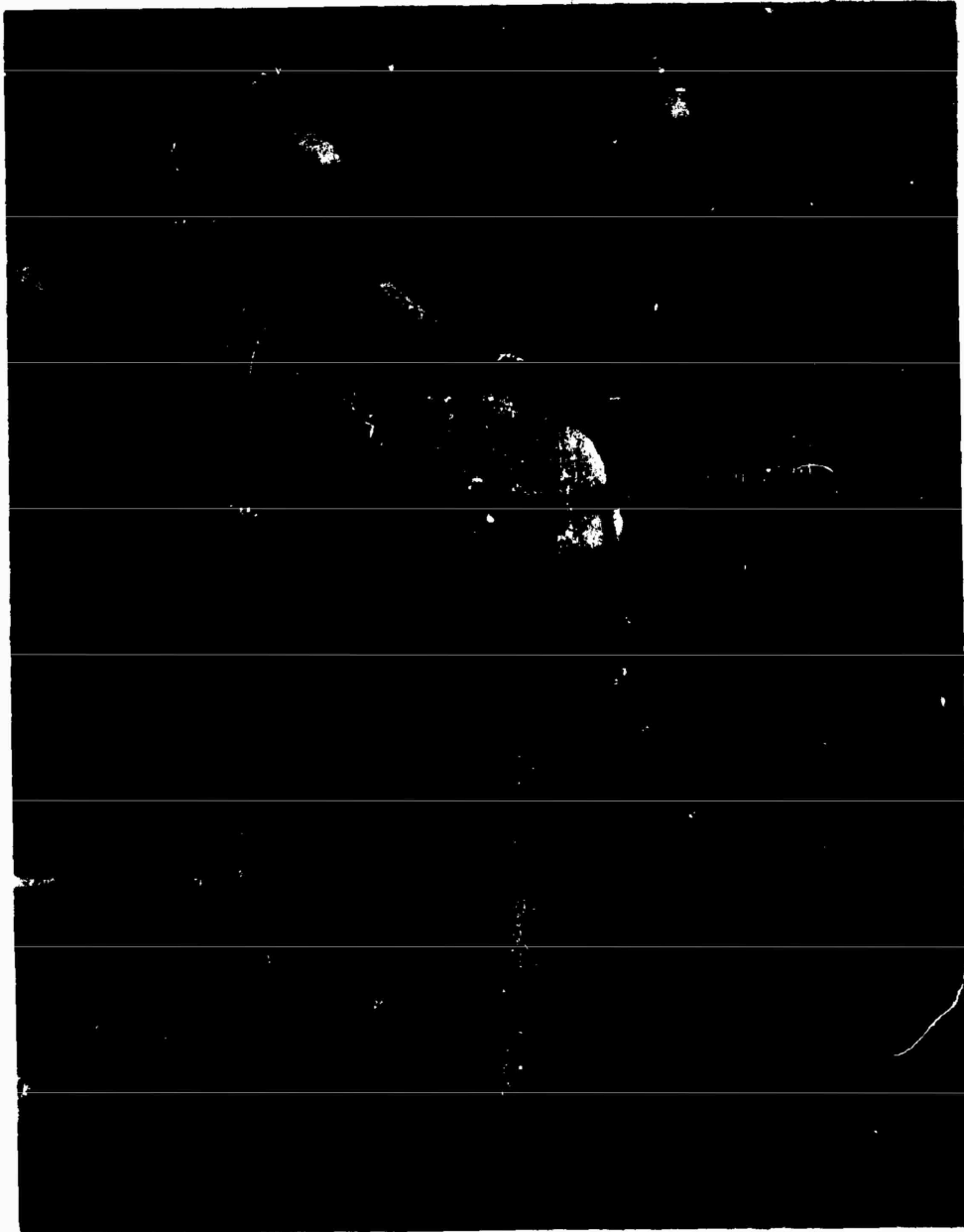


Figure 182. Ames 40 x 80-foot Wind Tunnel Installation of 33-Foot-Diameter Stopped-Rotor Model.

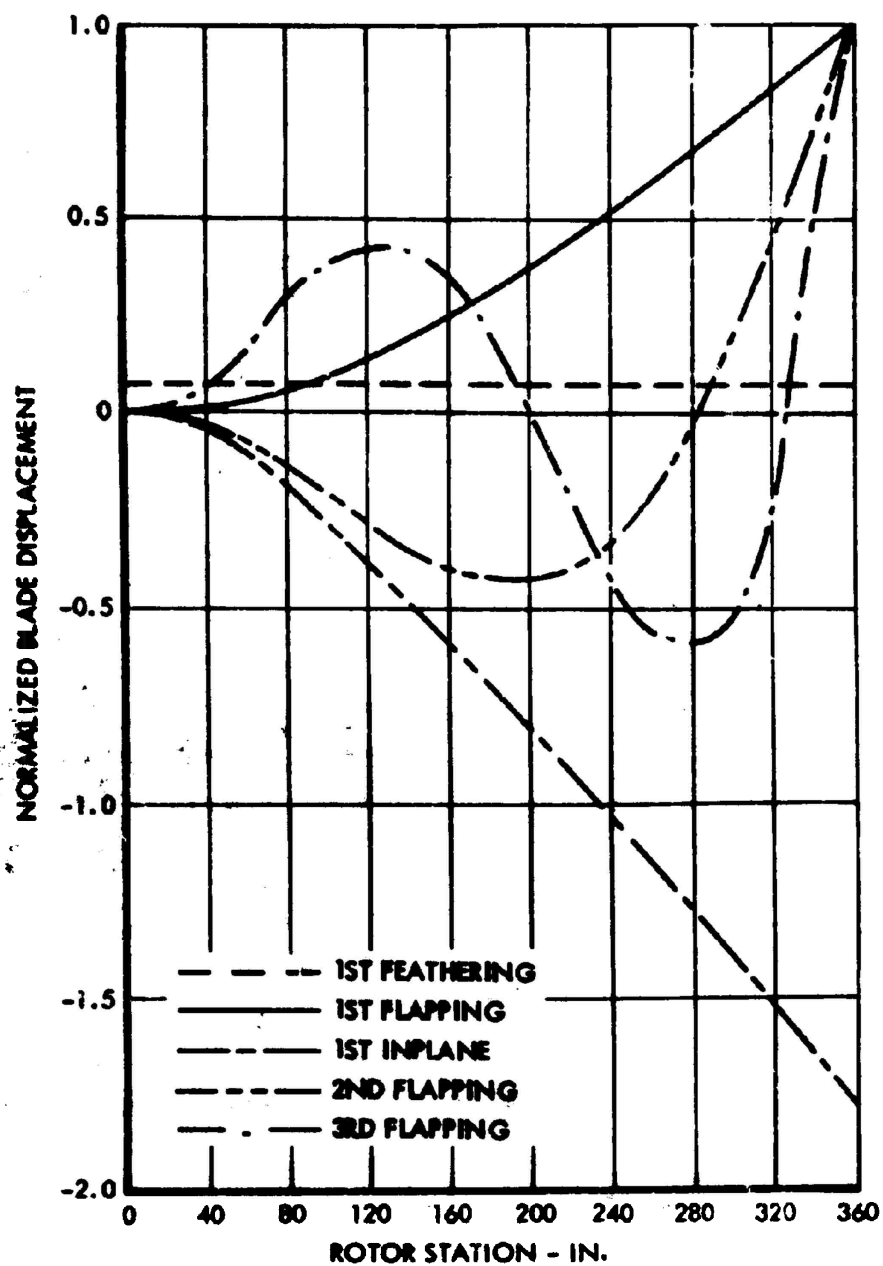


Figure 183. Mode Shapes Used for Modalization Analyses.

The cyclic stability of gyro-controlled, rigid-rotor systems is achieved primarily by the selection of a control gyro size and gearing ratio which is compatible with blade sweep and rotor power loading. Likewise, collective stability is achieved by providing for adequate collective control stiffness. The stability of advance rotary modes of rigid rotors is effectively controlled by proper selection of gyro cant angle and blade sweep and droop. The possibility of high-frequency blade flutter is precluded by providing for adequate frequency separation and a chordwise center-of-gravity distribution which is virtually on the blade quarter-chord in the outboard region of the blade.

HIGH-SPEED GYRO CHARACTERISTICS

The CRA rotor will be controlled by a high-speed gyro; that is, by a gyro whose spin speed, Ω_G , is considerably greater than that of the rotor, Ω . This is a departure from gyro systems incorporated in previous gyro-controlled rigid-rotor helicopters, but it can be shown that the high-speed gyro system provides the regressive once-per-revolution natural frequency characteristics essential to the function of the rotating swash plate. The high-speed gyro system will also produce a very high frequency "wobble" which will be of an advancing mode at $(2\Omega_G - \Omega)$ per revolution if the gyro is spun in the same direction as that of the rotor; otherwise, it will be of a regressive mode at $(2\Omega_G + \Omega)$ per revolution. These latter high-frequency characteristics are extraneous, since they are very easily damped with low swash plate damping and do not interfere at all with the gyro stabilization function. For the conventional gyro systems, with $\Omega_G = \Omega$, gyro nutation or "wobble" occurs at twice-per-revolution, and even at this frequency it is easily damped.

In the case of the high-speed gyro system, a desired rate of precession can be achieved using a gyro whose moment of inertia is proportionately lower than its spin speed, so that a much lighter gyro is possible. The high-speed gyro system is desirable from an aerodynamic standpoint also, since it may be conveniently concealed within the bounds of the fuselage.

TAIL ROTOR AEROELASTIC STABILITY

The CRA employs a universally mounted four-bladed tail rotor which will permit cyclic teetering motions during forward flight in the compound-helicopter mode. During flight transitions, however, the tail rotor will be restrained at reduced angular speeds in order to preclude excessive teetering angles and attendant high loads. The four-bladed tail rotor does not require the high support stiffness or damping which would be required to assure the mechanical stability of a two-bladed tail rotor. Furthermore, the oscillating loads which filter into the stationary fuselage structure through a four-bladed tail rotor are substantially lower than those which could be attained with a two-bladed tail rotor.

MECHANICAL STABILITY

The CRA rotor system, which has no lead-lag hinge, provides for a fundamental in-plane bending frequency that is well above once per revolution throughout the entire operating range (Figure 150). Rotors possessing this characteristic are frequently referred to as supercritical rotors, since they are completely free of so-called ground resonance phenomena without a requirement for mechanical damping in the blades or landing gear. In essence, ground resonance is a mechanical instability resulting from self-excited oscillations of the rotor-fuselage system. More specifically, ground resonance results from adverse coupling of blade inplane motions with a fuselage frequency. This phenomenon can occur only if the in-plane frequency of the blade is less than once per revolution.

VIBRATION

While operating in the compound helicopter mode, the CRA will respond to aerodynamically induced harmonic excitations associated with the rotors. Of course, the higher flight speeds of the CRA will be accompanied by substantial reductions in collective and cyclic blade angles, due to the transfer of lift from the rotor to the wing and use of the propellers to produce virtually all of the required thrust. Consequently, aerodynamic excitation of the main rotor at high flight speeds will be markedly less than would be associated with a pure helicopter at the same flight speeds, and there will be correspondingly lower blade cyclic loads and aircraft vibration levels.

Forced vibratory response of the CRA fuselage will occur predominantly at the three-per-revolution (3P) frequency characteristic of a three-bladed rotor system. Additional vibration will be induced by the 2P advancing and 4P regressive response of the main rotor to aerodynamic harmonic excitations. Therefore, the proximity of the main rotor blade frequencies to these harmonics and the proximity of the fuselage natural frequencies to 3P are important factors in ascertaining fuselage vibration levels. The effects of tail rotor and propeller excitations, which occur at considerably higher frequencies, will be highly localized by comparison.

BLADE FREQUENCY SPECTRUM

Minimized rotor response to aerodynamic harmonic excitations has been achieved by tailoring the design of the main rotor to provide for adequate separation from these excitations.

The reduction in cyclic aerodynamic excitation which accompanies the higher forward flight speeds limits the range of collective angles that have to be considered to assure adequate separation of blade natural frequencies from the aerodynamic excitation frequencies.

The natural frequencies of the main rotor blades were computed using a detailed description of the mass and stiffness properties. A 27-element

description was used to analyze the system, incorporating coupled bending in the flapwise and chordwise directions and torsion. The natural frequencies were computed at rotor speeds of 0, 50, 100, 150, 200, 239, and 265 rpm at a collective angle of 10 degrees. To study the effect of collective angle variations on frequencies, solutions were also obtained at collective angles of 0, 5, 10, and 15 degrees. Figure 150 summarizes the results of these analyses and indicates the separation of the various modes from the integer multiples of the rotor speed. It can be seen that the first flapping frequency is about 1.27 per revolution. The stiffness characteristics that affect this mode are dictated by the static divergence and rotor stiffness requirements. The second flapping frequency at operating rotor speed is approximately 3.6P, which assures minimum response to 3P and 4P excitations. The third flapping and the first torsion mode are above 5P at operating rotor speed and thus are of minimal interest.

Mode shapes obtained from the frequency analyses are presented in Figures 184, 185, and 186. Negligible torsional participation accompanied the first three modes; thus, these figures do not display torsional displacement.

The effect of collective angle variation on blade frequencies is shown in Figure 187. In the range of interest, the blade frequencies maintain adequate separation from excitation harmonics.

Vibration characteristics of the tail rotor depend on the success with which certain multiples of rotor speed are avoided in the rpm and collective angle ranges of operation. The flapwise stiffness characteristics dictated by static divergence considerations place the flapping frequencies higher than those of conventional helicopters.

Frequency separation from 2P aerodynamic excitation for both reactionless symmetric flapping and in-plane modes must be assured. Due to the stiff blade design, the second antisymmetric flapping mode is well above 3P. High torsional stiffness has been obtained in the blade, and a compatible control stiffness for both the cyclic and the collective mode will provide a flutter-free tail rotor design.

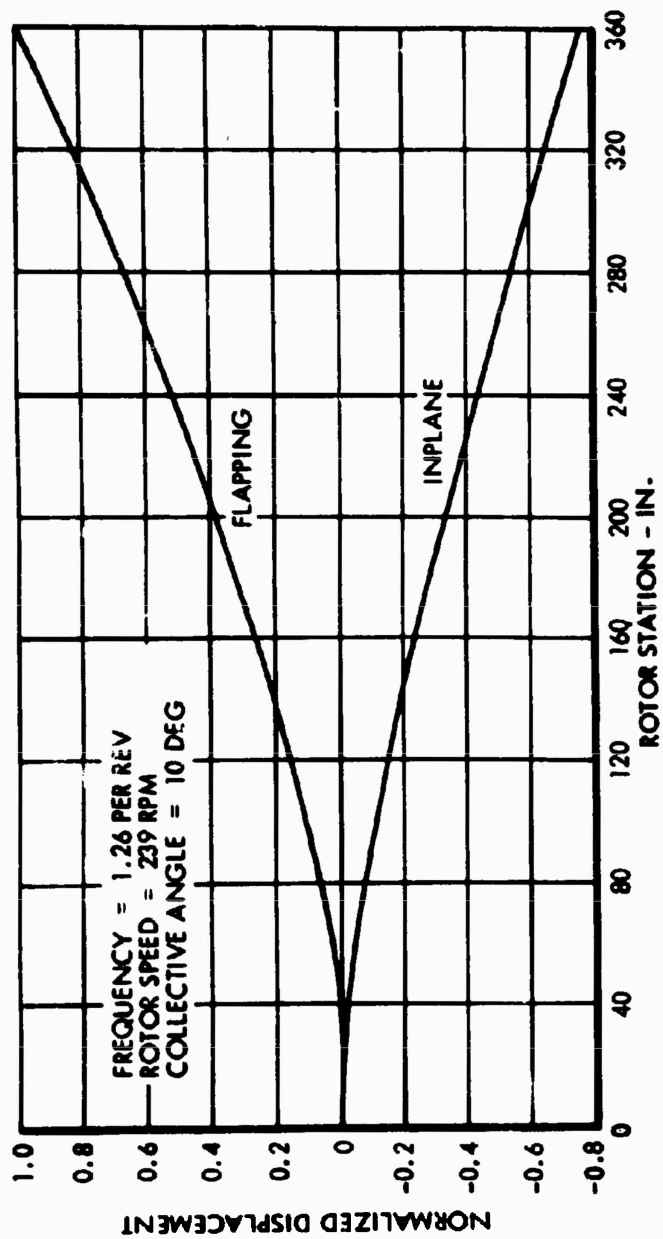


Figure 184. Main Rotor First Coupled Mode - CRA.

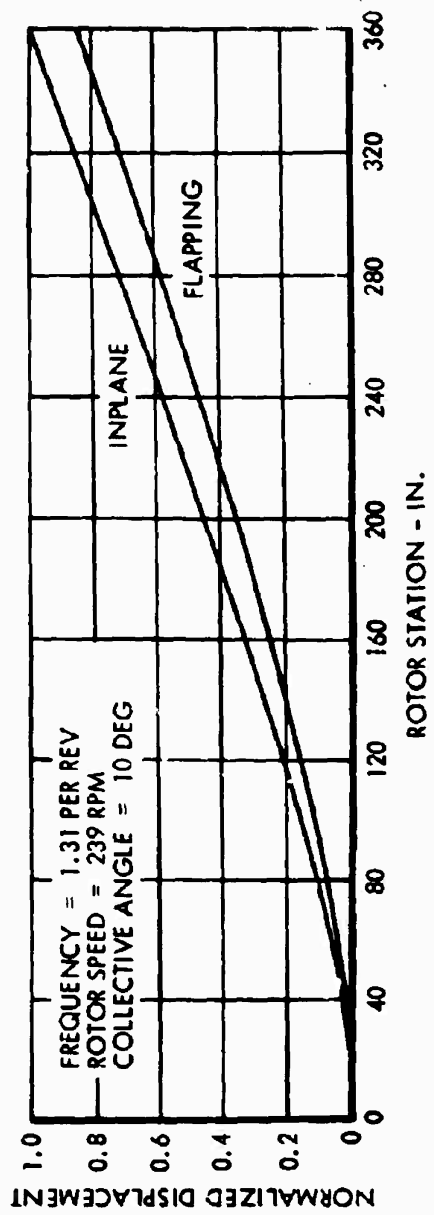


Figure 185. Main Rotor Second Coupled Mode - CRA.

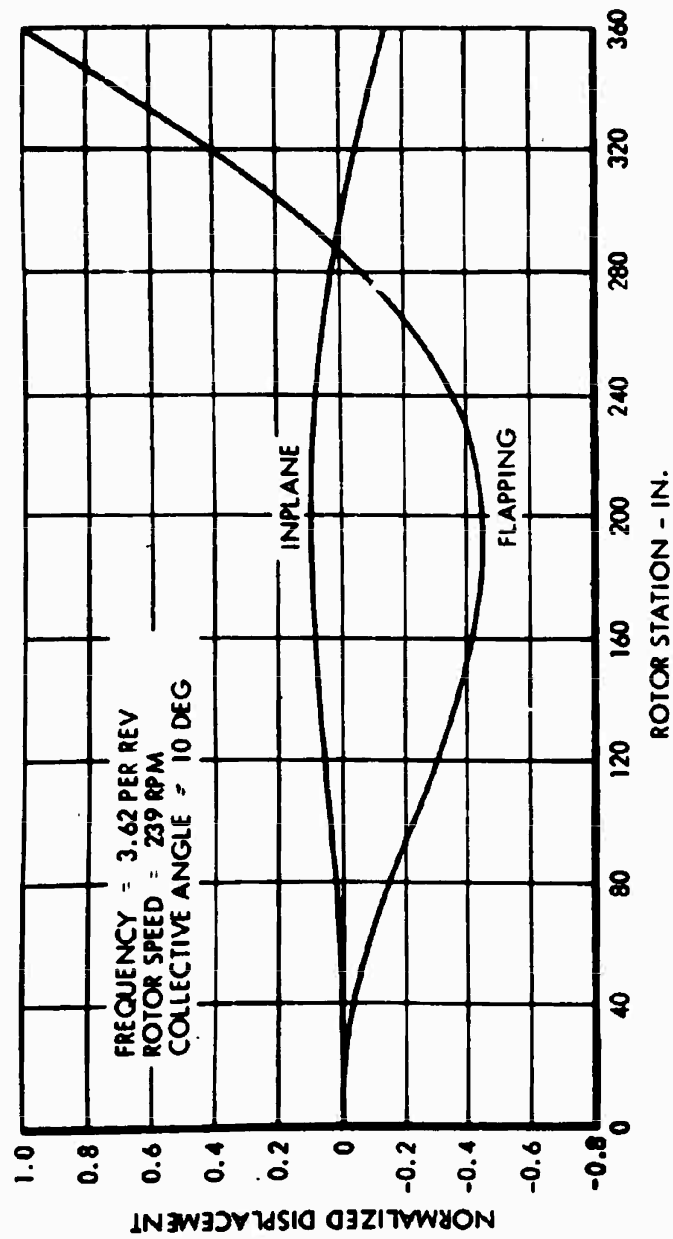


Figure 186. Main Rotor Third Coupled Mode - CRA.

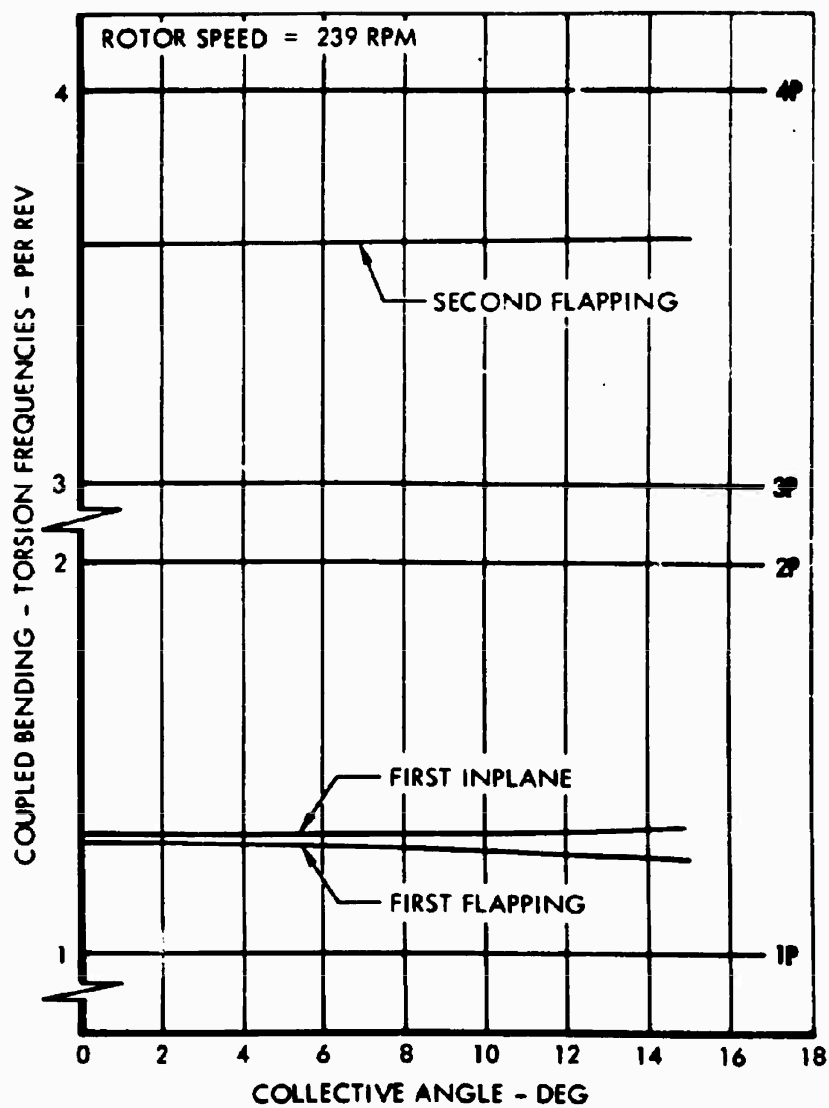


Figure 187. Main Rotor Frequency Variation with Respect to Collective Angle - CRA.

SECTION 22

TRANSITIONAL FLIGHT

At about 130 knots, the design speed for flight transition, the CRA will maintain lift for level flight completely on the wing. The untwisted rotor blades will be at virtually zero collective angles, and the rotor will be trimmed at zero rotor angle of attack. Under these ideal conditions, as the rotor is allowed to decelerate and is braked to a stop, no appreciable aircraft excursions would be anticipated. With the rotor thus stopped and stowed, the CRA will be in an essentially conventional airplane mode of flight and will exhibit stability and control characteristics similar to those of fixed-wing aircraft (References 44 and 45).

The foregoing discussion briefly described the transitional events normally expected. However, gust disturbances during transitions must also be considered. At the higher rotor angular velocities, the free-feathering gyro-stabilized rigid rotor is relatively insensitive to gusts. At the low rotor angular velocities and high advance ratios which prevail during rotor starts and stops, the authority of the gyro is gradually supplanted by a rotor blade pitch-bias system which provides for stability characteristics similar to those evidenced at high angular velocities.

MAIN ROTOR AEROELASTIC STABILITY

Under Bureau of Naval Weapons Contract NOW-66-0246-f, a program for investigating the transitional characteristics of a 33-foot-diameter stopped-rotor system was recently conducted at the NASA 40-foot by 80-foot wind tunnel, Ames Aeronautical Laboratory. A photograph of the test installation is shown in Figure 179. Briefly described, the test article is a relatively stiff three-bladed rigid rotor incorporating special systems for in-flight stopping, starting, and folding, and mounted on an inertia frame which is enclosed with a body shell to simulate aerodynamic characteristics.

In the course of the program, the 33-foot-diameter rotor system was subjected to 54 start-and-stop sequences at various tunnel speeds and rotor angles of attack. The number of start-and-stop sequences accrued at particular combinations of tunnel speed and rotor angle of attack are enumerated in Table XXVII.

The dearth of start-and-stop sequences represented at the higher tunnel speeds was primarily occasioned by the excitation of certain resonant frequencies of the wind tunnel support system. Most apparent was a lateral mode of the main support struts which was excited at a rotor rotational speed of about 110 revolutions per minute. This condition is indicated by a dilatation of the time-history envelopes presented in Figures 188, 189 and 190. The magnitude of the response to resonant modes of the wind tunnel support system was augmented by the inability of the model drive

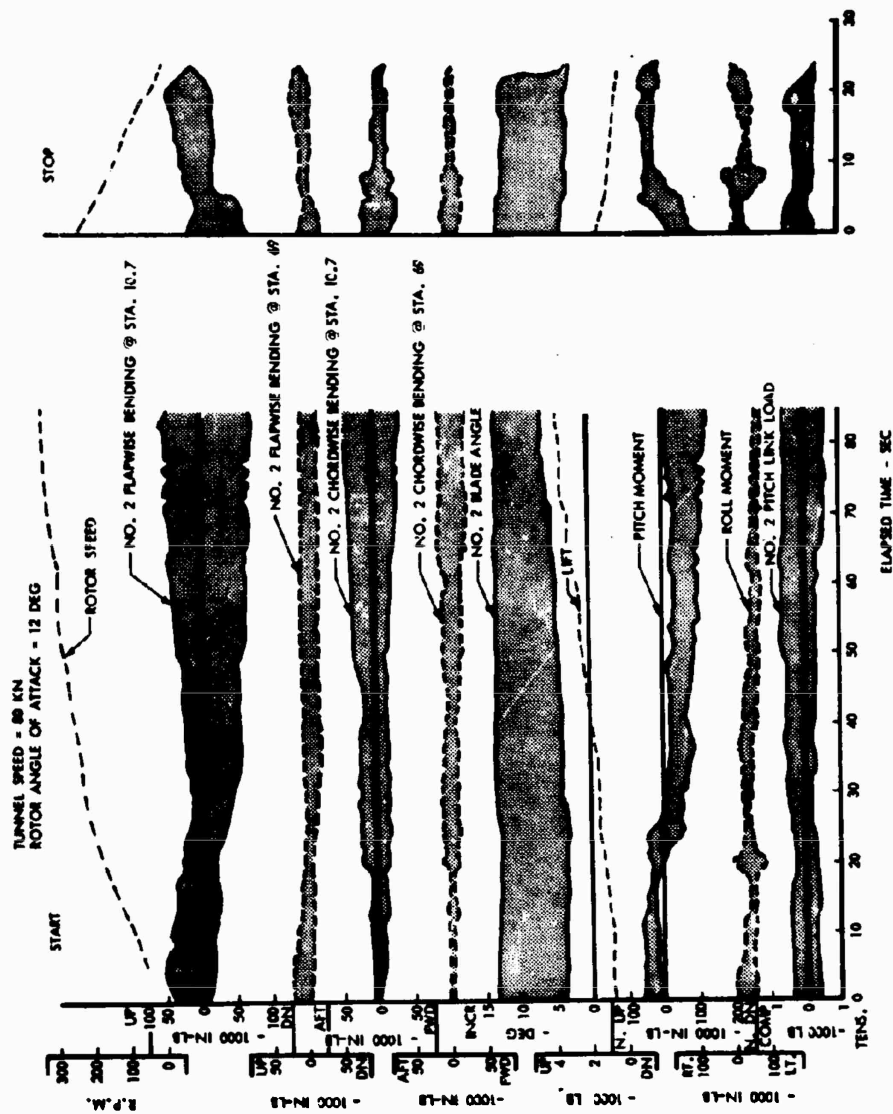


Figure 188. Time History of Stop-and-Start Sequence for 33-Foot-Diameter Rotor at 80 Knots

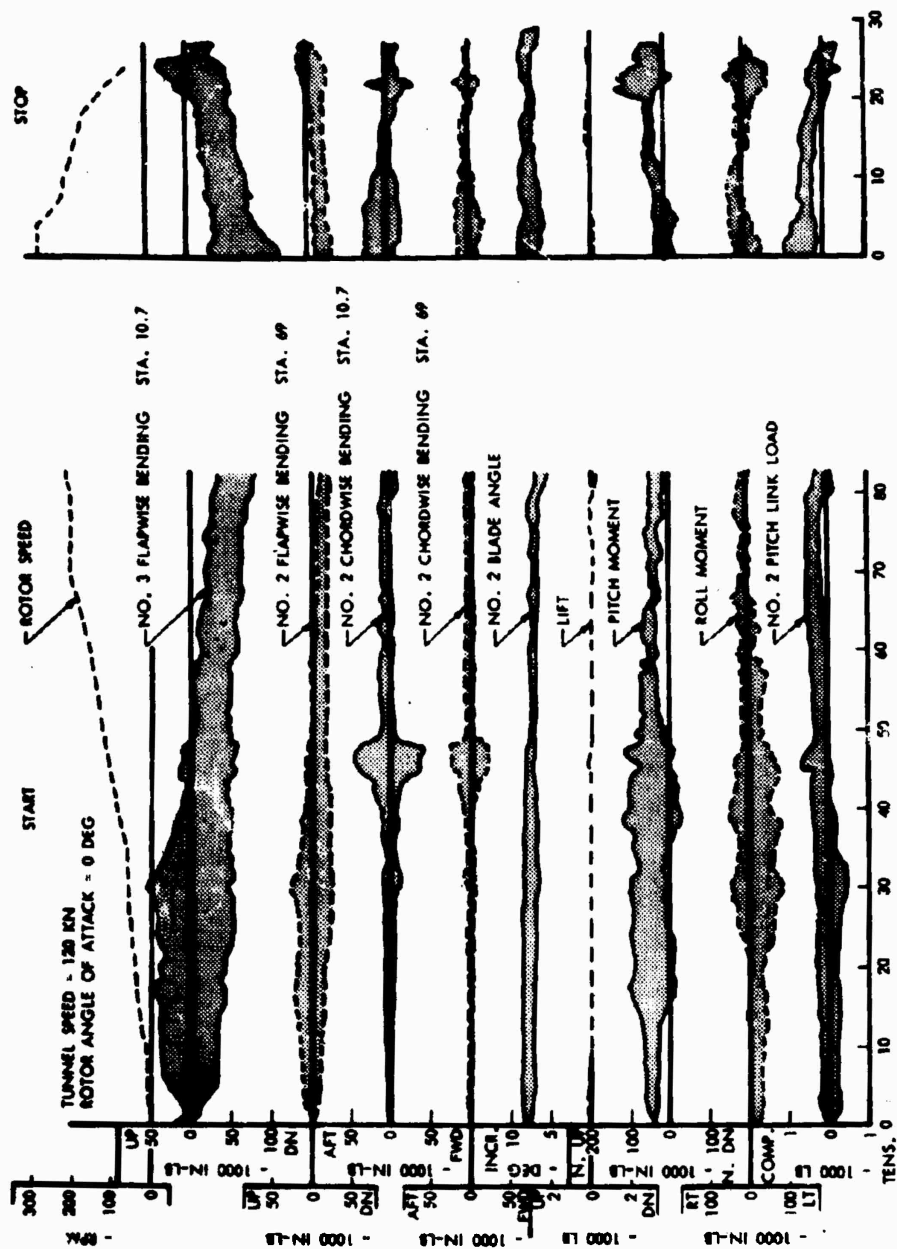


Figure 189. Time History of Stop-and-Start Sequence for 33-Foot-Diameter Rotor at 120 Knots.

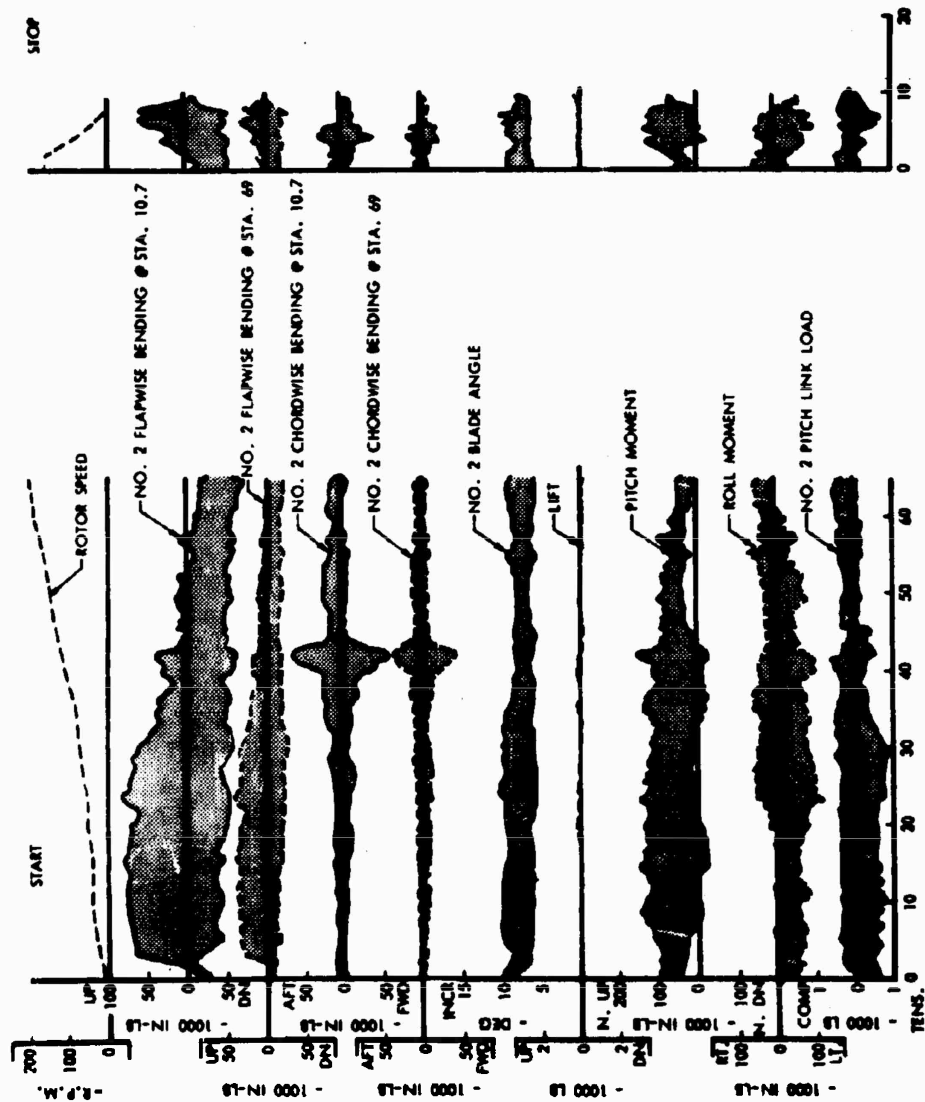


Figure 190. Time History of Stop-and-Start Sequence for 33-Foot-Diameter Rotor at 140 Knots.

TABLE XXVII. START/STOP SEQUENCES VS TUNNEL-SPEED/ANGLE-OF-ATTACK						
Rotor Angle of Attack (degrees)	Tunnel Speed (knots)					
	40	80	100	120	130	140
0	2	8	3	6	1	1
2		3	1	3		
3		7				
4		3	1			
6		10	1			
8		1				
9		1				
10		1				
12		1				

system to accelerate the rotor rapidly through the resonant frequencies. Deceleration through these resonant frequencies, as the rotor was braked to stops, was relatively rapid, and the duration and magnitude of response were diminished accordingly. Conversely, resonant modes of the support system would be expected to cause less interference during starting sequences if the acceleration capability of the rotor drive system were enhanced. Although additional accelerating torque can be obtained in autorotative states, the autorotation must, of course, be accomplished with a well-trimmed rotor if it is to be used to alleviate the resonance problem.

ROTOR CONTRIBUTION TO AIRCRAFT STABILITY

It has been demonstrated that a blade pitch-bias system of the basic type to be installed in the CRA can virtually eliminate unstable contributions of the rotor to overall aircraft stability (Reference 33). Stopping and starting time-history investigations were conducted both in a low-speed wind tunnel and in the NASA 40-foot by 80-foot wind tunnel on models dynamically similar to the CRA. The results of such stopped-rotor tests can be applied to a wide range of stopped-rotor vehicles by dynamic scaling. Although certain stability characteristics of the CRA could be approximated by such dynamic scaling, the results obtained therefrom would not reflect the most advanced stopped-rotor technology so far developed. For example, the aerodynamically stabilized blade pitch-bias system of the dynamic models has been significantly improved upon for application to the CRA. However, in order to provide some indication of how the CRA would be expected to respond during stopping sequences, the results obtained from the recent wind tunnel tests of the 33-foot-diameter stopped-rotor vehicle will be discussed. Some important properties of this vehicle are summarized in Table XXVIII.

TABLE XXVIII. SIGNIFICANT PROPERTIES OF 33-FOOT-DIAMETER STOPPED-ROTOR VEHICLE

Number of Blades	3
Blade Chord (in.)	24.00
Rotor Diameter (in.)	336.0
Approximate Weight (lb)	1000.0
Rotor Design Tip Speed (fps)	613.4
Rotor Rotational Speed (rpm)	355.0

The aircraft handling qualities during transition are derivable in terms of the vertical and angular accelerations of the fuselage which are induced by rotor loads transmitted through the shaft. Figure 191 compares rotor pitching and rolling moments, undergone during starts, with 30 percent of the available aerodynamic control power planned for the 33-foot stopped-rotor flight article. These results show that the elevator and aileron control power levels far exceed the fuselage pitch and roll moments produced by the rotor during rotor starts and stops. It should be emphasized, however, that the aforementioned figures are included solely for the purpose of giving some indication of the trends that may be anticipated during transitional flight of the CRA.

The actual schedule of the rotor blade pitch-bias system operated off-design during the course of the tests conducted at the higher tunnel speeds. The optimum swash plate schedule was realized at about 80 knots. The blade pitch-bias system provided for good response characteristics in the course of tests conducted at a tunnel speed of 80 knots, even at a rotor angle of attack of 12 degrees. Although the excursions seemed large, they were merely the result of the large cyclic blade pitch-angle variation required to trim the rotor at the designated test condition. The steady loads are low. The response to resonant modes of the main support struts are hardly apparent, which may be attributed to both the low level of steady rotor loads and the more rapid acceleration of the rotor at the designated test condition. These general characteristics were attained at all rotor angles of attack at 80 knots.

To ascertain the effectiveness of the blade pitch-bias system, a start-stop was made at 80 knots and a rotor angle of attack of 3 degrees, with the blade bias system inoperative. The levels of rotor response with the bias system operative were two-thirds those obtained with the swash plate fixed. In both cases, loads were low; but at higher speeds and larger angles of attack, the bias control would be expected to be more important.

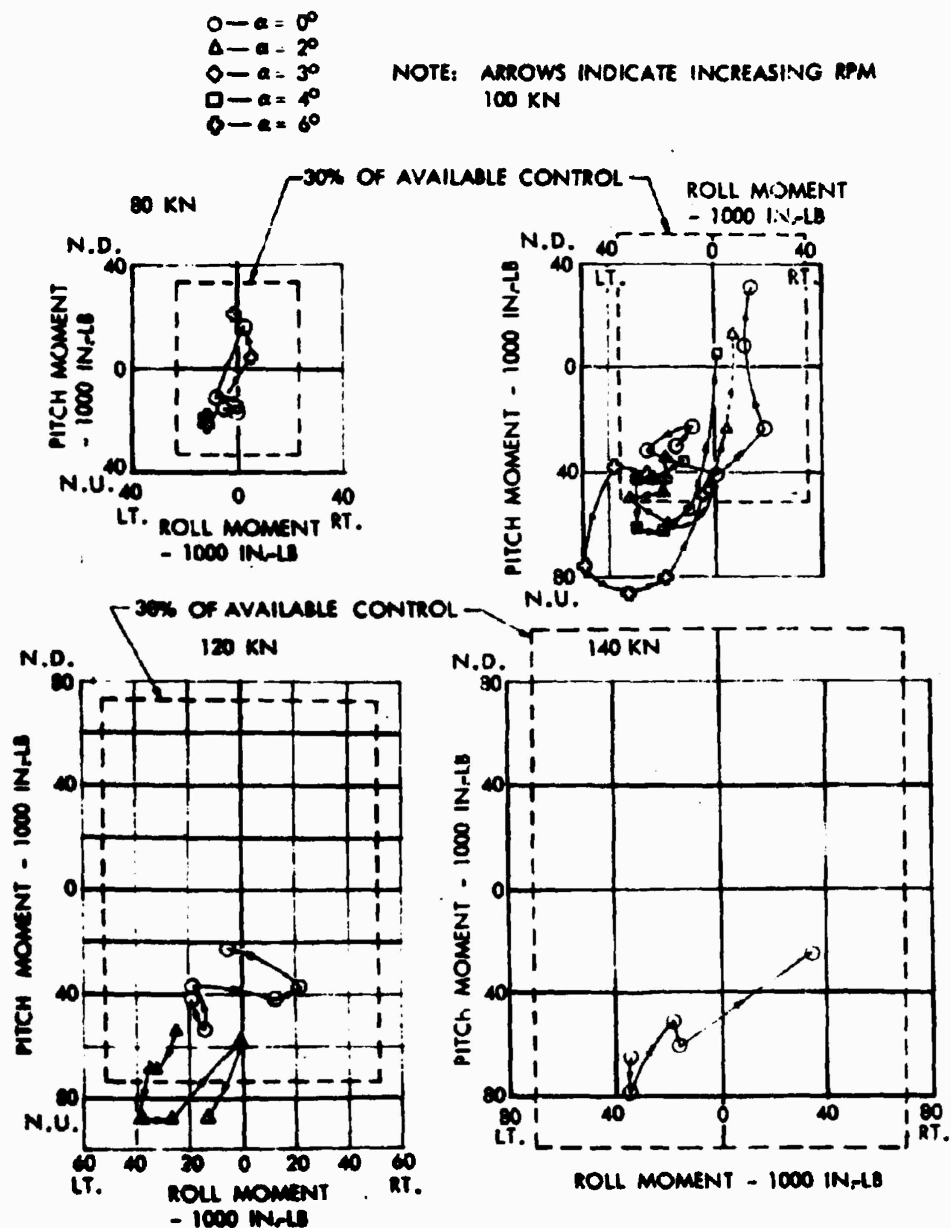


Figure 191. Rotor Moments During Start Sequences of 33-Foot-Diameter Rotor-System at Several Speeds.

SECTION 23
STOPPED-ROTOR FLIGHT

The main rotor stopping procedure will be performed with the rotor virtually unloaded, and it will be initiated by disengaging the main and tail-rotor drive systems. For a period of approximately 20 seconds, the rotors will be allowed to decelerate aerodynamically, but final stopping and indexing will be accomplished with a brake-and-detent system which will require an additional 15 seconds.

Once the rotors are stopped, the principal factors which must be considered are static aeroelastic stability of the rotor systems and aircraft handling qualities.

MAIN ROTOR AEROELASTIC STABILITY

The experimental program regarding transitional characteristics of the 33-foot-diameter stopped-rotor system included investigation of the static aeroelastic characteristics of the rotor as affected by rotor indexing, forward velocity, rotor angle of attack, and collective blade angle. Figure 192 summarizes some of the more severe loading conditions investigated. Figures 193 and 194 illustrate a variety of effects of variations in tunnel speed, rotor angle of attack, and blade collective angle. While the ultimate blade distortion due to the aerodynamic loading is a function of the initial angle of attack, in general, the divergence speed is not. (As discussed later, the divergence characteristics of a blade near an azimuth position of 180 degrees constitute an exception.) Specifically, static blade divergence corresponds to a physical condition where the increment in aerodynamic loading, due to an arbitrary change in angle of attack, is equal to the corresponding increment in elastic restoring moment. It is apparent from Figures 192 and 193 that, in general, both the highest aerodynamic loadings and the largest increments in aerodynamic loadings occur at an azimuth position of about 120 degrees. But it is also apparent that for small angles of attack, the divergence characteristics at about 225 degrees are virtually identical to those at 120 degrees; although for corresponding increases in angle of attack at the two azimuth positions, the azimuth position of 225 degrees actually becomes less critical as a consequence of earlier stalling of the blade in reverse flow. Nevertheless, for analytical purposes, a blade azimuth position of 225 degrees has generally been assumed to be most critical since - from a purely theoretical point of view - the streamwise angle of attack, due to flap-bending at this position, is augmented by the increased torsional deflection resulting from a larger offset of the line-of-aerodynamic-centers relative to the blade structural axis. What is more important, however, is that an analysis of the divergence stability of the blade at an azimuth position of 225 degrees actually results in a conservative estimate of the blade divergence speed.

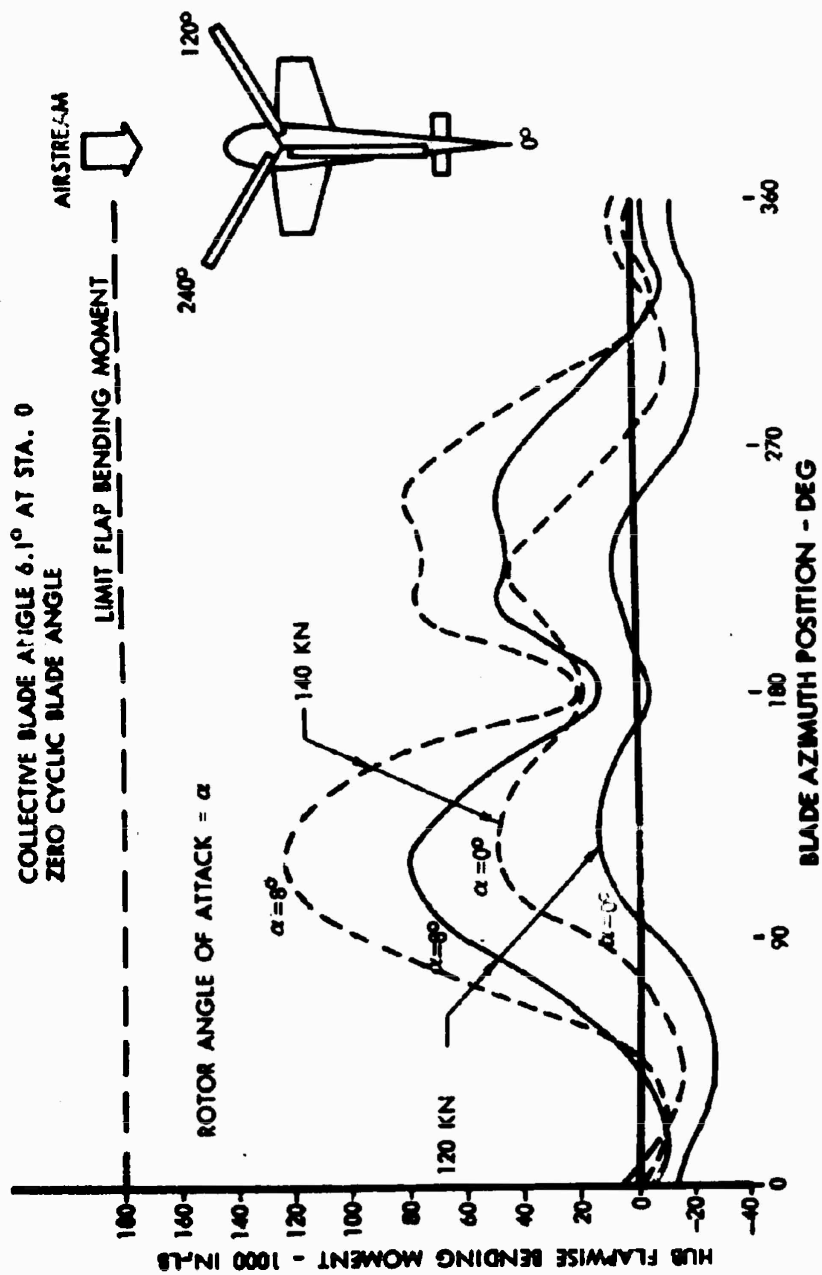


Figure 192. Summary of Nonrotating Flapwise Bending Moments for Stopped-Rotor, 33-Foot-Diameter.

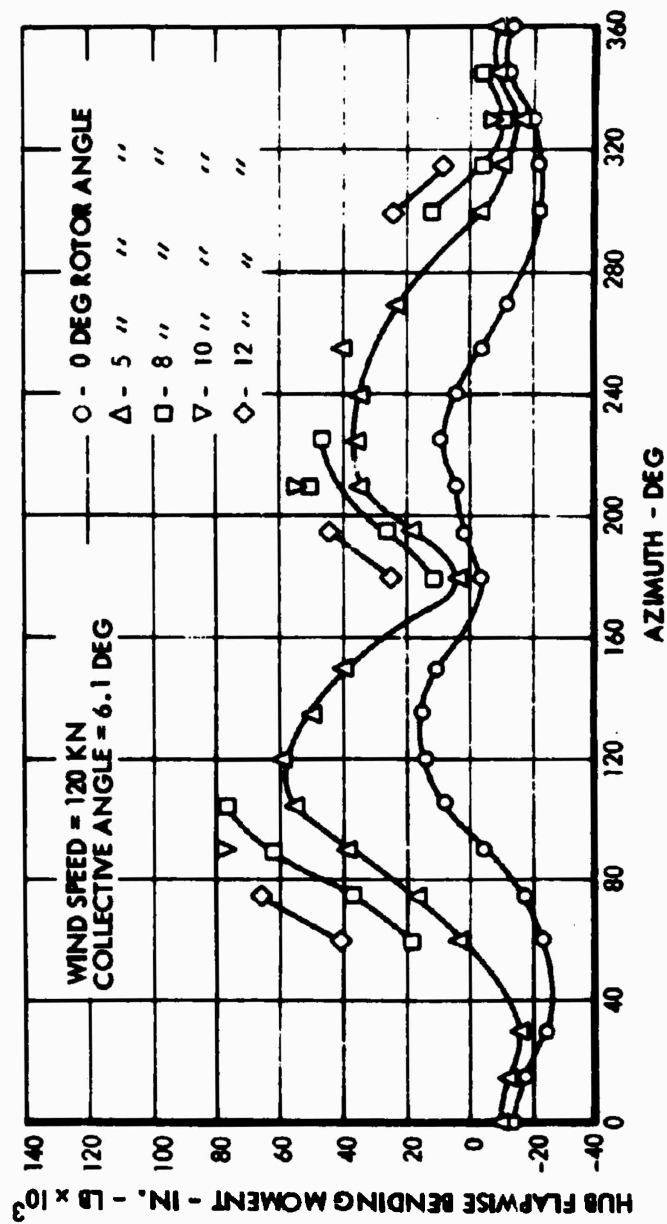


Figure 193. Nonrotating Flapwise Bending Moments as a Function of Rotor Angle for 33-Foot-Diameter Stopped-Rotor Full-Scale Model.

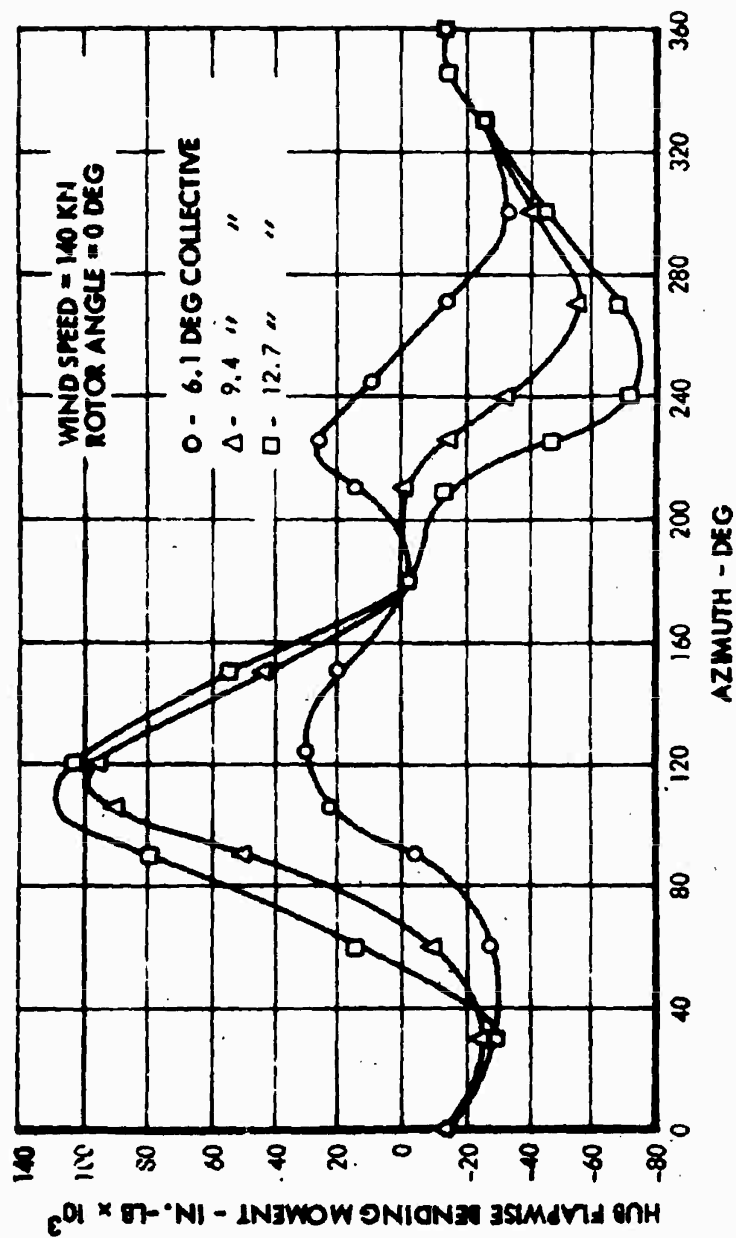


Figure 194. Nonrotating Flapwise Bending Moments as a Function of Collective Angle for 33-Foot-Diameter Stopped-Rotor Full-Scale Model.

Figures 195 and 196 show curves of root flap-bending moment, and their inverse, as a function of wind speed for two critical azimuth positions. Although somewhat limited in definition, these curves permit some evaluation of blade divergence characteristics and substantiate the analytical methods used to estimate stopped-rotor aeroelastic characteristics. It should be pointed out that the divergence characteristics of a blade at an azimuth position of 180 degrees are a function of rotor angle of attack because of a nonlinear viscous cross-flow phenomenon; consequently, the effects of gusts and up-flow induced by the fuselage forebody are of significance. These effects are transient since the rotor is stopped in the position shown in Figure 183.

The blades were successfully folded and deployed at various speeds up to 140 knots during this program.

Some of the analytical results obtained for the CRA main rotor blades are illustrated in Figures 197, 198, 199 and 200. As illustrated by Figure 201, the critical divergence speed of the CRA main rotor blades is at least 168 knots at an azimuth position of 225 degrees. Examination of the rotor bending stiffness distribution, shown on Figure 149, shows that the design load factor of 3g's has resulted in a reduced EI (flapping) from station 25 to station 70. Increased stiffness in this region will result in a substantial divergence speed increase.

The possibility of cyclic divergence of the rotor system due to swash plate displacement is precluded by a residual positive spring restraint between the swash plate and fuselage structure. This restraint is inherent in the design of the blade pitch-bias system.

The folding provisions are similar to those of the 33-foot-diameter rotor, the suitability of which has already been demonstrated in wind tunnel tests (Figure 190).

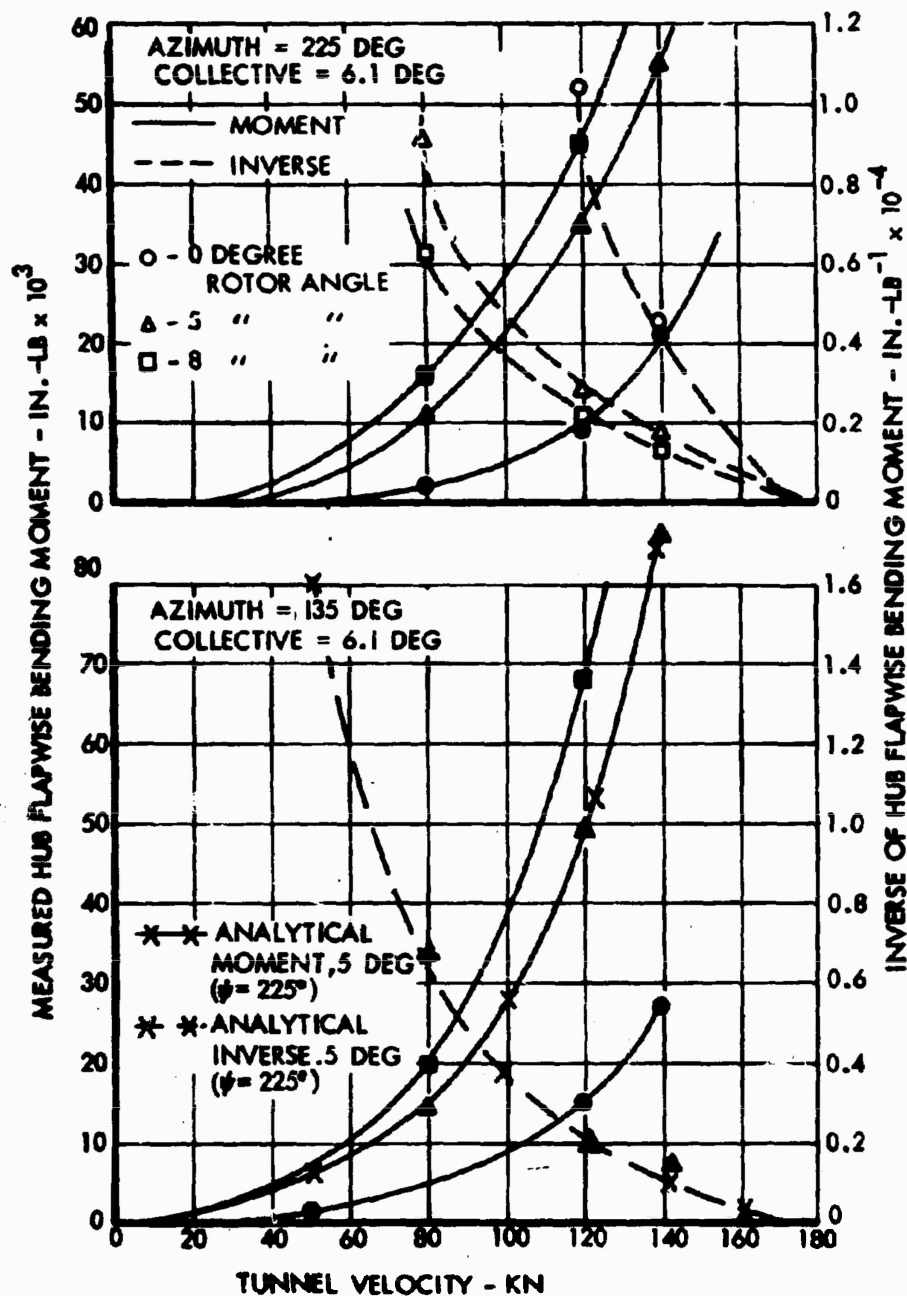


Figure 195. Hub Flapwise Bending Moment - 33-Foot-Diameter Rotor.

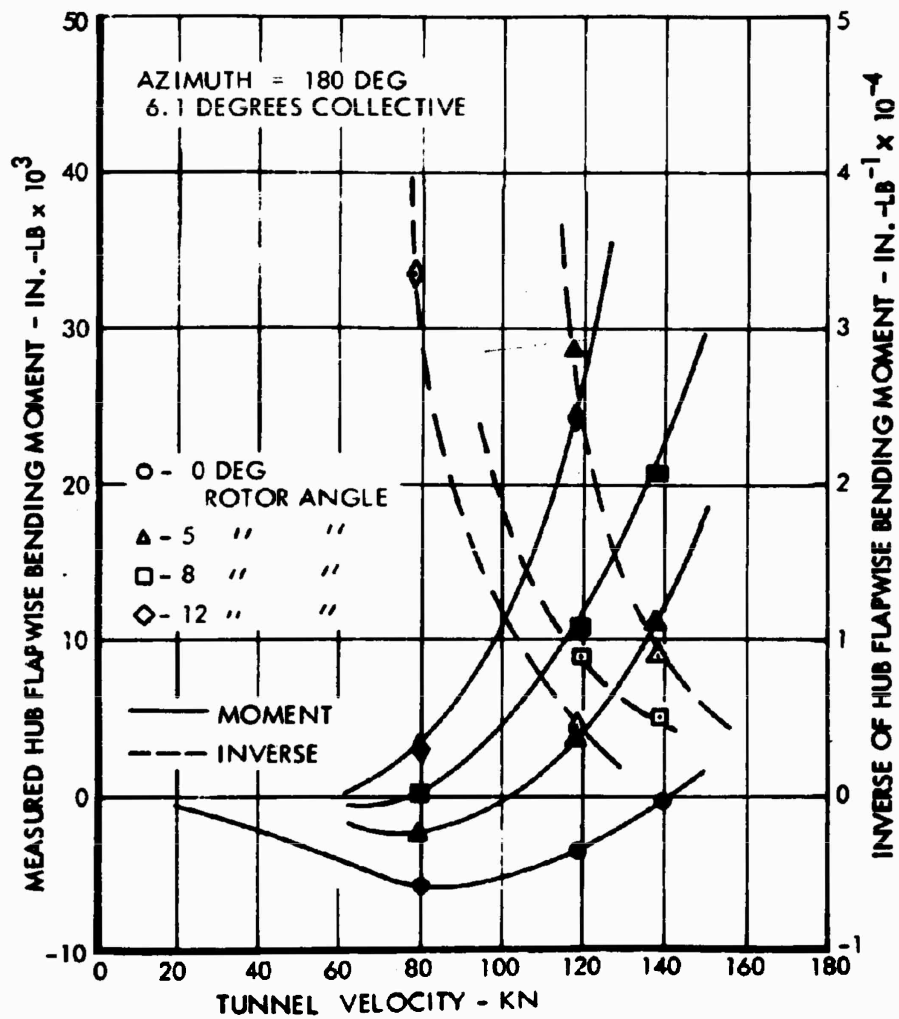


Figure 196. Hub Flapwise Bending Moment - 33-Foot-Diameter Rotor.

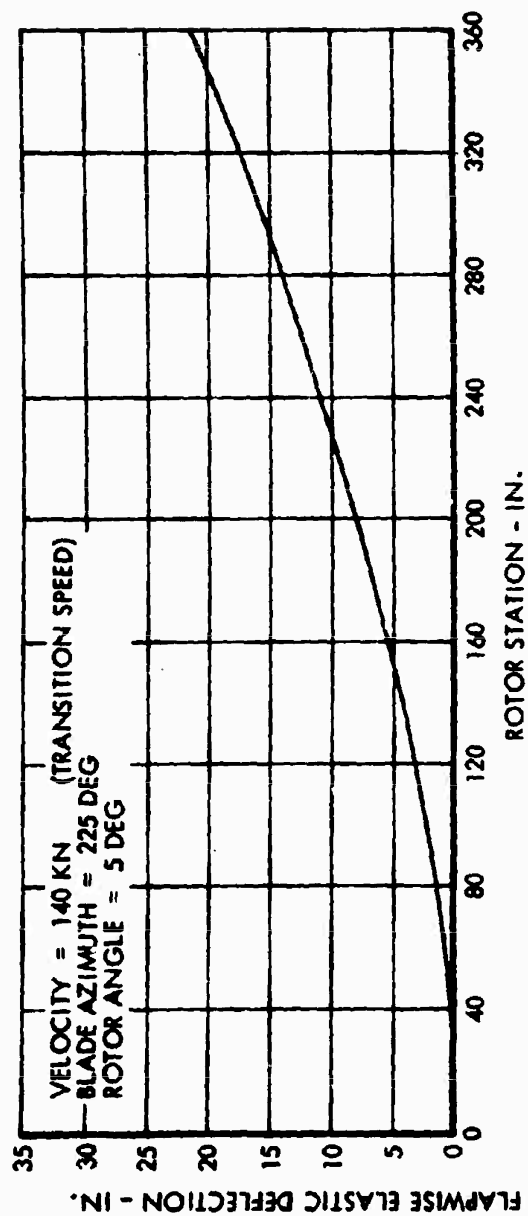


Figure 197. CRA Blade Flapwise Elastic Deflection.

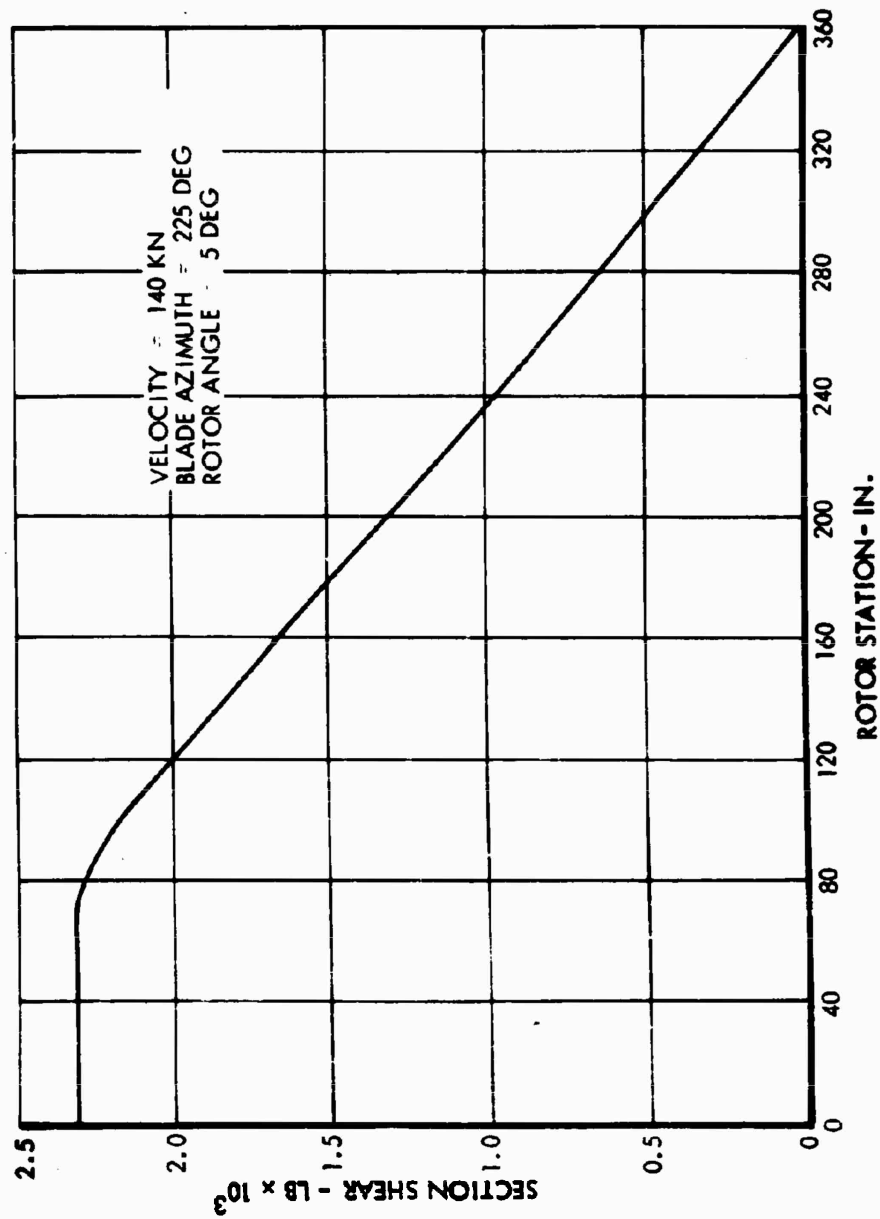


Figure 198. CRA Blade Section Shear.

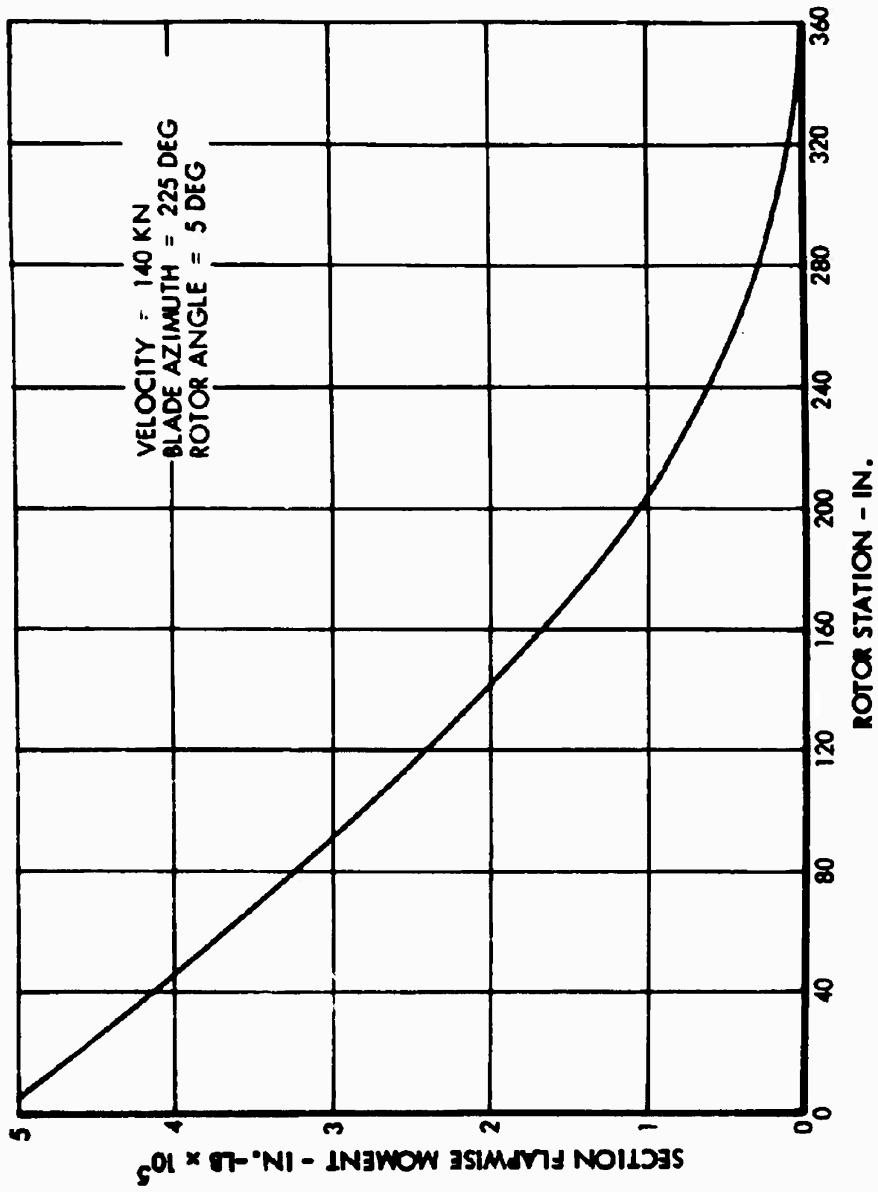


Figure 199. CRA Blade Section Flapwise Moment.

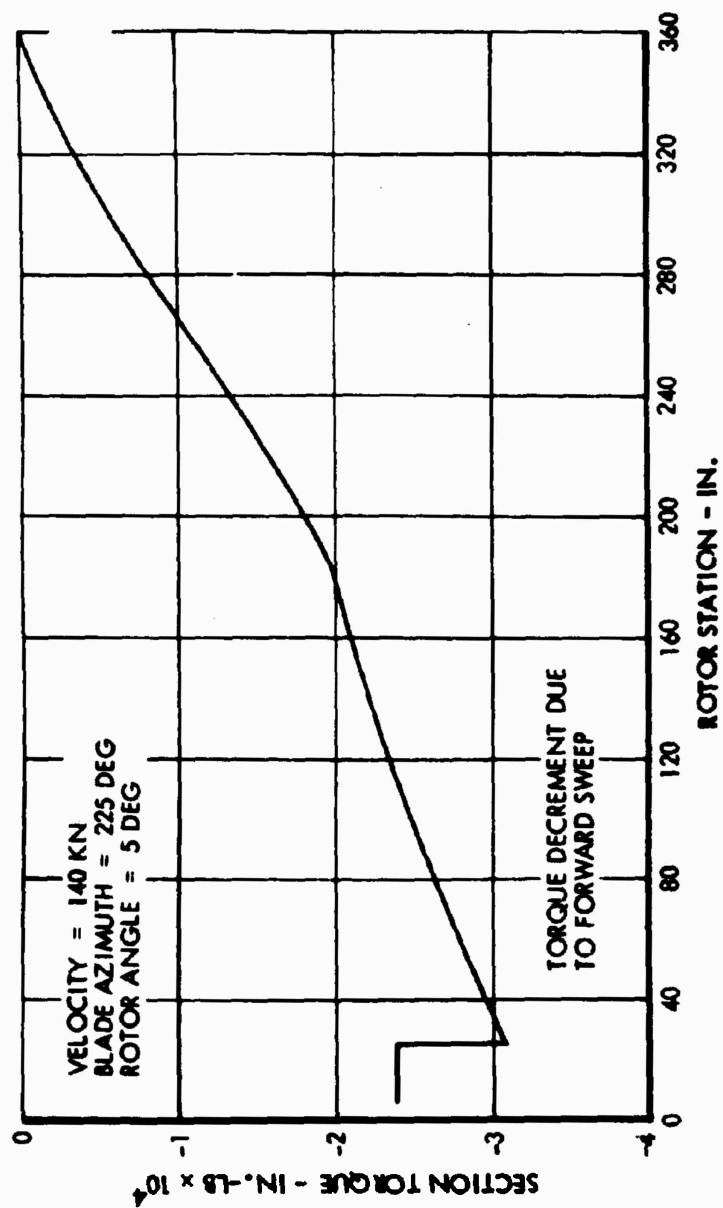


Figure 200. CRA Blade Section Torque.

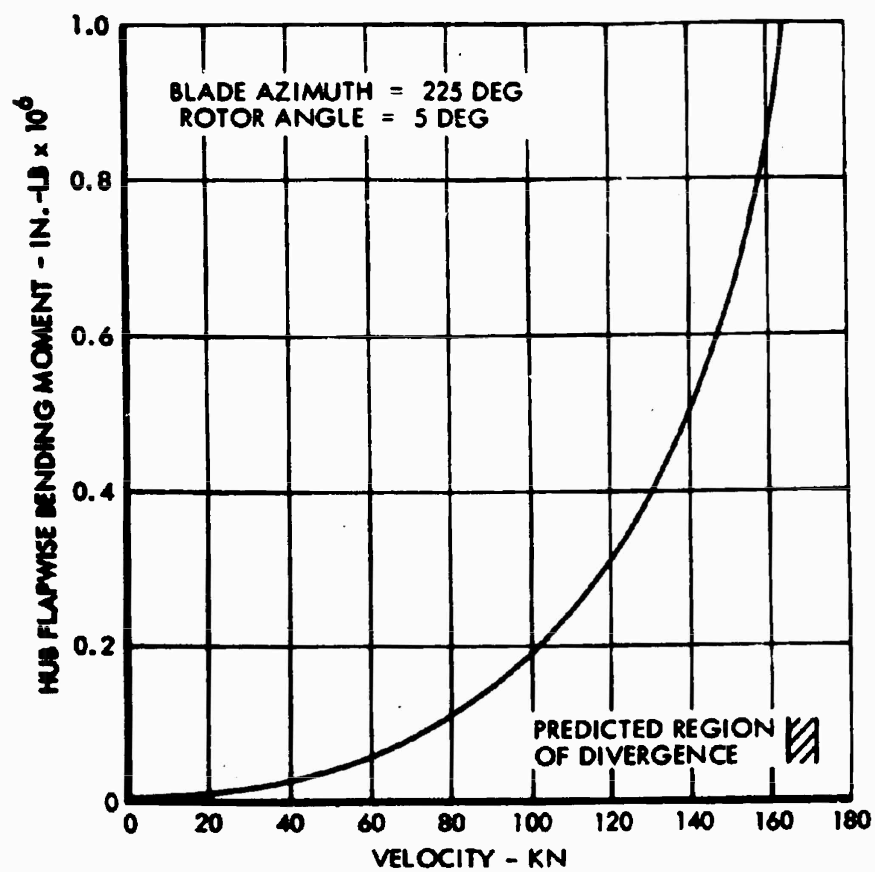


Figure 201. CRA Blade Divergence Region.

LITERATURE CITED

1. Breaks, J., LOW-SPEED WIND TUNNEL TEST ON THE CL-945 COMPOSITE RESEARCH AIRCRAFT, Lockheed-California Company; Lockheed Report LFL L-146, May 1966.
2. Daley, V.N. and Lord, D.R., AERODYNAMIC CHARACTERISTICS OF SEVERAL 6- PERCENT THICK AIRFOILS AT ANGLES OF ATTACK FROM 0° TO 20° AT HIGH SUPERSONIC SPEEDS, NACA TN3424, May 1955.
3. Wilson, H.B. and Horton, E.A., AERODYNAMIC CHARACTERISTICS AT HIGH AND LOW SUBSONIC MACH NUMBERS OF FOUR NACA 6-SERIES AIRFOIL SECTIONS AT ANGLES OF ATTACK FROM -2° TO 31° ; NACA RM L53C20, June 1953.
4. Abbot, I.H. and Von Doenhoff, A.E., THEORY OF WING SECTION, New York, Dover Publications.
5. Jewel, J.W. and Harrington, R.D., EFFECT OF COMPRESSIBILITY ON THE HOVERING PERFORMANCE OF TWO 10-FOOT-DIAMETER HELICOPTER ROTORS TESTED IN THE LANGLEY FULL-SCALE TUNNEL, NACA RM L58B19, April 1958.
6. Carpenter, P.J., LIFT AND PROFILE DRAG CHARACTERISTICS OF A NACA 0012 AIRFOIL SECTION AS DERIVED FROM MEASURED HELICOPTER ROTOR HOVERING PERFORMANCE, NACA TN4357, September 1958.
7. Pruyn, R.R. and Miller, N.J., STUDIES OF ROTOR CRAFT AERODYNAMIC PROBLEMS AIMED AT REDUCING PARASITE DRAG, ROTOR-AIRFRAME INTERFERENCE EFFECTS, AND IMPROVING AIRFRAME STATIC STABILITY, WADD TR 61-124, 1961.
8. Holford, F.R., PERFORMANCE ANALYSIS OF LOCKHEED VC-130, Lockheed-California Company; Lockheed Report LR 8705, June 1952.
9. Blackaby, J.R. and Watson, E.C., AN EXPERIMENTAL INVESTIGATION AT LOW SPEEDS OF LIP SHAPE ON THE DRAG AND PRESSURE RECOVERY OF A NOSE INLET IN A BODY OF REVOLUTION, NACA TN 3170, 1954.
10. Nichols, M.R. and Arvid, A.L., Jr., INVESTIGATION OF A SYSTEMATIC GROUP OF NACA 1-SERIES COWLINGS WITH AND WITHOUT SPINNERS, NACA TR 950, 1949.
11. DYNAMIC STABILITY AND CONTROL RESPONSE OF A COMPOUND HELICOPTER, Lockheed-California Company; Lockheed Aerodynamics Memo No. 23B.
12. Turner, A.W., FINAL SUMMARY REPORT - XH-51A RIGID ROTOR HELICOPTER PROGRAM, Lockheed-California Company; Lockheed Report LR 17545, February 1964.

LITERATURE CITED (Continued)

13. HOW TO USE AERODYNAMICS DEPARTMENT GENERALIZED TORQUE AND THRUST CHARTS FOR PROPELLERS INCORPORATING NACA 16-SERIES AIRFOIL SECTIONS, Hamilton Standard Aerodynamics Note No. 6, Supplement II.
14. Jepson, W.D., SOME CONSIDERATIONS OF THE LANDING AND TAKE-OFF CHARACTERISTICS OF TWIN ENGINE HELICOPTERS, PART I - WEIGHT-VELOCITY DIAGRAMS AND PART POWER DESCENTS, Journal of the American Helicopter Society, Vol. 7, No. 4, October 1962.
15. DeYoung, J. and Harper, C.W., THEORETICAL SYMMETRIC SPAN LOADING AT SUBSONIC SPEEDS FOR WINGS HAVING ARBITRARY PLAN FORM, NACA TR 921, 1948.
16. DeYoung, J., THEORETICAL SYMMETRIC SPAN LOADING DUE TO FLAP DEFLECTION FOR WINGS OF ARBITRARY PLAN FORM AT SUBSONIC SPEEDS, NACA TR 1071, 1952.
17. Kuhn, R.E. and Diaper, J.W., INVESTIGATION OF EFFECTIVENESS OF LARGE-CHORD SLOTTED FLAP ON DEFLECTING PROPELLER SLIPSTREAMS DOWNWARD FOR VERTICAL TAKE-OFF AND LOW-SPEED FLIGHT, NACA TN 3364, January 1955.
18. Smelt, R. and Davies, H., ESTIMATION OF INCREASE IN LIFE DUE TO SLIP-STREAM, ARC R & M, 1937.
19. Perkins, C.C. and Hage, R.E., AIRPLANE PERFORMANCE, STABILITY AND CONTROL; John Wiley and Sons, Inc., 1949.
20. Phillips, W.H., APPRECIATION AND PREDICTION OF FLYING QUALITIES, NACA TR 927, 1949.
21. Toll, T., SUMMARY OF LATERAL CONTROL RESEARCH, Langley Research Staff, NACA TR 868, 1947.
22. Sears, R.I., WIND TUNNEL DATA ON THE AERODYNAMIC CHARACTERISTICS OF AIRPLANE CONTROL SURFACES, NACA WR L-663, 1943.
23. Etkin, B., DYNAMICS OF FLIGHT; John Wiley and Sons, 1949.
24. USAF STABILITY AND CONTROL DATCOM, Air Force Flight Dynamics Laboratory, Wright-Patterson Air Force Base, October 1960, Revised July 1963.
25. Fischel, J. and Ivey, M., COLLECTION OF TEST DATA FOR LATERAL CONTROL WITH FULL SPAN FLAPS; NACA TN 1404, April 1948.
26. STRUCTURAL DESIGN REQUIREMENTS; HELICOPTERS, MIL-S-8698 (ASG), 1 July 1954, amended 28 February 1958.

LITERATURE CITED (Continued)

27. AIRPLANE STRENGTH AND RIGIDITY; FLIGHT LOADS, MIL-A-8861 (ASG), 18 May 1960.
28. Pratt, K.G. and Vennett, F.V., CHARTS FOR ESTIMATING THE EFFECTS OF SHORT-PERIOD STABILITY CHARACTERISTICS ON AIRPLANE VERTICAL-ACCELERATION AND PITCH-ANGLE RESPONSE IN CONTINUOUS ATMOSPHERIC TURBULENCE, NACA TN 3992, June 1957.
29. Beck, D.E., LT., USN; Wray, D.P., CPT., USA; Dummond, R.C.; Curry, P.R., MAJ., USA, FINAL REPORT, MILITARY RESEARCH EVALUATION OF THE LOCKHEED XH-51A, RIGID ROTOR HELICOPTER, U. S. Army; FT 23-4R-64, 7 January 1964.
30. Contract No. DA 44-177-AMC-372(T), Composite Research Vehicle (Including Statement of Work).
31. AIRPLANE STRENGTH AND RIGIDITY; LAND PLANE LANDING AND GROUND HANDLING LOADS, MIL-A-8862 (ASG), 18 May 1960.
32. GROUND LOADS, ANC-2, October 1952.
33. Goff, J.D., EXPERIMENTAL INVESTIGATION OF ROTOR MODEL STOP/START IN FORWARD FLIGHT, Lockheed-California Company, Lockheed Report LR 17865.
34. AIRPLANE STRENGTH AND RIGIDITY; GENERAL SPECIFICATION FOR, MIL-A-8860 (ASG), 18 May 1960.
35. LOCKHEED STRESS MEMO MANUAL, Lockheed-California Company.
36. Perry, D.J., AIRCRAFT STRUCTURES, New York, McGraw-Hill Book Company, Inc., 1950.
37. Roark, R.J., FORMULAS FOR STRESS AND STRAIN, New York, McGraw-Hill Book Company, Inc., 1943.
38. METALLIC MATERIAL AND ELEMENTS FOR AEROSPACE VEHICLE STRUCTURE, MIL-HDBK-5A, February 1964.
39. A SUMMARY OF DIAGONAL TENSION, NACA TN 2661, May 1952.
40. Hoblit, F.M., ANALYSIS OF LUGS AND SHEAR PINS IN ALUMINUM AND STEEL ALLOYS; Lockheed-California Company, Lockheed Report LR 8025, 31 March 1952.
41. Marlin-Rockwell Company, Jamestown, New York, 14701, MRC BALL AND ROLLER BEARINGS, CATALOG NO. 60, 1965.

LITERATURE CITED (Continued)

42. SKF Industries, Inc., Los Angeles, California 90007, SKF General Catalogue.
43. Danielson, H.G., SUMMARY OF STOPPED FOLDING ROTOR STATIC PROOF AND WHIRL TOWER TESTS, Lockheed-California Company, Lockheed Report LR 19314, 6 December 1965.
44. Celniker, L., Culver, I.H., and Theriault, P.W., CONSIDERATIONS RELATIVE TO STOPPING A ROTOR IN FORWARD FLIGHT, CL-870, American Helicopter Society Paper, 1965.
45. Celniker, L., Carlson, R.M., and Donham, R.E., STOPPED AND SLOW ROTOR AIRCRAFT CONFIGURATION, Paper presented at the National Aeronautic and Space Engineering and Manufacturing Meeting of the Society of Automotive Engineers, Los Angeles, California, 4-8 October 1965.

Unclassified

DOCUMENT CONTROL DATA - R & D		
(Security classification of title, body of abstract and indexing annotation must be entered when the overall report is classified)		
1. ORIGINATING ACTIVITY (Corporate author) Lockheed-California Company A Division of Lockheed Aircraft Corporation Burbank, California		2a. REPORT SECURITY CLASSIFICATION Unclassified
3. REPORT TITLE STOPPED-STOWED ROTOR COMPOSITE RESEARCH AIRCRAFT		2b. GROUP
4. DESCRIPTIVE NOTES (Type of report and inclusive dates) Final Report		
5. AUTHOR(S) (First name, middle initial, last name)		
6. REPORT DATE January 1969	7a. TOTAL NO. OF PAGES 430	7b. NO. OF REFS 45
8a. CONTRACT OR GRANT NO. DA 44-177-AMC-372(T)	8b. ORIGINATOR'S REPORT NUMBER(S) USAAVLABS Technical Report 68-40	
8c. PROJECT NO. Task 1F163204D15704	8d. OTHER REPORT NO(S) (Any other numbers that may be assigned this report) Lockheed Report LR 21722	
9. DISTRIBUTION STATEMENT This document has been approved for public release and sale; its distribution is unlimited.		
11. SUPPLEMENTARY NOTES	12. SPONSORING MILITARY ACTIVITY US Army Aviation Materiel Laboratories Fort Eustis, Virginia	
13. ABSTRACT This report describes the preliminary design of the Army VTOL Rotary Wing Composite Research Aircraft (CRA). The vehicle is configured to meet the requirements, and satisfy the objectives, of this program. This CRA design was the result of combining the most desirable features of a helicopter with those of a fixed-wing aircraft. The vehicle derived was capable of hovering as a helicopter with low rotor downwash velocity and yet cruise at high speed with economy and little noise or vibration. Use of the rigid-rotor system supplied positive control moments, in-flight rotor stop/start capability, and a simple blade-folding/stowing mechanism. The CRA can fly up to the conversion speed in the helicopter mode transfer lift and control to the conventional fixed-wing surfaces, stop the rotor, fold the blades and retract the rotor and blades into the top of the fuselage. This process is reversible to convert from the fixed-wing configuration to the helicopter. The results of this study indicate that the CRA is feasible and additional study and development should be undertaken.		

DD FORM 1473

REPLACES DD FORM 1473, 1 JAN 64, WHICH IS OBSOLETE FOR ARMY USE.

Unclassified

Security Classification

Unclassified

Security Classification

14.	KEY WORDS	LINK A		LINK B		LINK C	
		ROLE	WT	ROLE	WT	ROLE	WT
	Helicopter Slowed Rotor Stopped Rotor Stowed Rotor Rigid Rotor Composite Aircraft V/STOL Aircraft Folding Rotor High-Speed Helicopter Hingeless Rotor Winged Helicopter						

Unclassified

Security Classification